International Research Journal of Computer Science and Application
Vol. 2, No. 1, March 2018, pp. 1-181
Available Online at http://acascipub.com/Journals.php

Research article

d-dimensional analog of an inverse-gamma normal conjugate stratified by multivariate square summable discrete trajectories of finite anomalous nontrivial automorphic eco-endmembers based on Fréchet differentiability of Lipschitz maps recursively canonicalized between quasi-Banach spaces for tabularizng invariant Gaussianism injectable linearity and nonsensical maxima in an Cauchy integral formula employing holomorphic functions robustly regressively devised from eco-georeferenceable *Anopheline arabiensis s.s.* geo-spectrotemporal capture point geosampled prognosticators under the sparsity assumption: Objective Bayesian epistemological theory for evidentially deducing parasitological indicators of malaria transmission

Benjamin G. Jacob[1] **and Robert J. Novak**[1]

[1]**Global Infectious Disease Research Program, Department of** Public Health, College of Public Health, University of South Florida, 3720 Spectrum Blvd, Suite 304, Tampa, Florida, USA 33612

E-mail: bjacob1@health.usf.edu

International Research Journal of Computer Science and Application
Vol. 2, No. 1, March 2018, pp. 1-181
Available Online at http://acascipub.com/Journals.php

Abstract

Prior beliefs concerning malaria, transmission θ may be approximately modeled by a conjugate prior distribution π for optimally forecasting, hyperproductive, seasonal, malaria, mosquito, capture point, geolocations especially when X = (X1,…,Xp). Exploiting linearizability of capture point, aquatic, larval habitat, signature frequencies employing a p-variate normal distribution with an unknown mean vector θ = (θ1,…,θp) may reveal covariates associated with prolific seasonal foci. Further, an expectation of a random matrix Σ may statistically define an inferential dataset of wavelength, land use land cover (LULC), iteratable, signature,capture point prognosticators whose element in the i, j position could be the covariance between the i th and j thelements of a regressively elucidative, multivariate, random sequence, (e.g. a random tree, stochastic process, etc). In so doing, asymptotic properties of the matrix may reveal interpolative, LULC, properties which may reveal unknown, prolific, malaria, mosquito, aquatic, larval habitat geolocations by asymptotically expressing a capture point as a sequence of homoscedastic, scalar, krigable frequencies. Subsequently, the capture point, aquatic, larval habitat, sub-pixel signatures may stochastically, or deterministically, geo-spectrotemporally identify geolocations of un-geosampled, eco-georeferenceable, seasonal, hyperproductive, malaria, mosquito, capture points.We constructed an ento-endmember, multinomial, aquatic, larval, habitat, sub-meter resolution, geoclassifiable, LULC signature, frequency dataset of grid-stratified, quantile, distribution estimators which were tabularized employing a likelihood-free, Bayesian treatment for determining eco-georeferenecable, unknown, hyperproductive, malaria, mosquito, capture point, foci eigenvectors from an algorithmic, semi-parametric, autocorrelation, spatial filter,orthogonal, eigenfunction decomposition algorithm. Subsequently a probabilistic matrix factorization was performed in which model capacity was controlled automatically by integrating over all the model hyperparameters for deducing capture point, Gaussian, LULC priors for identifying unknown, hyperproductive, aquatic, larval habitats of *Anopheles arabiensis s.s.*, a malaria, mosquito vector, in Karima agro-village complex in the Mwea Rice Scheme in central Kenya. We considered an observation model of the form z (x) = y (x) + σ [y (x)] ξ (x), x ∈ X where X was the set of the sub-meter resolution, sensors, active, pixel positions, z was the actual raw LULC, signature, frequency capture point, aquatic,larval habitat, data output, y was the ideal output, ξ was zero-mean random noise with standard deviation (std) equal to 1, and σ was a function y, modulating the std of the overall noise component. The function σ (y) was the std function while σ2 (y) was the variance function. Since E {ξ (x)} = 0 we had E {z (x)} = y (x) and std {z (x)} = σ (E {z (x)}). There were no additional restrictions on the distribution of ξ (x), and different capture points were revealed with different distributions. A preference matrix described each habitat signature entry R*ij*, to find a factorization that minimized the root mean squared error on the test set. We defined I*ij* to be 1, if R*ij* was known (i.e., larval habitat i had an eco-endmember scatterplot j) and 0 otherwise in the model derivatives. Further, we let N(x|μ,σ2)=fX(x) with X∼N(μ,σ2)X∼N(μ,σ2).Accordingly, we quantitatively defined a conditional probability of the ratings with hyperparameter σ2p(R|U,V,σ2)=∏i=1N∏j=1M[N(R*ij*|UiTV*j*,σ2)]I*ij*(1)and priors on U and V with hyperparameters σU2,σV2p(U|σU2)=∏i=1NN(Ui|0,σU2I) and p(V|σV2)=∏i=1MN(Vi|0,σV2I). In the model estimator dataset, y maximized the log posterior over U and V where a substitute for the definition of N was explicated by taking the log[i.e., lnp(U,V,σ2,σ2V,σ2U)].Henceforth, 12σ2∑i=1N∑*j*=1MIij(Rij−UiTVj)2−12σU2∑*i*=1NUiTUi−12σV2∑i=1NViTVi−12(κlnσ2+NDlnσ2U+MDlnσ2V)+C(3) −12(κlnσ2+NDlnσU2+MDlnσV2)+C(3) was rendered where κ was the number of known, eco-georeferenceable, capture point, signature entries and C was a constant independent of the ento-endmember,LULC, geosampled, parameterizable estimators. We adjusted the three variance hyperparameters (which were observation noise variance and prior variances) as constants which reduced the optimization to the first three terms (i.e., a sum-of-squared minimization). Then defining λM=σ2/σM2 for M=U,V and multiplying by −σ2<0 resulted in the following objective function E=12(∑i=1N∑*j*=1MI*ij*(R*ij*−U*i*TV*j*)2+λU∑i=1N‖U*i*‖F2+λV∑i=1M‖Vi‖F2)where ‖A‖2F=∑mi=1∑nj=1|aij|2‖ whence F2=∑i=1m∑j=1n|aij|2 was the Frobenius norm. Since all the uncoalesceable, interpolative, signature, wavelength, iterable, habitat values were known [i.e. Iij=1∀(i,j)], σU2,σV2→∞ was reduced to a singular value decomposition.The objective function, was then minimized employing the method of steepest descent which was linearizable based on the geosampled habitat observations. The dot product specific feature vectors were passed through the logistic function g(x)=1/[1+exp(−x)] which bounded the range of habitat signature predictions.We employed a simple linear-Gaussian model which revealed vulnerability explanative forecasts outside of the range of the known capture point values. As well, the ratings from 1 to K were mapped to the [0,1] interval employing the

function t(x)=(x−1)/(K−1). This ensured that the range of the interpolatable, habitat, LULC frequencies matched the range of predictions made by the model. Thus, p(R|U,V,σ2)=∏Mi=1∏Nj=1[N(Rij|g(UTiVj)σ2)]. Proprieties of the posterior distribution in the model, integrated the observed, Anopheles data conditioned on a categorical, outcome variable (i.e., immature, seasonal, frequency, density count). A generative model was devised where b~N(0,σb)a~N(0,σW)zn~ (W)xn~p(·|β,zn)tn~Weibull[log(1+exp(z^Tna+b)]k. The latent input z_i came from a geosampled, An. arabiensis, capture point, regressable, LULC explicator. The seasonal, immature habitat, likelihood distribution was p(t|x)=∫zp(t|z)p(z|x)dz which accounted for all the noise in the sub-pixel, LULC, eco-endmember, signature, frequency paradigm employing the Bayes' theorem. In particular, a sequential Monte Carlo (SMC) algorithm that was adaptive in nature approximated a cloud of weighted, random, hyperproductive, seasonal, eco-georeferenceable, capture point samples which were subsequently propagated over time. Quantile distributions were constructed based on a copula from the iterative, Bayesian, computation algorithms. An informative prior was generated. A recognition algorithm expressed signature habitat images in terms of orthogonal two dimensional Gaussian-Hermite moments (2D-GHMs). Motivation for developing 2D-GHM-based recognition algorithm here included capturing higher-order, hidden, nonlinear, 2D structures within the LULC images while quantitating the invariance of certain linearized combinations of the moments to the geometric distortions in the capture point, grid-stratified images. The 2D-GHMs based on a set of orthonormal polynomials captured rotation and translation invariants in the frequency LULC model which proved that the construction forms of geometric moment invariants were valid in the linearized combinations. The moments stored the image information with minimal redundancy. A function was defined on an inner product space which possessed the rotation-invariant property. Since the moments were definable on the continuous domain, suitable transformations of the eco-endmember, An. arabiensis, capture point foci were needed to regressively quantitate these moments. Besides the discretization error derived from the approximation of various integrals, the inevitable uncertainty in the vulnerability forecasts were reconstructed with binary and gray-level, LULC, habitat images. The obtained results revealed the quality from Gaussian-Hermite moments were superior to known Legendre, discrete Tchebichef and Krawtchouk moments. Habitat properties of the modified, capture point, LULC, polynomials, specifically orthogonality and orthogonal invariance revealed an interval on the center of [-1,1] covered more zeros than did that on the edge of [-1,1]. A set of octiles was trialed as well as functions which exposed the unknown, hyperproductive, capture point, LULC geolocations with all symmetrical values (e.g. uncorrelatedness, scale, skewness and kurtosis) accounted for. The summary statement revealed a broad range of temporal trend derivatives in both the mean and variance. A computation of the probability of inclusion from the SMC output was specified. Variable selection was applied to the lags in the simulation, making it possible to infer the lag order from the regressed, capture point, aquatic, larval habitat, signature, frequency, count data simultaneously with all the other geosampled wavelength estimators. The Fisher information matrix for a two-parameter gamma distribution revealed un-geosampled, hyperproductive, An. arabiensis, seasonal, capture point, aquatic, larval habitat, LULC, descriptors employing $F'(z) = \psi_1(z+1)$. Sums and differences of $\psi_1(r/s)$ for small integral r and s were frugally extractable in terms of t k and π. For example, $\psi_1\left(\frac{1}{4}\right)=\pi^2+8K, \psi_1\left(\frac{1}{3}\right)=\frac{2}{3}\pi^2+3\sqrt{3}\ \mathrm{Cl}_2\left(\frac{2}{3}\pi\right), \psi_1\left(\frac{1}{2}\right)=\frac{1}{2}\pi^2, \psi_1\left(\frac{2}{3}\right)=\frac{2}{3}\pi^2-3\sqrt{3}\ \mathrm{Cl}_2\left(\frac{2}{3}\pi\right), \psi_1\left(\frac{3}{4}\right)=\pi^2-8K, \psi_1(1)=\zeta(2)=\frac{1}{6}\pi^2, \psi_1\left(\frac{5}{4}\right)=\pi^2+8K-16, \psi_1\left(\frac{3}{2}\right)=\frac{1}{2}\pi^2-4$ and $\psi_1(2)=\frac{1}{6}\pi^2-1.$ Here, the Fisher information matrix was I(θ)= trigamma(α)−1/λ −1/λ α/λ^2.Its determinant revealed| I(θ)| trigamma(α)−1/λ −1/λ α/λ^2=α trigamma(α) − 1 λ^2 and the Jeffreys prior was articulated as g(α, λ)=p α trigamma(α) – 1 whence g was the Catalan's constant which we approximated in the malaria, mosquito model by $K=\sum_{k=0}^{\infty}\frac{(-1)^k}{(2k+1)^2}$. The probability distribution revealed capture point signature, eco-endmember, frequency, gridde, LULC data conditional on a particular, discrete, aquatic, larval habitat, frequency, density, count value which was optimally devisable by Np(μ, A), whence μ and A were normalized. It may be desirable to estimate θ under the quadratic loss L (θ, δ) = (θ − δ)tQ(θ − δ) whence regressively forecasting grid-stratifiable, malaria, mosquito, capture point, sub-meter resolution, sub-pixel, robustifiable, LULC, interpolative covariates for precisely asymptotically geo-spectrotemporally, targeting un-geosampled, hyperproductive, eco-georeferenceable, seasonal foci. Sequential estimation of iteratable, ento-endmember,topological, prognosticators of unknown, seasonal, capture point, An. arabiensis foci may reveal risk factors to malaria transmission based on eigen-decomposable, sub-pixel, grid-stratifiable, geoclassifiable, LULC,signature, frequency co-factors (e.g., Euclidean distance of an eco-georeferenced, seasonal, prolific, agro-irrigated, African, riceland, aquatic, larval habitat, capture point to the nearest, remotely calculable, agro-village,

centroid), unless the geosampled count sequence is considered a realization of a random, zero-mean autocorrelated, diagnostic, capture point variable. Intuitively, main effects and interaction explicators quantized from an eco-endmember, eigenfunction, eigendecomposable, spatial filter, eigenvector An. arabiensis, vulnerability regression equation may satisfy the constraint $R(\theta, \delta) \leq tr(Q\Sigma) + c$, $R(\theta, \delta)$. Although employing prime computing ratios of normalizing constants in common measurable geospace can define correlation and non-orthogonality in such frequency paradigms, the residuals may not equate to causality in any krigeable, LULC, signature, frequency dataset of synthetic, capture point, orthogonal,capture point eigenvectors.Maximizing the log-posterior over an empirical uncoalesced, eco-entomological, geoclassifiable, eco-endmember LULC dataset of eco-georeferenceable, seasonal, frequency, capture point, non-negatively autorrelated, sub-meter resolution, An. arabiensis, geosampled, geo-spectrotemporal, attribute features with hyperparameters (i.e. the observation noise variance and prior variances) and simulating the data in probability space may minimize the sum-of-squared-errors objective function employing quadratic regularization terms for prevention of overfitting. Here a parallelizable expectation-maximization algorithm was constructed which we found applicable to large-scale, sub-meter resolution, grid-stratifiable, capture point, seasonal, malaria, mosquito, aquatic, larval, habitat, eco-epidemiological, uncertainty, risk, mapping applications. Regardless, our main result in this research is that an Lipschitz map quantitated between separable quasi-Banach spaces is Fréchet differentiable Γ-almost everywhere in an eco-endmember, sub-meter resolution, geoclassifiable, georeferenceable, An arabenisis, grid-stratifiable, capture point, geo-spectrotemporal, signature, frequency, prognosticative, LULC model provided that it is regularly Gˆateaux differentiable Γ-almost everywhere in the model and the derivatives stay within a norm separable space of operators. It is easy to see that wavelength, capture point, seasonal, malaria, mosquito, sub-pixel, interpolatable, signature, risk maps with the Radon-Nikodym property are Gˆateaux differentiable Γ. Moreover, Gˆateaux differentiability implies regular Gˆateaux differentiability with exception of another kind of negligible sets, (i.e., σ-porous sets). An eco-georeferenceable, seasonal, hyperproductive, capture point, sub-meter resolution, An. arabiensis, LULC, prognosticative, signature, frequency model is positive in every space in which every σ-porous sub-set is Γ-null. We show that this holds for C(K) with K countable compact, *the Tsirelson space and for all subspaces of c0, but that it fails for Hilbert spaces.*

Keywords: *Anopheline arabiensis*, trigamma(α), Gaussian-Hermite moments, Bayesian, Lipschitz map Fr´echet differentiable Gˆateaux differentiability.

Introduction

Unbiasedly, geo-spectrotemporally regressing sub-meter resolution, land use land cover (LULC), parameterizable, wavelength estimator datasets of malaria, mosquito, aquatic, larval habitat, eco-endmember, signature descriptors [e.g., visible an near infra-red (NIR) reflectance, capture point covariates] rest on four principal assumptions which justify the usage of frequentism for optimally prognosticating, geolocations of un-geosampled, hyperproductive, seasonal foci: (i) the coefficient of determination, (R^2) can reveal the proportion of the variance in the dependent variable (e.g., monthly, tabulated, malaria prevalence for an agro-irrigated, African, riceland, agro-village, ecosystem) from the endemic, emissivity-oriented and field geosampled, topological variables (ii) optimization of the independence of the discretization errors or the serial correlation will indicate an immature, habitat, Gaussian distribution; and, (iii) constant variance is expressable in the probability distribution in the formulated data.

For example, suppose there is an *n*, empirical, normalized, uncoalesced, dataset of ento-endmember, LULC, signature, ,geosampled, malaria, mosquito, seasonal, capture point, frequencies (e.g., discontinuously, canopied, hyperproductive, aquatic, larval, habitat, NIR density, count values), {yi,xi}which are employed as independent variables in an oviposition, linear, sub-meter resolution, forecast, vulnerability model where i=1,2,…,ni=1,2,…,*n*. Normalizations in ento-epidemiological, signature, LULC models include quantitating non-dimensional ratios of errors, devising residuals, scaling invariant means and standard deviations, eliminating effects of certain gross influences (e.g.,anomalous time series),procuring probability density functions and assessing percentiles[1]. Regressively, quantitatively interpolating an empirical dataset of multivariate, geosampled, signature, malaria, mosquito, aquatic, larval habitat, iterable, LULC quantities (e.g., orthogonal functions) whose sampling distribution does depend on the

parameters in an ordinary krige-based algorithm (e.g., weighted inverse distance matrix) may then reveal eco-georeferenceable, geolocations of unknown, seasonal, hyperproductive, LULC foci. The goal in aggregating an endemic epi-entomological dataset of parameterizable or semi-parameterizable, forecastable, eco-georeferenceable, vulnerability, model, signature, frequencies from normalized, geosampled, vector arthropod, grid-stratifiable, geoclassifiable, LULC, wavelength regressors is to locate the equation of the straight line (i.e., $y=\alpha+\beta xy=\alpha+\beta x$) [1] which may provide an optimal fit for precisely asymptotically determining geolocations of un-geosampled, seasonal, eco-georefernceable hyperproductive,eco-endmember foci.

Normalization of an input sub-meter resolution, experimental eco-georeferenceable, geo-spectrotemporal, multinomial, eco-endmember, explanatory LULC dataset derived from visible and NIR ento-epidemiological, empirical, frequency prognosticators can assure that geosampled, capture point, aquatic, larval habitat, regressable features representing geosampled, geoclassifiable, signature, wavelength explanators are in the same range of the values (i.e. [-1 1]) which may be appropriate whence the vector arthropod, remotely sensed data is processed in minimization algorithms. Gradient Descent (GD) is a first-order iterative optimization algorithm for finding the minimum of a function [3]. To find a local minimum of a function employing GD for an, eco-epidemiological, oviposition sub-meter resoluton, geo-spectrotemporal, grid-stratifiable, geoclassifiable, orthogonal, LULC datatset of unmixed, signature eco-endmember frequencies, a malariologist, medical entomologist or other experimenter may proportionally quantitate the approximate gradient of the geosampled signature regressands for determining the function at a predicted, unknown, eco-georeferenceable, capture point, seasonal, hyperproductive, aquatic, larval, habitat foci. Optimally, given a differentiable scalar field f(x) and x_1, a GD will transfer the, eco-epidemiological, LULC, eco-endmember, signature, model output toward values of f (e.g., geosampled, aquatic, larval habitat, prolific, frequency, count,) by taking steps in the direction of the negative gradient - λ f(x) for optimally deducing non-productive, seasonal, eco-georeferenceable, capture point geolocations. Locally, the negated gradient would be the steepest descent direction, (i.e., the direction that x_1 would need to move in order to decrease f in the model). Conversely moving to a positive gradient should reveal geolocations of un-geosampled, seasonal, eco-endmember, hyperproductive, capture point, eco-georeferenceable foci. The algorithm typically will converge to a local minimum, but it may rarely reach a saddle point, or not move at all if x_1 lies at a local maximum (e.g., a seasonal, prolific, foci, noisy outlier).

In mathematics, a saddle point or minimax point is a point on the surface of the graph of a function where the slopes (derivatives) of an eco-georeferenceable, expurgational geoclassifiable, function may be elucidatively employable for defining the surface transitioning to zero which may be employable in an LULC, signature, forecast-oriented, vulnerability, malaria, mosquito, eco-endmember model but it may not be a local extremum on both axes. An example of a saddle point is when there is a critical point with a relative minimum along one axial direction (between peaks) and at a relative maximum along the crossing axis [2]. However, a saddle point in an ento-epidemiological, malaria, mosquito, LULC, model for asymptotically, optimally, geo-spectrotemporally targeting eco-georeferenceable, seasonal, unknown, hyperproductive, eco-endmember foci need not be in such a form. For example, the function in such a predictive risk model may be based on a known, hyperproductive, signature foci, geosampled, feature attribute which may be a saddle point since it would not be a relative maximum, nor relative minimum in the model. Hence the geosampled, capture point, model renderings could have a relative maximum or relative minimum in any direction. A simple criterion for remotely validating if a given grid-stratifiable, ento-endmember, geoclassifiable, LULC, capture point, sub-meter resolution, oviposition, malaria, mosquito, signature frequency dataset derived from a real-valued, aquatic, larval habitat, function $F(x,y)$ derived from an uncoalesced, iterated interpolation, of a regressable, geosampled covariate (e.g., irradiance, of an un-geosampled, prolific, seasonal foci) for example, is to determine if the saddle point is able to be computated by the function's Hessian matrix at that point: if the Hessian is indefinite, then that capture point trait would be a saddle point.

In mathematics, the Hessian matrix or Hessian is a square matrix of second-order of a scalar-valued function, or scalar field [2]. Specifically, suppose $f: \mathbb{R}^n \to \mathbb{R}$ is a function taken as input where a vector $x \in \mathbb{R}^n$ is outputting a scalar $f(x) \in \mathbb{R}$ in an oviposition, sub-meter resolution, prognosticative, malaria, mosquito, eco-endmember, geo-spectrotemporal, signature, frequency, LULC model. If all second partial derivatives of f exist and are continuous over the domain of the function, in the ento--epidemiological, vulnerability model, then the Hessian matrix H of f would be a square $n \times n$ matrix which may be orthogonally, employable for precisely, aymptotically targeting, eco-georeferenceable,seasonal, grid-stratifiable, un-geosampled, hypeproductive, aquatic, larval habitats employing iteratively, interpolative,(co-kriged), eco-endmember,LULC foci, signature frequencies.

In linear algebra, a symmetric $n \times n$ real matrix is said to be positive definite if the scalar is positive for every non-zero column vector of real numbers [4] (e.g., empirical, geosampled, uncoalesced, seasonal, grid-stratifiable, malaria mosquito, aquatic, larval, habitat, geoclassfied, LULC, eco-endmember, capture point frequencies). More generally, an $n \times n$ Hermitian matrix is said to be positive definite if the scalar is real and positive for all non-zero column vectors of complex numbers. If the quadratic term 1/2 Y^T H Y is always positive for any nonzero y, then H is said to be positive definite [3]. However, a Hessian that is positive definite everywhere may not be required to obtain parsimonious quadratic convergence in an epi-entomological, eco-endmember, geoclassifiable, LULC, wavelength, uncoalesced dataset of geosampled, malaria, mosquito, sub-meter resolution, grid-stratifiable, signature, frequency, model estimators for optimally, asymptotically, geo-spectrotemporally targeting, eco-georeferenceable, seasonal, hyperproductive, unknown, aquatic, larval habitat, capture point foci. Quadratic convergence means that the square of the error at one iteration is proportional to the error at the next iteration [3]. If the quadratic term has positive and negative values, then H would be indefinite in any forecast, vulnerability, eco-epidemiological, sub-pixel, geoclassifiable, geo-spectrotemporal, LULC model for, targeting, eco-georeferenceable, prolific aquatic, larval habitat, foci based on optimally krigeable, signature frequencies. If the quadratic term is zero or positive in the endmember frequency model then H would be positive semi-definite. A positive semidefinite matrix is a Hermitian matrix all of whose eigenvalues are nonnegative [4].

Eigenvalues are a special set of scalars associated with a linear system of equations (i.e., a matrix equation) that are sometimes also known as characteristic roots, characteristic values proper values, or latent roots [2]. The determination of the eigenvalues and eigenvectors of a system is extremely important in physics and engineering, where it may be equivalent to matrix diagonalization and arises in such common applications as stability analysis, the physics of rotating bodies, and small oscillations of vibrating systems, to name only a few. Each geo-spectrotemporally extractable, eco-georeferenceable, aquatic, larval habitat, optimally, remotely, calculable eigenvalue may be paired with a corresponding so-called frequency,LULC eigenvector (or, in general, a corresponding right eigenvector and a corresponding left eigenvector; there is no analogous distinction between left and right for eigenvalues)[4]. Henceforth synthetic, orthogonal, spatial, filter, autocorrelation, eigenvectors may be employable to compute eco-geographically varying regression coefficients associated to a prolific, oviposition, geoclassfiable, LULC, signature, capture point, eco-endmember foci. These coefficients, which may be analogous to weighted regression coefficients, may display preferable properties whence optimally, iteratively, quantitatively, interpolating sub-meter resolution, capure point, geo-classifiable, grid-stratifiable, ento-endmember, LULC, malaria, mosquito, interpolative, signature frequencies for asymptotically, geo-spectrotemporally, elucidatively targeting unknown seasonal, hyperproductive, capture point foci.

Geographically weighted regression (GWR) has been receiving considerable attention in the literature. Maps of its coefficients tend to exhibit large degrees of multicollinearity as well as strong positive spatial autocorrelation. Meanwhile, spatial filtering furnishes a methodology for the better understanding of multicollinearity and for accounting for spatial autocorrelation. Interfacing these two approaches to quantitative, ento-epidemiological, empirical, geosampled, , geo-spectrotemporal, malaria, mosquito,eco-endmember, LULC, time series, signature, wavelength datasets may reveal that GWR could be viewed as a special case of spatial filtering that includes interaction terms between spatial filtering and sub-meter resolution, geometrically imaged, capture point, vector arthropod, seasonal, geosampled, discontinuous, attribute variables (percentage of intermittent canopy for a post tillering, agro-village, agro-irrigated, malaria, mosquito, aquatic, larval, habitat, eco-endmember, LULC foci) . This perspective may help clarify the degrees-of-freedom issue associated with GWR for optimally, asymptotically, geo-spectrotemporally targeting, seasonal, eco-georeferenceable, prolific, un-geosampled, malaria, mosquito, capture point, aquatic, larval habitats, while illuminating multicollinearity problems that plague it, which could indicate how to construct a more parsimonious solution to the eco-geographically, varying, linear, regression, coefficients problem for these epi-entomological, signature, wavelength paradigms. Further, forecast, vulnerability signature, capture point, malaria, mosquito, geo-spectrotemporal, eco-endmember, frequency models may contribute to the critique of GWR, adding to the discussion of multicollinearity complications outlined by Wheeler and Tiefelsdorf (2005) and addressed by Wheeler (2007) for optimal decomposition.

The frequency decomposition of a square matrix A into eigenvalues and eigenvectors is known as eigen-decomposition, and the fact that this decomposition is always possible as long as the matrix consisting of the eigenvectors frequency of A is square is known as the eigen-decomposition theorem. Eigenvector spatial filtering (ESF) is a spatial modeling approach, which has been applied in urban and regional studies, epi-ecological studies, and

so on. with non-approximated eigenvector spatial filtering and Monte Carlo simulation experiments which may be suitable for asymptotically quantitating, sub-meter resolution, LULC frequencies of geosampled, malaria, mosquito, capture points for robustly targeting un-geosampled, seasonal, hyperprouctive, aquatic, larval, habitat foci. The result may suggest that the proposed approaches effectively remove positive spatial dependence in the residuals with very small approximation errors whence the number of eigenvectors considered is a specific *n* geosampled, capture point, larval habitat, frequency, count value (e.g., 300 or more). Note that these ESF approaches may not deal with negative spatial dependence in eco-georeferenceable, oviposition, eco-endmember optimizable LULC signature datasets of iteratively interpolative, geoclassifiable, grid-stratifiable, geoclassifiable, unmixed frequencies. The proposed approaches are implementable in an R or SAS package. Let P be a matrix of eigenvectors of a given square matrix A and D be a diagonal matrix with the corresponding eigenvalues on the diagonal in a sub-meter resolution, eco-endmember, geoclassifiable, LULC, oviposition, signature, frequency, forecast, vulnerability model for optimally, asymptotically, geo-spectrotemporally, targeting eco-georeferenceable, seasonal, un-geosampled, hyperproductive foci. Henceforth, as long as P is a square matrix, A can be written as an eigen-decomposition $A=PDP^{-1}$ whence D is a diagonal matrix in the model. Thus, if a malariologist,medical entomologist or other experimenter lets P be a matrix of eigenvectors of a given square matrix A , in an aquatic, larval habitat, eco-endmember, explanatory, forecast, vulnerability,oviposition,malaria.mosquito, eco-georeferenceable, signature, frequency, capture point, sub-meter resolution, grid-stratifiable,LULC model and then lets D be a diagonal matrix with the corresponding eigenvalues, then A would be symmetric and the columns of P . In so doing, orthogonal vectors may asymptotically, enable optimal, remote targeting of unknown, seasonal, hyperproductive, eco-endmember, malaria, mosquito, LULC foci by employing an orthogonal, iteratable, interpolative, signature as a dependent variable in the model. If P is not a square matrix [e.g., the geospace of eigenvectors of $\begin{bmatrix} 1 & 1 \\ 0 & 1 \end{bmatrix}$ would be one-dimensional (1-D) in the epi-entomological, seasonal, prognosticative, signature, risk model] and as such then P cannot have a matrix inverse and A would not have an eigen-decomposition.

However, if P is *m x n* (with *m>n*), in the geo-spectrotemporal, eco-endmember, oviposition, LULC, malaria, mosquito, signature model then A may be written employing a singular value decomposition. In so doing, the model, frequencies may be able to asymptotically, geo-spectrotemporally, robustly target unknown, eco-georeferenceable, seasonal, hyperproductive, aquatic, larval habitat, eco-endmember, LULC foci. If *A* is an *m x n* real matrix with *m >n* in the model output then *A* may be written employing a so-called singular value decomposition. Note that there are several conflicting notational conventions in use in the literature. Press et al. (1992) defined *U* to be an *m x n* matrix, *D* as *n x n*, and *V* as *n x n*. However, the Wolfram Language defines *U* as an *m x n*, *D* as *m x n* , and *V* as *n x n*. In both systems, *U* and *V* will have orthogonal columns so that $U^T U = I$ and $V^T V = I$ where the two identity matrices may have different dimensions, and *D* has entries only along the diagonal.Singular value decomposition is implementable in the Wolfram Language as SingularValue Decomposition[*m*], which commonly returns a list $\{U, D, V\}$, where *U* and *V* are matrices and *D* is a diagonal matrix made up of the singular data (e.g., geosampled, malaria, mosquito, aquatic, larval habitat, capture point, geoclassifiable, grid-stratifiable, LULC, signature, frequency values of *m*). In so doing, a complex matrix A may asymptotically, geo-spectrotemporally, remotely target un-geosampled, hyperpoductive, seasonal, eco-endmember foci from a sub-meter resolution, empirical optimizable dataset of, grid-stratifiable, LULC model, estimators employing the singular value decomposition which may parsimoniously provide optimal eigen-decomposition of the optimal krigeable, signature frequencies ewhich may employ the form $A = U D V^H$,whence *U* and *V* are unitary matrices, V^H is the conjugate transpose of *V*, and *D* is a diagonal matrix whose elements are the singular values of the original matrix.

Let *M* be an $n \times n$ Hermitian matrix in an eco-endmember, geo-spectrotemporal, oviposition, malaria, mosquito, sub-meter resolution, eco-endmember, geoclassifiable, LULC, interpolative, signature, frequency, vulnerability, aquatic, larval habitat, iterative model for asymptotically geo-spectrotemporally, remotely targeting, seasonal, unknown, eco-georeferenceable foci in an interpolation field. The following capture point, eco-endmember, LULC properties would then be equivalent to *M* being positive definite in the paradigm: All its eigenvalues would be positive. Let $P^{-1}DP$ be an eigen-decomposition of *M* where *P* may be a unitary complex matrix whose rows comprise an orthonormal basis of eigenvectors of *M*, and *D* is a real diagonal matrix in the ento-epidemiological, signature model whose main diagonal may contain the corresponding orthogonal, grid-stratifiable, wavelength eigenvalues of a known, eco-georeferenceable, geosampled, hyperproductive, aquatic, larval habitat, capture point, eco-endmember

foci. The matrix *M* may be then regarded as a diagonal matrix *D* which may be re-expressable in terms of an unknown, seasonal, hyperproductive, aquatic, larval habitat, foci, explicator, coordinate dataset on the basis of *P*. In particular, the one-to-one change of a geosampled, geoclassifiable, LULC, hyperproductive, capture point, eco-endmember, wavelength, iteratively interpolative, explanator $y = Pz$ may reveal that z^*Mz is real and positive for any complex vector *z* if and only if, y^*Dy is real and positive for any *y*; in other words, *D* would be positive definite. For a diagonal, eigen-decomposable, ento-epidemiological, forecast-oriented, eco-endmember, geoclassifiable, LULC, oviposition, sub-meter resolution, grid-stratifiable, geo-spectrotemporal,regression, model matrix to render viable vulnerability, eco-georeferenceable,signature, frequency forecasts (e.g., precise geolocations of unknown, hyperproductive, seasonal, capture point, aquatic, larval habitats), each element of the main diagonal—that is, every eigenvalue of *M* must be positive. Since the spectral theorem guarantees all eigenvalues of a Hermitian matrix to be real[4], the positivity of an uncoalesced, frequency, LULC dataset of eco-endmember, sub-meter resolution, grid-stratifiable, geoclassified, capture point, malaria, mosquito, aquatic, larval habitat, signature, wavelength eigenvalues may be validated employing Descartes' rule of alternating signs whence the characteristic polynomial of a real, symmetric matrix *M* is optimally employable in the epi-entomological, capture point, eco-epidemiological eigenvector analyses. Descartes' rule of signs, is a technique for determining an upper bound on the number of positive or negative real roots of a polynomial (it is not a complete criterion, because it does not provide the exact number of positive or negative roots)[3].

In linear algebra and functional analysis, a spectral theorem is a result about when an eco-endmember, geo-spectrotemporal, signature, wavelength, geoclassifiable, LULC, operator or matrix can be diagonalized (that is, represented as a diagonal matrix in some basis). This may be extremely useful in time series, vulnerability, malaria, mosquito, eco-endmember, LULC, signature, frequency, forecast models whence asymptotically, geo-spectrotemporally, remotely, targeting, un-geosampled, seasonal, eco-georeferenceable, hyperproductive, sub-meter resolution, grid-stratefiable, aquatic, larval habitat as computations involving a diagonalizable, stratifiable matrix may be reducible to much simpler computations involving the corresponding diagonal matrix (e.g., a large diagonalization of mapped prolific, capture point, unknown, oviposition, eco-endmember operators on finite-dimensional vector spaces modified for dimensional spaces in an African, riceland, agro-village, agro-irrigated environment). In general, the spectral theorem can aid in asymptotically identifying a class of linear operators in any multinomial, LULC, geo-spectrotemporal, eco-epidemiological, sub-meter resolution, vector arthropod, aquatic, larval habitat, vulnerability eco-endmember, signature, prognosticative analyses which may be modeled by multiplication operators. In so doing, the frequency grid-stratifiable, eco-georeferenceable, model output may be able to optimally, asymptotically, geo-spectrotemporally target seasonal, unknown, hyperproductive, aquatic, larval, habitat, eco-endmember, LULC foci. In more abstract language, the spectral theorem is a statement about commutative C*-algebras [2].

A C*-algebra is a complex algebra *A* of continuous linear operators on a complex Hilbert space with two additional properties:*A* is a topologically closed set in the norm topology of operators[4]. *A* is closed under the operation of taking adjoints of operators. C*-algebras are now an important tool in the theory of unitary representations of locally compact groups, which may be also asymptotically employable in algebraic formulations of quantum mechanics, or for optimally geo-spectrotemporally, remotely discriminating hyperproductive, un-geosampled, capture point, malaria, mosquito, seasonal, eco-georeferenceable, eco-endmember,sub-meter resolution, LULC foci. A C*-algebra, *A*, may be a Banach algebric term of a hyperproductive seasonal, un-geosampled, sub-meter resolution, frequency, density count, together in an eco-endmember, geoclassifiable, LULC, grid-stratifiable, aquatic, larval habitat, risk map $* : A \rightarrow A$ which may be purposefully employable for asymptotically, targeting seasonal, eco-georeferenceable, unknown, capture point,vector arthropod foci. One writes x^* for the image of an element *x* of *A* [4].

In mathematics, more specifically in functional analysis, a Banach space is a complete normed vector space [3]. Thus, a Banach space is a vector space with a metric that allows the computation of vector length and distance between vectors in a capture point, aquatic, larval habitat, malaria, mosquito, epi-entomological, LULC, signature, frequency, forecast, vulnerability, geo-spectrotemporal model which would be complete in the sense that a Cauchy sequence of vectors always converges to a well defined limit (i.e., eco-georeferenceable, seasonal, aquatic, larval habitat, mean, count value) that is within the space (i.e., time series sample frame). A Cauchy sequence (e.g., a line sequence of seasonal, flooded, African, riceland, malaria, mosquito, aquatic, larval habitat, oviposition, agro-irrigated, grid-stratifiable, LULC, eco-endmember, eco-georeferenceable foci) may be iteratively definable as frequency, explanative, density counts and other capture point, remotely sensed, geosampled elements which may become arbitrarily close to each other as the season progresses. The criterion for convergence in these paradigms may depend only on the terms of the sequence itself, as opposed to the definition of convergence, which commonly utilizes the limit value as well as the terms for quantiatation of potential, unbiased, frequency, model estimators.

More precisely, given any trivial, frequentistically, quantifiable, Euclidean, LULC, habitat, distance, measurement all but a finite number of elements of the calculable, capture point, geoclassifiable, orthogonal, eco-endmember sequences would be tabulated as immature, habitat, distance measurement, signature frequencies (e.g., distance from a hyperproductive, capture point to a agro-village, gridded centroid) in an iteratable, interpolative, epi-entomological, eco-georeferenceable dataset, The utility of Cauchy sequences for determining unknown, seasonal, eco-georeferenceable, oviposition, hyperproductive, aquatic, larval, habitat, eco-endmember, explanative prognosticators may lay in the fact that in a complete metric space (one where all such sequences are known to converge to a limit), the criterion for convergence (e.g., geosampled, seasonal, maximum, aquatic, larval habitat, wavelength, density counts) would depend only on the terms of the quantitable signature sequence itself, as opposed to the definition of convergence, which could employ the limit value as well as the model terms for optimal regression. This feature may be exploitable employing unmixing algorithms where an iterative process may be shown relatively easily to produce a Cauchy sequence, consisting of the known, geosampled, aquatic, larval habitat iterates, thus fulfilling a logical condition, such as termination at a un-geosampled, potential, geolocation of an eco-georeferenceable, malaria, mosquito,hyperproductive, capture point, geoclassifiable, LULC, eco-endmember foci.

Examples of operators to which the spectral theorem applies are self-adjoint operators or more generally normalized operators on Hilbert spaces[2].The mathematical concept of a Hilbert space, generalizes the notion of Euclidean space.It extends the methods of vector algebra and calculus from the two-dimensional (2-D) Euclidean plane and three-dimensional (3-D)space to spaces with any finite number of dimensions(e.g., un-geosampled, seasonal, geoclassifiable, eco-endmember, hyperproductive, LULC foci) An oviposition, sub-meter resolution, malaria, mosquito LULC, signature, specified Hilbert space may hence optimally quantitate an abstract vector space possessing the structure of an inner product which may allow length and angle to be remotely measurable whence non-heuristically robustifying, grid-stratifiable, geosampled, aquatic, larval habitat, epi-entomological, capture point, prognosticative, risk mapping, impartial explicators of an unknown, seasonal, hyperproductive, iteratively interpolatable, eco-endmember foci. In linear algebra, an inner product space is a vector space with an additional structure called an inner product [3]. This additional structure may geo-spectrotemporally, non-frequentistically (i.e., inferencial Bayesianism) associate each pair of geoclassifiable, sub-pixel, LULC grid-stratifiable, signature, capture point vectors in geospace with a scalar quantity known as the inner product of the vectors.

Inner products may allow the rigorous introduction of intuitive, geometrical, LULC notions such as the length of an unknown, seasonal, eco-georeferenceable, oviposition, hyperproductive, malaria, mosquito, capture point, eco-endmember foci based on known, empirical dataset of unmixed, geosampled, aquatic, larval habitat, geo-spectrotemporal, eco-endmember, signature frequencies. These capture point eco-endmember wavelengths may be subsequently employable as a dependent variable in an interpolative, stochastic or deterministic kriged-based algorithm.

An inner product is a generalization of the dot product [2]. The name "dot product" is derived from the centered dot " $\cdot$ " that is often used to designate this operation; the alternative name "scalar product" emphasizes that the result is a scalar, rather than a vector, which is the case for the vector product in three-dimensional space.I n mathematics, the dot product or scalar product[is an algebraic operation that takes two equal-length sequences of numbers (usually coordinate vectors) and returns a single number[4]. Algebraically, the dot product is the sum of the products of the corresponding entries of the two sequences of numbers. Geometrically, it is the product of the Euclidean magnitudes of the two vectors and the cosine of the angle between them. These definitions are equivalent when employing Cartesian coordinates (e.g., eco-georferenecd, eco-endmember, capture point, seasonal, predicted hyperproductive, aquatic, larval, habitat foci). In modern geometry, Euclidean spaces are often defined by using vector spaces. In this case, the dot product is used for defining lengths (the length of a vector is the square root of the dot product of the vector by itself) and angles (the cosine of the angle of two vectors is the quotient of their dot product by the product of their lengths).

In vector space, multiply vectors may be quantizable together, with the result of this multiplication being a scalar.More precisely, for a real vector space in an oviposition, grid-stratifiable, sub-meter resolution, forecast-oriented, malaria, mosquito, vulnerability, signature, frequency model for asymptotically optimally, remotely targeting eco-georeferenceable, seasonal, hyperproductive, aquatic, larval habitat, foci an inner product $\langle \cdot, \cdot \rangle$ may satisfy the following four properties. Let u, v, and w be vectors and α be a scalar, then: 1. $\langle u + v, w \rangle = \langle u, w \rangle + \langle v, w \rangle$.2. $\langle \alpha v, w \rangle = \alpha \langle v, w \rangle$.3. $\langle v, w \rangle = \langle w, v \rangle$.4. $\langle v, v \rangle \geq 0$ and equal if and only

if $v = 0$[4].The fourth condition in the list may be the positive-definite condition of the model matrix. Related thereto, note that some authors define an inner product to be a function $\langle \cdot , \cdot \rangle$ satisfying only the first three of the above conditions with the added (weaker) condition of being (weakly) non-degenerate (i.e., if $\langle v, w \rangle = 0$ for all w, then $v \equiv 0$). In such literature, functions satisfying all four such conditions are typically referred to as positive-definite inner products (see Ratcliffe 2006), though inner products which fail to be positive-definite are sometimes called indefinite to avoid confusion. This difference, though subtle, introduces a number of noteworthy phenomena: For example, inner products in forecast, vulnerability, signature, eco-endmember, LULC frequency, sub-meter resolution, grid-stratifiable models which fail to be positive-definite may give rise to "norms" which may subsequently yield an imaginary magnitude for certain vectors (i.e., spacelike). These vectors may induce "metrics" which fail to be actual metrics in the epi-entomological geo-spectrotemporal signature, frequency paradigms. The Lorentzian inner product is an example of an indefinite inner product[4].A vector space together with an inner product on it is called an inner product space. This definition also applies to an abstract vector space over any field[2].Examples of inner product spaces include:1. The real numbers $\mathbb{R}$, where the inner product is given by $\langle x, y \rangle = x\, y$.2. The Euclidean space $\mathbb{R}^n$, where the inner product is given by the dot product $\langle (x_1, x_2, \ldots, x_n), (y_1, y_2, \ldots, y_n) \rangle = x_1\, y_1 + x_2\, y_2 + \cdots x_n\, y_n$ [4]. The vector space of real functions whose domain is an closed interval $[a, b]$ in a malaria, mosquito eco-endmeber, grid-stratifiable, sub-mter resolution, LULC model may be able to optimally asymptotically, geo-spectrotemporally targeting seasonal, eco-georeferenceable, prolific foci which may have an inner product $\langle f, g \rangle = \int_a^b f\, g\, d\, x.$

When given a complex vector space, the inner product for a sub-meter resolution, grid-stratifiable, eco-endmember, frequency, signature, geoclassifiable, LULC, asymptotical model for discerning, un-geosampled, seasonal, hyperproductive, oviposition, malaria, mosquito, capture point,eco-georeferenceable, aquatic, larval habitat may be replaced by $\langle v, w \rangle = \overline{\langle w, v \rangle}$, where $\overline{z}$ refers to complex conjugation. With this property, the inner product (i.e.,a Hermitian inner product and a complex vector space with a Hermitian inner product) may also reveal a Hermitian inner product space.Every inner product space is a metric space[2]. The metric in the prognosticative, vector arthropod, LULC, eco-endmember, eco-epidemiological, signature, frequency model may be given by $g\,(v, w) = \langle v - w, v - w \rangle$.If this process results in a complete metric space, it would be a Hilbert space in the model. Since every inner product naturally induces a norm of the form $|\mathbf{x}| = \sqrt{\langle \mathbf{x}, \mathbf{x} \rangle}$, whereby it follows that every inner product space[4], this model location may be a normed space. Inner products which fail to be positive-definite yield "metrics" - and hence, "norms" - which are actually due to failing their respective positivity conditions. For example, n-dimensional Lorentzian Space (i.e., the inner product space consisting of $\mathbb{R}^n$ with the Lorentzian inner product) comes equipped with a metric tensor of the form $(d\, s)^2 = -d\, x_0^2 + d\, x_1^2 + \cdots + d\, x_{n-1}^2$ and a squared norm of the form $|\mathbf{v}|^2 = -v_0^2 + v_1^2 + \cdots + v_{n-1}^2$. As such, inner product may then provide the means of optimally defining orthogonality between eco-georeferenceable, geosampled, capture point, vector habitats (zero inner product) in a malaria, mosquito, forecast, vulnerability, grid-stratifiable, geoclassefiable, LULC, signature, frequency model.

An inner product naturally induces an associated norm; thus, an inner product space may also be a normed vector space in a frequency-oriented, prognosticative, vulnerability, sub-meter resolution, grid-stratifiable, signature, malaria, mosquito, frequency, LULC model. Henceforth eco-georeferenceable, hyperproductive, seasonal, capture point, aquatic, larval habitat, eco-endmember, geoclassfiable, LULC foci from an iteratively interpolatable, empirical dataset of pameterizable and or semi-paramterizable, unbiased estimators may asymptotically, optimally, geo-spectrotemporally, remotely, target un-geosampled, prolific, habitat geolocations. In mathematics, a normed vector space is a vector space over the real or complex numbers, on which a norm is definable[2]. A norm in an uncoalesced frequency, capture point eco-endmember dataset of vector arthropod, grid-stratifiable, wavelength, vulnerability, LULC, signature, model estimators may be based on the formalization and the generalization to real vector spaces which may be based on intuitive, Euclidean, habitat, distance measurements. Hence, let V be a normed vector space in an eco-epidemiological, aquatic, larval habitat geo-spectrotemporal, forecast, vulnerability, signature, frequency, geoclassifiable, sub-meter resolution, LULC model for asymptotically optimally targeting unknown, seasonal, capture point, malaria, mosquito, eco-endmember foci. Then $\|v - w\| \geq | \|v\| - \|w\| |$, $\forall$ v, w $\in$ V. Henceforth, by letting v, w $\in$

V in the vector arthropod prognosticative model, a malariologist or medical entomologist may show that $\|v - w\| \geq \|v\| - \|w\|$ and $\|v - w\| \geq \|w\| - \|v\|$ (1.1) in the model renderings which may reveal un-geosampled, seasonal, hyperproductive, aquatic, larval habitat, eco-endmember, geoclassifiable, LULC, foci. The proofs of these two inequalities may be similar, so an experimenter may only need to prove the first perpective. Using the condition in equation.1.1, $\|v\| = \|(v - w) + w\| \leq \|v - w\| + \|w\|$ may also optimally asymptotically reveal, unknown prolific, seasonal, foci, capture point explanators.

A malariologist or medical entomologist may consider a bounded interval $[a, b] \subset R$, and let $C[a, b]$ denote the set of continuous functions $f : [a, b] \to C$, i.e., $C[a, b] := \{f : [a, b] \to C \mid\}$ where f is continuous, in a grid-stratifiable, sub-meter resolution, eco-endmember, signature, frequency, prognosticative, LULC, model estimator, empirical, geo-spectrotemporal, geosampled, oviposition dataset. $C[a, b]$ may be the optimal natural operations of addition and scalar multiplication that may aid then in asymptotically,optimally identifying un-geosampled, seasonal, eco-georeferenceable, hyperproductive,capture point, aquatic, larval habitat, iteratable, interpolative, eco-endmember foci. Each function $f \in C[a, b]$ may be bounded and may assume a maximum value; hence, let $\|f\|\infty := \max x\in[a,b] |f(x)|$ (1.2). Subsequently, a malariologist or medical entomologist may verify that $\| \cdot \|\infty$ is a viable model realization which could then define a norm on $C[a, b]$, (i.e., that it satisfies the requirements in 1.1). In so doing, $\|f\|\infty \geq 0$ for all $f \in C[a, b]$ may reveal aniteratively interpolative dataset of signature, geoclassified, grid-stratified, orthogonal, LULC, spectro-temporal, eco-endmember frequencies of an unknown, prolific foci. In such circumstances the function $f = 0$ would belong to $C[a, b]$ which may satisfy that $\|f\|\infty = 0$ in the model renderings. On the other hand, if $\|f\|\infty = 0$ for some geoclassifiable, eco-endmember, iteratively, interpolative, grid-stratifiable, LULC, capture point, aquatic, larval, habitat function $f \in C[a, b]$, then the definition of $\|\cdot\|\infty$ may reveal that $f(x) = 0$ for all $x \in [a, b]$, (i.e., $f = 0$) which would also verify.1.1. Once this property is clearly satisfied in the signature, frequency, vulnerability, malaria, mosquito, eco-endmember, prognosticative model, an experimenter may determine $f,g \in C[a, b]$. Then, for each $x \in [a, b]$, $|f(x) + g(x)|\leq|f(x)| + |g(x)| \leq \|f\|\infty + \|g\|\infty$; because this would hold for all $x \in [a, b]$ in the derivative,LULC, model, wavelength dataset. Hence it follows that $\|f + g\|\infty = \max x\in[a,b] |f(x) + g(x)| \leq \|f\|\infty + \|g\|\infty$ may optimally asymptotically, geo-spectrotemporally, target, seasonal, eco-georeferenceable, un-geosampled, hyperproductive, capture point, aquatic, larval habitat, eco-endmember,LULC foci. This may be verifiable by determining if $\|\cdot\|\infty$ defines a norm on $C[a, b]$ (i..e, supremums-norm).

Let K be a T2-topological space and let F be the space of all bounded complex-valued continuous functions definable on K in an eco-endmember, sub-meter resolution, malaria, mosquito, signature, frequency, grid-stratifiable, geoclassifiable, LULC, prognosticative, capture point model. A topological space fulfilling the T_2-axiom may determine if two capture points have disjoint neighborhoods. In the terminology of Alexandroff and Hopf (1972), a T_2-space is called a Hausdorff space. In topology and related branches of mathematics, a Hausdorff space, separated space or T_2 space is a topological space in which distinct points have disjoint neighbourhoods[2]. Of the many separation axioms that can be imposed on a topological space, the "Hausdorff condition" (T_2) is the most frequently used and discussed. It implies the uniqueness of limits of sequences, nets, and filters.A T_2-space is sometimes said to "have Hausdorff topology" or "be Hausdorff."[4] An Etale space provides an example of a space that is not T_2. Regardless, the supremum norm is the norm definable on F by $\|f\| = \sup_{x\in K} |f(x)|$. Hence, Fwould be a commutative Banach algebraic variable with identity in a sub-mter resolution, grid-startfiaible, geo-spectrotemproal, forecast, vulnerability, signature frequency model for optimally asymptotically targeting un-geosampled, eco-georeferenceable, hyperproductive, aquatic, larval habitat, capture point foci.

A Banach algebra is an algebra B over a field F endowed with a norm $\|\cdot\|$ such that B is a Banach space under the norm $\|\cdot\|$ where $\|x\, y\| \leq \|x\|\, \|y\|$. F is frequently taken to be the complex numbers (i.e., operational, empirical, sub-meter resolution, eco-endmember, grid-stratifiable, LULC, signature, capture point, uncoalesced, interpolative frequencies) in order to ensure that the operator spectrum fully characterizes an operator[i.e., the spectral theorems for normal or compact normal operators do not, in general, hold in the operator spectrum over real numbers for iteratively discerning, eco-georeferenceable, un-geosampled, malaria, mosquito aquatic, larval habitat, eco-endmember, geoclassfieid, LULC, hyperproductive foci. If B is commutative and has a unit, then $x \in B$ is invertible if $\hat{x}(\phi) \neq 0$ for all ϕ, where $x \mapsto \hat{x}$ is the Gelfand transform in the model formulation process.

The Gelfand transform $x \mapsto \hat{x}$ is defined as follows. If $\phi : B \to \mathbb{C}$ is linear and multiplicative in the sense $\phi(a\,x + b\,y) = a\,\phi(x) + b\,\phi(y)$ and $\phi(x\,y) = \phi(x)\,\phi(y)$, where B is a commutative Banach algebra, then $\hat{x}(\phi) = \phi(x)$[4]. The Gelfand transform would be automatically bounded in any signature, sub-meter resolution, grid-stratfiable, malaria, mosquito, capture point, prognosticative, vulnerability, eco-endmember, LULC, frequency model. For example, if $B = L^1(\mathbb{R})$ with the usual norm, then B would be Banach algebra under convolution and the Gelfand transform would be the Fourier transform. In fact, R may be replaced by any locally compact Abelian group, and then B in the malaria mosquito model where h may have a signature iteratively interpolative LULC unit if and only if the group is discrete.

An Abelian group is a group for which the elements commute (i.e., $A\,B = B\,A$ for all elements A and B) [2]. Abelian groups therefore correspond to groups with symmetric multiplication tables. All cyclic groups are Abelian, but an Abelian group is not necessarily cyclic [4]. All subgroups of an Abelian group are normal[2]. In an Abelian group, each element is in a conjugacy class by itself, and the character table involves powers of a single element known as a group generator.In the Wolfram Language, the function AbelianGroup[{$n1$, $n2$, ...}] represents the direct product of the cyclic groups of degrees n_1, n_2, ...No general formula is known for giving the number of non-isomorphic finite groups of a given group order for an oviposition, grid-stratifiable, malaria, mosquito, signature, frequency, sub-meter resolution, eco-georeferenceable, forecast-oriented, eco-endmember, geoclassifiable, LULC, geo-spectrotemporal model in the literature.Regardless, the number of non-isomorphic, Abelian, finite groups $a(n)$ of any given group order n in these models may be given by writing n as $n = \prod_i p_i^{\alpha_i}$, where the p_i are distinct prime factors. In so doing, then $a(n) = \prod_i P(\alpha_i)$, whence $P(k)$ may be the partition function, in the model which is implementable in the Wolfram Language as FiniteAbelianGroupCount[n]. The values of $a(n)$ for $n = 1$, 2, ... are 1, 1, 1, 2, 1, 1, 1, 3, 2, ... (OEIS A000688).

The smallest orders for which $n = 1$, 2, 3, ... nonisomorphic Abelian groups exist are 1, 4, 8, 36, 16, 72, 32, 900, 216, 144, 64, 1800, 0, 288, 128, ... (OEIS A046056), where 0 denotes an impossible number (i.e., not a product of partition numbers) of non-isomorphic Abelian, groups. The "missing" values are 13, 17, 19, 23, 26, 29, 31, 34, 37, 38, 39, 41, 43, 46,.. (OEIS A046064). The incrementally largest numbers of Abelian groups as a function of order are 1, 2, 3, 5, 7, 11, 15, 22, 30, 42, 56, 77, 101, ... (OEIS A046054), which occur for orders 1, 4, 8, 16, 32, 64, 128, 256, 512, 1024, 2048, 4096, 8192, ... (OEIS A046055).The Kronecker decomposition theorem states that every finite Abelian group can be written as a group direct product of cyclic groups of prime power group order[see 4]. If the group order of a finite group is a prime p,in a sub-meter resolution, grid-stratifiable, malaria, mosquito, eco-epidemiological, predictive, risk model for asymptotically, geo-spectrotemporally, optimally, targeting seasonal, eco-georeferenceable, hyperproductive, aquatic, larval, habitat foci then there exists a single Abelian group of order p (denoted $\mathbb{Z}_p$) and no non-Abelian groups. If the group order is a prime squared (p^2), then there are two Abelian groups denotable $\mathbb{Z}_{p^2}$ and $\mathbb{Z}_p \times \mathbb{Z}_p$. If the group order is a prime cubed p^3, then there are three Abelian groups (denoted $\mathbb{Z}_p \times \mathbb{Z}_p \times \mathbb{Z}_p$, $\mathbb{Z}_p \times \mathbb{Z}_{p^2}$, and $\mathbb{Z}_{p^3}$), and five groups total. If the order is a product of two primes p and q, then there exists exactly one Abelian group of group order $p\,q$ (denoted $\mathbb{Z}_p \times \mathbb{Z}_q$)[4]..Another interesting result is that if $a(n)$ denotes the number of nonisomorphic Abelian groups of group order n in a sub-meter resolution, malaria, mosquito, geo-spectrotemporal LULC model then $\sum_{n=1}^{\infty} a(n)\,n^{-s} = \zeta(s)\,\zeta(2\,s)\,\zeta(3\,s)\cdots$, where $\zeta(s)$ is the Riemann zeta function.

The Riemann zeta function is an extremely important special function of mathematics and physics that arises in definite integration and is intimately related with very deep results surrounding the prime number theorem. The prime number theorem gives an asymptotic form for the prime counting function $\pi(n)$, which counts the number of primes less than some integer n. Legendre (1808) suggested that for

large n, $\pi(n) \sim \frac{n}{\ln n + B}$, with $B = -1.08366$ (where B is sometimes called Legendre's constant), a formula which is correct in the leading term only, may be $\frac{n}{\ln n + B} \sin \frac{n}{\ln n} - B \frac{n}{(\ln n)^2} + B^2 \frac{n}{(\ln n)^3} + \ldots$ (Nagell 1951, p. 54; Wagon 1991, Havil 2003,). Legendre's constant is the number 1.08366 in Legendre's guess at the prime number theorem $\pi(n) = \frac{n}{\ln n - A(n)}$ with $\lim_{n\to\infty} A(n) \approx 1.08366$. Legendre first published a guess the form $\frac{n}{A \ln n + B}$ in This *Essai sur la Théorie des Nombres* (Edwards 2001, p. 3; Havil 2003, p. 177), but in the third edition (renamed *Théorie des nombres*), modified it to the form above (Derbyshire 2004, pp. 55 and 369).This expression is correct to leading term only, since it is actually true that this limit approaches 1 (Rosser and Schoenfeld 1962, Panaitopol 1999)., Gauss proposed that $\pi(n) \sim \frac{n}{\ln n}$.Gauss later refined his estimate to $\pi(n) \sim \mathrm{Li}(n)$, where $\mathrm{Li}(n) = \int_2^n \frac{dx}{\ln x}$ is the logarithmic integral. Gauss did not publish this result, which he first mentioned in an 1849 letter to Encke. It was subsequently posthumously published in 1863 (Gauss 1863; Havil 2003, pp. 174-176).Note that $\mathrm{Li}(n)$ has the asymptotic series about ∞ of $\mathrm{Li}(n) \sim \sum_{k=0}^{\infty} \frac{k!\, n}{(\ln n)^{k+1}}$.

While many of the properties of this function have been investigated, there remain important fundamental conjectures (most notably the Riemann hypothesis) that remain unproved to this day. The Riemann zeta function $\zeta(s)$ may be definable over the complex plane for one complex discontinuous, eco-endmember, geosampled, malaria, mosquito, oviposition, capture point, covariate which may be conventionally denoted s (instead of the usual z) in deference to the notation used by Riemann in his 1859 paper that founded the study of this function (Riemann 1859). The function is implementable in the Wolfram Languageas Zeta[*s*]

The numbers of Abelian groups of orders $\leq n$ are given by 1, 2, 3, 5, 6, 7, 8, 11, 13, 14, 15, 17, 18, 19, 20, 25, ... (OEIS A063966) for $n = 1$, 2, ... Srinivasan (1973) has also shown that $\sum_{n=1}^{N} a(n) = A_1 N + A_2 N^{1/2} + A_3 N^{1/3} + O\left[N^{105/407} (\ln N)^2\right]$, where the interpolative, vulnerability equations $A_k \equiv \prod_{j=1, j\neq k}^{\infty} \zeta\left(\frac{j}{k}\right) = \begin{cases} 2.294856591\ldots & \text{for } k=1 \\ -14.6475663\ldots & \text{for } k=2 \\ 118.6924619\ldots & \text{for } k=3 \end{cases}$ (OEIS A021002, A084892, and A084893) and $\zeta(s)$ is again the Riemann zeta function. Note that Richert (1952) incorrectly gave $A_3 = 114$. The sums A_k can also be written in the explicit forms $A_1 = \prod_{j=2}^{\infty} \zeta(j)$, $A_2 = \zeta\left(\frac{1}{2}\right) \prod_{j=3}^{\infty} \zeta\left(\frac{1}{2} j\right)$ and $A_3 = \zeta\left(\frac{1}{3}\right) \zeta\left(\frac{2}{3}\right) \prod_{j=4}^{\infty} \zeta\left(\frac{1}{3} j\right)$. in a sub-mter resolution, grid-stratifiable, eco-endmember, geo-spectrotemporal, prognosticative, geoclassfiiable, LULC, signature, frequency model for optimally asymptotically, geo-spectrotemporally, remotely targeting, eco-georeferenceable, hyerproductive, aquatic, larval habitat, seasonal, foci.

The Fourier transform is a generalization of the complex Fourier series in the limit as $L \to \infty$. Replace the discrete A_n with the continuous $F(k)\, dk$ while letting $n/L \to k$. Then change the sum to an integral, and the equations become $f(x) = \int_{-\infty}^{\infty} F(k)\, e^{2\pi i k x}\, dk$ and $F(k) = \int_{-\infty}^{\infty} f(x)\, e^{-2\pi i k x}\, dx$. Here, $F(k) = \mathcal{F}_x[f(x)](k) = \int_{-\infty}^{\infty} f(x)\, e^{-2\pi i k x}\, dx$ which may be the forward ($-i$) Fourier transform in a grid-stratifiable, sub-meter resolution, capture point, eco-endmember, LULC prognosictative, frequency-oriented, vulnerability model for asymptotically geo-spectrotemporally identifying, eco-georeferenceable, seasonal, un-geosampled, hyperproductive, malaria, mosquito foci,

and $f(x)=\mathcal{F}_k^{-1}[F(k)](x)=\int_{-\infty}^{\infty}F(k)\,e^{2\pi i k x}\,dk$ [i.e., the inverse $(+i)$ Fourier transform}. The notation $\mathcal{F}_x[f(x)](k)$ is introduced in Trott (2004), and $\hat{f}(k)$ and $\check{f}(x)$ are sometimes also used to denote the Fourier transform and inverse Fourier transform, respectively (Krantz 1999).

Note that some authors (especially physicists) prefer to write the transform in terms of angular frequency $\omega\equiv 2\pi\nu$ instead of the oscillation frequency ν. However, this would destroy the symmetry, in an eco-endmember, grid-stratifiable, sub-meter resolution, eco-georeferenceable, geo-spectrotemporal, LULC model especially whenceoptimally asymptotically targeting un-geosampled, hyperproductive, aquatic, larval habitat, eco-endmember foci, resulting in the transform pair $H(\omega)=\mathcal{F}[h(t)]=\int_{-\infty}^{\infty}h(t)\,e^{-i\omega t}\,dt$ where $h(t)=\mathcal{F}^{-1}[H(\omega)]=\frac{1}{2\pi}\int_{-\infty}^{\infty}H(\omega)\,e^{i\omega t}\,d\omega.$ To restore the symmetry of the transforms, the convention $g(y)=\mathcal{F}[f(t)]=\frac{1}{\sqrt{2\pi}}\int_{-\infty}^{\infty}f(t)\,e^{-iyt}\,dt$ where $f(t)=\mathcal{F}^{-1}[g(y)]=\frac{1}{\sqrt{2\pi}}\int_{-\infty}^{\infty}g(y)\,e^{iyt}\,dy$ may be remotely usable for asymptotically, identifying geolocations of un-geosampled, aquatic, larval habitat, capture points. In general, the Fourier transform pair may be definable in a sub-meter resolution, malaria, mosquito model by employing two arbitrary constants a and b as $F(\omega)=\sqrt{\frac{|b|}{(2\pi)^{1-a}}}\int_{-\infty}^{\infty}f(t)\,e^{ib\omega t}\,dt$ and $f(t)=\sqrt{\frac{|b|}{(2\pi)^{1+a}}}\int_{-\infty}^{\infty}F(\omega)\,e^{-ib\omega t}\,d\omega.$ .The Fourier transform $F(k)$ of afunction $f(x)$ may be robustly implementable in the Wolfram Language as FourierTransform[*f*, *x*, *k*], where different choices of a and b can be used by passing the optional FourierParameters-> {*a*, *b*} option. By default, the Wolfram Language takes FourierParameters as $(0, 1)$. Unfortunately, a number of other conventions are in widespread use. For example, $(0, 1)$ is used in modern physics, $(1, -1)$ is used in pure mathematics and systems engineering, $(1, 1)$ is used in probability theory for the computation of the characteristic function, $(-1, 1)$ is used in classical physics, and $(0, -2\pi)$ is used in signal processing. In Bracewell (1999,), it was always assumed that $a=0$ and $b=-2\pi$ unless otherwise stated. This choice may result in greatly simplified, eco-endmember, capture point, malaria, mosquito, aquatic, larval habitat, signature, frequency, geoclassifiable, LULC, orthogonal transforms quantitated on common functions such as 1, $\cos(2\pi k_0 x)$, etc.

Since any eco-endmember, LULC, explanatory, frequency function can be split up into even and odd portions $E(x)$ and $O(x)$, $f(x)=\frac{1}{2}[f(x)+f(-x)]+\frac{1}{2}[f(x)-f(-x)]=E(x)+O(x)$, a Fourier transform for a sub-meter resolution, grid-stratifiable, geoclassfiiable, orthogonal, malaria, mosquito, oviposition, epi-entomological, signature model for asymptotically forecasting geolocations of unknown, seasonal, aquatic, larval habitat, hyperproductive, eco-georeferenceable, foci may be expressable in terms of the Fourier cosine transform and Fourier sine transform as $\mathcal{F}_x[f(x)](k)=\int_{-\infty}^{\infty}E(x)\cos(2\pi k x)\,dx-i\int_{-\infty}^{\infty}O(x)\sin(2\pi k x)\,dx.$ A function $f(x)$ has a forward and inverse Fourier transform such that $f(x)=\begin{cases}\int_{-\infty}^{\infty}e^{2\pi i k x}\left[\int_{-\infty}^{\infty}f(x)\,e^{-2\pi i k x}\,dx\right]dk & \text{for } f(x) \text{ continuous at } x\\ \frac{1}{2}[f(x_+)+f(x_-)] & \text{for } f(x) \text{ discontinuous at } x,\end{cases}$ provided that\1. $\int_{-\infty}^{\infty}|f(x)|\,dx$ exists. There are a finite number of discontinuities [4]. The function has bounded variation.A sufficient weaker condition is fulfillment of the Lipschitz condition (Ramirez 1985). The smoother a function (i.e., the larger the number of continuous derivatives), the more compact its Fourier transform [2].

The Fourier transform is linear, since if $f(x)$ and $g(x)$ have Fourier transforms $F(k)$ and $G(k)$, then $\int [a f(x) + b g(x)] e^{-2\pi i k x} dx = a \int_{-\infty}^{\infty} f(x) e^{-2\pi i k x} dx + b \int_{-\infty}^{\infty} g(x) e^{-2\pi i k x} dx = a F(k) + b G(k)$. Therefore, $\mathcal{F}[a f(x) + b g(x)] = a \mathcal{F}[f(x)] + b \mathcal{F}[g(x)] = a F(k) + b G(k)$.The Fourier transform may also be symmetric in an eco-endmember, sub-meter resolution, malaria, mosquito, capture point, vulnerability, signature, frequency model for aymptotically , geospectrotemporally, remotely identifying eco-georeferenceable, seasonal, hyperproductive, eco-endmember, grid-stratifiable, LULC foci. since $F(k) = \mathcal{F}_x[f(x)](k)$ implies $F(-k) = \mathcal{F}_x[f(-x)](k)$.Let $f * g$ denote the convolution in a sub-meter resolution, grid-startfiable, eco-endmember, LULC model for targeting un-geosampled, seasonal, prolific foci. In so doing, the transforms of convolutions of functions may have particularly quantizable, non-heuristically optimizable, ento-endmember transforms,[e.g., $\mathcal{F}[f * g] = \mathcal{F}[f]\mathcal{F}[g], \mathcal{F}[f g] = \mathcal{F}[f] * \mathcal{F}[g], \mathcal{F}^{-1}[\mathcal{F}(f)\mathcal{F}(g)] = f * g, \mathcal{F}^{-1}[\mathcal{F}(f) * \mathcal{F}(g)] = f g$.The first of these may be asymptotically derived in the vector arthropod, signature,frequency,LULC model as follows: $\mathcal{F}[f * g] = \int_{-\infty}^{\infty}\int_{-\infty}^{\infty} e^{-2\pi i k x} f(x') g(x - x') dx' dx = \int_{-\infty}^{\infty}\int_{-\infty}^{\infty} \left[e^{-2\pi i k x'} f(x') dx'\right]\left[e^{-2\pi i k (x - x')} g(x - x') dx\right] =$ $\left[\int_{-\infty}^{\infty} e^{-2\pi i k x'} f(x') dx'\right]\left[\int_{-\infty}^{\infty} e^{-2\pi i k x''} g(x'') dx''\right] = \mathcal{F}[f]\mathcal{F}[g]$, where $x'' \equiv x - x'$.There is also a somewhat surprising and extremely important relationship between the autocorrelation and the Fourier transform known as the Wiener-Khinchin theorem[4].

Recall the definition of the autocorrelation function $C(t)$ of a function $E(t)$, $C(t) \equiv \int_{-\infty}^{\infty} \overline{E}(\tau) E(t + \tau) d\tau$. Also recall that the Fourier transform of $E(t)$ may be defined by $E(\tau) = \int_{-\infty}^{\infty} E_\nu e^{-2\pi i \nu \tau} d\nu$, giving a complex conjugate of $\overline{E}(\tau) = \int_{-\infty}^{\infty} \overline{E}_\nu e^{2\pi i \nu \tau} d\nu$. Plugging $\overline{E}(\tau)$ and $E(t + \tau)$ into the autocorrelation function of a sub-meter resolution, eco-endmember, geoclassifiable, LULC, geo-spectrotemporal, malaria, mosquito, prognosticative signature, frequency model therefore may render $C(t) = \int_{-\infty}^{\infty}\left[\int_{-\infty}^{\infty} \overline{E}_\nu e^{2\pi i \nu \tau} d\nu\right]\left[\int_{-\infty}^{\infty} E_{\nu'} e^{-2\pi i \nu' (t+\tau)} d\nu'\right] d\tau = \int_{-\infty}^{\infty}\int_{-\infty}^{\infty}\int_{-\infty}^{\infty} \overline{E}_\nu E_{\nu'} e^{-2\pi i \tau (\nu' - \nu)} e^{-2\pi i \nu' t} d\tau d\nu d\nu' =$ $\int_{-\infty}^{\infty}\int_{-\infty}^{\infty} \overline{E}_\nu E_{\nu'} \delta(\nu' - \nu) e^{-2\pi i \nu' t} d\nu d\nu' = \int_{-\infty}^{\infty} \overline{E}_\nu E_\nu e^{-2\pi i \nu t} d\nu = \int_{-\infty}^{\infty} |E_\nu|^2 e^{-2\pi i \nu t} d\nu = \mathcal{F}_\nu\left[|E_\nu|^2\right](t)$,.Henceforth the autocorrelation may be simply given by the Fourier transform of the absolute square of E_ν whence asymptotically geo-spectrotemporally, remotely identifying, un-geosampled, malaria, mosquito, aquatic, larval habitat, eco-endmember, eco-georeferenceable, hyperproductive foci. The Wiener-Khinchin theorem is a special case of the cross-correlation theorem with $f = g$ [4].

Let $\mathcal{F}_x[f(x)](k) = F(k)$, and $\overline{f}$ denote the complex conjugate of f, then the Fourier transform of the absolute square of $F(k)$ may be given by $\mathcal{F}_k\left[|F(k)|^2\right](x) = \int_{-\infty}^{\infty} \overline{f}(\tau) f(\tau + x) d\tau$. in an empirically regressed, oviposition, uncoalesced, signature dataset of eco-endmember, frequency-oriented, malaria, mosquito, prognosticative, vulnerability model unbiased estimators for aymptotically identifying unknown, seasonal, eco-georeferenceable, capture point, prolific foci. The Fourier transform of a derivative $f'(x)$ of a function $f(x)$ is commonly related to the transform of the function $f(x)$ itself[4]. A malariologist, medical entomologist or other experimenter may consider $\mathcal{F}_x[f'(x)](k) = \int_{-\infty}^{\infty} f'(x) e^{-2\pi i k x} dx$. for optimal remote quantitation of an empirical geo-spectrotemporal, geosampled, eco-georeferenced, geoclassfiable, LULC, oviposition dataset of capture point, iteratable, interpolative, capture point, signature frequencies.Using integration by

parts $\int v\,du=[uv]-\int u\,dv$ with $du=f'(x)\,dx$, $v=e^{-2\pi ikx}$ and $dv=-2\pi ike^{-2\pi ikx}\,dx$, t could occur in the residual dataset. In so doing, then $\mathcal{F}_x[f'(x)](k)=\left[f(x)e^{-2\pi ikx}\right]_{-\infty}^{\infty}-\int_{-\infty}^{\infty}f(x)\left(-2\pi ike^{-2\pi ikx}\,dx\right).$ The first term in the malaria, LULC, forecast model would consist of a function times $f(x)$. But if the function is bounded so that $\lim_{x\to\pm\infty}f(x)=0$ (as any geophysically, interpolative ,significant, LULC signal must be); then the capture point, eco-endmember,capture point, signature term would vanish, leaving $\mathcal{F}_x[f'(x)](k)=2\pi ik\int_{-\infty}^{\infty}f(x)e^{-2\pi ikx}\,dx=2\pi ik\mathcal{F}_x[f(x)](k).$ This process may be iterated for the nth derivative to yield $\mathcal{F}_x\left[f^{(n)}(x)\right](k)=(2\pi ik)^n\mathcal{F}_x[f(x)](k)$ whence asymptotically targeting seasonal, hyperproductive, aquatic, larval habitat, eco-georefernceable, eco- endmember foci.

The important modulation theorem of Fourier transforms allows $\mathcal{F}_x[\cos(2\pi k_0x)f(x)](k)$ to be robustly geo-spectrotemporally expressed in terms of $\mathcal{F}_x[f(x)](k)=F(k)$ as follows, $\mathcal{F}_x[\cos(2\pi k_0x)f(x)](k)\equiv\int_{-\infty}^{\infty}f(x)\cos(2\pi k_0x)e^{-2\pi ikx}\,dx=\frac{1}{2}\int_{-\infty}^{\infty}f(x)e^{2\pi ik_0x}e^{-2\pi ikx}\,dx+\frac{1}{2}\int_{-\infty}^{\infty}f(x)e^{-2\pi ik_0x}e^{-2\pi ikx}\,dx=\frac{1}{2}\int_{-\infty}^{\infty}f(x)e^{-2\pi i(k-k_0)x}\,dx+\frac{1}{2}\int_{-\infty}^{\infty}f(x)e^{-2\pi i(k+k_0)x}\,dx=\frac{1}{2}[F(k-k_0)+F(k+k_0)].$ Since the derivative of the Fourier transform is given by $F'(k)\equiv\frac{d}{dk}\mathcal{F}_x[f(x)](k)=\int_{-\infty}^{\infty}(-2\pi ix)f(x)e^{-2\pi ikx}\,dx,$ [4] it follows that in a sub-meter resolution, eco-endmember, geoclassifiable, LULC geo-spectrotemporal, forecast, vulnerabilitym signature, frequency model[i.e., $F'(0)=-2\pi i\int_{-\infty}^{\infty}xf(x)\,dx.$] may aymptotically,optimize. targeting seasonal, grid-stratifiable, eco-georeferenceable foci. Iterating the LULC signal further may render the general formula $\mu_n\equiv\int_{-\infty}^{\infty}x^nf(x)\,dx=\frac{F^{(n)}(0)}{(-2\pi i)^n}.$ The variance of a Fourier transform may be $\sigma_f^2=\left\langle(xf-\langle xf\rangle)^2\right\rangle,$ then which may be true when $\sigma_{f+g}=\sigma_f+\sigma_g$ in the malaria model output.If $f(x)$ has the Fourier transform $\mathcal{F}_x[f(x)](k)=F(k)$, then the Fourier transform in the signature, frequency, LULC, vector, arthropod model may have the shift property $\int_{-\infty}^{\infty}f(x-x_0)e^{-2\pi ikx}\,dx=\int_{-\infty}^{\infty}f(x-x_0)e^{-2\pi i(x-x_0)k}e^{-2\pi i(kx_0)}\,d(x-x_0)=e^{-2\pi ikx_0}F(k),$ so then $f(x-x_0)$ will be the Fourier transform $\mathcal{F}_x[f(x-x_0)](k)=e^{-2\pi ikx_0}F(k).$ If $f(x)$ has a Fourier transform $\mathcal{F}_x[f(x)](k)=F(k)$, then the Fourier transform obeys a similarity theorem $\int_{-\infty}^{\infty}f(ax)e^{-2\pi ikx}\,dx=\frac{1}{|a|}\int_{-\infty}^{\infty}f(ax)e^{-2\pi i(ax)(k/a)}\,d(ax)=\frac{1}{|a|}F\left(\frac{k}{a}\right),$ so $f(ax)$ has the Fourier transform $\mathcal{F}_x[f(ax)](k)=|a|^{-1}F\left(\frac{k}{a}\right).$ The "equivalent width" of a Fourier transform in the epi-entomological, prognosticative, geoclassifiable, grid-stratfiable, sub-meter resolution, signature, LULC model for optimally, asymptotically, geo-spectrotemporally, targeting, un-geosampled, eco-georeferenceable, aquatic, larval habitat, seasonal foci then would be by deducing whether $w_e\equiv\frac{\int_{-\infty}^{\infty}f(x)\,dx}{f(0)}=\frac{F(0)}{\int_{-\infty}^{\infty}F(k)\,dk}.$ whence the remotely quantiated "autocorrelation width" is $w_a\equiv\frac{\int_{-\infty}^{\infty}f\star\bar{f}\,dx}{[f\star\bar{f}]_0}=\frac{\int_{-\infty}^{\infty}f\,dx\int_{-\infty}^{\infty}\bar{f}\,dx}{\int_{-\infty}^{\infty}f\bar{f}\,dx},$ whence $f\star g$ denotes the cross-correlation of f and g and $\bar{f}$ is the complex conjugate in the frequency model. Any operation on $f(x)$ which leaves its

eco-endmember signature, frequencies unchanged leaves $F(0)$ unchanged, since $\int_{-\infty}^{\infty} f(x)\,dx = \mathcal{F}_x[f(x)](0) = F(0).$ [4] Table 1 summarizes some common Fourier transform pairs which may be optimally usable for robustly quantiating a a sinc function in the time domain in an eco-empirical, geosampled, geo-spectrotemporal, forecast, vulnerability, geoclassifiable, LULC signature, frequency model for asymptotically, optimally, geo-spectrotemporally targeting eco-georeferenceable, unknown, aquatic, larval habitat, prolific, capture point, eco-endmember foci.

Table 1: Fourier Transforms for a malaria mosquito, signature, endmember model

function	$f(x)$	$F(k) = \mathcal{F}_x[f(x)](k)$
Fourier transform--1	1	$\delta(k)$
Fourier transform--cosine	$\cos(2\pi k_0 x)$	$\frac{1}{2}[\delta(k-k_0)+\delta(k+k_0)]$
Fourier transform--delta function	$\delta(x-x_0)$	$e^{-2\pi i k x_0}$
Fourier transform--exponential function	$e^{-2\pi k_0 \lvert x\rvert}$	$\frac{1}{\pi}\frac{k_0}{k^2+k_0^2}$
Fourier transform--Gaussian	$e^{-a x^2}$	$\sqrt{\frac{\pi}{a}}\,e^{-\pi^2 k^2/a}$
Fourier transform--Heaviside step function	$H(x)$	$\frac{1}{2}\left[\delta(k)-\frac{i}{\pi k}\right]$
Fourier transform--inverse function	$-PV\frac{1}{\pi x}$	$i[1-2H(-k)]$
Fourier transform--Lorentzian function	$\frac{1}{\pi}\frac{\frac{1}{2}\Gamma}{(x-x_0)^2+\left(\frac{1}{2}\Gamma\right)^2}$	$e^{-2\pi i k x_0 - \Gamma\pi\lvert k\rvert}$
Fourier transform--ramp function	$R(x)$	$\pi i\,\delta'(2\pi k) - \frac{1}{4\pi^2 k^2}$

In2-D, , the Fourier transforbecomes $F(x,y)=\int_{-\infty}^{\infty}\int_{-\infty}^{\infty} f(k_x,k_y)\,e^{-2\pi i(k_x x+k_y y)}\,dk_x\,dk_y$ whence $f(k_x,k_y)=\int_{-\infty}^{\infty}\int_{-\infty}^{\infty} F(x,y)\,e^{2\pi i(k_x x+k_y y)}\,dx\,dy.$ [4]. Similarly, the n-dimensional Fourier transform can be defined for $\mathbf{k}, \mathbf{x}\in\mathbb{R}^n$ by $F(\mathbf{x})=\int_{-\infty}^{\infty}\cdots\int_{-\infty}^{\infty} f(\mathbf{k})\,e^{-2\pi i\mathbf{k}\cdot\mathbf{x}}\,d^n\mathbf{k}$ or $f(\mathbf{k})=\int_{-\infty}^{\infty}\cdots\int_{-\infty}^{\infty} F(\mathbf{x})\,e^{2\pi i\mathbf{k}\cdot\mathbf{x}}\,d^n\mathbf{x}.$. A periodic, continuous, malaria, mosquito, capture point, eco-endmember,LULC continuous signal may be a spectrum $F(u,v)=\int\int_{-\infty}^{\infty} f(x,y)e^{-j2\pi(ux+vy)}dx\,dy\; f(x,y)=\int\int_{-\infty}^{\infty} F(u,v)e^{j2\pi(ux+vy)}du\,dv$ where u and v are spatial frequencies in x and y directions, respectively, and $F(u,v)$ is the 2D spectrum of $f(x,y)$ .Conversely a periodic, discrete, habitat continuous, signal, may be delineated robustly remotely as $F(u,v)=\sum_{m=-\infty}^{\infty}\sum_{n=-\infty}^{\infty} f[m,n]e^{-j2\pi(umx_o+vny_o)}$ and

$$f[m,n] = \frac{1}{UV}\int_0^U \int_0^V F(u,v)e^{j2\pi(umx_o+vny_o)}du\,dv$$ where x and y are the spatial intervals between consecutive ,immature, habitat, signal samples in the x and y directions, respectively,whence $U = 1/x_o \quad V = 1/y_o$ and are sampling rates in the two directions, and they are also the periods of the spectrum $F(u,v)$ .A periodic, continuous signal, discrete, aperiodic, , sub-meter resolution, grid-stratefiable, geoclassified, LULC, aquatic,larval habitat, captire point spectrum for optimally, asymptotically, remotely targeting unknown, seasonal, prolific foci may be quantitaed using $F[k,l] = \frac{1}{XY}\int_0^X \int_0^Y f_{XY}(x,y)e^{j2\pi(kxu_o+lyv_o)}dx\,dy f_{XY}(x,y) = \sum_{k=-\infty}^{\infty}\sum_{l=-\infty}^{\infty} F[k,l]e^{-j2\pi(xku_o+ylv_o)}$.

A complete space with an inner product is called a Hilbert space. An (incomplete) space with an inner product is called a pre-Hilbert space, since its completion with respect to the norm induced by the inner product is a Hilbert space[2]. Inner product spaces over the field of complex numbers are sometimes referred to as unitary spaces. Hilbert space is a vector space H with an inner product $\langle f, g\rangle$ such that the norm defined by $|f| = \sqrt{\langle f, f\rangle}$ turns H into a complete metric space[2]. If the metric defined by the norm is not complete, then H is instead known as an inner product space.Examples of finite-dimensional Hilbert spaces include1. The real numbers $\mathbb{R}^n$ with $\langle v, u\rangle$ the vector dot product of v and u.2. The complex numbers $\mathbb{C}^n$ with $\langle v, u\rangle$ the vector dot product of v and the complex conjugate of u.An example of an infinite-dimensional Hilbert space is L^2, the set of all functions $f : \mathbb{R} \to \mathbb{R}$ such that the integral of f^2 over the whole real line is finite[4]. In this case, the inner product is $\langle f, g\rangle = \int_{-\infty}^{\infty} f(x)\,g(x)\,dx.$

In mathematics, orthogonality is the generalization of the notion of perpendicularity to the linear algebra of bilinear forms [3]. Two elements u and v of a vector space with bilinear form B are orthogonal when B (u, v) = 0[4]. When the bilinear form corresponds to a pseudo-Euclidean space in an eco-endmember, frequency-oriented, sub-meter resolution, malaria, mosquito, prognosticative, geo-spectrotemporal, vulnerability, LULC model there may be non-perpendicular vectors that are hyperbolic-orthogonal.Regressively quantitating orthogonal, geoclassifiable, grid-stratified, LULC capture point, eco-endmember, attribute features may enable precise targeting of unknown, seasonal, hyperproductve, malaria, mosquito, aquatic, larval habitat, eco-georeferenceable, foci.

In plane geometry, two lines are hyperbolic orthogonal when they are reflections of each other over the asymptote of a given hyperbola [2]. In the case of function spaces, families of orthogonal functions are used to form a basis.Hence, two particular hyperbolas may be employable in the plane:(A) $xy = 1$ with $y = 0$ as a asymptote in an eco-georeferenceable, geo-spectrotemporal, vector arthropod, forecast, vulnerability, malaria, mosquito, geometrical, grid-stratifiable, LULC, eco-endmember,signature, aquatic, larval habitat, capture point model which may be reflected in the x-axis and within a line $y = mx$ which may subsequently become $y = -mx$. In this case the lines would be hyperbolic orthogonal if their slopes are additive inverses (B) $x^2 - y^2 = 1$ where $y = x$ are asymptote. For lines $y = mx$ in an ento-ecoepidemiological, geo-spectrotemporal, malaria, mosquito, eco-endmember, LULC, signature, frequency model estimation where $-1 < m < 1$, t $x = 1/m$, may be then $y = 1$, for example.Hence an unknown seasonal, eco-georefereneable, seasonal, hyperproductive, capture point $(1/m , 1)$ on the regression line may be optimally reflected across $y = x$ to $(1, 1/m)$.Further, the reflected line of the prolific, malaria, aquatic, larval habitat, capture point, quantitable explanative, slope 1/m and the slopes of hyperbolic orthogonal lines could be reciprocals of each other.The relation of hyperbolic orthogonality in the prognosticative, vulnerability model may asymptotically, geo-spectrotemporally target seasonal, hypeproductive, unknown, eco-georeferenceable, malaria, mosquito, aquatic, larval, habitat,capture point foci by employing geoclassifiable, signature, LULC, eco-endmember classes of parallel lines in the plane, where any particular line may represent the known capture point. Thus, for a given hyperbola and asymptote A in an oviposition, sub-meter resolution, geosampled, geo-spectrotemporal, malaria, mosquito, LULC model for optimally targeting unknown, hyperproductive seasonal, aquatic, larval habitat foci, a pair of lines (a,b) may be hyperbolic orthogonal if there is a pair (c,d) such that c is the reflection property of the radius being orthogonal to

d across *A*. As such, the tangent at the curve in the eco-endmember, LULC, signature, frequency, geoclassifiable, hyperproductive, capture point, seasonal foci may be extended from an endemic, eco-georeferenceable, grid-stratifiable geolocation to the hyperbola by the hyperbolic orthogonal concept. In doing so, the inner product of the model may identify seasonal, unknown, prolific, aquatic, larval habitat, capture points.

Inner product spaces may generalize Euclidean spaces in which the inner product is the dot product, (also known as the scalar product) to vector spaces of any calculable, seasonal, hyperproductive, eco-georeferenceable, sub-meter resolution,malaria, mosquito, geosampled, aquatic, larval habitat, remotely sensed, grid-stratifiable, LULC eco-endmember, wavelength dimension. In mathematics, the dot product or scalar product is an algebraic operation that takes two equal-length sequences of numbers (usually coordinate vectors) and returns a single number [3]. In Euclidean geometry, the dot product of the Cartesian coordinates of two vectors is widely used and often called inner product (or rarely projection product)[4]. Hence, an ento-epidemiological, geoclassfiable, forecast, vulnerability LULC, signature,eco-endmember, signature, frequency, geo-spectrotemporal model may optimally asymptotically target unknown. seasonal, eco-georeferenceable, hyperproductive, malaria, mosquito, grid-stratifiable,capture point, geosampled, attribute features by employing a functional analysis.

Functional analysis is a branch of mathematical analysis, the core of which is formed by the study of vector spaces endowed with some kind of limit-related, structure (e.g. inner product, norm, topology, etc.). The linear functions may be optimally asymptotically definable for remotely, geo-spectrotemporally targeting, unknown, malaria, mosquito, hyperproductive, aquatic, larval habitat, ento-ecoepidemiological, geoclassified, LULC capture points in a suitable sense. The historical roots of functional analysis lie in the study of spaces of functions and the formulation of properties of transformations of functions such as the Fourier transform as transformations defining continuous, unitary etc. operators between function spaces[4]. The Fourier transform of a function of time itself is a complex-valued function of frequency, whose absolute value represents the amount of that frequency present in the original function, and whose complex argument is the phase offset of the basic sinusoid in that frequency[2]. A functional, frequency, eco-endmember, geo-spectrotemporal, invasive, LULC, signature, frequency analyses would be particularly useful for the study of differential and integral equations which may be employable for precisely, parsimoniously, asymptotically, targeting seasonal, eco-georeferenceable, sub-meter resolution, un-geosampled, hyperproductive, malaria, mosquito, aquatic, larval habitats.

An inner product may induce an associated norm, in an oviposition, prognosticative, eco-endmember, malaria, mosquito, LULC, signature, risk model for optimally asymptotically targeting unknown, hyperproductive, eco-georefernceable, seasonal, capture point, aquatic, larval habitats. In such circumstances an inner product space may be also a normed vector space in the signature paradigm. A complete space with an inner product is called a Hilbert space[4]. An (incomplete) space with an inner product is called a pre-Hilbert space, since its completion with respect to the norm induced by the inner product is a Hilbert space [2]. Since Hilbert spaces in an ento-epidemiological, geoclassifiable, geo-spectrotemporal, oviposition, endemic, LULC, malaria, mosquito, forecast, vulnerability, eco-endmember, signature frequency model would be complete there would be enough limits in the space to allow the techniques of calculus to be employable for optimally forecasting eco-georeferenceable, geolocations of unknown, seasonal, hyperproductive, aquatic, larval, habitat foci.

Calculus of variations is a type of mathematics involving maxima and minima,that science has used to produce significant theories. It is a field of mathematical analysis that employs variations, which are small changes in functions and functionals, to find maxima and minima of functionals, which may be represented as signature capture point, aquatic, larval habitat, forecast vulnerability mappings from a set of functions derived from an empirical optimizable, frequency dataset of geosampled, discrete, finite, integer values eco-cartographically, delineating eco-georeferenceable, hyperproductive, malaria mosquito, density, seasonal, LULC, frequency, count values). Functionals are often expressed as definite integrals involving functions and their derivatives [2]. Functions that maximize or minimize functionals in an oviposition, capture point, ento-epidemiological, geoclassifiable, time series, malaria, mosquito, forecast, vulnerability, LULC model for asymptotically targeting seasonal, hyperproductive, eco-georeferenceable, unknown, eco-endmember foci may be found using the Euler–Lagrange equation of the calculus of variations.

In the calculus of variations, the Euler–Lagrange equation, Euler's equation, or Lagrange's equation is a second-order, partial, differential equation whose solutions are the functions for which a given functional is stationary[3]. Because a differentiable functional is stationary at its local maxima and minima, the Euler–Lagrange equation may be useful for solving optimization problems in which, given some functional, a malariaologist, medical entomologist or

other experimenter seeks the function for minimizing or maximizing a geosampled, vector arthropod, geo-spectrotemporal, forecast, vulnerability, grid-stratifiable, frequency model for asymptotically geo-spectrotemporally targeting, unknown, hyperproductive, seasonal, eco-georeferenceable, capture point, ento-endmember,aquatic, larval, habitat foci from an iteratively interpolative sub-meter resolution, geoclassifiable, robustly krigable, LULC signature. This may be analogous to Fermat's theorem in calculus, stating that at any point (e.g., seasonal hyperproductive, un-geosampled foci) where a differentiable function attains a local extremum its derivative is zero [see 4]. In mathematics, Fermat's theorem (also known as interior extremum theorem) is a method to find local maxima and minima of differentiable functions on open sets by showing that every local extremum of the function is a stationary point (e.g., the function derivative is zero at a unknown, hyperproductive, seasonal, aquatic, larval habitat, malaria, mosquito, geoclassifiable, LULC, sub-meter resolution, capture point,eco-endmember, foci). A gradient technique may be developed for computing a class of non-isolated, signature, frequency seasonal, hyperproductive, eco-endmember, capture point (i.e., *C*-stationary points), for a real functional *F* defined on a Hilbert space in a forecast, vulnerability, ento-epidemiological, geoclassifiable, LULC, oviposition model.It may be shown that the least-squares solutions of the operator equation $Ax=b$ are *C*-stationary, seasonal, prolific, malaria, mosquito, aquatic, larval habitat, capture points for the functional $(1/2)\|Ax-b\|^2$ whence *R(A)* is closed and that certain orthogonal eigenvectors of the general eigen-problem $Ax=\lambda Bx$ are *C*-stationary points for the functional $1/2\|Ax-(<Ax, Bx>/<Bx, Bx>) Bx\|^2$.

Hilbert spaces arise naturally and frequently in mathematics and physics, typically as infinite-dimensional function spaces. They are indispensable tools in the theories of partial differential equations, quantum mechanics, Fourier analysis (which includes applications to signal processing and heat transfer)—and ergodic theory, which forms the mathematical underpinning of thermodynamics. Hilbert space methods for functional analysis may be applicable for ento-epidemiological, malaria, mosquito, oviposition, sub-mter resolution, grid-stratifiable, LULC research. Apart from the classical Euclidean spaces, examples of Hilbert spaces include spaces of square-integrable functions, spaces of sequences, consisting of generalized functions, and Hardy spaces of holomorphic functions.

In complex analysis, the Hardy spaces (or Hardy classes) H^p are certain spaces of holomorphic functions on the unit disk or upper half plane. In mathematics, a holomorphic function is a complex-valued function of one or more complex variables that is complex differentiable in a neighborhood of every point in its domain[2].

Geometric intuition plays an important role in many aspects of Hilbert space theory. The theory of Hilbert space is a fundamental tool for non-relativistic quantum mechanics. Applying this theory linear, topological, metric, and normed spaces may be all aymptotically addressed in an ento-epidemiological, geoclassfiable, oviposition, sub-meter resolution, gri-stratifiable, forecast, vulnerability, eco-endmember, LULC, signature, malaria, mosquito, frequency model for optimally aymptotically, geo-spectrotemporally targeting, seasonal, eco-georeferenceable, unknown, hyperproductive foci. Exact analogs of the Pythagorean theorem and parallelogram law hold in a Hilbert space [4]. At a deeper level, perpendicular projection onto a subspace (the analog of "dropping the altitude" of a triangle) plays a significant role in optimization problems and other aspects of the theory.

An element of a Hilbert space may be uniquely specified for in an oviposition, malaria, mosquito, aquatic, larval habitat,empirical, geoclassifiable non-heuristically optimizable, LULC, regressable dataset of uncoalesced, eco-georefereneced, sub-meter resolution, eco-endmember, geosampled, habitat coordinates based on capture point, coordinate axes. Thereafter based on orthonormality, prolific, seasonal, ento-endmember geo-spectrotemporal, capture points may be identified in a prognosticative, signature, frequency, vulnerability, LULC model framework in analogy with Cartesian coordinates in the plane.When that set of axes is countably finite, this means that the Hilbert space can also usefully be thought of in terms of the space of sequences [4], which may be usable for optimally asymptotically, geo-spectrotemporally targeting, unknown, seasonal, sub-pixel, LULC, hyperproductive, eco-endmember foci.

The L^p spaces are function spaces defined using a natural generalization of the *p*-norm for finite-dimensional vector spaces [4]. They are sometimes called Lebesgue spaces. L^p spaces form an important class of Banach spaces in functional analysis, and of topological vector space which may optimally asymptotically, geo-spectrotemporally target, unknown, seasonal, eco-georeferenceable, malaria, mosquito, oviposition, sub-meter resolution, hyperproductive, aquatic, larval habitat, LULC, eco-endmember, capture point foci. The elements of topological vector spaces are typically functions or linear operators acting on topological vector spaces, and the topology is often defined so as to capture a particular notion of convergence of sequences of functions[4].

The notions above are not as unfamiliar as they might at first appear. The customary acceptance of the fact that any geosampled, eco-georeferenceable, ento-ecoepidemiological, sub-meter resolution, grid-stratifiable, geo-spectrotemporal, eco-endmember,geosampled, LULC *x*, signature, frequency, eco-cartographic variable representing a seasonal, unknown, hyperproductive, malaria, mosquito, endmember foci has a decimal expansion is an implicit acknowledgment that a particular Cauchy sequence of rational numbers (e.g., frequency, density, larval counts whose terms are the successive truncations of the decimal expansion of *x*) has the real limit *x*. In some cases it may be difficult to geoclassify and describe *x* independently in an eco-endmember, vector, arthropod, prognosticative, endemic, malaria, mosquito, signature, aquatc, larval habitat, LULC, vulnerability model. In such circumstances, a limiting process may be employable for optimally log-tranforming, geosampled, regression-related, eco-endmember, unmixed, LULC, capture point outliers.An associated sesquilinear form may be an inner product in an oviposition, sub-pixel, ento-epidemiological, endemic,oviposition, prognosticative, ento-geoclasssified, geospectrotemporal, LULC, malaria, mosquito model which may be defined by *M* where the function from $C^n \times C^n$ to C mayis all *x* and *y* in C^n, and y^* is the complex conjugate of *y* whence optimally asymptotically targeting unknown, seasonal, prolific foci. In mathematics, a sesquilinear form is a generalization of a bilinear form that, in turn, is a generalization of the concept of the dot product of Euclidean space[4]. A bilinear form is linear in each of its arguments, but a sesquilinear form allows one of the arguments to be "twisted" in a semilinear manner[2]. For any complex matrix *M*, this form may be linear in each optimizable, mosaicked, LULC signature frequency, model estimate employed for optimally asymptotically targeting seasonal, eco-georeferenecable,unknown, hyperproductive, oviposition, malaria, mosquito, aquatic, larval habitat, sub-meter resolution,imaged, grid-stratifiable capture points. Hence, the model form would involve an inner product in the prognosticative, vulnerability, ento-endmember, signature LULC,capture point estimate dataset on C^n which would occur if and only if the geosampled,eco-georefereneceable,ento-epidemiological,known, hyperproductive, regressable, geo-spectrotemporal, geoclassifiable, signature, foci estimators are positive for all nonzero *z*; that is if and only if *M* is positive definite. Optimally every inner product on C^n in the model would arise in this fashion from a Hermitian positive definite matrix which may enable optimally asymptotically targeting, un-geosampled, seasonal, capture point, aquatic, larval habitat, endemic foci.

A Gram matrix of linearly independent vectors may be optimally employable as a grid-stratifiable, optimizable, ento-endmember, LULC, signature, frequency, estimator in an ento-epidemiological, sub-meter resolution, oviposition, forecast, vulnerability, signature, capture point, malaria, mosquito, forecast,vulnerability model. If a malariologist or medical entomologist applies a list of *n* linearly independent, eco-endmember, geoclassified, LULC, oviposition, malaria mosquito, capture point, geosampled vectors of some complex vector space with an inner product, he or she may be able to optimally regressively select, hyperproductive, eco-georferenceable, aquatic, larval habitat,capture point, endmember foci. It may be verifiable in SAS that the Gram matrix *M* of those vectors, defined by the ento-ecoepidemiological, prognosticative, endemic, oviposition,sub-meter resolution, LULC model is always positive definite. Conversely, if *M* is positive definite in the, prognosticative, vulnerability, ento-endmember, signature, frequency, oviposition, LULC model it will have an eigen-decomposition co-factor which may be measurable by $P^{-1}DP$ where *P* is unitary, *D* diagonal, and all diagonal elements $D_{ii} = \lambda_i$ of *D* are real and positive. Let *E* be the real diagonal matrix with entries in a malaria mosquito, signature model for optimally aympototically forecasting LULC, endemic, capture point, ento-ecoendmember,signature, frequency foci thereafter, then the columns of *EP* would be linearly independent and *M* would be the Gram matrix which could employ the standard inner product of C^n for optimally targeting, unknown, eco-georeferenceable, sub-meter resolution, seasonal, grid-stratifiable, hyperproductive, aquatic, larval habitats.

The *k*th leading principal minor of a matrix *M* is the determinant of its upper-left *k* by *k* sub-matrix. Its leading principal minors are all positive. It turns out that a matrix is positive definite if and only if all these determinants are positive [2]. This condition is known as Sylvester's criterion, and provides an efficient test of positive definiteness of a symmetric real matrix.

In mathematics, Sylvester's criterion is a necessary and sufficient criterion to determine whether a Hermitian matrix is positive-definite. Sylvester's criterion states that a Hermitian matrix *M* is positive-definite if and only if all the following matrices have a positive determinant:1)the upper left 1-by-1 corner of *M*, 2) the upper left 2-by-2 corner of *M*,3) the upper left 3-by-3 corner of *M*; and, 4) M itself[3]. In other words, all of the leading principal minors must be positive in order for an ento-endmember, geo-spectrotemporal, geoclassifiable, sub-meter resolution, prognosticative, LULC, signature model to robustly asymptotically, optimally target seasonal, eco-georeferenceable hyperproductive,

malaria, mosquito, aquatic, larval, habitat, capture points. In linear algebra, a minor of a matrix A is the determinant of some smaller square matrix, cut down from A by removing one or more of its rows or columns[2]. Minors obtained by removing just one row and one column from square matrices (first minors) are required for calculating matrix cofactors, which in turn are useful for computing both the determinant and inverse of square matrices[4].

An analogous theorem holds for characterizing positive-semidefinite Hermitian matrices, for optimally,aymptotically targeting seasonal, hyperproductive, eco-georeferenceable, malaria, mosquito,aquatic, larval habitat ungeosampled foci;therefore, it may be no longer sufficient to consider only the leading principal minors in these ento-epidemiological, LULC, forecast, vulnerability, eco-endmember, signature, geo-spectrotemporal, frequency paradigms. A Hermitian matrix *M* is positive-semidefinite if and only if all principal minors of *M* are nonnegative [2]. A positive semidefinite matrix is a Hermitian matrix all of whose eigenvalues are nonnegative [4].

A square matrix is called Hermitian if it is self-adjoint. Thus, a positive-semidefinite, sub-meter resolution, grid-stratifiable, eco-endmember, LULC, geo-spectrotemporal,oviposition, malaria, mosquito, forecast, capture point, aquatic, larval habitat, explanatory, regression model may be optimally usable for asymptotically targeting seasonal, hyperproductive, malaria, mosquito, eco-georeferenceable, foci. A Hermitian matrix $\mathbf{A}=(a_{ij})$ may be optimally definable as one for which $\mathbf{A}=\mathbf{A}^{\mathrm{H}}$,whence $\mathbf{A}^{\mathrm{H}}$ exists in the ento-epidemiological, LULC, malaria, mosquito model for asymptotically, optimally targeting, eco-georeferenceable, seasonal, hyperproductive, eco-endmember foci but only if it denotes the conjugate transpose. The conjugate transpose of an $m\times n$ matrix $\mathbf{A}$ could be the $n\times m$ matrix defined by $\mathbf{A}^{\mathrm{H}}\equiv\overline{\mathbf{A}}^{\mathrm{T}}$,where $\mathbf{A}^{\mathrm{T}}$ denotes the transpose of the matrix $\mathbf{A}$ and $\overline{\mathbf{A}}$ denotes the conjugate matrix [2]. Conjugate matrix is a matrix $\overline{\mathbf{A}}$ obtained from a given matrix $\mathbf{A}$ by taking the complex conjugate of each element of $\mathbf{A}$ [4](i.e., $\overline{(a_{ij})}=(\overline{a}_{ij})$,) .

Employing a matrix X in a similarity transformation $\mathbf{X}^{-1}\mathbf{A}\mathbf{X}$ of a given matrix $\mathbf{A}$ is also known as conjugating $\mathbf{A}$ by $\mathbf{X}$[4]. In this case, $\mathbf{B}=\mathbf{X}^{-1}\mathbf{A}\mathbf{X}$ and $\mathbf{A}$ are known as similar matrices.Two square matrices $\mathbf{A}$ and $\mathbf{B}$ that are related by $\mathbf{B}=\mathbf{X}^{-1}\mathbf{A}\mathbf{X}$,where $\mathbf{X}$ is a square nonsingular matrix are said to be similar [2]. A transformation of the form $\mathbf{X}^{-1}\mathbf{A}\mathbf{X}$ is called a similarity transformation, or conjugation by X [4]. For example, $\begin{bmatrix}0&1\\0&0\end{bmatrix}$and $\begin{bmatrix}0&0\\1&0\end{bmatrix}$ in an oviposition, LULC, eco-endmember, ento-epidemiological, geo-spectrotemporal, forecast, vulnerability, oviposition, malaria, mosquito, sub-meter resolution, signature, frequency, model ouptput would be similar under conjugation by $\mathbf{C}=\begin{bmatrix}0&1\\1&0\end{bmatrix}$. whence asymptotically geo-spectrotemporally, targeting unknown, hyperproductive, seasonal, malaria, mosquito,aquatic, larval habitat, eco-georeferenceable, capture points. Similar matrices may represent the same linear transformation after a change of basis for the domain and range simultaneously in the geo-spectrotemporal, geosampled, grid-stratified, LULC, model output. Recall that a matrix corresponds to a linear transformation, and a linear transformation corresponds to a matrix after choosing abasis b_i, $T\left(\sum\lambda_i\, b_i\right)=\sum a_{ji}\,\lambda_i\, b_j$[see 4]. Changing the coefficients of the matrix, [e.g., $T\left(\sum\gamma_i\, e_i\right)=\sum a'_{ji}\,\gamma_i\, e_j$]may aid in asymptotically, precisely targeting unknown, iteratively, interpolative, seasonal, hyperproductive, aquatic, larval habitat, eco-endmember, eco-georeferenceable foci as rendered from a sub-meter resolution, geosampled, malaria, mosquito, sub-meter resolution, grid-stratifiable, capture point, oviposition, multivariate, krigable, LULC dataset of uncoalesced, signature frequencies employing the standard basis vectors, where T is the matrix $C\,A\,C^{-1}$ utilizing the basis vectors $b_i=C\,e_i$. In so doing, the conjugate transpose or Hermitian transpose of an *m*-by-*n* matrix *A* with complex entries obtained from *A* may regressively quantitate the complex conjugate of each geosampled, oviposition, geoclassifiable, LULC, sub-meter resolution, malaria, mosquito, regression, grid-stratifiable, model entry. In so doing, unknown, hyperproductive, eco-endmember, eco-georeferenceable, seasonal, hyperproductive, unknown, mosquito, aquatic, larval habitats may be remotely identified.

The conjugate transpose of a matrix A is implementable in the Wolfram Language as ConjugateTranspose[*A*].If a matrix is equal to its own conjugate transpose, it is said to be self-adjoint and is called a Hermitian[4].The conjugate transpose of a matrix product is given by $(a\,b)^H_{i\,j} \equiv [\overline{(a\,b)^{\mathrm{T}}}]_{i\,j}$.[2].Using the identity for the product of transpose in an oviposition, sub-meter resolution, grid-stratifiable, malaria mosquito, forcast, vulnerability,eco-endmember, LULC, signature, frequency model could render $(\overline{(a\,b)^{\mathrm{T}}})_{i\,j} = (\overline{b^{\mathrm{T}}\,a^{\mathrm{T}}})_{i\,j} = \overline{b^T_{i\,k}\,a^T_{k\,j}} = (\overline{b^{\mathrm{T}}})_{i\,k}\,(\overline{a^{\mathrm{T}}})_{k\,j} = b^H_{i\,k}\,a^H_{k\,j} = (b^{\mathrm{H}}\,a^{\mathrm{H}})_{i\,j}$,when Einstein summations are employed to sum over repeated indices of geosampled, capture point, frequency, larval, density counts. Hence it follows that$(\mathbf{A}\,\mathbf{B})^{\mathrm{H}} = \mathbf{B}^{\mathrm{H}}\,\mathbf{A}^{\mathrm{H}}$.could occur in the frequency, vulnerability, model, diagnostic output whence asymptotically, geo-spectrotemporally, targeting seasonal, eco-endmember, unknown, eco-georeferenceable,hyperproductive, aquatic, larval, habitat foci.

Einstein summation is a notational convention for simplifying expressions including summations of vectors, matrices, and general tensors[4]. There are essentially three rules of Einstein summation notation, namely:1)Repeated indices are implicitly summed over, 2)Each index can appear at most twice in any term: and, 3) Each term must contain identical non-repeated indices of quantitable, products (e.g., signature malaria mosquito, oviposition, regression model tabulizable eco-endmember, LULC values) [6].The first item on the above list may be employable to greatly simplify and shorten equations involving tensors in an eco-endmember, sub-meter resolution, geo-spectrotemporal, oviposition, malaria, mosquito, forecast, vulnerability,geo-spectrotemporal LULC, signature model for asymptotically, targeting unknown, seasonal, hyperproductive, aquatic, larval habitat, grid-stratifiable, eco-georeferenceable, frequency-related, capture point foci.

An nth-rank tensor in m-dimensional space is a mathematical object that has n indices and m^n components and obeys certain transformation rules. Each index of a tensor ranges over the number of geoclassifiable dimensions of space.For example, in Einstein's theory of Special Relativity, Euclidean three-space plus time (the "fourth dimension") are unified into the so-called Minkowski space. Minkowski space is a four-dimensional space possessing a Minkowski metric, (i.e., a metric tensor having the form $d\tau^2 = -(dx^0)^2 + (dx^1)^2 + (dx^2)^2 + (dx^3)^2$.[4]. Unfortunately, the dimension of the space is largely irrelevant in most tensor equations employed in medical entomological literature (with the notable exception of the contracted Kronecker delta used by Griffth 2005 and Jacob et al. 2009). In mathematics, the Kronecker delta is a function of two variables, usually just positive discrete integers(e.g., aquatic larval geosampled, malaria, mosquito, eco-endmember, LULC,geosampled, geo-spectrotemporal data)[2]. Tensors are generalizations of scalars (that have no indices), vectors (that have exactly one index), and matrices (that have exactly two indices) to an arbitrary number of indices [4].

The notation for a tensor is similar to that of a matrix (i.e., $\mathbf{A} = (a_{i\,j})$), except that a tensor $a_{i\,j\,k\,\ldots}$, $a^{i\,j\,k\,\ldots}$, $a_i{}^{j\,k}{}_{\ldots}$, etc., may have an arbitrary number of indices especially in a sub-meter resolution, ento-epidemiological, prognosticative, geo-spectrotemporal, malaria, mosquito, oviposition, eco-endmember, LULC, signature, frequency model employed for asymptotically, geo-spectrotemporally,optimally targeting seasonal,unknown, hyperproductive foci. In addition, a tensor with rank $r + s$ may be of mixed type (r, s), consisting of r so-called "contravariant" (upper) indices and s "covariant" (lower) indices. Note that the positions of the slots in which contravariant and covariant indices are placeable in an ento--epidemiological, vector arthropod, geo-spectrotemporal, frequency, LULC, signature model which may be significant for rendering timely vulnerability forecasts of seasonal, un-geosampled, aquatic, larval habitat, eco-endmember, hyperproductive foci. For example, $a_{\mu\nu}{}^{\lambda}$ would be distinct from $a_{\mu}{}^{\nu\lambda}$ in an, oviposition, endemic, malaria, mosquito, grid-stratifiable, forecast, endmember, signature model, whence asymptotically targeting, unknown sub-meter resolution, geo-specrotemporal, ento-ecoepidemiological, hyperproductive, malaria, mosquito, eco-georeferenceable, aquatic, larval habitat, seasonal foci.

While the distinction between covariant and contravariant indices must be made for general tensors, the two are equivalent for tensors in 3-D Euclidean space, and such tensors are known as Cartesian

tensors.In geometry and linear algebra, a Cartesian tensor employs an orthonormal basis to represent a tensor in a Euclidean space in the form of components (uncoalesced, eco-endmember, sub-mter resolution, grid-stratified, malaria , mosquito, seasonal, hyperproductive, un-geosampled ,aquatic, larval, habitat, foci)[4]. A set of vectors form an orthonormal set if all vectors in the set are mutually orthogonal and all of unit length [2]. Converting a tensor's components from one such basis to another in a sub-meter resolution, eco-georefereneceable, geo-spectrotemporal, oviposition, malaria, mosquito, forecast, vulnerability, grid-stratifiable, LULC model for optimally asymptotically, geo-spectrotemporally targeting unknown hyperproductive, aquatic, larval habitat, eco-endmember, geoclassifiable, capture points may utilize an orthogonal transformation. The construction of orthogonality of vectors is motivated by a desire to extend the intuitive notion of perpendicular vectors to higher-dimensional spaces [4]. In the Cartesian plane, two vectors are said to be perpendicular if the angle between them is 90° (i.e. if they form a right angle [2]). This definition can be formalized in Cartesian space for optimally eco-cartographically robustly predicting, unknown, eco-georeferenceable, un-geosampled, geolocations of sub-meter resolution sub-pixel, grid-stratifiable, orthogonal, seasonal, LULC, hyperproductive, malaria, mosquito foci by delineating the dot product and specifying that two vectors in the plane that are orthogonal but only if their dot product is zero. Similarly, the construction of the norm of a vector in a forecast, vulnerability, malaria, mosquito, capture point, oviposition,LULC, signature, sub-meter resolution, frequency model may be motivated by a desire to extend the intuitive notion of the length of a remotely captured, malaria mosquito, seasonal, vector arthropod, aquatic larval habitat,capture point to higher-dimensional spaces whence optimally, asymptotically, geo-spectrotemporally targeting seasonal, unknown, eco-endmember, eco-georeferenceable, hyperproductive foci. In Cartesian space, the norm of a vector may be the square root of the vector dotted with itself [2].

The most familiar coordinate systems are the 2-D and 3-D Cartesian coordinate systems [4]. Cartesian tensors may be employable within any Euclidean space, or more technically, for any finite-dimensional vector space, field of signature, geosampled, sub-meter resolution, grid-stratifiable, geo-spectrotemporal, oviposition, malaria, mosquito, geoclassifiable, LULC, eco-endmember, LULC, capture points that have an inner product for optimally, asymptotically, geo-spectrotemporally targeting sesasonal, hyperproductive, eco-georeferenceable, un-geosampled, aquatic, larval habitat, foci.Use of Cartesian tensors occurs in physics and engineering, such as with the Cauchy stress tensor and the moment of inertia tensor in rigid body dynamics[6].

Sometimes general curvilinear coordinates are convenient, as in high-deformation continuum mechanics, or even necessary, as in general relativity. While orthonormal bases may be found for some such coordinate systems (e.g. tangent to spherical, explanative, LULC, frequency, empirical datasets of seasonal, malaria, mosquito, hyperproductive, un-geosampled, eco-georeferenceable, capture point coordinates), Cartesian tensors may provide considerable simplification. Further, applications in which rotations of rectilinear coordinate axes are required in a vector arthropod, LULC, ento-endmember, signature, frequency model may be non-heuristically optimizable employing sub-meter resolution, forecast, vulnerability, geo-spectrotemporal, risk model, capture point estimators for asymptotically, targeting seasonal, eco-georeferenceable, hyperproductive, unknown foci. The transformation would be a passive transformation, since the ento-geosampled seasonal, prolific, capture point, LULC coordinates would be changed but not in the physical prognosticative, eco-endmember, aquatic, larval habitat, modeling system.

Objects that transform like zeroth-rank tensors are called scalars while those that transform like first-rank tensors are called vectors, and those that transform like second-rank tensors are called matrices [4]. In tensor notation in a sub-meter resolution, grid-stratifiable, eco-endmember, LULC, malaria, mosquito, forecast, vulnerability, geo-spectrotemporal, frequency, risk model, a vector $\mathbf{v}$ could be written v_i, where $i = 1, \ldots, m$, and matrix is a tensor of type $(1, 1)$, which could be written $a_i{}^j$ in tensor notation.Tensors may be operated on by other tensors (such as metric tensors, the permutation tensor, or the Kronecker delta), or by tensor operators (such as the covariant derivative)[2]. The manipulation of tensor indices in an ento-epidemiological, oviposition, sub-meter resolution, grid-stratifiable, forecast, vulnerability, eco-endmember, geoclassifiable, LULC, signature, frequency model may enable asymptotically, geo-spectrotemporally targeting unknown, eco-georeferenceable, seasonal, hyperproductive, aquatic, larval habitat,capture point foci by producing identities.This includes index lowering and index raising as special cases. These can be achieved through multiplication by a so-called metric tensor g_{ij}, g^{ij}, $g_i{}^j$, etc., e.g., $g^{ij}A_j = A^i$, $g_{ij}A^j = A_i$[3]. Tensor notation may provide a very concise way of writing vector and more general identities in these forecast ento—epidemiological, LULC models. For example, for optimally quantitating tensor notation in an oviposition, malaria, mosquito, predictive, geo-spectrotemporal, sub-meter resolution, geoclassifiable, LULC, signature, frequency

vulnerability model for asymptotically targeting, seasonal, unknown, eco-endmember, hyperproductive, aquatic, larval habitat foci, the dot product $\mathbf{u}\cdot\mathbf{v}$ may be simply written as $\mathbf{u}\cdot\mathbf{v}=u_i\,v^i$,where repeated geosampled, larval, count indices may be summed over Einstein summations. The generalization of the dot product applied to tensors is called tensor contraction, and consists of setting two unlike indices equal to each other and then summing using the Einstein summation convention[2]. Similarly, the cross product may be concisely written as$(\mathbf{u}\times\mathbf{v})_i=\epsilon_{i\,j\,k}\,u^j\,v^k$,where $\epsilon_{i\,j\,k}$ may be the permutation tensor in an eco-endmember, geo-spectrotemporal, sub-meter resolution, signature, forecast, vulnerability, frequency, LULC model for asymptotically geo-spectrotemporally targeting seasonal, eco-georeferenceable, foci. The permutation tensor, also called the Levi-Civita tensor is a pseudotensor which is antisymmetric under the interchange of any two slots[4]. Recalling the definition of the permutation symbol in terms of a scalar triple product of the Cartesian unit vectors, $\epsilon_{i\,j\,k}\equiv\hat{\mathbf{x}}_i\cdot\left(\hat{\mathbf{x}}_j\times\hat{\mathbf{x}}_k\right)=\left[\hat{\mathbf{x}}_i,\hat{\mathbf{x}}_j,\hat{\mathbf{x}}_k\right]$,[6], the pseudotensor in an oviposition, LULC sub-meter resolution, geo-spectrotemporal, grid-stratifiable, eco-endmember, forecast, vulnerability model for optimally asymptotically targeting unknown, seasonal, eco-georeferenceable, hyperproductive, aquatic, larval habitat, capture point foci may be a generalization to an arbitrary basis as defined by$\epsilon_{\alpha\beta\ldots\mu}=\sqrt{|g|}\;[\alpha,\beta,\ldots,\mu]$ and$\epsilon^{\alpha\beta\ldots\mu}=\dfrac{[\alpha,\beta,\ldots,\mu]}{\sqrt{|g|}}$, where $[\alpha,\beta,\ldots,\mu]=\begin{cases}1 & \text{the arguments are an even permutation}\\ -1 & \text{the arguments are an odd permutation}\\ 0 & \text{two or more arguments are equal,}\end{cases}$. Also $g\equiv\det\left(g_{\alpha\beta}\right)g_{\alpha\beta}$ are the metric tensor. $\epsilon(\mathbf{x}_1,\ldots,\mathbf{x}_n)$ which may be nonzero if the vectors are linearly independent in the model.When viewed as a tensor, the permutation symbol is sometimes known as the Levi-Civita tensor[2]. The permutation tensor $\epsilon^{\alpha\beta\delta\gamma}$ of rank four is important in general relativity which has components which may be definable as $(\epsilon)^{\alpha\beta\gamma\delta}=\begin{cases}+1 & \text{if } \alpha\beta\gamma\delta \text{ is an even permutation of 0123}\\ -1 & \text{if } \alpha\beta\gamma\delta \text{ is an odd permutation of 0123}\\ 0 & \text{otherwise}\end{cases}$ [3]. The rank four permutation tensor may satisfy the identity$\epsilon_{\alpha\beta\gamma\delta}=-\epsilon^{\alpha\beta\gamma\delta}$ in an oviposition, geo-spectrotemporal, geosampled, aquatic, larval habitat, malaria, mosquito, predictive vulnerability, grid-stratifiable, LULC, signature, frequency, eco-endmember model. A transformation of the geosampled, ento-epidemiological, illuminative, geosampled, variables of a tensor may change the tensor into another whose asymptotically regressable aquatic, larval, habitat, malaria, mosquito, capture point components are linear homogeneous functions of the components of the original tensor. In so doing, unknown, seasonal, eco-georeferenceable, malaria, mosquito, capture point, iteratively, interpolative, eco-endmember foci may be optimally, remotely identified.

A tensor space of type (r,s) may be geo-spectrotemporally definable as a vector space tensor product between r copies of vector fields and s copies of the dual vector fields, (i.e., one-forms) in an ento-endmember, sub-meter resolution, grid-stratifiable, forecast, vulnerability, oviposition, LULC model for optimally, asymptotically, remotely targeting unknown, seasonal, eco-georefernceable, malaria, mosquito, hyperproductive, capture point foci. For example, $T^{(3,1)}=T\,M\otimes T\,M\otimes T\,M\otimes T^*\,M$may be the vector bundle of $(3,1)$-tensors on a manifold M, in an ento-epidemiological, LULC, vector arthropod, forecast, sub-meter resolution, grid-stratifiable, signature, vulnerability, frequency model where $T\,M$ is the tangent bundle of M and $T^*\,M$ is its dual. Tensors of type (r,s) form a vector space [2]. This description may be generalizable to any tensor type in any vulnerability,eco-endmember, malaria mosquito, oviposition, LULC model, and an invertible linear map $J:V\to W$may be induced for robustly constructing, interpolative, seasonal, unknown, hyperproductive, aquatic, larval habitat, capture point, eco-endmember, explanative, foci, time series, probilistic, risk maps (e.g., $\tilde{J}:V\otimes V^*\to W\otimes W^*$), whence V^* is the dual vector space and J the Jacobian is optimally definable by$\tilde{J}\,(v_1\otimes v_2^*)=\left(J\,v_1\otimes\left(J^{\mathrm{T}}\right)^{-1}\,v_2^*\right)$, whence J^{T} is the pullback map of a form as defined employing the transpose of the Jacobian. This definition can be extended similarly to other tensor products of V and V^* in any, forecast, vulnerability, seasonal, malaria, mosquito, capture point, geo-spectrotemporal,signature,eco-endmember, capture point,LULC sub-meter resolution, model output. When there is a change of eco-georeferenceable, coordinates, then tensors transform similarly, with $J$the Jacobian of the linear

transformation [6].This may be associated to the condition $a_{ij} = \bar{a}_{ji}$, where $\bar{z}$ denotes the complex conjugate in the grid-stratifiable, aquatic, larval, habitat vector arthropod, geo-spectrotemporal, geosampled paradigm.

As a result of this definition the diagonal elements a_{ii} of a Hermitian matrix could be the geosampled, aquatic, habitat, count,capture point,eco-georeferenceable, frequency,larval density counts as rendered from a sub-meter resolution imaged, grid-stratifiable, hyperproductive, seasonal, malaria, mosquito foci (since $a_{ii} = \bar{a}_{ii}$), while other elements may be complex.Examples of 2×2 Hermitian matrices include $\begin{bmatrix} 1 & -i \\ i & 1 \end{bmatrix}, \begin{bmatrix} 2 & -i \\ i & 1 \end{bmatrix}$ and the Pauli matrices $\begin{bmatrix} 0 & 1 \\ 1 & 0 \end{bmatrix}, = \begin{bmatrix} 0 & -i \\ i & 0 \end{bmatrix}$ and $\sigma_3 = \begin{bmatrix} 1 & 0 \\ 0 & -1 \end{bmatrix}$. [2].Examples of 3×3 Hermitian matrices may also be included whence regressively optimally quantitating an empirical, frquency dataset of uncoalesced, oviposition, capture point, iteratively interpolative, signature, LULC frequencies [see 1].An integer or real matrix is Hermitian if it is symmetric[4]. A matrix m may be tested to see if it is Hermitian using the Wolfram Language functionHermitianQ[m_List?MatrixQ] :=m === Conjugate@Transpose@m which may be frequentistically employable in a sub-meter resolution, eco-endmember,oviposition, ento-epidemiological, LULC, signature, model for optimally asymptotically, geo-spectrotemporally targeting seasonal, eco-georeferenceable, hyperproductive, capture point, aquatic, larval, habitat foci.

Hermitian matrices have real eigenvalues whose eigenvectors form a unitary basis which may be employable for optimally constructing geo-spectrotemporal, geosampled, malaria, mosquito, eco-endmember, geoclassifiable, LULC, signature, frequency models for optimally asymptotically targeting, eco-georeferenceable, seasonal, hyperproductive, aquatic, larval habitat foci. For real matrices, Hermitian is the same as symmetric [5].Any matrix C which is not Hermitian can be expressed as the sum of a Hermitian matrix and a antihermitian matrix [4].

A continuous, explanatorial, differentiable function of several eco-endmember LULC, geosampled, malaria mosquito, oviposition, capture point, wavelength, discontinuous variables may be convex on a convex set if and only if its Hessian matrix of second partial derivatives is positive semidefinite on the interior of the convex set. ... f(x) ≤ a} with a ∈ R are convex sets. Let f(x) be a differentiable function in an explanatorial, diagnostic, eco-endmember, sub-meter resolution, oviposition, malaria, mosquito, aquatic, larval habitat, forecast, vulnerability, geo-spectrotemporal, LULC, frequency,grid-stratifiable model. In so doing, the quadratic approximation to f(x) near some unknown, seasonal, eco-georeferenceable, un-geosampled, LULC, hyperproductive, capture point, ento-epidemiological, eco-endmember grid-stratifiable foci x_0 may be given by f(x) = f(x0) + fx(x0)(x-x0) + ½fxx(x0)(x-x0)2 or, equivalently df = fx(x0)dx + ½fxx(x0)(dx)2 where dx=(x-x_0) and df=f(x)-f(x_0). A critical point in such an LULC, geoclassifiable, vector arthropod, prognosticative, signature, frequency model would be the value of x_0 such that $f_x(x_0)=0$. If $f_x(x_0)=0$ then df = $\frac{1}{2}f_{xx}(x_0)(dx)^2$ in the model renderings.

For optimally tabulating a minimum in an eco-endmember, signature, prognosticative, geoclassifiable, grid-stratifiable, LULC malaria, mosquito, oviposition, aquatic, larval habitat, explanative, time series, df and $(dx)^2$ would have to be positive. Hence $f_{xx}(x_0)$ has to be positive as well in the ento-ecoepidemiological, forecast, vulnerability, frequency, sub-meter resolution, LULC, capture point, grid-stratifiable, model output. On the other hand, for a maximum df to be negative requires $f_{xx}(x_0)$ be negative in the frequency model [4]. The Hessian matrix for this case would be just then be 1×1 matrix $[f_{xx}(x_0)]$. Thereafter, the capture point at which the second set of geosampled, ento-endmember, LULC, aquatic, larval, habitat,probabilistic, capture point, iterative, interpolative derivatives evaluated may not be expressed explicitly so the Hessian matrix would have to optimized by f_{xx}. There would be no corresponding constrained optimization problems in any single geosampled, eco-endmember, geoclassified LULC, explanatory,signature, frequency, thereafter, in any seasonal, malaria, mosquito, oviposition, vulnerability, modeling, case scenario but the forecasted, ento-epidemiological ouput would not be able to determine geolocations of, sub-meter resolution, grid-stratifiable, geoclassifiable, unknown, seasonal, hyperproductive, capture point, eco-endmember, eco-georeferenceable foci.

In an eco-endmember, grid-stratifiable, LULC, signature, aquatic, larval habitat,geo-spectrotemporal, vulnerability signature, frequency, eco-endmember model two variable case scenarios may be expected; the quadratic approximation would be about the seasonal, geosampled, geo-spectrotemporal, hyperproductive, sub-meter resolution, geoclassifiable,capture point (x_0, y_0) where a differentiable eco-endmember, geosampled, LULC function f(x,y) may be asymptotically defined as $df = f_x dx + f_y dy + ½[f_{xx}dxdx + f_{xy}dxdy + f_{yx}dydx + f_{yy}dydy]$.This forecast, vulnerability, oviposition, predictive, malaria, mosquito, capture point, eco-endmember, geo-spectrotemporal, geo-spectrotemporal, signature, frequency,LULC model may also be expressed in the form df = fxdx + fydy + ½(dx, dy)H(dx, dy)T where (dx, dy)T may be the column vector which may be the transpose of the row vector (dx, dy) and H= f_{xx} f_{xy} |or f_{yx} f_{yy}.

For parsimoniously constructing an unconstrained, geosampled, sub-meter resolution, geo-spectrotemporal, malaria, mosquito, eco-endmember, oviposition, LULC, forecast, vulnerability, geo-spectrotemporal model, a critical point may be one such that $f_x=0$ and $f_y=0$ so $df = ½(dx, dy)H(dx, dy)^T$ for asymptotically targeting seasonal, unknown, hyperproductive, eco-georeferenceable foci. For a minimum the second order condition is that H be a positive definite matrix [4]. The conditon for a matrix to be positive definite is that its principal minors all be positive [2]. For a maximum, H must be a negative definite matrix which will be the case scenario if the principal minors alternate in sign in any ento-epidemiological, oviposition, sub-meter resolution, grid-stratifiable, signature, forecast, vulnerability model unbiased, frequency estimator for asymptotically targeting, hyperproductive, eco-georeferenceable, malaria, mosquito, aquatic, larval habitat, geo-spectrotemporal, eco-endmember, LULC foci.

For the constrained oviposition, ento-epidemiological, malaria, mosquito, eco-endmember, geo-spectrotemporal, frequency, LULC model, a hyperproductive, capture point may be optimally definable in terms of the Lagrangian multiplier method. In mathematical optimization, the method of Lagrange multipliers is a strategy for finding the local maxima and minima of a function subject to equality constraints [4]. Suppose the constraint is $p_x x + p_y y = 1$ in an aquatic, larval habitat, prognosticative, ento-ecoepidemiological, vulnerability, vector, arthropod, LULC, signature, capture point model. Then the first orders would be $f_x = \lambda p_x$ and $f_y = \lambda p_y$ where λ, the Lagrangian multiplier may be chosen so as to have critical values which may satisfy the constraint in the model. In so doing, the quadratic approximation in the model may be expressed as $df = \lambda p_x dx + \lambda p_y dy + ½(dx, dy)H(dx, dy)^T$.Since any deviations from the critical point must also satisfy the constraint $p_x dx + p_y dy = 0$ in an ento-ecoepidemiological, eco-georeferenceable, eco-geoclassifiable, signature, LULC, predictive,sub-meter resolution, oviposition, geo-spectrotemporal, risk model [see[1], then $df = \lambda(p_x dx + p_y dy) + ½(dx, dy)H(dx, dy)^T = ½(dx, dy)H(dx, dy)^T$ may occur in the data output when asymptotically targeting geo-spectrotemporal, geosampled, unknown, hyperproductive,capture point, aquatic, larval, habitat, eco-endmember foci. H may have to be either positive or negative definite for an extreme (maximum or minimum) as dx and dy may not be unrestricted (i.e., only dx and dy such that $p_x dx + p_y dy = 0$ would be allowed) in the entomological LULC model output. This makes specifying the conditions such as asymptotically targeting seasonal, malaria, mosquito, aquatic, larval habitat,eco-georeferenceable, frequency, eco-endmember, LULC, foci on H very crucial.

For a trinary function f (x,y,z) the quadratic approximation of the deviations as rendered in an oviposition eco-endmember, malaria, mosquito, sub-meter resolution, grid-stratifiable, LULC eco-georeferenceable, forecast, vulnerability, signature, frequency model $df = f_x dx + f_y dy + f_z dz + ½(dx, dy, dz)H(dx, dy, dz)^T$ may be given by

$$H = \begin{vmatrix} f_{xx} & f_{xy} & f_{xz} \\ f_{yx} & f_{yy} & f_{yz} \\ f_{zx} & f_{zy} & f_{zz} \end{vmatrix}$$

As in the one and two variable unconstrained case scenario, the first orderm eco-endmemberm oviposition, ento--epidemiological, capture point, geo-spectrotemporal, eco-geoclassifiable, LULC terms would vanish and the conditions for a minimum would be based soley on the positive definiteness of H and similarly negative definiteness for the maximum which would be apparent in the eco-georeferenecable, prognosticative, malaria, mosquito, signature model, output dataset. Those conditions in turn can be stated in terms of the signs of the principal minors of H in the LULC model output in ArcGIS. The significance of this case is that the constrained two variable case scenario can be restated in terms of a three variable case through the use of the Lagrangian multiplier method for optimally geo-

spectrotemporally asymptotically targeting seasonal, eco-georeferenceable, hyperproductive, capture point, aquatic, larval habitat, eco-endmember foci.

In the Lagrangian multiplier method the optimization problem of minimizing f(x,y) with respect to x and y subject to the constraint $p_x x + p_y y = I$ may be transformed into a three variable problem of unconstrained minimizing $L(x,y,\lambda) = f(x,y) - \lambda(p_x x + p_y y - I)$with respect to x, y and λ for optimally asymptotically targeting unknown, seasonal, eco-georeferenceable, malaria, mosquito, hyperproductive, signature, aquatic, larval, habitat foci frequencies. The first order condition for λ is $L_\lambda = p_x x + p_y y - I = 0$ which may be equivalent to satisfying the constraint in the oviposition, sub-meter resolution, grid-stratifiable, eco-endmember, geoclassifiable, LULC, malaria mosquito, capture point, model.The quadratic approximation for L(x,y,λ) could then be optimally described as $dL = L_x dx + L_y dy + L_\lambda d\lambda + ½(dx, dy, d\lambda)H^*(dx,dy,d\lambda)^T$ which on the basis of the definition of L in the ento-epidemiological, forecast, vulnerability, model could reduce to $dL=f_x dx+f_y dy+(p_x x+p_y y-I)d\lambda+½(dx,dy,d\lambda)H^*(dx,dy,d\lambda)^T$ for the first order conditions to $dL=\lambda p_x dx+\lambda p_y dy+(p_x x+p_y yI)d\lambda + ½(dx, dy, d\lambda)H^*(dx, dy, d\lambda)^T$. Because of the contentment of the constraints, the first two terms in the eco-epidemiological, explanatory, LULC residual, sub-meter resolution, signature, frequency, model output will reduce to zero and likewise the third term. Thus, the value of dL could be given by $dL = + ½(dx, dy, d\lambda)H^*(dx, dy, d\lambda)^T$whence optimally asymptotically geo-spectrotemporally, targeting seasonal, eco-georeferenceable, hyperproductive, capture point, aquatic, larval habitat, eco-endmember foci on specific geoclassified LULCs (e.g., post-tillering, agro-irrigation, riceland ditches).

The second order conditons for the constrained two variable case in an oviposition, sub-meter resolution, grid-stratifiable, eco-endmember, LULC, malaria, mosquito, forecast, vulnerability, eco-epidemiological, signature, frequency model for optimally asymptotically, remotely, geo-spectrotemporally targeting, seasonal, eco-georeferenceable,unknown, hyperproductive, aquatic, larval, habitat foci can be stated in terms of the Hessian H* for the corrsponding three variable case scenario. The character of H* may be given by first noting that$L_x=f_x-\lambda p_x$ $L_y=f_y\lambda p_y$ and $L_\lambda = -(p_x x + p_y y - I)$ in the,forecast, model preliminary output. Consequently, the second derivatives for the ento-ecoepidemiological eco-endmember oviposition, malaria, mosquito, geosampled, geo-spectrotemporal, capture point, signature, LULC data may be given as:

$$H^* = \begin{vmatrix} f_{xx} & f_{xy} & -p_x \\ f_{yx} & f_{yy} & -p_y \\ -p_x & -p_y & 0 \end{vmatrix}$$

Suppose *f* is a function of one geosampled, sub-meter resolution, grid-stratifiable, eco-endmember, malaria, mosquito, orthogonal, LULC geosampled signature, variable in an non-heuristically optimizable, frequency, prognosticative, vulnerability model framework that is at least two times continuously differentiable around a seasonal, hyperproductive, capture point x^* in its domain, when $f'(x^*) \neq 0$. Then, there would exist $\varepsilon > 0$ such that for any $x^{(0)} \in (x^* - \varepsilon, x^* + \varepsilon)$. The sequence may be parsimoniously extractable by applying Newton's method for root-finding a function of one eco-endmember, sub-resolution, geosampled, signsture, frequency, grid-stratifiable, geoclassifiable, spectrotemporal, geosampled, LULC variable starting from $x^{(0)}$ which would either reach the root in finitely many steps or via quadratic convergence or higher-order convergence to the root x^* .

A Newton method based on the Hessian approximation $H=g'(x) * g'(x)\partial x$ may be employable to optimally quantitate, eco-epidemiological, geosampled, oviposition, geo-spectrotemporal, empricial, regressable, malaria, mosquito, geoclassifiable, LULC datsets of eco-georeferenceable, seasonal, hypeproductive, aquatic, larval habitat, oviposition, capture point, sub-meter resolution, unknown, eco-endmember foci Technically, a malariologist or medical entomologist may only quantitate first-derivatives in these models. According to Jacob et al. [1] a sequence {xi}subscriptxi\{x_{i}\} in an epi-entomological, vector arthropod, oviposition, prognosticative, geo-spectrotemporal, eco-endmember, LULC, sub-meter resolution, vulnerability, grid-stratifiable, frequency model in metric space (X,d)Xd

is said to converge quadratically to x*superscriptxx^{*} if there is a constant 1>c>01c01>c>0 such that d⁢(xi+1,x*)≤c⁢d⁢(xi,x*).

To obtain a robust expression for optimally, asymptotically, targeting, prolific, seasonal, malaria, mosquito, hyperproductive, aquatic, larval habitat, signature, eco-endmember, eco-georefernceable foci, a malariologist or medical entomologist may need information about how the second-derivative of J is constructed and not just g in a forecast, vulnerability, LULC, sub-meter resolution, malaria, mosquito model. Under the right assumptions, a superlinear convergence may be obtainable for conducting an approximation for an ento-endmember, oviposition, signature, geo-specified, LULC dataset of uncoalesced, seasonal, eco-georeferenceable, hyperproductive, capture point, malaria, mosquito, aquatic, larval habitat, seasonal foci.

The Ostrowski theorem is a classical result which ensures the attraction of all the successive approximations *xk*C1G (*xk*) near a fixed, oviposition, malaria, mosquito, capture point *x** (e.g., agro-irrigated eco-georeferenceable, geosampled, seasonal, hypeproductive, aquatic, larval, habitat, LULC foci). Let $\mathsf{A} = a_{i\,j}$ be a matrix with positive coefficients and λ_0 be the positive eigenvalue in the Frobenius theorem, then the $n-1$ tabulated eigenvalues $\lambda_j \neq \lambda_0$ may satisfy the inequality $|\lambda_j| \leq \lambda_0 \frac{M^2 - m^2}{M^2 + m^2}$, where $M = \max_{i,j} a_{i\,j}$ and $m = \min_{i,j} a_{i\,j}$ and $i,\ j = 1$, 2, ..., n [3].

In mathematics, Frobenius' theorem gives necessary and sufficient conditions for finding a maximal set of independent solutions of an underdetermined system of first-order homogeneous, linear, partial differential equations[2]. For an eco-endmember, sub-meter resolution, geo-spectrotemporal, LULC,frequency dataset of malaria, mosquito, capture point, predictive, risk model, grid-stratifiable, geometric terms, the theorem could provide necessary and sufficient conditions for the existence of a foliation by maximal integral manifolds, each of whose tangent bundles may be spanned by a given family of eco-georeferenceable, aquatic, larval habitat, vector fields. In so doing, the integrability condition in the capture point, ento-epidemiological, eco-endmember, LULC model may be satisfied in much the same way that an integral curve may be assigned to a single vector field. Although the theorem is foundational in differential topology and calculus on manifolds, in its most elementary form, the theorem can address the problem of finding a maximal set of independent solutions for a regular system of first-order, linear, homogeneous, partial differential equations for geo-spectrotemporally, asymptotically optimally, remotely, targeting unknown, hyperproductive, eco-georeferenceable, eco-endmember,sub-meter resolution, LULC, oviposition, malaria, mosquito, seasonal, aquatic, larval habitat, capture points.

Different seasonal, eco-endmember, grid-stratified, oviposition, LULC conditions based on the magnitude of *G′*(*x**) may provide lower bounds for the convergence order in an frequency-oriented, seasonal, malaria, mosquito, forecast, vulnerability, sub-meter resolution, immature,capture point model, construction process. Characterizing high convergence orders in the signature model terms may help aid in optimally asymptotically, remotely quantitating some eco-georeferenceable eco-endmember, LULC elements of *G′*(*x**)(e.g., levels of infrequently shading in a capture point, seasonal, hyperproductive, geo-spectrotemporal, LULC, grid-stratifiable, imaged, aquatic, laval habitat,) for optimally asymptotically targeting un-geosampled, hyperproductive foci. A malariologist or medical entomologist may obtain a set of trajectories with high convergence orders for example, which may be restricted to some subspaces, regardless of the nonlinearity of *G* in an ento-epidemiological, time series, LULC, orthogonal, eco-endmember, signature, frequency, model output. A malariologist or medical entomologist may also analyze the stability of the successive approximations under perturbation assumptions.

If a malariologist, medical entomologist or other experimenter identifies a root of a system of equations F(x)=0, he or she may be able to asymptotically, target, seasonal, hyperproductive, eco-georeferenceable, malaria, mosquito, epi-entomological, LULC foci employing an oviposition, geosampled, datastet of uncoalesced, krigeable, sub-meter resolution, signature, geo-spectrotemporal,model, frequency estimators where x=(x 1 ,…,x n) .Further, he or she may globalize Newton's method which could formulate the problem as the optimization problem by employing min x f(x)wheref(x):=12 ‖F(x)‖ 2 , in the forecast, vulnerability, eco-endmember model whence F(x)=⎡⎣⎢ f 1 (x)…f m (x) ⎤⎦⎥,‖F(x)‖ 2 =∑ i=1 m f i (x) 2 . In so doing, the gradient and Hessian of f may be robustly computed for the oviposition geosampled model, hyperproductive, capture point, geoclassifiable, LULC, signature,

regressable, aquatic, larval habitat, wavelength covaraites in terms of : $\nabla f(x)=J(x)^T F(x), \nabla^2 f(x)=J(x)^T J(x)+\sum_{i=1}^{m} i f(x)\nabla^2 f_i(x)$, where J is the Jacobian of F, (i.e., the matrix whose i -th row is $\nabla f_i(x)^T \nabla f_i(x)^T$).

By applying Newton's method to f and globalizing it employing a line search, (e.g., an Armijo line search) precise, eco-georeferenceable, eco-endmember, oviposition, LULC, grid-stratified targets of seasonal, hyperproductive, malaria, mosquito, aquatic, larval habitat, capture point foci may be established. The procedure could be as follows:

1. Compute Newton's direction by solving $\nabla^2 f(x_k)d_k=-\nabla f(x_k)$ $\nabla^2 f(x_k)d_k=-\nabla f(x_k)$ in the optimizable, geosampled, geo-spectrotemporal, eco-endmember, malaria model, aquatic, larval, habitat, frequency, signature, count, density estimates.
2. Compute a step size $t\in(0,1]$ such that $f(x_k+td_k)\leq f(x_k)+\alpha t\nabla f(x_k)^T d_k$ starting from t=1 and halving t until the inequality is satisfied (i.e., the model converges on a seasonal, hyperproductive, capture point foci). If d_k is a descent direction, this procedure is guaranteed to succeed.
3. Set $x_{k+1}=x_k+td_k$ for statistical verification of all ento-ecoepidemiological, geoclassified, LULC, eco-georeferenceable, grid-stratfiable, model outputs.

Because of the form of $\nabla^2 f(x_k)\nabla^2 f(x_k)$,it may be necessary to modify an LULC, sub-meter resolution, grid-stratifiable, oviposition, malaria, mosquito, aquatic, larval habitat, capture point, hyperproductive, eco-endmember, foci, forecast, vulnerability model to ensure that dk is a descent direction. If a malariologist or medical entomologist locally assumes that an ento-ecoepidemiological, frequency, LULC eco-endmember, oviposition, model can be a minimizer, it would not be necessary to modify any geosampled, grid-stratifiable, parameterizable, or semi-paramterizable, capture point estimators (e.g., total seasonal, aquatic, larval habitat, frequency. density counts). If the sub-meter resolution, ento-epidemiological model converges, a minimizer could be established for the vector arthropod, geoclassifiable, LULC data when $\nabla^2 f$ is positive definite. The approach could guarantee that t=1 at all iterations would be asymptotic in the model output.

The drawback of this approach is that a malariologist or medical entomologist may converge to a stationary, oviposition, eco-endmember, gridded, frequency, LULC, malaria, mosquito, seasonal capture point, aquatic, larval, habitat, foci $x* \; x*$ of f (a minimizer) whence $F(x)\neq 0$. However, this can only happen if $J(x*)$ is rank deficient. A matrix is said to have full rank if its rank equals the largest possible for a matrix of the same dimensions, which is the lesser of the number of rows and columns[4]. A matrix is said to be rank deficient if it does not have full rank [2].

Newton's method may aid in quadratic convergance of an empirical, non-heuristically optimizable, frequency dataset of eco-georeferenceable,geosampled, oviposition,LULC unmixed, sub-meter resolution, oviposition, malaria, mosquito, geo-spectrotemporal,signature, model estimators for asymptotically targeting seasonal,geoclassifiable,hypeproductive, aquatic, larval, habitat, eco-endmember foci.This could be conducted within a certain radius, since a self-concordant function is employable during the forecast, vulnerability, capture point, LULC model, construction process. Let $\Omega \subseteq R^n$ be a convex open set in the model. Then $f : \Omega \rightarrow R$ may be self-concordant with parameter $r\sigma > 0$ at $x \in$[4]. The iteration will converge quadratically starting from any real initial guess a_0 except zero in the eco-endmember, sub-meter resolution, LULC, malaria, mosquito, vulnerability model. When a_0 is negative, Newton's iteration may converge to the negative square root of the geosampled, oviposition, malaria, mosquito, capture point, hyperproductive, aquatic, larval habitat, ento-endmember, un-geosampled, LULC foci. Quadratic convergence in the prognosticative, signature model then would mean that the square of the error $a_t - \sqrt{s}$ at one iteration could be calculable proportional to the error at the next interpolatble iteration employing $a_{t+1} - \sqrt{s} \quad \sim \quad (a_t - \sqrt{s})^2 = a_t^2 - 2a_t\sqrt{s} + s \quad > \quad 0$ [Equation 1.1]. So, for example if the error is recorded as a one significant digit employing one iteration in the model, then at the next iteration it would be two digits, then four, etc. A malariologist or medical entomologist may not be able to use equation [1.1] in place of the Newton iteration itself, as a capture point, oviposition, eco-endmember, LULC, frequency, model unbiased estimator, but he or she could employ $\sqrt{s}$ to achieve a_{t+1}.Further, the factor of proportionality may be required for optimally, asymptotically, remotely targeting the eco-georeferenceable, seasonal, hypeproductive,malaria, mosquito, aquatic, larval, habitat foci. Notice, however, if a malariologist or medical entomologist takes this factor to be $1/(2a_t)$, then $\sqrt{s}$ cancels and equation [1.1] becomes itself the Newton iteration.

Newton's iteration is an algorithm for computing the square root $\sqrt{n}$ of a number n via the recurrence equation $x_{k+1} = \frac{1}{2}\left(x_k + \frac{n}{x_k}\right)$, where $x_0 = 1$. This recurrence converges quadratically as $\lim_{k\to\infty} x_k$. Newton's iteration is simply an application of Newton's method for solving the equation $x^2 - n = 0$. For example, when applied numerically, the first few iterations to Pythagoras's constant $\sqrt{2} = 1.4142\ldots$ are 1, 1.5, 1.41667, 1.41422, 1.41421, ...The first few approximants x_1, x_2, ... to $\sqrt{n}$ may be then given by $1, \frac{1}{2}(1+n), \frac{1+6n+n^2}{4(n+1)}, \frac{1+28n+70n^2+28n^3+n^4}{8(1+n)(1+6n+n^2)}, \ldots$. These may be also given by the analytic formula $x_k = \sqrt{n}\left[1 + \frac{2}{\left(\frac{1+\sqrt{n}}{1-\sqrt{n}}\right)^{2^k} - 1}\right] = \sqrt{n}\coth\left(2^k \tanh^{-1}\left(\sqrt{n}\right)\right)$. which may be parsimoniously derived by noting that the recurrence can be written as $\frac{x_k - \sqrt{n}}{x_k + \sqrt{n}} = \left(\frac{x_{k-1} - \sqrt{n}}{x_{k-1} + \sqrt{n}}\right)^2$, which may have the closed-form solution $\frac{x_k - \sqrt{n}}{x_k + \sqrt{n}} = \left(\frac{1 - \sqrt{n}}{1 + \sqrt{n}}\right)^{2^k}$. Solving for x_k in the geo-spectrotemporal, predictive, malaria, mosquito, LULC,eco-endmember model derivatives may render the solution derived above.

Even though a malariologist or medical entomologist cannot estimate the rate of convergence by $a_t - \sqrt{s}$ in any eco-endmember, oviposition, sub-meter resolution, grid-stratifiable, LULC, ento-epidemiological, malaria, mosquito, forecast, vulnerability model (i.e.,*s*,), an estimate of it may be quantitated by looking at the difference between the intermediate solutions employing two consecutive steps. For example, from equation 1.1 a malariologist or medical entomologist may write $a_{t+1} - a_t = \frac{1}{2}\left(a_t + \frac{s}{a_t}\right) = \frac{a_t^2 + s}{2a_t} - a_t$ then $a_{t+1} - a_t = \frac{s - a_t^2}{2a_t}$. In so doing, the Newton iteration may not overestimate the ultimate square root in the oviposition, sub-meter resolution, signature, frequency model for geo-spectrotemporally, remotely targeting, seasonal, hyperproductive, eco-endmember, LULC, aquatic, larval, habitat foci.Since the second-order optimality conditions tell us that near the solution the Hessian will be positive definite, we can then rely on our convergence rate analysis under this assumption by using following notations.
x = input, malaria, mosquito,capture point, geosampled, endmember, data points m*2
y = labelled outputs(m) which may correspond to a seasonal, eco-georeferenceable, hyperproductive, aquatic, larval, habitat foci.

Eco-endmember, geo-spectrotemporal, prognosticative, signature, frequency, malaria, mosquito, capture point, sub-meter resolution, orthogonal, geoclassfiable, LULC paradigms for orthogonally, asymptotically targeting seasonal, unknown, eco-georeferenceable, hyperproductive foci could focus on the frequency, signature, conditional, probability distribution of y given x, rather than on the joint probability distribution of y and x, which would be the domain of multivariate analysis. In eco-georeferenceable, optimal, prognosticative, vector arthropod, aquatic, larval habitat, capture point,LULC, risk mapping given two jointly distributed geosampled, random variables *x* and *y*, (e.g., Depth of habitat, Differentially corrected GPS geolocation of a seasonal, hyperproductive, eco-georeferenceable, capture point), the conditional probability distribution of *y* given *x* would be the probability distribution of *y* when *x* is known to be a particular value (e.g., total, immature, density count values of a prolific foci)[1]. In some cases the conditional probabilities may be expressible as LULC eco-endmember, explanatory functions containing the unspecified, aquatic, aquatic, larval, habitat, regressable value *x* as a parameter. When both "x" and "y" are categorical, aquatic, larval habitat, oviposition, capture point, geosampled, LULC, time series, frequentistically optimizable signature, iteratively interpolative variables, a conditional probability table may be non-heuristically employable to

represent the conditional probability in an, oviposition, malaria, mosquito, eco-endmember model for optimally predictively targeting, unknown, eco-georeferenceable, seasonal, hyperproductive foci.

In the study of probability, given at least two explanatorial, grid-stratifiable, eco-georeferenceable,signature, oviposition, sub-meter resolution, geoclassfiable, LULC, geo-spectrotemporal orthogonal, signature, frequency-oriented, malaria, mosquito, aquatic, larval habitat, geosampled, capture point, eco-endmember, random variables *x*, *y*, ..., that are definable on a probability space, the joint probability distribution for *x*, *y*, ... could be a distribution that optimally renders the probability that each of *x*, *y*, ... falls in any particular range or discrete set of values specified for that variable[1]. The joint probability distribution may be then expressed from a regressed geomterical, geo-spectrotemporal, geosampled, frequency dataset of forecasted, seasonal, hyperproductive, malaria, mosquito, grid-stratifiable, eco-georeferenceable, capture points either in terms of a joint cumulative distribution function or in terms of a joint probability density function (in the case of continuous geosampled oviposition, geoclassifiable, LULC variables) or joint probability mass function (in the case of discrete, habitat, suitability variables). These vector arthropod, capture point, eco-endmember, LULC variables may be employable to find other types of unknown, geo-spectrotemporal, malaria, mosquito, oviposition, seasonal distributions. For example, a marginal distribution may be calculable for rendering the probabilities of any regressed geoclassified, geo-spectrotemporal, oviposition, LULC dataset of empirically geosampled, eco-georeferenceable, malaria, mosquito, prognosticative, hyperproductive, endmember, variables with no reference to any specific ranges of the capture point, frequency, habitat, larval, density counts.

However, the conditional probability distribution for rendering the probabilities for any subset of the unknown, eco-endmember, LULC oviposition, variables conditional on particular geo-spectrotemporal, aquatic, larval habitat, frqeuncy, count value may be tabulated and archived in a statistical database (e.g., PROC REG). Most commonly, the conditional mean of y given a geosampled, oviposition, frequency, capture point, optimizable, explanatory, geo-spectrotemporal, signature, LULC, malaria, mosquito, grid-stratfiable, eco-endmember value of x may be an affine function of x; less commonly, the median or some other quantile of the conditional, probabilistic distribution of y given x may be quantitatable as a linear function of x in a optical-geometric, forecast, eco-endmember, vulnerability, LULC ento-ecoepidemiological, geo-spectrotemporal model. In geometry, an affine transformation, affine map or an affinity is a function between affine spaces which preserves points, straight lines and planes [2].

Linear regression was the first type of regression analysis to be studied rigorously, and to be used extensively in seasonal, malaria, mosquito, aquatic larval habitat, predictive, LULC, risk mapping applications. This is because in general, oviposition, eco-endmember, grid-stratifiable, geoclassifiable, LULC malaria, mosquito, geo-spectrotemporal,signature, frequency models depend linearly on their seasonal, geosampled, parameterizable estimators and are easier to fit than vulnerability models which are non-linearly related to their capture point, vector arthropod-related, aquatic, larval habitat, eco-georeferenecable, ento-ecoepidemiological,signature prognosticators. Further, the statistical properties of the resulting LULC, diagnostic, endmember, sub-meter resolution, geoclassifiable estimators rendered from a linear regression algorithm would be easier to quantitate for optimally determining geolocations of seasonal, hyperproductive, grid-stratifiable, malaria, mosquito, eco-georeferenceable, capture point foci. If the goal is prediction or error reduction, linear regression can be employed to fit a model to an observed dataset of y and x values [2]. After developing an ento-epidemiological, sub-meter resolution, geoclassifiable, LULC, forecast, vulnerability, foci model, if an additional value of x is regressed without its accompanying value of y, the fitted model may still be employable to make an optimal forecast of an un-geosampled, eco-georeferenceable, malaria, mosquito, hypeproductive, aquatic, larval habitat, capture point, seasonal, frequency, signature, eco-endmember value.

An oviposition, time series geosampled, eco-endmember, prolific, grid-stratifiable, orthogonal, LULC, geosampled, malaria mosquito, optimizable variable y and a number of other ento--epidemiological, geosampled, sub-meter resolution, aquatic, larval habitat, capture point frquency explanators X_1, ..., X_p may be regressively related to y in a linear, malaria, mosquito, forecast, vulnerability, time series analysis. The model constant may be one of the diagnostic regressors. For example, a malariologist or medical entomologist may employ $x_{i1} = 1$ for $i = 1, ..., n$ in an aquatic, larval habitat, oviposition, sub-meter resolution, LULC, eco-endmember,prognosticative, signature model. The corresponding element of β in the vulnerability, malaria, mosquito, model would be then the intercept. According to Jacob et al. [5] employing the common convention that the horizontal axis represents an eco-endmember, eco-

georeferenceable, optimizable, ento-epidemiological, geoclassifiable, LULC,optimizable variable *x* whence the vertical axis represents a geosampled, geo-spectrotemporal, aquatic, larval, habitat, frequency, density count *y*,.Optimally this would render a *y*-intercept or vertical intercept which may be realized as a hyperproductive, seasonal, capture point realization where the graph of a function or relation intersects the *y*-axis of the coordinate system. Many statistical inference procedures for parsimoniously constructing, linear, oviposition, malaria, forecast, vulnerability, eco-endmember, frequency LULC models may then be able to target, un-geosampled, ento-ecoepidemiological signature variables which could require an intercept to be present. Sometimes one of the eco-endmember, capture point, diagnostic, grid-stratifiable, LULC, signature, frequency regressors may be considered a non-linear function of another explanatorial oviposition regressor, as in polynomial and segmented regression. In statistics, polynomial regression is a form of linear regression in which the relationship between the independent variable x and the dependent variable y is modelled as an *n*th degree polynomial. Segmented regression, also known as piecewise regression or 'broken-stick regression', is a method in regression analysis in which the independent variable is partitioned into intervals and a separate line segment is fit to each interval [2].

Nevertheless, an eco-endmember, sub-meter resolution, grid-stratifiable, geoclassifiable, LULC, ento-epidemiolgical, oviposition, forecast, vulnerability, eco-georeferenceable, malaria, mosquito model for asymptotically, geo-spectrotemporally, remotely targeting unknown hyperproductive foci will remain linear as long as it is linear in the parameter vector β. The geosampled, geo-spectrotemporal, capture point, immature habitat regressors x_{ij} may be viewed either as random variables, which may be simply observed by a malariologist or a medical entomologist, or they may be considered as predetermined fixed values. Both interpretations may be appropriate in various, grid-stratifiable, malaria, mosquito, prognosticative, vulnerability, LULC, signature, wavelength, endmember modelling, case scenarios for optimally aymptotically targeting, seasonal, unknown, eco-georeferenceable, hyperproductive, aquatic, larval, habitat foci which may lead to the same estimation procedures; however different approaches to asymptotic analysis are employable in these two situations. The endmember model outputs may be applicable to robustly quantify the strength of the relationship between y and the x_j, in the signature, endmember, frequency, malaria, mosquito, LULC signature, oviposition, probability model to assess which x_j may have no relationship with y at all. This method may also identify which subsets of the X_j in the regressed forecasted, ento-epidemiological, robustifiable dataset of seasonal, hyperproductive, aquatic, larval habitat, foci contain redundant information about y.

Linear regression models are often fitted employing the least squares approach, but they may also be fitted in other ways, such as by minimizing the "lack of fit" in some other norm (as with least absolute deviations regression), or by minimizing a penalized version of the least squares loss function as in ridge regression (L^2-norm penalty) and lasso (L^1-norm penalty). L1 and L2 penalized estimation methods shrink the estimates of the regression ceffcients towards zero relative to the maximum likelihood estimates [2]. The purpose of this shrinkage in an oviposition, sub-meter resolution, eco-endmember, malaria, mosquito, grid-stratifiable, prognosticative, vulnerability, sub-meter resolution, geo-spectrotemporal, LULC signature, frequency model would be to prevent over fitting arising due to either collinearity of the eco-georefereneced covariates or high-dimensionality. Although both methods are shrinkage methods, the effects of L1 and L2 penalization would be quite different in an endmember, LULC, malaria, mosquito, oviposition, aquatic, larval, habitat model. Applying an L2 penalty would tend to result in small but non-zero, eco-endmember, geo-spectrotemporal, capture point, regression coefficients, whereas applying an L1 penalty may tend to result in many regression LULC coeffcients shrunk exactly to zero and a few other residual variables (e.g., immature seasonal, unknown, hyperproductive, eco-endmember capture point, foci, frequency, density counts) with comparatively little shrinkage. Combining L1 and L2 penalties may render a result in between, with fewer regression coefficients set to zero than in a pure L1 setting, and more shrinkage of the other ento-ecoepidemiological, geosampled, endmember, geo-spectrotemporal, LULC coefficients.

The fused lasso penalty, an extension of the lasso penalty, encourages sparsity of the coefficients and their differences by penalizing the L1-norm for both of them at the same time[4], thus producing sparse and piecewise constant stretches of non-zero endmember, sub-meter resolution, LULC coefficients in a forecast, capture point,ento-ecoepidemiological, malaria, mosquito, vulnerability, aquatic, larval habitat model. A value of zero always means no shrinkage and hence the procedure would be similar to that of a maximum likelihood estimation) [4], whilst a mean value (e.g., aquatic, larval habitat, eco-georeferenced , hyperproductive, density count) would mean infinite shrinkage (i.e., setting all the geosampled malaria mosquito, endmember, LULC regression coefficients to zero).

Least absolute deviations (LAD), also known as least absolute errors (LAE), least absolute value (LAV), least absolute residual (LAR), sum of absolute deviations, or the L_1 norm condition[2], is a statistical optimality criterion and the statistical optimization technique that relies on it. Least squares techniques may parsimonioulsy locate a function such as a simple "trend line" in an endmember, oviposition, empirical,sub-meter resolution,LULC dataset of two-dimensional, malaria, mosquito, aquatic, larval habitat, capture point, geosamped, Cartesian coordinates which may closely approximate a set of (x,y),seasonal, grid-stratifiable, hyperproductive, capture point, foci covariates. Conversely, the least squares approach may be employable to fit a geo-spectrotemporal, oviposition, malaria, mosquito, endmember, forecast, vulnerability, LULC model that is not linear. Thus, although the terms "least squares" and "linear model" are closely linked, they may not be synonymous in prognosticative, malaria, mosquito, oviposition, geo-spectrotemporal, optiizable, eco-endmember, geoclassifiable, LULC, eco-georeferenceable paradigms for tareting seasonal, hyperproductive, unknown foci.

An optimal, least square, oviposition, sub-meter resolution, endmember, LULC, eco-georeferenecable, malaria, mosquito, oviposition, predictive, risk model may reveal un-geosampled geolocations of eco-georeferenceable, seasonal, hypeproductive, aquatic, larval, habitat, capture point foci. Here "optimal" in the least-squares approach may be understood to be a line that minimizes the sum of squared residuals of the geosampled, endmember, eco-geographical, LULC data (e.g Euclidean distance between hyperproductive, aquatic, larval habitats), or geometrical mean, oviposition, non-eco-geographical, endmember, explantive regressors [e.g., solar-induced chlorophyll fluorescence as measured by Photosynthetically Active Radiation (PAR) absorbed by chlorophyll at an intermittently canopied, seasonal, unknown, hyperproductive, malaria, mosquito, eco-georeferenecable foci].

The method of least squares is also a standard approach in regression analysis to the approximate solution of overdetermined systems, (i.e., optimizable, sub-meter, resolution, geo-spectrotemporal, oviposition, LULC datasets of vulnerability, vector arthropod, capture point, prognosticative, non-linear equations in which there are more equations than unknowns). The most important application in quantitative, ento-ecoepidemiological, LULC, endmember, capture point, predictive, regression, endemic, risk modeling for optimizing targeting of seasonal, eco-georeferenceable, hyperproductive, malaria, mosquito, aquatic, larval, habitat foci is in data fitting[1]. An overdetermined system in an endmember, seasonal, capture point, LULC model, endmember simulation may be inconsistent (it has no solution) when constructed with a random empirical dataset of geosampled, hyperproductive, capture point, malarial, mosquito, aquatic, larval habitat, geo-spectrotemporal, orthogonal, regression covariates.

As mentioned, defining the best fit in the least-squares sense for a vulnerability, forecast-oriented, geo-spectrotemporal, capture point, malaria, mosquito, LULC, endemic,aquatic, larval habitat model for targeting unknown, seasonal, hyperproductive, endmember foci may require minimizing the sum of squared residuals (an residual being: the difference between an observed, geosampled, immature count, capture point, measured,regressable value, and the fitted value provided by the aquatic, larval, habitat, oviposition model). Unfortunately, when such models have substantial, inconspicuous, propagational uncertainties (heteroscedasticity) in the independent variables, (the x variables), then simple regression and least-squares, vulnerability, eco-georeferenceable, LULC, endemic forecasts (e.g., endmember, grid-stratifiable, targets of seasonal, geo-spectrotemporal, hyperproductive, unknown, capture point foci) may be misspecified; in such cases, the methodology required for fitting errors-in-variables models may be considered instead of that for least squares.

In statistics, errors-in-variables models or measurement error models are regression models that account for measurement errors in the independent variables. In contrast, standard, forecast, vulnerability, ento-ecoepidemiological, grid-stratifiable, goclassifiable, optimizable, oviposition, malaria, mosquito, endmember,orthogonal, regression models for targeting unknown, seasonal, eco-georeferenceable, hyperproductive, capture point, aquatic, larval, habitat foci will assume that frequency, wavelength, signature, sub-meter resolution, explanatory, LULC,endmember regressors have been measured exactly, or observed without error; as such, those models may account only for errors in the dependent variables. The linear structural model is an example of an errors in response variable model, or measurement error model that have wide practical use in vector arthropod, geostatistical literature.

The classical measurement error assumption maintains that the measurement errors in any of the variables in a signature, frequency, wavelength dataset are independent of all the true variables that are the objects of interest [2]. The

only consequence of the presence of geosampled measurement errors in the dependent variables in an oviposition, forecast, vulnerability, geo-spectrotemporal, malaria, mosquito, capture point, endmember, ento-ecoepidemiological, sub-meter resolution, LULC model is that they would inflate the standard errors of the regressed coefficient estimates. On the other hand, independent errors that are present in an empirical, oviposition, ento-ecoepidemiological dataset of geosampled, eco-georeferenceable, aquatic, larval habitat, capture point, LULC observations of the regressand xi = x ∗ i + ηi may lead to attenuation bias in a simple univariate, regression, vulnerability, endemic, malaria, mosquito, capture point model and to any inconsistent unknown foci, coefficient estimates forecasted. Regression dilution, (or attenuation bias) also known as regression attenuation, is the biasing of the regression slope towards zero (or the underestimation of its absolute value), caused by errors in the independent variable [2].

In the measurement error Cox proportional hazards model, the naive maximum partial likelihood estimator (MPLE) is asymptotically biased [2]. A malariologist, medical entomologist or other experimenter may provide the formula of the asymptotic bias for constructing an additive measurement, error-less, Cox, forecast, vulnerability malaria, mosquito, model when regressively delineating uncertainty-oriented, eco-georeferenecable, geoclassifiable, aquatic, larval habitat, sub-meter resolution, oviposition, LULC model misspecified, grid-stratifiable, unknown, endmember estimators. By adjusting for such error, a malariologist or medical entomologist may derive an adjusted MPLE that is less biased. The bias can be further reduced by adjusting for the estimator second and even third time. An oviposition, sub-meter resolution, LULC, aquatic, larval habitat, endmember, capture point, oviposition estimator my have the advantage of being easy to apply when regressing orthogonal covariates associated to a dependent variable (e.g., geosampled, orthogonally decomposeable, eco-georeferenecable, seasonal, unknown hyperproductive, capture point, foci eigenvectors). The performance of the proposed orthogonal, endmember, LULC, spatial filter, synthetic estimators may be then evaluated through an ento-ecoepidemiological, time series, simulation study.

Proportional hazards models are a class of survival models in statistics. Survival models relate the time that passes before some event occurs to one or more covariates that may be associated with that quantity of time. In a proportional hazards model, the unique effect of a unit increase in a covariate is multiplicative with respect to the hazard rate [2]. There is a relationship between proportional hazards models and Poisson, probability, models which may fit approximate proportional hazards models constructed from eco-georeferenceable, seasonal, malaria, mosquito, oviposition, aquatic, larval habitat, capture point, regressed vulnerability, semi-parameterizable, geo-spectrotemporal, endemic, sub-meter resolution, endmember, LULC, orthogonal estimators.

Two explanatorial regression lines may occur when quantitating the range of linear regression possibilities in a prognosticative, ento-ecoepidemiological, malaria, mosquito, vulnerability, orthogonal, LULC, signature model employed for targeting seasonal, unknown, eco-georeferenceable, hyperproductive, capture point, endmember foci. The shallow slope in an uncoalesced empirical dataset of capture point, oviposition, grid-stratifiable, frequency, wavelength, sub-meter resolution, geosampled LULC, covariates may be then obtainable when the independent variable (or predictor) is on the abscissa (x-axis). The steeper slope is detectable when the independent variable is on the ordinate (y-axis) [3]. By convention, the more, explicative, an ento-ecoepidemiological, eco-georeferenceable, orthogonal, LULC dataset of aquatic, larval habitat, oviposition, endmember, signature, independent variables on the x-axis are, the shallower slope obtainable. Reference lines are averages within arbitary bins along each axis [2]. Note that the steeper regression estimates in an orthogonal, seasonal, forecast, malaria, mosquito, sub-meter resolution, eco-georeferenceable, geo-spectrotemporal, vulnerability, LULC model would be, the more consistent the regression quantitation of the diagnostic, observational, endmember, oviposition, ento-ecoepidemiological,geoclassifiable,optimizable,regressable, orthogonal, residuals (grid-stratifiable,seasonal, eco-georferenecable, unknown, hyperproductive, oviposition-related, foci geolocations) with smaller errors in the y-axis variable rendered.

In the case when some oviposition, eco-georeferenceable, hyperproductive, seasonal, aquatic, larval habitat, grid-stratfiable, non-ecographical, LULC,signature, frequeny, wavelength regressors have been measured with errors, estimation based on the standard assumption could lead to inconsistent, correlation, time series, endmember, coefficient estimates. For example, semi-parameterizable, LULC, geo-spectrotemporal, covariate estimates in a probabilistic, endmember, malaria, mosquito, sub-meter resolution, grid-stratifiable, capture point, oviposition model may not tend to the true, geosampled, larval, density, count values even in very large, ento-ecoepidemiological, regressable, geo-spectrotemporal, parameterizable or semi-paramterizable datasets. In non-linear, time series, dependent, sub-meter

resolution, prognosticative, vulnerability, endmember, eigenfunction, orthogonal, eigenfunction, orthogonal, decomposable, LULC models, the direction of the bias is likely to be very complicated. A malariologist or medical entomologist may consider fitting a straight line when quantitating the relationship of an outcome explanatory, LULC, eco-endmember, aquatic, larval habitat, seasonal, hyperproductive, geosampled variable y (e.g., levels of discontinuous canopy foliar traits geosampled at a capture point) to an eco-georeferenceable, sub-meter resolution, grid-stratifiable,optimizable, regressable, oviposition, parameterizable explanator x (immature density count) for estimating the slope of the line in a geomorphological, malaria, forecast, vulnerability, orthogonal, model output. Statistical variability, measurement error or random noise in the y variable may cause uncertainty in the estimated slope, but not bias: on average, the procedure could calculate the right slope of the model. However LULC, capture point, endmember signature, reflectance variability, geometrical measurement error or random noise in an non-optimizable geosampled, aquatic, larval habitat, explanatorial covariate in the model may cause bias in the estimated slope as well as imprecision in forecasts of seasonal, hyperproductive foci. The greater the variance in the x measurement in the oviposition, prognosticative, ento-ecoepidemiological, endmember, LULC, risk model the closer the estimated slope will approach zero instead of the true value [1].It may seem counter-intuitive that noise in an eco-georeferenecable, geosampled, aquatic, larval, habitat, geo-spectrotemporal, orthogonal or geomteric mean regression oviposition, LULC explanator x induces a bias, but noise in an outcome variable y will not. Linear regression is not symmetric: the line of best fit for predicting y from x (the usual linear regression) is not the same as the line of best fit for regressively optimally quantitating x from an ento-ecoepidemiological, geo-spectrotemporal, LULC dataset of uncoalesced, eco-georeferenceable, geoclassifiable, sub-meter resolution, capture point, orthogonal, grid-stratifiable, malaria, mosquito, signature, eco-endmember covariates.

In certain circumstances propagational uncertainties in an eco-georeferenceable, ento-ecoepidemiological, capture point, forecast, vulnerability, probabilistic, oviposition, geosampled, endmember, LULC paradigm may be corrected, but in order to do so, some knowledge of the nature and size of the both x and y errors must be known in the endmember model output. Typically this is not the case in predictive, orthogonal, oviposition, malaria, mosquito, endmember, LULC, risk mapping. Unfortunately, malariologists and other researchers (medical entomologists, vector ecologists) are often not cognoscente whether an eco-georeferenceable, aquatic, larval habitat, grid-stratifiable, x empirical, seasonal, geosampled, hyperproductive, geoclassified, discontinuous, LULC explanator is a ‘controlled optimizable variable’ with negligible error. Fortunately several techniques have been recently developed to estimate the error in the slope of these ento-ecoepidemiological, aquatic, larval, habitat, vulnerability, eco-endmember, foci models.

A controlled orthogonal, malaria, mosquito, oviposition, eco-georeferenceable, optimally regressable, geosampled, geo-spectrotemporal, capture point, explanatory, LULC variable can usually be attained in a controlled experiment, or when studying a time series of regressable, eco-georeferncable, capture point, seasonal, uncoalesced, sub-meter resolution, grid-stratifiable, hyperproductive,endmember foci provided that the date and time of capture point observations have been recorded and documented in a precise and consistent manner. Unfortunately this is typically not the case especially when multiple, capture point, grid-stratifiable, LULC, geoclassified, oviposition, ento-ecogeographical, endmember, data observations are retrieved from different eco-georeferenecable, seasonal, orthogonally, eigendecomposable reference, endmember, signature datasets.

One way to demonstrate the slope problem in an ento-ecoepidemiological,eco-georeferenecable, grid-stratfiied, oviposition, forecast, vulnerability, malaria, mosquito, sub-meter resolution, endmember, LULC model is to invert the x and y axes and repeat the ordinary least squre (OLS) fit. If the results are valid, irrespective of orientation, the first slope in the - endmember, LULC model output would be the reciprocal of second one. However, this is only the case when there is very small errors in the capture point, endmember variables or when the geosampled, aquatic, larval, habitat data is highly correlated (i.e., grouped closely around a straight line). In the case of one controlled, explicative, diagnostic, orthogonal, LULC, capture point, aquatic, larval habitat, hyperproductive, geosampled, eco-endmember variable and one error-prone, dependent variable in an exploratory, grid-stratifiable, sub-meter resolution, signature, probabilistic paradigm, the inverted result would be incorrect. In the case scenario of two regressable, seasonal, hyperproductive, capture point, aquatic, larval habitat, geomorphological, frequeny, LULC, parameterizable or semi-paramterizable, eco-georeferenceable, foci, estimator datasets containing multiple, geosampled, oviposition–related, observational error-prone, sub-meter reoslution, grid-stratified covariates, both results will be wrong and the correct result will generally lie somewhere in between.

Another way to check the result in an oviposition,orthogonal, tim series, dependent, LULC, ento-ecoepidemiological, sub-meter resolution, grid-stratifiable, endmember, empirical dataset of eco-georeferenceable, malaria, mosquito, capture point, vulnerability, model forecasts (e.g., hyperproductive, seasonal, aquatic, larval habitat geolocations), is by examining the cross-correlation between the residual and the independent variable (i.e., model – y vs x) then repeating it with incrementally larger frequency, explanatorial, discrete, immature, frequency, wavelength, density, count values of the fitted ratio. Depending on the nature of the endmember, signature, capture point, geo-spectrotemporal, orthogonal, LULC, frequency, signature data, it may be obvious that the Ordinary Least Square (OLS) result does not produce the minimum residual between the ordinate and the non-explicative regressor, (i.e. it does not optimally account for co-variability of the two geosampled, aquatic, larval, habitat quantities in the vulnerability model).

In the latter situation, the two regression fits can be taken as bounding the likely true value in the ento-ecoepidemiological, forecast, vulnerability, malaria, mosquito, LULC endmember, geo-spectrotemporal model when optimally targeting seasonal, eco-georeferenceable, hyperproductive, aquatic, larval, habitat foci, but some knowledge of the relative errors is needed to decide where in that range would be the finest estimation of a seasonal, sub-meter resolution, eco-endmember, empirical, LULC, capture point, signature, time series. There are a number of techniques such as bisecting the angle, taking the geometric mean (e.g., square root of the capture point, eco-georeferenceable, hyperproductive, aquatic, larval, habitat, geosampled density, count values), or some other average, but ultimately, they are no more objectives unless driven by some knowledge of the relative errors in such probabilistic, geo-spectrotemporal, endmember, LULC paradigms. Clearly bisection would not be correct if one geosampled, hyperproductive, seasonal, malaria, mosquito, endmember, oviposition, capture point, prognosticative, grid-stratifiable, LULC, explanatory variable has low error, since the true slope would then be close to the OLS fit conducted with that quantity on the x-axis.

Least-square problems fall into two categories: linear OLS and non-linear least squares, depending on whether or not the residuals are linear in all unknown. The linear least-squares problem occurs often in statistical, predictive, regression, endmember, orthogonal, ento-ecoepidemiological, forecast, vulnerability modelling of eco-georeferenceable, remotely sensed, malaria, mosquito, capture point, oviposition, seasonally hyperproductive, aquatic, larval habitat geo-spectrotemporal, geosampled, explicative, LULC variables; it has a closed-form solution. In mathematics, a closed-form expression is a mathematical expression that can be evaluated in a finite number of operations [2]. It may contain constants, and variable functions (e.g., *n*th root, exponent, logarithm, trigonometric functions, and inverse hyperbolic functions), but usually no limit. The nonlinear problem is usually solved by iterative refinement; at each iteration the system is approximated by a linear vulnerability, capture point, endmember, LULC estimator [see 1].

Polynomial least squares can describe the variance in the prediction of a dependent explanatorial, endmember variable such as total, seasonal, aquatic, larval habitat, capture point, LULC density counts as a function of an independent variable and the deviations from the fitted curve within any sub-meter resolution, grid-stratifiable, oviposition, malaria, mosquito, geo-spectrotemporal, vulnerability, regression model for targeting seasonal, un-geosampled, LULC, hypeprproductive, endemic foci. When eco-georeferenceable, capture point, geo-spectrotemporal, eco-endmember, aquatic, larval habitat, geosampled, unmixed, LULC, signature observations (e.g., non-continuous, infrequently canopied, malaria mosquito, capture point, sub-meter resolution, regression covariates) come from an exponential family, mild conditions are satisfiable and least-squares estimates and maximum-likelihood estimates are identical[1].

The method of least squares may also be optimally constructed as a method of moments in any forecast, vulnerability, geo-spectrotemporal, malaria, mosquito, aquatic, larval habitat,eco- endmember, oviposition, capture point, vulnerability, LULC model. In statistics, the method of moments is a method of estimation of population parameters [2].In order to qualitatively regressively quantitate a method of moments in an endmember, probabilistic, sub-meter resolution, grid-stratifiable, geo-spectrotemporal, forecast, vulnerability, ento-ecoepidemiological, eco-georeferenceable, vector arthropod, signture model, a malariologist or medical entomologist may have to start by deriving equations that relate the population moments (i.e., the expected values of powers of the geosampled, random, oviposition-oriented, geoclassified, LULC variable under consideration) to the capture point, signature, geo-spectrotemporal, parameterizable, endmember estimators of interest (e.g. aquatic, larval, habitat denisty count of a seasonal, hyperproductive, aquatic foci). The use of least squares is valid and practical for more general families of

functions [2]. Initially, an endmember, sub-meter resolution, malaria, mosquito, oviposition, aquatic, larval, habitat sample may be drawn and the population moments may be seasonally estimated from the sample. The regression equations may then then solve for the, eco-georeferenceable, capture point, parameterizable, eco-endmember, geoclassifiable, LULC, explanative, foci estimators of interest, employing the sample moments in place of the unknown population moments. In so doing, regression coefficient estimates of those ento-ecoepidemiological, geosampled, capture point, endmember, LULC prognosicators may be optimally orthogonally derivable whch may reveal other unknown, hyperproductive, eco-georeferenceable, malaria, mosquito, aquatic, larval habitat, foci, endemic geolocations. Also, by iteratively applying local quadratic approximation to the likelihood through Fisher information, the least-squares method may be robustly employable to fit a generalized, endemic, linear, oviposition, endmember, geoclassifiable, LULC, sub-meter resolution, malaria, mosquito, grid-stratifiable, forecast, vulnerability, signature model.

A Fisher scoring is a known methods for maximum likelihood computation [3]. A generalization for the method may be employable to determine geolocations of seasonal, geosampled, eco-georeferenecable, capture point, hyperproductive foci of malaria, mosquito, aquatic, larval habitat in a unified manner so that they can be used for maximum likelihood computation, when, for example, there exist constraints on the geosampled prognosticative, frequency, wavelength, signature, endmember, LULC, regression, vulnerability parameters. A generalized method may employ corresponding quadratic functions to validate the ento-ecoepidemiological regression forecasts. The model could proceed by repeatedly approximating the log-likelihood function with the quadratic functions in the geosampled, capture point, endmember neighborhoods (e.g., agro-village African, LULC pastureland foci) of the current iterates and optimize each quadratic function within the parameter space. It may be shown that each quadratic function has a weighted linear regression formulation, which can be conveniently solved in an LULC, sub-meter resolution, grid-stratifiable, malaria, mosquito, oviposition, forecast, vulnerability, aquatic, larval habitat, capture point model. This generalization may also extend the applicability of the Fisher scoring method for targeting eco-georeferenceable, seasonal, hyperproductive, aquatic, larval, habitat malaria, mosquito, capture point, ento-ecoepidmeiological foci when the expected Fisher information matrices may be unavailable in closed form. While the generalized method may suffer from large residual problems and the generalized Fisher scoring method may perform inconsistently in numerical experiments.

According to Jacob et al. [1] letting $\{P\theta\}\theta\in\Theta$ denote a parametric family of distributions in an exploratory, ento-ecoepidemiological, LULC, eco-georeferenceable, forecast, vulnerability, malaria, mosquito, oviposition, capture point, eco-endmember paradigm, in a probability space X, where $\theta \in \Theta \subset R$ (i.e., an uncoalesced dataset of frequency, orthogonal, aquatic, larval habitat, wavelength, sub-meter resolution, signature explanators) can index the distribution while denoting bias introduced by random measurement error. Random measurement error in an exposure variable can bias the estimates of regression slope coefficients towards the null [2]. Random measurement error in an outcome oviposition, eco-endmember, LULC variable will instead increase the standard error of the estimates and widen the corresponding confidence intervals, making results less likely to be statistically significant. Increasing the ento-ecoepidemiological, malaria mosquito, sample size may help minimize the impact of measurement error in an outcome, aquatic, larval habitat, oviposition, explanatory, geo-spectrotemporal, capture point, geosampled, LULC, prognosticative variable.

A malariologist, medical entomologist or other researcher may assume (with no real loss of generality) that each $P\theta$ in an ento-ecoepidemiological, geo-spectrotemporal, LULC, forecast, vulnerability, eco-georeferenceable, time series, malaria, mosquito, endmember, oviposition model has a density given by $p\theta$. Then the Fisher information associated with the model could be the matrix given by $I\theta := E\theta\, h\, \nabla\theta \log p\theta(X) \nabla \log p\theta(X)\, \top i = E\theta[\ \dot{}\ell\theta\ \dot{}\ell\ \top\theta\ ]$, where the score function $\ell\theta = \nabla\theta \log p\theta(x)$ would be the gradient of the log-likelihood at θ (implicitly depending on X) and the expectation $E\theta$ would denote expectation taken with respect to $P\theta$ in the model outcome. Intuitively, the Fisher information will capture the variability of the gradient $\nabla \log p\theta$ in a family of capture point, hyperproductive, aquatic, larval habitat habitat, computated, sub-meter resolution, frequency, wavelength, signature, seasonal distributions for which the score function $\ell\theta$ may have high, geo-spectrotemporal, endmember, geoclassifiable, LULC, irradiance variability. Expecting a non-biased, capture point, endmember, LULC regression estimation from an eco-georeferenecable, geosampled, hyperproductive, aquatic, larval habitat, orthogonal, geo-spectrotemporal, capture point, foci parameter θ would be naïve, however different θ changes in the behavior of $\ell\theta$ may be quantitated though the log-likelihood functional $\theta \rightarrow E\theta 0$ [log $p\theta(X)$]which may vary more in θ in erroneous, endmember, oviposition, capture point, foci frequency, wavelength models with non-robust, LULC signature properties.

For optimally regressively estimatng geosampled, ento-ecoepidemiological, LULC, model functions in an empirical, oviposition datset of eco-georeferenceable, malaria, mosquito,sub-meter resolution, capture point, geo-spectrotemporal, grid-stratifiable, endemic, risk model for optimally prognosticatively targeting, seasonal, hypeproductive, grid-stratifiable, malria, mosquito, aquatic, larval, habitat, endmember foci, a sum of geosampled, immature, count data and an objective function based on squared Euclidean distances (i.e., a least squares function approximation) may be employed. For time series comparisons, it has often been observed that z-score normalized Euclidean distances far outperform the unnormalized variant in ento-ecoepidemiological, forecast, vulnerability, endember, geo-spectrotemporal, vector arthropod, geoclassifiable, sub-meter resolution, optimizable models [5,6]. Hence a seasonal, hypeproductive foci may show that a z-score normalized, squared Euclidean Distance (e.g., measurements between eco-georeferenceable capture points) is, in fact, equal to a distance based on Pearson Correlation. This would have profound impact on many distance-based classification or clustering methods in any aquatic, larval habitat, malaria, mosquito, sub-meter resolution, oviposition, grid-stratifiable, capture point, eco-endmember, LULC model. It may be shown that the often used k-Means algorithm formally needs a modification to keep the interpretation as Pearson correlation strictly valid for defining seasonal, eco-georeferenceable, hyperproductive, malaria, mosquito, LULC, endmember foci. Experimental results may demonstrate that in many cases the standard k Means algorithm generally produces the same results. The summand may be: $(yi-\alpha-\beta xi)^2$ which may be same as in the expression of $P(\alpha,\beta)$ in an LULC, endemic, model output.

In mathematics, computer science and operations research, mathematical optimization or mathematical programming, is the selection of a best element (with regard to some criterion) from some set of available alternatives[4]. In the simplest case, an optimization in a regression equation for geo-spectrotemporally targeting, hyperproductive, oviposition, eco-georefereneceable, malaria, mosquito, aquatic, larval habitat, endemic foci consists of maximizing or minimizing a real function by optimizing, and precisely systematically choosing model input geosampled capture point values from within an allowed set and computing the value of the function. More generally, optimization includes finding "best available" values of some objective function given a defined domain (or input), including a variety of different types of objective functions and different types of domains.

Typically, an empirical oviposition,LULC dataset **A** of ento-ecoepidemiological, vector arthropod, aquatic, larval habitat geosampled, sub-meter resolution, signature, grid-stratifiable, eco-endmember, LULC,oviposition, signature prognosticators will have some subset of the Euclidean space R^n, often specified by a set of constraints, equalities or inequalities that the members of **A** have to satisfy. The domain **A** of f would then be based on the search space or the choice set, while the elements of **A** would be called candidate solutions or feasible solutions in the endmember, forecast, vulnerability, LULC model. The function f is called, an objective function, a loss function or cost function (minimization), a utility function or fitness function (maximization) [4]. A feasible solution that minimizes (or maximizes, if that is the goal) **A** would be the objective function may be an optimal solution (e.g., field-verified, predicted, seasonal, hyperproductive, LULC, endmember foci) derivied from a sub-meter resolution, ovipsoition, malaria mosquito, endmember, probabilistic, signature paradigm). Conventional optimization problems are usually stated in terms of minimization. Generally, unless both the objective function and the feasible region are convex in a minimization problem, there may be several local minima for **A**. A local minimum x* for an oviposition, LULC, sub-meter resolution, grid-stratifiable, endemic, forecast, vulnerability,optimizable, endmember, model defined as a hyperproductive capture point for which there exists some $\delta > 0$ such that for all x all of the function values are greater than or equal to geosampled, endmember value at that point. Local maxima in the ento-ecoepidemiological LULC, malaria, mosquito, aquatic, larval habitat, vulnerability model would be then geo-spectrotemporally defined similarly.

While a local minimum is at least as good as any nearby points, a global minimum is at least as good as every feasible point [7]. A global minimum**,** also known as an absolute minimum**,** is the smallest overall value of a set, function, etc., over its entire range [4]. Global minimum, also known as an absolute minimum, is the smallest overall value of a set, function, etc., over its entire range. It may be impossible to construct an algorithm that will find a global minimum for an arbitrary function. In a convex problem in an ento-ecoepidemiological, LULC, endmember malaria, mosquito model for targeting seasonal, hyperproductive,aquatic, larval habitat foci, if there is a local minimum that is interior (not on the edge of the set of feasible capture points), it may then also be the global minimum in the vulnerability model. However, a nonconvex problem in an endmember, oviposition endemic, geo-spectrotemporal, endmember, LULC, malaria mosquito, forecast, vulnerability model may have more than one local minimum all of which need not be global minima. A large number of algorithms proposed for solving nonconvex problems—including the majority of commercially available solvers—are not capable of making a distinction between locally optimal solutions and globally optimal solutions, and will treat the former as actual solutions to the original problem [4]. Global

optimization is the branch of mathematics and numerical analysis that is concerned with the development of deterministic algorithms that are capable of guaranteeing convergence in finite time to the actual optimal solution of a nonconvex problem[7].

The generator argmin does, as applied to a function, may pick out oviposition, hyperproductive, foci, endmember, geo-spectrotemporal, forecast, vulnerability, grid-stratifiable, LULC, model estimator in the function's domain at which the function takes its minimum value (assuming that the seasonal, eco-georeferenceable,capture point is unique based on geosampled larval density count).Argminw,bmaxα≥0f(w,b,α)arg⁡minw,bmaxα≥0f(w,b,α)[4].In so doing a value of (w,b)(w,b) may minimize maxα≥0f(w,b,α)maxα≥0f(w,b) for optimally targeting eco-georeferenceable, malaria, mosquito, aquatic, larval habitat, geosampled foci. The maxα≥0f(w,b,α)maxα≥0f(w,b,α) may be the maximum value the function achievable in an endmember, sub-meter resolution, LULC, prognosticative model subject to the constraint alpha greater than or equal to 0 but a malariologist or medical entomologist should be clear that this response would depend on the variable vector (w,b)(w,b): given any (w,b),(w,b); it could equal f(w,b,α0)for some (maximizing) α0⩾0α; that is, f(w,b,α0)⩾f(w,b,α)) for all α⩾0α⩾0 whenst targeting prolific habitats. In the paradigm α0 may depend on (w,b).

Hence quantitating argmin α and β, from an uncoalesced, sub-meter resolution, endmember, empirical datatset of geosampled, oviposition, capture point, frequency, aquatic, larval habitat, signature values of the objective function in a malaria mosquito model may optimally define ecogeoreferenceable orthogonal, oviposition, geo-spectrotemporal, LULC geolocations of unknown, prolific, seasonal foci. In such as ecogeographic, linear regression the L∞ norm or, equivalently, the Chebyshev approximation criterion, rather than the usual L2 norm may be optimally employable to minimize the sum of squared, vulnerability, endmember, ento-ecoepidemiological, grid-stratifiable, LULC residuals in an oviposition, signature, forecast, vulnerability model.

The Chebyshev criterion states: Let p(x) be a monic polynomial of degree *n*[4]. Hence the smallest least upper bound for p(x) in the interval [-1,+1] would be 1/2^(n-1 in a malaria, mosquito model for targeting seasonal, hyperproductive, capture point foci. The problem in an oviposition, sub-meter resolution, malaria, mosquito, aquatic, larval habitat, grid-stratifiable, LULC, forecast vulnerability for targeting seasonal, eco-georeferenceable, hyperproductive, aquatic, larval habitats is to minimize the maximum absolute value of the "criterion function" of the error[5]. By imposing a rather natural restriction on the criterion function, the problem may be solved completely; in these prognosticative endmember models where the existence of the uniqueness and the characterization of the best approximation may be optimally clarified and interesting relationships between the best approximations corresponding to different endmember, geospectrotemporal, LULC criterion functions may be quanatitated.

The Chebyshev theorem and the de la Vallée-Poussin theorem (see Appendix 1) remain valid for Chebyshev systems; all methods developed for the approximate construction of algebraic polynomials of best uniform approximation apply equally well as well based on the uniqueness theorem. The de la Vallée-Poussin alternation theorem: If a sequence of points $\{x_i\}$, $i = 0, \ldots, n+1$, in a closed set $Q \in [a, b]$ forms an alternation, then for the best approximation of a function f by multivariate, geo-spectrotemporal, LULC polynomials of the form $P_n(x) = \sum_{k=0}^{n} c_k s_k(x)$, the estimate $E_n(f) = \inf_{c_k} \sup_{x \in Q} \left| f(x) - \sum_{k=0}^{n} c_k s_k(x) \right| \geq \min_{0 \leq i \leq n+1} |f(x_i) - P_n(x_i)|$ is valid, where $\{s_k(x)\}_0^n$ is a Chebyshev system. According to the Chebyshev theorem, equality holds if and only if $P_n(x)$ is the polynomial of best approximation. Analogues ofi this theorem exist for arbitrary Banach spaces [2]. The theorem is employed in numerical methods for constructing polynomials of best approximation. If a function f(x) is parsimoniously, robustly, geo-spectrotemporally continuous on [a,b] and ifA=maxa≤x≤b|f(x)−Pn(x)|,A=maxa≤x≤b|f(x)−Pn(x)|,Pn(x)=∑k=0nakxk,Pn(x)=∑k=0nakxk,then Pn(x)Pn(x) is the polynomial of best uniform approximation for f(x), i.e. maxa≤x≤b|f(x)−Pn(x)|=min{ck}maxa≤x≤b|||f(x)−∑k=0nckxk|||,maxa≤x≤b|f(x)−Pn(x)|=min{ck}maxa≤x≤b|f(x)−∑k=0nckxk|,if and only if there exist n+2n+2 points a≤x0<⋯<xn+1≤ba≤x0<⋯<xn+1≤b in Chebyshev alternation, which means that the conditionf(xi)−Pn(xi)=ϵA(−1)i,i=0,…,n+1,f(xi)−Pn(xi)=ϵA(−1)i,i=0,…,n+1,is satisfied, where ϵ=1ϵ=1 or −1−1. This theorem was proved by P.L. Chebyshev in 1854 in a more general form, namely for the best uniform approximation of functions by rational functions with fixed degrees of the numerator and denominator. Chebyshev's theorem remains valid if instead of algebraic polynomials one considers polynomials Pn(x)=∑k=0nckϕk(x),Pn(x)=∑k=0nckϕk(x),

where {ϕk(x)}nk=0{ϕk(x)}k=0n is a Chebyshev system. The criterion formulated in Chebyshev's theorem leads to methods for the approximate construction of polynomials of best uniform (Chebyshev) approximation. In a somewhat different formulation Chebyshev's theorem can be extended to functions of a complex variable (cf. [2]) and to abstract functions (cf. [3]).

A theorem stating the uniqueness of a mathematical, eco-georeferenceable, geosampled, geo-spectrotemporal, geoclassified, LULC, geospatial object (e.g. seasonal, hyperproductive, malaria mosquito, aquatic, larval habitat,) may mean that there is only one object (capture point foci)fulfilling the given properties, or that all objects of a given class are equivalent (i.e., they can be represented by the same ento-ecoepidemiological forecast model). This may be expressed by stating that the seasonal, geosampled, prolific, aquatic, larval habitat foci is uniquely quantifiable by a certain set of wavelength, sub-meter resolution, capture point, grid-stratifiable, uncoalesced, LULC empirical, oviposition, endmember, frequency covariates. The object of many uniqueness theorems is the solution to a problem or an equation (e.g., prognosticative, geo-spectrotemporal, autocorrelation, frequency, signature, sub-meter resolution, imaged, capture point, LULC, signature, endmember, noise optimizer); in such cases, a uniqueness theorem is normally combined with an existence theorem.

The existence theorem is a theorem stating the existence of an object, (e.g., seasonal, hyperproductive, malaria, mosquito, aquatic, larval habitat, LULC, capture point, foci) which may help generate a solution to a problem or equation. Strictly speaking, it need not tell how many such objects there are, nor give hints on how to find them. Some existence theorems render explicit formulas for solutions [e.g., Cramer's rule (see Appendix 2)], while others describe in their proofs iteration processes for approaching them [e.g., Bolzano-Weierstrass theorem]. Other existence theorems are settled by nonconstructive proofs which simply deduce the necessity of solutions without indicating any method for quantitating them (e.g., the Brouwer fixed point theorem, which is proved by reductio ad absurdum, showing that nonexistence would lead to a contradiction).

Bolzano-Weierstrass theorem states that for $n = 1$, an infinite subset of a closed bounded set S has an accumulation point in S[4]. For example, given a bounded sequence a_n, in an optimizable, regressive, ento-ecoepidemiological, oviposition, eco-georeferenceable, forecast, vulnerability, eco-endmember, malaria, mosquito grid-stratified, signature, LULC model with $-C \leq a_n \leq C$ for all n, it must have a monotonic subsequence a_{n_k}. A time series, optimizable subsequence a_{n_k} must converge as it is monotonic and bounded[2]. Because S would be closed, the oviposition LULC, sub-meter resolution, eco-endmember, model would contain the limit of a_{n_k}. The Bolzano-Weierstrass theorem is closely related to the Heine-Borel theorem and Cantor's intersection theorem, each of which can be easily derived from either of the other two[6].

The Heine-Borel theorem states that a subspace of R^n (with the usual topology) is compact if it is closed and bounded [4]. Given a decreasing sequence of bounded nonempty closed sets $C_1 \supset C_2 \supset C_3 \supset \cdots$ with real numbers (e.g., empirical dataset of endmember, geosampled, eco-georeferenceable, ento-ecoepidemiological, capture point, seasonal, hyperproductive, larval density counts) then Cantor's intersection theorem states that there must exist a optimizable regressable point p in their intersection, $p \in C_n$ for all n.For example, $0 \in \bigcap[0, 1/n]$ may be true in higher dimensions of Euclidean space in an orthnormal, forecast, vulnerability, signature, weighted endmember, LULC, oviposition model. Note that the hypotheses stated above may be crucial for normalization of diagnostic, eco-georeferenecable, geoclassifiable, endmember, sub-meter resolution, geo-spectrotemporal, grid-stratifiable, endemic, oviposition, model output as it could reveal seasonal, eco-georeferenceable, hyperproductive, aquatic, larval habitat, LULC foci. The infinite intersection of open intervals may be empty, for example ,$\bigcap(0, 1/n)$ may be usable to optimally quantitate geolocations of eco-georeferenceable, LULC, seasonal, unknown, hyperproductive, endmember,capture point foci Also, the infinite intersection of unbounded closed sets in the vector arthropod, geospectrotemporal, malaria, mosquito, prognosticative, grid-stratfiiable, risk model may be empty, (e.g., $\bigcap[n, \infty]$).

Alternatively, Brouwer's fixed-point theorem states if g is a continuous function $g(x) \in [a, b]$ for all $x \in [a, b]$, then g has a fixed point in $[a, b]$[2]. This can be proven in an ento-ecoepidemiological, prognosticative, LULC, sub-meter resolution, malaria, mosquito, LULC, oviposition model by supposing

that $g(a) \geq a \quad g(b) \leq b g(a) - a \geq 0 \quad g(b) - b \leq 0.$ Since g is continuous, the intermediate value theorem guarantees that there would exist a $c \in [a, b]$ such that $g(c) - c = 0,$ in the endmember model. Furthermore, there must exist c such that $g(c) = c,$ in the endmember model output (e.g., eco-georeferenceable, residual targets of seasonal, hyperproductive, LULC foci) so there must exist a fixed capture point $\in [a, b]$.If f is continuous on a closed interval $[a, b]$, and c is any orthonormalized, discrete, integer, larval, density, count foci, measured value between $f(a)$ and $f(b)$ inclusive, then there would be at least one eco-georeferenceable, hyperproductive, seasonal, aquatic, habitat, density count value x in the closed interval such that $f(x) = c$.The theorem may be proven by observing that $f([a, b])$ is connected because the capture point, eco-georeferenced, image of a connected set under a continuous function may be connected, when $f([a, b])$ denotes the image of the interval $[a, b]$ under the function f in the frequency, wavelength, signature, ento-ecoepidemiological, geo-spectrotemporal, diagnostic, LULC model output. Since c is between $f(a)$ and $f(b)$, it must have estimators in the capture point, endmember paradigm. While Bolzano's used techniques which were considered especially rigorous for his time, they are regarded as nonrigorous in modern times [see 4].

Optimally regressively quantitating malaria, mosquito, ento-ecoepidemiological, forecast, sub-meter resolution, oviposition, grid-stratifiable, orthogonal, LULC, capture point, seasonal, hyperproductive, aquatic, larval habitat polynomials of best uniform employing the Chebyshev expansion, may explicitly determine the best uniform polynomial approximation employing the space of polynomials for optimally validating an eco-georeferenceable, vulnerability, hyperproductive, vector, arthropod, forecast, endmember, LULC modelling system. In so doing, new theorems about the best approximation of a class of rational functions may be parsimoniously devised for robustly targeting, endmember geo-spectrotemporal, malaria, mosquito, geosampled, seasonal, aquatic, larval habitat, hypeproductive foci. Lack of uniqueness may optimally regressively quantitate the numerical series of best approximations in ento-ecoepidemiological, capture point, endmember geo-spectrotemporal, prognosticated, aquatic, larval habitat, frequency, density count.

A malariologist or medical entomologist may study Chebyshev systems defined on an interval in an ento-ecoepidemiological, geo- eco-georeferenceable, malaria, mosquito, endmember, oviposition, prognosticative, orthogonal, endmember, LULC model whose constituent functions may be either complex or real–valued. As such, an invasive vulnerability analyses may be conducted in SAS applying differential equations for targeting geo-spectrotemporal, seasonal, hyperprproductive, malaria, mosquito, capture point, endmember foci. These derivatives (e.g., geolocations of aquatic, larval habitat, geo-spectrotemporal, endmember, capture point,hyperproductive foci) cannot be solved by a mere rewording of existing proofs, especially those dealing with the existence of an adjoined function. The extension of the interval of definition, and the problem of embedding a set of time series, geosampled, LULC, endmember, capture point, orthogonal, explanatorial functions into an extended complete Chebyshev System may be a laborious task. An important special case of a Chebyshev system is a Markov function system. This system $\{\phi v(x)\}nv=1$ $(n \leq \infty)$ of linearly independent, real-valued, continuous functions may be more easily orthogonally and ento-ecoepidemiologically definable on a finite interval [a,b] in an oviposition, forecast, vulnerability, malaria, vector, arthropod, LULC, eigenfunction, spatial autocorrelation, eigendecomposition, explanatory model whenst targeting eco-georeferenecable, hyperproductive, capture point, foci geolocations [2].

Consider an eco-georefereneceable, oviposition, malaria, mosquito, aquatic, larval habitat, ento-ecoepidemiological, orthogonal, LULC, risk map constructed employing P: R n+1 → C ([a, b]) which may be given as a tuple (a0, a1, a2, . . . an) polynomial anx n + an−1x n−1 + · · · + a0. In so doing, a mapping P: R n+1 → C ([a, b]) may be achievable in order to diagnosis seasonal, hypeproductive, LULC, endemic foci, eco-georeferenceable, eigenfunction eco-geolocations. This endmember, orthogonal, eigenvector, orthogonal, risk mapping would be continuous. This means that if the geosampled, geo-spectrotemporal, LULC coefficients are changed slightly, the eco-georeferenceable, capture point, grid-stratified polynomial will not change much in the uniform normality on [a, b]. Optimally a malariologist or medical entomologist wants to be able to show that he or she can restrict themselves to polynomials with small, robustly regressable, capture point, endmember, LULC, coefficient estimates of a seasonal, hyperproductive, aquatic, larval ,habitat foci[1]. Hence polynomials with large endmember, geo-spectrotemporal coefficients would not be good candidates in approximating, unknown, hyperproductive, endemic, malaria, vector

arthropod, oviposition, capture point, aquatic, larval habitat model endmember, grid-sratifiable, signature, sub-meter resolution, frequency, wavelength, LULC estimators.

More specifically, a malariologist or medical entomologist may want to show that if P has a coefficient of absolute value greater or equal to M in an eco-georeferenceable, time series, oviposition, malaria, mosquito, sub-meter resolution, prognosticative, eco-endmember, LULC, signature, orthogonal, risk model then $\|P\| \geq kM$ for some constant k may be usable for optimally targeting unknown, seasonal, hyperproductive, grid-stratifiable, eco-endmember, aquatic, larval, habitat foci. In particular, this means that if $kM > 2\|f\|$ in the model, then P will provide worse approximations to f than the trivial polynomial which may be identically zero, (e.g., $\|f - P\| \geq \|P\| - \|f\| \geq \|f\| = \|f - 0\|$ in the ento-ecoepidemiological, capture point, LULC, model output. Having shown this claim, existence of the best approximating polynomial would follow from compactness of [−M, M] n+1 in any robust, endmember, sub-meter resolution, prognosticative, ento-ecoepidemiological model for optimally targeting, seasonal, unknown, eco-georeferenceable, hyperproductive, grid-stratifiable, malaria, mosquito, oviposition, LULC, capture point foci.

One of the basic questions in approximation theory concerns the existence of best approximations. Specifically, let K be a subset of a normed linear space xEX in an eco-georeferenceable, LULC, oviposition, grid-stratifiable, orthogonal, capture point, malaria, mosquito, sub-meter resolution, endmember, signature, forecast, vulnerability, geo-spectrotemporal model, for example.The (possibly empty) set of best approximations to x from K may be then defined by PK(x) = {y E K 1 [j x - y II = 4x, K)j,where d(x, K) = inf(li x - y /; / JJ E K]. The set K would be proximinal [e.g., if PK(x) contains at least (resp. exactly)]to at least one, eco-georeferenecable, hyperproductive, LULC, endmember, capture point for every xEX]. The vulnerability, endmember, oviposition, aquatic, larval habitat, forecast, vulnerability LULC mapping PK (x) + 2K could then be quantitated as a metric projection onto K. In this terminology, the basic existence question may be phrased as: Which subsets of seasonal, geoclassified, malaria, mosquito, eco-endmember, aquatic, larval habitat, capture point, hyperproductive, LULC foci are proximinal to an eco-georeferenceable, village, grid-stratified, centroid? There is much that is unknown concerning existence of best approximations in ento-epidemiological, remote sensing, malaria, vector arthropod, vulnerability, endmember, LULC models which may be resolvable employing Pearsons, correlation coefficient (PCC)

In statistics, the PCC,) also referred to as the Pearson's r, Pearson product-moment correlation coefficient (PPMCC) or bivariate correlation, is a measure of the linear correlation between two variables X and Y [2]. In an ento-ecoepidemiological, forecast, vulnerability, malaria, mosquito, oviposition, capture point, endmember, LULC, regression, signature model, the PCC will have a value between +1 and −1, when 1 is total positive linear correlation, 0 is no linear correlation, and −1 is total negative linear correlation[1]. Hence, Pearson's correlation coefficients rendered from such a seasonal, oviposition, forecast, vulnerability, endmember model may be precisely tabulated in probability space employing the covariance of two, geosampled, time series, capture point, frequency, wavelength, LULC, endmember explanators divided by the product of their standard deviations. Defining the form of the approximate regressively, quantitable, orthogonal inferences (e.g., targets of geosampled, seasonal, hyperproductive, geo-spectrotemporal, capture point, endmember foci) would involve optimally determining a "product moment", that is, the mean (the first moment about the origin) of the product of the mean-adjusted, oviposition-related, capture point, geosampled, LULC, random variables. Hence the modifier product-moment should be theorectically optimally quantifiable in a robust, endmember, sub-meter resolution, frequency, capture point, signature, wavelength, malaria, mosquito, oviposition, eco-epidemiological, forecast, vulnerability, grid-stratifiable, LULC model for targeting seasonal, hyperproductive, aquatic, larval habitats. A value of 1 would imply that a linear equation describes the relationship between X and Y perfectly, with all geosampled, oviposition, capture points lying on a regression line for which Y increases as X increase. A value of −1 would imply that all the capture points lie on a line for which Y decreases as X increases. A value of 0 in the aquatic, larval, habitat, endemic model would imply that there is no linear correlation between the time series, geosampled, LULC variables. Factor-based, endmember, oviposition, malaria, mosquito models have been used extensively in the domain of collaborative filtering for eco-entomological, time series, forecast, vulnerability, capture point, modelling user preferences[1].

In eco-georeferenceable, endmember, malaria, mosquito, forecast vulnerability, oviposition, remotely sensed, regression, modeling, where sub-meter resolution, habitat signatures are the dependent variable, LULC factor variables may be assumed to be marginally independent whilst rating variables may be assumed to be conditionally independent.

The main drawback of such prognosticative, malaria, aquatic larval habitat, oviposition, orthogonal, endmember models is that inferring the posterior distribution over the factors given the ratings would reveal intractablity. Hence, many of the existing malaria, mosquito, capture point, predictive, endmember, LULC, risk modeling methods in literature resort to performing MAP estimation of eco-georeferenceable, oviposition, time series, geo-spectrotemporal, geosampled, capture point, aquatic, larval habitats and their, parameterizable estimators for optimally quantitating geolocations of seasonal foci and their covariates. Training such models amounts to maximizing the log-posterior over model parameters which may be conducted inefficiently due to large, non-parameterizable, diagnostic, clinical, field-operational and remotely time series, geosampled, aquatic larval, habitat, endmember, grid-stratified, eigenvector estimator, LULC datasets[1].

In statistics, an expectation–maximization (EM) algorithm is an iterative method to find maximum likelihood or MAP estimates of parameters in statistical models, where the model depends on unobserved latent variables [2]. The EM iteration alternates between performing an expectation (E) step, which creates a function for the expectation of the log-likelihood evaluated employing the current estimate for the parameters [2], and maximization (M) step, which may compute eco-georeferenceable, geo-specified, malaria, mosquito, geo-spectrotemporal, non-parameterizable, oviposition, endmember, LULC, orthogonal, eigenvector estimators maximizing the expected log-likelihood found on the E step. These parameter estimates may be employable to determine the distribution of the latent, eco-georeferenecable, eigendecomposed, geo-spectrotemporal, hyperproductive, aquatic, larval, habitat, capture point, seasonal, immature, geosampled endmember, grid-stratifiable, LULC, optimizable variables in the next E step.

Suppose a malariologist or medical entomologist has an estimation problem in which he or she has a training set {x (1), . . . , x(m)} consisting of *n* independent examples derived from an empricial, geo-spectrotemporal, optimizable, geoclassifiable, geosampled, eco-georeferenced, empirical, ento-ecoepidemiological dataset of aquatic, larval habitat, hyperproductive, capture point foci. If a malariologist or medical entomologist wishes to fit the LULC parameters of such a model p(x, z) to the empirical, seasonal, geosampled, malaria mosquito, signature data, the likelihood may be given by ℓ(θ) = Xm i=1 log p(x; θ) = Xm i=1 logX z p(x, z; θ) But, explicitly finding the maximum likelihood estimates of the geosampled oviposition, capture point, endmember parameters θ may be difficult. Here, the z (i) 's would be the latent random variables. In such a setting, the EM algorithm would render an efficient method for maximum likelihood estimation.

Maximizing ℓ(θ) explicitly might be difficult to do in an ento-ecoepidemiological, malaria, mosquito, LULC, risk model, thus the strategy may be shifted to instead repeatedly constructing a lower-bound on ℓ (E-step), and then optimizing thr lower-bound (M-step). Hence for each i, in the mosquito model let Qi be some distribution over the z's (P z Qi(z) = 1, Qi(z) ≥ 0). A malariologist or medical entomologist may then optimally target a seasonal, eco-georeferenecable, hyerproductive,capture point foci employing the following:1 X i log p(x (i) ; θ) = X i logX z (i) p(x (i) , z(i) ; θ) (1) = X i logX z (i) Qi(z (i)) p(x (i) , z(i) ; θ) Qi(z (i)) (2) ≥ X i X z (i) Qi(z (i)) log p(x (i) , z(i) ; θ) Qi(z (i)). The last step of this derivation would employ Jensen's inequality. Specifically, f(x) = log x would be a concave function, since f ″(x) = −1/x2 < 0 over its domain x ∈ R +. Also, the term X z (i) Qi(z (i)) p(x (i) , z(i) ; θ) Qi(z (i)) in the summation would just be an expectation of the quantity p(x (i) , z(i) ; θ)/Qi(z (i)) with respect to z (i) drawn according to the capture point, malaria, mosquito, aquatic, larval habitat, normalized, LULC, endmember distribution given by Qi. By Jensen's inequality, the ento-ecoepidemiological, oviposition, signature, forecast, vulnerability LULC model would have f Ez (i)∼Qi p(x (i) , z(i) ; θ) Qi(z (i)) ≥ Ez (i)∼Qi f p(x (i) , z(i) ; θ) Qi(z (i)) . Notice the "z (i) ∼ Qi" subscripts above indicate that the expectations are with respect to z (i) drawn from Qi. This would allow a malariologist or medical entomologist to go from iteratable interpolative equations efficiently for optimally determining statistically significant (e.g., 95% confidence interval) regressed endmember, geoclassified, LULC covariates which may be geo-spectrotemporally associated to a, eco-georeferenced, sub-meter resolution, grid-stratified, capture point, seasonal, hyperproductive foci.

Now, for determining eco-georeferenecable, optimizable, regression, LULC geoclassified, geolocations of seasonal, hypeproductive, capture point foci, from any set of distributions Qi, rendered from an orthogonal, malaria, mosquito model a lower-bound on ℓ(θ) must be provided. Unfortunately many possible choices for the Qis exist for these models. Which should a malariologist or medical entomologist choose? Well, if we have some current guess θ of an aquatic, larval habitat, ento-eco-epidemiological, geoclassified, LULC, sub-meter resolution, grid-stratifiable,

parameters, it seems natural to try to make the lower-bound tight at that endmember, geo-spectrotemporal, geosampled foci of θ. Hence a malariologist or medical entomologist could make the inequality above hold with equality at a particular seasonal, hyperproductive, larval density, value of θ. In so doing, ℓ(θ) may be proven to increase monotonically with successsive iterations of EM in an eco-georeferenceable, eto-ecoepidemiological, oviposition, predictive, risk-related, malaria, capture point, aquatic, larval habitat, grid-stratifiable, endmember, regression model. To make the bound tight for a particular geo-spectrotemporal, geosampled, prolific, eco-georeferenceable, geoclassified LULC, capture point value of θ, the reseachists may need to highlight the step involving Jensen's inequality since such a derivation could hold with equality. For this to be true in any seasonal, eco-georeferenecable, malaria, mosquito, oviposition, regression, LULC model output, however, it may require that the expectation be taken over a "non-constant"-valued, ento-ecoepidemiological, seasonal, geosampled, aquatic, larval habitat, capture point, explanatory, random variable [i.e., p(x (i) , z(i) ; θ) Qi(z (i)) = c for some constant c that does not depend on z (i)]. This is easily accomplished by choosing Qi(z (i)) ∝ p(x (i) , z(i) ; θ). Actually, if a malariologist or medical entomologist knows Pz Qi(z (i)) = 1 (as it is a normalized distribution), this further would allow the researchists to optimally quantiate Qi(z (i)) = p(x (i) , z(i) ; θ) P z p(x (i) , z; θ) = p(x (i) , z(i) ; θ) p(x (i) ; θ) = p(z (i) |x (i) ; θ).In so doing, seasonal, ecogeoreferenecable, hyperproductive, aquatic, larval, habitat foci may be identified, on geoclassifiable, sub-mter resolution, grid-stratifiable, LULCs. Thereafter, by simplying setting the Qi 's to be the posterior distribution of the z (i) x (i) and setting the geosampled, geo-spectrotemporal, capture point, geoclassified, grid-stratifiable, LULC signature, aquatic, larval habitat, orthogonal, endmember parameters θ seasonal, hyperproductive, foci in an sub-meter resolution, capture point, grid-stratfied image may be optimally targeted.

Now, for this choice of the Qi's,the oviposition, endmember,geo-spectrotemporal, LULC model should render a lower-bound on the loglikelihood ℓ that which the regression is trying to maximize. This is the E-step. In the M-step of the unmixing algorithm, the malaria researchers could maximize the formula with respect to the geosampled, capture point, aquatic, larval habitat, geo-spectrotemporal, endmember LULC parameters to obtain a new setting of the θ's in the orthogonal, oviposition, signature model. Repeatedly carrying out these two steps would allow the EM algorithm, to devise geolocations of eco-georeferenceable, malaria, mosquito, seasonal, hypeproductive foci based on geosampled capture point, seasonal, immature, discrete, geosampled, density, count values. This process may be repeated until convergence (E-step) For each i, set Qi(z (i)) := p(z (i) |x (i) ; θ). (M-step) would be able to define capture point, LULC covariates related to the prolific, aquatic larval habitats. By setting θ := arg max θ X i X z (i) Qi(z (i)) log p(x (i) , z(i) ; θ) Qi(z (i)), the seasonal, grid-stratifiable, hyperproductive, oviposition, eco-georeferenceable, aquatic, larval habitats could be mathematically described.

Interestingly EM could cause the likelihood to converge monotonically. In such a description of the EM algorithm, an oviposition, malaria, forecast, vulnerability, endmember, LULC, sub-meter, resolution model would run until convergence. Given the result that we just showed, one reasonable convergence test would be to check if the increase in ℓ(θ) in the data is between successive iterations. In so doing, some endmember variables smaller than some tolerance parameters may be able to declare convergence if EM is improving ℓ(θ) too slowly. Hence if a malariologist or medical entomologist defines J(Q, θ) = X i X z (i) Qi(z (i)) log p(x (i) , z(i) ; θ) Qi(z (i)) whenst conducting a malaria mosquito, risk mapping application , then it may be known that ℓ(θ) ≥ J(Q, θ) is derivable from the model diagnostic output. The EM can also be viewed a coordinate ascent on J, in which the E-step maximizes it with respect to Q whenst the M-step maximizes it with respect to θ.

This research presents a general approach to iterative computation of maximum-likelihood estimates whenst regressable, geosampled, geoclassified, grid-stratified, endmember, oviposition, sub-meter resolution, malaria, mosquito, (*An. arabiensis*), aquatic, larval habitat, hyperproductive, capture point, sub-meter resolution, LULC observations are viewed as incomplete data. Since eachiteration of the algorithm consists of an expectation step followed by a maximization step it is called the EM algorithm [2]. The EM process is remarkable in part because of the simplicity and generality of the associated theory, and in part because of the wide range of examples which fall under its umbrella[3]. When the underlying complete endmember, capture point, malaria, mosquito, oviposition parameterizable estimator data comes from an exponential family whose maximum-likelihood estimates are easily computed, then each maximization step of an EM algorithm is likewise easily computable. The term "incomplete data" in its general form implies the existence of two sample spaces in the model [3]. The EM algorithm may be usable to geolocate maximum likelihood, endmember LULC, parameters within an eco-georeferenceable, geoclassified, oviposition, malaria, mosquito, sub-meter resolution, signature, probabilistic paradigm especially in cases where the

equations cannot be solved directly [1]. Typically these models would incorporate latent geo-spectrotemporality and latent frequency, geosampled, capture point, endmember, oviposition, regressable LULC explanators in addition to unknown, malaria, mosquito, seasonal, hyperproductive, foci estimators. The EM algorithm is used to find (locally) maximum likelihood parameters of a statistical model [2]. The presumption would be either missing endmember LULC values exist amongst the geosampled malarial, ento-ecoepidemiological, empiricial, capture point, sub-meter resolution, endmember data, or that the eco-georeferenceable model can be formulated more simply by assuming the existence of further unobservable, oviposition, grid-stratifiable, endmember datasets of geosampled, geo-spectrotemporal, seasonal, aquatic, larval habitats. For example, a mixture model may be describable more simply by assuming that each observed, malaria, mosquito, aquatic, larval, habitat, endmember foci has a corresponding unobserved data measurable point, or latent extraneous variable, specifying the mixture component to which each capture point, geoclassified, LULC foci belongs. Thereafter, computing a liklihood solution would require optimally regressively quantitating the derivatives of the likelihood function with respect to all the unknown, orthogonal, capture point, endmember signature, LULC, habitat values, the parameters and the latent variables. In so doing, the capture point, forecast, vulnerability model, endmember output may simultaneously solve the resulting equations for optimally rendering robust realizations of eco-georeferenceable, geolocations of capture point, seasonal, hyperproductive, aquatic, larval, habitat foci.The result would be an interlocking solution which may require the geosampled, LULC endmember parameter estimator, geo-spectrotemporal, values to be regressively displayed in eco-geographic space. Unfortunately substituting any misspecified, endmember, LULC, signature prognosticators may render an unsolvable equation.

In the moment-related literature, there is an endless discussion and a number of comparative experiments about what type of moments that provides the maximum separability of geospatial, geo-spectrotemporal, grid-stratifiable, geoclassifiable, non-heuristic, LULC objects for maximum robustness which optimally requires minimum computational time. Individual experiments in vector, malaria, eco-entomology, forecast, vulnerability, aquatic, larval habitat, orthogonal, endmember LULC, mapping have exhibited significant results employing product moments optimally geolocating eco-georeferenceable, hyperproductive, capture point foci[1]. For practical, endemic oviposition, ento-ecoepidemiological, capture point, predictive, risk modeling, endmember, seasonal hyperproductive foci applications, moments may be computed employing sub-meter resolution, grid-stratifiable eco-georeferenceable, LULC images where the focus scan may be on orthogonal grid-stratfiable, sub-meter resolution polynomials. In mathematics, an orthogonal polynomial sequence is a family of polynomials such that any two different polynomials in the sequence are orthogonal to each other under some inner product [2].

In linear algebra, an inner product space is a vector space with an additional structure called an inner product [2]. This additional structure may associate each pair of ecogeoreferenceable, vector, aquatic, larval habitat, geo-spectrotemporal, malaria mosquito, sub-meter resolution, grid-stratifiable, LULC covariates regressively derived from an oviposition, mosquito, malaria, empiricial, optimally geosampled parameter estimator, geo-spectrotemporal, endmember dataset in eco-geographic space with a scalar quantity known as the inner product of the vectors. Inner products may allow the rigorous introduction of intuitive geometrical notions such as the length of a vector or the angle between two vectors in a time series, forecast vulnerability, endmember, malaria, mosquito model. The means of defining orthogonality between vectors (i.e, zero inner product) in eco-geographic space of eco-georeferenceable, geo-spectrotemporal, malaria, capture point, aquatic larval habitat, empricial datasets may hence robustly geolocate seasonal, endemic, hyperproductive, capture point, eco-entomological, foci.

Inner product spaces also generalize Euclidean spaces (in which the inner product is the dot product, also known as the scalar product) to vector spaces of any (possibly infinite) dimension [2].Quantized Euclidean distances from an eco-georeferenecable, capture point, hyperproductive, grid-stratified, orthogonal, high, malaria prevalence, African, riceland, agro-irrigated, village foci, or urban environment complex ecosystem, for example, may reveal seasonal, endemic, malaria transmission based on aquatic, larval, habitat geolocations and their specific, ento-ecoepidemiological,eco-geographical, attributes (e.g., seasonal, geosampled, larval density, count values). An inner product may induce associated norm, thus an inner product space in an eco-georeferenecd, vector, ento-ecoepidemiological, forecast, vulnerability, sub-meter resolution, grid-stratifiable, geoclassifed, LULC, geo-spectrotemporal, eco-georeferenceable, signature model could also be a normed vector space. In mathematics, a normed vector space is a vector space on which a norm is defined. In a vector space with 1- 2- or 3-dimensional vectors with real-valued entries, the idea of the "length" of a vector is intuitive [2].

Let V be a vector space over K in an eco-georeferenceable, geoclassifiable, robust, oviposition ento-ecoepidemiological, endmember, forecast, vulnerability, malaria, mosquito aquatic, larval, habitat, orthogonal, LULC map targeting seasonal, geosampled, eco-georeferenceable, hypeproductive foci. A norm in V in the seasonal map $x \rightarrow \|x\|$ from V to the set of non-negative, endmember, sub-meter resolution, grid-stratfiable, capture point, geosampled discrete integer,immature count, values would be quantifiable such that 1). $\|x\| = 0$ if and only if x = 0.2). $\|\alpha x\| = |\alpha|\|x\|$ for all $\alpha \in K$, $x \in V$ .3. $\|x + y\| \leq \|x\| + \|y\|$ for all x, y ∈ V. A normed vector space is a real or complex vector space in which a norm has been defined [2]. Formally, a normed vector space is a pair $(V, \|\cdot\|)$ where V is a vector space over K and $\|\cdot\|$ is a norm in V. This methodology usually refers to V as being the normed space. Unfortunately in an vulnerability, forecastable, oviposition, malaria, mosquito, prognosticative, geoclassifiable, LULC endmember, paradigm, a malariologist or medical entomologist has to consider more than one norm at the same time; then one u sub-indices on the norm symbol: $\|x\|1$, for example. When dealing with several normed spaces it is customary to refer to the norm of a space denoted byV by the symbol $\|\cdot\|V$[6]. Other symbols for norms include $|\cdot|$ and $\||\cdot|\|$.A complete space with an inner product is called a Hilbert space [2].

The mathematical concept of a Hilbert space, generalizes the notion of Euclidean space. It may extend the methods of vector algebra and calculus from the 2-D Euclidean plane and 3-D space to spaces with any finite LULC, malaria, mosquito, capture pont quantifiable number of dimensions. A Hilbert space is an abstract vector space possessing the structure of an inner product that allows length and angle to be measured [2]. Further, Hilbert spaces are complete: there are enough limits in the space to allow the techniques of calculus to be employed for optimally remotely targeting, eco-georeferenecable, seasonal, hyperproductive, capture point, sub-meter resolution, grid-stratifiable, oviposition, malaria, mosquito, immature habitats. Hilbert spaces are indispensable tools in the theories of partial differential equations, quantum mechanics, Fourier analysis (which includes applications to signal processing and heat transfer)—and ergodic theory, which forms the mathematical underpinning of thermodynamics. Apart from the classical Euclidean spaces, examples of Hilbert spaces include spaces of square-integrable functions, spaces of sequences, Sobolev spaces consisting of generalized functions, and Hardy spaces of holomorphic functions which may be important for optimally identifying eco-georeferenceable, seasonal, hyperproductive, malaria, mosquito, capture point endmember foci on sub-meter resolution, grid-stratifiable, LULC, geoclassified data.

Hilbert space is a vector space $H$with an inner product $\langle f, g\rangle$such that the norm defined by $|f| = \sqrt{\langle f, f\rangle}$ turns Hinto a complete metric space[2]. If the metric defined by the norm is not complete, then $H$is instead known as an inner product space. In linear algebra, an inner product space is a vector space with an additional structure called an inner product[3]. This additional structure may associate each pair of malaria, mosquito, aquatic, larval habitat, oviposition, LULC, sub-meter resolution, time series, grid-stratifiable, endmember vectors in the space with a scalar quantity known as the inner product of the vectors. Inner products allow the rigorous introduction of intuitive geometrical notions such as the length of a vector or the angle between two vectors [3]. They may provide the means of defining orthogonality between vectors (zero inner product).

Inner product, malaria, mosquito, aquatic larval habitat spaces generalize Euclidean spaces (in which the inner product is the dot product, also known as the scalar product) to vector spaces of any (possibly infinite) dimension. The dot produc may be definable for endmember, capture point, LULC, optimizable, vectors $\mathbf{X}$ and $\mathbf{Y}$ by$\mathbf{X}\cdot\mathbf{Y} = |\mathbf{X}|\,|\mathbf{Y}|\cos\theta$,where θ may be a quantifiable, geomterical, geolcassifiable, optimal angle between the vectors and $|\mathbf{X}|$ is the norm. It may then follow that $\mathbf{X}\cdot\mathbf{Y} = 0$ if $\mathbf{X}$ is perpendicular to $\mathbf{Y}$. The dot product therefore has th interpretation as the length of the projection of $\mathbf{X}$ onto the unit vector $\hat{\mathbf{Y}}$ when the two vectors are placed so that their tails coincide[3].

Examples of finite-dimensional Hilbert spaces may quantitate an empirical geosample datatset of sub-mter resolution wavenegth, malaria, mosquito, capture point, aquatic, larval habitats. The LULC, count larval denisties $\mathbb{R}^n$with $\langle v, u\rangle$the vector dot product of $v$and u. Then identy hyperproductive foci. The complex numbers $\mathbb{C}^n$with $\langle v, u\rangle$the vector dot product of $v$and the complex conjugate of u. An example of an infinite-dimensional Hilbert space is

L^2, the set of all functions $f : \mathbb{R} \to \mathbb{R}$such that the integral of f^2over the whole real line is finite[4]. The inner product is $\langle f, g \rangle = \int_{-\infty}^{\infty} f(x)\, g(x)\, dx$.

A Hilbert space is always a Banach space, but the converse need not hold in a malaria, mosquito, capture point, forecast, endmember LULC model.Banach space is a complete vector space $B$with a norm $\|\cdot\|$. Two norms $\|\cdot\|_{(1)}$and $\|\cdot\|_{(2)}$are called equivalent if they give the same topology, which is equivalent to the existence of constants $c$and Csuch that $\|v\|_{(1)} \le c\,\|v\|_{(2)}$and $\|v\|_{(2)} \le C\,\|v\|_{(1)}$hold for all v.[4]. In the finite-dimensional case, all norms are equivalent [3]. An infinite-dimensional space may have many different norms in an ovispoition, endmember, orthogonal, LULC, geo-spectrotemporal, prognosticative, grid-stratifiable, sub-meter,resolution, hyperproductive, foci model. A basic example is n-dimensional Euclidean space with the Euclidean norm. Usually, the notion of Banach space is only used in the infinite dimensional setting, typically as a vector space of functions. For example, the set of continuous functions on closed interval of the real line with the norm of a function $f$given by $\|f\| = \sup_{x \in \mathbb{R}} |f(x)|$ is a Banach space, where $\sup$denotes the supremum. On the other hand, the set of continuous functions on the unit interval $[0, 1]$with the norm of a function $f$may be given by $\|f\| = \int_0^1 |f(x)|\, dx$ which may not be a Banach space in the LULC model because it may not be complete. For instance, the Cauchy sequence of functions

$$f_n = \begin{cases} 1 & \text{for } x \le \frac{1}{2} \\ \frac{1}{2}n + 1 - nx & \text{for } \frac{1}{2} < x \le \frac{1}{2} + \frac{1}{n} \\ 0 & \text{for } x > \frac{1}{2} + \frac{1}{n} \end{cases}$$

may not converge to a continuous function when predictively, optimally targeting, eco-georeferenceable, LULC, hyperrpoductive, seasonal, malaria, mosquito foci.

Hilbert spaces with their norm given by the inner product may be examples of Banach spaces in an ento-ecoepidemiological, ovispsoition, sub-meter resolution, endemic, grid-stratifiable, LULC endmember model for targeting seasonal, hyperproductive, aquatic, larval habitat foci. While a Hilbert space is always a Banach space, the converse need not hold [see 4]. Therefore, it is possible for a Banach space in a forecast vulnerability ento-ecoepidemiological model not to have a norm given by an inner product. For example, the supremum norm cannot be given by an inner product in the model. An inner product is a generalization of the dot product[4]. A vector space, it is a way to multiply vectors together, with the result of this multiplication being a scalar[6]. More precisely, for a real vector space, an inner product $\langle \cdot, \cdot \rangle$satisfies the following four properties. Let u, v, and $w$be vectors and αbe a scalar, then: 1. $\langle u + v, w \rangle = \langle u, w \rangle + \langle v, w \rangle$. 2. $\langle \alpha v, w \rangle = \alpha \langle v, w \rangle$. 3. $\langle v, w \rangle = \langle w, v \rangle$. 4. $\langle v, v \rangle \ge 0$and equal if and only if $v = 0$[4].

The fourth condition in the list above is known as the positive-definite condition. Related thereto, note that some authors define an inner product to be a function $\langle \cdot, \cdot \rangle$satisfying only the first three of the above conditions with the added (weaker) condition of being (weakly) non-degenerate (i.e., if $\langle v, w \rangle = 0$for all w, then $v \equiv 0$). In such literature, functions satisfying all four such conditions are typically referred to as positive-definite inner products [4],though inner products which fail to be positive-definite are sometimes called indefinite to avoid confusion. This difference, though subtle, may introduce a number of noteworthy phenomena in an endmember, malaria, mosquito, aquatic, larval habitat, endmember LULC, sub-meter resolution, geo-spectrotemproal, prognosticative, capture point, models For example, inner products which fail to be positive-definite in such models may give rise to "norms" which yield an imaginary magnitude for certain vectors (such vectors are called spacelike) and which induce "metrics" which fail to be actual metrics for optimally targeting, seasonal, eco-georeferenecable, LULC, seasonal, hyperproductive, endmember foci.

The Lorentzian inner product is an example of an indefinite inner product which may be employable in a malaria, mosquito, oviposition, aquatic, larval habitat, endmember LULC, grid-stratifiable forecast, vulnerability model. A vector space together with an inner product on it is called an inner product space[3]. This definition may apply to an abstract vector space over any field in the model when targeting seasonal, hyperproductive, endmember foci. Examples of inner product spaces in the model may include $\mathbb{R}$, where the inner product may be given by $\langle x, y \rangle = x\, y$. The Euclidean space $\mathbb{R}^n$, where the inner product is given by the dot product $\langle (x_1, x_2, \ldots, x_n), (y_1, y_2, \ldots, y_n) \rangle = x_1\, y_1 + x_2\, y_2 + \cdots x_n\, y_n$ [3], in the endmember, LULC model vector space may reveal real functions whose domain is an closed interval $[a, b]$with inner product $\langle f, g \rangle = \int_a^b f\, g\, d\, x.$ for targeting seasonal, hyperrpoductive foci. When given a complex vector space, the third property may be replaced by $\langle v, w \rangle = \overline{\langle w, v \rangle}$,where $\bar{z}$refers to complex conjugation[6]. The inner product is called a Hermitian inner product and a complex vector space with a Hermitian inner product is called a Hermitian inner product space[2].

Every inner product space is a metric space. The metric is given by $g\,(v, w) = \langle v - w, v - w \rangle$.If this process results in a complete metric space in a sub-meter resolution, endmember, LULC, geo-spectrotemporal, endemic, forecast, vulnerability, grid-stratfiiable model, it may be a Hilbert space. What's more, every inner product in the ento-ecoepidemiological model output may naturally induce a norm of the form $|\mathbf{x}| = \sqrt{\langle \mathbf{x}, \mathbf{x} \rangle}$,whereby it follows that every inner product space is also a normed space. As noted above, inner products in the malaria model which fail to be positive-definite yield "metrics" - and hence, "norms" - which are actually something different due to the possibility of failing their respective positivity conditions. For example, n-dimensional Lorentzian Space (i.e., the inner product space consisting of $\mathbb{R}^n$with the Lorentzian inner product) may come equipped with a metric tensor of the form $(d\, s)^2 = -d\, x_0^2 + d\, x_1^2 + \cdots + d\, x_{n-1}^2$and a squared norm of the form $|\mathbf{v}|^2 = -v_0^2 + v_1^2 + \cdots + v_{n-1}^2$for all vectors $\mathbf{v} = (v_0, v_1, \ldots, v_{n-1})$.which may be usable for forecasting seasonal, hypeproductive, malaria, mosquito, aquatic, larval habitat, capture point foci In particular, a malarilogist or medial entomologist may have negative Euclidean distances and squared norms, as well as nonzero vectors whose vector norm is always zero in the model. As such, the metric (respectively, the norm) may actually be a habitat metric.

In mathematics, a Sobolev space is a vector space of functions equipped with a norm that is a combination of Lp-norms of the function itself and its derivatives up to a given order. The derivatives are understood in a suitable weak sense to make the space complete, thus a Banach space. Intuitively, a Sobolev space is a space of functions with sufficiently many derivatives for some application domain, such as partial differential equations, and equipped with a norm that measures both the size and regularity of a function. For $d \geq 1$, Ωan open subset of $\mathbb{R}^d$, $p \in [1; +\infty]$and $s \in \mathbb{N}$, the Sobolev space $W^{s,p}\left(\mathbb{R}^d\right)$is defined by $W^{s,p}(\Omega) = \{f \in L^p(\Omega) : \forall\, |\alpha| \leq s, \partial_x^\alpha f \in L^p(\Omega)\}$,where $\alpha = (\alpha_1, \ldots, \alpha_d)$, $|\alpha| = \alpha_1 + \ldots + \alpha_d$, and the derivatives $\partial_x^\alpha f = \partial_{x_1}^{\alpha_1} \cdots \partial_{x_d}^{\alpha_d} f$ are taken in a weak sense [4]. When endowed with the norm $\|f\|_{s,p,\Omega} = \sum_{|\alpha| \leq s} \|\partial_x^\alpha f\|_{L^p(\Omega)}$, $W^{s,p}(\Omega)$is a Banach space[7]. In the special case $p = 2$, $W^{s,2}(\Omega)$is denoted by $H^s(\Omega)$. This space is a Hilbert space for the inner product $\langle f, g \rangle_{s\Omega} = \sum_{|\alpha| \leq s} \langle \partial_x^\alpha f, \partial_x^\alpha g \rangle_{L^2(\Omega)} = \sum_{|\alpha| \leq s} \int_\Omega \partial_x^\alpha f\, \overline{\partial_x^\alpha g}\, d\, \mu.$.

In mathematics, more specifically in functional analysis, a Banach space is a complete normed vector space [2]. Thus, a Banach space is a vector space in an ento-ecoepidemiological, forecast, vulnerability, oviposition, predictive, endmember, sub-meter resolution, LULC, grid-stratified, risk model with a metric that allows the computation of vector length and distance between vectors which would be complete in the sense that a Cauchy sequence of vectors would always converge to a well defined limit (e.g., seasonal, geosampled, malaria mosquito, capture point, hypeprproductive, foci). In mathematics, a Cauchy sequence is a sequence whose elements become arbitrarily close to each other as the sequence progresses [2]. More precisely, given any small positive distance between oviposition, geosampled, geo-spectrotemporal, eco-georeferenced, malaria, mosquito, capture point, hyperproductive, aquatic, larval habitats all but a finite number of elements of the sequence would be less than that given distance from each other. Their importance would come from the fact that solutions of partial differential equations are naturally

found in Sobolev spaces, rather than in spaces of continuous functions and with the derivatives understood in the classical sense.

In mathematics, a holomorphic function is a complex-valued function of one or more complex variables that is complex differentiable in a neighborhood of every capture point in its domain. The existence of a complex derivative in an eco-georeferenced, geoclassified, geospectrotemporal neighborhood (e.g., seasonal, hyperproductive, malaria, mosquito, oviposition foci) implies that any holomorphic function is actually infinitely differentiable and equal to its own Taylor series (analytic). In mathematics, a Taylor series is a representation of a function as an infinite sum of terms that are calculable from the values of the function's derivatives at a single point (e.g., seasonal, eco-georeferenecd, malaria, mosquito, aquatic, larval habitat, capture point, endmember, sub-meter resolution, grid-stratified, LULC foci). Holomorphic functions are the central objects of study in complex analysis as complex differentiation is linear and obeys the product, quotient, and chain rules; the sums, products and compositions of holomorphic functions are holomorphic, and the quotient of two holomorphic functions is holomorphic wherever the denominator is not zero [2].

If a malariologist or medical entomologist identifies C with R2 in a grid-stratifiable, ento-ecoepidemiological, geosampled, vulnerability, malaria, mosquito, oviposition, capture point, aquatic, larval habitat, sub-meter resolution, orthogonal eigenfunction, spatial filter, model whilst targeting, eco-georeferenecable, seasonal, prolific foci, then the holomorphic functions would coincide with those functions of any geosampled, capture point, LULC, endmember, signature variable with continuous first derivatives which could solve the Cauchy–Riemann equations, a set of two partial differential equations. In the field of complex analysis in mathematics, the Cauchy–Riemann equations, consist of a system of two partial differential equations which, together with certain continuity and differentiability criteria, form a necessary and sufficient condition for a complex function (e.g., constructing an equation that contains unknown multivariable LULC functions and their eco-georeferenceable, orthogonal, prognosticative, ento-ecoepidemiological, endmember model, vulnerability, estimator, partial derivatives.) to be complex differentiable, that is, holomorphic. The Cauchy–Riemann equations on a pair of real-valued functions of two real variables u(x,y) and v(x,y) are the two equations[2].

Every holomorphic function can be separated into its real and imaginary parts, and each of these is a solution of Laplace's equation on R2[3]. In other words, if a malariologist or medical entomologist expresses a holomorphic function f(z) as u(x, y) + i v(x, y) in an orthogonal, prognosticative, time series dependent, regression, malaria, mosquito, oviposition, vulnerability, ento-ecoepidemiological, endmember, LULC, vulnerability, signature paradigm both u and v would be harmonic functions, whent v is the harmonic conjugate of u.

The scalar form of Laplace's equation is the partial differential equation $\nabla^2 \psi = 0$,where $\nabla^2$is the Laplacian[3]. The Laplacian for a scalar function $\phi$is a scalar differential operator defined by $\nabla^2 \phi = \frac{1}{h_1 h_2 h_3}\left[\frac{\partial}{\partial u_1}\left(\frac{h_2 h_3}{h_1}\frac{\partial}{\partial u_1}\right)+\frac{\partial}{\partial u_2}\left(\frac{h_1 h_3}{h_2}\frac{\partial}{\partial u_2}\right)+\frac{\partial}{\partial u_3}\left(\frac{h_1 h_2}{h_3}\frac{\partial}{\partial u_3}\right)\right]\phi$, where the $h_i$are the scale factors of the coordinate system [4]. Note that the operator $\nabla^2$is commonly written as $\Delta$by mathematicians [2]. Laplace's equation may be a special case of the Helmholtz differential equation $\nabla^2 \psi + k^2 \psi = 0$with $k = 0$, or Poisson's equation $\nabla^2 \psi = -4\pi\rho$with $\rho = 0$ in an oviposition, endmember,LULC,sub-meter resolution, malaria, mosquito, model for targetinh seasonal, hyperproductive, capture point foci.

The Helmholtz differential equation is an elliptic partial differential equation given by $\nabla^2 \psi + k^2 \psi = 0$,where $\psi$is a scalar function and $\nabla^2$is the scalar Laplacian, or $\nabla^2 \mathbf{F} + k^2 \mathbf{F} = 0$,where $\mathbf{F}$is a vector function and $\nabla^2$is the vector Laplacian whenst $k = 0$, the Helmholtz differential equation reduces to Laplace's equation[2]. Whenst $k^2 < 0$ (i.e., for imaginary k), the equation becomes the space part of the diffusion equation. The Helmholtz differential equation can be solved by separation of variables in only 11 coordinate systems, 10 of which (with the exception of confocal paraboloidal coordinates) are particular cases of the confocal ellipsoidal system: Cartesian, confocal ellipsoidal, confocal paraboloidal, conical, cylindrical, elliptic cylindrical, oblate spheroidal, paraboloidal, parabolic cylindrical, prolate spheroidal, and spherical coordinates (see Eisenhart 1934ab for more detail). Laplace's equation (the Helmholtz differential equation with $k = 0$ is separable in the two additional bispherical coordinates and toroidal coordinates[4]. If

International Research Journal of Computer Science and Application
Vol. 2, No. 1, March 2018, pp. 1-181
Available Online at http://acascipub.com/Journals.php

Helmholtz's equation is separable in a three-dimensional coordinate system, then an oviposition, ento-ecoepidemiological, vulnerability, malaria, mosquito, hyperproductive, seasonal, aquatic, larval habitat, eco-georeferenecable, predictive, endmember, geoclassifiable, optimizable, LULC model may show that $\frac{h_1 h_2 h_3}{h_n^2} = f_n(u_n) g_n(u_i, u_j)$, where $i \neq j \neq n$ formally regressively exists. The Laplacian is $\nabla^2 = \frac{1}{h_1 h_2 h_3}\left\{g_1(u_2, u_3)\frac{\partial}{\partial u_1}\left[f_1(u_1)\frac{\partial}{\partial u_1}\right] + g_2 (u_1, u_3)\frac{\partial}{\partial u_2}\left[f_2(u_2)\frac{\partial}{\partial u_2}\right] + g_3(u_1, u_2)\frac{\partial}{\partial u_3}\left[f_3(u_3)\frac{\partial}{\partial u_3}\right]\right\}$, [3]which simplifies to $\nabla^2 = \frac{1}{h_1^2 f_1}\frac{\partial}{\partial u_1}\left[f_1(u_1)\frac{\partial}{\partial u_1}\right] + \frac{1}{h_2^2 f_2}\frac{\partial}{\partial u_2}\left[f_2(u_2)\frac{\partial}{\partial u_2}\right] + \frac{1}{h_3^2 f_3}\frac{\partial}{\partial u_3}\left[f_3(u_3)\frac{\partial}{\partial u_3}\right]$. Such a coordinate system may obey the Robertson condition, which means that the Stäckel determinant is of the form $S = \frac{h_1 h_2 h_3}{f_1(u_1) f_2(u_2) f_3(u_3)}$. For the Helmholtz differential equation to be separable in a coordinate system, the scale factors h_i in the Laplacian $\nabla^2 = \sum_{i=1}^{3}\frac{1}{h_1 h_2 h_3}\frac{\partial}{\partial u_i}\left(\frac{h_1 h_2 h_3}{h_i^2}\frac{\partial}{\partial u_i}\right)$ and the functions $f_i(u_i)$ and Φ_{ij} defined by $\frac{1}{f_n}\frac{\partial}{\partial u_n}\left(f_n\frac{\partial X_n}{\partial u_n}\right) + \left(k_1^2\Phi_{n1} + k_2^2\Phi_{n2} + k_3^2\Phi_{n3}\right)X_n = 0$ must be of the form of a Stäckel determinant $S = |\Phi_{mn}| = \begin{vmatrix}\Phi_{11} & \Phi_{12} & \Phi_{13}\\ \Phi_{21} & \Phi_{22} & \Phi_{23}\\ \Phi_{31} & \Phi_{32} & \Phi_{33}\end{vmatrix} = \frac{h_1 h_2 h_3}{f_1(u_1) f_2(u_2) f_3(u_3)}$. [4].A Stäckel tdeterminant used to determine in which coordinate systems the Helmholtz differential equation is separable [3]. A determinant $S = |\Phi_{mn}| = \begin{vmatrix}\Phi_{11} & \Phi_{12} & \Phi_{13}\\ \Phi_{21} & \Phi_{22} & \Phi_{23}\\ \Phi_{31} & \Phi_{32} & \Phi_{33}\end{vmatrix}$ in which Φ_{ni} are functions of u_i alone is called a Stäckel determinant. A coordinate system is separable if it obeys the Robertson condition, namely that the scale factors h_i in the Laplacian $\nabla^2 = \sum_{i=1}^{3}\frac{1}{h_1 h_2 h_3}\frac{\partial}{\partial u_i}\left(\frac{h_1 h_2 h_3}{h_i^2}\frac{\partial}{\partial u_i}\right)$ which may be rewritten in terms of functions $f_i(u_i)$ which may be robustly defined by $\frac{1}{h_1 h_2 h_3}\frac{\partial}{\partial u_i}\left(\frac{h_1 h_2 h_3}{h_i^2}\frac{\partial}{\partial u_i}\right)_{,,} = \frac{g(u_{i+1}, u_{i+2})}{h_1 h_2 h_3}\frac{\partial}{\partial u_i}\left[f_i(u_i)\frac{\partial}{\partial u_i}\right] = \frac{1}{h_i^2 f_i}\frac{\partial}{\partial u_i}\left(f_i\frac{\partial}{\partial u_i}\right)$ such that S can $S = \frac{h_1 h_2 h_3}{f_1(u_1) f_2(u_2) f_3(u_3)}$ occurs in a malaria mosquito model output. When this is true, the separated equations are of the form $\frac{1}{f_n}\frac{\partial}{\partial u_n}\left(f_n\frac{\partial X_n}{\partial u_n}\right) + \left(k_1^2\Phi_{n1} + k_2^2\Phi_{n2} + k_3^2\Phi_{n3}\right)X_n = 0$ The Φ_{ij}s obey the minor, frequency forecast equations $M_1 = \Phi_{22}\Phi_{33} - \Phi_{23}\Phi_{32} = \frac{S}{h_1^2}$, $M_2 = \Phi_{13}\Phi_{32} - \Phi_{12}\Phi_{33} = \frac{S}{h_2^2}$ and $M_3 = \Phi_{12}\Phi_{23} - \Phi_{13}\Phi_{22} = \frac{S}{h_3^2}$, which may be mathematically, geo-spectrotemporally equivalent to $M_1\Phi_{11} + M_2\Phi_{21} + M_3\Phi_{31} = S_{,}M_1\Phi_{12} + M_2\Phi_{22} + M_3\Phi_{32} = 0$ and $M_1\Phi_{13} + M_2\Phi_{23} + M_3\Phi_{33} = 0$ also in a malaria model output.This gives a total of four equations in nine unknowns. Morse and Feshbach (1953, pp. 655-666) give not only the Stäckel determinants for common coordinate systems, but also the elements of the determinant (although it is not clear how these are derived).

For Helmhotz equation to be seperable in a coordinmate system for constructing a model for optimally targeting seasonal, eco-georerenceable, LULC, hyperproductive, malaria, mosquito, aquatic, larval habitat, endmember, sub-meter, resolution, grid-stratifiable, endmember, capture points, the scale factor in the Lapacian

$\nabla^2 = \sum_{i=1}^{3} \frac{1}{h_1 h_2 h_3} \frac{\partial}{\partial u_i} \left(\frac{h_1 h_2 h_3}{h_i^2} \frac{\partial}{\partial u_i} \right)$ must be solved. For the Helmholtz differential equation to be separable in a coordinate system, the scale factors $h_i$in the Laplacian and the functions $f_i(u_i)$and Φ_{ij}must be clearly defined by $\frac{1}{f_n} \frac{\partial}{\partial u_n} \left(f_n \frac{\partial X_n}{\partial u_n} \right) + \left(k_1^2 \Phi_{n1} + k_2^2 \Phi_{n2} + k_3^2 \Phi_{n3} \right) X_n = 0$ whichmay be of of the form of a Stäckel determinant $S = |\Phi_{mn}| = \begin{vmatrix} \Phi_{11} & \Phi_{12} & \Phi_{13} \\ \Phi_{21} & \Phi_{22} & \Phi_{23} \\ \Phi_{31} & \Phi_{32} & \Phi_{33} \end{vmatrix} = \frac{h_1 h_2 h_3}{f_1(u_1) f_2(u_2) f_3(u_3)}$. [4].

The vector Laplace's equation for an eco-endmember, oviposition, malaria, mosquito, grid-stratfiable, LULC model for targeting, capture point, seasonal, capture point, hyperproductive foci may be given by $\nabla^2 \mathbf{F} = \mathbf{0}$.A function ψwhich satisfies Laplace's equation is said to be harmonic[2]. A solution to Laplace's equation has the property that the average value over a spherical surface is equal to the value at the center of the sphere Gauss's harmonic function theorem states[4]. If a function $\phi$is harmonic in a sphere, then the value of ϕat the center of the sphere is the arithmetic mean of its value on the surface [2]. Solutions rendered from a mlaria mosquito, forecast, vulnerability model may have a local maxima or minima. Because Laplace's equation is linear, the superposition of any two solutions may also then be a solution in any seasonal, hyperproductive, malaria, mosquito, aquatic, larval habitat, eco-endmember, sub-meter, resolution, capture point, prognosticative, vulnerability oviposition,LULC model.

A solution to Laplace's equation for constructing a robust, endmember, eco-georeferenecable, geo-spectrotemporal, oviposition, forecast, vulnerability, eigendecomposable paradigm would be uniquely determined if (1) the value of the sub-meter resolution, grid-stratifiable, LULC function is specified on all endmember habitat boundaries (or (2) the normal derivative of the function is specified on all boundaries as specified Laplace's equation. This endmember orthogonal model may be solved by separation of the geosampled, endmember, aquatic, larval habitat, geosampled, geo-spectrotemporal, capture point, seasonal, hyperproductive foci variables in all 11 coordinate systems.

An elliptic partial differential equation given by $\nabla^2 \psi + k^2 \psi = 0$,where $\psi$is a scalar function and $\nabla^2$is the scalar Laplacian, or $\nabla^2 \mathbf{F} + k^2 \mathbf{F} = 0$, where $\mathbf{F}$is a vector function and $\nabla^2$is the vector Laplacian[4]. A second-order partial differential equation, i.e., one of the form $A u_{xx} + 2B u_{xy} + C u_{yy} + D u_x + E u_y + F = 0$,is called elliptic if the matrix[4]. $Z \equiv \begin{bmatrix} A & B \\ B & C \end{bmatrix}$is positive definite. Elliptic partial differential equations have applications in almost all areas of mathematics, from harmonic analysis to geometry to Lie theory, as well as numerous applications in physics. As with a general PDE, elliptic PDE may have non-constant coefficients and be non-linear. Despite this variety, the elliptic equations have a well-developed theory.The basic example of an elliptic partial differential equation is Laplace's equation $\nabla^2 u = 0$[5].in n-dimensional Euclidean space, where the Laplacian ∇^2 is defined by $\nabla^2 = \sum_{i=1}^{n} \frac{\partial^2}{\partial x_i^2}$.

Other examples of elliptic equations include the nonhomogeneous Poisson's equation $\nabla^2 u = f(x)$and the non-linear minimal surface equation.For an elliptic partial differential equation, boundary conditions are used to give the constraint $u(x, y) = g(x, y)$ on $\partial\Omega$, where $u_{xx} + u_{yy} = f(u_x, u_y, u, x, y)$holds in Ω.One property of constant coefficient elliptic equations is that their solutions can be studied using the Fourier transform. Consider Poisson's equation with periodic $f(x)$. The Fourier series expansion is then given by $-|\zeta|^2 \hat{u}(\zeta) = \hat{f}(\zeta)$,where $|\zeta|^2$ is called the "principal symbol," and so we can solve for u. In mathematics, a Fourier series (English: /ˈfʊəri eɪ/)[1] is a way to represent a function as the sum of simple sine waves. More formally, it decomposes any periodic function or periodic signal into the sum of a (possibly infinite) set of simple oscillating functions, namely sines and cosines (or, equivalently, complex exponentials)[4].

The discrete-time Fourier transform is a periodic function, often defined in terms of a Fourier series. In mathematics, the discrete-time Fourier transform (DTFT) is a form of Fourier analysis that is applicable to the uniformly-spaced samples of a continuous function[2]. The term *discrete-time* refers to the fact that the transform operates on discrete data (samples) whose interval often has units of time. Our assumption was the capture point vulnerability forecast, samples, it produces a function of frequency that is a periodic summation of the continuous Fourier transform of the original continuous function. Under certain theoretical conditions, described by the sampling theorem, the original continuous function can be recovered perfectly from the DTFT and thus from the original discrete samples[6]. Except for $\zeta = 0$, the multiplier was nonzero in the model.

In Jacob et al. (2013), the discrete-time, capture point, sub-meter resolution, grid-stratfied LULC signal was considered as a continuous signal $^{x(t)}$ geosampled at a rate $F = 1/t_0$ or $\Omega = 2\pi/t_0$, where t_0 was the sampling period (time interval between two consecutive habitat samples). The corresponding sampling function (comb function) was $comb(t) = \sum_{m=-\infty}^{\infty} \delta(t - mt_0)$.

The habitat, capture point, eco-endmember, LULC, sampling process was found to be $x_s(t) = x(t)\ comb(t) = x(t) \sum_{m=-\infty}^{\infty} \delta(t - mt_0) = \sum_{m=-\infty}^{\infty} x[m]\delta(t - mt_0)$ where $x[m] = x(mt_0)$ was the signature habitat, spectral value of $^{x(t)}$ at $t = mt_0$. The Fourier transform of this discrete signal was $X(j\omega) \int_{\infty}^{\infty} x_s(t)e^{-j\omega t}dt = \int_{\infty}^{\infty} [\sum_{m=-\infty}^{\infty} x[m]\delta(t - mt_0)]\ e^{-j\omega t}dt \sum_{m=-\infty}^{\infty} x[m] \int_{\infty}^{\infty} \delta(t - mt_0)\ e^{-j\omega t}dt = \sum_{m=-\infty}^{\infty} x[m]\ e^{-j\omega mt_0}$ We determined this to be the forward Fourier transform (analysis) of a discrete signal $^{x_s(t)}$. The spectrum $^{X(j\omega)}$ in the capture point, immature habitat, endmember.LULC model was periodic with $\Omega = 2\pi F = 2\pi/t_0$: $X(j(\omega+\Omega)) = \sum_{m=-\infty}^{\infty} x[m]e^{-j(\omega+\Omega))mt_0} = \sum_{m=-\infty}^{\infty} x[m]e^{-j\omega mt_0}e^{-j\Omega mt_0} = X(j\omega)$ as $e^{-j\Omega mt_0} = e^{-j2m\pi} = 1$.To get back the time signal $x[m]$ from its spectrum: $X(j\omega) = \sum_{m=-\infty}^{\infty} x[m]\ e^{-j\omega mt_0}$. The authors multiplied the equation by $e^{j\omega nt_0}/\Omega$ and integrated both sides with respect to ω over the period $\Omega = 2\pi F = 2\pi/t_0$ to obtain the inverse Fourier transform (synthesis) $\frac{1}{\Omega}\int_{\Omega} X(j\omega)e^{j\omega nt_0}d\omega = \frac{1}{\Omega}\int_{\Omega}[\sum_{m=-\infty}^{\infty} x[m]e^{-j\omega mt_0}]e^{j\omega nt_0}d\omega$ were Then they used $\sum_{m=-\infty}^{\infty} x[m]\frac{1}{\Omega}\int_{\Omega} e^{-j\omega(m-n)t_0}d\omega = \sum_{m=-\infty}^{\infty} x[m]\delta[m-n] = x[n]$ Note that the authors also used the expression $\frac{1}{\Omega}\int_{\Omega} e^{-j\omega(m-n)t_0}d\omega = \frac{1}{\Omega}\int_{\Omega} e^{-j(m-n)2\pi\omega/\Omega}d\omega = \delta[m-n] = \begin{cases} 1 & m = n \\ 0 & m \neq n \end{cases}$ which was compared this with $\frac{1}{T}\int_{T} e^{j(m-n)\omega_0 t}dt = \frac{1}{T}\int_{T} e^{j(m-n)2\pi t/T}dt = \delta[m-n] = \begin{cases} 1 & m = n \\ 0 & m \neq n \end{cases}$

To summarize, the spectrum of a given discrete habitat signal, Jacob et al. (2013) employed $x_s(t) = \sum_{m=-\infty}^{\infty} x[m]\delta(t - mt_0)$ which was found by forward Fourier transform to be: $X_\Omega(j\omega) = \mathcal{F}[x[m]] = \sum_{m=-\infty}^{\infty} x[m]e^{-j\omega mt_0} = \sum_{m=-\infty}^{\infty} x[m]e^{-j2\pi mt_0}$ and the signal was re- expressed by the inverse Fourier as $x[m] = \mathcal{F}^{-1}[X_\Omega(j\omega)] = \frac{1}{\Omega}\int_\Omega X_\Omega(j\omega)e^{j\omega mt_0}d\omega = \int_F X_F(f)e^{j2\pi mt_0}df$ It may be interesting to compare this discrete time Fourier transform pair with a Fourier series habitat expansion - the Fourier transform of a periodic, eco-endmember LULC, malaria mosquito signal: $X[n] = \mathcal{F}[x_T(t)] = \frac{1}{T}\int_T x_T(t)e^{-jn\omega_0 t}dt = \frac{1}{T}\int_T x_T(t)e^{-j2\pi nf_0 t}dt$ $x_T(t) = \mathcal{F}^{-1}[X[n]] = \sum_{n=-\infty}^{\infty} X[n]e^{jn\omega_0 t} = \sum_{n=-\infty}^{\infty} X[n]e^{j2\pi nf_0 t}$ ith discrete spectrum: $X(j\omega) = 2\pi\sum_{n=-\infty}^{\infty} X[n]\delta(\omega - n\omega_0)$ or $X(f) = \sum_{n=-\infty}^{\infty} X[n]\delta(f - nf_0)$. A symmetry between these two different forms of Fourier transform may be important for asymptotically quantitating a absolute iterative interpolative habitat signal for targeting unknow foci. If the signal $x(t) = x(t+T)$ is periodic, its spectrum $X(j\omega)$ is discrete, the coefficients of the Fourier series may have an interval $\omega_0 = 2\pi/T$. On the other hand, if $x(t)$ is discrete with interval $t_0 = 2\pi/\Omega$, its spectrum $X(j\omega) = X(j\omega + \Omega)$ may be periodic. In particular, if the unit of time is so chosen that the sampling period is $t_0 = 1$, then $\Omega = 2\pi/t_0 = 2\pi$, and the forward Fourier transform of a discrete signal may become: $X(j\omega) = \sum_{m=-\infty}^{\infty} x[m]e^{-jm\omega} = \sum_{m=-\infty}^{\infty} x[m]e^{-jm2\pi f}$ Other discrete habitat solutions may eb summarized as in Table 1 below.

Table 1 Dirichlet boundary conditions which may be employable for an endmember, oviposition, sub-meter resolution, malaria, mosquito, forecast, vulnerability, LULC model

Coordinate System	Variables	Solution Functions
Cartesian	$X(x)Y(y)Z(z)$	exponential functions, circular functions, hyperbolic functions
circular cylindrical	$R(r)\Theta(\theta)Z(z)$	Bessel functions, exponential functions, circular functions
conical		ellipsoidal harmonics, power
confocal ellipsoidal	$\Lambda(\lambda)M(\mu)N(\nu)$	ellipsoidal harmonics of the first kind
elliptic cylindrical	$U(u)V(v)Z(z)$	Mathieu function, circular functions
oblate spheroidal	$\Lambda(\lambda)M(\mu)N(\nu)$	Legendre polynomial, circular functions
parabolic		Bessel functions, circular functions
parabolic cylindrical		parabolic cylinder functions, Bessel functions, circular functions
paraboloidal	$U(u)V(v)\Theta(\theta)$	circular functions
prolate spheroidal	$\Lambda(\lambda)M(\mu)N(\nu)$	Legendre polynomial, circular functions

In addition to these 11 coordinate systems, separation can be achieved in two additional coordinate systems by introducing a multiplicative factor for optimally targeting, eco-georefernecable, hyperproductive, capture point, aquatic, larval, habitat,malaria mosquito, geoclassified, LULC, seasonal foci. In these coordinate systems, the separated form would be $\psi = \frac{X_1(u_1) X_2(u_2) X_3(u_3)}{R(u_1, u_2, u_3)}$, and setting $\frac{h_1 h_2 h_3}{h_i^2} = g_i(u_{i+1}, u_{i+2}) f_i(u_i) R^2$, where h_i are scale factors, may then give the Laplace's equation $\sum_{i=1}^{3} \frac{1}{h_i^2 X_i} \left[\frac{1}{f_i} \frac{d}{d u_i} \left(f_i \frac{d X_i}{d u_i} \right) \right] = \sum_{i=1}^{3} \frac{1}{h_i^2 R} \left[\frac{1}{f_i} \frac{\partial}{\partial u_i} \left(f_i \frac{\partial R}{\partial u_i} \right) \right]$. If the right side is equal to $-k_1^2 / F(u_1, u_2, u_3)$, where k_1 is a constant and F is any function, and if $h_1 h_2 h_3 = S f_1 f_2 f_3 R^2 F$, where S is the Stäckel determinant, then the equation can be solved using the methods of the Helmholtz differential equation.

The two systems where this is the case are bispherical and toroidal, bringing the total number of separable systems for Laplace's equation to 13 (Morse and Feshbach 1953, pp. 665-666). In two-dimensional bipolar coordinates, Laplace's equation is separable, although the Helmholtz differential optimal equation is not. $(a_0 x + b_0) y^{(n)} + (a_1 x + b_1) y^{(n-1)} + \ldots + (a_n x + b_n) y = 0$ may be Laplace equations which when solved may reveal gelocations of eco-georeferenecable, endmember, LULC, seasonal, hyperproductive, malaria, mosquito, aquatic, larval habitat, foci.

A Laplace operator for a function *f (x)* in an oviposition, malaria, mosquito model may be defined on a Hilbert space[2] in a seasonal, hyperproductive, aquatic, larval habitat, sub-meter, resolution, grid-stratifiable, eco-georeferenceable, capture point, forecast, vulnerability, LULC, endmember model. A Hilbert space is a vector space H with an inner product $\langle f, g \rangle$ such that q quantaifiable, norm defined by $|f| = \sqrt{\langle f, f \rangle}$ turns H into a complete metric space[3]. If the metric defined by the norm is not complete, then H is instead known as an inner product space. Examples of finite-dimensional Hilbert spaces include 1, the real numbers $\mathbb{R}^n$ with $\langle v, u \rangle$ the vector dot product of v and u.2[4]. The complex numbers $\mathbb{C}^n$ with $\langle v, u \rangle$ the vector dot product of v and the complex conjugate of u.may be employed in Hilbert space for targeting seasonal, prolific, vector arthropod, immature habitats. An example of an infinite-dimensional Hilbert space is L^2, the set of all functions $f : \mathbb{R} \to \mathbb{R}$ such that the integral of f^2 over the whole real line is finite[3]. In this case, the inner product is $\langle f, g \rangle = \int_{-\infty}^{\infty} f(x) g(x) d x$. .An (incomplete) space with an inner product is also called a pre-Hilbert space, since its completion with respect to the norm induced by the inner product is a Hilbert space[4]. Inner product spaces over the field of complex numbers such as geosampled, geo-spectrotemporal, eco-entoepidemiological, seasonal, malaria, mosquito, capture point, eco-georeferenceable, larval density counts are may be referred to as unitary spaces[1].

A malariologst or medical entomologist may develop basic properties of unitary Hilbert space representations of topological groups in an eco-georeferenced, ento-ecoepidemiological, malaria, mosquito, oviposition, endmember, sub-meter resolution, aquatic, larval habitat, oviposition, signature, vulnerability, LULC map. The groups G may be locally-compact, Hausdorff, and countably based. One purpose of such a quantitation would be to isolate techniques which may result in identifying seasonal, hyperproductive, capture points which may not be dependent upon additional structure of the groups. Much can be done in the representation theory of compact groups without anything more than the compactness [3]. Similarly, the discrete decomposition of L 2 (Γ\G) for compact quotients Γ\G may depend upon nothing more than quantiting compactness in an vulnerability, malaria,oviposition model. Schur orthogonality and inner product relations can then be proven for discrete time series, eco-georeferenced, aquatic, larval habitat, capture point,orthogonal, prognosticative representations inside regular representations which may be discussed without further hypotheses. The purely topological treatment of compact groups in an oviposition, malaria, forecast, vulnerability, capture point, seasonal, endmember, LULC, risk map may reveal a degree of commonality between subsequent treatments of Lie groups and of p-adic groups, whose rich details might otherwise obscure the simplicity of some geosampled habitat properties. By reviewing Haar measure, and proving the some basic things about invariant

measures on quotients H\G may be regressively discernible in an eco-georefereneced,LULC datatset of oviposition malaria, mosquito, geoclassifiable, grid-stratifiable, sub-meter resolution, seasonal, hyperproductive, aquatic, larval habitat, capture point, endmember, signature foci.This notation may refer to a quotient on the left, consisting of cosets Hg in the model. Hence by considering Gelfand-Pettis integrals for continuous, compactly-supported, vector valued, aquatic, larval, habitat functions with their immature, geosampled, geo-spectrotemporal, endmember, density, county values in Hilbert spaces eco-georeferenceable, capture point, hyperproductive foci may be remotely identifiable.

Emphasizing discretely occurring representations unfortunately may neglect continuous Hilbert integrals of these habitat representations. Nevertheless these discrete series may be suffice for sub-meter resolution, vulnerability, forecast endmember malaria, mosquito, LULC modeling compact groups in emprically regressable, malaria mosquito, capture point, empirical ento-ecoepidemiological datasets. Though it entails some complications, throughout the model construction process, attention to closed central subgroups Z of groups G, may distinguish various spaces of functions on G by their behavior under Z in a malaria model whenst targeting eco-georeferenecable seasonal, hyperproductive, aquatic, larval habitat, endmember, sub-meter, resolution, grid-stratifiable, capture points. These complications may be genuine. This issue may come up a with GL(2, R) and GL(2, Qp), which have discrete series representations modulo within their centers, but not otherwise However, moments produced using orthogonal basis sets may exist for modeling seasonal, hyperproductive, malaria mosquito, sub-meter resolution, grid-stratified, endmember,LULC data. These orthogonal moments may have the advantage of needing lower precision to represent differences (e.g., seasonal productive discrete, aquatic, larval habitat, capture point, explanatory, endmember, integer values quantitated seasonally) to the same accuracy as the monomials. The orthogonality condition would then simplify the reconstruction of the original function from the generated moments which may be employable to target, eco-georefereneceable, LULC, endmember, hyperproductive, capture point foci.

Compared to geometric moments, orthogonal moments may be suitable for oviposition, malaria, mosquito, endmember, reference, signature regression considerations whenst targeting, for seasonal, hyperproductive eco-georeferenecable, LULC foci based on geosampled, immature, ento-ecoepidemiological, endmember, capture point,geo-spectrotemporal, count data because of their simplicity. Amongst various orthogonal moments Gaussian–Hermite (GH) moments play a special role. The GH polynomials and moments may be introduced into grid-stratified, sub-meter resolution, malaria, mosquito, capture point, image analysis of an optimizable, seasonal, hyperproductive, capture point, ento-ecoepidemiological, foci geolocation which may prove to be very robust to additive noise compared to other common endmember moments. GH polynomials are orthogonal on a rectangular area[3], which may be suitable when working with digital images of malaria, mosquito, seasonal, hyperproductive, immature habitats The polynomials orthogonal on a disk, such as Zernike, radial Chebyshev, and similar polynomials, would require polar resampling of the capture point, aquatic, larval, habitat image, which not only would increase the computation time but also lead to the loss of precision in the forecasted vulnerability targets (i.e., seasonal, hyperproductive, eco-georeferenecable, foci, LULC geolocations). Generally, it would be difficult to construct rotation invariants, which are important for object recognition in a sub-meter resolution, grid-stratifiable, malaria, mosquito, capture point, endmember, habitat signature image from moments orthogonal on a rectangle (on the contrary, the moments orthogonal on a disk can be made rotation-invariant easily. The GH moments are the only moments orthogonal on a rectangle which offer a possibility of an easy and efficient design of rotation invariants [3]. This is guaranteed by the Yang's Theorem, which holds in 2D. In case of other common moments in a sub-meter resolution, capture point, malaria mosquito, seasonal hyperproductive, grid-stratified, LULC image, the scaling invariance may be achieved easily by normalizing the moments in the regression model by employing a mean gray level of the image.

Analysis of covariance for optimally conducting malaria, mosquito, immature habitat, capture point, parameter estimator, geoclassifiable, orthogonal, ento-epidemiological, LULC approximation (i.e., statistical significance validating) for a general capture point, linear model could blend ANOVA and regression. ANCOVA may evaluate whether a geosampled, eco-georeferenceable, aquatic, larval, habitat, sub-meter resolution, capture point, geo-spctrotemporal, empirical, geosampled, LULC dataset of population frequency means of an eco-entomological, explanatory, dependent variable (e.g., total seasonal, immature counts) are quantitable across levels of categorical independent variables, whilst statistically controlling for the grid-stratified, endmember, LULC effects of other continuous variables that may be primary interest, (e.g., nuisance, capture point variables). Mathematically, ANCOVA will decompose the variance in the dependent variable into explainable residual variance [2].

Intuitively, ANCOVA can be employed for 'adjusting' the dependent variable in an ento-ecoepidemiological, sub-meter resolution, grid-stratifiable, eco-georeferenecable, LULC, oviposition, orthogonal, malaria, mosquito, endmember, forecast, vulnerability model for seasonally targeting hyperproductive foci by the group means of the conditional variance. ANCOVA may be also employable to increase statistical power (e.g., the ability to find a significant difference at 95% confidence interval between multivariate, geoclassified empirical, LULC groups) by reducing the within-group error variance. In order to understand this regression methodology for optimally targeting, seasonal, oviposition, eco-georeferenceable, aquatic, larval habitat, endmember, hyperproductive foci it may be necessary for the malariologist medical entomologist or other experimenter to understand the test used to evaluate differences between the endmember LULC groups, (i.e.,the F-test).

The F-test is computed by dividing the explained variance between groups (e.g., eco-georeferenceable, seasonal, hyperproductive, malaria mosquito, oviposition, sub-meter resolution, grid-stratified, LULC imaged, capture points) by the unexplained variance within the groups. If the analysis of covariance in the oviposition, forecast, vulnerability, endmember, geo-spectrotemporal model reveals a significant difference between the tabulated slopes in the regression lines in the ento-ecoepidemiological, grid-stratified, LULC, geoclassifiable, malaria model output, there may be evidence that the linear relationship between X and Y varies with the value of the blocking factor in the model.

If multiple values of Y are collected at the same capture point, X, this can act as another type of blocking, with the unique geo-spectrotemporal, sub-meter resolution, grid-stratfiable, (i.e., orthogonal), malaria, mosquito geosampled, aquatic, larval habitat values of X acting as blocks. These multiple Y capture point, immature habitat, eco-georeferenced, LULC measurements may be less variable than the overall variation in Y, and, given their common value of X, they may not truly be independent of each other. If there are many replicated X endmember, oviposition, forecast, vulnerability, regressable,LULC values in the ento-ecogeoreferenceable, orthogonal model and if the variation between Y at replicated values is much smaller than the overall, quantitated, tabulated, residual variance, then the variance of the estimate of the slope may be too small, making the test of whether the slope is 0 (and, equivalently, the test of the goodness of linear fit) anticonservative (i.e., more likely than the stated significance level to reject the null hypothesis, even when it is true). In this case, an alternative method may be employable for optimally regressively quantitating sub-meter resolution, grid-stratifiable,seasonal, endmember, malaria, mosquito, hyperproductive,oviposition foci from an empirical, operational, LULC dataset of geo-spectrotemporal, capture point, aquatic, larval habitat, eco-georefernceable estimators by replacing each replicated X value (e.g., single, geosampled foci, count) with the average Y value, and then performing the regression analysis with the new dataset of geomorphological, geo-spectrotemporal, geosampled, independent variables. A possible drawback to this method may be that by reducing the number of geosampled, oviposition, capture points, explicative, diagnostic, terrain-related descriptors the degrees of freedom associated with the residual error may be reducable, thus potentially reducing the power of the test.

Whether the Y values are independent of each other in an ento-ecoepidemiological, prognosticative, sub-meter resolution, grid-stratifiable, oviposition, malaria, mosquito, forecast, vulnerability, endmember, LULC model may be determined by the structure of the experiment from which they arise. Y values collected over time may be serially correlated whenst time is the implicit factor, for example. If the ento-ecoepidemiological data are in a particular order, the possibility of dependence may be considered in the model. If the row order of the geosampled, malaria, mosquito, grid-stratified, capture point,sub-meter resolution, geo-spectrotemporal, oviposition, LULC data reflect the order in which the data were collected, an index plot of the explanatory, immature, eco-georeferenceable, frequency, wavelength, count data values plotted against row numbers (e.g., seasonal geosampled larval counts) in a covariance matrix may reveal patterns in the plot that could suggest possible seasonal effects. An index plot is a scatterplot of data plotted serially against the observation (case) number within a sample dataset (e.g., original geosampled, oviposition, sub-meter resolution, capture point, seasonal, hyperproductive, eco-georeferenceable, geoclassifiable, endmember, LULC observations) or some regressively deriveable measure, such as residuals or predicted values [2]. For quantitating, orthogonal, geosampled, serially correlated, endmember, hyperproductive, malaria, ento-ecoepidemiological, oviposition, capture point, Y values in a forecast, vulnerability, linear model, the estimates of the slope and intercept must be unbiased, otherwise the estimates of their variances may not be reliable.

Values may not be identically distributed because of the presence of outliers in an oviposition, malaria, ento-ecoepidemiological, sub-meter, resolution, grid-stratifiable, forecast, vulnerability, endmember model. Outliers are

anomalous values in the data [2]. Outliers may have a strong influence over the fitted slope and intercept, giving a poor fit to the bulk of geosampled, malaria, mosquito, endemic, geo-spectrotemporal, endmember, LULC, signature, sub-meter resolution, grid-stratifiable, hyperproductive, capture points, for example. Outliers may tend to increase the estimate of residual variance in the endmember ento-ecoepidemiological model lowering the chance of rejecting the null hypothesis. This may be due to recording errors in the malaria model, which may be correctable, or they may be due to the Y values not all being geosampled from the same capture point, geosampled, aquatic, larval, habitat population. Apparent outliers may also be due to the Y values being from the same, but non-normal, non-spectrotemporal, geosampled populations. Outliers may show up clearly in a X-Y scatterplot of the oviposition, endmember, signature, orthogonal, optimizable, time series, geosampled, aquatic, larval, habitat, capture point, geoclassifiable, LULC data, as ento-ecoepidemiological, hyperproductive, seasonal, eco-georeferenceable, aquatic, larval, habitat, capture points that do not lie near the general linear trend of the data. A seasonal, ento-ecoepidemiological, explanatory, eco-georeferenecable, predictor variable may be an unusual value in either X or Y without necessarily being an outlier in the scatterplot. Once the regression line has been fitted, the boxplot and normal probability plot (i.e., normal Q-Q plot) for regressed residuals may suggest the presence of outliers in an ento-ecoepidemiological, forecast, vulnerability, malaria, mosquito, geo-spatiotemporal, sub-meter resolution, ento-ecoepidemiological, eco-endmember, LULC empirical, grid-stratifiable, capture point, oviposition, geosampled dataset.

In statistics, a Q–Q plot ("Q" stands for quantile) is a probability plot, which is a graphical method for comparing two probability, endmember,LULC prognosticated, malaria, mosquito,capture point distributions by plotting their quantiles against each other. First, the set of intervals for the quantiles have to be chosen. In terms of oviposition, geo-spectrotemporal, sub-meter resolution, grid-stratifiable, malaria, mosquito, geosampled parameter estimator, endmember, LULC, forecast, vulnerability, regression data analyses, an eco-georeferenceable, capture point (i.e.,seasonal hyperproductive foci) (x, y) on the plot may correspond to one of the quantiles of the second distribution (y-coordinate) plotted against the same quantile of the first distribution (x-coordinate). Thus, the line in the forecast, vulnerability, oviposition, endmember, LULC model would be a parametric curve with the parameter which may be the interval for the quantile when targeting seasonal, hyperproductive foci. Hence, a 95% confidence interval for the q quantile can be found by an application of the Binomial distribution whenst conducting a sub-meter resolution, grid-stratifiable, malaria, mosquito, capture point, seasonal, invasive, orthogonal, eco-georeferenceable, geoclassifiable, regressable, ento-ecoepidemiological, LULC, geo-spectrotemporal, endmember, data analyses.

q-quantiles are values that partition a finite set of values into q subsets of (nearly) equal sizes [2]. There are $q - 1$ of the q-quantiles, one for each integer k satisfying $0 < k < q$. In some cases the value of a quantile in an endmember, oviposition, mosquito, malaria, forcast, vulnerability, signature, grid-stratifiable, sub-meter resolution, probabilistic LULC paradigm may not be uniquely determined, as can be the case for the median (2-quantile) of a uniform probability distribution on a set of even size. Quantiles can also be applied to continuous endmember LULC distributions rendered from an oviposition, eco-georeferenecable, prognosticative, ento-ecoepidemiological, forecast,vulnerability model for targeting seasonal, unknown, eco-georferenceable capture point, endmember, hyperproductive foci by providing a way to generalize rank statistics to continuous variables. When the cumulative distribution function (CDF) of a random geosampled, geo-entoecoepidemiological, endemic, explanatorial, time series, orthogonal LULC variable is known, the q-quantiles may be quantitatable by the application of the quantile function (the inverse function of the CDF) to the capture point, geosampled, oviposition sub-meter resolution, grid-stratifiable, endmember geosampled values $\{1/q, 2/q, \ldots, (q - 1)/q\}$[1].

More abstractly given two CDFs F and G, with associated quantile functions F^{-1} and G^{-1} the inverse function of the CDF may be the quantile function in an oviposition, malaria, mosquito, LULC endmember, model for targeting seasonal, hyperproductive foci. The Q–Q plot generated from an eco-georeferenceable, oviposition, malaria, mosquito, capture point, sub-meter resolution, time series would then draw the q-th quantile of F against the q-th quantile of G for rendering a range of ento-ecoepidemiological, forecast vulnerability, capture point, orthogonal, LULC, decomposed values of q. Thus, the Q–Q plot would be a parametric curve indexed over [0,1] whose immature, geosampled, geoclassifable density count values exists in the real plane R^2 in the oviposition, vulnerability, endmember, grid-stratifiable, capture point model.

In mathematics, parametric equations define a group of quantities as functions of one or more independent variables ("parameters) [2] Parametric equations are commonly employed to express the coordinates of points that make up a geometric object (e.g., seasonal, eco-georeferenceable, malaria, mosquito, hyperproductive, aquatic, larval, habitat,capture point, LULC, endmember foci) such as a curve or surface, in which case the equations are collectively called a parametric representation or parameterization of the object. Note that parametric representations are generally nonunique in sub-meter resolution, malaria, oviposition, mosquito, eco-entomological, grid-stratifiable, empirical, orthogonal, forecast, vulnerability, LULC datasets[see1], so the same endmember wavelength frequency quantities [e.g., sub-meter resolution visible and near-infra-red (NIR) reflectance, oviposition data), may be expressed by a number of different LULC parameterizations.

In addition to curves and surfaces, parametric equations may describe manifolds and algebraic varieties in a, time series, robust, ento-ecoepidemiological, capture point, oviposition, prognosticative, malaria, mosquito, orthogonal, vulnerability, LULC model of higher dimension, with the number of geosampled aquatic, larval habitat, geo-spectrotemporal, parameterizble estimators being equal to the dimension of the manifold or variety, and the number of equations being equal to the dimension of the space(i.e, seasonal, oviposition, sub-meter resolution, capture point, orthogonal grid). The manifold or variety may be considered for quantitating curves of various dimensions in the empirical oviposition dataset which may require the estimators employed for determining surface,capture point LULC, aquatic, larval habitat dimensions. Thereafter, regressively quantitating the empirical, geo-spectrotemporal, geosampled, endmember, LULC dataset of uncoalesced, sub-meter resolution, grid-stratfiable, eco-georeferenceable, seasonal, malaria, mosquito, capture point, aquatic, larval habitat, ento-ecogeoreferenecable,ovipoistion dataset.

Parametric equations are commonly used in kinematics, where the trajectory of an object is represented by equations depending on time as the parameter. Because of this application, a single parameter is often labeled in a parametric model, hence, geo-spectrotemporally, eco-georeferenceable, geosampled sub-meter resolution, grid-stratifiable oviposition, LULC parameters of imaged, seasonal, hyperproductive foci may represent other physical quantities (e.g., geometric, malaria ,mosquito, capture point, seasonal endmember, non-continuous, canopied, or soil moisture, aquatic, larval habitat variables) or can be selected arbitrarily for convenience. Parameterizations are non-unique; more than one set of parametric equations can specify the same curve [4].

In statistics and in particular in regression analysis, leverage is a measure of how far away the independent variable values of an observation are from those of the other observations[6]. High-leverage points in a vulnerability, immature habitat, sub-meter resolution, eco-georferenceable, grid-stratifiable, malaria, ento-ecoepidemiological, capture point, forecast, regression, LULC, vulnerability model are those observations, if any, made at extreme or outlying values of the independent variables such that the lack of neighboring observations means that the fitted regression model will pass close to that particular observation (e.g., eco-georeferenceable, LULC, seasonal, hyperproductive, aquatic, larval, habitat foci). Modern computer packages for statistical analysis for uncoalesced, time series, endmember, immature, malaria, capture point, mosquito, LULC signature data include, as part of their facilities for regression analysis, various quantitative measures for identifying influential observations; amongst these measures is partial leverage, a measure of how a variable contributes to the leverage of a datum.

The method of least squares involves minimizing the sum of the squared vertical distances between each data point and the fitted line [2]. Because of this, a fitted line in an oviposition, sub-meter resolution, grid-stratifiable signature, malaria, mosquito, ento-eco-epidemiological, endmember,oviposition, LULC, prognosticative, sub-meter rersolution, grid-stratifiable, eco-georferenceable, vulnerability, model can be highly sensitive to outliers. In other words, least squares regression may not be resistant to outliers, and thus, neither is the fitted slope estimate in a malaria, mosquito predictive, capture point, forecast, vulnerability oviposition, LULC model. A seasonal, eco-georeferenceable, capture point vertically removed from the other geo-spectrotemporal, oviposition, geosampled, immature habitat,capture points may cause the fitted line to pass close to it, instead of following the general linear trend of the rest of the empirical, malaria, endmember data, especially if the capture point is relatively far horizontally from the centroid of the data (e.g., the eco-georeferenced capture point represented by the mean of X and the mean of Y). Such malaria, mosquito, endmember, oviposition, signature, aquatic, larval, habitat, LULC, capture points are said to have high leverage: the centroid acts as a fulcrum, and the fitted line pivots toward high-leverage, capture points (i.e., possible prolific, LULC foci), perhaps fitting the main body of the oviposition geosampled data poorly. A sub-meter resolution,

eco-georferenceable, orthogonal, grid-stratifiable, hyperproductive, geoclassified, capture point that is extreme in Y but lies near the center of the geosampled data horizontally will not have much effect on the fitted slope, but by changing the estimate of the mean of Y, it may affect the fitted estimate of the intercept. A nonparametric or other alternative regression method may be a better method in such a situation.

The values in a geosampled, sub-meter resolution, oviposition, grid-stratifiable, endmember, malaria, mosquito, signature, regression LULC dataset may indeed be from the same population, but not from a normal one. Signs of non-normality in an ento-ecoepidemiological, geosampled, malaria model are skewness (lack of symmetry) or light-tailedness or heavy-tailedness[1]. The boxplot, histogram, and normal probability plot (normal Q-Q plot), along with the normality test may provide information on the Gaussianism of an endmember, oviposition, malaria, mosquito, immature habitat, LULC, prolific, capture point, population distribution. However if there are only a small number of eco-georeferenceable, capture points, non-normality can be hard to detect. If there are a great many eco-georeferenced, capture points in the empirical, geo-spectrotemporal, geoclassified, eco- endmember, oviposition dataset the normality test may detect statistically significant in a ento-ecoepidemiological LULC model but trivial departures from normality may not be detected (e.g., the t statistic for the test of the slope will converge in probability to the standard normal distribution by the law of large numbers).

In probability theory, the law of large numbers (LLN) is a theorem that describes the result of performing the same experiment a large number of times. According to the law, the average of the results obtained from a large number of trials should be close to the expected value, and will tend to become closer as more trials are performed. For heuristically extracting optimal, oviposition, sub-meter resolution, grid-stratifiable, time series malaria, mosquito, geo-spectrotemporal, eco-georeferenceable, geosampled, ento-ecoepidemiological, endmember,LULC data from a normalized probability plot may approximate straight lines, and boxplots may be symmetric (median and mean together, in the middle of the box) with no outliers. Except for substantial non-normality that leads to outliers in the X-Y data, if the number of prognosticated, seasonal, hyperproductive, geo-spectrotemporal, LULC, capture points is not too small, then the linear regression statistic will not be much affected even if the endmember geosampled population distributions are skewed. Unless the LULC sample sizes are small (less than 10), light-tailedness or heavy-tailedness may have little effect on the linear regression [2].

Statistical tests may operate well across a wide variety of endmember, sub-meter resolution, malarial, oviposition, seasonal, capture point, eco-georeferenceable, geosampled, geo-spectrotemporal, aquatic, larval habitat, forecasted, normalizable distributions. A test can be robust for validity, meaning that it provides P values close to the true ones in the presence of (slight) departures from its assumptions [2]. It may also be robust for efficiency in an optimizable, hierarchical, explanatory, linear, parameter estimation, eco-endmember, time series analyses meaning that the residual prognosticative, vulnerability residuals (e.g., eco-georefereneced, sub-meter resolution, grid-stratified, eco-geolocations of seasonal, hyperproductive, aquatic, larval, habitat foci) maintains its statistical power (e.g., the probability that a true violation of the null hypothesis will be detected by the test) in the presence of those departures. Linear regression is fairly robust for validity against non-normality in oviposition, sub-meter resolution, grid-stratifiable, malaria, oviposition, orthogonal or geometric mean regression models, but it may not be the most powerful test available for a given non-normal distribution, (e.g., regression test assumptions are not met) when targeting seasonal, hyperproductive foci. In the case of violations of assumtpions (non-normality) in a optimizable, nonparametric, orthogonal, optimization, eigendecomposable, eigenvector, LULC, frequency, diagnostic, regression, endmember method, a transformation of X may result in endmember, capture point misspecifications whenst quantitating seasonal, hyperproductive, oviposition, aquatic, larval habitat, eco-georefernceable, sub-meter resolution, grid-stratifiable, malaria, mosquito, geoclassified, LULC, capture point geolocations.

A nonparametric or resistant regression method, a transformation, a weighted least squares linear regression, or a nonlinear,diagnostic, grid-stratifiable, LULC model output may result in a better time series, oviposition, malaria, mosquito, forecast, vulnerability, endmember, sub-meter resolution, orthogonal model fit. If the population variance for Y is not constant, a weighted least squares linear regression or a transformation of Y may provide a means of fitting a regression adjusted for optimally quantitating the inequality of the variances in the forecast, vulnerability, endmember model. Often, the impact of an assumption violation on ento-ecoepidemiological malarial, vector, arthropod, endemic,

oviposition, endmember, signature, capture point, linear regression results depends on the extent of the violation (e.g., how inconstant the variance of Y is, or how skewed the Y geosampled, eco-georeferenceable, sub-meter resolution, tabulated, population distribution is) (see Jacob et al [1]). Some small violations may have little practical effect on the time series, capture point, oviposition, aquatic, larval habitat, regression grid-stratifiable, signature, vulnerability, endmember LULC analysis, whilst other violations may render the gridded linear, prognosticative, malaria, model results (e.g., eco-georeferenceable, targeted geolocations of seasonal, endmember, hyperproductive foci) uselessly incorrect or uninterpretable. Hence insights yielded from eco-geographical, eco-georferenceable, time series, vulnerability endmember forecasts, (e,g., geostatistically targeted, ento-ecoepidemiological, hyperproductive, capture points) rendered from an endemic, transmission-oriented LULC, endmember, signature model confidence intervals may be biased.

Asymptotic theories for test statistics in linear, seasonal, vector arthropod-related, optimally semi-parameterizable, malaria-oriented, time series, sub-meter resolution, grid-stratifiable, geoclassifiable, LULC, panel models may be utilized to determine robustness to heteroskedasticity and other probabilistic, residual, diagnostic non-normalities in multiple, vulnerability, algorithmic, (e.g., an eigenfunction spatial filter eigendecomposition) model outputs. In so doing, optimal targeting of eco-georefernceable, seasonal, hyperproductive, capture point, malaria, mosquito, endmember foci may be conducted. A medical entomologist or a malarialogist may consider a standard mathematical, geo-spectrotemporally, quantizable, regressively optimizable, fixed-effects, diagnostic, oviposition, ento-ecoepidemiological, endmember, orthogonal, LULC geoclassified, panel model given by equation it=xit′β+ai+uit,i=1,2,…,nt=1,2,…,T (1.1) in PROC PANEL where yityit, ai and uit maye be plausible scalars and xit and β are k×1 vectors. These data may be autoregressed in an empirical regressively, optimizable uncoalesced endmember dataset of geo-spectrotemporal, geosampled malaria, mosquito, aquatic, larval habitat parsitological, hyperrpoductive, capture point, oviposition, eigendecomposition, autocorrelation model. Often time period fixed-effects are included in regresseable, malaria, mosquito, immature, habitat estimates which could render the predictive risk model equation yit=xit′β+ai+ft+uit as in Jacob et al. [5].

The model statement in PROC PANEL may be specified like the MODEL statement in other SAS regression procedures: the dependent variable (e.g., uncoalesced, sub-meter resolution, wavelength, frequency-oriented, seasonal, malaria, mosquito, oviposition, LULC, grid-stratifiable, eco-georeferenceable, iteratively, interpolatable, grid-stratifiable, endmember signature) may be listed first, followed by an equal sign, followed by the list of regressor variables, as shown in the following statements:

```
proc panel data=a;

 id state date;

malaria model y = x1 x2;

run;
```

The major advantage of employing PROC PANEL is that a malariologist, medical entomologist or other experimenter may incorporate an endmember, grid-stratifiable, oviposition, orthogonal, LULC signature, aquatic, larval habitat, seasonal, eco-georeferenceable, capture point, geo-spectrotemporal, model estimators for determining the structure of the random errors. It is important to consider what kind of probabilistic, geoclassifiable, error structure model is appropriate whenst regressing malaria, oviposition, geo-spectrotemporal, geosampled, capture point, endemic, LULC data[1]. The error structure options supported by the PANEL procedure are FIXONE, FIXONETIME, FIXTWO, RANONE, RANTWO, PARKS, DASILVA, GMM and ITGMM (iterated GMM)(http://support.sas.com/). Jacob et al. [5] fit a Fuller-Battese one-way random-effects, oviposition, endmember, malaria, capture point, moderate resolution (5m spatial resoln), grid-stratified LULC model of immature habitats of malaria mosquito vector *Anopheles gambiae* s.l., in two urban towns (Malindi and Kisumu) in Kenya. The asymptotic distribution of the F-statistic in the models were derived as the number of grid-stratfiable, LULC, categorical or continuous, explanatory, time series, diagnostic, clinical, field–operational, and remote-specified, endemic, seasonal, hyperproductive, capture point, aquatic larval, habitat covariates. The result was used to establish an approximate test for the significance of the random effect variance component in both urban, ento-ecoepidemiological, eco-endmember, forecast, vulnerability, *An. gambiae* s.l. oviposition, capture point models. Robustness of the established approximate test was regressively quantitated and the

asymptotic distribution of the F-statistic for the LULC, random-effects models with p unknown parameters under an arbitrary design matrix of rank p. Here the number of endmember, explicative, observations, ni was the number of observations from the ith group and t was the number of habitat groups.

Jacob et al. [5] tackled two different assumptions on the ni's where the ni's were assumed to be either fixed or large which provided robustness of the asymptotic distribution of the F-statistic in the LULC, oviposition, endmember, malaria, mosquito, ento-ecoepidemiological, aquatic, larval, habitat, endmember models. The ni's are only assumed to be fixed and robustness of the asymptotic distribution of the F-statistics are not commonly given [2]. Two different assumptions on the ni's led to the same asymptotic results since the asymptotic distribution of the F-statistic was unique in both oviposition, ento-ecoepidemiological, eco-endmember, grid-stratified, risk model, orthogonally parameterizable, geo-spectrotemporal, signature datasets. The authors considered the analysis of variance (ANOVA) type design matrix. They used the technique where the asymptotic distribution of the F-statistic was reduced to the asymptotic distribution of the difference mean square error (MSE) in the models. The MSE converged in probability to the constant in the vulnerability forecasts.

A malariaologist, medical entomologist or other experimenter may consider the asymptotic behavior of the one-way analysis of variance (ANOVA) F statistic whenst the number of levels or endmember, LULC groups of grid-stratifiable, seasonal, endmember, eco-georeferenceable, hyperproductive capture point foci is large in an signature, sub-meter resolution, prognosticative, oviposition model. The results obtained may be under the assumption of homoscedasticity and in such circumstances the sample or group sizes ni may remain fixed as the number of groups tends to infinity. It may be imperative to study both weighted and unweighted test statistics in the heteroscedastic case whenst constructing an oviposition, malaria, LULC, endmember, sub-meter resolution, signature, capture point, aquatic, larval habitat, ento-ecoepidemiological prognosticative, vulnerability model. The unweighted statistic may be employable even with small group size oviposition, endmember signature, eco-georeferenecable, capture point, empirical datasets. It may be demonstrated that an asymptotic approximation to the distribution of the weighted statistic in these models is possible only if the group sizes tend to infinity suitably. An investigation may reveal local, aquatic, larval habitat, hyperproductivegeoclassifiable, optimizable, endmember signature, seasonal, geo-spectrotemporal, ento-ecoepidemiological, geosampled, aquatic, larval habitat, data alternatives for constant regression in the case of replicated, seasonal, hyperproductive, eco-georeferenceable, LULC observations and the case of no replications, which may require smoothing techniques.

The asymptotic theory may employ a novel application of the projection principle which may regressively quantitate the asymptotic distribution of endmember, LULC, quadratic forms in an oviposition, sub-meter resolution, grid-stratifiable, malaria, mosquito, signature, forecast, vulnerability, geo-spectrotemporal, optimizable, aquatic, larval habitat, hyperproductive, eco-georeferenceable model. It is interesting that the asymptotic distribution of the F-statistic for the random effects model under an arbitrary design matrix X has never been considered for optimally regressively quantitating uncoalesced, malaria, mosquito, oviposition, LULC endmembers. The model under an arbitrary design matrix X may reduce to the one-way random-effects model or the split plot design with appropriate design matrix for parsimoniously predicting eco-georeferenceable, seasonal, hyperproductive, capture point, aquatic, larval habitat, endemic foci, geolocation, endmember explanators precisely. The results presented may be applicable for the asymptotic distribution of F-statistic to all types of seasonal malaria, mosquito, aquatic, larval habitat, capture point, oviposition, endmember, LULC models, (e.g., agro-irrigation, urban residential etc.). In so doing, the approximate F-test for a null variance ratio may be proposed in the presence of non-normality for these models. The proposed test may be useful when the assumption of normality for random effect and error of the ento-ecoepidemiological,geosampled, seasonal, capture point, aquatic, larval, habitat, malaria, mosquito, geo-spectrotemporal,oviposition model estimators which may not coincide with the approximate F-test under normality when a kurtosis of random effect and error are taken to be zero. The power of the approximate F-test is based on the violation of the normality assumption [2].

In order to aid in endmember, oviposition, ento-ecoepidemiological, forecast, vulnerability, geo-spectrotemporal, malaria, mosquito, capture point, aquatic, larval habitat, model specification, two specification test statistics may be applied. The first is an F statistic that tests the null hypothesis that the fixed-effects, capture point, grid-stratifiable, oviposition-related, time series, geosampled, vulnerability parameters are all zero. The second is a Hausman m statistic that provides information about the appropriateness of the random-effects endmember specification in the aquatic, larval habitat, ento-ecoepidemiological, LULC, geosampled data. The m statistic is based on the idea that, under the null hypothesis of no correlation between the effects variables and the regressors, Ordinary

Least Square may be consistent. Hence, a test in an oviposition, ento-ecoepidemiological, forecast, vulnerability, eco-georeferenceable, seasonal, capture point, aquatic, larval, habitat, oviposition, malaria, mosquito, optimizable, signature, LULC model can be based on the result that the covariance of an efficient grid-stratfiable, geosampled estimator with its difference from an inefficient estimator is zero. Rejection of the null hypothesis may suggest that the fixed-effects model is more appropriate in the model.

In statistics, a fixed effects model is a statistical model in which the model parameters are fixed or non-random quantities. This is in contrast to random effects LULC models and mixed endmember models in which all or some of the model parameters are considered as random variables. In many applications including endmember, malaria, mosquito, capture point, signature, grid-stratifiable, forecast, vulnerability, geosampled, LULC models, a fixed effects model refers to a regression model in which the group means are fixed (non-random) as opposed to a random effects model in which the group means are a random sample from a seasonal, geo-spectrotemporal, aquatic, larval, habitat population. Generally, empirical, oviposition, endmember, malaria mosquito data can be grouped according to several observed factors. The group means should be modeled as fixed or random effects for each grouping [6]. In a fixed effects LULC, ento-ecoepidemiological, eco-georeferenecable, forecast, vulnerability model each group mean would a group-specific fixed quantity. In panel data where longitudinal observations exist for the same subject, fixed effects represent the subject-specific means [2]. In geo-spectrotemporal, ento-ecoepidmiological, malaria, mosquito, aquatic, larval habitat, eco-georeferenceable, forecast, vulnerability, endmember, data analysis the term fixed effects capture point, ovipsoition estimator may refer to an estimator for the LULC coefficients in the model including those fixed effects (one time-invariant intercept for each seasonal, hyperproductive foci geosampled subject).

An OLS procedure may also provide the pseudo- R square measure in an oviposition, endmember, malaria, geoclassifiable, mosquito, capture point, endmember grid-stratifiable, sub-meter resolution, LULC, signature model. This number would be interpretable as a measure of the proportion of the endmember transformed sum of squares of the dependent variable (e.g., eco-georeferenceable, seasonal, aquatic, larval, habitat, density count) that is attributable to the influence of the geosampled, capture point, wavelength, frequency, LULC independent variables. In the case of OLS estimation, the R square measure is equivalent to the usual R square measure. Conversely, a more generalizable, seasonal, multivariate, vector, arthropod-related, aquatic, larval habitat, malaria, mosquito, endemic, transmission-oriented, predictive, oviposition, capture point, LULC, risk model might include individual geo-spectrotemporal, capture point trends. In so doing, the asymptotic limiting variables may then remain unchanged when additional grid-stratifiable, endmember, heuristically optimizable, LULC timeseries descriptors are included in the oviposition model, however the results may not be applicable to the estimated coefficients (e.g., seasonal, hyperproductive, eco-georeferenceable, malaria, mosquito, aquatic, immature, density, count data, geosampled in an agro-irrigated riceland agro-ecosystem) themselves. The focus would instead be on estimtion and inference about β whenst optimally eco-cartographically, remotely geo-spectrotemporally targeting, hyperproductive, eco-georeferenceable, capture point, seasonal ento-ecoepidemiological, vulnerability foci. According to Gu and Novak (2005) oviposition, malaria, mosquito, seasonal, eco-georeferenceable, immature, prolific LULC sites should be field prioritized for optimally determining geolocations of clustering, prolific, seasonal, immature habitat, capture points for implementing control strategies [e.g., Integrated Vector Management(IVM)].

For instance, consider the fixed-effects OLS estimator of β as rendered by a time series, progressive, field-operationizable, sub-meter resolution, evidentially probabilistic, malaria, mosquito, capture point, LULC, seasonal, hyperproductive foci, model, forecast equation where β′ is equal to $(\sum i=1n\sum t=1Tx\tilde{}itx\tilde{}it')-1\sum i=1n\sum t=1Tx\tilde{}ity\tilde{}$. In such circumstances the optimizable, geosampled, geo-spectrotemporal, malaria, oviposition, grid-stratifiable, capture point, regression variable i $y\tilde{}it=yit-\bar{y}i, x\tilde{}it=xit-\bar{x}i$, may be $\bar{y}i=T-1\sum t=1Tyit$ and $\bar{x}i=T-1\sum t=1Txit$. In a seasonal, vector, arthropod-related, endmember, risk model this equation could render explicative, time series, robust forecasts of seasonal hyperproductive, capture point, aquatic, larval habitat, eco-georeferenecable foci employing $y\tilde{}it=yit-yi-1n\sum j=1n(yjt-yj), x\tilde{}it=xit-xi-1n\sum j=1n(xjt-xj)$. Plugging in the diagnostic, residual ento-ecoepidemiological, time series, explanatorial, vulnerability forecasts $\tilde{y}_{it}\tilde{}$would then subsequently optimally render $\beta-\beta=(\sum i=1n\sum t=1Tx\tilde{}itx\tilde{}it')-1\sum i=1n\sum t=1Tx\tilde{}ituit$. If a medical entomologist or malarialogist then lets $v\tilde{}it=x\tilde{}ituit$ and defines $\hat{v}it=x\tilde{}it\hat{u}it$ in the LULC model where $\hat{u}it$ are the OLS residuals is given by $\hat{u}it=y\tilde{}it-x\tilde{}it'\beta$, the partial sums of $\hat{v}it$ as $\hat{S}i[rT]=\sum t=1[rT]\hat{v}it$ could be optimally definable in the endemic, endmember, probabilistic, parasitological, ento-ecoepidemiological, risk model, residual derivatives for eco-geographically targeting hypeproductive foci seasonally whenst $r\in(0,1]$. In such circumstances rT would be the integer part of the residual eco-georeferenceable, vulnerability

forecasts (e.g., targeted, eco-georeferenceable, hyperproductive, *Anopheles*, seasonal, capture point, aquatic, larval habitats). The sample variance–covariance matrix could then be employable to obtain the standard errors in the prognosticative, endmember, oviposition, signature,LULC model which could take the sandwich form T(∑i=1n∑t=1Tx˜itx˜it′)−1(∑i=1nT−1ŝiTŝiT′)(∑i=1n∑t=1Tx˜itx˜it′)−1.

In employing a sandwich estimator, a malarialogist or medical entomologist could show that the middle term in an oviposition, ento-ecoepidemiological, forecast, vulnerability, malaria, mosquito, LULC model is a special case of a more generalizable class of an empirical, optimizable, uncoalesced dataset of prognosticative, seasonal, vector, arthropod-related, evidentially probabilistic, variance–covariance, diagonal, eigenfunction, orthogonally eigen-decomposable, sub-meter resolution, covariance matrix estimators.Henceforth, by letting Γj(i)=T−1∑t=j+1Tv̂itv̂it−j′for defining the residual, diagnostic, explanative, vulnerability, hyperproductive, capture point, regressively optimizable endmember, orthogonal, optimizabe, vulnerability forecasts by Ω̃i=Γ̃0(i)+∑j=1T−1k(jM)(Γ̃j(i)+Γ̃j(i)′), the explicative, nonparametric kernel heteroskedasticity and autocorrelation consistent (HAC) covariance matrix estimator for cross-sectional individual grid-stratifiable, eco-georefereneced geosampled, immature habitats in a sample frame may optimally quantitate propagational geo-spectrotemporal, probabilistic uncertainties employing the kernel, k(x), and bandwidth M.

An equivalent expression for $\widehat{\Omega}_i$Ω may also be provided also by Ω̃i=T−1∑t=1T∑s=1TKtsv̂itv̂is′. In so doing, Kts=k(|t−s|M) may unbiasedly render iteratively, interpolative, seasonal, eco-entomological, time series, optimizable, vector, arthropod-related, optimally regressively, robustifiable, capture point, parameterizable, dataset of endmember, sub-meter resolution, grid-stratified LULC covariate coefficients. For example, if a medical entomologist or malarialogist considers the time series sample, regression-based, variance–covariance matrix V̂ave(n)=T(∑i=1n∑t=1Tx˜itx˜it′)−1(∑i=1nΩ̃i)(∑i=1n∑t=1Tx˜itx˜it′)−1is parsimoniously employed for constructing a multivariate, expositiorial, prognosticative seasonal, vector, arthropod-related, malaria,mosquito, eco-entomological, endmember, oviposition, eco-georeferenceable, LULC, risk model, the subscript, ave(n) may indicate the "average" of the *n* individual-by-individual geo-spectrotemporally geosampled, hyperproductive, capture point foci. Hence endmember HAC estimators could be employable to construct the middle matrix of the sandwich in a malaria, mosquito, oviposition, forecast, vulnerability model.

For the case where k(x)=1k(x)=1 for |x|≤1|x|≤1 and k(x)=0 [i.e. k(x)k(x)], an ento-ecoepidemiological dataset of oviposition, seasonal, time series, diagnostic, vulnerability, hyperproductive, capture point, malaria, mosquito, oviposition, endmember, eco-georeferenecable, vulnerability forecasts may be the truncated kernel, which could robustly reveal if M=TM=T, $\widehat{\Omega}_i = T^{-1}\widehat{S}_{iT}\widehat{S}'_{iT}$Ω̃i=T−1ŝiTŝiT exists in the residual, diagnostic, model output. In such circumstances, the variance-covariance estimator for the traditional standard errors can be easily provided for the endemic, transmission-oriented, oviposition, goclassifiable forecast, vulnerability, endemic, seasonal, hyperproductive, remotely sensed, grid-stratifiable, LULC model and their geostatistical, eco-georeferenceable, ento-ecoepidemiological, geosampled, capture point, endmember, sub-meter resolution, parameterizable estimators. The traditional standard errors are a special case of "cross-section averages of HACs" standard errors [2].

Jacob et al. [6] studied properties of the truncated kernel function γ^2 in an ento-ecoepidemiological, grid-stratified, eco-georeferenceable, malarial,oviposition, capture point, forecast, vulnerability, geo-spectrotemporal, sub-meter resolution, remotely sensed, geostatistical, endmember,LULC model defined on integers n ≥ 0 by γ(n)/P(n), where γ(n) = ∏ p|n p where the w kernel function and P(n) was the largest empirical, time series, aquatic, larval habitat, unbiased, parameter estimator in an eco-georeferenceable, temporally geosampled dataset in Uganda. In particular, the authors proved that the maximal order of $\gamma^2(n)$ for n ≤ x is (1 + o(1))x/log x as x → ∞ and that ∑ n≤x 1/γ2(n) = (1 + o(1))ηx/log x, where η = ζ(2)ζ(3)/ζ(6) for any oviposition, endmember, optimizable, sub-meter resolution, geo-spectrotemporal, signature, malaria, mosquito, geosampled dataset at the ento-ecoepidemiological study site. The authors further show that, given any geosampled, oviposition, malaria, grid-stratified, parameterizable, optimizable, aquatic, larval habitat, capture point, endmember,LULC estimator u < 1, limx→ ∞ 1 x #{n ≤ x: γ2(n) < xu} = limx→ ∞ 1 x #{n ≤ x: n/P(n) < xu} = 1 − ρ(1/(1 − u)), whenst ρ is the Dickman function. The probability that a random integer between 1 and x will have its greatest prime factor $\leq x^{\alpha}$ approach a limiting value $F(\alpha)$ as $x \to \infty$,

whenst $F(\alpha)=1$ for $\alpha>1$ and $F(\alpha)$ is defined through the integral equation $F(\alpha)=\int_0^{\alpha} F\left(\frac{t}{1-t}\right)\frac{dt}{t}$ for $0\le\alpha\le 1$ (Dickman 1930,).

Jacob et al. [1] employed the orthogonal function analytically in a time series, malaria, oviposition, remote sensing, capture point, forecast, vulnerability, geo-spectrotemporal, LULC model for $1/2\le\alpha\le 1$ by $F(\alpha)=1-\int_{\alpha}^{1} F\left(\frac{t}{1-t}\right)\frac{dt}{t}=1-\int_{\alpha}^{1}\frac{dt}{t}=1+\ln\alpha$ [2]. The authors show that n/P(n) can very often be much larger than γ2(n) in these oviposition models namely by proving that, given any c ∈ [1, ξ), where ξ is the unique solution to ξ log 2 = log(1 + ξ) + ξ log(1 + 1/ξ), then #{n ≤ x: γ2(n) ≥ n/(c log n)} = o (#{n ≤ x: n/P(n) ≥ n/(c log n)}) (x → ∞). In particular, the authors revealed that the maximal order in the paradigm of γ2 (n) for n ≤ x was (1 + o(1))x/log x as x → ∞ such that ∑ n≤x 1/γ2(n) = (1 + o(1))ηx/log x, whenst η = ζ(2)/ζ(n)

The geostatistical properties of test statistics optimally constructed employing traditional clustered standard errors are well developed in the literature beginning with Arellano [1987]. A paper by Hansen [2004] provides a thorough analysis that extends the traditional fixed-T, large-n results to include large-T, large-n results and large-T, fixed-n results. Unfortunately, Hansen [2006] did not provide results for the case where time period dummies are included (e.g., PROG REG). A key assumption in showing that the traditional time series, positively autocorrelated, orthogonally clustered, standard errors are valid in optimizable, sub-meter resolution, grid-stratifiable, endemic, malaria, oviposition, mosquito, aquatic, larval habitat dataset is that the vulnerability forecast regressors and the error terms are independent across the neighbourhood [see 2]. This assumption rules out the possibility of correlation across predictive, seasonal, vector, arthropod-related, endemic, oviposition, optimally parameterizable, empiricial geosampled, capture point, covariate coefficients [i.e. spatial autocorrelation in the cross-section is not quantitable]. Whenst there is spatial correlation in the cross-section, traditional, clustered, geo-spatiotemporal, ecto-entoepidemiological, empirical datset, standard errors derived are no longer valid[2].

As shown by Driscoll and Kraay [1988] it is possible however to obtain standard errors in a panel, seasonal, multivariate, predictive, risk model that are robust to general forms of spatial correlation in the cross-section. These standard errors would retain robustness to heteroskedasticity and serial correlation in the diagnostic residual plots (e.g., Q-Q) in a vulnerability, prognosticative, endemic, forecast-oriented, malaria oviposition, endmember, geoclassifiable, sub-meter resolution, grid-stratifiable,orthogonal, LULC model though the serial correlation would be weakly time series dependent. For instance, by stacking the k×1 vectors $\hat{v}_{1t},\hat{v}_{2t},\ldots,\hat{v}_{nt}$ v̂1t,v̂2t,…,v̂nt into an nk×1vector $\hat{v}_t$ v̂t with transpose $\hat{v}_t'=[\hat{v}_{1t}',\hat{v}_{2t}',\ldots,\hat{v}_{nt}']$ v̂t′=[v̂1t′,v̂2t′,…,v̂nt′], a medical entomologist or malarialogist could theoretically define $\hat{\bar{v}}_t=\sum_{i=1}^{n}\hat{v}_{it}$. v¯̂t=∑i=1nv̂it in an ent-eco-epidemiological, evidential, probabilistic, malarial, immature habitat, oviposition, prognosticative, capture point, ento-ecoepidemiological, sub-meter resolution, grid-stratifiable, geo-spectrotemporal, geosampled, risk model. Note that $\hat{\bar{v}}_t$ v¯̂t would be n times the cross-section average of $\hat{v}_{it}$ v̂it in the oviposition model. For instance, suppose a medical entomologist malarialogist or other experimenter computes a HAC estimator for a prognosticative, qualitatively optimizable, regression-related, vulnerability, malaria, mosquito LULC, endmember model employing the $\hat{\bar{v}}_t$ v¯̂t as follows:equation $\hat{\bar{\Omega}}=\hat{\bar{\Gamma}}_0+\sum_{j=1}^{T-1}k\left(\frac{j}{M}\right)\left(\hat{\bar{\Gamma}}_j+\hat{\bar{\Gamma}}_j'\right),\quad \hat{\bar{\Gamma}}_j=T^{-1}\sum_{t=j+1}^{T}\hat{\bar{v}}_t\hat{\bar{v}}_{t-j}'.$ Ω=Γ¯̂0+∑j=1T−1k(jM)(Γ¯̂j+Γ¯̂j′),Γ¯̂j=T−1∑t=j+1Tv¯̂tv¯̂t−j′.An equivalent expression for $\hat{\bar{\Omega}}$ Ω¯̂ could then be given by $\hat{\bar{\Omega}}=T^{-1}\sum_{t=1}^{T}\sum_{s=1}^{T}K_{ts}\hat{\bar{v}}_t\hat{\bar{v}}_s'$, Ω¯̂=T−1∑t=1T∑s=1TKtsv¯̂tv¯̂s′,where Kts may be definable as $\hat{\bar{\Omega}}$ Ω¯̂ which may be employable for regressively quantitating the middle term of any, geosampled, ento-ecoepidemiological, dependent, regressively optimizable, endmember, estimatator,variance–covariance matrix whenst V̂HACSC=T(∑i=1n∑t=1Tx˜itx˜it′)−1Ω¯̂(∑i=1n∑t=1Tx˜itx˜it′)−1. Notice that V̂HACSC and V̂ave(n) are very similar except that V̂HACSC uses the “HAC of the cross-section averages” whereas V̂ave(n) employs “cross-section averages of HACs.

Note that putting full weight on all the sample geoclassified, LULC autocovariances in an oviposition, geo-spectrotemporal, geosampled, malaria, ento-eco-epidemiological, forecast vulnerability, capture point, model regression framework is not an option in practice for $\widehat{\widehat{\Omega}}\hat{\Omega}$ as $\bar{\Omega}=\bar{\Gamma}0+\sum j=1T-1(\bar{\Gamma}j+\bar{\Gamma}j')=T-1S\bar{T}S\bar{T}=0$, employing $S\bar{T}=\sum t=1Tv\bar{t}=\sum t=1T\sum i=1n\hat{v}it=\sum t=1T\sum i=1nx\tilde{i}t\hat{u}it=0$. Placing full weight on the aquatic, larval habitat, endmember, LULC sample autocovariances could however render an endemic, vulnerability, parasitological, parametric estimator that is identically zero for any seasonal, geo-spectrotemporal, geosampled, vector, arthropod-related, empirical, malaria, mosquito, capture point, field-operational, clinical, or remote geosampled, ento-ecoepidemiological, endmember sub-meter resolution, grid-stratifiable, optimizable dataset.

An interesting twist on kernel HAC estimators that are special cases of $\hat{V}ave(n)$ and $\hat{V}HACSC$ is BCH. BCH can consider covariance matrix estimators in generalizable situations where an empirical, optimizable, ento-ecoepidemiological, geospectrotemporal geosampled, malarial, mosquito, oviposition sub-meter resolution, grid-stratfiiable, empirical, capture point, endmember dataset can be divided into clusters that are asymptotically independent. In so doing, for a given time dimension, the seasonal, geosampled, malaria, mosquito, vector, arthropod-related, probabilistically regressable, ento-eco-epidemiological, empirical datasets can be optimally analyzed by dividing the time dimension into contiguous (i.e., non-overlapping), non-exhaustive groups (e.g., time-related, diagnostic, geo-spectrotemporally prioritized clusters) corresponding to timeperiods$\{1,\ldots,[\lambda 1T]\}\{1,\ldots,[\lambda 1T]\},\{[\lambda 1T]+1,\ldots,[\lambda 2T]\},\ldots,\{[\lambda G-1T]+1,\ldots,T\}\{[\lambda 1T]+1,\ldots,[\lambda 2T]\},\ldots,\{[\lambda G-1T]+1,\ldots,T\}$ where $0<\lambda 1<\lambda 2<\cdots<\lambda G-1<10<\lambda 1<\lambda 2<\cdots<\lambda G-1<1$, for example. Hence setting $\lambda 0=0$ and $\lambda G=1$could optimally render geostatistically significant, explanatory, sub-meter resolution, grid-stratifiable, capture point, oviposition, covariate coefficients in regressable residual, forecast, vulnerability, malaria mosquito, grid-stratifiable, dataset. Also by letting Kts=1, the time periods t and s would be geolocated in the same seasonal, geosampled, time period, autocorrelated cluster and Kts=0 which would lead to the BCH–HAC oviposition, estimators[i.e.,$\Omega\hat{i}BCH=T-1\sum t=1T\sum s=1TKts\hat{v}it\hat{v}is'=T-1\sum g=1G[(\sum t=[\lambda g-1T]+1[\lambda gT]\hat{v}it)(\sum t=[\lambda g-1T]+1[\lambda gT]\hat{v}it')]$. These probabilistic, endmember, residual, prognosticative, oviposition, malaria model, parameterizable, aquatic, larval, habitat estimators can thereafter be viewed as a generalization of the variance-covariance matrix estimator of a forecasting, multivariate, vector, arthropod-related, eco-entomological, endemic transmission, parasitological, risk model.

Alternatively, it may be possible to obtain standard errors in a panel, seasonal, vector, arthropod-related, ento-ecoepidemiological, forecast, vulnerability, endemic, malarial, mosquito, sub-meter resolution, grid-stratfiiable, endmember, risk model that are robust to general forms of spatial correlation in the cross-section. For example, by stacking the $k\times 1$ vectors $\hat{v}1t,\hat{v}2t,\ldots,\hat{v}nt$ into an $nk\times 1$ vector $\widehat{v}_t\hat{v}t$ with transpose $\hat{v}t'=[\hat{v}1t',\hat{v}2t',\ldots,\hat{v}nt']$, a seasonal, multivariate, vector, arthropod-related, ento-ecoepidemiological, predictive, sub-meter resolution, grid-stratifiable, geo-spectrotemporal, geosampled, ovipositon, risk model may define $\widehat{v}_t = \sum_{i=1}^{n} \widehat{v}_{it}$. $v\bar{t}=\sum i=1n\hat{v}it$ which can then render $\widehat{\widehat{v}}_t v\bar{t}$ n times the cross-section average of $\widehat{v}_{it}\hat{v}it$. Suppose the medical entomologist or malarialogist computes a diagnostic, HAC estimator[i.e., $\widehat{\widehat{v}}_t v\bar{t}$] I an oviposition model as follows: $\bar{\Omega}=\bar{\Gamma}0+\sum j=1T-1k(jM)(\bar{\Gamma}j+\bar{\Gamma}j'),\bar{\Gamma}j=T-1\sum t=j+1Tv\bar{t}v\bar{t}-j'(1.1)$. An equivalent robust expression for $\widehat{\widehat{\Omega}}\hat{\Omega}$ could then be also given by $\bar{\Omega}=T-1\sum t=1T\sum s=1TKtsv\bar{t}v\bar{s}'$, where Kts is defineable by equation (1.1). In so doing, $\widehat{\widehat{\Omega}}\hat{\Omega}$ could be usable as the middle term of the estimate variance–covariance matrix, for optimally regressively deriving the predictive, LULC, optimizable, equation $\hat{V}HACSC=T(\sum i=1n\sum t$ where $tx\tilde{i}t')-1\bar{\Omega}(\sum i=1n\sum t=1Tx\tilde{i}tx\tilde{i}t')-1$ may geolocate an unknown, un-geosampled, eco-georeferenceable, hyperproductive, LULC, capture point, seasonal,aquatic, larval habitat foci. Notice that $\hat{V}HACSC$ and $\hat{V}ave(n)$ are very similar except that $\hat{V}HACSC$ uses the "HAC of the cross-section averages" while $\hat{V}ave(n)$ uses "cross-section averages of HACs".

Unfortunately putting full weight on all the sample autocovariances would then be not an option in practice for $\hat{\Omega}$ in the malaria, oviposition, forecast, endmember, vulnerability, LULC model as then $\bar{\Omega}=\bar{\Gamma}0+\sum j=1T-1(\bar{\Gamma}j+\bar{\Gamma}j')=T-1S\bar{T}S\bar{T}'=0$, whenst $S\bar{T}=\sum t=1Tv\bar{t}=\sum t=1T\sum i=1n\hat{v}it=\sum t=1T\sum i=1nx\tilde{i}t\hat{u}it=0$. Fortunately, placing full weight on the sample autocovariances gives an estimator that is identically zero for any uncertainty dataset.

Currently, two classes of standard errors have been thoroughly analyzed in ento-ecoepidemiological, oviposition, malaria, mosquito, capture point, endemic, endmember, forecast, vulnerability modelling in literature for

testing non-normality in multivariate, seasonal, transmission-oriented, ento-ecoepidemiological, signature, LULC, risk analyses. Both are based on HAC covariance matrix estimators. The first class is based on averages of HAC estimators across individual, seasonal, geo-spectrotemporal, geosampled, multivariate, vector, arthropod-related, explanatory, endemic transmission-oriented, geosampled, eco-georeferenceable, aquatic larval, sub-meter resolution, grid-stratfiiable, prognosticative, endmember variables employing the averages of HACs. This class also includes various well known cluster standard errors. The second class is based on the HAC of cross-section averages as proposed. Unfortunately, the"HAC of averages" standard errors are non-robust whenst there exists heteroskedasticity and multicollinearity; thus, they are weak dependent in the time dimension.

Conversely, a fixed-*b* asymptotic malaria, endmember, oviposition, forecast, vulnerability, sub-meter resolution, grid-stratifiable, signature, capture point, aquatic, larval, habitat, LULC model based on both classes of standard errors in seasonal, multivariate, ento-ecoepidemiological, vector, arthropod,capture point, eco-georferenceable models with individual time fixed-effects dummy variables may be employable for targeting hypeproductive, seasonal, sub-mter resolution, oviposition foci. The presence of heteroskedastic or autocorrelated ovispoition, variables in a ento-ecoepidemiological, forecast, vulnerability, endemic, signature, frequency model may not be conspicuous. The covariance matrix of the geo-spectrotemporal geosampled, oviposition, parameterizable, orthogonal, LULC, endmember estimator of an endemic, seasonal, malaria model may be estimated employing a non-paramteric kernel method that involves a lag truncation parameter. Depending on whether this lag truncated parameter is specified, will then determine growth rate which will also be dependent on sample size of the parameterizable covariate, endmember dataset. Two types of asymptotic approximations: the small asymptotics and the fixed-b asymptotics. Employing techniques for quantitating the probabilioty distribution rendered from the oviposiiton, ento-ecoepidemiological, endmember, signature, LULC eco-georeferenceable, geo-spectrotemporal model may determine higher order of expansion in the geosampled, malaria, capture point, model, foci, explanatory estimators. It may be shown that a fixed b asymptotic approximation provides a more robust order of refinement than a first order small-b asymptotics whenst optimally interpreting a geosampled oviposition, endmember, optimizable dataset for determining seasonal hypeporductive foci. This result may provide a justification to utize the fixed b asymptotic approximation in empirical applications whenst mapping prolific, ento-ecoepidemiological, capture point,aquatic, larval habitats.

The asymptotics can then be carried out for time sample empirical, geosampled, capture point datasets employing both fixed and large cross-sectional sample sizes. Extensive simulations may reveal that the fixed-*b* approximation is also much better than the traditional normal or chi-square approximation especially for the Driscoll–Kraay standard errors whenst contructing a robust, endemic, transmission-oriented, vector, arthropod-related, ento-ecoepidemiological, sub-meter resolution, grid-stratifiable, geospectrotemporal, endmember, risk model. Further, the use of fixed-*b* critical values could lead to more reliable inferences in the endemic, transmission-oriented, oviposition, risk model construction practice especially for tests of joint hypotheses. Although "averages of HACs" standard errors are robust to heteroskedasticity including the nonstationary unfortunately, they are not valid in the presence of spatial autocorrelation.

Spatial autocorrelation measures the correlation of a variable with itself through geographic space [2]. Thus, if a medical entomologist or malarialogist, lets $\{a_i\}_{i=0}^{N-1}$ be a periodic sequence, then the autocorrelation of the sequence

$$\rho_i = \sum_{j=0}^{N-1} a_j \, \bar{a}_{j+i},$$

would be the sequence where $\bar{a}$ denotes the complex conjugate and the final subscript is understood to be taken modulo N. Similarly, for a periodic array $a_{i\,j}$ with $0 \le i \le M-1$ and $0 \le j \le N-1$, the autocorrelation, capture point, aquatic, larval habitat, endmember, sub-meter resolution, grid-stratifiable, coefficients in a time series, vector arthropod-related, endemic, transmission-oriented,predictive, vulnerability, multivariate, malaria, grid-stratfiiable, seasonal, oviposition, sub-meter resolution, prioritization,LULC model could be quantitated employing a

$$\rho_{i\,j} = \sum_{m=0}^{M-1} \sum_{n=0}^{N-1} a_{m\,n} \, \bar{a}_{m+i,n+j},$$

$(2M)\times(2N)$-dimensional matrix given by where the final subscripts are understood to be taken modulo M and N, respectively. By definition, the complex conjugate satisfies $\bar{\bar{z}} = z$.[3]. The conjugate is $\overline{z_1 + z_2} = \bar{z}_1 + \bar{z}_2$ distributive under complex addition,

since $\overline{(a_1 + i\,b_1) + (a_2 + i\,b_2)} = \overline{(a_1 + a_2) + i\,(b_1 + b_2)} = (a_1 + a_2) - i\,(b_1 + b_2) = (a_1 - i\,b_1) + (a_2 - i\,b_2)$ and $\overline{a_1 + i\,b_1} + \overline{a_2 + i\,b_2}$, . Further, $\overline{z_1\,z_2} = \overline{z}_1\,\overline{z}_2$, may be a distributive over complex multiplication scheme in an orthogonal, multivariate, seasonal, prognosticative, vector arthropod-related, endemic, transmission oriented, eco-epidemiological, vulnerability,geo-spectrotemporal, endemic, model since $\overline{(a_1 + b_1\,i)\,(a_2 + b_2\,i)} = (a_1\,a_2 - b_1\,b_2) - i\,(a_1\,b_2 + a_2\,b_1) = (a_1 - i\,b_1)\,(a_2 - i\,b_2) \overline{a_1 + i\,b_1}\;\overline{a_2 + i\,b_2}$.For a complex function f, the eigenfunction autocorrelation coefficients in an empirical orthogonally eigendecomposed endmember datasets of ento-ecoepidemiological, time series, residual,LULC, vulnerability forecasts would then be defineable by $f \star f = \int_{-\infty}^{\infty} \overline{f}\,(\tau)\,f\,(\tau + t)\,d\,\tau$, where $\star$denote cross-correlation and $\overline{f}$ is the complex conjugate. Note that the notation $\rho_f\,(t)$is sometimes used for $f \star f$and that the quantity $R_f\,(t) \equiv \lim_{T\to\infty} \frac{1}{2\,T} \int_{-T}^{T} f\,(\tau)\,f\,(t + \tau)\,d\,\tau$ is sometimes known as the autocorrelation of a continuous real function $f\,(t)$[3].

Thus, if we let X be some repeatable process (e.g., measured, aquatic, larval habitat, oviposition, density, count value), and i be some point in time after the start of that process in a seasonal, predictive, multivariate, vector, arthropod related, malarial, endemic, transmission-oriented, regression-based, LULC, predictive, risk model, i may be an integer for a discrete-time process, or a geo-spectrotemporally geosampled, explanatory, endemic, transmission-oriented, parameterizable, endmember, covariate, coefficient value for a continuous-time process. Then X_i would be the value or realization optimally rendered by a given run of the process at time i. For example, suppose that the endemic, vector, arthropod-related, endemic, disease transmission is known to have well-defined field and remote geo-spectrotemporally geosampled, explanatory, oviposition, sub-meter resolution, grid-stratifiable, geosampled,endmember, LULC, covariate, coefficient value for mean μ_i and variance σ_i^2 for all seasonal sample times i. Then the definition of the autocorrelation in a robustifiable, vector arthropod-related, seasonal, predictive, risk model between times s and t would be denotable employing $R(s,t) = \frac{\mathrm{E}[(X_t - \mu_t)(X_s - \mu_s)]}{\sigma_t \sigma_s}$, where "E" is the expected value operator. Note that this expression would not be well-defined for all time series or processes in the predictive, seasonal, multivariate, vector, arthropod-related, eco-epidemiological, oviposition, risk, LULC model, ento-epidemiological, residual forecasts (e.g.,geolocations of eco-georferenecable, seasonal hyperproductive foci) as the variance may be zero especially for a constant process.

Theoretically, if the function R is well-defined in an oviposition, predictive, grid-stratifiable, seasonal, multivariate, vector, arthropod-related, endemic, transmission oriented, malaria, LULC, endmember, sub-meter resolution, risk model, its value must lie in the range $[-1, 1]$, with 1 indicating perfect correlation and -1 indicating perfect anti-correlation.

Additionally, if X_t is a second-order stationary process then the mean μ and the variance σ^2 are time-independent, and the autocorrelation in the expositorial, eco-epidemiological, residual, forecast \-oriented, vector, arthropod-related, explanatory, observational, endmember, parasitological, malaria, mosquito, aquatic, larval, habitat endmember LULC, predictors would depend only on the lag between t and s. Further, in the ento-ecoepidemiological, sub-mter reoslution, grid-stratfiied, vulnerability forecasts (seasonal, prolific, eco-georeferenceable foci), the correlation would depend only on the time-distance values (e.g. prevalence rates, geosampled, aquatic, larval habitat, frequency, wavelength, count indicators) but, not on their position in time. This implies that the autocorrelation in a predictive, multivariate, seasonal, malaria, endemic, transmission-oriented, optimizable, eco-entomological, endmember, geoclassifiable, LULC eco-georeferenecable, oviposition, risk model may be expressed as a function of the time-lag. In so doing, the diagnostic, endmember forecasts (e.g., targeted, hyperproductive, immature, seasonal, capture point, autocorrelated, grid-stratified, quantitable, orthogonal geo-spectrotemporal eco-georeferenceable, cluster) would render an even function of the lag $\tau = s - t$. This would provide the form $R(\tau) = \frac{\mathrm{E}[(X_t - \mu)(X_{t+\tau} - \mu)]}{\sigma^2}$. Fortunately, the fact that this is an even function can be stated as $R(\tau) = R(-\tau)$ in the forecasts targeting the

statictically significant explanatory, geosampled, vector, arthropod-related, endemic, transmission-oriented, foci clustering, parameterizable, covariate coefficients.

Regardless, normalization would still be important in any, robust, endemic, seasonal, predictive, vector, arthropod-related, transmission-oriented, sub-meter resolution, grid-stratifiable, ento-ecoepidemiological, endmember,LULC malaria, oviposition, risk model since the interpretation of the autocorrelation as a correlation coefficient can provide a scale-free measure of the strength of statistical dependence. Normalization will have an effect on the immature, capture point endmember, uncoalesced habitat properties of the estimated seasonal, serially correlated, endmember, predictor variables. Since autocorrelation can be quantifiable as the correlation amongst values of a single variable in a robust, vector, arthropod-related, malarial, oviposition, endemic, transmission-oriented, endmember, LULC, risk model, strictly attributable to their relatively close geolocational positions on a two-dimensional surface, introducing a deviation from the independent observations assumption of classical statistics[1], it may be vital to seasonally quantitate this component in a seasonal, malaria, orthogonal, vector arthropod, capture point, risk model, endmember framework whenst eco-georefernecable, targeting hyperproductive, seasonal, ento-ecoepidemiological foci.

Unfortunately, currently, in seasonal, multivariate, prognosticative, vector, arthropod-related, probabilistic, malarial, eco-epidemiological, sub-mter reoslution,geoclassifiable, optimizable, grid-stratifiable, endmember, LULC, risk models, the above definition is often employed without the normalization, that is, without subtracting the mean and dividing by the variance. As such, when the autocorrelation function is normalized by mean and variance in the endemic, LULC, orthogonal, risk model, it would act as an autocorrelation coefficient. In a seasonal, predictive, vector, arthropod-related, eco-georferenecable, endemic, transmission-oriented, oviposition, malaria, endemic, risk model. Given a signal $f(t)$, the continuous autocorrelation $R_{ff}(\tau)$ may be defined as the continuous cross-correlation integral of $f(t)$with itself, at lag τ.whenst $R_{ff}(\tau) = (f(t) * \overline{f}(-t))(\tau) = \int_{-\infty}^{\infty} f(t+\tau)\overline{f}(t)\,\mathrm{d}t = \int_{-\infty}^{\infty} f(t)\overline{f}(t-\tau)\,\mathrm{d}t$where $\overline{f}$ represents a seasonal, hyperproductive foci.

Methods Materials

Study area: The studies were conducted 100 km northeast of Nairobi, in Karima village within Mwea Rice Scheme in Kenya. Mwea occupies the lower altitude zone of the Kirin-yaga District in an expansive low-lying, formally wet-savannah ecosystem. The Mwea rice irrigation scheme is lo-cated in the west central region of Mwea Division and coversan area of approximately 13,640 hectares. More than 50% of the scheme area is used for rice cultivation. The remaining area is used for subsistence farming, grazing, and communityactivities. The mean annual precipitation is 950 mm withmaximum rainfall occurring in April–May and October–November. The average temperatures range from 16°C to26.5°C. Relative humidity varies from 52% to 67%. The study site village Karima has approximately 358 homesteads with more than 2250 residents. Cows, goats, chick-ens, and donkeys are the primary domestic animals and theyare kept within 5 meters of most houses. More than 90% of the houses have mud walls with iron roofing.

Rice cultivation.: In Karima, the beginning of each croppingcycle is scheduled according to the water availability throughthe irrigation water distribution scheme. The schedule of in-dividual rice husbandry also differs within the water availability time limits from one group of rice fields to another. Most fields are cultivated once a year, although some farmers cul-tivate a second crop. The typical cultivation cycle includes asowing–transplanting period (June–August), a growing pe-riod (August–November), and an post-harvest period (No-vember–December). The second crop is cultivated prior tothe short rainy period between January and May. The dura-tion of the rice cycle varies between 120 and 150 days de-pending on the rice variety. The cycle includes a flooded vegetative period when plants develop and grow, a reproductivephase with limited water during which plants stop growingand orient towards the development of the panicles andgrains, and a ripening phase (water is drained) in which plantssenesce and their water content drops. Rice plants are usually transplanted from flooded small seed beds when 20–30 days old, and the vegetative phase lasts 45–60 days, including the seedling transplant, tillering, and stem elongation stages.Tillering extends from the appearance of the first tiller untilthe maximum tiller number is reached. In previois literature (Muturi et al. 2007, Mwangamgi et al 2008), ric-tillering aquatic, larval habitats were found to be the mosqt productive for emrging immatures. Jacob et al. (2009) constructed a rice ecosystem, real-time ArcGIS cyberenvironment for remotely capturing *An. arabienis* aquatic, lareval habitat, seasonal, frequency, density, count values in Karima village, which allowed

detereming a sub-meter resolution ento-ecoepidmeiological, foreast matris and a sub-pixel eco-endmember, vulanreability analyses.

In Karima, 207 temporary, permanent,and semipermanent aquatic habitat sites were located, andmapped using a CSI-Wireless differentially corrected globalpositioning system (DGPS) Max receiver using a OmniStarL-Band satellite signal with a positional accuracy of less than1 meter (Advanced Computer Resources Corp., Nashua,NH). Water bodies were inspected for mosquito larvae usingstandard dipping techniques with a 350-mL dipper to collect the mosquito larvae.The number of dips per habitat was afunction of habitat size (e.g., paddies 0.3–1 hectares) andranged from 15 to 25. All data from the habitat characterization of each aquatic larval habitat was recorded on a fieldsampling form (see Table 2).

Table 2. Environmental sampled within cluster based varying and constant covariates of *immature An, arabiensis* study site as entered in SAS®

Variable	Description	Units
GCP	Ground control points	Decimal-degrees
DISCAP	Distance from capture point	Meters
ELEV	elevation	Meters
DEPTH	Capture point	Meters
CANVEG	Canopy vegetation	Percentage
SEA	Rice-cycle	Meters
DISHAB	Distance between	Meters

Base maps for this study including major roads and hydrography were created using ArcGIS 10.3. Aquatic larval habitat with its associated land coverattributes from Karima were entered into a Vector ControlManagement System (VCMS) (Advanced Computer Re-sources Corp.) database. The VCMS database supported mobile field data acquisition in Karima through a Pock-etPC™. All two-way, remote synchronization of data, geo-coding, and spatial display were processed using the embedded geographic information system (GIS) Interface Kit™ that was built using MapObjects™ 2 technology (Earth SystemsResearch Institute). The VCMS database plotted and update GPS ground coordinates of the geosampled, *An. arabiensis* aquatic larval habitat,capture point, eco-georeferenceable, seasonal information and supported exporting LULC data in spatial format whereby any combination of larval habitats and supporting data can be described in a shapefile format (En-vironmental Systems Research Institute, Redlands, CA) for use in an ArcGIS. The database displayed this information onto auser-defined field base map.

2.3 Regression analyses: The relationship between geosampled, immature, sub-meter, oviposition, grid-stratified, eco-georeferenecd, *An. arabiensis*, capture point, aquatic, larval habitats and each individual geo-spatiotemporal, geosampled, endmember, endemic, transmission-oriented, predictive risk–related, explanatory, LULU, sub-meter covariate, at the Mwea study site, was then investigated by single variable regression analysis employing PROC MIXED. Since parasite prevalence data are binomial fractions, a regression model was used, as is standard practice for the analysis of such data. Poisson regression analyses were used to determine the relationship between *An. arabiensis*, capture point, aquatic, habitat larval count data, village –level, prevalence rates and the geosampled characteristics

The regression analyses assumed independent counts (i.e. *Ni*), taken at geosampled habitat locations i=1, 2… n. The *An. arabiensis* larval counts were described by a set of variables denoted by matrix X_i, where a $1\times p$ vector of

eco-georeferenceable, oviposition, capture point, covariate coefficient, indicator values for a geosampled,aquatic, larval habitat geolocation *i*. The expected value of these data was given by $\mu_i (X_i) = n_i (X_i) \exp (X_i\beta)$, where β was the vector of non-redundant parameters in the *An. arabiensis*,capture point, eco-georeferenced, oviposition, ento-ecoepidemiological, LULC risk model and the Poisson rates parameter was given by $\lambda_i (X_i) = \mu_i (X_i)/n_i (X_i)$ [3]. The rates parameter $\lambda_i (X_i)$ was both the mean and the variance of the Poisson distribution for each eco-georeferenceable,capture point, foci geolocation *i*. The dependent variable wastotal geosampled, frequency, larval density count. The Poisson regression model assumed that the geosampled, aquatic, larval, habitat, geo-spectrotemporal data was equally dispersed-that is, that the conditional variance equaled the condition mean. The procedure used maximum likelihood estimation to find the endmember regression coefficients. The capture point LULC data was log-transformed before analyses to normalize the distribution and minimize standard error

There was considerable overdispersion in the regression-based, capture point, oviposition *An. arabiensis* forecast, vulnerability. ento-ecoepidemiological, endmember model; thus, we employed a negative binomial model with a non-homogeneous mean to determine parameters associated to the seasonal, geosampled, *An. arabiensis*,sub-meter resolution, aquatic, larval, habitat, geo-spectrotemporal, grid-straified, LULC data. Overdispersion is often encountered when fitting very simple parametric models, such as those based on the Poisson distribution [2]. If overdispersion is a feature in a vector, arthropod, capture point, eco-georeferenceable, ento-ecoepidemiological, forecast, vulnerability, distribution model, an alternative endmember model with additional free parameters may provide a better fit [3]. In this research, a Poisson mixture model with a negative binomial distribution was employed, where the mean of the Poisson distribution was itself a random variable drawn from the gamma distribution; thereby, introducing an additional free parameter in the geo-spectrotemporal geosampled, grid-stratified, eco-georeferenced, eco-geoclassified, LULC, aquatic, larval habitat, endmember, distribution model. The family of negative binomial distributions is a two-parameter family which uses several parameterizations for treating overdispersed data [2].The Poisson distribution has one free parameter and does not allow for the variance to be adjusted independently of the mean [3].

A parameterization technique was employed such that two geosampled, capture point, geo-spectrotemporal aquatic, larval, habitat, endmember, capture point, LULC variables p and r with $0 < p < 1$ and $r > 0$. Under this parameterization, the probability mass function of the ento-ecological geosampled, *An. arabiensis*, endemic transmission-oriented, oviposition-related, endmember, explanatory, predictor variables with a NegBin(r, p) distribution took the following form: for $k = 0, 1, 2,$ where: $f(k;r,p) = \binom{k+r-1}{k} \cdot p^r \cdot (1-p)^k$ $\binom{k+r-1}{k} = \frac{\Gamma(k+r)}{k!\cdot\Gamma(r)} = (-1)^k \cdot \binom{-r}{k}$ and $\Gamma(r) = (r-1)!$ We also employed an alternative parameterization for the geosampled, capture point, eco-endmember, LULC data using the mean λ: $\lambda = r \cdot (p^{-1} - 1)$ $p = \frac{r}{r+\lambda}$ and the mass function which then became: $g(k) = \frac{\lambda^k}{k!} \cdot \frac{\Gamma(r+k)}{\Gamma(r)(r+\lambda)^k} \cdot \frac{1}{\left(1+\frac{\lambda}{r}\right)^r}$ where λ and r were the, eco-georeferenecable, geosampled, geo-spectrotemporal parameters.

Under this parameterization, we were able to generate: $\lim_{r\to\infty} g(k) = \frac{\lambda^k}{k!} \cdot 1 \cdot \frac{1}{\exp(\lambda)}$ which was the mass function of a Poisson-distributed random variable with Poisson rate λ. In other words, the alternatively parameterized, negative, binomial distribution generated from the regressed, ovipoition, eco-georeferenecd, malaria, aquatic, larval habitat explanatory, sub-meter resolution, grid-stratfied, endmember, geosampled, LULC, predictor covariates converged to the Poisson distribution, and r controlled the deviation from the Poisson. This made the negative, binomial, habitat model suitable as a robust alternative to the Poisson model for modeling the geo-spectrotemporal,

immature, endmember, capture point, *An. arabiensis* seasonal, geosampled, endemic, transmission-oriented, oviposition, grid-stratified, endmember, LULC, signature, risk–related covariates.

The negative binomial distribution of the geosampled sub-meter resolution, explanatory, geo-spectrotemporal, capture point, observational predictors arose as a continuous mixture of Poisson distributions, where the mixing distribution of the Poisson rate was a gamma distribution. The mass function of the negative binomial distribution of the capture point, eco-georeferenceable, *An. arabiensis* aquatic, larval habitat, predictor variables was written as $f(k)=\int_0^\infty Poisson(k|\lambda)\cdot Gamma(\lambda|r,(1-p)/p)d\lambda = \int_0^\infty \frac{\lambda^k}{k!}\exp(-\lambda)\cdot\frac{\lambda^{r-1}\exp(-\lambda p/(1-p))}{\Gamma(r)((1-p)/p)^r}d\lambda$

$$=\frac{1}{k!\Gamma(r)}p^r\frac{1}{(1-p)^r}\int_0^\infty \lambda^{(r+k)-1}\exp(-\lambda/(1-p))d\lambda = \frac{1}{k!\Gamma(r)}p^r\frac{1}{(1-p)^r}(1-p)^{r+k}\Gamma(r+k)=\frac{\Gamma(r+k)}{k!\Gamma(r)}p^r(1-p)^k$$

2.4 Bayesian matrix: We then considered a regression problem where the dependent variable to be predicted was not a single real-valued scalar but an *m*-length vector of correlated real geosampled, geo-spectrotemporal, hyperproductive, *An. arabiensis* capture point, aquatic, larval habitats. As in the standard regression setup, there were *n* (31) seasonal, oviposition, endemic, transmission-oriented, sub-meter resolution, grid-stratified, eco-endmember, aquatic, larval habitat, signature, geosampled LULC observations, where each,eco-georeferenced, capture point observation *i* consisted of *k*-1 explanatory variables, grouped into a vector $\mathbf{x}_i$of length *k* where a dummy variable with a value of 1 had been added to allow for an intercept coefficient. Our model was viewable as a set of *m* related regression problems for each, eco-georeferenced, explanatory, *An. arabiensis*, endemic, transmission oriented, regresseable, geo-spectrotemporal, geosampled, capture point,foci observation *i*: $y_{i,1}=\mathbf{x}_i^{\mathrm{T}}\boldsymbol{\beta}_1+\epsilon_{i,1}\ldots y_{i,m}=\mathbf{x}_i^{\mathrm{T}}\boldsymbol{\beta}_m+\epsilon_{i,m}$ where the set of errors $\{\epsilon_{i,1},\ldots,\epsilon_{i,m}\}$were all assumed to be correlated. Equivalently, thus, the oviposition, forecast, vulnerability model was viewed as a single regression problem where the outcome is a row vector $\mathbf{y}_i^{\mathrm{T}}$ and the regression coefficient vectors were stacked next to each other, as follows: $\mathbf{y}_i^{\mathrm{T}}=\mathbf{x}_i^{\mathrm{T}}\mathbf{B}+\boldsymbol{\epsilon}_i^{\mathrm{T}}$. The coefficient matrix B was a $k\times m$matrix where the coefficient vectors $\boldsymbol{\beta}_1,\ldots,\boldsymbol{\beta}_m$for each regression problem stacked horizontally: $\mathrm{B}=\left[\begin{pmatrix}\\ \boldsymbol{\beta}_1\\ \\ \end{pmatrix}\cdots\begin{pmatrix}\\ \boldsymbol{\beta}_m\\ \\ \end{pmatrix}\right]=\left[\begin{pmatrix}\beta_{1,1}\\ \vdots\\ \beta_{1,k}\end{pmatrix}\cdots\begin{pmatrix}\beta_{m,1}\\ \vdots\\ \beta_{m,k}\end{pmatrix}\right]$. The noise vector $\boldsymbol{\epsilon}_i$for each, eco-georeferenced, *An. arabiensis*, endemic, transmission-oriented, geo-spectrotemporal, geosampled, oviposition, geoclassifiable, capture point, eco-georeferenceable, aquatic, larval habitat, endmember, LULC observation *i* was jointly normal, so that the outcomes for a given observation were correlated: $\boldsymbol{\epsilon}_i\sim N(0,\boldsymbol{\Sigma}_\epsilon^2)$. We wrote the entire regression problem in matrix form as: $\mathbf{Y}=\mathbf{XB}+\mathbf{E}$, where Y and E were $n\times m$matrices. The design matrix X was an $n\times k$matrix with the geosampled observations stacked vertically, as in the standard linear regression setup: $\mathbf{X}=\begin{bmatrix}\mathbf{x}_1^{\mathrm{T}}\\ \mathbf{x}_2^{\mathrm{T}}\\ \vdots\\ \mathbf{x}_n^{\mathrm{T}}\end{bmatrix}=\begin{bmatrix}x_{1,1}&\cdots&x_{1,k}\\ x_{2,1}&\cdots&x_{2,k}\\ \vdots&\ddots&\vdots\\ x_{n,1}&\cdots&x_{n,k}\end{bmatrix}$. A classical, frequentist, linear, least squares solution was then derived by regressively estimating the matrix of regression coefficients $\hat{\mathbf{B}}$ using the Moore-Penrose pseudoinverse: $\hat{\mathbf{B}}=(\mathbf{X}^{\mathrm{T}}\mathbf{X})^{-1}\mathbf{X}^{\mathrm{T}}\mathbf{Y}$

We employed an Moore-Penrose generalized matrix inverse i$m\times n$matrix This matrix was independently defined by Moore in 1920 and Penrose (1955), and variously known as the generalized inverse, pseudoinverse, or Moore-Penrose inverse. All the vector arthropod-related, malaria, mosquito, oviposition, eco-georeferenced, endemic, sub-meter resolution, grid-stratifiable, transmission-oriented, sub-meter resolution, LULC, endmember, covariate coefficients were entered into a matrix 1-inverse, which was implemented in *Mathematica* as PseudoInverse[*m*]. The Moore-Penrose inverse satisfies $\mathrm{B}\,\mathrm{B}^+\,\mathrm{B}$=B, $\mathrm{B}^+\,\mathrm{B}\,\mathrm{B}^+$=B, $(\mathrm{B}\,\mathrm{B}^+)^{\mathrm{H}}=\mathrm{B}\,\mathrm{B}^+$,$(\mathrm{B}^+\,\mathrm{B})^{\mathrm{H}}=\mathrm{B}^+\,\mathrm{B}$,where $\mathrm{B}^{\mathrm{H}}$was the conjugate transpose [3]. It is also true that $\mathbf{z}=\mathrm{B}^+\,\mathbf{c}$ is the shortest length least squares solution to the problem $\mathrm{B}\,\mathbf{z}=\mathbf{c}$.In the ento-epidemiological, eco-georferenecable, prognosticative, vulnerability, endmember, aquatic, larval, habitat, LULC model

the inverse of $(\mathsf{B}^{\mathsf{H}}\,\mathsf{B})$existed, thus $\mathsf{B}^{+}=(\mathsf{B}^{\mathsf{H}}\,\mathsf{B})^{-1}\,\mathsf{B}^{\mathsf{H}}$, was seen by premultiplying both sides by $\mathsf{B}^{\mathsf{H}}$to create a square matrix which we subsequently inverted to $\mathsf{B}^{\mathsf{H}}\,\mathsf{B}\,\mathbf{z}=\mathsf{B}^{\mathsf{H}}\,\mathbf{c}$, rendering z=$(\mathsf{B}^{\mathsf{H}}\,\mathsf{B})^{-1}\,\mathsf{B}^{\mathsf{H}}\,\mathbf{c}$=$\mathsf{B}^{+}\,\mathbf{c}$,in the diagnostic residual estimates.

To obtain the iterative Bayesian solution we needed to specify the conditional likelihood and then find the appropriate conjugate prior. As with the univariate case of linear Bayesian regression, we found that we could specify a natural conditional conjugate prior which was scale dependent. We wrote our conditional likelihood, ento-ecoepidemiological, capture point, risk model as$\rho(\mathbf{E}|\mathbf{\Sigma}_\epsilon)\propto(\mathbf{\Sigma}_\epsilon^2)^{-n/2}\exp(-\frac{1}{2}\mathrm{tr}(\mathbf{E}^{\mathrm{T}}\mathbf{\Sigma}_\epsilon^{-1}\mathbf{E}))$, and the error E in the seasonal geosampled endemic trasnmission-oriented sub-meter resolution, oviposition, grid-stratified, endmember, signature, *An. arabiensis*, habitat model, iterative, quantitatively interpolative terms of $\mathbf{Y},\mathbf{X}$,and B which yielded$\rho(\mathbf{Y}|\mathbf{X},\mathbf{B},\mathbf{\Sigma}_\epsilon)\propto(\mathbf{\Sigma}_\epsilon^2)^{-n/2}\exp(-\frac{1}{2}\mathrm{tr}((\mathbf{Y}-\mathbf{XB})^{\mathrm{T}}\mathbf{\Sigma}_\epsilon^{-1}(\mathbf{Y}-\mathbf{XB})))$.We sought a natural conjugate prior—a joint density $\rho(\mathbf{B},\sigma_\epsilon)$which was of the same functional form as the likelihood. Since the likelihood was quadratic in B in the endemic transmission-oriented, predictive, oviposition, geo-spectrotemporal, geosampled, risk model, we re-wrote the likelihood so it was normal in $(\mathbf{B}-\hat{\mathbf{B}})$(i.e., the deviation from classical sample *An. arabiensis*, aquatic, larval habitat, eco-endmember,LULC estimate). Using the same technique as with Bayesian linear regression, we decomposed the exponential term using a matrix-form of the sum-of-squares technique. Here, however, we needed to use Kronecker product transformations.

Given an $m\times n$matrix A and a $p\times q$ matrixB, their Kronecker product $\mathsf{C}=\mathsf{A}\otimes\mathsf{B}$, also called their matrix direct product, is an $(m\,p)\times(n\,q)$matrix with elements defined by $c_{\alpha\beta}=a_{i\,j}\,b_{k\,l}$, where α=$p\,(i-1)+k$ and β=$q\,(j-1)+l$.[3]. The matrix direct product was implemented in *Mathematica* as KroneckerProduct[*a*, *b*]. The matrix direct product rendered the LULC, oviposition, seasonal, geo-spectrotemporal, geosampled endemic, transmission-oriented, sub-meter resolution, grid-stratfied, endmember, signature, capture point, *An. arabiensis* related, regression-based matrix of the linear transformation induced by the vector space tensor product of the original vector spaces in the model. The Kronecker product of the endmember, sub-meter resolution, grid-stratfied, forecast, vulnerability model was denoted by ⊗ which was based an operation on two matrices of arbitrary size resulting in a block matrix. Hence, our matrix was a generalization of the outer product from vectors to matrices, which rendered the matrix of the tensor product with respect to a standard choice of basis. Initially, we employed A which was an *m* × *n* matrix and B which was a *p* × *q* matrix . In so doing, the Kronecker product A ⊗ B was the *mp* × *nq* block matrix: $\mathbf{A}\otimes\mathbf{B}=\begin{bmatrix}a_{11}\mathbf{B} & \cdots & a_{1n}\mathbf{B}\\ \vdots & \ddots & \vdots\\ a_{m1}\mathbf{B} & \cdots & a_{mn}\mathbf{B}\end{bmatrix}$, more explicitly:

$$\mathbf{A}\otimes\mathbf{B}=\begin{bmatrix}a_{11}b_{11} & a_{11}b_{12} & \cdots & a_{11}b_{1q} & \cdots & \cdots & a_{1n}b_{11} & a_{1n}b_{12} & \cdots & a_{1n}b_{1q}\\ a_{11}b_{21} & a_{11}b_{22} & \cdots & a_{11}b_{2q} & \cdots & \cdots & a_{1n}b_{21} & a_{1n}b_{22} & \cdots & a_{1n}b_{2q}\\ \vdots & \vdots & \ddots & \vdots & & & \vdots & \vdots & \ddots & \vdots\\ a_{11}b_{p1} & a_{11}b_{p2} & \cdots & a_{11}b_{pq} & \cdots & \cdots & a_{1n}b_{p1} & a_{1n}b_{p2} & \cdots & a_{1n}b_{pq}\\ \vdots & \vdots & & \vdots & \ddots & & \vdots & \vdots & & \vdots\\ \vdots & \vdots & & \vdots & & \ddots & \vdots & \vdots & & \vdots\\ a_{m1}b_{11} & a_{m1}b_{12} & \cdots & a_{m1}b_{1q} & \cdots & \cdots & a_{mn}b_{11} & a_{mn}b_{12} & \cdots & a_{mn}b_{1q}\\ a_{m1}b_{21} & a_{m1}b_{22} & \cdots & a_{m1}b_{2q} & \cdots & \cdots & a_{mn}b_{21} & a_{mn}b_{22} & \cdots & a_{mn}b_{2q}\\ \vdots & \vdots & \ddots & \vdots & & & \vdots & \vdots & \ddots & \vdots\\ a_{m1}b_{p1} & a_{m1}b_{p2} & \cdots & a_{m1}b_{pq} & \cdots & \cdots & a_{mn}b_{p1} & a_{mn}b_{p2} & \cdots & a_{mn}b_{pq}\end{bmatrix}.$$

We noted that if A and B represent linear transformations $V_1\to W_1$ and $V_2\to W_2$, respectively in the endemic, transmission-oriented, geo-spectrotemporal, ento-ecoepidemiological, geosampled dataset of capture point, foci endmember, prognosticators then A ⊗ B represented the tensor product of the eco-georeferenced, *An. arabiensis*,

explanatory, LULC, observation model estimator $V_1 \otimes V_2 \rightarrow W_1 \otimes W_2$. We then calculated the sum-of-squares to obtain expression for the likelihood $\rho(\mathbf{Y}|\mathbf{X},\mathbf{B},\mathbf{\Sigma}_\epsilon) \propto \mathbf{\Sigma}_\epsilon^{-(n-k)/2}\exp(-\mathrm{tr}(-\frac{1}{2}\mathbf{S}^{\mathrm{T}}\mathbf{\Sigma}_\epsilon^{-1}\mathbf{S}))(\mathbf{\Sigma}_\epsilon^2)^{-k/2}\exp(-\frac{1}{2}\mathrm{tr}((\mathbf{B}-\hat{\mathbf{B}})^{\mathrm{T}}\mathbf{X}^{\mathrm{T}}\mathbf{\Sigma}_\epsilon^{-1}\mathbf{X}(\mathbf{B}-\hat{\mathbf{B}})))$, $\mathbf{S} = \mathbf{Y} - \hat{\mathbf{B}}\mathbf{X}$ We also developed a robust conditional form for the priors: $\rho(\mathbf{B},\mathbf{\Sigma}_\epsilon) = \rho(\mathbf{\Sigma}_\epsilon)\rho(\mathbf{B}|\mathbf{\Sigma}_\epsilon)$, where r$\rho(\mathbf{\Sigma}_\epsilon)$ was an inverse-Wishart distribution and $\rho(\mathbf{B}|\mathbf{\Sigma}_\epsilon)$ was some form of normal distribution in the matrix B. This was accomplished employing the vectorization transformation, which converted the likelihood from a function of the matrices $\mathbf{B},\hat{\mathbf{B}}$ to a function of the vectors $\boldsymbol{\beta} = \mathrm{vec}(\mathbf{B}), \hat{\boldsymbol{\beta}} = \mathrm{vec}(\hat{\mathbf{B}})$ We then wrote the residual LULC endmember model $\mathrm{tr}((\mathbf{B}-\hat{\mathbf{B}})^{\mathrm{T}}\mathbf{X}^{\mathrm{T}}\mathbf{\Sigma}_\epsilon^{-1}\mathbf{X}(\mathbf{B}-\hat{\mathbf{B}})) = \mathrm{vec}(\mathbf{B}-\hat{\mathbf{B}})^{\mathrm{T}}\mathrm{vec}(\mathbf{X}^{\mathrm{T}}\mathbf{\Sigma}_\epsilon^{-1}\mathbf{X}(\mathbf{B}-\hat{\mathbf{B}}))$ We formulated the expression $\mathrm{vec}(\mathbf{X}^{\mathrm{T}}\mathbf{\Sigma}_\epsilon^{-1}\mathbf{X}(\mathbf{B}-\hat{\mathbf{B}})) = (\mathbf{\Sigma}_\epsilon^{-1}\otimes\mathbf{X}^{\mathrm{T}}\mathbf{X})\mathrm{vec}(\mathbf{B}-\hat{\mathbf{B}})$, where $\mathbf{A}\otimes\mathbf{B}$ denoted the Kronecker product of matrices A and B. A generalization of the outer product was multiplied for tabularizing an $m \times n$ matrix by a $p \times q$ matrix to generate an $mp \times nq$ matrix, consisting of every combination of products of elements from the two matrices. Then $\mathrm{vec}(\mathbf{B}-\hat{\mathbf{B}})^{\mathrm{T}}(\mathbf{\Sigma}_\epsilon^{-1}\otimes\mathbf{X}^{\mathrm{T}}\mathbf{X})\mathrm{vec}(\mathbf{B}-\hat{\mathbf{B}}) = (\boldsymbol{\beta}-\hat{\boldsymbol{\beta}})(\mathbf{\Sigma}_\epsilon^{-1}\otimes\mathbf{X}^{\mathrm{T}}\mathbf{X})(\boldsymbol{\beta}-\hat{\boldsymbol{\beta}})$ which consequently lead to a likelihood quantification which was normalized [i.e. $(\boldsymbol{\beta}-\hat{\boldsymbol{\beta}})$].With the likelihood in a more tractable form, we found a natural (i.e., conditional) conjugate prior for the predictive, oviposition, geo-spectrotemporalendemic trasnmission-oriented, endmember, sub-meter resolution, oviposition, grid-stratified, endmember, geosampled, *An. arabiensi*,s endemic transmission-oriented, forecast, vulnerability model.

To obtain the Bayesian solution, we specified the conditional likelihood and then found the appropriate conjugate prior in the eco-georeferenced, seasonal, geosampled, endemic trasnmission-oriented, *An. arabiensis* signature, related, endemic, transmission-oriented, risk model LULC, endmember estimators. As with the univariate case of linear Bayesian regression, we found that we could specify a natural conditional conjugate prior which was scale dependent. We then wrote our conditional likelihood as $\rho(\mathbf{E}|\mathbf{\Sigma}_\epsilon) \propto (\mathbf{\Sigma}_\epsilon^2)^{-n/2}\exp(-\frac{1}{2}\mathrm{tr}(\mathbf{E}^{\mathrm{T}}\mathbf{\Sigma}_\epsilon^{-1}\mathbf{E}))$, writing the error E in terms of $\mathbf{Y},\mathbf{X}$, and B which yielded $\rho(\mathbf{Y}|\mathbf{X},\mathbf{B},\mathbf{\Sigma}_\epsilon) \propto (\mathbf{\Sigma}_\epsilon^2)^{-n/2}\exp(-\frac{1}{2}\mathrm{tr}((\mathbf{Y}-\mathbf{X}\mathbf{B})^{\mathrm{T}}\mathbf{\Sigma}_\epsilon^{-1}(\mathbf{Y}-\mathbf{X}\mathbf{B})))$, We sought a natural conjugate prior—a joint density $\rho(\mathbf{B},\sigma_\epsilon)$ which was of the same functional form as the likelihood. Since the likelihood was quadratic in B in the. sub-meter resolution, oviposition, grid-stratified capture point, ento-ecoepidemiological, eco-georeferenecable, LULC endmember model, we re-wrote the likelihood so it was normal in $(\mathbf{B}-\hat{\mathbf{B}})$.

Employing the same technique as with Bayesian linear regression, we eigendecomposed the exponential term using a matrix-form of the sum-of-squares technique. Here, however, we needed to use Matrix Differential Calculus (i.e., Kronecker product and vectorization transformations).First, we let the sum-of-squares quantitate a new expression for the likelihood: $\rho(\mathbf{Y}|\mathbf{X},\mathbf{B},\mathbf{\Sigma}_\epsilon) \propto \mathbf{\Sigma}_\epsilon^{-(n-k)/2}\exp(-\mathrm{tr}(-\frac{1}{2}\mathbf{S}^{\mathrm{T}}\mathbf{\Sigma}_\epsilon^{-1}\mathbf{S}))(\mathbf{\Sigma}_\epsilon^2)^{-k/2}\exp(-\frac{1}{2}\mathrm{tr}((\mathbf{B}-\hat{\mathbf{B}})^{\mathrm{T}}\mathbf{X}^{\mathrm{T}}\mathbf{\Sigma}_\epsilon^{-1}\mathbf{X}(\mathbf{B}-\hat{\mathbf{B}})))$ $\mathbf{S} = \mathbf{Y} - \hat{\mathbf{B}}\mathbf{X}$. We robustly developed a conditional form for the priors: $\rho(\mathbf{B},\mathbf{\Sigma}_\epsilon) = \rho(\mathbf{\Sigma}_\epsilon)\rho(\mathbf{B}|\mathbf{\Sigma}_\epsilon)$, where $\rho(\mathbf{\Sigma}_\epsilon)$ was an inverse-Wishart distribution and $\rho(\mathbf{B}|\mathbf{\Sigma}_\epsilon)$ was some form of normal distribution in the matrix B. This was accomplished using the vectorization transformation which converted the likelihood from a function of the seasonal, oviposition, geosampled, endemic, transmission-oriented, sub-meter resolution, grid-stratified, rco-endmember, *An. arabiensis*, regression-based, signature-related, multivariate matrices $\mathbf{B},\hat{\mathbf{B}}$ to a function of the vectors $\boldsymbol{\beta} = \mathrm{vec}(\mathbf{B}), \hat{\boldsymbol{\beta}} = \mathrm{vec}(\hat{\mathbf{B}})$. We optimistically calculated the geosampled, LULC, capture point, variable, seasonal distribution and established $\mathrm{tr}((\mathbf{B}-\hat{\mathbf{B}})^{\mathrm{T}}\mathbf{X}^{\mathrm{T}}\mathbf{\Sigma}_\epsilon^{-1}\mathbf{X}(\mathbf{B}-\hat{\mathbf{B}})) = \mathrm{vec}(\mathbf{B}-\hat{\mathbf{B}})^{\mathrm{T}}\mathrm{vec}(\mathbf{X}^{\mathrm{T}}\mathbf{\Sigma}_\epsilon^{-1}\mathbf{X}(\mathbf{B}-\hat{\mathbf{B}}))$.. Therefater, for robuslty quantitating the variables we let $\mathrm{vec}(\mathbf{X}^{\mathrm{T}}\mathbf{\Sigma}_\epsilon^{-1}\mathbf{X}(\mathbf{B}-\hat{\mathbf{B}})) = (\mathbf{\Sigma}_\epsilon^{-1}\otimes\mathbf{X}^{\mathrm{T}}\mathbf{X})\mathrm{vec}(\mathbf{B}-\hat{\mathbf{B}})$, where $\mathbf{A}\otimes\mathbf{B}$ denoted the Kronecker product of matrices A and B.Next, a generalization of the outer product multiplied an $m \times n$ matrix by a $p \times q$ matrix to generate an $mp \times nq$ matrix, consisting of every combination of products of elements from the two matrices. Then $\mathrm{vec}(\mathbf{B}-\hat{\mathbf{B}})^{\mathrm{T}}(\mathbf{\Sigma}_\epsilon^{-1}\otimes\mathbf{X}^{\mathrm{T}}\mathbf{X})\mathrm{vec}(\mathbf{B}-\hat{\mathbf{B}})$ which led to a likelihood which was normal in $(\boldsymbol{\beta}-\hat{\boldsymbol{\beta}})$.With the likelihood in a more tractable form, we then found a natural (i.e., conditional) conjugate prior for the seasonal, geo-spectrotemporal, eco-georeferenced, capture point, aquatic, larval habitat, geosampled endemic, sub-meter resolution, oviposition, grid-stratified, eco-endmember, signature, transmission-oriented,LULC risk model.

We began with a "prior distribution" which was based on the relative likelihoods of the geosampled, *An. arabiensis*, explanatory, endemic, transmission-oriented time series, "Bayesianized" predictive, risk –related, capture point, eco-georeferenced, geo-spectrotemporal, aquatic, larval, habitat covariates. In practice, it is common to assume a uniform distribution over the appropriate range of values for the prior distribution [3].We then calculated the likelihood of the observed distribution as a function of the endmember, sub-meter resolution, oviposition, grid-stratified, parameter values, multiplied this likelihood function by the prior distribution, and then normalized the parameters to obtain a unit probability over all possible values (i.e., posterior distribution). The mode of the distribution was then the parameter estimate, and "probability intervals". These intervals represented the Bayesian analog of confidence intervals in the regression-based distribution model.

In our Bayesian formulation, the specification of aquatic, larval habitat, the *An. arabiensis*, forecast, vulnerability, eco-endmember, signature, LULC, frequency model was completed by assigning priors to all unknown parameters. We used our dataset of geo-spatiotemporal empirical LULC observations, where each x_i for $i = 1 \ldots n$ was assumed to be distributed according to some distribution $p(x_i \mid \theta)$.

In this research, θ was a parameter that was unknown and had to be inferred from the geosampled, ento-ecoepidemiological, eco-georeferenced capture point, LULC data. Our Bayesian procedure began by assuming that θ was distributed according to some prior distribution $p(\theta \mid \alpha)$, where the parameter α was a hyperparameter. The joint probability of the geosampled, endemic, transmission-oriented, sub-meter resolution, oviposition, endmember, signature, predictive, risk-related, ento-ecoepidemiological, geo-spectrotemporal, geosampled, capture point, grid-stratified, habitat data was then determined using: $p(\mathbf{X}|\theta) = p(x_1, \ldots, x_n|\theta) = \prod_{i=1}^{n} p(x_i|\theta)$;whereby, $p(\mathbf{X}|\theta, \alpha) = p(\mathbf{X}|\theta)$ and $p(x_i|\theta, \alpha) = p(x_i|\theta)$ were conditionally independent on the hyperparameters. Bayesian inference then determined the posterior distribution of the parameter $p(\theta|\mathbf{X}, \alpha)$ employing the robust regressable expression: $p(\theta|\mathbf{X}, \alpha) = \frac{p(\theta, \mathbf{X}, \alpha)}{p(\mathbf{X}, \alpha)} = \frac{p(\theta, \mathbf{X}, \alpha)}{\int_\theta p(\theta, \mathbf{X}, \alpha) d\theta} = \frac{p(\mathbf{X}|\theta)p(\theta|\alpha)}{\int_\theta p(\mathbf{X}|\theta)p(\theta|\alpha)\,\mathrm{d}\theta} = \frac{[\prod_{i=1}^{n} p(x_i|\theta)]p(\theta|\alpha)}{\int_\theta [\prod_{i=1}^{n} p(x_i|\theta)]p(\theta|\alpha)\,\mathrm{d}\theta}$. For the fixed, capture point, geosampled, geoclassified, LULC, geo-spectrotemporal, eco-endmember,aquatic, larval, habitat, signature, predictive, regression parameters, we chose a diffuse prior, [i.e., $p(\gamma) \propto const$,] A prior distribution of a parameter is the probability distribution that represents your uncertainty about the parameter before the current data are examined. [2] Multiplying the prior distribution and the likelihood function together leads to the posterior distribution of the parameter. You use the posterior distribution to carry out all inferences[4], A second-order Gaussian random walk prior was then employed to allow enough flexibility in the malaria, forecast, vulnerability model while penalizing abrupt changes in the function.

Thereafter, we generated heterogeneous random walks in one dimension for determining, eco-georeferenecable, geolocations of seasonal, hyperproductive, malaria mosquito foci at the Mwea study siste. A way for simulating such a random walk is when first drawing a random number out of a uniform distribution that determines the propagation direction according to the transition probabilities, and then drawing a random time out of the relevant different jumping time probability density functions JT-PDF[2]. The interval in our geosampled, endemic, trasnmission-oriented, sub-meter resolution, oviposition, grid-stratified, endmember, signature, predictive, LULC endmember data was discrete. In a discrete system, the connections are among adjacent stat while the dynamics are either Markovian, Semi-Markovian, or even not-Markovian depending on the model [2]. Heterogeneous random walks in 1D have jump probabilities that depend on the location in the system, and/or different jumping time (JT) probability density functions (PDFs) that depend on the location in the system [3].Known important results in simple systems include a symmetric Markovian random walk, the Green's function (i.e.,PDF) of the walker for occupying state *i* which is commonly Gaussian and has a variance that scales like time [2].This result holds in a system with discrete time and space, yet also in a system with continuous time and space. Here we used a completely heterogeneous semi Markovian random walk in a discrete system of *L* (>1) where the Green's function was found in Laplace space for determining unknown, geo-spectrotemporal, aquatic, larval habitat, hyperproductive, *An. arabiensis*, oviposition, eco-georeferenced, geo-spectrotemporal, geosampled, capture points. The Laplace transform of a function was t\defined with, $\bar{f}(s) = \int_0^\infty e^{-st} f(t) dt$). In this research the system was defined through the jumping time (JT) PDFs: $\psi_{ij}(t)$ connecting states *i* with state *j*. The jump was from state *i*. The solution was based on the path representation of the

Green's function, calculated by including all the path PDFs of all the geosampled, eco-georeferenced, aquatic, larval, habitat, explanatory, endmember, eco-georeferenced, aquatic, larval habitat, LULC endmember, predictor covariates using : $\bar{G}_{ij}(s) = \bar{\Gamma}_{ij}(s)\frac{\bar{\Phi}(s,\tilde{L})}{\bar{\Phi}(s,L)}\bar{\Psi}_i(s).$

We subsequently quantitatively derived $\bar{\Psi}_i(s) = \Sigma_j \bar{\Psi}_{ij}(s)$ and $\bar{\Psi}_{ij}(s) = \frac{1-\bar{\psi}_{ij}(s)}{s}$ from $\bar{G}_{ij}(s) = \bar{\Gamma}_{ij}(s)\frac{\bar{\Phi}(s,L)}{\bar{\Phi}(s,L)}\bar{\Psi}_i(s).$ Thereafter, we used these equations to generate the following equations in PROC MCMC : $\bar{\Gamma}_{ij}(s) = \Pi_{c=0}^{i\mp1}\bar{\psi}_{c\pm1c}(s)$, and $\bar{\Phi}(s,L) = 1 + \Sigma_{c=1}^{[L/2]}(-1)^c\bar{h}(s,c;L)$ and $\bar{f}_{k_j}(s) = \bar{\psi}_{k_jk_j+1}(s)\bar{\psi}_{k_j+1k_j}(s)$. Here, $L=1$, $\bar{\Phi}(s;L) = 1$. The symbol $[L/2]$ that appeared in the upper bound in the Σ in these algorithms was the floor operation which essentially entailed rounding off the geo-spectrotemporal, geosampled ecogeoreferenced, sub-meter resolution, grid-stratified, capture point, *An. arabiensis*, endemic, transmission-oriented, oviposition, LULC, signature, prognosticative, eco-endmember covariates towards zero. In this research the factor $\Phi(s,\tilde{L})$ I) had the same form as in $\bar{\Phi}(s;L)$ which was calculated on a lattice $\tilde{L}$. Lattice $\tilde{L}$ was constructed from the original lattice generated from the geosampled, endemic, trasnmission-oriented, sub-meter resolution, aquatic, larval habitat endmember signature, dataset by taking out from it the states *i* and *j* and the states between them, and then connecting the obtained two fragments. When each fragment is a single state, $\bar{\Phi}(s;\tilde{L}) = 1$ [2].

A random walk having a step size that varied according to a normal distribution of the geosampled, eco-georeferenced $= (\boldsymbol{\beta} - \hat{\boldsymbol{\beta}})(\boldsymbol{\Sigma}_\epsilon^{-1} \otimes \mathbf{X}^{\mathrm{T}}\mathbf{X})(\boldsymbol{\beta} - \hat{\boldsymbol{\beta}})$ aquatic, larval habitat, endemic transmission-oriented,forecast, vulnerability–related, explanatory, LULC. endmember covariates was used to geolocate validate geolocations of unknown seasonal, hyperproductive foci. The Black–Scholes formula used a Gaussian random walk as an underlying assumption. Here, the step size was the inverse cumulative normal distribution $\Phi^{-1}(z,\mu,\sigma)$ where $0 \le z \le 1$ were the geosampled, aquatic, larval habitat, density, seasonal, count values and μ and σ were the mean and standard deviations of the normal distribution, respectively. The Black–Scholes equation we used was a partial differential equation. The equation was $\frac{\partial V}{\partial t} + \frac{1}{2}\sigma^2 S^2 \frac{\partial^2 V}{\partial S^2} + rS\frac{\partial V}{\partial S} - rV = 0.$ our data followed a classic geometric Brownian motion (GBM). That is, $\frac{dS}{S} = \mu\, dt + \sigma\, dW$ where *W* was a Brownian motion. The GBM (i.e. Exponential Brownian motion) is a continuous-time stochastic process in which the logarithm of the randomly varying quantity follows a Brownian motion [2].Brownian motion is the presumably random drifting of suspended particles or the mathematical model used to describe such random movements [3].Note that *W*, and consequently its infinitesimal increment *dW*, were the only source of uncertainty in our model. Intuitively, *W (t)* is a process that fluctuates up and down in such a random way that its expected change over any time interval is 0. The variance over time *T* in *W(t)* when we constructed the Gaussian random walks for the geo-spectrotemporal, vector, insect sub-meter resolution, oviposition, grid-stratified aquatic, larval habitat, endmember distribution,LULC models was essentially equal to *T*;therefore in the model the expected value of *μ is dt* with a variance of $\sigma^2 dt$.

In this research, the stochastic process $S_t = (\boldsymbol{\beta} - \hat{\boldsymbol{\beta}})(\boldsymbol{\Sigma}_\epsilon^{-1} \otimes \mathbf{X}^{\mathrm{T}}\mathbf{X})(\boldsymbol{\beta} - \hat{\boldsymbol{\beta}})$ generated from the, empirical, clinical, field and remote, geo-spatiotemporally geosampled larval habitat, LULC endmember, parameter estimates was said to follow a GBM which satisfied the following stochastic differential equation (SDE): $dS_t = \mu S_t\, dt + \sigma S_t\, dW_t$ where W_t was a Brownian motion and μ ('the percentage drift') and σ were constants. For an arbitrary initial value S_0 the above SDE had the analytic solution under Itō's interpretation: $S_t = S_0 \exp\left(\left(\mu - \frac{\sigma^2}{2}\right)t + \sigma W_t\right)$, which in the malaria, mosquito, sub-meter resolution, oviposition, grid-stratified, eco-georefrenceable, forecast, vulnerability, endmember, signature model was for any value of t, a log-normally distributed explanative, vector arthropod-related immature random variable with expected value $\mathbb{E}(S_t) = S_0 e^{\mu t}$ and variance $\mathrm{Var}(S_t) = S_0^2 e^{2\mu t}\left(e^{\sigma^2 t} - 1\right)$. The correctness of this solution was checked using Itō's lemma.

In its simplest form, Itō's lemma states the following: for an Itō drift-diffusion process $dX_t = \mu_t\,dt + \sigma_t\,dB_t$ and any twice differentiable function $f(t, x)$ of two real variables t and x, one has $df(t, X_t) = \left(\frac{\partial f}{\partial t} + \mu_t\frac{\partial f}{\partial x} + \frac{\sigma_t^2}{2}\frac{\partial^2 f}{\partial x^2}\right)dt + \sigma_t\frac{\partial f}{\partial x}\,dB_t.$ [3].This immediately implies that $f(t, X)$ is itself an Itō drift-diffusion process in any sub-meter resolution, oviposition, grid-stratified, malaria, mosquito, capture point, eco-georrferenced, forecast, vulnerability, endmember,LULC model used for seasonally targeting unknown, hypeproductive, aquatic, larval habitats. In higher dimensions, Ito's lemma explanative, time seres states $df\,(t, X_t) = \dot{f}_t\,(t, X_t)\;dt + \nabla_{X_t}^T f \cdot dX_t + \frac{1}{2}\,dX_t^T \cdot \nabla_{X_t}^2 f \cdot dX_t$ where $X_t = (X_{t,1}, X_{t,2}, \ldots, X_{t,n})^T$ is a vector of Itō processes, $\dot{f}_t\,(t, X)$ is the partial differential w.r.t. t, $\nabla_X^T f$ is the gradient of f w.r.t. X, and $\nabla_X^2 f$ is the Hessian matrix of f w.r.t. X. More generally, the above formula also holds for any continuous d-dimensional semimartingale $X = (X^1, X^2, \ldots, X^d)$, and twice continuously differentiable and real valued function f on R^d. Some people prefer to present the formula in another form with cross variation shown explicitly as follows, $f(X)$ is a semimartingale satisfying $df(X_t) = \sum_{i=1}^{d} f_i(X_t)\,dX_t^i + \frac{1}{2}\sum_{i,j=1}^{d} f_{i,j}(X_t)\,d[X^i, X^j]_t.$ In this expression, the term f_i represents the partial derivative of $f(x)$ with respect to x^i, and $[X^i, X^j]$ is the quadratic covariation process of X^i and X^j.

Finally, for the spatial components, *VI*, a Markov random field (MRF) prior was assigned for quantiating inconspicuous uncertainty (e.g., spatial heteroskedascity) in the endmember, model, capture point, vulnerability, prognosicators. The conditional distribution of *VI*, given an adjacent eco-georeferenced, explanatory, aquatic, larval habitat, geosampled, geo-spectrotemporal, LULC, endmember, predictor covariate, *VJ*, was a univariate normal distribution with mean equalling the average *VJ* coefficient values of *VI's* neighboring geosampled capture point, where the variance was equal to τ_v^2 divided by the number of total adjacent *An. arabiensis.* sub-meter resolution, oviposition, grid-stratified, parameterizable, eco-endmember, capture point, frequency,LULC estimators. This lead to a joint density of the form: $p\left(v|\tau_v^2\right)\alpha\exp\left(-\frac{\tau_v^2}{2}\sum_{i\sim j}\left(v_i - v_j\right)^2\right)$ where $i \sim j$ denoted geosampled habitats i adjacent to j, and where the parameterizable,capture point,eco-georeferenecable LULC endmember estimates *VI* and *VJ* in the adjacent sampled aquatic, larval habitats were similar. The degree of uncertainty in the geo-spectrotemporal, geosampled data was then determined by the unknown precision parameter τ_v^2.

By writing $f_j = Z_j\beta_j$, $h = Z_k\beta_k$, $u = Z_l\beta_l$, and $v = Z_m\beta_m$ for a well- defined design matrix Z, a vector of regression parameters β, with all different priors, was expressed in a general Gaussian form employing the expression: $p\left(\beta_j|\tau_j^2\right)\alpha\exp\left(-\frac{1}{2\tau_j^2}\beta_j' K_j \beta_j\right)$ with an appropriate penalty matrix K_j. The model structure was dependent on the geosampled eco-georeferenced explanatory, LULC, endmember, predictor, aquatic, larval habitat covariates and smoothness of the function. In most cases, K_j is rank deficient and, hence, the prior for β_j is improper[2]. For the variances τ_j^2 inverse Gamma priors IG (a_j, b_j) was assumed, with hyperparameters a_j, b_j chosen such that this prior was weakly informative.

The Bayesian framework in this research was defined by conditional probabilities constructed from the geosample, time series, *An. arabiensis* ento-ecoepidmiological,eco-georefernecable, aquatic, larval habitat, endmeber LULC data. The observation nodes in the Bayesian estimation model were denoted by a vector $x = (x_1, x_2, \ldots, x_N)$, and the set of states of the observation node x_j generated from the sampled data that was represented by $x_j \in \{1, 2, \ldots, Y_j\}$.

In the malaria, mosquito, sub-meter resolution, oviposition, grid-stratified, endmember, forecast, vulnerability model the hidden nodes were denoted by $z_k \in \{1, 2, \ldots, T_k\}$. The probability that the state of the hidden node z_k was i, $1 \le i \le T_k$, was expressed as $a_{(k,i)} := P(z_k = i)$. Because $\{a_{(k,i)}, i = 1, 2, \ldots, T_k\}$ was a probability distribution,

$\sum_{i=1}^{T_k} a_{(k,i)} = 1$ which held for $k = 1, 2, \ldots, K$ in the model, the conditional probability was the *j*th observation node x_j and *l*,$(1 \leq l \leq Y_j)$ which was based on the condition that the states of hidden nodes $[z = (z]_1, z_2, \ldots, z_K)$, which were generated by $b_{(j,l|z)} = P(x_j = l|z)$. We defined $a := \{a_{(k,i)}\}$, $b := \{b_{(j,l|z)}\}$ and let $\omega = \{a, b\}$ be the set of all the geosampled *An. arabiensis*, aquatic, larval habitats, geo-spatiotemporal parameters in the Mwea study site. Then the joint probability that the states of observation nodes were $x = (x_1, x_2, \ldots, x_N)$ and the states of hidden nodes were then $[z = (z]_1, z_2, \ldots, z_K)$ which was based on $P(x, z|\omega) = \prod_{k=1}^{K} a_{(k,z_k)} \prod_{j=1}^{N} b_{(j,x_j|z)}$.

The marginal probability that the states of hypeprproductive observation the nodes were *x* was generated using $P(x, z|\omega) = \sum_z P(x, z|\omega) = \left\{\prod_{k=1}^{K} \sum_{zk=1}^{T_k} \square\right\} \prod_{k=1}^{K} a_{(k,z_k)} \prod_{j=1}^{N} b_{(j,x_j|z)}$. We employed the notation $\sum_z = \left\{\prod_{k=1}^{K} \sum_{zk=1}^{T_k} \square\right\} := \sum_{z_1=1}^{T_1} \sum_{z_2=1}^{T_2} \cdots \sum_{z_K=1}^{T_K} \square$ for the summation over all states of hidden nodes. We assumed the geosampled ecogeoreferenced, endmember, *An. arabiensis*, aquatic, larval habitat, -spectrotemporal, endemic transmission-oriented, predictive, risk-related, observational covariates $X_n = \{X_1, X_1, \ldots, X_n\}$ were independently and identically taken from the true distribution $p_0(x)$. In Bayesian learning, the prior distribution $\varphi(\omega)$ on the parameter ω is set [2]. Here, the posterior distribution $p(\omega|X^n)$ was computed from the eco-georeferenecd, geo-spectrotemporal, capture point, oviposition, ento-ecoepidemiological, aquatic larval habitat,eco-endmember LULC dataset and the prior by $p(\omega|X^n) = \frac{1}{Z(X^n)} \exp(-nH_n(\omega))\, \varphi(\omega)$ which was generated employing the expression$H_1 n\ (\omega) = 1/n\ \Sigma_1 (i = 1)^{\uparrow} n \square \log (po\{X_{\downarrow} i\}) / (p\{X_{\downarrow} i\ )|\omega))$, and $Z(X^n)$(i.e., the normalization constant). The Bayesian predictive distribution $p(x|X^n)$ was provided by averaging the model over the posterior distribution as follows, $p(x|X^n) = \int [p(x|\omega) p(\omega|\square] X^n) d\omega$. The Bayesian stochastic complexity *F* (*Xn*) was defined by $F(X^n) = -\log Z(X^n)$ which was used as a criterion by which the oviposition, forecastable, ento-ecoepidemiological, eco-georeferenced, model estimtors was selected and the vulnerabityhyperparameters in the prior were optimized. We then let $E_{X^n}[\cdot]$ be the expectation over all the geosampled *An. arabiensis*, aquatic, larval habitat, endmember, LULC parameters. The Bayesian stochastic complexity had the following asymptotic form:$E_1(X^{\uparrow} n\ )\ [F(X^{\uparrow} n) \approx \lambda \log n - (m - 1) \log\log n + O(1)$ where λ and *m* were the hyperproductive, seasonal, capture point, geosampled and their indicator, immature, density, count values, respectively. In regular models, 2λ is equal to the number of parameters and $m = 1$, while in non-identifiable models, 2λ is not larger than the number of parameters and $m \geq 1$ [25].However, Bayesian frameworks employing the time series, ento-ecoepidemiological, geo-spectrotemporal, clinical, field and remote-sampled aquatic, larval habitat,LULC endmemver data required integration over the posterior distribution, which typically could not be performed analytically.

We let $\{X^n, Z^n\}$ be the geo-spectrotemporal, endemic, geosampled, *An. arabiensis*, aquatic, larval,habitat, parameterizable,LULC eco-endmebmber,orthogonal estimates corresponding to the hidden error variables in the equation$Z^n = \{Z_1, Z_1, \ldots, Z_n\}$. The variational framework approximated the Bayesian posterior $p(Z^n, \omega|X^n)$ of the hidden variables and the malarial parameters employing the variational posterior$q(Z^n, \omega|X^n)$, which was factorized using$q(Z^n, \omega|X^n) = Q(Z^n|X^n) r(\omega|X^n)$, where $Q(Z^n|X^n)$ and $r(\omega|X^n)$ were posteriors based on the inconspicuous, sub-meter resolution, grid-stratified, geosampled capture point, error coefficients in the empirical, endmember, aquatic, larval, habitat, oviposition, forecasted datasets respectively. The variational posterior $q(Z^n, \omega|X^n)$ was chosen to

minimize the functional $\overline{F}[q]$ which here was defined by $\overline{F}[q] = \sum_{z^n} \int \frac{q(Z^n, \omega | X^n) \log\left(q(Z^n, \omega | X^n) po(X^n)\right)}{p(X^n, Z^n, \omega)} d\omega$ which was then further defined by s$= F(X^{\uparrow} n) + K(q(Z^{\uparrow} n, \omega | X^{\uparrow} n) || p(Z^{\uparrow} n, \omega | X^{\uparrow} n))$ employing the geo-spectrotemporal, geosampled capture point, endmember, frequency, parameters, where $K(q(Z^{\uparrow} n, \omega | X^{\uparrow} n) || p(Z^{\uparrow} n, \omega | X^{\uparrow} n))$, the true Bayesian posterior was $p(Z^n, \omega | X^n)$ and the variational posterior was$q(Z^n, \omega | X^n)$. This led to the functional $\overline{F}[q]$ being minimized under the constraint and tthe variation posteriors, $r(\omega | X^n)$ and $Q(Z^n | X^n)$ being parsimoniously computed employing the equation $r(\omega | X^n) = \frac{1}{C_r} \varphi(\omega) \mathbf{exp} < \log p(X^n | Z^n | \omega) > Q$ and $Q(Z^n | X^n) = \frac{1}{C_Q} \mathbf{exp} < \log p(X^n, Z^n | \omega) > r$ where C_r *and* C_Q were the normalization constants. It is important to note that these equations gave only necessary conditions for the functional $\overline{F[q]}$ to be minimized in the *An. arabiensis*, aquatic, larval habitat, forecast, vulnerability, endmember, capture point, eco-georferenceable, oviposition, LULC, endmember, distribution model. The variational posteriors were computed by an iterative algorithm. We defined the variational stochastic complexity $\overline{F(X^n)}$ by the minimum value of the functional $\overline{F[q]}$ which was $\overline{F}(X^n) = \min_{r,Q} \overline{F[q]}$, thereafter based on the difference between $\overline{F(X^n)}$ and the Bayesian stochastic complexity$F(X^n)$.

Next, we generated variational posterior for the estimation matrix for the malaria, mosquito model. We assumed that the prior distribution φ (ω) of the *An. arabiensis* aquatic, larval habitat geosampled, eco-endmember LULC parameters $\omega = \{a, b\}$ was the conjugate prior distribution. Hence, φ (ω) was given by $\varphi(a_k) = \frac{\Gamma(T_k \phi_0)}{\Gamma(\phi_0)^{T_k}} \prod_{z_k=1}^{T_k} a_{(k,z_k)}^{\phi_0 - 1}, k = 1, 2 \ldots, K$, and the geosampled, eco-georeferenced explanatory, signature, geoclassied,LULC, predictor covariates estimates were given by $\varphi(b_{(j,\cdot|z)}) = \frac{\Gamma(Y_j \xi_0)}{\Gamma(\xi_0)^{Y_j}} \prod_{x_j=1}^{Y_j} b_{(j,x_j|z)}^{\xi_0 - 1}, \quad j = 1, 2 \ldots, N$, which were Dirichlet distributions with hyperparameters generated using $\phi_0 > 0$ and $\xi_0 > 0$. The Dirichlet distribution [i.e.,Dir(α)] is a family of continuous multivariate probability distributions parameterized by the vector α of positive reals which can generate the multivariate generalization of the beta distribution, and conjugate prior of the categorical distribution and multinomial distribution in Bayesian statistics for quantification of predictive, vector, larval habitat, LULC data [2].The Dirichlet distribution is the multinomial extension to the beta distribution for a binomial process which can also be used in quantifying probabilities in predictive larval habitat probability models [3].

We then let $\delta(n)$ be 1 when n = 0 and 1 otherwise, and then defined the sampled capture point, sub-meter resolution, oviposition, grid-stratified, LULC endmember, parameter, uncertainty estimates using $n_{(k,z_k)}^{z} := \sum_{i=1}^{n} (\delta(Z_i^{(k)} - z_k))_Q$. We also employed $n_{(j,x_j|z)}^{x} := \sum_{i=1}^{n} \delta\left(X_i^{(j)} - x_j\right) (\prod_{k=1}^{K} \delta(Z_i^{(k)} - z_k))_Q$. In these equations, $X_i^{(j)}$ was the state of the *j*th capture point, seasonal, hyperproductive, foci observation node and $Z_i^{(k)}$ was the state of the *k*th hidden node. The variational posterior distribution of the endmember parameters $\omega = \{a, b\}$ was given by using the equation $r(a_k | X^n) = \frac{\Gamma(n + T_k \phi_0)}{\prod_{z_k=1}^{T_k} \Gamma\left(n_{(k,z_k)}^{z} + \phi_0\right)} \prod_{z_k=1}^{T_k} a_{(k,z_k)}^{\overline{n}_{(k,z_k)}^{x} + \phi_0 - 1}$, where each geosampled, geo-spectrotemporal, *An. arabiensis*, aquatic, larval habitat,LULC endmember, explanatory predictor covariate was

generated using the equation $\bar{n}_{\downarrow}z^{\uparrow}x \square(:=) \Sigma_{\downarrow}(i=1)^{\uparrow}n \cong (\prod_{\downarrow}(\mathbf{k}=1)^{\uparrow}\mathbf{K} \equiv [\delta(Z_{\downarrow}i^{\uparrow}((k)) - z_{\downarrow}k \,]_{\downarrow}Q$ It then followed that $\bar{n}_z^x = \sum_{x_{j=1}}^{Y_j} \bar{n}_{(j,x_j|z)}^x$, for $j = 1, \ldots, N,$ and $\bar{n}_{(k,z_k)}^z = \sum_{z_{-k}} \bar{n}_z^x$ denoted the sum over $z_i (i \neq k).$

2.5 Eigenvector analyses: Initially, a misspecification perspective for the uncertainty-oriented, vector arthropod, endmember, forecast, vulnerability estimation model endmember estimators was generated assuming that the geo-spatiotemporal,aquatic, larval habitat, endemic, transmission-oriented, capture point, ento-ecoepidemiological , prognosticative estimators were able to be quantitated by $y = X\beta + \varepsilon^*$ (i.e. regression equation) had autocorrelated disturbances ε^*, which decomposed into a white-noise component, ε, and a set of unspecified and/or misspecified models that had the structure $y = XB + \underbrace{E\gamma + \varepsilon}_{=\varepsilon^*}$. White noise is a univariate or multivariate discrete-time stochastic process whose terms are independent and identically distributed (i.i.d.) with a zero mean [2]. In this research, the misspecification term was $E\gamma$. Endmember quantification of the topographic, sub-meter resolution, oviposition, grid-stratified, endmember, LULC patterns rendered from the distribution of the eco-georeferenced, explanatory, endemic, transmission-oriented, geo-spectrotemporal, oviposition, capture point, observational, geosampled eco-georeferenced, *An. arabiensis* larval habitat, explanatory, prognosticative, aquatic, larval habitat covariates was required to describe independent key dimensions of the underlying spatial processes in the sampled habitat data and for defining a spatial pattern in the misspecification term.

A spatial autoregressive model was then generated that employed a geosampled, *An. arabiensis*, oviposition, aquatic larval, habitat, eco-endmember LULC variable, Y, as a function of nearby geosampled habitat Y explanatory, predictor, covariate indicator value I (i.e., an autoregressive response) and/or the residuals of Y as a function of nearby sampled habitat Y residuals (i.e., an SAR or spatial error specification). For vector arthropod, aquatic, larval habitat, malaria, oviposition, endmember, predictive modeling the SAR model furnishes an alternative specification that frequently is written in terms of matrix W [1].As such, its spatial covariance was a function of the matrix $(I - \rho CD^{-1})(I - \rho D^{-1}C) = (I - \rho W^T)(I - \rho W)$, where T denoted matrix transpose. The resulting matrix was symmetric, and was considered a second-order specification as it included the product of two spatial structure matrices (i.e., W^TW) – adjacent geosampled, aquatic, larval habitats as well as those having a single intervening unit involved in the autoregressive function. This matrix restricted positive values of the autoregressive parameter to the more intuitively interpretable range of $0 \leq \hat{\rho} \leq 1$.

In this research distance between geosampled, geosampled, eco-georeferenced, aquatic, larval habitats was defined in terms of an *n*-by-*n* geographic weights matrix, C, whose c_{ij} values were; 1 if the *An. arabiensis* ,capture point, foci geolocations *i* and *j* were deemed nearby, and 0 otherwise. Adjusting this matrix by dividing each row entry by its row sum gave C1, where 1 was an *n*-by-1 vector of ones, converted this matrix to matrix W. The resulting SAR model specification, with no geosampled, larval, habitat covariates present (i.e., the pure spatial autoregression specification), took on the following form: $\mathbf{Y} = \mu(1 - \rho)\mathbf{1} + \rho\mathbf{WY} + \boldsymbol{\varepsilon}$, where μ was the scalar conditional mean of Y, and $\boldsymbol{\varepsilon}$ was an *n*-by-1 error vector whose endmeber LULC parameters were statistically dependent ,.normal, random variates. The spatial covariance matrix for analyzing the geosampled, eco-georeferenced, capture point, foci, predictor covariates was $E[(\mathbf{Y} - \mu\mathbf{1})'(\mathbf{Y} - \mu\mathbf{1})] = \boldsymbol{\Sigma} = [(\mathbf{I} - \rho\mathbf{W}')(\mathbf{I} - \rho\mathbf{W})]^{-1}\sigma^2$, where E (•) denoted the calculus of expectations, I was the *n*-by-*n* identity matrix denoting the matrix transpose operation, and σ^2 was the error variance.

Next, an autoregressive, endmemberm model specification was generated. The model was written as: $X_t = c + \sum_{i=1}^{p} \varphi_i X_{t-i} + \varepsilon_t.$ where $\varphi_1, \ldots, \varphi_p$ were the clinical, field and remote, geo-spectrotemporal, geosampled, aquatic, larval habitat, sub-meter resolution, oviposition, grid-stratified, eco-endmember ,LULC parameters of the model, *c* was a constant and ε_t was the white noise. When coupled with regression and the normal probability model, an autoregressive specification results in a covariation term characterizing spatial autocorrelation by

denoting the autoregressive parameter that with ρ, a conditional autoregressive covariance specification [1] which in this research involved the matrix (I - ρ C), where I was an *n*-by-*n* identity matrix. In an autoregressive expression; however, the response variable is on the left-side of the equation, while the spatial lagged version of this variable is on the right side. Therefore, one of the main objectives in this research was to bring the spatially unlagged, aquatic, larval habitat, ovipsoition, endogenous variable, y exclusively on the left-hand side of the regression equation in order to decorrelate the geosampled, eco-georeferenced, *An. arabiensis*, aquatic, larval habitat, endemic, trasnmission-oriented, predictive, risk-related, explanatory, endmeber,LULC, geo-spectrotemporal covariates. In this research, this was accomplished by expanding the matrix term: $(I-\rho V)^{-1}=\sum_{k=0}^{\infty}\rho^k V^k$, as an infinite power series, which was feasible under the assumption that the underlying spatial process in the geosampled ento-ecological,LULC,ovisposition, eco-georeferenecable, datasets was stationary. The simultaneous autoregressive,capture point, forecast, vulnerability, error model was then rewritten as $y-\rho Vy=X\beta-\rho VX\beta+\varepsilon$. Substituting this transformation rendered: $y=(I-\rho V)^{-1}[X\beta-\rho V(X\beta)+\varepsilon]$, $y=\sum_{k=0}^{\infty}\rho^k V^k(X\beta-\rho VX\beta+\varepsilon)$,

$$y=\sum_{k=0}^{\infty}\rho^k V^k X\beta-\sum_{k=0}^{\infty}\rho^{k+1}V^{k+1}(X\beta)+\sum_{k=0}^{\infty}\rho^k V^k\varepsilon,\ y=X\beta+\underbrace{\sum_{k=1}^{\infty}\rho^k V^k X\beta-\sum_{k=1}^{\infty}\rho^k V^k(X\beta)}_{k=0}+\sum_{k=0}^{\infty}\rho^k V^k\varepsilon,$$

$$y=X\beta+\underbrace{\sum_{k=1}^{\infty}\rho^k V^k\varepsilon}_{misspecificationterm}+\varepsilon$$

The misspecification term $\sum\rho^k V^k\varepsilon(k=1,\mathrm{K},\infty)$ remained uncorrelated with the exogenous variable, X , as the standard OLS assumption of the disturbances, ε , were uncorrelated in the endmember,capture point, sub-meter resolution, oviposition, grid-stratified,LULC predictor variables generated from the parameter estimates. (b). the spatial lag model on the other hand, was expressed as: $(I-\rho V)y=X\beta+\varepsilon$ .Substituting the transformation generated: $y=\sum_{k=0}^{\infty}\rho^k V^k(X\beta+\varepsilon)$ and $y=X\beta+\underbrace{\sum_{k=1}^{\infty}\rho^k V^k(X\beta+\varepsilon)}_{misspecificationterm}+\varepsilon$. The misspecification term $\sum\rho^k V^k(X\beta+\varepsilon)(k=1,\mathrm{K},\infty)$ included the exogenous,aquatic, larval, habitat variables X . Consequently, the exogenous variables were correlated with the misspecification term. Under this condition, standard OLS results for the basic regression model $y=X\beta+\varepsilon^*$, generated from the geosampled, eco-georeferenced aquatic, larval habitat, endmeber, explanatory predictor covariates provided biased estimates $\hat{\beta}$ of the underlying regressed, sub-meter resolution, oviposition, grid-stratified, endmeber LULC parameters β .

The correlation, or lack thereof, between the exogenous variables and the misspecification terms of both endemic,capture point, *An. arabiensis*, larval habitat, e= transmission-oriented predictive, risk, ento-ecoepidmeiological, eco-georefernecable, endmember LULC models were then used to design spatial proxy variables, so that the habitat properties of either model could be satisfied. We considered two different projection matrices, $M_{(1)}\equiv I-1(1^T1)^{-1}1^T$ and $M_{(X)}\equiv I-X\left(X^TX\right)^{-1}X^T$. The projection matrix $M_{(1)}$ is a special case of the more general projection matrix $M_{(X)}$ [3]. .The general projection matrix $M_{(X)}$ included, in addition to the constant unity vector 1, additional exogenous variables. The set of spatial filter, eigenfunction eigen-decomposable eigenvectors $\{e_1,\mathrm{K},e_n\}_{SAR}$ was extracted from the quadratic form $\{e_1,\mathrm{K},e_n\}_{SAR}\equiv evec\left[M_{(X)}\frac{1}{2}(V+V^T)M_{(X)}\right]$ (2.1) was designed

orthogonal to the exogenous variable X . The projection matrix $M_{(X)}$ imposed this constraint. In contrast, the set of eigenvectors $\{e_1,\mathrm{K}\ ,e_n\}_{Lag}$ that was extracted from $\{e_1,\mathrm{K}\ ,e_n\}_{Lag} \equiv evec\left[M_{(1)}\frac{1}{2}(V+V^T)M_{(1)}\right]$ (2.2),

These two different sets of eigenvectors established a basis for constructing an LULC, geo-spectrotemporal, autocorrelation, *An. arabiensis*, aquatic, aquatic, larval habitat regression-based oviposition, endmember, distribution model. Both expressions were solely defined in terms of exogenous information. This model feature enabled us to also use the eigenvector spatial filtering approach for predictions of the endogenous variable y . The associated sets of ovipsoition, aquatic, larval habitat, explanatory, eco-georeferenceable, LULC,spatial filter, eigenvalues $\{\lambda_1,\mathrm{K}\ ,\lambda_n\}_{Lag}$ and $\{\lambda_1,\mathrm{K}\ ,\lambda_n\}_{SAR}$, with $\lambda_i \geq \lambda_{i+1}$, range, were used for properly standardizing adjacent link matrices V that were related to irregular spatial tessellations, generated from the geosampled eco-georeferenced,capture point, geo-spectrotemporal, ento-ecoepidemiological, endmember LULC covariates.

The components of each capture point, eigenvector, e_i, when mapped onto an underlying spatial tessellation, exhibited a distinctive topographic pattern ranging from positive spatial autocorrelation,(PSA), (i.e., similar values of log-transformed, aquatic, larval,habitat, LULC count data aggregating in geographic space) for $\lambda_i > E(I)$, to negative spatial autocorrelation (NSA) (i.e., dissimilar log-values aggregating in geographic pace) for, $\lambda_i > E(I)$. Each seasonal, hypeproductive, capture point, endmember, eigenvector was mapped where $E(I)$ was the expected value of Moran's I under the assumption of (a) spatial independences and (b) use of the related projection matrix $M_{(1)}$ or $M_{(X)}$, respectively. The associated Moran's I autocorrelation coefficient, of each eigenvector, e_i generated, was equal to its associated eigenvalue $\lambda_i = \left[e_i^T(V+V^T)e_i\right]/(2e_i^T e_i)$, if V was scaled to satisfy $\left[1^T(V+V^T)1\right]/2 = n$. Moran's autocorrelation often denoted as *I* is an extension of Pearson's product moment correlation coefficient can be used to measure the amount of autocorrelation in an ecological-sampled datasets of vector insect arthropod-related habitat weighted estimators[1].

We employed the Pearson's correlation coefficient between two geo-spectrotemporal geosampled, eco-georferenced, sub-meter resolution, grid-stratified, *An. arabiensis*, aquatic, larval habitat, predictor variables to defined the covariance of any two explanatory endmeber regressors divided by the product of their standard deviations using $\rho_{X,Y} = \frac{\operatorname{cov}(X,Y)}{\sigma_X \sigma_Y} = \frac{E[(X-\mu_X)(Y-\mu_Y)]}{\sigma_X \sigma_Y}$, . The formula defined the geosampled, aquatic, larval habitat, geosampled population correlation coefficient. Substituting estimates of the covariances and variances also provided the sample correlation coefficient, commonly denoted *r*: $r = \frac{\sum_{i=1}^{n}(X_i-\bar{X})(Y_i-\bar{Y})}{\sqrt{\sum_{i=1}^{n}(X_i-\bar{X})^2}\sqrt{\sum_{i=1}^{n}(Y_i-\bar{Y})^2}}$. An equivalent expression rendered the correlation coefficient as the mean of the products of the standard scores. Based on paired, geo-spectrotemporal geosampled, eco-georferenced, sub-meter resolution, grid-stratified, aquatic, larval habitat ,hyperproductive, seasonal, LULC, endmember data, denisty, immature count values (i.e., X_i, Y_i), the sample Pearson correlation coefficient was $r = \frac{1}{n-1}\sum_{i=1}^{n}\left(\frac{X_i-\bar{X}}{s_X}\right)\left(\frac{Y_i-\bar{Y}}{s_Y}\right)$ where $\frac{X_i-\bar{X}}{s_X}, \bar{X},$ and s_X was the standard score, sample mean, and sample standard deviation, respectively. The spatial filter, orthogonal eigenvectors yielded distinct risk-oriented,capture point, map pattern descriptions of latent spatial autocorrelation in the *An. arabiensis*, aquatic, larval ,habitat , ento-ecoepidemiolgical, endmember, LULC data. This was interpreted as synthetic map variables that represented specific natures (i.e., positive or negative) and degrees (i.e., negligible, weak, moderate, strong) of potential spatial autocorrelation. For the immature *An. arabiensis* mosquitoes, two counteracting spatial autocorrelation effects were conceptualized (i.e., common factors leading to positive and competitive factors leading to negative spatial autocorrelation materializing) at the same time, with a possible net effect being global detection of near-zero spatial autocorrelation. If a parsimonious set of eigenvectors is to be selected for a vector arthropod-related, geo-

spectrotemporal geosampled, eco-georferenced, sub-meter resolution, grid-stratified, larval habitat distribution,endmember LULC model then eigenvectors depicting near-zero spatial autocorrelation should be avoided, since such a set of latent vectors associated with a matrix equation fail to capture any geographic information.

The eigenvector spatial filtering approach added a minimally sufficient set of eigenvectors as proxy-variables to the set of linear predictors, in the geo-spectrotemporal geosampled, eco-georferenced, sub-meter resolution, grid-stratified, *An. arabiensis*, aquatic, larval habitat, endemic trasnmission-oriented, predictive, risk-related model by inducing mutual independence in the geosampled, endmember, parameter estimator datasets. The regression,LULC capture point, geo-spectrotemporal, oviposition, ecogeoreferenced, residuals represented spatially independent variable ,eco-endmember components. The spatial pattern in the eigenvectors was synthetic: for positive global autocorrelation in the local patterns of the aquatic, larval habitat, endmember parameters exhibited only positive local autocorrelation and vice versa for negative global autocorrelation The eigenvectors e_i and e_j within each set of eigenvectors, were mutually orthogonal, as the symmetry transformation $\frac{1}{2}\left(V+V^T\right)$ was a quadratic form as revealed in equations (2.1) and (2.2).

As mentioned previously, the eigenvectors of specification (2.1) were orthogonal to the exogenous,capture point,aquatic, larval habitat variables X of the regression model constructed employing the geosampled eco-georeferneced, *An. arabiensis*, capture point, endmember, LULC, ento-ecoepidemiological, covariates; whereas, the eigenvectors of specification (2.2) were orthogonal only to the constant unity vector 1 in X . This orthogonality had implications for modeling the spatial misspecification terms, in the aquatic, larval habitat, forecast, vulnerability, grid-stratified, model and allowed us to link each collection of geo-spectrotemporal geosampled, eco-georeferenced, sub-meter resolution eigenvectors to its specific autoregressive model by letting E_{SAR} be a matrix whose vectors were subsets of $\{e_1,\mathrm{K}\,,e_n\}_{SAR}$. A linear combination of this subset was then approximated by using the misspecification term of the simultaneous autoregressive version of the endmember, *An. arabiensis* aquatic, larval habitat, distribution prognosticative, vulnerability –related,LULC model; (i.e., $E_{SAR}\gamma \approx \sum_{k=1}^{\infty}\rho^k V^k \varepsilon$). (2.3)

The linear combination $E_{SAR}\gamma$ remained orthogonal to exogenous variables X and, consequently, the estimated time series, geosampled, clinical, field and remote-sampled, geo-spectrotemporal, endmember, LULC, specified, predictor variables $\hat{\beta}$ were unbiased. Furthermore, as a property of the OLS estimator, the estimated term $E_{SAR}\gamma$ was also orthogonal to the,capture point, eco-georeferenced, frequency, sub-meter resolution, grid-stratified, model residuals $\hat{\varepsilon}$. The model $y = X\hat{\beta} + E_{SAR}\hat{\gamma} + \hat{\varepsilon}$ eigen-decomposed the endogenous variable y into a systematic trend component, a stochastic signal component, and some white-noise residuals. The term $E_{SAR}\hat{\gamma}$ removed variance inflation in the mean squared error (MSE) term attributable to spatial autocorrelation.

Alternatively, for the spatial lag model (2.3), E_{Lag} was a matrix of those eigenvectors that were a subset of $\{e_1,\mathrm{K}\,,e_n\}_{Lag}$. The approximation of the misspecification term became $E_{Lag}\gamma \approx \sum_{k=1}^{\infty}\rho^k V^k\left(X\beta+\varepsilon\right)$. Since $E_{Lag}\gamma$ is correlated with the exogenous variables X [2], its incorporation into the geo-spectrotemporal geosampled, eco-georeferenced, sub-meter resolution, grid-stratified, *An. arabiensis*, aquatic, larval habitat, predictive, LULC endmember, risk model distribution model corrected the bias of estimated plain OLS parameters $\hat{\beta}$ in the spatial lag model. The model $y = X\hat{\beta} + E_{Lag}\hat{\gamma} + \hat{\varepsilon}$, generated from the geosampled eco-georeferenced, aquatic, larval habitat, explanatory, capture point, predictor covariates was a decomposition of the spatial lag model into a systematic trend component, a stochastic signal component, and some white-noise residuals. However, for the geo-spectrotemporal,

geosampled, aquatic, larval habitat, ento-ecoepidemiological, oviposition, endemic, trasnmission-oriented, capture point, predictive, risk LULC, distribution model, the trend and the stochastic signal were no longer uncorrelated, and, again, the MSE was deflated.

The set of eigenvectors $\{e_1, \mathrm{K}, e_n\}_{Lag}$ of the spatial lag model (2.3) was then calculated independently of the exogenous, eco-georeferenced, sub-meter resolution, grid-stratified, capture point, aquatic, larval, habitat variables X. In this research, this calculation was dependent on the underlying spatial link matrix V. Consequently, this filtering approach was more adaptable to an exploratory specification search of relevant exogenous habitat, endmember LULC variables and spatial predictions with changing explanatory endmeber, predictor variable values. In contrast, for the simultaneous autoregressive, geo-spectrotemporal, aquatic, larval, habitat model (2.2), the eigenvectors $\{e_1, \mathrm{K}, e_n\}_{SAR}$ depended, through the projection of $M_{(X)}$, on the exogenous variables X. Thus, any change in the underlying malaria, mosquito, oviposition, ento-ecoepidmeiological, endmember, model structure required a recalculation of the eigenvectors for generating the tessellations. Spatial filtering, of either the spatial lag model or the simultaneous autoregressive model with a common factor constraint, requires identification of only one set of selected eigenvectors, namely E_{SAR} or E_{Lag}, respectively [2].The relevant set of eigenvectors was applied simultaneously to all the empirical, clinical, field and remote geosampled eco-georeferenced, aquatic, larval, habitat, endemic, trasnmission-oriented, predictive, risk –related, explanatory, capture point, endmember LULC covariates in either model. For the generic autoregressive model (2.1); however, spatial filtering was applied individually to each geosampled, explanatory, predictor, covariate coefficients. The generic specification of autoregressive, eco-georeferenced, sub-meter resolution, grid-stratified, spatial models associates a specific spatial lag factor with the endogenous y variable and other specific spatial lag factors for each geosampled, aquatic, larval habitat, exogenous, geo-spectrotemporal, eco-georeferenced LULV variable. We employed the eigenvectors $\{e_1, \mathrm{K}, e_n\}_{Lag}$ to filter spatial autocorrelation in the generic, autoregressive, *An. arabiensis*, eco-endmember, LULC, capture point, aquatic, larval, habitat model from each geosampled endmember estimator.

The next step was to identify suitable and parsimonious subsets of eigenvectors E_{SAR} or E_{Lag} from the geo-spectrotemporal, *An. arabiensis*, aquatic, larval habitat endemic, transmission-oriented , geosampled, forecast, vulnerability, endmember, geo-spectrotemporal, LULC model specification (2.1) or (2.2). A particular subset of eigenvectors is suitable, if the residuals $\hat{\varepsilon}$ of the resulting spatially filtered model become stochastically independent with respect to the underlying sampled habitat spatial structure V [2], In addition, parsimony in the model estimation in this research was defined as the smallest possible subset of geosampled, eco-georeferenced, sub-meter resolution, grid-stratified, capture point, geo-spectrotemporal eigenvectors which led to spatial independence in the malaria, aquatic, larval habitat, distribution, endmember LULC, model residuals being identified. The spatial patterns of different eigenvectors express independent and uncorrelated dimensions of spatial autocorrelation [2].This approach to filter spatial autocorrelation out of regression,capture point, endmember, model residuals has been explicitly formalized for the geo-spatiotemporal geosampled, eco-georeferenced, vector, insect, aquatic, larval, habitat, orthogonal LULC covariates by Jacob et al. (2005b) which has been used in previous research for spatially extrapolating eco-georeferenced, habitat, predictor covariates associated to prolific larval habitats. For example, in Jacob et al. (2008a) an eigenfunction decomposition algorithm was used along with a forward stepwise regression to add eigenvectors to regression-based *An. gambiae s.l.* and *Cx. quinqueasciatus*, aquatic larval habitat, endmember LULC models for targeting, eco-georferenceable, prolific habitats in Gulu, Uganda until the spatial autocorrelation in the resulting residuals ^e dropped below a critical level. The linear combination of the selected geo-spectrotemporal geosampled, eco-georeferenced, grid-stratified, eigenvectors then expressed the stochastic signal within the vector in the model. The measures of clustering of *An. gambaie s.l.* and *Cx. quinquefasciatus*, aquatic larval habitats were reported. Estimation results from SAS PROC GENMOD for all models were generated. In the models both positive and negative spatial autocorrelation eigenvectors were selected by the stepwise negative binomial regression procedure. Positive and negative spatial autocorrelation spatial filter component pseudo-R^2 values were reported using GLMM estimation results from SAS PROC NLMIXED. The spatial autocorrelation components suggested the presence of roughly 12% to 28% redundant information in the larval count. Spatially pseudoreplicated, endmember, capture point, LULC data can generate a mispecified model [1].

Results and Discussion

Initally, ODEs were constructed employing the geosampled, geo-spectrotemporal, sub-meter resolution, *An. arabeinsis*, aquatic, larval habitat, grid-stratified, eco-endmember, LULC data. We noted a time zero value for each first-order differential equation. We employed a first-order ODE equation $\frac{dy}{dx} = F(x, y),$ where $F(x, y)$ was expressed using separation of the geosampled, *An. arabiensis*,capture point, LULC variables as $F(x, y) = X(x)\,Y(y),$ The equation was expressed as $\frac{dy}{Y(y)} = X(x)\,dx$ and the equation was solved by integrating both sides to obtain $\int \frac{dy}{Y(y)} = \int X(x)\,dx.$ We employed a first-order ODE of the form $\frac{dy}{dx} + p(x)\,y = q(x)$ which was solved by finding an integrating factor $\mu = \mu(x)$ such that $\frac{d}{dx}(\mu y) = \mu\frac{dy}{dx} + y\frac{d\mu}{dx} = \mu\, q(x).$ Dividing through by $\mu\, y$ yielded $\frac{1}{y}\frac{dy}{dx} + \frac{1}{\mu}\frac{d\mu}{dx} = \frac{q(x)}{y}$ in the capture point, eco-endmember, prognosticative, signature, LULC, vulnerability, model derivatives (e.g., covariates of eco-georeferenecable, seasonal, hyperproductive, foci explanators) However, this condition enabled us to explicitly determine the appropriate μ for arbitrary p and q in the model renderings. To accomplish this,we took $p(x) = \frac{1}{\mu}\frac{d\mu}{dx}$ from the capture point, LULC, prognosticative signature, grid-stratfiiable, eco-endmember equation, from which we recovered the original equation (◇),, in the form $\frac{1}{y}\frac{dy}{dx} + p(x) = \frac{q(x)}{y}.$ We integrated both sides of the *An. arabiensis*, geo-spectrotemporal, seasonal, geosampled, predictive model to obtain $\int p(x)\,dx = \int \frac{d\mu}{\mu} = \ln\mu + c$ $\mu = e^{\int p(x)\,dx}$.Now integrating both sides of (◇) rendered $\mu\, y = \int \mu\, q(x)\,dx + c$ (with μ a known function), which we solved for y to obtain $y = \frac{\int \mu\, q(x)\,dx + c}{\mu} = \frac{\int e^{\int_x p(x')\,dx'}\, q(x)\,dx + c}{e^{\int_x p(x')\,dx'}},$ where c was an arbitrary constant of integration.

After quantitating the geosampled, geo-spectrotemporal, *An. arabiensis*, forecast, vulnerability, model estimators employing grid-stratfiiable, sub-meter resolution, nth-order linear ODE with constant coefficients $\frac{d^n y}{dx^n} + a_{n-1}\frac{d^{n-1} y}{dx^{n-1}} + \ldots + a_1\frac{dy}{dx} + a_0\, y = Q(x),$ we then solved the characteristic equation obtained by writing $y \equiv e^{rx}$ and setting $Q(x) = 0$ to obtain the n complex roots.The LULC, eco-endmember, forecast, vulnerability, spectral model rendered $r^n e^{rx} + a_{n-1} r^{n-1} e^{rx} + \ldots + a_1 r e^{rx} + a_0 e^{rx} = 0 r^n + a_{n-1} r^{n-1} + \ldots + a_1 r + a_0 = 0.$ Factoring can render the roots $r_i, (r - r_1)(r - r_2)\cdots(r - r_n) = 0.$[6].For a nonrepeated real root r, the corresponding solution in the model required $y = e^{rx}$.If a real root r is repeated k times, the solutions are degenerate and the linearly independent solutions are $y = e^{rx}, y = x\,e^{rx}, \ldots, y = x^{k-1}\,e^{rx}$.[7]Complex roots from the habitat signature, eco-endmember model were realized as complex conjugate pairs, $r_{\pm} = a \pm i\,b$. For nonrepeated complex roots, the solutions were $y = e^{ax}\cos(bx), y = e^{ax}\sin(bx).$ When the complex roots were repeated k times, the linearly independent solutions were $y = e^{ax}\cos(bx), y = e^{ax}\sin(bx), \ldots, y = x^{k-1}\,e^{ax}\cos(bx), y = x^{k-1}\,e^{ax}\sin(bx).$

Linearly combining solutions of the appropriate LULC types with arbitrary multiplicative ento-endmember, capure point, prognosticated constants then rendered the complete solution (asymptotically iteratable,

quantitatively.geo-spectrotemporally interpolative, aquatic, larval habitat, signature frequencies). If initial conditions are specified, the constants can be explicitly determined [6]. For example, we considered the sixth-order linear ODE $(\tilde{D}-1)(\tilde{D}-2)^3(\tilde{D}^2+\tilde{D}+1)y=0,$ for targeting unknown foci which had the characteristic equation $(r-1)(r-2)^3(r^2+r+1)=0.$ The roots of the malaria, mosquito, geo-spectrotemporal, LULC paradigm was 1, 2 (three times), and $(-1\pm\sqrt{3}\ i)/2$, so the solution $y=A\,e^{x}+B\,e^{2x}+C\,x\,e^{2x}+D\,x^{2}\,e^{2x}+E\,e^{-x/2}\cos\left(\frac{1}{2}\sqrt{3}\ x\right)+F\,e^{-x/2}\sin\left(\frac{1}{2}\sqrt{3}\ x\right).$. The general solution for the model was $y(x)=\sum_{i=1}^{n}c_i\,y_i(x)+y^*(x),$ where was the solutions to the linear equations which were $y_1(x)$, $y_2(x)$, ..., $y_n(x)$, where $y^*(x)$ was the particular solution (i.e.,seasonal, hyperproductive unknown, foci, LULC data).

We onsidered a first-order ODE in the slightly different form $p(x,y)\,dx+q(x,y)\,dy=0.$ Such an equation we assumed to be exact if $\frac{\partial p}{\partial y}=\frac{\partial q}{\partial x}.$ This statement is equivalent to the requirement that a conservative field exists, so that a scalar potential can be defined for an empirically geosampled, geo-spectrotemporally regressable, uncoalesceable, frequency dataset of seasonal, unknown , capture point, aquatic, larval, habitat foci) . For an exact equation, the quantitated solution is $\int_{(x_0,y_0)}^{(x,y)}p(x,y)\,dx+q(x,y)\,dy=c,$ where c is a constant.A first-order ODE (◇) is said to be inexact if $\frac{\partial p}{\partial y}\neq\frac{\partial q}{\partial x}.$ [6].For a nonexact equation, the solution may be obtained by defining an integrating factor μ of (◇) so that the new equation $\mu\,p(x,y)\,dx+\mu\,q(x,y)\,dy=0$ satisfied $\frac{\partial}{\partial y}(\mu\,p)=\frac{\partial}{\partial x}(\mu\,q),$

T he following first-order system of ODEs provided an ento-ecoepidemiological, capture point, oviposition-related, capture point, eco-endmember, LULC signature initial value for each ODE. We modeled a system of first-order, *An. arabiensis*, aquatic, larval habitat, capture point, differential equations. We also wrtote the following 2nd order differential equation as a system of first order, linear, differential equations. $2y''-5y'+y=0 \qquad y(3)=6 \qquad y'(3)=-1$ We wrote higher order differential equations as a system with a very simple change of larval habitat variable. We defined the following two, signature LULC function., $x_2(t)=y'(t)$ which we subsequently differentiatedin the model. I so doing we obtained $x_2'=y''=-\frac{1}{2}y+\frac{5}{2}y'=-\frac{1}{2}x_1+\frac{5}{2}x_2$ Note the use of the differential equation in the second equation. converted the initial conditions over to the new functions (i.e., $x_1(3)=y(3)=6$))Putting all of this together rendered a system of differential equations for optimally quanatiating the empricial geosampeld, datset of eco-georgferemnecable, sub-myter resolution, grid-stratifiable, LULC signature iterators..

We considered the differential equations $y''=by'+cy$ when y_0=0 and y_0'=1 which we wrote as the system of differential equations where $y'=z, z'=by'+cy$ and y_0=0 and z_0=1.This differential system was simulated as follows for the geosampled, *An. arabiensis* habitat data t;

time=0; output;
time=1; output;
time=2; output;

```
run;
proc model capture point data=t ;
  dependent y 0 z 1;
  parm b -2 c -4;
  dert.y = z;
  dert.z = b * dert.y + c * y;
  solve y z / dynamic solveprint;
run;
```

The preceding statements produced the output shown in Table 3.

Table 3 Simulation Results for the oviposition, *An. arabiensis*, LULC habitat, forecast, vulnerability, endmember, modeling differential system

Simultaneous Simulation

Observation	1		**Missing**	2	**CC**	-1.000000	
			Iterations	0			
Solution Values							
y	**z**						
0.000000	1.000000						
Observation	2	**Iterations**	0	**CC**	0.000000	**ERROR.y**	0.000000
Solution Values							
y	**z**						
0.2516892	-.3169643						
Observation	3	**Iterations**	0	**CC**	7.352802	**ERROR.y**	-0.172505
Solution Values							
y	**z**						
-.0657833	.25751						

The differential, geo-spectrotemporally, geosampled, *An. arabienis*, aquatic, larval habitat, prognosticative, eco-endmember, eco-geoclassfiied, LULC, capture point, ento-ecoepidemiological, LULC variables were distinguished by their derivative with respect to time [i.e., (DERT.) prefix]. The differential equations were expressed in normal form.

The TIME variable was implied with respect to the endmember, geosampled, LULC, capture point, aquatic, larval habitat variables for all DERT explanators. We provided initial values for the differential equations in an optimizable, sub-meter resolution, capture point dataset. We specified the initial values as

```
proc model An. arabiensis data=t ;
  dependent y z ;
  parm b -1 c -4;
  if ( time=0 ) then
    do;
      y=0;
      z=1;
    end;
  else
    do;
      dert.y = z;
      dert.z = b * dert.y + c * y;
    end;
  end;
```

```
solve y z / dynamic solveprint;
run;
```

The differential equation for the ento-ecoepidemiological, oviposition, malaria mosquito, LULC, eco-endmember, geo-spectrotemporal, signature modeling process was $\frac{dconc}{dt} - k_u - k_e conc conc_0 = 0$. The analytical solution to the model was $conc = (k_u/k_e)(1 - \exp(-k_e t))$ An ordinary differential equation (*ODE*) is an equation containing a unknown function of one real or complex variable *x*, its derivatives, and some given functions of *x*[6]. An ordinary differential equation (frequently called an "ODE," "diff eq," or "diffy Q") is an equality involving a function and its derivatives [4]. Our ODE of order n I was initially an equation of the form $F\left(x, y, y', \ldots, y^{(n)}\right) = 0$, where y was a function of x, $y' = d\,y/d\,x$ which was the first derivative with respect to x, and $y^{(n)} = d^n\,y \,/\, d\,x^n$ and the nth derivative with respect to x[7].Nonhomogeneous ordinary differential equations can be solved if the general solution to the homogenous version is known, in which case the undetermined coefficients method or variation of parameters can be used to find the particular solution[6].The ordinary differential vector arthropod, iteratively, interpolative ento-ecoendmember, geo-spectrotemporal, prognosticative LULCm equations were solved exactly in the Wolfram Language using DSolve[*eqn*, *y*, *x*], and numerically using NDSolve[*eqn*, *y*, {*x*, *xmin*, *xmax*}].The sub-meter resolution, gri-stratfiiable, eco-endmember, ODE of order n was linear since $a_n(x)\,y^{(n)} + a_{n-1}(x)\,y^{(n-1)} + \ldots + a_1(x)\,y' + a_0(x)\,y = Q(x)$.A linear ODE where $Q(x) = 0$ is said to be homogeneous[6].

While there are many general techniques for analytically solving classes of ODEs, the only practical solution technique for complicated equations is to use numerical methods (Milne 1970, Jeffreys and Jeffreys 1988). The most popular of these is the Runge-Kutta method, but many others have been developed, including the collocation method and Galerkin method. A vast amount of research and huge numbers of publications have been devoted to the numerical solution of differential equations, both ordinary and partial (PDEs) as a result of their importance in fields as diverse as physics, engineering, economics, and electronics.Here the solutions to an ODE satisfied the existence and uniqueness of an sub-meter resolution, grid-stratified dataset of imaged, capture point, *An. arabiensis*, aquatic, larval habitat, eco-endmember, geo-spectrotemporal, signature, LULC, wavelength properties. The first-order ODE was given by $\frac{d\,x_i}{d\,t} = f_i(x_1, \ldots, x_n, t)$, for $i = 1, \ldots, n$ /We let the functions $f_i(x_1, \ldots, x_n, t)$, where $i = 1, \ldots, n$, all be defined in a domain D of the $(n+1)$- in dimensional space . In so doing, the geosampled, capture point, gridded, LULC variables $x_1, \ldots, x_n, t$. were found to be useful for remotely identifying seasonal, eco-georeferenceable, unknown foci by determing estimators associated with known, hyperproductive foci.We let these functions be continuous in D and have continuous first partial derivatives $\partial f_i \,/\, \partial x_j$ for $i = 1, \ldots, n$ and $j = 1, \ldots, n$ in D. . We then let $\left(x_1^0, \ldots, x_n^0\right)$ be D. In so doing, there existed a solution given by $x_1 = x_1(t), \ldots, x_n = x_n(t)$ for $t_0 - \delta < t < t_0 + \delta$ (where $\delta > 0$) which satisfied the initial conditions $x_1(t_0) = x_1^0, \ldots, x_n(t_0) = x_n^0$.Further, the solution was unique, so that if $x_1 = x_1^*(t), \ldots, x_n = x_n^*(t)$ was a second solution of (◇) for the model $t_0 - \delta < t < t_0 + \delta$, the derivatives satisfied (◇). Subsequently $x_i(t) \equiv x_i^*(t)$ for $t_0 - \delta < t < t_0 + \delta$.was rendered. Because every nth-order ODE can be expressed as a system of n first-order ODEs[6], this theorem also may apply to the single nth-order OD, sub-meter resolution, eco-endmember, LULC, signature, grid-stratifiable, forecast, vulnerability, geo-spectrotemporal model for asymptotically geo-spectrotemporally targe4ting seasonal, eco-georeferenecable, aquatic, larval habitat, un-geosdampled, foci..

An exact first-order ordinary differential equation of the form $p(x, y)\,d\,x + q(x, y)\,d\,y = 0$, was then extracted where $\frac{\partial p}{\partial y} = \frac{\partial q}{\partial x}$. We noted that an equation of the form (◇) with $\frac{\partial p}{\partial y} \neq \frac{\partial q}{\partial x}$ was nonexact. An integrating factor is a function by which an ordinary differential equation can be multiplied in order to make it integrable[7]. For example, a linear, first-order,*An. arabiensis*, eco-endmember, sub-meter resolution, geo-spectrotemporal, forecast, vulnerability,

signature ordinary differential equation of type $\frac{dy}{dx} + p(x)\,y(x) = q(x),$ where p and q are given continuous functions, can be made integrable by letting $v(x)$ be a function such that $v(x) = \int p(x)\,dx$ and $\frac{dv(x)}{dx} = p(x).$. In so doing, $e^{v(x)}$ would be the integrating factor such that multiplying by $y(x)$. In so doing, the expression $\frac{d}{dx}\left[e^{v(x)}\,y(x)\right] = e^{v(x)}\left[\frac{dy(x)}{dx} + p(x)\,y(x)\right] = e^{v(x)}\,q(x)$ could be rendered employing the product rule. Integrating both sides with respect to x in the habitat signature, An. arabiensis, oviposition, LULC model for asymptotically, optimally, remotely, targeting, eco-georeferenecable, hyperproductive, seasonal foci then may render the solution $y(x) = e^{-v(x)} \int e^{v(x)}\,q(x)\,dx.$

For robustly, parsimoniously quantitating the empirical, regressed dataset of the geosampled, empirical, eco-georeferenceable, geo-spectrotemporal, *An. arabiensis*, aquatic, larval habitat, capture point, geo-spectrotemporal, LULC eco-endmember $\frac{\frac{\partial p}{\partial y} - \frac{\partial q}{\partial x}}{q} = f(x)$ in (◇),an x-dependent variable we, integrated all the signature frequency factosr. If $\frac{\frac{\partial q}{\partial x} - \frac{\partial p}{\partial y}}{x\,p - y\,q} = f(x\,y)$ in (◇) was it had an $x\,y$-dependent integrating factor. If $\frac{\frac{\partial q}{\partial x} - \frac{\partial p}{\partial y}}{p} = f(y)$ in (◇), but only if it had a y-dependent integrating factor, for example,.

```
 input day conc;
datalines;

0.0   0.0
1.0   0.15
2.0   0.2
3.0   0.26
4.0   0.32
6.0   0.33
```

To fit this model in differential form, we employed the following statements:

```
proc model data=Anopheles;
  parm ku ke;

  dert.conc = ku - ke * conc;

  fit conc / time=day;
run;
```

The results from the eco-endmember, capture point, oviposition, LULC estimation is shown In Table 4.

Table 4 The MODEL Procedure estimation revealing the quantitated, endmember,` LULC results from the *An. arabienisis* capture point model output

Nonlinear OLS Parameter Estimates				
Parameter	**Estimate**	**Approx Std Err**	**t Value**	**Approx Pr > |t|**
ku	0.126743	0.0116	2.33	0.0031
ke	0.345398	0.2783	3.54	0.0528

To perform a dynamic estimation of the geosampled, aquatic, larval habitat, signature, LULC ento-endmember differential equation, we added the DYNAMIC option to the FIT statement.

```
proc model data=Anopheles;
  parm ku .5 ke .7;

  dert.conc = ku - ke * conc;

  fit conc / time = day dynamic;
run;
```

The equation DERT.CONC was integrated from $conc(0) = 0$. The results from this estimation are shown in Table 5 .

Table 5. Dynamic estimation results for the o*An.arabiensis*, capture point model

The MODEL Procedure **Parameter**	**Estimate**	**Approx Std Err**	**t Value**	**Approx Pr > |t|**
ku	0..376 34	0.3683	6.27	0.0005
ke	0.522235	0.0364	7.48	0.0080

A comparison of the endmember sub-meter resolution, oviposition, malaria, mosquito, LULC, orthogonal, endmember model data results amongst the seasonal, forecast ,vulnerability model outputs revealed that the two dynamic estimations and the analytical estimation rendered nearly identical results (identical to the default precision). The two dynamic capture point, endmember, vector arthropod, LULC model, frequency estimations were identical because the initial, capture point, seasonal hyperproductive, eco-georeferenced, aquatic, larval habitat sample value was very close to the initial geosampled value employed in the first, dynamic, habitat parameter (0).

Note also that the static model did not require an initial guess for the parameter values. Static estimation, in general, is more forgiving of bad initial, grid-stratifiable, time series, orthogonal, LULC endmember values (www.esri.com). preferable form of the regression estimation for an oviposition, sub-meter resolution, grid-stratifiable, empricial, geo-spectrotemporal, oviposition, LULC dataset of, capture point, malaria mosquito, hyperproductive, eco-georeferenecable, aquatic, larval habitats, may depend mostly on the model and seasonal geosampled, ento-ecoepidemiological data[1]. If a very accurate initial, geosampled, aquatic, larval habitat, malaria, mosquito, capture point, geo-spectrotemporal endmember, tabulated, LULC geosampled value is known, then a dynamic estimation makes sense. If, additionally, the model can be written analytically, then the analytical, endmember, LULC estimation may be computationally simpler. If an approximate initial value is known and not modeled as an unknown, seasonal, LULC, ecogeoreferenecable, hyperproductive, foci parameter initially, the static estimation may be less sensitive to errors in the capture point, aquatic, larval habitat,eco-georeferenecable, geolocations and their density, count values prognosticated.

The form of the error in the endmember oviposition, ento-ecoepidemiological, endmember, LULC model is also an important factor in choosing the form of the capture point, forecast, vulnerability, geospectrotemporal, capture

point, uncertainty-oriented paradigm. If the error term is additive and independent of previous error, then the dynamic mode is appropriate. If, on the other hand, the errors are cumulative in the ento-ecoepidemiological, vector arthropod, capture point, aquatic, larval habitat, orthogonal, LULC endmember dataset, a static estimation may be more appropriate.

Auxiliary equations may be parsimoniously useable with various time series, malaria, mosquito, aquatic, larval habitat, oviposition, endmemebr, orthogonal, differential equations. These are equations that may need to be satisfied with the differential equations at each capture point between each eco-georeferenecable, geosampled, geo-spectrotemporal, larval, density count value, endmember, prognosticated, seasonal, hyperproductive geolocation. Here, the aquatic, larval habitat, LULC data was automatically added to the system, so we did not need to specify them in the SOLVE or FIT statement.

A time induced, endmember, LULC ento-coepidemiological variable was identified in the *An. arabiensis* aquatic, larval, habitat, ento-ecoepidemiological,oviposition dataset. The name of the time variable defaulted to TIME in the model construction process. Other geosampled, endmember, LULC variables may be employable in future oviposition, forecast, vulnerability, *An. arabiensis*, capture point, aquatic, larval habitat, mapping applications for seasonally targeting eco-georeferenecable, hyperproductive foci as the time variable by specifying the TIME= option in the FIT or SOLVE statement. Here, the time intervals for the ento-ecoepidemiological, LULC endmember, capture point, orthogonal dataset were not evenly spaced. If the time dependent, predictor variable for the current observation is less than the time variable for the previous observation, the integration is restarted [2].

We considered the following differential equation $y' = a*x$ for fitting the sub-meter resolution, endmember, LULC, *An. arabiensis*, aquatic, larval habitat, capture point, geo-spectrotemporal, geosampled oviposition, explanatory dataset

```
data t2;
  y=0; time=0; output;
  y=2; time=1; output;
  y=3; time=2; output;
run;
```

The problem we were trying to resolve was to find the seasonal, hyperproductive, endemic, LULC foci, eco-georeferenecable, *An. arabiensis* capture point, geosampled, larval density,frequency, count values for X that satisfied the differential equation in SAS (see Table 6) and the ento-ecoepidemiological, geo-spectrotemporal, endmember data in the oviposition dataset. This problem was solved with the following statements:

```
proc model data=t2;
  independent x 0;
  dependent y;
  parm a 5;
  dert.y = a * x;
  solve x / out=goaldata;
run;

proc print data=goaldata;

run;
```

Table 6 The output from the PROC PRINT

Obs	_TYPE_	_MODE_	_ERRORS_	x	y	time
1	PREDICT	SIMULATE	0	0.0	0	0
2	PREDICT	SIMULATE	0	0.7	2	5
3	PREDICT	SIMULATE	0	-0.3	3	1

Note that an initial value of 0 was provided for the x variable in the forecast, vulnerability *An. arabiensis*, capture point, LULC model because it was undetermined at TIME = 0. Hence x was treated as a linear function between each geosampled, eco-georeferenecable, LULC, geosampled, geo-spectrotemporal, capture point. We optimally integrated the equation $y' = ax$ as $x(t) = \frac{t_f - t}{t_f - t_o} x_o + \frac{t - t_o}{t_f - t_o} x_f$, $y_f - y_o = \int_{t_o}^{t_f} ax(t)dt = a\frac{1}{t_f - t_o}\left(t(t_f x_o - t_o x_f) + \frac{1}{2}t^2(x_f - x_o)\right)\Big|_{t_o}^{t_f}$. This frequency signature LULC model reduced to $y_f - y_o = \frac{1}{2}a * x_f$ (see Table 7).

Table 7. An *An. arabiensis* aquatic, larval habitat observation reduced to $2.5 * x_f$

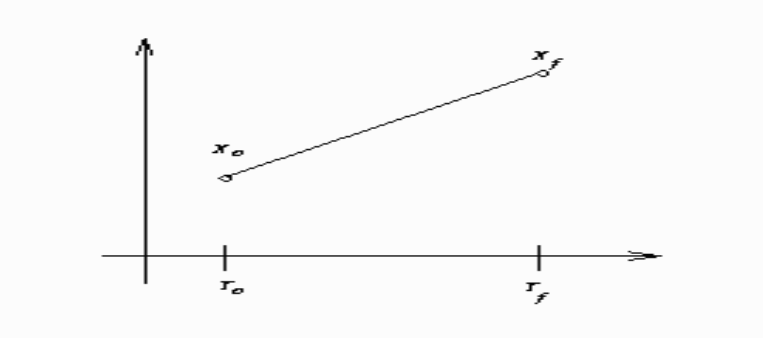

Employing the BOUNDS and RESTRICT statements, PROC MODEL we computed optimal LULC, *An. arabienis*, aquatic, larval, habitat, sub-meter resolution, grid-stratifiable, eco-endmember, signature, frequency estimates subject to equality or inequality constraints on capture points, parameter estimates. Equality restrictions were written as a vector function: $\mathbf{h}(\theta) = 0$. Inequality restrictions are either active or inactive [6]. When an inequality restriction is active, it is treated as an equality restriction [2]. All inactive inequality restrictions in the oviposition, capture point, LULC, malaria, mosquito, forecast, vulnerability, signature model was written as a vector function: $F(\theta) \geq 0$

The strict inequalities, in the vector arthropod, capture point, LULC, orthogonal, endmember function $(f(\theta) > 0)$, was transformed into inequalities as $f(\theta) \times (1 - \varepsilon) - \varepsilon \geq 0$, where the tolerance ε was controlled by the EPSILON= option in the FIT statement which defaulted to 10^{-8}. The *i*th inequality restriction became active if $F_i < 0$ and remained active until its Lagrange multiplier became negative. Lagrange multipliers in the eco-georeferenecable, capture point, endmember, *An. arabiensis*, aquatic, larval habitat, LULC, model estimators were computed for all the non-redundant equality restrictions and all the active inequality restrictions.

During the construction process of the ento-ecoepidemiological, explanatory, eco-endmember, LULC, oviposition,capture point, signature, frequency, geo-spectrotemporal model we assumed the vector $\mathbf{h}(\theta)$ contained all the current active restrictions. The constraint matrix $\mathbf{A}$ was $\mathbf{A}(\hat{\theta}) = \frac{\partial \mathbf{h}(\hat{\theta})}{\partial \hat{\theta}}$ .The covariance matrix for the restricted, LULC, signature, *An. arabiensis*, aquatic, larval habitat, geosampled, optimizable, parameterizable estimates which was computed as $\mathbf{Z}(\mathbf{Z}'\mathbf{H}\mathbf{Z})^{-1}\mathbf{Z}'$ where $\mathbf{H}$ was Hessian or approximation to the Hessian of the objective function $(\mathbf{X}'(\text{diag}(\mathbf{S})^{-1} \otimes \mathbf{I})\mathbf{X})$ for OLS. In so doing, $\mathbf{Z}$ was the last $(np - nc)$ columns of $\mathbf{Q}$. We derived this result from an LQ factorization of the constraint matrix, *nc* which was based on the number of active constraints in the LULC forecast, vulnerability, malaria mosquito, model for asymptotically targeting unknown, hyperproductive foci,

whence *np* is the number of geosampled, aquatic, larval habitat, geo-spectrotemporalm ento-endmember, oviposition, eco-epidemiological, eco-georeferenceable, signature, frequency, capture point parameters.

The LQ factorization for the oviposition, ento-ecoepidemiological, forecast, vulnerability, LULC, eco-endmember, grid-stratified model for asymptotically, optimally, geo-spectrotemporally targeting hyperproductive, unknown, *An. arabiensis*, aquatic, larval habitats was given by $A = \begin{pmatrix} L & 0 \end{pmatrix} Q = \begin{pmatrix} L & 0 \end{pmatrix} \begin{pmatrix} Q_1 \\ Q_2 \end{pmatrix} = LQ_1, \quad \text{if } m \leq n,$ where *L* was *m*-by-*m* lower triangular, *Q* was *n*-by-*n* orthogonal (or unitary), *Q* consisted of the first *m* rows of *Q*, and Q_2 was the remaining *n* - *m* rows. This factorization was computed by the routine xGELQF. *Q* was represented in the ento-ecoepidemiological, eco-endmember, signature, LULC model as a product of elementary reflectors; xORGLQ which here generated all or part of *Q*, and xORMLQ (or xUNMLQ) which we post-multiplied with a given matrix[i.e., Q^T Q^H(if *Q* is complex)]. The LQ factorization of *A* was essentially the same as the *QR* factorization of A^T (^{AH} if *A* is complex) in the model renderings since $A = \begin{pmatrix} L & 0 \end{pmatrix} Q \iff A^T = Q^T \begin{pmatrix} L^T \\ 0 \end{pmatrix}.$ The *LQ* factorization was then employed to find a minimum norm solution of an underdetermined system of linear equations *Ax* = *b* where *A* was *m*-by-*n* with *m* < *n* and had rank *m* in the *An. arabiensis* model The solution was given by $x = Q^T \begin{pmatrix} L^{-1}b \\ 0 \end{pmatrix}$ which was be computed by calls to xTRTRS and xORMLQ. See Gill, Murray, and Wright (1981) for more details on LQ factorization.

The covariance column summarized the Hessian approximation employed for each capture point, geosampled, *An. arabiensis*, geoclassified, LULC, sub-meter resolution, aquatic, larval habitat, grid-stratified, eco-endmember, capture point, in the non-heuristic, geo-spectrotemporal estimation method. In mathematics, the Hessian matrix or Hessian is a square matrix of second-order partial derivatives of a scalar-valued function, or scalar field. It describes the local curvature of a function of many variables[4]. The covariance matrix for the explicative, LULC endmember, regressable, *An. arabiensis*, aquatic, larval habitat, Lagrange multipliers in the oviposition, aquatic, larval habitat, forecast, orthogonal, geoclassifiable, ento-ecoepidemiological, vulnerability model estimator dataset was computed as $(\mathbf{A}\mathbf{H}^{-1}\mathbf{A}')^{-1}$The *p*-value reported for a restriction in the model was computed from a beta distribution rather than a *t* distribution as the numerator and the denominator of the *t* ratio for the estimated Lagrange multiplier were not independent. The Lagrange multipliers for the active restrictions were quantifiable with the geosampled, oviposition, endmember, *An. arabiensis*, LULC, orthogonal, parameterized estimates. The Lagrange multiplier estimates were then computed employing the relationship $\mathbf{A}'\lambda = \mathrm{g}$ where the dimensions of the constraint matrix $\mathbf{A}$ was based on the number of constraints, and the number of eco-endmember, eco-georeferenceable, capture point, LULC, geosampled, geo-spectrotemporal, oviposition, habitat signature parameters, λ which was based on the vector of Lagrange multipliers where *g* was the gradient of the objective function of the final prognosticated dataset of eco-georeferenceable, unknown, seasonal, hyperproductive,foci estimates.

The final gradient included the effects of the estimated $\mathbf{S}$ matrix in the *An. arabiesnsis* forecast, vulnerability, LULC model. For example, in the aquatic, larval habitat, OLS, the final gradient was: $\mathrm{g} = \mathbf{X}'(\mathrm{diag}(\mathbf{S})^{-1} \otimes \mathbf{I})r$ where *r* was the residual vector. Note that when nonlinear restrictions were imposed onto the capture point, eco-endmember, geocassifiable, LULC, frequency, model estimators the convergence measured the geosampled, larval density, seasonal, count values greater than one for other geosampled variable iterations.

In general, the hypothesis tested was written as $H_0 : \mathbf{h}(\theta) = 0$ where $\mathbf{h}(\theta)$ was a vector-valued function of the geosampled, capture point, eco-georeferenced, aquatic, larval habitat, eco-endmember, signature, LULC, multivariate, oviposition, parameters θ given by the *r* expressions specified on the TEST statement. We let $\hat{\mathbf{V}}$ be the estimate of the covariance matrix of $\hat{\theta}$. We also let $\hat{\theta}$ be the unconstrained, frequency, endmember estimate of θ and $\tilde{\theta}$ be the constrained estimate of θ such that $h(\tilde{\theta}) = 0$. We then let $\mathbf{A}(\theta) = \partial h(\theta)/\partial \theta \,|_{\theta}$ during the quantitation of the un-geosampled, aquatic, larval habitat, seasonal, hyperproductive, ento-ecoepidemiological, model

parameters. We let *r* be the dimension of $h(\theta)$ and *n* be the number of capture point, geosampled LULC observations. Using this notation, the statistics for the tests were computed in SAS.

The Wald test statistic was defined as $W = h^{'}(\hat{\theta})\left(\mathbf{A}(\hat{\theta})\hat{\mathbf{V}}\mathbf{A}^{'}(\hat{\theta})\right)^{-1}h(\hat{\theta})$. The Wald test is not invariant to reparameterization of the model (see Gregory and Veall 1985; Gallant 1987,). The choice between a *z*-value or a *t*-value depends on how the standard error of the coefficients has been calculated [2]. Because the Wald statistic was asymptotically distributed as a standard normal distribution in the eco-endmember, *An. arabienis*, aquatic, larval habitat, grid-stratified, sub-meter resolution, prognosticative, LULC, capture point, forecast, vulnerability model, we employed the *z*-score to calculate the p-value. In addition to quantitating the spectral coefficients, we had to estimate the residual variance, a *t*-value instead of the *z*-value.

In the OLS, normalized, linear regression of the ento-ecoepidemiological, geo-spectrotemporal, datset of empirically regressed, eco-georeferenecable, sub-meter resolution, geoclassifed, malaria mosquito, seasonal, hyperproductive, LULC, eco-endmembers, the variance-covariance frequency, signature, regression, time sreis dependnet matrix of the coefficients was Var[β^|X]=σ2(X′X)−1Var[β^|X]=σ2(X′X)−1 where σ2 was the variance of the residuals (here unknown had to be estimated from the geosampled endmember data) and X was the design matrix. The standard errors of the coefficients in the *An. arabiensis*, signature, habitat model was the square roots of the diagonal elements of the variance-covariance, geo-spectrotemporal, geoclassified, LULC matrix.

Because we did know σ2 we had to replace it by its estimate which here was described as σ^2=s2so: seˆ(βj^)=s2(X′X)−1j in the *An. arabiensis*, model framework Because we had to estimate the variance of the frequency, LULC signature, sub-mter resolution residuals to calculate the standard error of the grid-stratified, capture point, aquatic, larval habitat coefficients in the eco-endmember, forecast, vulnerability model, we needed to use a *t*-value and the *t*-distribution. For more information about the theoretical properties of the Wald test, see Phillips and Park (1988).

The Lagrange multiplier test statistic was $R = \lambda^{'}\mathbf{A}(\tilde{\theta})\tilde{\mathbf{V}}\mathbf{A}^{'}(\tilde{\theta})\lambda$ where λ was the vector of Lagrange multipliers from the computation of the restricted, endemic, explanatory, oviposition, *An. arabiensis*, capture point, seasonal, hyperproductive, eco-endmember, signature, LULC estimate $\tilde{\theta}$. The Lagrange multiplier test statistic was equivalent to Rao's efficient score test statistic: $R = (\partial L(\tilde{\theta})/\partial\theta)^{'}\tilde{\mathbf{V}}(\partial L(\tilde{\theta})/\partial\theta)$where L was the log-likelihood function for the estimation method used for determining geolocations of eco-georeferenceable, sub-meter resolution, grid-stratifiable, unknown, seasonal, hyperproductive foci.The likelihood function in the orthogonal, aquatic, larval habitat, geo-spectrotemporal, geoclassified, LULC signature, forecast, vulnerability, geo-spectrotemporal, ento-ecoepidemiological, endmember model was computed as$L = \text{Objective} \times Nobs/2$.

For OLS and 2SLS, the Lagrange multiplier test statistic in the oviposition ento-ecoepidemiological, signature, LULC model was aympoptically optimally computed as: $R = [(\partial\hat{S}(\tilde{\theta})/\partial\theta)^{'}\tilde{\mathbf{V}}(\partial\hat{S}(\tilde{\theta})/\partial\theta)]/\hat{S}(\tilde{\theta})$where $\hat{S}(\tilde{\theta})$ was the corresponding objective, frequency, capture point,, geosampled, eco-endmember, capture point, regressable, linearizable function, (i.e., value of a constrained, eco-georeferenceable, unknown, seasonal, hyperproductive, aquatic, larval, habitat, foci, explanatory estimate). The likelihood ratio test statistic was$T = 2\left(L(\hat{\theta}) - L(\tilde{\theta})\right)$where $\tilde{\theta}$ represented the constrained, capture point, endmember, grid-stratified, signature, frequency LULC estimate of θ and L was the concentrated log-likelihood value.For OLS and 2SLS, the likelihood ratio test statistic was computed as: $T = (n - nparms) \times (\hat{S}(\tilde{\theta}) - \hat{S}(\hat{\theta}))/\hat{S}(\hat{\theta})$.This capture point, test statistic was an approximation from $T = n \times log\left(1 + \frac{rF}{n - nparms}\right)$ whence the frequency, geo-spectrotemporal, immature, density count value of $rF/(n - nparms)$ in the geosampled, aquatic, larval habitat,capture point, *An. arabiensis*, forecast, vulnerability model was small(< than 12 immatures).

For each kind of test, under the null hypothesis, the test statistic for optimally quantitating the geo-spectrotemporal, eco-georeferenecable, *An. arabiensis,* aquatic, larval habitat, geosampled eco-endmember, signature, grid-stratified, LULC data was asymptotically distributed as a χ^2 random variable with *r* degrees of freedom, where *r* was the number of expressions in the TEST statement. The *p*-values reported for the tests were computed from the $\chi^2(r)$ distribution and were only asymptotically valid. When both RESTRICT and TEST statements were used in the PROC MODEL step, test statistics for summarizing, the geosampled, oviposition, *An. arabiensis*, eco-endmember, LULC, predictive, risk model estimators was computed by taking into account the constraints imposed by the RESTRICT statement.

We performed a likelihood ratio test for a compound hypothesis. test a*exp(-k) = 1-k, d = 0 ,/ lr. It is important to keep in mind that although individual *t* tests for each LULC, grid-stratfiied, sub-meter resolution, geo-spectrotemporal, *An. arabienis,* geosampled, aquatic larval habitat, seasonal, ecogeoreferenceable, un-geosampled, hypeproductive, capture point, endmember, foci covariate was printed by default into the parameter estimates table, they were only asymptotically valid for the nonlinear geo-spectrotemporally prognosticated models. In statistics, a likelihood ratio test is a statistical test used for comparing the goodness of fit of two statistical models, one of which (the null model) is a special case of the other (the alternative model)[2]. The likelihood ratio, and its logarithm, was employed to compute a *p*-value to decide whether or not to reject the *An. arabiensis* null model.When the logarithm of the likelihood ratio is used, the statistic is known as a log-likelihood ratio statistic, and the probability distribution of this test statistic, assuming that the null model is true, can be approximated employing Wilks' theorem [see Appendix 2].

Suppose we have a family of ento-ecoepidemiological, oviposition, eco-endmember, geo-spectrotemporal, LULC, capture point, geosampled, signature, malaria, mosquito, hyperproductive, aquatic, larval habitat, endmember foci probability density or mass functions f(θ, x) > 0.Furthermore, suppose this vector arthropod data was dependent on a *d*-dimensional capture point parameter θ which ranged over a parameter space H1. Then theorectically θ could be written as (θ1, . . . , θd).In general, however, H1 will not necessarily be a Euclidean space Rd or an open subset of one in any oviposition,ento-ecoepidemiological, endmember, sub-meter resolution, forecast, vulnerability, malaria, mosquito, LULC probabilistic, geo-spectrotemporal, signature, interpolative, iterative paradigm. It may be a curved surface or manifold in a higher-dimensional space, on which θ1, ..., θd could be local coordinates of a seasonal, eco-georeferenceable, empirical geosampeld dataset of hyperproductive, aquatic larval, habitat, , LULC eco-endmember,unknown foci. Here, Pθ would denote the probability distribution of x given θ ∈ H1, and Eθ could be the expectation under the distribution, for X1, ..., Xn in the independently distributed Pθ in the vector arthropod model.

Let L(θ, x) := log f(θ, x) be the log likelihood function in a malaria, mosquito, capture point, oviposition, endmember,sub-meter resolution, grid-stratifiable, LULC model.In so doing, partial derivatives ∂ log f(θ, x)/∂θi will occur at each θ ∈ H1, continuous with respect to θ in the ento-ecoepidemiologcal model, diagnostic output. In statistics, a likelihood function (often simply the likelihood) is a function of the parameters of a statistical model given data[2]. Likelihood functions play a key role in statistical inference, in vector arthropod, forecast, vulnerability, geo-spectrotemrpoal, ento-ecoepidemiological, LULC oviposition, eco-georeferenecable, endmember,capture point,malaria, mosquito model especially in methods of estimating a parameter from a set of statistics [1].

Partial derivatives of the eco-endmember, LULC, oviposition, ento-ecoepidemiological, aquatic, larval habitat were defined as derivatives of a function of multiple, unmixed signature variables especially when all but the variable of interest were held fixed during the differentiation. $\frac{\partial f}{\partial x_m} \equiv \lim_{h \to 0} \frac{f(x_1, \ldots, x_m + h, \ldots, x_n) - f(x_1, \ldots, x_m, \ldots, x_n)}{h}$. The partial derivative was denoted f_{x_m} for brevity. Partial derivatives were quantitable with respect to multiple, eco-endmember, oviposition, sub-meter resolution, grid-stratifiable, oviposition, geosampeld, *An. arabiensis,*capture point LULC variables, as denoted for examples $\frac{\partial^2 f}{\partial x^2} = f_{x\,x}$, $\frac{\partial^2 f}{\partial x\,\partial y} = f_{x\,y}$ and $\frac{\partial^3 f}{\partial x^2\,\partial y} = f_{x\,x\,y}$.For a "nice" two-dimensional (2-D) function $f(x, y)$ (i.e., one for which $f, f_x, f_y, f_{x\,y}, f_{y\,x}$ existed andwere continuous in the agro-irrigated, Riceland, agro-village, African, geosampled neighborhood (a, b)), then $f_{x\,y}(a, b) = f_{y\,x}(a, b)$.More generally, for "nice" ento-

endmember, LULC, prognosticated signature, frequency functions, mixed, partial derivatives had to be equal regardless of the order in which the differentiation was performed. We noted that that $f_{x\,x\,y} = f_{x\,y\,x} = f_{y\,x\,x}$ was tru in the model output. If the continuity requirement for mixed partials was dropped, during the ento-ecoepidemiological, forecast, vulnerability model construction for geo-spectrotemporally, aymptotically targeting seasonal, hyperproductive,capture point, eco-endmember, LULC processes it may be possible to construct functions for which mixed partials are not equal. An example may be the function $f(x,y) = \begin{cases} \frac{x\,y\,(x^2 - y^2)}{x^2 + y^2} & \text{for } (x,y) \neq (0,0) \\ 0 & \text{for } (x,y) = (0,0), \end{cases}$ which has $f_{x\,y}\,(0,0) = -1$ and $f_{y\,x}\,(0,0) = 1$. Abramowitz and Stegun (1972) give finite difference versions for partial derivatives.

A partial differential equation (PDE) is an equation involving functions and their partial derivatives; for example, the wave equation $\frac{\partial^2 \psi}{\partial x^2} + \frac{\partial^2 \psi}{\partial y^2} + \frac{\partial^2 \psi}{\partial z^2} = \frac{1}{v^2}\frac{\partial^2 \psi}{\partial t^2}$. A differential equation expressing one or more quantities in terms of partial derivatives is called a partial differential equation[8].An oviposition,eco-endmember, signature, malaria, mosquito, ento-ecoepidemiological, sub-meter resolution, grid-stratifiable, capture point, LULC, aquatic, larval habitat, partial differential equation for asymptotically, geo-spectrotemporally targeting seasonal, hyperproductive, eco-georeferenecable,LULC foci may be solved exactly in the Wolfram Language using DSolve[*eqn*, *y*, {*x1*, *x2*}], and numerically employing NDSolve[*eqns*, *y*, {*x*, *xmin*, *xmax*}, {*t*, *tmin*, *tmax*}].In general, partial differential equations are much more difficult to solve analytically than ordinary differential equations[7]. The ento-ecoepidemioloigcal, immature, forecast, vulnerability, endmember LULC,model may be solved using a Bäcklund transformation, characteristics, Green's function, integral transform, Lax pair, separation of variables, or via quantitation of finite differences for targeting, unknown, seasonal, prolific foci, Fortunately, partial differential equations of second-order are often amenable to analytical solution. Such PDEs are of the form $A\,u_{x\,x} + 2\,B\,u_{x\,y} + C\,u_{y\,y} + D\,u_x + E\,u_y + F = 0$.Linear second-order,ento-ecoepidemiological, LULC, endmember PDEs may then be classified according to the properties of the matrix $Z \equiv \begin{bmatrix} A & B \\ B & C \end{bmatrix}$as elliptic, hyperbolic, or parabolic.If Z is a positive definite matrix in a sub-meter resolution, grid-stratifiable oviposition, eco-georeferenecable, endmember, LULC, prognosticative, geo-spectrotemporal, geosampled model (i.e., det (Z)>0) the PDE may be be elliptic. Laplace's equation and Poisson's equation are examples.

Thereafter boundary conditions may be employable in a sub-mterv reoslition, oviposition, forecast, vulnerability, eco-endmember,grid-stratifiable, LULC model for rendering the constraint $u\,(x,y) = g\,(x,y)$ on $\partial\Omega$, where $u_{x\,x} + u_{y\,y} = f\,(u_x, u_y, u, x, y)$ to determine if it holds in Ω.If det (Z)>0, the PDE is said to be hyperbolic[see 7]. The wave equation is an example of a hyperbolic partial differential equation which may help optimally, symptotically, geo-spectrotemporally, remotely, target, seasonal, eco-georeferenceable, hyperproductive, malaria mosquito aquatic, larval habitat, capture point foci Initially, boundary conditions may be employable for robustly parsimoniously rendering $u\,(x,y,t) = g\,(x,y,t)$ for $x \in \partial\Omega,\, t > 0 u\,(x,y,0) = v_0\,(x,y)$ in Ω and $u_t\,(x,y,0) = v_1\,(x,y)$ in Ω, where $u_{x\,y} = f\,(u_x, u_t, x, y)$ holds in Ω in the model output. If the PDE is said to be parabolic[4]. A sub-meter resolution, ento-eco-epidemiological, malaria, oviposition, vector arthropod, LULC eco-endmember, diffusion equations would be an example. Initial-boundary conditions may then be parsimoniously, robustly employed to give $u\,(x,t) = g\,(x,t)$ for $x \in \partial\Omega,\, t > 0 u\,(x,0) = v\,(x)$ for $x \in \Omega$, where $u_{x\,x} = f\,(u_x, u_y, u, x, y)$ holds in Ω in det (Z)> the model for optimally, targeting, seasonal, hypeproductive foci.

Suppose that all the geosampled, sub-meter resolution, endmember, geoclassified, grid-stratifiable, explanatory, eco-georeferenceable, oviposition LULC,spatial filter, orthogonal elements in a grid-stratified,malaria, vector arthropod, prognosticative, geo-spectrotemporal, uncertainty-oriented,probabilistic matrix Iij (θ) := Eθ ∂L(θ, x) ∂θi ∂L(θ, x) ∂θj , i, j = 1, ..., d, are well-defined and finite. Then Iij (θ) would be a symmetric $d \times d$ matrix, (i.e, the

Fisher information matrix) at θ. It can be easily seen that the ento-ecoepidemiological, eco-endmember, geo-spectrotemporal, LULC, signature, frequency model would be nonnegative definite whence targeting unknown seasonal, hyperproductive foci, since for any t = (t1, . . . , td), there would be X d i,j=1 Iij (θ)titj = Eθ X d i=1 ti ∂L(θ, x) ∂θi !2 ≥ 0. It may be assumed that the Fisher information matrix is strictly positive definite in the model for all θ, in other words, in the last inequality, "≥ 0" is replacable by "> 0" if at least one ti = 0 in the model output. This will assure that the model H1 is truly *d*-dimensional. For example, if for some i = 1, . . . , d, ∂L(θ, x)/∂θi = 0 for all θ in an oviposition, sub-meter resolution, eco-endmember, malaria, mosquito, forecast, vulnerability,grid-stratified, geo-spectrotemporal, ento-ecoepidemiological, LULC model and x, then Iij (θ) = 0 for all j, Iij would not be positive definite in the predicted output (e.g., geolocation of eco-georeferenecable, seasonal, hyperproductive, LULC , unknown, aquatic, larval habitat, capture point, iteratively intyerpolated, signature foci) and the true dimension of model H1 would be d − 1 or less. Although not necessary for the given definition of Iij (θ), it may be often convenient to assume that second partial derivatives Hij (x, θ) := ∂ 2 log f(θ, x)/∂θi∂θj exist for i, j = 1, ..., d in these model circumstances.

The Fisher information matrix is important in vector epi-entomological, prognosticative signature statistics, For example, this matrix may render an honest definition of the dimensions of an empirical geosampled, geo-spectrotemporal, unmixed, oviposition dataset of ento-ecoepidemiological, empirically regressable, ecogeoreferenecable, sub-meter resolution, grid-stratifiable, LULC, capture point, *An. arabiensis*, aquatic, larval habitat, prognosticators in a , vulnerability, geo-spectrotemporal, eco-endmember model. Let H0 be an m-dimensional subset of H1 for some m < d in the predictive, risk model for asymptotically, remotely targeting eco-georeferenceable, seasonal, unknown, prolific foci. It may be assumed then that H0 is "smooth" in the sense that at any hyperproductive, seasonal, capture point, ento-ecoepidemiological foci of H0. As such, a malariologist or medical entomologist could select of the geosampled, *An. arabiensis*, aquatic, larval habitat, vulnerability, endmember, geo-spectrotemporal, LULC, grid-stratified,oviposition parameters, say for example θ1, ..., θm, for which the other d − m parameters are twice differentiable functions of θ1, ..., θm. Or, H0 may be given by way of an *m*-dimensional, capture point, geosampled, eco- endmember, signature dataset of LULC parameters φ = (φ1, ..., φm) with a mapping φ → θ(φ) of H0 into H1, such that the geo-spectrotemporal, eco-georeferenceable, malaria, mosquito, orthogonal, endmember, forecasted, partial derivatives ∂/∂φj and ∂ 2/∂φj∂φk of f(θ(φ), x) exist in the model outpt and have the same endmember properties with respect to φ as were assumed with respect to θ.

Consider the family of all spectrotemporal, normal distributions N(μ, σ2), with d = 2 as rendered from a vector arthropod, oviposition, forecast, vulnerability, endmember, sub-meter resolution, grid-stratified, eco-georeferenecable, *An. arabiensis*, LULC model. Here μ can be any real, geosampled, aquatic, larval habitat, capture point, hyperproductive, eco-georeferenceable, ento-eco-epidemiological foci and σ or σ 2 any number > 0. As such, thesubfamily with μ = 0 will then have dimension m=1. In a trinomial distribution, there may be *n* independent experimental trials with multiple possible, forecast, vulnerability, capture point, outcomes, having respective endmember, hyperproductive, eco-georefereneceable, aquatic, larval, habitat malaria, mosquito, oviposition, LULC endmember, geo-spectrotemporal probabilities (p1, p2, and p3) occurring on each trial. Then pj ≥ 0 and p1 + p2 + p3 = 1. Suppose a malariologist or medical entomologist assumes that pj > 0 for each j in the habitat, signature, LULC model.This parameter space H1 may have a dimension d = 2. He or she may then take for example, p1 and p2 as eco-georeferenecable, capture point, seasonal, hyperproductive, LULC, eco-endmember, foci coordinates, where p3 ≡ 1 − p1 − p2. One lower-dimensional submodel H0 is the family of Hardy–Weinberg equilibrium distributions in which for some p with 0 < p < 1 and q ≡ 1 − p, p1 = p 2 , p2 = 2pq, and p3 = q 2[2] . Hence, in the oviposition, eco-endmember, prognosticative, LULC model φ = φ1 = p would be the optimal, geoclassifiable, capture point, aquatic,malaria mosquito, larval habitat geosampled unknown parameter for H0, which may have dimension m = 1, and θ(p) = {θj (p)} 3 j=1 = {pj (p)} 3 j=1 = (p 2 , 2pq, q2). So the *An. arabiensis*, aquatic, larval habitat, eco-endmember, oviposition, orthogonal, LULC, signature, risk mapping θ(·)would be nonlinear (quadratic), but the derivatives with respect to p of all orders would exist and would be continuous in the model output whence optimally seasonally asymptotically, targeting unknown, seasonal, hyperproductive, eco-georeferenecable,endmember foci.

A malariologist or a medical entomologist may assume that an empirical, geospectrotemporal, geosampled, regressable ento-ecoepidemiological, oviposition, dataset of eco-georeferenecable, grid-stratified, geoclassified, LULC, sub-meter resolution, malaria, mosquito, capture point, aquatic, larval, habitat observations X1, . . . , Xn are independently distributed with likelihood function f(θ, x) for some θ ∈ H1. A malariologist or medical entomologist

may then want to test the hypothesis that θ ∈ H0. This can be conducted by letting L(θ) = Πn j=1f(θ, Xj) be the likelihood function in the ento-ecoepidemiological, forecast, vulnerability, LULC model. Let MLd be the maximum of the likelihood for θ in H1, in other words. In so doing, MLd = L(ˆθd) where θbd would be the maximum likelihood estimate of θ in H1, provided it exists in regression space. Let MLm be, likewise, the maximum of the likelihood for θ in H0 in the forecast, vulnerability, endmember, oviposition, LULC, *An. arabiensis*, risk model. Then MLm ≤ MLd would exist in the model renderings because H0 ⊂ H1. Let Λ be the likelihood ratio, Λ = MLm/MLd, so that 0 < Λ ≤ 1. The malariologist or medical entomologist could then reject H0 if Λ is small, or sufficiently less than 1, depending on n, but not reject it if Λ is close to 1 in the model output (seasonal, targeted, unknown, hyperproductive, aquatic, larval habitat, eco-endmember foci).

S. S. Wilks in 1938 proposed the following test: let W = −2 log Λ, so that 0 ≤ W < ∞. Wilks found that if the hypothesis H0 is true, then the distribution of W converges as n → ∞ to a χ 2 distribution with d−m degrees of freedom, which may not be dependent on true θ = θ0 ∈ H0 values. Thus, H0 would be rejected in a signature *An. arabeinsis*, sub-meter resolution, eco-endmember, signature, LULC model if W is too large in terms of the tabulated χ 2 d−m distribution rendered from the ento-ecoepidemiological, prognosticative, malaria, mosquito, orthogonal, oviposition, endmember, non-linear vector arthropod model. In a multinomial, trinomial, capture point, seasonal hyperproductive, unknown variable tabulated probability distribution for which the jth outcome has probability pj, the jth outcome may be Xj times in n trials. Hence since Xj has a binomial (n, pj) distribution[2], the maximum likelihood estimate of pj in an *An. arabiensis*, endmember, sub-meter resolution, LULC, predictive, oviposition, risk model for asymptotically targeting, capture point, eco-georeferenceable, seasonal, hyperproductive, aquatic, larval habitat foci would be Xj/n for each j. For the Hardy–Weinberg, aquatic, larval habitat, quantitated, LULC endmember, *An. arabiensis*, submodel of the trinomial, the maximum likelihood estimate of p may be easy to tabulate: the likelihood function may be defined as (p2) X1 (2pq) X2 (q 2) X3 times factors not depending on p, or p 2X1+X2 q X2+2X3 times such factors. Such a geosampled, geo-spectrotemporal, malaria, mosquito, ento-ecoepidemiological, eco-endmember, signature, LULC, forecast, vulnerability, capture point model may have the form of a binomial likelihood function for success probability p and 2n trials. So it is theoretically possible to find the likelihood ratio and Wilks statistic Λ and W respectively in such a model for optimally, asymptotically, remotely, targeting unknown, seasonal, eco-georeferenceable, hyperproductive, aquatic, larval habitat, eco-endmember, geo-spectrotemporal foci

Recall in our previous malaria, eco-endmember, sub-meter resolution, oviposition, LULC, predictive, risk model example where H1 was the set of all normal distributions with d = 2, and H0 was μ = 0, having dimension m = 1. In this case another test of H0 could be optimally conducted whence the 0 is outside the 1 − α confidence interval for μ in the model output. Question: is this test, or the Wilks test, preferable in this case when optimally quantitating an empirical geosampled, geospectrotemporal, eco-endmember, signature, iteratable, interpolative, LULC, oviposition dataset of regressable, geosampled, sub-meter resolution, grid-stratifiable, explanators? The Wilks test is only applicable when *n* is large and with an approximation, whereas the test based on a confidence interval would employ the t distribution which is exact for any n ≥ 2[4]. The likelihood ratio test of a multinomial hypothesis for k categories a special case of Wilks's test with d = k – 1[6].

The Wilks's statistic may render an asymptotic distribution for any seasonal, eco-georeferenecable, regressed, geosampled, sub-meter resolution, grid-stratifiable, unknown, malaria, mosquito, vulnerability mapped dataset of signature frequency variables associated with a targeted hyperproductive,eco-endmember,unknown, LULC, seasonal, capture point,aquatic, larval habitats if H0 is true. Wilks's statistic (n, p, q), also sometimes denoted by Un.p,q, is widely used for various statistical tests in multivariate analysis since it, supposedly, plays the same role as the Fisher–Snedecor F1,2 in univariate statistics. The distribution of Wilks's statistic is, however, difficult to track, because, its density lacks a closed form expression, except for some simple values of its parameters. Derived distributions, such as geo-spectrotemporal, geosampled, signature, frequency, LULC aquatic, larval habitat, ento-ecoepidemiological, un-geosampled, eco-georeferenecable, capture point, oviposition, malaria, mosquito, prognosticative, sub-meter resolution, aquatic, larval habitat, vulnerability forecasts overlaid on grid-stratified, geoclassified, endmember densities may be based on the product and ratio of two independent Wilks's statistics which may be computed in SAS.

Here we also examined asymptotic distributions of the canonical correlations between x1;q×1 and x2;p×1 with q≤p, based on a sample of size of N=n+1 in the forecast, vulnerability, ento-

ecoepidemiological,sub-meter resolution, grid-stratified, endmember ,LULC model for asymptotically, remotely targeting seasonal, hyperproductive, eco-georeferenceable, *An. araibiensis,*capture points. The asymptotic distributions of the canonical, malaria, mosquito, vector arthropod, aquatic, larval habitat geosampled, geo-spectrotemporal correlations were studied extensively when the dimensions q and p were fixed. However, these approximations worsed when q or p was large in comparison to *n*. To overcome this weakness,we propose employing first derived, asymptotic distributions of the canonicalized, eco-endmember, signature, frequency, sub-mter resolution, grid-stratfiable, geoclassfiiable, LULC correlations under a high-dimensional framework such that q is fixed, m=n−p→∞ and c=p/n→c0∈[0,1).If a malariologist or medical entomologist assumes that x1 and x2 has a joint (q+p)-variate normal distribution then an extended Fisher's z-transformation may be proposed for targeting seasonal, hypeprproductive, eco-georeferenecable, sub-meter resolution, grid-stratified, unknown, aquatic, larval habitat, capture point foci. The asymptotic distributions may be improved further by deriving their asymptotic expansions. Numerical simulations may reveal that eco-endmember, geo-spectrotemporal, geosampled, grid-stratified, optimizable, LULC approximations asymptotically,target, eco-georeferenceable, seasonal, hyperproductive, unknown, *An.arabiensis*, aquatic, larval habitats with more accuracy than the classical eco-endmember, signature, iteratively interpolatable, LULC, orthogonal approximations for a large range of p,q, and n and for optimally quanitating population canonical correlations.

Various approaches have been suggested in the literature to approximate the density of (n, p, q). For example, Ulyanov, Wakakiand Fujikoshi [2006] give the Berry–Esseen bound for high dimensional asymptotic approximation of (n, p, q). In probability theory, the central limit theorem states that, under certain circumstances, the probability distribution of the scaled mean of a random sample converges to a normal distribution as the sample size increases to infinity[2]. Under stronger assumptions, the Berry–Esseen theorem, or Berry–Esseen inequality, renders a more quantitative result, as it also specifies the rate at which this convergence takes place by giving a bound on the maximal error of approximation between the normal distribution and the true distribution of the scaled sample mean. The approximation may be robustly parsimoniously measured in an eco-georeferenecable, grid-stratified, geo-classified, geo-spectrotemporal, geosampled, ento--epidemiological, sub-meter resolution, eco-endmember,signature, frequency, LULC, malaria mosquito, oviposition, vulnerability, ento-ecoepidemiological, forecast, model by employing the Kolmogorov–Smirnov distance.

In statistics, the Kolmogorov–Smirnov test (K–S test or KS test) is a nonparametric test of the equality of continuous, one-dimensional probability distributions which may be employable to compare a sample in an eco-georeferenceable, geo-spectrotemporal, aquatic, larval habitat vector arthropod (riceland,oviposition, *An. arabiensis,*seasonal, hyperproductive, geo-spectrotemporal, geosampled foci), sub-meter resolution, grid-stratifiable, geoclassifiable, LULC, endmember model with a reference probability distribution (one-sample K–S test), or to compare two samples (two-sample K–S test). The Kolmogorov–Smirnov statistic quantifies distances between empirical distribution function of a sample geosampled, dataset and the cumulative distribution function of the reference distribution, or between the empirical distribution functions of two datasets[2]. In probability theory and statistics**,** the CDF of a real-valued random variableX (e.g., sub-meter resolution, eco-georeferenceable, capture point, aquatic, larval habitat, grid-stratified, endmember, LULC, eco-georeferenecable, hyperproductive foci) or just distribution function of X, evaluated at x, is the probability that X will take a value less than or equal to x[1]. The null distribution of this statistic may be calculable under the null hypothesis that the sample is drawn from the reference distribution (in the one-sample case) or that the samples are drawn from the same distribution (in the two-sample case). In each case, the multivariate, vector arthropod, aquatic, larval habitat, capture point, uncertainty-oriented,probabilistic, eco-endmember, LULC signature distributions for a seasonal, eco-georeferenecable, unknown prognosticated, capture point, hyperproductive foci may be considered under the null hypothesis based on continuous distributions which may be otherwise unrestricted. The two-sample K–S test is one of the most useful and general nonparametric methods for comparing two samples, as it is sensitive to differences in both location and shape of the empirical CDFs of the two samples [2].

The Kolmogorov–Smirnov test can be modified to serve as a goodness of fit test. The goodness of fit of a statistical model describes how well it fits a set of observations [2]. Measures of goodness of fit typically can summarize the discrepancy between observed, sub-meter resolution, grid-stratifiable, geoclassifiable, eco-endmember malaria, mosquito, aquatic, larval habitat, capture point, oviposition, geo-spectrotemporal geosampled,LULC siganture, iterative interpolative values and the values expected under an eco-georeferenceable, seasonal, hyperproductive

reference, sub-meter resolution, LULC model in question. Such measures can be used in statistical hypothesis testing, (e.g. to quantitate for normality of capture point target residuals, to test) whether two seasonal, eco-georeferenceable, unknown, forecasted, vector arthropod, aquatic, larval, habitat samples are drawn from identical distributions (e.g., Kolmogorov–Smirnov tests) for determining ungeosampled, hyperproductive, *An. arabeinsis*, geo-spectrotemporal, eco-endmember, signature foci, or whether outcome immature density frequencies follow a specified distribution (e.g., Pearson's chi-squared test). In the analysis of variance, one of the components into which the variance may be partitioned which may be due to a lack-of-fit sum of squares. In statistics, a sum of squares due to lack of fit, or more commonly a lack-of-fit sum of squares, is one of the components of a partition of the sum of squares in an analysis of variance, used in the numerator in an F-test of the null hypothesis that can state that a proposed model fits well[2].

In the special case of testing for normality of the distribution as rendered from a sub-meter resolution, eco-endmember, LULC dataset of empricially regressable, eco-georeferenceable, oviposition, geo-spectrotemporal, malaria, mosquito, aquatic, larval habitat, hyperproductive, oviposition, capture point samples may be standardizable and as usch comparable with a standard normal distribution of non-prolific, seasonal, foci. This may be equivalent to setting the mean and variance of the reference distribution equal to the geosampled, geo-spectrotemporal, immature, capture point, density, frequency count estimates to define the specific reference, siganture, distribution, endmember LULC changes in the null distribution of the test statistic. Various studies have found that, even in this corrected form, the test is less powerful for testing normality than the Shapiro–Wilk test or Anderson–Darling test[see 8 and 9]. However, these other tests have their own disadvantages. For example, the Shapiro–Wilk test is known not to work well in samples with many identical values.

Here, explanatory, independent, malaria, mosquito, aquatic, larval habitat geo-spectrotemporal, geosampled, eco-endmember, LULC, sub-meter resolution, capture point samples, the convergence rate was $n^{-1/2}$, where n was the sample size, and the constant was estimated in terms of the third absolute normalized moments. In mathematics, a moment is a specific quantitative measure, employed in both mechanics and statistics, of the shape of a set of points. If the points represent mass, then the zeroth moment is the total mass, the first moment divided by the total mass is the center of mass, and the second moment is the rotational inertia[3]. If the points represent probability density such as in our *An. arabiensis*, aquatic, larval habitat, capture point, forecast, vulnerability model, then the zeroth moment is the total probability (i.e. one), the first moment is the mean, the second central moment is the variance, the third central moment is the skewness, and the fourth central moment (with normalization and shift) is the quantizable kurtosis.

In probability theory and statistics, kurtosis is a measure of the "tailedness" of the probability distribution of a real-valued, random, orthogonal, geosampled variable (e.g., geo-spectrotemporal, eco-georeferenceable, sub-meter resolution, vector arthropod, aquatic, larval habitat, capture point, seasonal, hypeproductive, frequency, larval, density, count). In a similar way to the concept of skewness, kurtosis can be a descriptor of the shape of an ento-ecoepidemiological, endmember, LULC, probability distribution and, just as for skewness, there are different ways of quantifying it for constructing a theoretical or field operational, prognosticative, malaria, mosquito, capture point, model and corresponding the observational, output (e.g., seasonally eco-georeferenceable, unknown, targeted, hyperproductive, capture point) to a sample from a sesonal, aquatic,larval habitat, geosampled population. Depending on the particular measure of kurtosis that is employed for quantatiting the uncertainty in the ento-ecoepidemiological, forecast, vulnerability, endmember, LULC signature model there are various interpretations of kurtosis, and of how particular measures should be interpreted in SAS.

The standard measure of kurtosis in the eco-georeferenecable, sub-meter resolution, *An. arabiensis*, geoclassifiable, oviposition, LULC, eco-endmember model was based on a scaled version of the fourth moment of the geo-spectrotemporal, geosampled,unmixed, signature data and immature, geosampled, vector arthropod, aquatic, larval, habitat population. This number was related to the tails of the distribution, not its peak. Higher kurtosis in an oviposition, sub-meter resolution, grid-stratifiable, LULC, endmember model for aymptotically targeting seasonal, eco-georeferenecable, hyperproductive, aquatic, larval habitat, capture point foci may be the result of infrequent extreme deviations (or outliers) in an empricial geosampled oviposition, malaria, mosquito, geosampled, empirical dataset of parameterizable spectral paramaters as opposed to frequent modestly sized deviations.

The kurtosis of any univariate normal distribution is 3[2]. It is common to compare the kurtosis of a distribution to this value. Distributions with kurtosis less than 3 would be platykurtic in an eco-georeferenecable, sub-meter resolution, geoclassifiable, *An. arabiensis*, grid-,stratifiable, LULC, oviposition, forecast, vulnerability model although this does not imply the distribution is "flat-topped" as sometimes reported in literature. Rather, it means the distribution produces fewer and less extreme outliers than does the normalized, geo-spectrotemporal, malaria, vector arthropod, geosampled, capture point, eco-endmember, signature distributions. An example of a platykurtic distribution is the uniform distribution which does not produce outliers [2].

Malaria mosquito, oviposition, endmember, LULC, model probability distributions with kurtosis greater than 3 would be leptokurtic. An example of a leptokurtic distribution in an ento-ecoepidemiological, eco-georeferenecable, geo-spectrotemporal, oviposition, sub-meter resolution, grid-stratifiable, *An. arabiensis*, LULC, aquatic, larval habitat, oviposition, endmember,capture point model, is the Laplace distribution.This distribution which has tails that asymptotically approach zero more slowly than a Gaussian, produces more outliers than the normal distribution. It is also common practice to use an adjusted version of Pearson's kurtosis, the excess kurtosis, which is the kurtosis minus 3, to provide the comparison to the normal distribution [4]. Alternative measures of kurtosis are: the L-kurtosis, which is a scaled version of the fourth L-moment; measures based on four population or sample quantiles. These are analogous to the alternative measures of skewness that are not based on ordinary moments.

An ento-ecogeoreferenecable, geo-spectrotemporal, *An. arabeinsis*, oviposition, capture point, LULC, signature, eco-endmember, sub-meter resolution, geoclassifiable, grid-stratifiable, forecast, vulnerability, signature model for asymptotically targteing seasonal, eco-georeferenecable, hyperproductive aquatic, larval, habitat foci may be established such that (n, p, q) has the same density as a product of independent univariate beta variables.In Consul [1967], for example, the author employed Meijer functions to express that density in a theoretical context, when simple values of the parameters are considered. In this article, we first established the density of the general (n, p, q) under a closed form expression, employing H-function probability density which resulted in drawing the aquatic, larval habitat, geosampled, endmember, capture point, eco-georefereneceable, LULC densities using MAPLE. Percentiles of this distribution were obtained for unknown, seasonal, hypeprproductive, *An. arabiensis*, aquatic, larval habitats forecasts accurately employing the exact distribution which served as a reference to which all other capture point approximate distributions were compared. Considering two explanatorial, geosampled, geo-spectrotemporal, independent, generalized Wilks's statistics 1(n1, p1, q1) and 2 (n2, p2, q2), where capture point, seasonal, hypeproductive, aquatic, larval habitat, eco-endmember, sub-meter resolution signature frequencies may take LULC, non-integer values can establish expressions of prognosticated immature densities of P = 1,2, and R = 1/2 in closed form. The likelihood ratio statistic intimately related to Wilks's statistic may then be considered, in different contexts (e.g., seasonal, targeting of unknown, malaria mosquito, hyperproductive foci).

Wilks's statistic is often compared to the Fisher–Snedecor variable F1,2 in univariate statistics but it should rather be compared to the standard beta variable and to the matrix variate beta, in matrix variate, ento-ecoepidemiological, sub-meter resolution, grid-stratifiable, malaria ,mosquito, geo-spectrotemporal, LULC, prognosticative, eco-endmember, prognosticative, vulnerability analysis when optimally asymptotically remotely targeting seasonal, eco-georeferenecable, hypeproductive foci. The determinant of the matrix beta variate, of both types I
and II may also be studied in these models. An alternate form of the generalizedWilks's statistic, may be found to be more closely related to F1,2 in such forecast, vulnerability, vector, arthropod models.

Distinguishing between two explanatory, eco-georeferenceable, eco-endmember, sub-meter resolution, grid-stratifiable, LULC,capture point, aquatic, larval habitat, oviposition, forecast, vulnerability models, each of which has no unknown parameters, may require the use of the likelihood ratio test which may be justifiable by the Neyman–Pearson lemma. In so doing, a malariologist or medical entomologist may demonstrate that such a test has the highest power among all competitors. If there exists a critical region $C$of size $\alpha$and a nonnegative constant $k$such that $\frac{\prod_{i=1}^{n} f(x_i \mid \theta_1)}{\prod_{i=1}^{n} f(x_i \mid \theta_0)} \geq k$ for a multiple, seasonal, eco-georeferenceable, *An.arabiensis*, LULC, hyperproductive,capture point, geo-spectrotemporal,ento-ecoepidemiological,oviposition dataset in $C$and $\frac{\prod_{i=1}^{n} f(x_i \mid \theta_1)}{\prod_{i=1}^{n} f(x_i \mid \theta_0)} \leq k$ not in C, then Cwould be

the best critical region of size α in the entomological, vector arthropod, geosampled, ento-endmember, empirical,LULC, non-heuristically optimizable, geo-spectrotemporal dataset.

Employing a Chebyshev polynomial of the first kind $T(x)$ we were able to,define $c_j = \frac{2}{N}\sum_{k=1}^{N} f(x_k)\,T_j(x_k) = \frac{2}{N}\sum_{k=1}^{N} f\left[\cos\left\{\frac{\pi\left(k-\frac{1}{2}\right)}{N}\right\}\right]\cos\left\{\frac{\pi j\left(k-\frac{1}{2}\right)}{N}\right\}$. in the *An. arabiensis*, eco-endmember,oviposition, signature, LULC,operational model for optimally, aymptotically targeting seasonal, eco-georeferenecable, hyperproductive,capture point, aquatic, larval habitat foci.Then $f(x) \approx \sum_{k=0}^{N-1} c_k\,T_k(x) - \frac{1}{2}\,c_0.$ It was exact for the N zeros of $T_N(x)$ in the ento-ecoepidemiological, LULC, geosampled, empirical dataset.This type of approximation is important for malaria mosquito,prognosticative,vulnerability endmember, sub-meter resolution, risk mapping because, when truncated, the error in the model would spread smoothly over $[-1, 1]$. Our Chebyshev approximation formula was very close to a minimax polygon (an approximating polynomial which has the smallest maximum deviation from the true function).

Optimization of an eco-endmember, geo-spectrotemporal, ento-ecoepidmeiological, sub-meter resolution, grid-stratifiable, orthogonal, LULC, capture point, malaria, mosquito, aquatic, larval habitat, oviposition, forecast, vulnerability model for satellite applications is often performed using an iterative process that adjusts coefficients of the surface expansion based on some norm of the far-field directivity[1]. Traditionally, this involves sampling the far-field, directivity, LULC, endmember patterns on a fixed uniform stratified grid within the specification polygon (see Sorensen, S.B., 1993). Here we presented a procedure that optimized an ento-ecoepidemiological, oviposition, LULC, grid-stratifiable, eco-endmember, sub-meter resolution LULC dataset for asymptotically targeting, unknown, ecogeoreferenceable, *An. arabiensis*, capture point, aquatic, larval habitats in a riceland African agro-ecosystem employing the minimax criteria. The new procedure exploited the filtering aspects of the geosampled larval habitat, seasonal ric-cycle LULC pattern in order to obtain improved results from the optimization exercise. The specification coverage polygon was analogous to the mask of a harmonic filter.

We replaced the capture point, geoclassified, grid-stratified, LULC *An. arabiensis*, eco-georeferenced eco-endmember, geo-spectrotemporal polygons by a sequence of contracting polygons beginning with a circumscribing ellipse and ending with the specification polygon. The problem for targeting seasonal, hyperproductive foci at the agro-irrigated study site was solved essentially by a sequence of optimizations. We also employed an adaptive grid method which more efficiently defined the endmember LULC sample pattern by recognizing the filtering aspects of the habitat, capture point shape. The method achieved significantly improved results at the cost of an extremely slow convergence. It is anticipated that for many commercial, seasonal, vector, arthropod, malaria, mosquito, aquatic, larval habitat, control applications this cost can be justified, given the significant improvement in predictive power that is possible in these vulnerability, porognostictaive paradigms.

The Chebyshev polynomials of the first kind generated an eco-georeferenecable, endmember, geo-spectrotemporal, geoclassifiable, LULC, grid-stratified, oviposition, sub-meter resolution, explanatory, unmixed dataset of orthogonal capture point, *An. arabiensis*, aquatic, larval habitat, endmember polynomials. The vector arthropod,capture point, orthogonal polynomials were revealed in SAS as a class of polynomials $\{p_n(x)\}$ defined over a range $[a, b]$ that follwed an orthogonality relation $\int_a^b w(x)\,p_m(x)\,p_n(x)\,dx = \delta_{mn}\,c_n,$ where $w(x)$ was a weighting function and δ_{mn} was the Kronecker delta. In mathematics, the Kronecker delta is a function of two variables, usually just positive integers where the Kronecker delta δij is a piecewise function of variables i and j [2].

The simplest interpretation of the Kronecker delta in the eco-endmember, LULC, prognosticative, geo-spectrotemporal, malaria, mosquito, sub-resolution, forecast, vulnerability model was the discrete version of the delta

International Research Journal of Computer Science and Application
Vol. 2, No. 1, March 2018, pp. 1-181
Available Online at http://acascipub.com/Journals.php

function which we defined by $\delta_{ij} \equiv \begin{cases} 0 & \text{for } i \neq j \\ 1 & \text{for } i = j. \end{cases}$ The Kronecker delta was implemented in the Wolfram Language as KroneckerDelta[*i*, *j*], employing a generalized form KroneckerDelta[*i*, *j*, ...] that returned 1 if all arguments were equal and 0 in the, vulnerability, time series, malaria model output It had the contour integral representation $\delta_{mn} = \frac{1}{2\pi i} \oint_\gamma z^{m-n-1}\, dz,$ whence γ was a contour corresponding to the unit circle and m and n were the integers. In three-space, the Kronecker delta of the *An. arabiensis*, aquatic, larval habitat, ento-ecoepidemiological, eco-georeferenecable, capture point, oviposition, LULC, geo-spectrotemporal signmature, frequency model satisfied the identities $\delta_{ii} = 3$, $\delta_{ij}\, \epsilon_{ijk} = 0$, $\epsilon_{ipq}\, \epsilon_{jpq} = 2\, \delta_{ij}$ and $\epsilon_{ijk}\, \epsilon_{pqk} = \delta_{ip}\, \delta_{jq} - \delta_{iq}\, \delta_{jp}$, based on the orthogonal polynomials where $w(x)$ (see Table 8).

Table 7. Orthogonal eco-endmember *An.arabiensis*, larval habitat polynomials where $w(x)$ was the weighting function and $c_n \equiv \int_a^b w(x)\, [p_n(x)]^2\, dx$

Polynomial	interval	$w(x)$	c_n
Chebyshev polynomial of the first kind	$[-1, 1]$	$(1-x^2)^{-1/2}$	$\begin{cases} \pi & \text{for n} = 0 \\ \frac{1}{2}\pi & \text{otherwise} \end{cases}$
Chebyshev polynomial of the second kind	$[-1, 1]$	$\sqrt{1-x^2}$	$\frac{1}{2}\pi$
Gegenbauer polynomial	$[-1, 1]$	$(1-x^2)^{\alpha-1/2}$	$\begin{cases} \frac{2^{1-2\alpha}\,\pi\,\Gamma(\text{n}+2\alpha)}{\text{n!}\,(\text{n}+\alpha)\,[\Gamma(\alpha)]^2} & \text{for } \alpha \neq 0 \\ \frac{2\pi}{\text{n}^2} & \text{for } \alpha = 0. \end{cases}$
Hermite polynomial	$(-\infty, \infty)$	e^{-x^2}	$\sqrt{\pi}\ 2^n\, n!$
Jacobi polynomial	$(-1, 1)$	$(1-x)^\alpha\,(1+x)^\beta$	h_n
Laguerre polynomial	$[0, \infty)$	e^{-x}	1
generalized Laguerre polynomial	$[0, \infty)$	$x^k\, e^{-x}$	$\frac{(n+k)!}{n!}$
Legendre polynomial	$[-1, 1]$	1	$\frac{2}{2n+1}$

The roots of the orthogonal, *An. arabiensis*, capture point, geo-spectrotemporal, grid-stratified, signature, LULC polynomials possessed many useful properties for optimally targeting, hypeproductive, aquatic, larval habitat, eco-georeferenecable, endmember foci For example we let $x_1 < x_2 < \ldots < x_n$ be the roots of $p_n(x)$ with $x_0 = a$ and $x_{n+1} = b$ in the malaria mosquito model. In so doing, then each interval $[x_\nu, x_{\nu+1}]$ in the model for $\nu = 0$, 1, ..., n contained exactly one root of $p_{n+1}(x)$. Between two roots of $p_n(x)$ there was at least one root of $p_m(x)$ for $m > n$ in the LULC, model output.

We then let c be an arbitrary real constant in the ento-ecoepidemiological, eco-endmember, *An. arabiensis*, geo-spectrotemporal model. In so doing, a capture point, grid-stratifiable, geo-spectrotemporal, eco-georeferenecable, oviposition, geoclassified, LULC polynomial (i.e, $p_{n+1}(x) - c\, p_n(x)$) had $n+1$ distinct real roots. If $c > 0$ ($c < 0$), these roots lay in the interior of $[a, b]$ of the model, with the exception of the greatest (least) root which lay

in $[a, b]$ only for $c \le \frac{p_{n+1}(b)}{p_n(b)} \quad \left(c \ge \frac{p_{n+1}(a)}{p_n(a)}\right)$. An eco-endmember, geo-spectrotemporal, geoclassifiable, LULC, variance decomposition was performed which subsequently revealed partial fractions $\frac{p_n(x)}{p_{n+1}(x)} = \sum_{\nu=0}^{n} \frac{l_\nu}{x - \xi_\nu}$, held in the model residual, parameterized derivatives whence the roots of $p_{n+1}(x)$ and $l_\nu = \frac{p_n(\xi_\nu)}{p'_{n+1}(\xi_\nu)} = \frac{p'_{n+1}(\xi_\nu)\, p_n(\xi_\nu) - p'_n(\xi_\nu)'\, p_{n+1}(\xi_\nu)}{[p'_{n+1}(\xi_\nu)]^2} > 0.$ occurred in the output.

Another interesting property in the ento-ecoepidemiological, malaria, mosquito, geo-spectrotemporal, oviposition, LULC model was obtained by letting $\{p_n(x)\}$ be the orthonormal set of grid-stratified, eco-endmember, signature, frequency, capture point, geosampled polynomials associated with the distribution $d\alpha(x)$ on $[a, b]$. Then the convergents R_n / S_n of the continued fraction $\frac{1}{A_1 x + B_1} - \frac{C_2}{A_2 x + B_2} - \frac{C_3}{A_3 x + B_3} - \ldots - \frac{C_n}{A_n x + B_n} + \ldots$ was robustly, parsimoniously given by $R_n = R_n(x) = c_0^{-3/2} \sqrt{c_0\, c_2\, c_1^2} \int_a^b \frac{p_n(x) - p_n(t)}{x - t}\, d\alpha(t)$ whence the capture point model residuals were $S_n = S_n(x) = \sqrt{c_0}\; p_n(x)$, where $n = 0$, 1, ... and $c_n = \int_a^b x^n\, d\alpha(x).$ Further, the roots of the, vulnerability, prognosticative, geo- orthogonal, endmember, malaria, capture point, eco-georeferenecable, LULC polynomials $p_n(x)$ was associated with the distribution $d\alpha(x)$ on the interval $[a, b]$ which were distinct and were geolocated in the interior of the interval $[a, b]$.

Subsequently, the prognosticative, Chebyshev, differential, aquatic, larval habitat, empirical LULC, eco-endmember, sub-meter resolution, signature, grid-stratified dataset of oviposition, geo-spectrotemporal, eco-georeferenecable, *An. arabiensis*, aquatic,larval habitat, model, frequency estimatators were used as an approximation to a non-linear,least squares fit, For nonlinear least squares fitting to a number of unknown parameters, linear least squares fitting may be applicable iteratively to a linearized form of the function in an oviposition, endmember, geo-spectrotemporal, eco-georeferenecable, *An. arabiensis*, aquatic,larval habitat, sub-meter resolution, LULC model,until convergence is achieved[1]. It may be possible to linearize a nonlinear capture point, geo-spectrotemporal, orthogonal, eco-endmember, signature, LULC function at the outset and still use linear methods for determining unknown, prolific, aquatic, larval habitat, fit parameters without resorting to iterative procedures. This approach may violate the implicit assumption that the distribution of errors is normal, but may still render acceptable results (e.g., field-verifiable, eco-georeferenecable, *An. arabiensis*, aquatic, larval habitat seasonal, hyperproductive, geosampled, LULC, sub-meter resolution, foci prognosticators) employing normalized equations. Depending on the type of fit and initial parameters chosen, the nonlinear endmember, orthogonal, LULC fit may have good or poor convergence properties in these probabilistic, geo-spectrotemporal, vector arthropod, oviposition paradigms. If uncertainties (in the most general case, error ellipses) are given for the capture points, the ento-ecoepidemiological, vector arthropod, model ouput may be weighted differently in order to optimally render the hyperproductive, aquatic, larval habitat, unknown capture points and their weights.

Vertical least squares fitting proceeds may geolocate the sum of the squares of the vertical deviations R^2 for a set of n malaria, mosquito, geosampled, geo-spectrotemporal, eco-georeferenceable, unknown, seasonal, hyperproductive, *An. arabiensis*, geosampled, capture point, aquatic, larval habitats employing $R^2 \equiv \sum [y_i - f(x_i, a_1, a_2, \ldots, a_n)]^2$ from a function f. Note that this procedure will not minimize the actual deviations from the regression line (which should be measured perpendicular to the given function). In addition, although the unsquared sum of habitat distances might seem a more appropriate quantity to minimize in an eco-georeferenecable, ento-ecoepidemiological, oviposition, geo-spectrotemporal, sub-mter resolution, grid-stratifiable, *An. arabiensis*, aquatic, larval habitat, vulnerability model for asymptotically, geo-spectrotemporally, remotely, targeting seasonal, hyperproductive, eco-georeferenecable, eco-endmember signature, iteratable or interpolative foci,employing

the absolute value, the output may have discontinuous, non-orthogonal, fractionalized, habitat derivatives which cannot be treated analytically. The square deviations from each geosampled, geo-spectrotemproal, LULC, capture point could however be summed, and the resulting residual could be minimized to find the best fit line. This procedure may result in optimally outlying, seasonal, hyperproductive, eco-georeferenecable, LULC endmember, oviposition, capture points which may subsequently render disproportionately large weighting. The condition for R^2 to be a minimum in such a model is that $\frac{\partial(R^2)}{\partial a_i} = 0$ for $i = 1, ..., n$. For a linear fit, $f(a, b) = a + b\,x$, may geosampeld, capture point, seasonal LULC endmeber variables may be expressable. Hence, the expressions, $R^2(a, b) \equiv \sum_{i=1}^{n} [y_i - (a + b\,x_i)]^2$, $\frac{\partial(R^2)}{\partial a} = -2\sum_{i=1}^{n} [y_i - (a + b\,x_i)] = 0$, and $\frac{\partial(R^2)}{\partial b} = -2\sum_{i=1}^{n} [y_i - (a + b\,x_i)]\,x_i = 0$ iterations could lead to the equations $n\,a + b\sum_{i=1}^{n} x_i = \sum_{i=1}^{n} y_i$ and $a\sum_{i=1}^{n} x_i + b\sum_{i=1}^{n} x_i^2 = \sum_{i=1}^{n} x_i\,y_i$. for aympoptically targeting seasonal, eco-georeferenceable, eco-endmember, sub-meter resolution, grid-stratifiable, signature, LULC, hyperproductive foci.

In matrix form, $\begin{bmatrix} n & \sum_{i=1}^{n} x_i \\ \sum_{i=1}^{n} x_i & \sum_{i=1}^{n} x_i^2 \end{bmatrix} \begin{bmatrix} a \\ b \end{bmatrix} = \begin{bmatrix} \sum_{i=1}^{n} y_i \\ \sum_{i=1}^{n} x_i\,y_i \end{bmatrix}$, so $\begin{bmatrix} a \\ b \end{bmatrix} = \begin{bmatrix} n & \sum_{i=1}^{n} x_i \\ \sum_{i=1}^{n} x_i & \sum_{i=1}^{n} x_i^2 \end{bmatrix}^{-1} \begin{bmatrix} \sum_{i=1}^{n} y_i \\ \sum_{i=1}^{n} x_i\,y_i \end{bmatrix}$. The 2 x 2 matrix inverse is $\begin{bmatrix} a \\ b \end{bmatrix} = \frac{1}{n\sum_{i=1}^{n} x_i^2 - (\sum_{i=1}^{n} x_i)^2} \begin{bmatrix} \sum_{i=1}^{n} y_i \sum_{i=1}^{n} x_i^2 - \sum_{i=1}^{n} x_i \sum_{i=1}^{n} x_i\,y_i \\ n\sum_{i=1}^{n} x_i\,y_i - \sum_{i=1}^{n} x_i \sum_{i=1}^{n} y_i \end{bmatrix}$, so $\frac{\sum_{i=1}^{n} y_i \sum_{i=1}^{n} x_i^2 - \sum_{i=1}^{n} x_i \sum_{i=1}^{n} x_i\,y_i}{n\sum_{i=1}^{n} x_i^2 - (\sum_{i=1}^{n} x_i)^2}$ c=,b= $\frac{\bar{y}\left(\sum_{i=1}^{n} x_i^2\right) - \bar{x}\sum_{i=1}^{n} x_i\,y_i}{\sum_{i=1}^{n} x_i^2 - n\,\bar{x}^2}$,c= $\frac{n\sum_{i=1}^{n} x_i\,y_i - \sum_{i=1}^{n} x_i \sum_{i=1}^{n} y_i}{n\sum_{i=1}^{n} x_i^2 - (\sum_{i=1}^{n} x_i)^2}$ and d= $\frac{(\sum_{i=1}^{n} x_i\,y_i) - n\,\bar{x}\,\bar{y}}{\sum_{i=1}^{n} x_i^2 - n\,\bar{x}^2}$ (see Kenney and Keeping 1962). These can be rewritten in a simpler form in an oviposition, malaria, mosquito, eco-georefereneceable, sub-meter resolution, grid-stratifiable, geoclassifable, endmember, LULC, forecast, vulnerability model by optimally remotely, parsimoniously defining the sums of squares $SS_{xx} = \sum_{i=1}^{n} (x_i - \bar{x})^2 = \left(\sum_{i=1}^{n} x_i^2\right) - n\,\bar{x}^2$, $SS_{yy} = \sum_{i=1}^{n} (y_i - \bar{y})^2 = \left(\sum_{i=1}^{n} y_i^2\right) - n\,\bar{y}^2$ and $SS_{xy} = \sum_{i=1}^{n} (x_i - \bar{x})(y_i - \bar{y}) = \left(\sum_{i=1}^{n} x_i\,y_i\right) - n\,\bar{x}\,\bar{y}$,

A forecast, vulnerability, oviposition, malaria mosquito, LULC, sub-meter resolution, grid-stratifiable, endmember signature model may also be written as $\sigma_x^2 = \frac{SS_{xx}}{n}$, $\sigma_y^2 = \frac{SS_{yy}}{n}$ and $\mathrm{cov}(x, y) = \frac{SS_{xy}}{n}$. Here, $\mathrm{cov}(x, y)$ would be the covariance and σ_x^2 and σ_y^2 would be the model variances. Note that the quantities $\sum_{i=1}^{n} x_i\,y_i$ and $\sum_{i=1}^{n} x_i^2$ can also be interpreted as the dot products [e.g., $\sum_{i=1}^{n} x_i^2 = \mathbf{x} \cdot \mathbf{x}$, $\sum_{i=1}^{n} x_i\,y_i = \mathbf{x} \cdot \mathbf{y}$.] In mathematics, the dot product or scalar product (sometimes inner product in the context of Euclidean space, or rarely projection product for emphasizing the geometric significance), is an algebraic operation that takes two equal-length sequences of numbers (usually coordinate vectors) and returns a single number [7]. This operationmay be definable either algebraically or geometrically in an oviposition, ento-epidemiological, forecast, vulnerability, sub-meter resolution, endmember, grid-stratifiable, LULC model for aymptotically targeting, eco-georeferenecable, seasonal, hyperproductive, capture point, aquatic, larval, habitat foci

In terms of the sums of squares, in our oviposition, ento-epidemiological, LULC model *An. arabiensis*, forecast, vulnerability model, the regression coefficient, eco- endmember signature coefficients b was given by

$b = \frac{\operatorname{cov}(x, y)}{\sigma_x^2} = \frac{\mathrm{ss}_{xy}}{\mathrm{ss}_{xx}}$, and $a$was given in terms of $b$using (◇) as $a = \bar{y} - b\,\bar{x}$.The overall quality of the fit was then parameterized in terms of a quantity known as the correlation coefficient, which we defined in the LULC model by $r^2 = \frac{\mathrm{ss}_{xy}^2}{\mathrm{ss}_{xx}\,\mathrm{ss}_{yy}}$, .This rendered the proportion of ss_{yy}which was accounted for by the regression of the ento-epidemiological, geo-spectrotemporal, geosampled, empiricial, geosampled, regressed, oviposition,capture point,aquatic, larval, habitat variables.

We let $\hat{y}_i$be the vertical coordinate of the best-fit line with x geosampled, eco-endmember seasonal, hypeproductive,signature, foci coordinate x_i, so $\hat{y}_i \equiv a + b\,x_i$.In so doing, the error between the actual vertical point $y_i$and the fitted, *An. arabiensis*, aquatic, larval habitat, prolific, capture point was given by $e_i \equiv y_i - \hat{y}_i$. .Therefater, we defined s^2as an estimator for the variance in e_i, $s^2 = \sum_{i=1}^{n} \frac{e_i^2}{n-2}$. Subsequently, s was be given by $s = \sqrt{\frac{\mathrm{ss}_{yy} - b\,\mathrm{ss}_{xy}}{n-2}} = \sqrt{\frac{\mathrm{ss}_{yy} - \frac{\mathrm{ss}_{xy}^2}{\mathrm{ss}_{xx}}}{n-2}}$.

The standard errors for $a$and $b$are$\mathrm{SE}(a) = s\sqrt{\frac{1}{n} + \frac{\bar{x}^2}{\mathrm{ss}_{xx}}}$ are a special case of the Gegenbauer polynomial with $\alpha = 0$[4].The ento-ecoepidemiological, geo-spectrotemporal, eco-georeferenecable, *An. arabiensis*, aquatic, larval habitat, endmember, polgonized, LULC, foci covariates $C_n^{(\lambda)}(x)$ were solutions to the Gegenbauer differential equation for integer n. They were generalizations of the associated Legendre polynomials to $(2\lambda + 2)$-D space, and were proportional to (or, depending on the normalization, equal to) the ultraspherical polynomials $P_n^{(\lambda)}(x)$. The Legendre polynomials, sometimes called Legendre functions of the first kind, Legendre coefficients, or zonal harmonics (see Whittaker and Watson 1990) and are solutions to the Legendre differential equation. If l is an integer, they are polynomials[4].

The Legendre polynomials $P_n(x)$ for the oviposition, eco-endmember, orthogonal, *An.arabiensis* aquatic, larval habitat, sub-meter resolution, grid-stratifiable, LULC, optimizable dataset were illustrated for $x \in [-1, 1]$ and $n = 1$, 2, ..., 5. They were implemented in the Wolfram Language as LegendreP[*n*, *x*].We noted that the geo-spectrotemporally bassociated Legendre signature LULC polynomials $P_l^m(x)$ and P_l^{-m} were solutions to the associated Legendre differential equation, when l did represent an unknown , endmember, capture point , frequency, immature density, or LULC, count value and $m = 0$, ..., l at a forecasted, eco-geoerferenceable, aquatic , larval habitat.

The ecogeoreferenecable, geoclassfiied, LULC, *An. arabiensis*, aquatic, larval habitat, geo-spectrotemporal, -meter resolution, capture point, sub Legendre polynomial $P_n(z)$ was defined by the contour integral $P_n(z) = \frac{1}{2\pi i} \oint (1 - 2tz + t^2)^{-1/2}\, t^{-n-1}\, dt$, where the contour enclosed the origin which was traversed in a counterclockwise direction. Contour integration is a method of evaluating certain integrals along paths in the complex plane [7]. We let $P(x)$and $Q(x)$be polynomials of polynomial degree $n$and $m$with coefficients b_n, ..., $b_0$and c_m, ..., c_0. We took the contour in the upper half-plane, replaced $x$by z, and wrote $z \equiv R\,e^{i\theta}$ in the frequency ento-

ecoepidemiological model. Then $\int_{-\infty}^{\infty}\frac{P(z)\,dz}{Q(z)}=\lim_{R\to\infty}\int_{-R}^{R}\frac{P(z)\,dz}{Q(z)}$. .We defined a path γ_R which was straight along the real axis from $-R$ to R and made a circular half-arc to connect the two ends in the upper half of the complex plane. The residue theorem then rendered $\lim_{R\to\infty}\int_{\gamma_R}\frac{P(z)\,dz}{Q(z)}\ \lim_{R\to\infty}\int_{-R}^{R}\frac{P(z)\,dz}{Q(z)}=\lim_{R\to\infty}\int_0^{\pi}\frac{P\left(R\,e^{i\theta}\right)}{Q\left(R\,e^{i\theta}\right)}i\,R\,e^{i\theta}\,d\theta\ 2\pi i\sum_{I[z]>0}\mathrm{Res}\left[\frac{P(z)}{Q(z)}\right]$, where $\mathrm{Res}\,[z]$ denoted the complex residues. By solving, $\lim_{R\to\infty}\int_{-R}^{R}\frac{P(z)\,dz}{Q(z)}=2\pi i\sum_{I[z]>0}\mathrm{Res}\,\frac{P(z)}{Q(z)}-\lim_{R\to\infty}\int_0^{\pi}\frac{P\left(R\,e^{i\theta}\right)}{Q\left(R\,e^{i\theta}\right)}i\,R\,e^{i\theta}\,d\theta.$ we were optimally able to aymptotically, define $I_R=\lim_{R\to\infty}\int_0^{\pi}\frac{P\left(R\,e^{i\theta}\right)}{Q\left(R\,e^{i\theta}\right)}i\,R\,e^{i\theta}\,d\theta\ \lim_{R\to\infty}\int_0^{\pi}\frac{b_n\left(R\,e^{i\theta}\right)^n+b_{n-1}\left(R\,e^{i\theta}\right)^{n-1}+\ldots+b_0}{c_m\left(R\,e^{i\theta}\right)^m+c_{m-1}\left(R\,e^{i\theta}\right)^{m-1}+\ldots+c_0}i\,R\,d\theta$ which was equal to $\lim_{R\to\infty}\int_0^{\pi}\frac{b_n}{c_m}\left(R\,e^{i\theta}\right)^{n-m}i\,R\,d\theta\ \lim_{R\to\infty}\int_0^{\pi}\frac{b_n}{c_m}R^{n+1-m}\,i\left(e^{i\theta}\right)^{n-m}d\theta$ and set $\epsilon\equiv-(n+1-m)$, the the model output which subsequently revealed $I_R\equiv\lim_{R\to\infty}\frac{i}{R^{\epsilon}}\frac{b_n}{c_m}\int_0^{\pi}e^{i(n-m)\theta}\,d\theta.$ Now, $\lim_{R\to\infty}R^{-\epsilon}=0$ for $\epsilon>0$. That meant that for $-n-1+m\geq 1$, or $m\geq n+2$, $I_R=0$, so $\int_{-\infty}^{\infty}\frac{P(z)\,dz}{Q(z)}=2\pi i\sum_{I[z]>0}\mathrm{Res}\left[\frac{P(z)}{Q(z)}\right]$ for $m\geq n+2$. We applied Jordan's lemma (see Appendix 3) with $f(x)\equiv P(x)/Q(x)$. In so doing, thes malaria model output was $\lim_{x\to\infty}f(x)=0,$ so we required $m\geq n+1$. Then $\int_{-\infty}^{\infty}\frac{P(z)}{Q(z)}e^{iaz}\,dz=2\pi i\sum_{I[z]>0}\mathrm{Res}\left[\frac{P(z)}{Q(z)}e^{iaz}\right]$ for $m\geq n+1$ and $a>0$. The model was henceforth extended to $\int_{-\infty}^{\infty}\frac{P(x)}{Q(x)}\cos(ax)\,dx=2\pi\,\mathrm{R}\left\{\sum_{I[z]>0}\mathrm{Res}\left[\frac{P(z)}{Q(z)}e^{iaz}\right]\right\}\int_{-\infty}^{\infty}\frac{P(x)}{Q(x)}\sin(ax)\,dx=2\pi\,\mathrm{I}\left\{\sum_{I[z]>0}\mathrm{Res}\left[\frac{P(z)}{Q(z)}e^{iaz}\right]\right\}.$

Jordan's lemma revealed the value of the integral $I\equiv\int_{-\infty}^{\infty}f(x)\,e^{iax}\,dx$ along the infinite upper semicircle and with $a>0$ is 0 in the *An. arabiensis* , aquatic, larval habitat ,eco-endmember, orthogonal, geo-spectrotemporal, LULC signature functions which satisfied $\lim_{R\to\infty}\left|f\left(R\,e^{i\theta}\right)\right|=0$. Thus, the integral along the real axis in the eco-entomological, gridded, *An. arabiensis*, asquatic, larval habitat, capture point, forecast, vulnerability model was just the sum of complex residues in the contour. The model renderings was established using a contour integral I_R that satisfied $\lim_{R\to\infty}|I_R|\leq\frac{\pi}{a}\lim_{R\to\infty}\epsilon=0.$ To derive the forecast datset we wrote $x=R\,e^{i\theta}=R\,(\cos\theta+i\sin\theta)=i\,R\,e^{i\theta}\,d\theta$, and defined the eco-endmeber, sub-mter resolution, oviposition, LULC, capture point, contour integral $I_R=\int_0^{\pi}f\left(R\,e^{i\theta}\right)e^{i\,a\,R\cos\theta-a\,R\sin\theta}\,i\,R\,e^{i\theta}\,d\theta$ Then $|I_R|\leq R\int_0^{\pi}\left|f\left(R\,e^{i\theta}\right)\right|\left|e^{i\,a\,R\cos\theta}\right|\left|e^{-a\,R\sin\theta}\right||i|\left|e^{i\theta}\right|d\theta=$ $R\int_0^{\pi}\left|f\left(R\,e^{i\theta}\right)\right|e^{-a\,R\sin\theta}\,d\theta\ 2R\int_0^{\pi/2}\left|f\left(R\,e^{i\theta}\right)\right|e^{-a\,R\sin\theta}\,d\theta.$ Now, $\lim_{R\to\infty}\left|f\left(R\,e^{i\theta}\right)\right|=0$ was choosen. In so doing,

an ϵ such that $|f(R e^{i\theta})| \le \epsilon$, so $|I_R| \le 2R\epsilon \int_0^{\pi/2} e^{-aR\sin\theta}\, d\theta.$ in the model output. But, for $\theta \in [0, \pi/2]$, $\frac{2}{\pi}\theta \le \sin\theta,$ so

$$\lim_{R\to\infty} |I_R| \le \frac{\pi}{a} \lim_{R\to\infty} \epsilon = 0 \quad |I_R| \le 2R\epsilon \int_0^{\pi/2} e^{-2aR\theta/\pi}\, d\theta = 2\epsilon R \frac{1-e^{-aR}}{\frac{2aR}{\pi}} = \frac{\pi\epsilon}{a}\left(1-e^{-aR}\right).$$

Jordan's lemma yielded a simple way to calculate the integral along the real axis of functions $f(z) = e^{i\,a\,z}\, g(z)$ holomorphic on the upper half-plane and continuous on the closed upper half-plane, at a finite number of simulated un-geosampeld, seasonal, hyperproductive,*An. arabiensis* aquatic, larval habitat,capture points $z_1, z_2, \ldots, z_n$. We then considered the closed contour C, which was the concatenation of the paths C_1 and C_2. If one identifies **C** with $\mathbf{R}^2$, then the holomorphic functions coincide with those functions of two real variables with continuous first derivatives which solve the Cauchy–Riemann equations, a set of two partial differential equations[7].

Every holomorphic function detrmined by the vector arthropod, ento-ecoepidemiological, forecast, vulnerability, eco-endmember model was separated into its real and imaginary parts, and each of these was a solution of Laplace's equation on $\mathbf{R}^2$. Inso doing, if we expressed a holomorphic function $f(z)$ as $u(x, y) + i\,v(x, y)$ both u and v were harmonic functions, where v was the harmonic conjugate of u. Cauchy's integral theorem implies that the contour integral of every malarai, mosquiot holomorphic function along a loop vanished from the model output[1]. Here γ was a rectifiable path in a simply connected open subset U of the complex plane **C** whose start point was equal to a seasonal, eco-georeferenceable, unknown, prolific, capture point,LULC whence $f : U \to \mathbf{C}$ was a holomorphic function.

Contour integration is closely related to the calculus of residues a method of complex analysis[4]. One use for contour integrals in a forecast, vulnerability, sub-meter resolution, ,vector arthropod, ento-ecoepidemiological, aquatic, larval habitat, prognosticative, ecogeoreferenecable, LULC, oviposition, model is the evaluation of integrals along the real line that are not readily found by using only real variable endmember methods. Our contour integration methods included1)direct integration of a complex-valued LULC function along a curve in the complex plane (a contour)2) application of the Cauchy integral formula3) application of the residue theorem (see Table 9).

Table 9 The residue theorem applied to the function $f(z) = \frac{3}{(z-1)^2} + \frac{2}{z-i} - \frac{2}{z+i} + \frac{i}{z+3-2i} + \frac{5}{z+1+2i}.$ **in the *An. arabiensis*, model whose values of the contour integral were given by** $\int_\gamma f(z)\,dz = 2\pi i\,(0+2) = 4\pi i.$

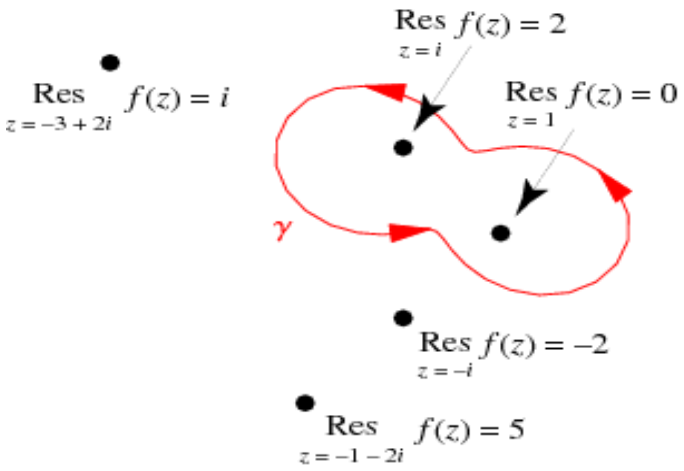

International Research Journal of Computer Science and Application
Vol. 2, No. 1, March 2018, pp. 1-181
Available Online at http://acascipub.com/Journals.php

An analytic function $f(z)$whose Laurent series was given by $f(z)=\sum_{n=-\infty}^{\infty} a_n (z-z_0)^n,$ for the ento-ecoepidemiological, oviposition, forecast, vulnerability, capture point, endmember , LULC model which was an integrated term by term employing a closed contour γencircling z_0, $\int_\gamma f(z)\,dz \sum_{=n=-\infty}^{\infty} a_n \int_\gamma (z-z_0)^n\,dz \sum_{=n=-\infty}^{-2} a_n \int_\gamma (z-z_0)^n\,dz + a_{-1}\int_\gamma \frac{dz}{z-z_0} + \sum_{n=0}^{\infty} a_n \int_\gamma (z-z_0)^n\,dz.$ The Cauchy integral theorem requires that the first and last terms vanish, so we were left with $\int_\gamma f(z)\,dz = a_{-1}\int_\gamma \frac{dz}{z-z_0},$ where $a_{-1}$was the complex residue[7].. Using the contour $z=\gamma(t)=e^{it}+z_0$in the eco-endmember, aquatic, larval habitat, malaria, mosquito prognosticative,LULC, orthogonal, geospectrotemporal model rendered $\int_\gamma \frac{dz}{z-z_0} = \int_0^{2\pi} \frac{i\,e^{it}\,dt}{e^{it}} = 2\pi i,$ so we then had $\int_\gamma f(z)\,dz = 2\pi i\, a_{-1}.$ If the contour γencloses multiple poles, then the theorem gives the general result $\int_\gamma f(z)\,dz = 2\pi i \sum_{a\in A} \operatorname{Res}_{z=a_i} f(z),$ where $A$is the set of poles contained inside the contour[4]. The value of a contour integral for any contour in the complex plane depended only on the properties of a few very few *An. arabiensis*, aquatic, larval habitat, eco-endmember, geoclassifiable, LULC, grid-stratifiable, sub-meter resolution, capture points inside the contor.

We employed a combination of methods, for the purpose of finding the seasonal, hyperproductive, eco-georeferenceable, geo-spectrotemrporal, geosampled, capture point, endmember, *An. arabiensis* , oviposition, LULC integrals.We noted in the model renderings that the first few constructed Legendre polynomials were$P_0(x)$=1, $P_1(x)$=x, $P_2(x)=\frac{1}{2}(3x^2-1), P_3(x)=\frac{1}{2}(5x^3-3x), P_4(x)=\frac{1}{8}(35x^4-30x^2+3), P_5(x)=\frac{1}{8}(63x^5-70x^3+15x), P_6(x)=\frac{1}{16}(231x^6-315x^4+105x^2-5).$When ordered from smallest to largest powers and with the denominators factored out, the triangle of nonzero coefficients was 1, -1, 3, -3, 5, -30, ... The leading denominators were 1, 2, 8, 16, 128, 256, ... The first few powers in terms of ento-ecoepidemiological, oviposition, geospecified, eco-endmember, LULC Legendre, aquatic, larval habitat, geospecified geo-spectrotemporal, capture point, polynomials were quantitated as x=$P_1(x), x^2=\frac{1}{3}[P_0(x)+2P_2(x)], x^3=\frac{1}{5}[3P_1(x)+2P_3(x)], x^4=\frac{1}{35}[7P_0(x)+20P_2(x)+8P_4(x)], x^5=\frac{1}{63}[27P_1(x)+28P_3(x)+8P_5(x)]$ and $x^6=\frac{1}{231}[33P_0(x)+110P_2(x)+72P_4(x)+16P_6(x)]$. A closed form for these was given by $x^n=\sum_{l=n,n-2,\ldots} \frac{(2l+1)n!}{2^{(n-l)/2}\left(\frac{1}{2}(n-l)\right)!\,(l+n+1)!!}P_l(x)$ For Legendre polynomials and powers up to exponent 12, [see Abramowitz and Stegun (1972)].

The eco-georeferenecable, eco-endmember,LULC, signature, *An. arabiensis*,capture point, oviposition, capture point, aquatic, larval habitat, Legendre polynomials were also generated employing Gram-Schmidt orthonormalization in the open interval $(-1, 1)$ with the weighting function The Schmidt orthogonalization, (also called the Gram-Schmidt process), is a procedure which takes a non-orthogonal set of linearly independent functions and constructs an orthogonal basis over an arbitrary interval with respect to an arbitrary weighting function $w(x)$[8].

Applying the Gram-Schmidt process to the eco-endmember, oviposition, malaria, mosquito, ,sub-meter resolution, LULC functions 1, x, x^2, ... on the interval $[-1, 1]$ with the inner product L^2 rendered the Legendre, geospecified, *An. arabiensis*, capture point, polynomials.Given an original set of linearly independent, sub-mter resolution, eco-endmember, LULC, malaria, mosquito, geosampled, geo-spectrotemporal, aquatic, larval habitat

International Research Journal of Computer Science and Application
Vol. 2, No. 1, March 2018, pp. 1-181
Available Online at http://acascipub.com/Journals.php

,functions $\{u_n\}_{n=0}^{\infty}$, we let $\{\psi_n\}_{n=0}^{\infty}$ denote the orthogonalized (but not normalized) functions, $\{\phi_n\}_{n=0}^{\infty}$ which subsequently denoted the orthonormalized, vector, arthropod, immature, habitat functions, and defined $\psi_0(x)=u_0(x)$ and $\phi_0(x)=\frac{\psi_0(x)}{\sqrt{\int {\psi_0}^2(x)\,w(x)\,dx}}$. We then took $\psi_1(x)=u_1(x)+a_{10}\,\phi_0(x)$, where we were required to tabulate $\int \psi_1\,\phi_0\,w\,dx=\int u_1\,\phi_0\,w\,dx+a_{10}\int {\phi_0}^2\,w\,dx=0$. By definition, $\int {\phi_0}^2\,w\,dx=1$, so $a_{10}=-\int u_1\,\phi_0\,w\,dx$. in the forecast, vulnerability, eco-endmember, siganture model output. The first orthogonalized function was $\psi_1=u_1(x)-\left[\int u_1\,\phi_0\,w\,dx\right]\phi_0$, in the aquatic, larval habitat, eco-endmeber model and the corresponding normalized signature, iteratively interpolative, LULC function was $\phi_1=\frac{\psi_1(x)}{\sqrt{\int {\psi_1}^2\,w\,dx}}$. By mathematical induction, it followed that $\phi_i(x)=\frac{\psi_i(x)}{\sqrt{\int {\psi_i}^2\,w\,dx}}$, where $\psi_i(x)=u_i+a_{i0}\,\phi_0+a_{i1}\,\phi_1\ldots+a_{i,j-1}\,\phi_{i-1}$ in the,ento-ecoepidemiological, eco-endmember paradigm when $a_{ij}\equiv-\int u_i\,\phi_j\,w\,dx$.

When the *An. arabiensis* aquatic, larval habitat, capture points functions were normalized to N_j instead of 1, then the model rendered $\int_a^b\left[\phi_j(x)\right]^2 w\,dx=N_j^2$, $\phi_i(x)=N_i\frac{\psi_i(x)}{\sqrt{\int {\psi_i}^2\,w\,dx}}$ and $a_{ij}=-\frac{\int u_i\,\phi_j\,w\,dx}{N_j^2}$. The oviposition, ento-ecoepidemiological, endmember, signature, frequency LULC, aquatic, larval habitat, endmember, orthogonal polynomials were easy to generate using Gram-Schmidt orthonormalization. We parsimoniously, robustly, geo-spectrotemporally employed the notation $\langle x_i\,|\,x_j\rangle=\langle x_i\,|\,w\,|\,x_j\rangle=\int_a^b x_i(x)\,x_j(x)\,w(x)\,dx$, where $w(x)$ was a weighting function, which defined the first few polynomials, $p_0(x)=1$ and $p_1(x)=\left[x-\frac{\langle x\,p_0\,|\,p_0\rangle}{\langle p_0\,|\,p_0\rangle}\right]p_0$. Here, p_0 and p_1 were orthogonal, capture point, LULC endmember,polynomials, which were validated by $\langle p_0\,|\,p_1\rangle=\left\langle\left[x-\frac{\langle x\,p_0\,|\,p_0\rangle}{\langle p_0\,|\,p_0\rangle}\right]p_0\right\rangle=\langle x\,p_0\rangle-\frac{\langle x\,p_0\,|\,p_0\rangle}{\langle p_0\,|\,p_0\rangle}\langle p_0\rangle=\langle x\,p_0\rangle-\langle x\,p_0\rangle=1$. A weight function $w(x)$ was then employed to normalize the endmember, orthogonal, LULC functions $\int[f_n(x)]^2\,w(x)\,dx=N_n$. The functions $f(x)$ and $g(x)$ were orthogonal over the interval $a\le x\le b$ with weighting function $w(x)$ if $\langle f(x)\,|\,g(x)\rangle\equiv\int_a^b f(x)\,g(x)\,w(x)\,dx=0$. in the model.

We employed the recurrence relation $p_{i+1}(x)=\left[x-\frac{\langle x\,p_i\,|\,p_i\rangle}{\langle p_i\,|\,p_i\rangle}\right]p_i-\left[\frac{\langle p_i\,|\,p_i\rangle}{\langle p_{i-1}\,|\,p_{i-1}\rangle}\right]p_{i-1}$ to construct all higher order, eco-endmember, *An. arabiensis* habitat, geospecified, grid-stratified, LULC polynomials.To verify that this procedure we produced orthogonal, eco-endmember, polynomials. Weexamined $\langle p_{i+1}\,|\,p_i\rangle=\left\langle\left[x-\frac{x\,p_i\,|\,p_i}{p_i\,|\,p_i}\right]p_i\,\middle|\,p_i\right\rangle-\left\langle\frac{p_i\,|\,p_i}{p_{i-1}\,|\,p_{i-1}}\,p_{i-1}\,\middle|\,p_i\right\rangle=\langle x\,p_i\,|\,p_i\rangle-\frac{\langle x\,p_i\,|\,p_i\rangle}{\langle p_i\,|\,p_i\rangle}\langle p_i\,|\,p_i\rangle-\frac{\langle p_i\,|\,p_i\rangle}{\langle p_{i-1}\,|\,p_{i-1}\rangle}\langle p_{i-1}\,|\,p_i\rangle=-\frac{\langle p_i\,|\,p_i\rangle}{\langle p_{i-1}\,|\,p_{i-1}\rangle}\langle p_{i-1}\,|\,p_i\rangle=-\frac{\langle p_i\,|\,p_i\rangle}{\langle p_{i-1}\,|\,p_{i-1}\rangle}\left[-\frac{\langle p_{i-1}\,|\,p_{j-1}\rangle}{\langle p_{j-2}\,|\,p_{j-2}\rangle}\langle p_{j-2}\,|\,p_{j-1}\rangle\right]=(-1)^j\frac{\langle p_j\,|\,p_j\rangle}{\langle p_0\,|\,p_0\rangle}\langle p_0\,|\,p_1\rangle$ =1 since $\langle p_0\,|\,p_1\rangle=0$. We found

International Research Journal of Computer Science and Application
Vol. 2, No. 1, March 2018, pp. 1-181
Available Online at http://acascipub.com/Journals.php

that all the polynomials $p_i(x)$ were orthogonal in the eco-georeferenecable, vector, arthropod, malaria, mosquito, aquatic, larval habitat, capture point, orthogonal,LULC model, Another eco-georeferenceable, frequency, capture point, eco-endmember, ento-ecoepidemiological, forecast, vulnerability, oviposition model was constructed which optimally rendered $P_0(x)$-1, $P_1(x)=,\left[x-\frac{\int_{-1}^{1}x\,dx}{\int_{-1}^{1}dx}\right]\cdot 1\ P_2(x)=\ x\left[x-\frac{\int_{-1}^{1}x^3\,dx}{\int_{-1}^{1}x^2\,dx}\right]-\left[\frac{\int_{-1}^{1}x^2\,dx}{\int_{-1}^{1}dx}\right]\cdot 1\ ,P_{2(x)=}P_3(x)=x^2-\frac{1}{3}\left[x-\frac{\int_{-1}^{1}x\left(x^2-\frac{1}{3}\right)^2dx}{\int_{-1}^{1}\left(x^2-\frac{1}{3}\right)^2dx}\right]\left(x^2-\frac{1}{3}\right)-\left[\frac{\int_{-1}^{1}\left(x^2-\frac{1}{3}\right)^2dx}{\int_{-1}^{1}x^2\,dx}\right]x$

Normalizing the seasonal, malaria, eco-endmember, geo-spectrotemporal, LULC model $P_n(1)=1$ rendered the expected, larval habitat, seasonal, unknown, hyperproductive, *An. arabiensis*, LULC foci, Legendre polynomials. The "shifted" Legendre polynomials were a set of functions analogous to the Legendre polynomials which were defined on the interval (0, 1). They followed the orthogonality relationship $\int_0^1 \overline{P}_m(x)\,\overline{P}_n(x)\,dx=\frac{1}{2n+1}\delta_{mn}.$ The first few outputs were $\overline{P}_0(x)=1,\ \overline{P}_1(x)=2x-1, \overline{P}_2(x)=6x^2-6x+1$ and $\overline{P}_3(x)=20x^3-30x^2+12x-1.$ The Legendre polynomials were orthogonal over $(-1,1)$ with weighting function 1 which in our research model satisfied $\int_{-1}^{1}P_n(x)\,P_m(x)\,dx=\frac{2}{2n+1}\delta_{mn},$ whence δ_{mn} was the Kronecker delta.

The Legendre polynomials are a special case of the Gegenbauer polynomials with $\alpha=1/2$, a special case of the Jacobi polynomials $P_n^{(\alpha,\beta)}$ with $\alpha=\beta=0$, and can be written as a hypergeometric function using Murphy's formula $P_n(x)=P_n^{(0,0)}(x)=_2F_1\left(-n,n+1;1;\tfrac{1}{2}(1-x)\right)$ (see Bailey 1933; Koekoek and Swarttouw 1998). The Rodriguez representation provided the forecast, vulnerability, endmember, ento-epidemiological, LULC, *An. arabiensis*, aquatic, larval habitat,capture point, prognostictive, LULC, orthogonal formula $P_l(x)=\frac{1}{2^l\,l!}\frac{d^l}{dx^l}\left(x^2-1\right)^l,$ as which yielded the expansion $P_l(x)=\frac{1}{2^l}\sum_{k=0}^{\lfloor l/2\rfloor}\frac{(-1)^k(2l-2k)!}{k!\,(l-k)!\,(l-2k)!}x^{l-2k}=\frac{1}{2^l}\sum_{k=0}^{\lfloor l/2\rfloor}(-1)^k\binom{l}{k}\binom{2l-2k}{l}x^{l-2k}$ where $\lfloor r\rfloor$ was the floor function [also called the greatest integer function or integer value]. We noted that the largest integer was less than or equal to x. Rodrigues representation is an operator definition of a function [2].

Here we converted the Rodriguez formula into a Schläfli integral which was the integral representation of $J_n(z)=\frac{1}{\pi}\int_0^{\pi}\cos(n\theta-z\sin\theta)\,d\theta+$ the Bessel functions for any n where $-\frac{\sin n\pi}{\pi}\int_0^{\infty}e^{-n\theta-z\sinh\theta}\,d\theta,$ when $\mathrm{Re}\,z>0$. In the oviposition, geo-spectrotemrpoal, eco-endmember, malaria, endmember, *An. arabiensis*, LULC model, orthogonal, grid-stratified, weight function $Z_n(x)$ was defined by the recurrence relations $Z_{n+1}+Z_{n-1}=\frac{2n}{x}Z_n$ and $Z_{n+1}-Z_{n-1}=-2\frac{dZ_n}{dx}.$ The Bessel functions are more frequently defined as solutions to the differential equation $x^2\frac{d^2y}{dx^2}+x\frac{dy}{dx}+\left(x^2-n^2\right)y=0.$ [7]. There are two classes of solution, called the Bessel function of the first kind $J_n(x)$ and Bessel function of the second kind $Y_n(x)$. A Bessel function of the third kind, more commonly called a Hankel function, is a special combination of the first and second kinds.) [2]. Several related ento-ecoepidemiological, forecast vulnerability, geo-spectrotemporal, eco-endmember, signature, model ,LULC functions were also defined for asymptotically targeting eco-georeferenecable seasonal,

unknown, aquatic, larval habitat, *An. arabiensis*, capture point, hyperproductive, foci by slightly modifying the defining equations.

We noted that the model was valid for all geosampled, geo-spectrotemporal, uncoalesced, hyperproductive, capture point, *An. arabiensis*, aquatic, larval habitats. The formula was optimally derived from $J_n = \frac{z^n}{2^{\pi+1}\,\pi\,i} \int_{-\infty}^{(0+)} t^{-n-1} \exp\left(t - \frac{z^2}{4t}\right) dt.$ .An integral representation of the Legendre polnomials was displayed employing $P_n(z) = \frac{1}{2\pi i} \int_C \frac{(t^2-1)^n}{2^n (t-z)^{n+1}}\, dt,$ where C was a contour making one contour-clockwise turn around z.

The Iverson bracket for the oviposition, endmember, geoclassified, eco-georeferenecable, LULC, *An. arabiensis*, aquatic, larval habitat,prognosticative, capture point, vulnerability model as implemented as a built-in function in the Wolfram Language as Boole[*S*]. Unfortunately, in many older and current works (e.g., Honsberger 1976,; Steinhaus 1999; Shanks 1993; Ribenboim 1996; Hilbert and Cohn-Vossen 1999; Hardy 1999), the symbol $\lceil x \rfloor$ is used instead of $\lfloor x \rfloor$ (Graham et al. 1994). In fact, this notation harks back to Gauss in his third proof of quadratic reciprocity in 1808. However, because of the elegant symmetry of the floor function and ceiling function symbols $\lfloor x \rfloor$ and $\lceil x \rceil$,in our forecast, vulnerability, *An. arabiensis*, aquatic, larval habitat, sub-meter resolution, eco-endmemeber, LULC model and because $\lceil x \rfloor$ was such a useful symbol when interpreted as an Iverson bracket in the oviposition ento-epidemiological model [see Table 11], the use of $\lceil x \rfloor$ may denote the floor function in these paradigms (see Table 11.The symbol $\lceil x \rfloor$ is used to denote the nearest integer function since it naturally falls between the $\lfloor x \rfloor$ and $\lceil x \rceil$symbol[4]

Then, an element [A] ∈ {0, 1} was defined as follows: We set [A] = (1, if A is true; 0, if A is false. For example, [1 + 1 = 2] = 1 and [1 + 1 = 3] = 0. The notation [A] for the truth value of A is known as the Iverson bracket notation[4]. If A and B are two equivalent logical statements, then [A] = [B]. If A is any logical statement, then [not A] = 1 − [A]. If A and B are two logical statements, then [A ∧ B] = [A] [B]. (d) If A and B are two logical statements, then [A ∨ B] = [A] + [B] − [A] [B][2]. If A, B and C are three logical statements, then [A ∨ B ∨ C] = [A] + [B] + [C] − [A] [B] − [A] [C] − [B] [C] + [A] [B] [C] [7]. Hence, we assumed if A is true; 0, if A is false = (1, if B is true; 0, if B is false in the sub-meter resolution, LULC, grid-stratifiable, forecast, vulnerability , eco-endmember,model.

We considered an observation model of the form z (x) = y (x) + σ (y (x)) ξ (x), x ∈ X, (1) where X was the set of the submeter resolution sensors active endmember, LULC, pixel positions, z was the actual raw signature, frequency, data output, y was the ideal output, ξ was zero-mean random noise with standard deviation equal to 1, and σ was a function y, modulating the standard-deviation of the overall noise component. The function σ (y) was the standard-deviation function while σ2 (y) was the variance function. Since E {ξ (x)} = 0 we had E {z (x)} = y (x) and std {z (x)} = σ (E {z (x)}). There were no additional restrictions on the distribution of ξ (x), and different capture points were revealed with different distributions. A preference matrix described each habitat signature entry Rij, to find a factorization that minimized the root mean squared error on the test set. We defined Iij to be 1, if Rij was known (i.e., habitat i had an eco-endmember scatterplot j) and 0 otherwise in the residual, LULC, model derivatives. Further, we let N(x|μ,σ2)=fX(x) with X∼N(μ,σ2)X∼N(μ,σ2). Then, we defined a conditional probability of the ratingswith hyperparameter σ2p(R|U,V,σ2)=∏i=1N∏j=1M[N(Rij|UiTVj,σ2)]Iij(1)and priors on U and V with geo-spectrotemporal, ento-ecoepidmeiological, forecastable, regressable, LULC hyperparameters σU2,σV2p(U|σU2)=∏i=1NN(Ui|0,σU2I)and p(V|σV2)=∏i=1MN(Vi|0,σV2I). In the paradigm, y maximized the log posterior over U and V to optimally derive a substitute for the definition of N by invasively taking the log[i.e., lnp(U,V,σ2,σ2V,σ2U)]. In so doing, 12σ2∑i=1N∑j=1MIij(Rij−UiTVj)2−12σU2∑i=1NUiTUi−12σV2∑i=1NViTVi−12(κlnσ2+NDlnσ2U+MDlnσ2V)+C(3) −12(κln⁡σ2+NDln⁡σU2+MDln⁡σV2)+C(3) was rendered where κ was the number of known, habitat, ento-endmember, signature entries and C was a constant independent of the geosampled, capture point, aquatic, larval,

habitat parameters. We adjusted the three variance hyperparameters (which were observation noise variance and prior variances) as constants which reduced the optimization to the first three terms (i.e., a sum-of-squared minimization). Then defining $\lambda M=\sigma 2/\sigma M2$ for M=U,V and multiplying by $-\sigma 2<0$ resulted in the following objective function$E=12(\sum i=1N\sum j=1MIij(Rij-UiTVj)2+\lambda U\sum i=1N\|Ui\|F2+\lambda V\sum i=1M\|Vi\|F2$where $\|A\|2F=\sum mi=1\sum nj=1|aij|2\|$ whence $F2=\sum i=1m\sum j=1n|aij|2$ was the Frobenius norm. Since all the uncoalesced, iterable, interpolative, signature, habitat values were known [i.e. $Iij=1\forall(i,j)$] $\sigma U2,\sigma V2\rightarrow\infty$ was reduced to a singular value decomposition.

Table 11 The floor function was generalized to complex geosampled, *An. arabiensis*, aquatic, larval habitat,signature capture point larval density seasonal values of z

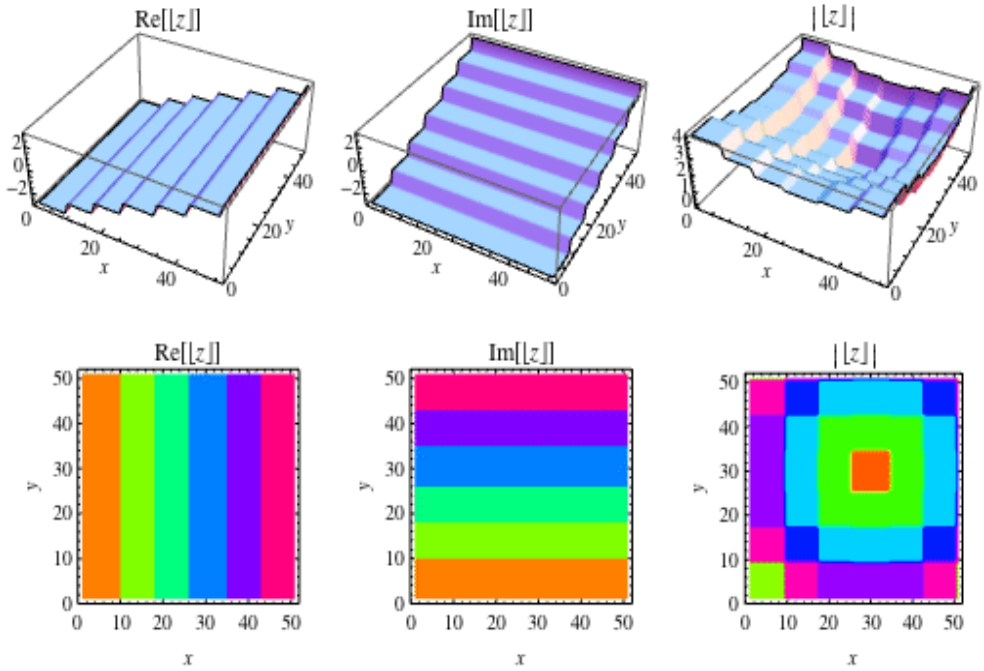

We quantitated the eco-endmember, aquatic, larval habitat, sub-mter resolution, capture point, fractional, part/value and integer part/value for the geosampled, sub-meter resolution, LULC, grid-stratifiable, orthogonal, ecogeoreferenceable, forecast, vulnerability, model estimators employing Table 11.

Table 11 A summary of names and notation implemented in the Wolfram Language as Floor[z], for the oviposition, *An. arabiensis*, aquatic, larval, habitat , endemic foci, geo-spectrotemporal endmember model

notation	name	S&O	Graham et al.	Wolfram Language
$\lceil x \rceil$	ceiling function	--	ceiling, least integer	Ceiling[x]
$\mathrm{mod}\,(m, n)$	congruence	--	--	Mod[m, n]
$\lfloor x \rfloor$	floor function	$\mathrm{Int}\,(x)$	floor, greatest integer, integer part	Floor[x]
$x - \lfloor x \rfloor$	fractional value	$\mathrm{frac}\,(x)$	fractional part or $\{x\}$	SawtoothWave[x]
$\mathrm{sgn}\,(x)\,(\lvert x \rvert - \lfloor \lvert x \rvert \rfloor)$	fractional part	$\mathrm{Fp}\,(x)$	no name	FractionalPart[x]
$\mathrm{sgn}\,(x)\,\lfloor \lvert x \rvert \rfloor$	integer part	$\mathrm{Ip}\,(x)$	no name	IntegerPart[x]

$\text{nint}(x)$	nearest integer function	--	--	Round[x]
$m\backslash n$	quotient	--	--	Quotient[m, n]

The floor function satisfied the identity $\lfloor x+n\rfloor=\lfloor x\rfloor+n$ for all the geosampled, malaria, mosquito, geosampled, oviposition, geo-spectrotemporal, LULC, discrete, C integers n.A number of geometric-like sequences with a floor function in the numerator were solved analytically. For example,, sums of the form $\sum_{n=1}^{\infty}\frac{\lfloor n\,x\rfloor}{k^n}$ was quantitated analytically for rational x. For $x=1/m$ a unit fraction, $\sum_{n=1}^{\infty}k^{-n}\left\lfloor\frac{n}{m}\right\rfloor=\frac{k}{(k-1)(k^n-1)}$. was formulated. For irrational $\alpha>0$, the continued fraction converged to p_n/q_n, and $\epsilon_n\equiv q_n\,\alpha-p_n$, $\lfloor n\,\alpha+\epsilon_N\rfloor=\begin{cases}\lfloor n\,\alpha\rfloor & \text{for } n<q_{N+1}\\ \lfloor n\,\alpha\rfloor+(-1)^N & \text{for } n=q_{N+1}\end{cases}$ This lead to the result relating sums of the floor function of multiples of α to the continued fraction of α by $\sum_{n=1}^{\infty}\lfloor n\,\alpha\rfloor\,z^n=\frac{p_0\,z}{(1-z)^2}+\sum_{n=0}^{\infty}(-1)^n\frac{z^{q_n}\,z^{q_{n+1}}}{(1-z^{q_n})(1-z^{q_{n+1}})}$.Additionally, t sum formulas were generated for determining the geosampled hypeproductive eco-endmember, LULC, foci, signature covariates which included $P_l(x)=\frac{1}{2^l}\sum_{k=0}^{l}\binom{l}{k}^2(x-1)^{l-k}(x+1)^k\sum_{=k=0}^{l}\binom{l}{k}\binom{-l-1}{k}\left(\frac{1-x}{2}\right)^k$.

In terms of hypergeometric functions, for the oviposition, sub-meter resolution, LULC, *An. arabiensis*, aquatic, larval habitat, capture point, prognostic ative, model , they were written $P_n(x)=\left(\frac{x-1}{2}\right)^n{}_2F_1\left(-n,-n;1;(x+1)/(x-1)\right)$, $P_n(x)\binom{2n}{n}\frac{x^n}{2^n}{}_2F_1\left(-n/2,(1-n)/2;1/2-n;x^{-2}\right)$, $P_n(x)={}_2F_1\left(-n,n+1;1;(1-x)/2\right)$ A generating function for $P_n(x)$ was subsequently provided by $g(t,x)=\left(1-2\,x\,t+t^2\right)^{-1/2}=\sum_{n=0}^{\infty}P_n(x)\,t^n.$ for aymptotically, optiamlly targeting seasonal, eco-georeferenceable, unknown, hyperproductive, *An. arabiensis*, LULC, capture points.We took $\partial g/\partial t$, $-\frac{1}{2}\left(1-2\,x\,t+t^2\right)^{-3/2}(-2\,x+2\,t)=\sum_{n=0}^{\infty}n\,P_n(x)\,t^{n-1}.$ We generated $-t\left(1-2\,x\,t+t^2\right)^{-3/2}(-2\,x+2\,t)=\sum_{n=0}^{\infty}2\,n\,P_n(x)\,t^n$ and added $\left(1-2\,x\,t+t^2\right)^{-3/2}\left[\left(2\,x\,t-2\,t^2\right)+\left(1-2\,x\,t+t^2\right)\right]=\sum_{n=0}^{\infty}(2\,n+1)\,P_n(x)\,t^n$ This expansion was useful for quantitating the geosampled, geo-spectrotemporal, eosample,d *An. arabiensis*, endmember, LULC covariates since the Heyney-Greenstein phase function computed the distribution on a sphere. Another generating function was then given by $\sum_{n=0}^{\infty}\frac{P_n(x)}{n!}z^n=e^{x\,z}\,J_0\left(z\sqrt{1-x^2}\right),$ where $J_0(x)$ is a zeroth order Bessel function of the first kind .

The Legendre polynomials satisfied the recurrence relation $(l+1)\,P_{l+1}(x)-(2\,l+1)\,x\,P_l(x)+l\,P_{l-1}(x)=0$.In addition, $\left(1-x^2\right)P_n'(x)=-n\,x\,P_n(x)+n\,P_{n-1}(x)=(n+1)\,x\,P_n(x)-(n+1)\,P_{n+1}(x)$ corrected any residual probabilistic, incospicious uncertaities. A complex generating function was generated as $P_l(x)=\frac{1}{2\,\pi\,i}\int\left(1-2\,z\,x+z^2\right)^{-1/2}z^{-l-1}\,dz,$ and the Schläfli integral was $P_l(x)=\frac{(-1)^l}{2^l}\,\frac{1}{2\,\pi\,i}\int\frac{\left(1-z^2\right)^l}{(z-x)^{l+1}}\,dz.$

International Research Journal of Computer Science and Application
Vol. 2, No. 1, March 2018, pp. 1-181
Available Online at http://acascipub.com/Journals.php

Integrals in the LULC, *An.arabiensis*, forecast, vulnerability model was conducted over the interval $[x, 1]$which included the general formula $\int_x^1 P_m(x)\,dx = \frac{(1-x^2)}{m(m+1)}\frac{dP_m(x)}{dx}$ for $m \neq 0$ from which the specialcase $\int_0^1 P_m(x)\,dx = \frac{P_{m-1}(0) - P_{m+1}(0)}{2m+1} = \begin{cases} 1 & m = 0 \\ 0 & m \text{ even } \neq 0 \\ (-1)^{(m-1)/2}\frac{m!!}{m(m+1)(m-1)!!} & m \text{ odd} \end{cases}$ For the integral over a product of the eco-endmember *An. arabiensis*, capture point, Legendre functions , $\int_x^1 P_m(x)P_n(x)\,dx = \frac{(1-x^2)[P_n(x)P'_m(x) - P_m(x)P'_n(x)]}{m(m+1) - n(n+1)}$ for $m \neq n$, which gave $\int_0^1 P_m(x)P_n(x)\,dx = \begin{cases} \frac{1}{2n+1} & m = n \\ 0 & m \neq n,\ m, n \text{ both even or odd} \\ f_{m,n} & m \text{ even}, n \text{ odd} \\ f_{n,m} & m \text{ odd}, n \text{ even} \end{cases}$ where $f_{m,n} \equiv \frac{(-1)^{(m+n+1)/2}\,m!\,n!}{2^{m+n-1}(m-n)(m+n+1)\left[\left(\frac{1}{2}m\right)!\right]^2\left\{\left[\frac{1}{2}(n-1)\right]!\right\}^2}$

The latter was a special case of $\int_0^1 P_\mu(x)P_\nu(x)\,dx = \frac{A\sin\left(\frac{1}{2}\pi\nu\right)\cos\left(\frac{1}{2}\pi\mu\right) - A^{-1}\sin\left(\frac{1}{2}\pi\mu\right)\cos\left(\frac{1}{2}\pi\nu\right)}{\frac{1}{2}\pi(\nu-\mu)(\mu+\nu+1)}$, where $A \equiv \frac{\Gamma\left(\frac{1}{2}(\mu+1)\right)\Gamma\left(1+\frac{1}{2}\nu\right)}{\Gamma\left(\frac{1}{2}(\nu+1)\right)\Gamma\left(1+\frac{1}{2}\mu\right)}$ and $\Gamma(z)$ was a gamma function over the integrals over $[-1, 1]$ with weighting functions x and x^2 which here was given by the expression $\int_{-1}^1 x\,P_L(x)P_N(x)\,dx = \begin{cases} \frac{2(L+1)}{(2L+1)(2L+3)} & \text{for } N = L+1 \\ \frac{2L}{(2L-1)(2L+1)} & \text{for } N = L-1 \end{cases}$ and

$$\int_{-1}^1 x^2 P_L(x)P_N(x)\,dx = \begin{cases} \frac{2(L+1)(L+2)}{(2L+1)(2L+3)(2L+5)} & \text{for } N = L+2 \\ \frac{2\left(2L^2+2L-1\right)}{(2L-1)(2L+1)(2L+3)} & \text{for } N = L \\ \frac{2L(L-1)}{(2L-3)(2L-1)(2L+1)} & \text{for } N = L-2 \end{cases}$$

The Laplace transform in the eco-epidemiological, *An. arabeisnis* aquatic, larval habitat, sub-meter resolution, eco-endmember, LULC geo-spectrotemporal, signature model was given by:

$$\mathcal{L}[P_n(t)](s) =$$

$$\begin{cases} \frac{1}{2}\sqrt{\pi}\left[\sqrt{\frac{2}{s}}\,I_{-n-1/2}(s) - \frac{1}{2}s\,{}_1F_2\left(1; 2+\frac{1}{2}n, \frac{1}{2}(3-n); \frac{1}{4}s^2\right)\right] & \text{for } n \text{ even} \\ \frac{1}{2}\sqrt{\pi}\left[\sqrt{\frac{2}{s}}\,I_{-n-1/2}(s) + {}_1F_2\left(1; \frac{1}{2}(3+n), 1-\frac{1}{2}n; \frac{1}{4}s^2\right)\right] & \text{for } n \text{ odd}, \end{cases}$$

where $I_n(s)$ was a modified Bessel function of the first kind. A sum identity is given by $1-[P_n(x)]^2=\sum_{\nu=1}^{n}\frac{1-x^2}{1-x_\nu^2}\left[\frac{P_n(x)}{P_n'(x_\nu)(x-x_\nu)}\right]^2$, where x_ν is the νth root of $P_n(x)$ [4]. A similar identity was also constructed employing $\sum_{\nu=1}^{n}\frac{1-x_\nu^2}{(n+1)^2[P_{n+1}(x_\nu)]^2}=1$, which was responsible for the fact that the sum of weights in Legendre-Gauss quadrature was always equal to 2 throughout the eco-endmember, LULC forecast, vulnerability, ento-ecoepidemiological, eco-georeferenecable, signature model construction process.

In this work, Gegenbauer polynomials were given in terms of the Jacobi polynomials $P_n^{(\alpha,\beta)}(x)$ with $\alpha=\beta=\lambda-1/2$ by $C_n^{(\lambda)}(x)=\frac{\Gamma\left(\lambda+\frac{1}{2}\right)}{\Gamma(2\lambda)}\frac{\Gamma(n+2\lambda)}{\Gamma\left(n+\lambda+\frac{1}{2}\right)}P_n^{(\lambda-1/2,\lambda-1/2)}(x)$ as in Szegö (1975), thus making them equivalent to the Gegenbauer polynomials implemented in the Wolfram Language as GegenbauerC[*n*, *lambda*, *x*]. These polynomials were also given by the generating function $\frac{1}{(1-2xt+t^2)^\lambda}=\sum_{n=0}^{\infty}C_n^{(\lambda)}(x)t^n$. The first few Gegenbauer polynomials were $C_0^{(\lambda)}(x)=1$, $C_1^{(\lambda)}(x)=2\lambda x$, $C_2^{(\lambda)}(x)=-\lambda+2\lambda(1+\lambda)x^2$ and $C_3^{(\lambda)}(x)=-2\lambda(1+\lambda)x+\frac{4}{3}\lambda(1+\lambda)(2+\lambda)x^3$. In terms of the hypergeometric functions, [i.e., $\binom{n+2\lambda+1}{n}\left(\frac{x+1}{2}\right)^n{}_2F_1\left(-n,-n-\lambda+\frac{1}{2};\lambda+\frac{1}{2};\frac{x-1}{x+1}\right)$.]. They were normalized by $\int_{-1}^{1}(1-x^2)^{\lambda-1/2}\left[C_n^{(\lambda)}\right]^2dx=2^{1-2\lambda}\pi\frac{\Gamma(n+2\lambda)}{(n+\lambda)\Gamma^2(\lambda)\Gamma(n+1)}$ for $\lambda>-1/2$. Derivative identities optimally derived from the malaria model included $\frac{d}{dx}C_n^{(\lambda)}(x)=2\lambda C_{n-1}^{(\lambda+1)}(x)$, $(1-x^2)\frac{d}{dx}\left[C_n^{(\lambda)}\right]$ $[2(n+\lambda)]^{-1}\left[(n+2\lambda-1)(n+2\lambda)C_{n-1}^{(\lambda)}(x)-n(n+1)C_{n+1}^{(\lambda)}(x)\right]=-nxC_n^{(\lambda)}(x)+(n+2\lambda-1)C_{n-1}^{(\lambda)}(x)=$ $(n+2\lambda)xC_n^{(\lambda)}(x)-(n+1)C_{n+1}^{(\lambda)}(x)$, $nC_n^{(\lambda)}(x)=x\frac{d}{dx}\left[C_n^{(\lambda)}(x)\right]-\frac{d}{dx}\left[C_{n-1}^{(\lambda)}(x)\right]$, $(n+2\lambda)C_n^{(\lambda)}(x)=$ $\frac{d}{dx}\left[C_{n+1}^{(\lambda)}(x)\right]-x\frac{d}{dx}\left[C_n^{(\lambda)}(x)\right]$, $\frac{d}{dx}\left[C_{n+1}^{(\lambda)}(x)-C_{n-1}^{(\lambda)}(x)\right]=2(n+\lambda)C_n^{(\lambda)}(x)=2\lambda\left[C_n^{(\lambda+1)}(x)-C_{n-2}^{(\lambda+1)}(x)\right]$ which helped aymptotically, geo-spectrotemporally, remotely. target seasonal, hyperproductive, *An. arabiensis*, aquatic, larval habitat, eco-endmember, LULC, capture points.

A recurrence relation is $nC_n^{(\lambda)}(x)=2(n+\lambda-1)xC_{n-1}^{(\lambda)}(x)-(n+2\lambda-2)C_{n-2}^{(\lambda)}(x)$ for $n=2$ also existed in the LULC, eco-endmember, *An. arabiensis*,, aquatic, larval habitat, signature model for optimally targeting seasonal, hypeprproductive, eco-georferenecable, capture point, foci whence $C_{2\nu}^{(\lambda)}(x)=\binom{2\nu+2\lambda-1}{2\nu}{}_2F_1\left(-\nu,\nu+\lambda;\lambda+\frac{1}{2};1-x^2\right)=(-1)^\nu\binom{\nu+\lambda-1}{\nu}{}_2F_1\left(-\nu,\nu+\lambda;\frac{1}{2};x^2\right)$ and $C_{2\nu+1}^{(\lambda)}(x)$ $=\binom{2\nu+2\lambda}{2\nu+1}x{}_2F_1\left(-\nu,\nu+\lambda+1;\lambda+\frac{1}{2};1-x^2\right)=(-1)^\nu 2\lambda\binom{\nu+\lambda}{\nu}x{}_2F_1\left(-\nu,\nu+\lambda+1;\frac{3}{2};x^2\right)$. This model gave representations in terms of elliptic functions for $\lambda=-3/4$ and $\lambda=-2/3$.

A $(1-x^2)\frac{d^2y}{dx^2}-x\frac{dy}{dx}+\alpha^2y=0$ expression was then generated from the eco-georferenced, sub-meter resolition, grid-stratified, frequencies for $|x|<1$. The Chebyshev differential equation had a regular singular, signature,

An. arabiensis, aquatic, larval habitat, ,LULC capture points at -1, 1, and ∞. and a power series solution about x0=0x for the Chebyshev differential equation(1−x2)y′′−xy′+n2y=0, as a function of the integer n . We showed that the solutions form a terminating expansion for each value of n This equation was solved by series solution employing the geosampled, signature, frequency model signature, expansions $y=\sum_{n=0}^{\infty} a_n x^n$,$y' = \sum_{n=0}^{\infty} n\, a_n x^{n-1}$,$= \sum_{n=1}^{\infty} n\, a_n x^{n-1} = \sum_{n=0}^{\infty} (n+1)\, a_{n+1} x^n$ and $y'' = \sum_{n=0}^{\infty} (n+1)\, n\, a_{n+1} x^{n-1} = \sum_{n=1}^{\infty} (n+1)\, n\, a_{n+1} x^{n-1}$ .Now, we plugged these equations into the original equation (◇) to obtain the following $(1-x^2)\sum_{n=0}^{\infty} (n+2)(n+1)\, a_{n+2} x^n - x\sum_{n=0}^{\infty} (n+1)\, n_{n+1} x^n + \alpha^2 \sum_{n=0}^{\infty} a_n x^n = 0$,which then we decomposed into $\sum_{n=0}^{\infty} (n+2)(n+1)\, a_{n+2} x^n - \sum_{n=0}^{\infty} (n+2)(n+1)\, a_{n+2} x^{n+2} - \sum_{n=0}^{\infty} (n+1)\, a_{n+1} x^{n+1} + \alpha^2 \sum_{n=0}^{\infty} a_n x^n = 0$ whence $\sum_{n=0}^{\infty} (n+2)(n+1)\, a_{n+2} x^n - \sum_{n=2}^{\infty} n(n-1)\, a_n x^n - \sum_{n=1}^{\infty} n\, a_n x^n + \alpha^2 \sum_{n=0}^{\infty} a_n x^n = 0$. Further we solved for $2\cdot 1\, a_2 + 3\cdot 2\, a_3 x - 1\cdot a\, x + \alpha^2 a_0 + \alpha^2 a_1 x + \sum_{n=2}^{\infty} \left[(n+2)(n+1)\, a_{n+2} - n(n-1)\, a_n - n\, a_n + \alpha^2 a_n\right] x^n = 0$ .Then $\left(2\, a_2 + \alpha^2 a_0\right) + \left[\left(\alpha^2 - 1\right) a_1 + 6\, a_3\right] x + \sum_{n=2}^{\infty} \left[(n+2)(n+1)\, a_{n+2} + \left(\alpha^2 - n^2\right) a_n\right] x^n = 0,$ so $2\, a_2 + \alpha^2 a_0 = 0$ while $\left(\alpha^2 - 1\right) a_1 + 6\, a_3 = 0,$ and by induction, $a_{n+2} = \dfrac{n^2 - \alpha^2}{(n+1)(n+2)}\, a_n$ for $n = 2$, 3, ... (see Table 11). In Morris and Horner [1977], the Chebyshev series solution of a linear fourth-order homogeneous differential equation was discussed in relation to eigenvalue problems associated with simple boundary conditions. Its approximate solution was represented in the reproducing kernel space. It was proved that models can converges uniformly to the exact solution . Moreover, the derivatives of are also convergent to model derivatives. That investigation provided a systematic method for obtaining the recurrence relation for the coefficients in a Chebyshev series solution.

Here ideas were applied to the solution of both homogeneous and inhomogeneous sub-meter resolution, grid-stratifiable, eco-endmember, LULC, forecast, vulnerability model equations of orders one to four. In so doing we were able to obtain Chebyshev series expansions for certain rational functions. We studied the nonlinear fourth-order differential equation with integral boundary conditions in the reproducing kernel space: $u(4)\,(x) - \lambda f\,(x, u\,(x)) = 0$, $0 < x < 1$, $u\,(0) = u\,(1) = \int 1\ 0\ h1\,(s)\ u\,(s)\ ds$, $u\,(0) = u\,(1) = \int 1\ 0\ h2\,(s)\ u\,(s)\ ds$, The arguments were based upon a specially constructed cone and the fixed point theory. First, the conditions for determining solution in (1) were imposed on the reproducing kernel space and therefore the reproducing kernel satisfying the conditions for determining a solution (vulnerability forecasts of seasonal, unknown, hyperproductive, aquatic, larval habitat, malaria, mosquito, LULC foci..We used the kernel to solve problems. Second, the iterative sequence $un(x)$ was emoployed to approximate solutions convergence in $C4$ to the solution $u(x)$.

International Research Journal of Computer Science and Application
Vol. 2, No. 1, March 2018, pp. 1-181
Available Online at http://acascipub.com/Journals.php

Table 11 Solutions to the Chebyshev differential *An. arabiensis* aquatic, larval habitat prognostic ative, eco-endmember, LULC equation denoted by $T_n(x)$.

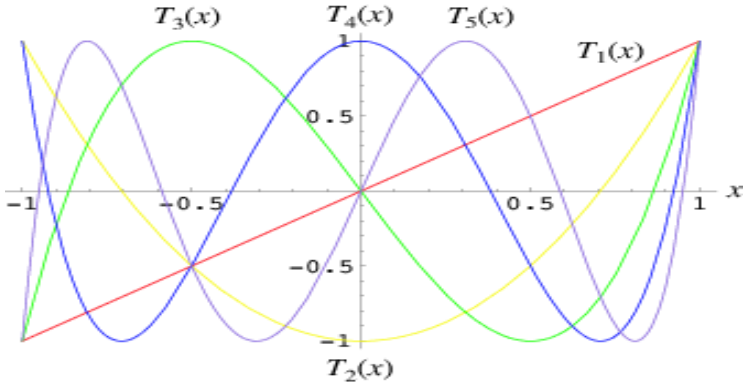

`

The Chebyshev, eco-epidemiological, forecast, vulnerability, *An. arabiensis* aquatic, larval habitat, geo-spectrotemporal, endmember, LULC polynomials of the first kind were denoted $T_n(x)$, and were implemented in the Wolfram Language as ChebyshevT[*n*, *x*]. They were normalized such that $T_n(1) = 1$. The first few polynomials for $x \in [-1, 1]$ and $n = 1$,….The Chebyshev polynomial of the first kind $T_n(z)$ was defined by the contour integral $T_n(z) = \frac{1}{4\pi i} \oint \frac{(1-t^2)\, t^{-n-1}}{(1-2tz+t^2)}\, dt$, where the contour encloses the origin and was traversed in a counterclockwise direction (see Arfken 1985).

The first few *An. arabiensis*-related Chebyshev polynomials of the first kind were $T_0(x)=1$, $T_1(x)=x$, $T_2(x)=2x^2-1$, $T_3(x)=4x^3-3x$, $T_4(x)=8x^4-8x^2+1$, $T_5(x)=16x^5-20x^3+5x$, $T_6(x)=32x^6-48x^4+18x^2-1$. (See Figure 1)

Figure 1 Ordered from smallest to largest powers, the triangle of nonzero coefficients was 1; 1; -1, 2; -3, 4; 1, -8, 8; 5, -20, 16, ...

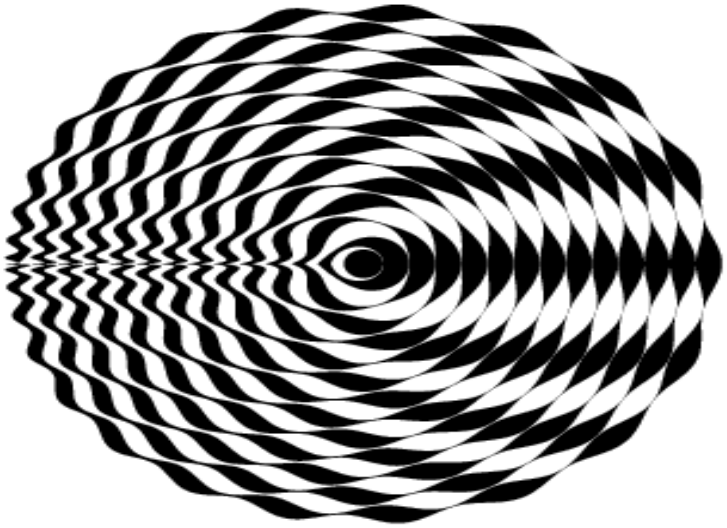

A beautiful plot was obtained by plotting $T_n(x)$ radially, increasing the radius for each predicted, *An. arabiensis*, aquatic, larval habitat value of n, and filling in the areas between the curves. The Chebyshev polynomials of the first kind generated from the empirical geosampled, geo-spectrotemporal, sub-meter resolution, eco-endmember LULC signature, frequency dataset were defined through the identity $T_n(\cos\theta) = \cos(n\theta)$. The Chebyshev polynomials of the first kind were obtained from the training, geosampled, *An. arabiensis* capture point dataset by generating functions $g_1(t,x) = \frac{1-t^2}{1-2xt+t^2} = T_0(x) + 2\sum_{n=1}^{\infty} T_n(x)\,t^n$ and $g_2(t,x) = \frac{1-xt}{1-2xt+t^2} = \sum_{n=0}^{\infty} T_n(x)\,t^n$ for $|x| \le 1$ and $|t| < 1$.

.

A direct representation of the eco-endmember, *An. arabiensis* aquatic larval habitat, oviposition, capture point, ento-ecoepidemiological, forecast, vulnerability,LULC model was given by $T_n(z) = \frac{1}{2} z^2 \left[\left(\sqrt{1-\frac{1}{z^2}} + 1 \right)^n + \left(\sqrt{1-\frac{1}{z^2}} \right)^n \right]$. The polynomials were defined in terms of the sums $T_n(x) = \frac{n}{2} \sum_{r=0}^{\lfloor n/2 \rfloor} \frac{(-1)^r}{n-r} \binom{n-r}{r} (2x)^{n-2r} = \cos\left(n \cos^{-1} x\right) = \sum_{m=0}^{\lfloor n/2 \rfloor} \binom{n}{2m} x^{n-2m} \left(x^2-1\right)^m$, when $\binom{n}{k}$ was a binomial coefficient and $\lfloor x \rfloor$ was the floor function, or the product $T_n(x) = 2^{n-1} \prod_{k=1}^{n} \left\{ x - \cos\left[\frac{(2k-1)\pi}{2n} \right] \right\}$.

In the sub-mter resolution, *An. arabiensis* , aquattic, larval habitat frequency model T_n also satisfied the curious determinant equation $T_n = \begin{vmatrix} x & 1 & 0 & 0 & \cdots & 0 & 0 \\ 1 & 2x & 1 & 0 & \ddots & 0 & 0 \\ 0 & 1 & 2x & 1 & \ddots & 0 & 0 \\ 0 & 0 & 1 & 2x & \ddots & 0 & 0 \\ 0 & 0 & 0 & 1 & \ddots & 1 & 0 \\ \vdots & \ddots & \ddots & \ddots & \ddots & \ddots & 1 \\ 0 & 0 & 0 & 0 & \cdots & 1 & 2x \end{vmatrix}$. The Chebyshev polynomials of the first kind are a special case of the Jacobi polynomials $P_n^{(\alpha,\beta)}$ with $\alpha = \beta = -1/2$, $T_n(x) = \frac{P_n^{(-1/2,-1/2)}(x)}{P_n^{(-1/2,-1/2)}(1)} = {}_2F_1\left(-n, n; \frac{1}{2}; \frac{1}{2}(1-x)\right)$, where ${}_2F_1(a, b; c; x)$ is a hypergeometric function [6]. Zeros occur when $x = \cos\left[\frac{\pi\left(k-\frac{1}{2}\right)}{n} \right]$ for $k = 1$, 2, ..., n. Extrema occurred in the *An. arabiensis*, forecast, vulnerability, LULC, eco-endmember, signature, frequency model for $x = \cos\left(\frac{\pi k}{n}\right)$, where $k = 0, 1, \ldots, n$ and att maximum, $T_n(x) = 1$, and at minimum, $T_n(x) = -1$.

The eco-endmember, LULC, *An. arabiensis*, aquatic larval habitat, capture point, eco-georeferenceable, Chebyshev polynomials were orthogonal polynomials with respect to the weighting function $\left(1-x^2\right)^{-1/2}$ $\int_{-1}^{1} \frac{T_m(x)\,T_n(x)\,dx}{\sqrt{1-x^2}} = \begin{cases} \frac{1}{2}\pi\delta_{nm} & \text{for } m \neq 0, n \neq 0 \\ \pi & \text{for } m = n = 0, \end{cases}$ where δ_{mn} was the Kronecker delta.

International Research Journal of Computer Science and Application
Vol. 2, No. 1, March 2018, pp. 1-181
Available Online at http://acascipub.com/Journals.php

Chebyshev polynomials of the first kind satisfied the additional discrete identity $\sum_{k=1}^{m} T_i(x_k)\, T_j(x_k) = \begin{cases} \frac{1}{2}\, m\, \delta_{ij} & \text{for } i \neq 0,\ j \neq 0 \\ m & \text{for } i = j = 0, \end{cases}$ where x_k for $k = 1$, ..., m are the m zeros of $T_m(x)$.They also optimally, remotely, geo-spectrotemporally satisfied the recurrence relations $T_{n+1}(x) = 2x\, T_n(x) - T_{n-1}(x)$, $T_{n+1}(x) = x\, T_n(x) - \sqrt{(1-x^2)\{1-[T_n(x)]^2\}}$ for $n \geq 1$ in the *An. arabiensis*, capture point, signature, eco-endmember, LULC model output as well as $(x-1)[T_{2n+1}(x)-1] = [T_{n+1}(x) - T_n(x)]^2$, $2(x^2-1)[T_{2n}(x)-1] = [T_{n+1}(x) - T_{n-1}(x)]^2$. The derivatives had a complex integral representation which was represented in the forecast, vulnerability, model as $T_n(x) = \frac{1}{4\pi i} \int_\gamma \frac{(1-z^2) z^{-n-1}\, dz}{1 - 2xz + z^2}$ and a Rodrigues representation which was solved as $T_n(x) = \frac{(-1)^n \sqrt{\pi}\, (1-x^2)^{1/2}}{2^n \left(n - \frac{1}{2}\right)!} \frac{d^n}{dx^n} \left[(1-x^2)^{n-1/2}\right]$.

Using a fast Fibonacci transform the *An. arabiensis* capture point, oviposition, frequency,signature, LULC model rendered $(T_{n+1}(x), -T_n(x)) = (T_1(x), -T_0(x))(1,0)^n$.Using Gram-Schmidt orthonormalization in the range $(-1,1)$ with weighting function $(1-x^2)^{(-1/2)}$ then rendered $p_0(x) = 1, p_1(x) = \left[x - \frac{\int_{-1}^{1} x (1-x^2)^{-1/2}\, dx}{\int_{-1}^{1} (1-x^2)^{-1/2}\, dx}\right] = x - \frac{\left[-(1-x^2)^{1/2}\right]_{-1}^{1}}{\left[\sin^{-1} x\right]_{-1}^{1}} = x, p_2(x) = \left[x - \frac{\int_{-1}^{1} x^3 (1-x^2)^{-1/2}\, dx}{\int_{-1}^{1} x^2 (1-x^2)^{-1/2}\, dx}\right] x - \left[\frac{\int_{-1}^{1} x^2 (1-x^2)^{-1/2}\, dx}{\int_{-1}^{1} (1-x^2)^{-1/2}\, dx}\right] \cdot 1 =$ $[x-0]\, x - \frac{\frac{\pi}{2}}{\pi} = x^2 - \frac{1}{2}$,Normalizing $T_n(1) = 1$ in the model then rendered the Chebyshev polynomials of the first kind.(see Figure 2).

Figure 2.The *An. arabiensis* predicted capture point resultants $\rho(T_n(x), T_k(x))$

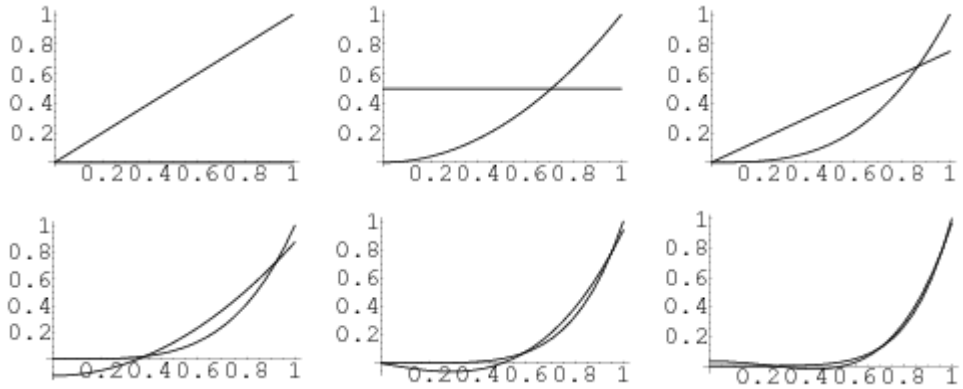

The EM algorithm proceeded from the geo-spectrotemporal geosampled oviposition, eco-georeferenecable, aquatic, larval habitat, explanatory foci, LULC observations and solve sets of equations numerically. The EM algorithm (Dempster, Laird, and Rubin 1977) is a technique that finds maximum likelihood estimates in parametric models for incomplete data. The books by Little and Rubin (2002), Schafer (1997), and McLachlan and Krishnan (1997) provide a detailed description and applications of the EM algorithm.The EM algorithm is an iterative procedure that finds the maximum likelihood estimation of the parameter vector[4].Given the set of *An. arabiensis*, capture point, aquatic, larval habitat, parameter, eco-endmeber estimates, including the mean vector and covariance matrix for the

multivariate normal distribution, the E-step calculated the conditional expectation of the complete-data log likelihood given the observed capture point data and the sub-meter resolution, LULC, orthogonal, oviposition, parameter estimates.Thereafter, a complete-data log likelihood was conducted and the M-step found the *An. arabiensis*, hyperproductive, capture point, unknown, parameter estimates which maximized the complete-data log likelihood from the E-step.The two steps iterated until the iterations converged.

In the EM process, the *An. arabiensis* aquatic, larval habitat, capture point, observed, LULC eco-endmember data log likelihood did not nondecrease at each iteration. For the multivariate,ento-ecoepidemiological,oviposition geosampled, LULC data, there were a G groups with distinct missing topological patterns. The observed eco-endmember, malaria, mosquito,sub-meter resolution, data log likelihood being maximized was then expressed as $\log L(\theta|Y_{obs}) = \sum_{g=1}^{G} \log L_g(\boldsymbol{\theta}|Y_{obs})$ which was the observed-data log likelihood from the gth group whence $\log L_g(\boldsymbol{\theta}|Y_{obs}) = -\frac{n_g}{2}\log|\Sigma_g| - \frac{1}{2}\sum_{ig}(\mathbf{y}_{ig} - \boldsymbol{\mu}_g)'\boldsymbol{\Sigma}_g^{-1}(\mathbf{y}_{ig} - \boldsymbol{\mu}_g)$ where n_g was the number of prognosticated, hyperproductive, eco-endmember *An. arabiensis*, capture point,observations in the gth group. The summation was over observations in the gth group, whence $\mathbf{y}_{ig}$ was a vector of observed geosampled, geospectrotemporal, endemic, sub-pixxel LULC values corresponding to observed variables whence $\boldsymbol{\mu}_g$ was the corresponding mean vector, and $\boldsymbol{\Sigma}_g$ was the associated covariance matrix.

A sample covariance matrix was computed at each step of the EM algorithm. If the covariance matrix is singular, the linearly dependent variables for the observed data are excluded from the likelihood function [8]. Hence for each predicted eco-endmember, capture point, *An. arabiensis*, LULC observation with linear dependency amongst its observed capture point, aquatic, larval habitat variables, the dependent variables were excluded from the likelihood function. Note that this can result was an unexpected change in the likelihood between iterations prior to the final convergence.

PROC MI used the means and standard deviations from available eco-epidemiological, eco-endmember, signature LULC, immature habitat data as the initial estimates for the EM algorithm. The correlations were set to zero. These initial estimates provided a good starting value with positive definite covariance matrix. We specified the convergence criterion with the CONVERGE= option in the EM statement. The iterations were considered to have converged when the maximum change in the geosampled, oviposition, orthogonal,*An. arabiensis* LULC, parameter estimates between iteration steps was less than the value specified. We specified the maximum number of iterations used in the EM algorithm with the MAXITER= option.

The MI procedure displayed the tables of the geosampled, *An. arabiensis*, capture point, LULC signature, parameter estimates to begin the EM process along with the maximum likelihood parameter estimates derived from EM. You can display the EM iteration history with the ITPRINT option[www.sas.com]. PROC MI listed the iteration number, the likelihood _2 log L, and the capture poit, unknown seasonal habitat parameter values $\boldsymbol{\mu}$ at each iteration. We saved the ovipoition, LULC , eco- endmembers, derived from the EM algorithm in a SAS data set by specifying the OUTEM= option.

Here we employed the EM algorithm to compute the maximum likelihood estimates for the sub-meter resolution, umixed, frequency signature,a quatic larval habitat, multivariate, normally, distributed iteratively interpolatale, LULC data with missing values. To use EM, we employed the given ,capture point, geosampled eco-georeferenced, observed data y, a parametric density p(y | θ), a description of the geosampled, larval habiotat, frequency data x and the parametric density p(x | θ). At this point, we assumed what the complete habitat dataset x could be modeled as a continuous random explanatory variable X with density p(x | θ), where θ ∈ Θ. The treatment of discrete random variables is very similar: one only need to replace the probability density function with probability mass function and integral with summation[2] We assumed that the support X of X, where X was the closure of the geosampled empricial regressable dataset x p(x | θ) > 0 , did not depend on θ. For example, we did not address the case whence θ was the end capture point of a uniform distribution.: Notation Summary y ∈ R d1 measurement habitat observation had Y ∈ R d1 random measurement. We assumed we had a realization y of Y x ∈ R d2 complete eco-

endmeber LULC dataset for asymptotically targeting seasonal unknown, eco-geoerferenecable, prolific foci but instead we had y = T(x) X ∈ R d2, a random complete dataset;

The intuition behind EM is an old one: alternate between estimating the unknowns Θ and the hidden variables J. This idea has been around for a long time. However, instead of finding the best J ∈ J given an estimate Θ at each iteration for our sub-mter resolution, *An. arabiensnis*, grid-startfiaible, prognosticative, LULC signature eco-endmeber model , the EM computed a distribution over the space J . One of the earliest papers on EM is (Hartley, 1958), but the seminal reference that formalized EM and provided a proof of convergence is the "DLR" paper by Dempster, Laird, and Rubin (Dempster et al., 1977). A recent book devoted entirely to EM and applications is (McLachlan and Krishnan, 1997), whereas (Tanner, 1996) is another popular and very useful reference. One of the most insightful explanations of EM, that provides a deeper understanding of its operation than the intuition of alternating between variables, is in terms of lowerbound maximization (Neal and Hinton, 1998; Minka, 1998). In this derivation, the E-step was interpreted as constructing a local lower-bound to the posterior distribution in the *An. arabiensis* eco-endmember, capture point, predictive, vulnerability,LULC model for asymptotically optimally remotely geo-spectrotemporally targeting seasonal, eco-georeferenecable, hyperproductive aquatic, larval habitat seasonal foci ,whereas the M-step optimized the bound, thereby improving the estimate for the unknowns.

The following statements invoked the MI procedure and requested the EM algorithm to compute the hyperproductive capture points using $(\boldsymbol{\mu}, \boldsymbol{\Sigma})$ from the input dataset

proc mi data=*An. arabiensis* =151 simple nimpute=0;

em itprint outem=outem;

var Oviposition geosample larval habitat ;

run;

Note that when we specify the NIMPUTE=0 option, the missing values wewre not imputed.The "Model Information" table (see Table 12) described the method and options employed in the procedure when a geosampled, *An. arabiensis*, aquatic, larval habitat was specified in the NIMPUTE= option.

Table 12. The MI procedure for the *An. arabiensis* aquatic, larval habitat, spectral model

Model Information	
Data Set	***An. arabiensis.***
Method	**MCMC**
Multiple Imputation Chain	**Single Chain**
Initial Estimates for MCMC	**EM Posterior Mode**
Start	**Starting Value**
Prior	**Jeffreys**
Number of Imputations	**0**

Model Information	
Number of Burn-in Iterations	**200**
Number of Iterations	**100**
Seed for random number generator	**151**

The "Missing Data Patterns" table in the oviposition, sub-meter resolution, grid-stratfiable, listed, distinct, missing LULC data patterns with corresponding frequencies and percentages. Here, a value of "X" meant that the geosampled, *An. arabiensis,* aquatic, larval habitat, eco-georeferenecd, LULC variable was observed in the corresponding group and a value of "." meant that the variable was missing. The model output displayed the group-specific, oviposition, LULC, geo-spectrotemporal, endmember variable means.

With the SIMPLE option, the procedure displayed simple descriptive univariate statistics for the eco-georeferenceable, hyperproductive, oviposition, LULC, capture points employing univariate statistics which included correlations from pairwise available *An. arabiensis* aquatic, larval habitats as in Table 13. This option displayed simple descriptive statistics (mean, standard deviation, minimum and maximum) for each explanatory geosampled, sub-meter resolution, grid-stratfiied, geoclassifiable, ento-endmember LULC, signature, frequency variable in the MODEL statement. The SIMPLE option generates a breakdown of the simple descriptive statistics for the entire empirical ovispoition, capture point, regressed dataset and also for individual response levels.

Table 13: Univeraite statistics for the *An. arabeisnis* LULC signature model

Variable	N	Mean	Std Dev	Minimum	Maximum	Missing Values	
						Count	Percent
Levels of water	**8**	**47.11**	**5.41**	**37.3**	**60.0**	**3**	**9.68**
Larval count	**8**	**90.3**	**7.11**	**86**	**140**	**113**	**96**
Distance from capture point	**8**	**1.71**	**1.01**	**1.48**	**1.86**	**.911**	**1.03**

The expectation-maximization (EM) algorithm is a technique for maximum likelihood estimation in parametric models for incomplete data[2]. The EM statement used the EM algorithm to compute the MLE for (μ, Σ), in the sub-meter resolution, geo-spectrotemporal, grid-startified, LULC, eco-endmember, signature model for optimally asymptotically geolocation unknown seasonal, eco-georeferenecable, hypeporductive foci. The means and covariance matrix, of a multivariate normal distribution from the input data set was employed to determine missing values in the empricially regressable, frequency unmixed signature, iteratively interpolative estimators. The means and endmeber covariances from complete cases or the means and standard deviations from available cases can be used as the initial estimates for the EM algorithm[7]. We specified the correlations for the unknow, capture point, prolific estimates from the available geosampled sub-pixel LULC dataset. We employed the EM statement with the NIMPUTE=0 option in the PROC MI statement to compute the EM estimates without multiple imputation. PROC CORR also estimates a correlation by using the eco-endmember uncoalesced, frequency, sub-meter resolution, datasets with nonmissing, LULC values. In so doing the available data, revealed optimal resulting correlation matrix but it was not positive definite. We employed the EM statement,

```
proc mi data=FitMiss An. araiensis data nimpute=0;
   em itprint outem=outem;
   var RunTime RunPulse;
run;
```

where the MI procedure displayed the initial oviposition, eco-endmeber, *An. arabiensis* LULC, spectral-temporal, hyperproductive, aquatic larval habitat, capture point, eco-georeferenced, geoclassified, parameter estimates for the EM algorithm in the "Initial Parameter Estimates (Table 14).

Table 14 The ITPRINT option in the EM statement, the "EM (MLE) Iteration History" to display the iteration history for the EM algorithm for the *An. arabiensis* forecast model.

EM (MLE) Iteration History				
Iteration	**-2 Log L**	**Larval count**	**Distance to capture point**	**Levels of vegetaion**
0	**289.544782**	**47.116179**	**10.688214**	**171.863636**
1	**263.549489**	**47.116179**	**10.688214**	**171.863636**
2	**255.851312**	**47.139089**	**10.603506**	**171.538203**
3	**254.616428**	**47.122353**	**10.571685**	**171.426790**
4	**254.494971**	**47.111080**	**10.560585**	**171.398296**
5	**254.483973**	**47.106523**	**10.556768**	**171.389208**
6	**254.482920**	**47.104899**	**10.555485**	**171.385257**

In this paper, we consider an extension of the EM-algorithm presented in Laird & Ware (1982) for parameter estimation in a bivariate response random-effects model. We presented the algorithm for two possible types of 'missing' data structures. In the first case both aquatic, larval habitat, eco-endmember, characteristics were observed at each habitat, though the number and timing of the geosampled, geo-spectrotemporal, *An. arabiensis*, endemic foci,capture point, LULC observations differed from individual habitat to individual habitat (i.e., the larval data were complete in number of observations per experimental unit). We employed the EM-algorithm for obtaining maximum likelihood or restricted maximum likelihood (REML) estimates for the oviposition, endmember, geosampled, *An. arabiensis*, geo-spectrotemporal, grid-stratified, LULC parameters. It should be noted that the estimate was easily obtained via a closed form solution by Generalized Least Squares (GLS).

We let r index the iterations for r = O, 1,2, ... m, where r = O denoted the geosampled *An. arabiensis*, grid-stratified oviposition, sub-meter resolution, endmember,LULC signature values. The sufficient statistics for the model frequency estimators were ~(Ei) and ~(~i) respectively. Since Ti and ei = vec(E;) were unobservable, the algorithm computed the expectations of the sufficient statistics and then solved for maximum likelihood. The algorithm employed the joint density of yi, vi, ei to obtain the conditional expectations of the sufficient statistics. In the E-step we let @ be the vector of unknown seasonal, un-geosampled, hyperproductive, *An. arabiensis*, eco-endmember, geo-spectrotemrpoal, geosampled, LULC parameters in E and D and O(r) which we denoted by their larval habitat values at the end of the ~th iteration. The estimate for B given values was i=l where P~') = Vi(')'1 and Vi = Var(yi) =

[Z$DZ~' + Y @ Ii]. Letting ri('j = yi – xt~t') and B@2 = B', the expectations of the Jh term of the sufficient statistics was given by: q(%)(%'ylyi, @),@TJ = {E[-yi[yi,e(7),p(T)]}@'2+v[-/ily;, d'), p(T)] .E[(Eij)'(Ei~)lyi, d7), fI(T)] = EIE~jly~,6(7), @T)]'EIEiklyi,/3@),@T)] (~), p(0)], j,k = 1,2. + tr[Cov(Eij, EMlYi, ~. These expectations were easily obtained using the conditional mean and covariance matrix of the ento-ecoepidemiologically, tabulated, multivariate normal distribution. In the M-step, X('+l) and D('+l) were found by equating them to the expected value of their sufficient statistics. For the ovispsoition, capture point,ML estimates the iterative equations were: N D(7+1) = [Hq(-f;)(~i)'lyi, 0 1]/ (~),p(~)] ~, i=l (T+l) _ rjk-[~ni]-l[~[E[(Eij),(Ei~) Iyi,~(T),P(T)I]], j,k=l,2'i=l. The model output was addressed in detail with the estimating equations being derived for both ML and REML estimation.

The following statements used the restricted maximum likelihood (REML) for estimation which produce Table 14

```
proc varcomp method=reml data=a;
  class a b;
  model y=a|b / fixed=1;
run;
```

Table 15 REML estimation of the *An. arabiensis* aquatic, larval habitat model

Iteration	Objective	Var(b)	Var(a*b)	Var(Error)
0	63.4134144942	1269.52701	0	91.5581191305
1	63.0446869787	1601.84199	32.7632417174	76.9355562461
2	63.0311530508	1468.82932	27.2258186561	78.7548276319
3	63.0311265148	1464.33646	26.9564053003	78.8431476502
4	63.0311265127	1464.36727	26.9588525177	78.8423898761

REML Estimates	
Variance Component	Estimate
Var(b)	1464.4
Var(a*b)	26.95885
Var(Error)	78.84239

Asymptotic Covariance Matrix of Estimates			
	Var(b)	Var(a*b)	Var(Error)
Var(b)	4401703.8	1.29359	-273.39651
Var(a*b)	1.29359	3559.1	-502.85157
Var(Error)	-273.39651	-502.85157	1249.7

The "REML Iterations" in Table 15 showed that the REML optimization of the *An.arabeisnis* aquatic, larval habitat, oviposition, eco-endmember, LULC data required four iterations to converge.The REML estimated all corresponding ML estimates and adjusted for potential downward bias. Type I estimates were rectified. The asymptotic covariance matrix of the ento-ecoepidemiological, eco-georeferenceable, grid-stratified, eco-endmember LULC, frequency estimates" in Table 15 revealed that the error variance component endmember, iteratively interpolative,

signature estimate was negatively correlated with the other variance component estimates, and the estimated variances were all larger than their ML counterparts.

To obtain REML estimates, at the E-step conditioned only on y, we employed the aquatic, larval habitat, density, endme,ber,LULC, simuatedcounts since ~ was integrated out of the likelihood using a flat prior. Using the posterior distribution of ,B we obtained the conditional expectations of the sufficient statistics: + tTIUjkIi– (~ljIilujzIi)@i (61kIi[6kzIi)']j j] k = lj 2. For obtaining starting values for the geosampled, geo-spectrotemporal, *An. arabiensis* ,capture point, hyperproductive, eco-endmember, LULC, signature foci we conducted an OLS for each grid-stratified , LULC unit and requisited a minimum number of repeat measurements. The model used to fit by OLS was equivalent to the random design, Yi = ZJ~i +ei. This yielded vi(o) and ei(o) = vec[Ei(0)]. From these we obtained ~(o) using (2), and D(o) and E(o) which was obtained employing the following equations N D(o) = [Z(Vi(o) – ~ Nvi(o)) @21/N, and Y(o) = i=l [f(Ei(0))'] / ~ni.

A malariologist or medical entomologist may pick arbitrary, malaria, mosquito, immature habitat, seasonal geosampled, frequency, density, count values for one of the two sets of unknowns, and then use them to estimate the second set. In so doing, the new values may find a better estimate of the first set. Hence by alternating between the two geosampled, LULC datasets, the resulting values would be both estimateable since they would converge to fixed capture points (i.e., seasonal, hyperproductive, aquatic, larval habitat, eco-georrferenceable,LULC, eco-entomological foci). It may be proven that in forecast, vulnerability, malaria, endmember, sub-meter resolution, grid-stratifiable, LULC modelling context that the derivative of the likelihood is arbitrarily close to zero at the capture point, foci which in turn would mean that the point is either a maximum or a saddle point.

In general, multiple maxima may occur, with no guarantee that the global maximum is quantifiable in an eco-endmember, prognosticative, malaria, mosquito, sub-meter resolution, vulnerability, oviposition, LULC, signature model. Some likelihoods in these models may have also have singularities in them, (i.e., nonsensical maxima). For example, one of the solutions that was found by EM in our mixture, model was attained by setting one of the eco-endmember grid-stratified, LULC components (Euclidean distance from capture point to village centroid) to have zero variance and the mean, eco-endmember, geo-spectrotemporal, LULC parameter for the same component to be equal to one of the known, eco-georefereneced, hyperproductive, seasonal, capture point.

Whenst searching for the MLE of a likelihood in an oviposition, malaria, mosquito, endmember, sub-meter resolution, ento-ecoepidemiological,signature, forecast, vulnerability model of the form∫f(x,z|β)dz, the EM- algorithm should optimally proceed by iteratively maximizing (M) expected (E) complete log-likelihoods, which may result in maximizing β at iteration for rendering a quantitative explanatory, time series, quantitable LULC function which may be devisable from Q(β|βi)=∫log f(x,z|β)f(z|x,βt)dz.The algorithm may identify the latent explanatory, endmember LULC variable z and its conditional distribution in the ento-ecoepidemiological, forecast, vulnerability, endmember, signature, malaria model. In so doing an eco-georeferenceable, seasonal, hyperproductive, malaria, mosquito, oviposition, ento-ecoepidemiological, capture point, aquatic, larval habitat foci may be distinguishable on a sub-meter resolution, grid-stratified, orthogonal image.

A polynomial furnishing the best approximation of an endmember, oviposition, function $\boldsymbol{x}(t)$ can occur in some metric, relative to all optimizable *An. arabiensis* ,aquatic, larval, habitat, polynomials constructed from a given (finite) system of eco-endmember, grid-stratfiable, sub-meter resolution LULC, siganture functions . If **x** is a normed linear function space in an eco-georeferenecable, capture point, oviposition, sub-meter resolution, grid-stratifiable, malaria, mosquito, capture point, endmember, signature model (such as $C[a,b]$or $L_p(a,b)$, $p \geq 1$), and if $U_n = \{u_1(t),..., u_n(t)\}$ is a system of linearly independent, frequency-oriented, aquatic, larval, habitat,time series, LULC, endmember, sub-meter resolution, grid-stratifiable, signature functions in **x**, then for any $\boldsymbol{x} \in \boldsymbol{X}$the generalizable LULC polynomial of best approximation $\hat{u}(t) = \hat{u}(x,t) = \sum_{k=1}^{n} c_k u_k(t),$ may be defined by the relation $\|x - \hat{u}\| = \min_{\{c_k\}} \left\| x - \sum_{k=1}^{n} c_k u_k \right\|,$ which may or may not exist in the output. The polynomial of best approximation would be unique for all $\boldsymbol{x} \in \boldsymbol{X}$, malaria, mosquito, capture points if $\boldsymbol{X}$ is a space with a strictly convex norm (i.e. if

$\|x\| = \|y\|$and $x \neq y$, then $\|x+y\| < \|x\| + \|y\|$). This was the case for $L_p(a,b)$, $1 < p < \infty$ in our model derivative dataset. In $C[a,b]$, which had a norm that was not strictly convex in our model, the polynomial of best approximation for any $x \in C[a,b]$ seasonal, hyperproductive, aquatic, larval habitat foci was unique if U_n was a Chebyshev system on $[a,b]$, (i.e. if each capture point polynomial $u(t) = \sum_{k=1}^{n} c_k u_k(t) \neq 0$ and at most $n-1$ zeros occurred on $[a,b]$.

For any finite k≤nk≤n the functions ϕ1(x),…,ϕk(x)ϕ1(x),…,ϕk(x) forms a Chebyshev system on (a,b)[4]. Examples of Markov function systems which may be applicable for regressively quantiating an uncoalesced LULC dataset of sub-mteer resolution, capture point, oviposition, endmember, geo-spectrotemporal, geosampled, malaria mosquito, ento-ecoepidemiological, geo-spectrotemporal, prognosticative, risk modeling frequencies may include a) 1,x,x2,…,1,x,x2,…, on any interval [a,b]; b) 1,cosx,cos2x,…, ,…, on [0,π]; c) sinx,sin2x,…, on [0,π] for optimally targeting seasonal, eco-georferenceable, hyperproductive, capture point foci.

In particular, a malariologist or medical entomologist could quantitate uniqueness in the case of the (usual) algebraic polynomials in $C[a,b]$, and also for the trigonometric, endmember grid-stratifable polynomials in the space $C_2\,\pi$of continuous $2\,\pi$-periodic functions on the real line, with the uniform metric for adjusting erroneous variability in an oviposition, geo-spectotemporal, ento-ecoepidemiological, sub-meter resolution, capture point, forecast, vulnerability, ecogeoreferenceable, endmember,LULC model. If the polynomial of best approximation exists in the signature, oviposition, sub-meter resolution, model and is unique for any $x \in X$, (e.g., geolocation of a capture point, seasonal, eco-georeferenceable, hyperproductive, aquatic, larval habitat foci) the oviposition model may have a continuous function of x.

Necessary and sufficient conditions for a polynomial to be a best approximation in the spaces $C[a,b]$and $L_p\,[a,b]$ in a sub-meter resolution, oviposition, malaria mosquito, grid-stratifiable, forecast, vulnerability, endmember,LULC model may be also known. For example, if a malariologist or medical entomologist employs Chebyshev's theorem in an aquatic, larval habitat, endmember, risk model U_n would have a Chebyshev system when the endmember LULC geo-spectrotemporal, ento-ecoepidemiological polynomial (*) is a polynomial of best approximation for a function $x \in C[a,b]$in the metric of $C[a,b]$if and only if there exists a system of $n+1$ field-verifiable, eco-georeferenecable, capture points t_i, $a \leq t_1 < \square \ldots < t_n + 1 \leq b$, at which the difference $\Delta(t) = x(t) - \tilde{u}(t)$assumes, discrete integer, frequency, denisty, habitat, count values $\pm \max_{a \leq t \leq b} |\Delta(t)|$ and, moreover, $\Delta(t_{i+1}) = -\Delta(t_i), \quad i = 1, \ldots, n$. The polynomial (*) is a polynomial of best approximation for a function $x(t) \in L_p\,[a,b]$, $p > 1$, in the metric of that space, if and only if for $k = 1, \ldots, n$, $\int_a^b u_k(t) |x(t) - \tilde{u}(t)|^{p-1} \operatorname{sign}\,[x(t) - \tilde{u}(t)]\,dt = 0$.

[4]. If $L_1\,[a,b]$ occurs in the ento-ecoepidemiological, endmember LULC, oviposition model, the conditions $\int_a^b u_k(t) \operatorname{sign}\,[x(t) - \tilde{u}(t)]\,dt = 0, \quad k = 1, \ldots, n,$ may be suffice for optimally quantitating $\tilde{u}(t)$ so as to be a polynomial of best approximation for $x \in L_1\,[a,b]$ in a sub-meter resolution, malaria, mosquito, forecast, vulnerability, grid-stratifiable model. If the measure of the set of all geo-spectrotemporal, geosampled, eco-georeferenceable, aquatic, larval habitat, capture points $t \in (a,b)$at which $x(t) = \tilde{u}(t)$is zero,this would allow enabling a malariologist, medical entomologist or other experimenter to exploit effectively the endmeber LULC polynomial and the error of best integral approximation of a function f. This was established by A.A. Markov in 1898.

Hence, if a malariologist or medical entomologist lets $\{\phi_k(x)\}$, $k = 1, \ldots, n$, be a system of linearly independent, explanative, capture point, eco-georferenecable, grid-stratifiable, malaria mosquito, endmember, geo-spectrotemporal,geoclassifiable, LULC functions continuous in an signature, oviposition, sub-meter resolution,

prognosticative,vulnerability model on the interval $[a, b]$, and let the continuous function ψchange sign at an unknown, seasonal, hyperproductive, capture point then $x_1 < \ldots < x_r$in (a, b) would be quantifiable such that $\int_a^b \phi_k(x) \operatorname{sgn} \psi(x)\, dx = 0, \quad k = 1, \ldots, n$. occurs in the model output. If the malaria, mosquito polynomial $P_n^*(x) = \sum_{k=1}^{n} c_k^* \phi_k(x)$ has the property that the difference $f - P_n^*$changes sign at the seasonal, hyperproductive, capture points $x_1, \ldots, x_r$, and only at those points, then P_n^* would be the polynomial of best integral approximation to $f$and $\inf_{\{c_k\}} \int_a^b \left| f(x) - \sum_{k=1}^{n} c_k \phi_k(x) \right| dx = \int_a^b \left| f(x) - P_n^*(x) \right| dx = \left| \int_a^b f(x) \operatorname{sgn} \psi(x)\, dx \right|$. Further the system $\{1, \cos x, \ldots, \cos nx\}$on $[0, \pi]$, ψmay be taken to be $\cos(n+1)x$; in the model for quantitating the system $\{\sin x, \ldots, \sin nx\}$, $0 \le x \le \pi$, ψ which may be be taken to be $\sin(n+1)x$; when targeting seasonal, hyperproductive, malaria, mosquito, aquatic, larval, habitat, foci. $\{1, x, \ldots, x^n\}$.Hence $-1 \le x \le 1$, $\psi(x) = \sin((n+2) \arccos x)$.

More generally, note that (Xi − X)(Yi − Y) is positive in an ento-ecoep idemiological, prognosticative, malaria, capture point, aquatic,larval habitat,capture point,oviposition, regression-related, LULC, endmember model if and only if Xi and Yi lie on the same side of their respective means. Thus, the correlation coefficient for an eco-georeferenceable, sub-meter resolution, seasonal, hyperproductive grid-stratfiable, eco-endmember foci would be positive if Xi and Yi tend to be simultaneously greater than, or simultaneously less than, their respective means. The correlation coefficient would be negative if Xi and Yi tend to lie on opposite sides of their respective means in the model. Moreover, the stronger the anti-correlation tendency in the ento-ecoepidemiological, geo-spectrotemporal, oviposition, endmember LULC model output, the larger would be the absolute value of the correlation coefficient in the model.

Geometerically there would be a quantitative relationship between the correlation coefficient in an oviposition, vulnerability, forecast, capture point, sub-meter resolution, endmember, LULC, signature,orthogonal model and the angle φ between the two regression lines, y = gx(x) and x = gy(y) which may be regressively obtainable by quantitating y on x and x on y respectively. Here φ may be measured within the first quadrant formed around the lines' intersection point if r > 0, or counterclockwise from the fourth to the second quadrant if r < 0.)A malariologist, medical entomologist or other experimenter may determine that if the standard deviations are equal in an oviposition, prognosticative, endemic, risk model, then r = sec φ − tan φ, where sec and tan are trigonometric functions. For robustly centered, geosampled malaria, mosquito, capture point, eco-georeferenceable, geo-spectrotemporal, geoclassified, LULC endmember observations (i.e., eco-georeferenecable, seasonal, hyperproductive aquatic, larval habitat data which have been shifted by the sample means of their respective variables so as to have an average of zero for each variable), the correlation coefficient can also be viewed as the cosine of the angle θ between the two vectors of samples in *n*-dimensional space (for *n* samples of each grid-stratifiable oviposition prognosticator).

Both the uncentered (non-Pearson-compliant) and centered correlation endmember, grid-stratfiable, LULC, ento-ecoepidemiological, coefficients can be determined for an empricial regressable optimizable oviposition, dataset of eco-georeferened, geosampled, malaria, mosquito, capture point regressors. In so doing, an eco-entomological, forecast, vulnerability, endmember LULC, model framework may be developed by conceiving a quantity of the total larval productivity in an ento-ecepidemiological, intervention or control, study site area, partitioned into its constituent parts from individual capture point, aquatic, larval hyperproductive, seasonal geosampled,eco-georeferenecd, habitats to determine impacts on parasitological, geospectrotemporal, endmember indicators of malaria transmission.

Regardless, in a regression, forecast, vulnerability, endemic endmember equation if the x or y geosampled, eco-georeferenecable, capture point, malaria, mosquito, seasonal, surveyed, capture point, larval habitat populations are quantitatively analyzed violations of one or more of assumptions, within a statistical algorithm (e.g.,binary logistic)

would render incorrect or misleading, LULC forecasts (e.g., false explanators of seasonal, hyperproductive foci). If the assumption of independence is violated in an ento-ecoepidemiological, prognosticative, time series, malaria, mosquito, capture point, empirical, regressed,edmember, LULC dataset, then quantitating linearity would not be appropriate for determining type I error [e.g., incorrect rejection of a true null hypothesis (a "false positive")]. Hence, if the assumption of normality is violated, or outliers are present in an empirical LULC dataset of eco-georeferenced, geo-spectrotemporal, sub-meter resolution,grid-stratified, malaria, mosquito, ento-ecoepidemiological, capture points with their geosampled aquatic, larval, habitat count variables, then the linear regression goodness of fit test may not be the most powerful test available for predicting, hyperproductive, oviposition, seasonal, malaria, mosquito, immature habitat endmember foci.

Apparent lack of independence in fitted y values in an oviposition, sub-meter resolution, malaria, mosquito, ento-ecoepidemiological, forecast, vulnerability, endmember, sub-meter resolution, grid-stratifiable, LULC, signature model may be caused by the existence of an implicit x variable in the geosampled data. Thus, an x variable may not be explicitly usable in the linear model for forecasting, orthogonal, capture point, seasonal, hyperproductive foci. In this case, the best model for optimally regressively quantitating, empirical, geosampled, malaria, mosquito, aquatic, larval habitat, parameterizable, frequency, signature, geo-spectrotemporal, eco-georeferenecable, LULC, endmember covariates may still be linear, but may not include the original x variable. If there is a linear trend in the plot of the uncoalesced, regression residuals against the fitted values, in the malaria, mosquito, prognosticative, endmember, frequency model then an implicit x variable may be the cause. A plot of the residuals against the prospective new X geosampled regressed, oviposition- sub-meter resolution, LULC variables could reveal whether there is a systematic variation exists in the grid-stratified, endmember, model output. If there is, a malariologist, medical epidemiologist or other experimenter may consider adding a new x variable to the linear, ento-ecoepidemiological, forecast, vulnerability, eco-endmember model.

If an implicit x variable is not included in a fitted, malaria, mosquito forecast-oriented, exploratory,LULC risk model, the fitted oviposition, estimates for the slope and intercept may be biased, and hence may not render precise data,(i.e, non verifiable, geolocations of eco-georeferenecable, seasonal, hyperproductive foci) and the fitted y values may not be accurate. Another possible cause of apparent misspecification in an oviposition, malaria, mosquito, regression, forecast, vulnerability, sub-meter resolution, LULC geo-spectrotemporal model for optimally targeting hyperproductive, aquatic, larval, habitat foci may be due to the presence of an implicit block effect in the model ento-ecoepidemiological estimators. The block effect can be considered as another type of implicit X variable, albeit a discrete one in any prognosticative, endmember, sub-meter resolutionoviposition, ento-ecoepidemiological, LULC, risk model. If a blocking regressable capture point grid-stratfiable, oviposition, geo-spectrotemporal, malaria, mosquito, endmember, larval habitat, geosampled explanatory variable is suspected, an analysis of covariance may be performed, essentially dividing the data into different regression lines based on the value of the blocking variable.

If two explicative, time series, oviposition, *An. arabiensis*, mosquito, seasonal, regressed, normalized distributions are being compared for similarity, the LULC, endmember, capture points in the Q–Q plot will approximately lie on the line y = x. If the distributions are linearly related, the points in the Q–Q plot will approximately lie on a line, but not necessarily on the line y = x. Q–Q plots may also be employable as a graphical means for optimally estimating, eco-georeferenecable, eco-geographical, ento-ecoepidemiological, geosampled, sub-meter resolution, grid-stratifiable, geo-spectrotemporal, *An.arabiensis* immature, habitat, capture point, frequency, signature, parameter estimators employing a location-scale family of distributions.

Further, a Q–Q plot may be employable to compare the shapes of sub-meter resolution, grid-stratifiable, *An. arabiensis* capture point, oviposition, geosampled,tabulated, endmember, LULC estimator distributions, for providing a graphical view of how properties such as geolocation scale, and skewness of regressed habitat data are similar or different in two probability, seasonal distributions. Q–Q plots can be used to compare collections of data, or theoretical distributions [2]. The use of Q–Q plots to compare two samples of regressed, *An. arabensis*, aquatic, larval habitat, empirical, capture point geosampled, data distributions may be viewed as a non-parametric approach to comparing their underlying distributions. A Q–Q plot is generally a more powerful approach to do this than the common technique of comparing histograms of the two samples, but requires more skill to interpret [3]. An assessment of "goodness of fit" may be generated that is graphical in ArcGIS for generating a numerical summary of eco-georferenceable, grid-

stratifiable sub-meter resolution, eco-georeferenceable, seasonal hyperproductive foci of endmember, capture point, *An. arabiensis*. Since Q–Q plots compare distributions, there would be no need for the geosampled, endmember, LULC, geo-spectrotemporal values to be observed as endmember pairs, as in a scatter plot.

The term "probability plot" sometimes refers specifically to a Q–Q plot, sometimes to a more general class of plots, and sometimes to the less commonly used P–P plot . The probability plot is a graphical technique for assessing whether or not a dataset follows a given distribution such as the normal or Weibull. According to Jacob et al. [1] the formula for the probability density function of a generalizable, Weibull, malaria, mosquito (i.e., *Anopheles gambiae* s.l.) endmember LULC, geo-spectrotemporal,grid-stratfiiable, optimizable distribution is $f(x)=\gamma\alpha(x-\mu\alpha)(\gamma-1)\exp(-((x-\mu)/\alpha)\gamma)x\geq\mu;\gamma,\alpha>0$where γ is the shape parameter, μ is the aquatic, larval habitat, endmember, signature, geosampled geolocation parameter and α is the scale parameter. The case where μ = 0 and α = 1 is called the standard Weibull distribution[2]. In Jacob et al. [1] the case where μ = 0 in an *An. arabiensis* forecast, vulnerability regression model was the 2-parameter Weibull distribution. The equation for the standard Weibull distribution then reduced the malaria, mosquito, oviposition, regression distribution to $f(x)=\gamma x(\gamma-1)\exp(-(x\gamma))x\geq 0;\gamma>0$. The authors of Jacob et al. [1] plotted the geosampled sub-meter resolution, grid-stratified, time series, oviposition, mosquito, endmember, aquatic, larval, habitat data against a theoretical distribution in such a way that the capture points formed approximately a straight line. According to the authors departures from this straight line then indicated departures from the specified distribution.

The correlation coefficient associated with the linear fit to the data in the probability plot is a measure of the goodness of the fit [2]. Estimates of the location and scale parameters of malaria, mosquito, aquatic, larval habitat distribution are given by the intercept and slope [1]. Probability plots may be generated for several competing oviposition, malaria, mosquito, capture point, endmebr LULC, regression distributions to determine which provides the best fit. The probability plot generating the highest correlation coefficient rendered from say for example,a sub-meter resolution, mosquito, endmeber, signature, vulnerability, prognosticative model may be the best choice since it may generate the straightest probability plot.

For sub-meter resolution, malaria mosquito, oviposition tabulated LULC endmember distributions with shape parameters (not counting location and scale endmember parameters), may also generate a probability plot. For example, for a capture point, regressed, malaria, mosquito, oviposition foci, empirical distribution with a single shape parameter, the probability plot correlation coefficient (PPCC) plot may provide an method for estimating the an unknown, hyperrpoductive, eco-georeferenceable,oviposition, geo-spectrotemporal, ento-ecoepidemiological, endmember LULC signature, forecast, vulnerability model. The probability plot correlation coefficient may be a quantity derived from the Q–Q plots. The model may measure the agreement of a fitted distribution with observed geosampled oviposition, endmember, grid-stratifiable, malaria, mosquito data which may be also used as a means of fitting a distribution to the data. After the fit, outliers may be detected by examining the regression residuals or the high-leverage capture points.

The relationship between prevalence of each individual potential,explanatorial, capture point, aquatic, larval habitat, sub-meter resolution, predictor variable geosampled in the Mwea study site was investigated by single variable regression analysis in PROC MIXED. We employed the regression line $(y_i-\bar{y})=(\hat{y}_i-\bar{y})+(y_i-\hat{y}_i)$ to generate a pseudo R^2 value where the first term was the total variation in the response *y* (larval density count of seasonal, geosampled, *An. arabiensis* capture point habitats) and the second term was the variation in mean response based on the sampled parameters. The third term was the residual value in the model estimates. Squaring each of these terms and adding over all of the sampled ento- epidemiological, endmember LULC observations generated the equation $\sum(y_i-\bar{y})^2=\sum(\hat{y}_i-\bar{y})^2+\sum(y_i-\hat{y}_i)^2$. This equation was then written as SST = SSM + SSE, where SS was notation for sum of squares and T, M, and E were the notation for total, model, and error, respectively. The square of the sample correlation was equal to the ratio of the estimates while the sum of squares was related to the total sum of squares: r^2 = SSM/SST. This formalized the interpretation of R^2 as explaining the fraction of variability in the geo-spectrotemporal, geosampled, immature, An. arabiensis, aquatic, larval habitat data explained by the regression model. The sample variance s_y^2 was equal to $\sum\frac{(y_i-\bar{y})^2}{n-1}$, which in turn was equal to the SST/df, the total sum of squares divided by the total DF. A regression equation was then constructed using the mean square model (i.e., MSM)

$=\sum\frac{(\hat{y}_i-\bar{y})^2}{l}$, which was equal to the SSM/df. The corresponding mean square error (i.e, MSE) was $\sum\frac{(y_i-\hat{y}_i)^2}{n-2}$, which was equal to SSE/df and the estimate of the variance about the regression line (i.e., σ^2). The MSE is an estimate of σ^2 for determining whether or not the null hypothesis is true [2].

For the geo-spectrotemporal, geosampled, eco-georeferenceable, sub-meter resolution, grid-stratifiable, explanatoryendmeber LULC variables,(*p)* the capture point, *An. arabiensis*, aquatic, larval, habitat modeled the DFM which in this research was equal to *p*, and the error degrees of freedom (dfe) which was equal to (*n* - *p* - 1), and the total degrees of freedom (dft) which was equal to (*n* - 1), the sum of DFM and DFE. The explanatory and response ento-ecoepidemiological, endmeber LULC variables were numeric. The relationship between the mean of the response variable (i.e. total, geosampled, density, larval count) and the level of the explanatory, geo-spectrotemporal eco-georeferenced, sub-meter resolution, grid-stratified, predictor covariates in the regression equation were assumed to be approximately linear (i.e.,straight line). The corresponding table generated each the clinical, field and remote-sampled malaria-related, aquatic, larval habitat, geoclassified, endmember parameters in SAS.

In the multiple regression analyses, the test statistic MSM/MSE had an F (p, n - p - 1) distribution. The null hypothesis was $\beta_1 = \beta_2 = ... = \beta_p = 0$, and the alternative hypothesis was at least one of the geo-spectrotemporally geosampled, *An. arabiensis*, aquatic, larval habitat, endemic, transmission-oriented, predictive, endmember, risk parameters$\beta_j \neq$ 0, j = 1, 2, ,,, p. The F test did not indicate which of the parameters $\beta_j \neq$ was not equal to zero, only that at least one of them was linearly related to the capture point, endmebr LULC, grid-stratified, response variable. The ratio SSM/SST = R^2 (i.e., squared multiple correlation coefficient) was the proportion of the variation in the response variable that was explained by the immature, habitat data. The square root of R^2 (i.e., the multiple correlation coefficient) was the correlation between the geosampled, *An. arabiensis*, *aquatic*, larval, habitat geo-spectrotemporal, endmeber LULC observations (i.e., $y_{i)}$ and the fitted values (i.e., $\hat{y}_{i.}$). Additionally, from the sampling distribution, generated from the geosampled *t* parameters, the probability of obtaining an F was large or larger than the one was calculated. The *t*-test and the F-test were equivalent; the relation between ANOVA and *t* was given by $F = t^2$. Significant differences by ANOVA were noted for the geosampled, larval count density discrete integer values of the seasonal, hyperproductive capture points throughout the sampling frame (F = 41.3, DF = 1).

A Poisson regression analyses was then constructed in PROC MIXED to determine the relationship between the geosampled, *An. arabiensis*, frequency, signature, sub-mter resolution, larval, density, count data and the sampled habitat LULC characteristics. The Poisson models were built using the clinical, field and remote-sampled habitat, endemic transmission-oriented, predictive risk data. A negative binomial regression had to be employed, however, as an examination of the data indicated that overdispersion was a significant problem in the Poisson model. The Poisson distribution is a special case of the negative binomial distribution, where the mean approximates the standard deviation (see Neter 1992). We assumed that the log of the meanμ was a linear function of independent variables, log (μ) = intercept + b1*X1 +b2*X2 + ...+ b3*Xm in the geo-spectrotemporal geosampled, eco-georeferenced, sub-meter resolution, grid-stratified, capture pointmodel which implied that μ was the exponential function of independent variables when μ = exp (intercept + b1*X1 +b2*X2 + ...+ b3*Xm) (see Jacob et al. 2008b). Therefore, instead of assuming that the distribution of the geosampled, aquatic, larval habitat, eco-georeferenced,. explanatory, endemic, transmission-oriented, geo-spectrotemporal, oviposition, observation, parameter estimates (i.e., Y) was Poisson, we were able to assume that Y had a negative binomial distribution. We relaxed the assumption about equality of mean and variance (i.e., Poisson distribution property), since the variance of negative binomial was equal to $\mu + k\mu^2$, where $k>= 0$ was a dispersion parameter. The maximum likelihood method was used to estimate *k*, as well as the geosampled, aquatic, larval habitat endmember, parameters of the regression model for log(μ). For the negative binomial distribution, the variance was equal to the mean + k $mean^2$ (i.e.,k>= 0) as the negative binomial distribution reduced to Poisson when k was 0.

In the regression analyses the null hypothesis was: H_0: k=0 and the alternative hypothesis was: H_a: k>0. We recorded the log-likelihood (i.e., LL) for the models we used the likelihood ratio (LR) test to compute the LR statistic using -2(LL) (Poisson) and the LL (i.e., negative binomial). The asymptotic distribution of the LR statistic

had probability mass of one half at zero and one half – chi-square distribution with 1 df. To test the null hypothesis at the significance level α, we used the critical value of chi-square distribution corresponding to significance level 2α, that was rejection of H_0 , if LR statistic > χ^2 (1-2α , 1 df). We generated the log of the mean, μ, which in this research was a linear function of independent variables, log(μ) = intercept + b1*X1 +b2*X2 + ...+ b3*Xm, in the. eco-georeferenced, sub-meter resolution, grid-stratified, *An. arabiensis*,aquatic, larval habitat endemic trasnmission-oriented prognosticative, vulnerabilty, endmember model which implied that μ was the exponential function of the independent variables when μ = exp(intercept + b1*X1 +b2*X2 + ...+ b3*Xm).

A Poisson distribution with parameter $\lambda > 0$ was then generated employing the empirical dataset of the *An. arabiensis*, endemic, transmission-oriented, capture point, oviposition endmember covariates by $f(k;\lambda) = \Pr(X = k) = \frac{\lambda^k e^{-\lambda}}{k!}$, where was the base of the natural logarithm (*e* = 2.71828...) and where *k*! was the factorial of *k*. $\lambda = \lambda T$, The positive, real, sampled, explanatory, covariate coefficient λ was then equal to the expected value of *X* and also to its variance[e.g., $\lambda = \mathrm{E}(X) = \mathrm{Var}(X)$. The expected value of a Poisson-distributed random variable was then equal to λ and so was its variance. The coefficient of variation was $\lambda^{-1/2}$, while the index of dispersion was 1. The mean deviation about the mean in the geo-spectrotemporal geosampled, malaria, mosquito, eco-georeferenced, sub-meter resolution, grid-stratified, capture point, regression model,was $\mathrm{E}\,|X - \lambda| = 2\exp(-\lambda)\frac{\lambda^{\lfloor\lambda\rfloor+1}}{\lfloor\lambda\rfloor!}$. The mode of a Poisson-distributed random variable with non-integer λ was then equal to $\lfloor\lambda\rfloor$, which was the largest integer less than or equal to λ. When λ is a positive integer, the modes are λ and λ – 1(see Homer and Lemeshew 2000) All of the cumulants of the Poisson distribution were then equal to the expected value λ in the model residual, vulnerability forecasts. The *n*th factorial moment of the Poisson distribution was λ^n.

Bounds for the median (*ν*) of the distribution was then quantitated as $\lambda - \ln 2 \leq \nu < \lambda + \frac{1}{3}$. The higher moments m_k of the Poisson distribution about the origin were Touchard polynomials in λ: $m_k = \sum_{i=1}^{k} \lambda^i \left\{ {k \atop i} \right\}$, where the {braces} denoted Stirling numbers of the second kind The coefficients of the polynomials had a combinatorial meaning. In fact, when the expected value of the Poisson distribution was 1. If $X_i \sim \mathrm{Pois}(\lambda_i)\, i = 1, \ldots, n$ are independent, and $\lambda = \sum_{i=1}^{n} \lambda_i$, $Y = \left(\sum_{i=1}^{n} X_i\right) \sim \mathrm{Pois}(\lambda)$ [3]. Further since the Poisson distributions rendered by the empirical dataset of. The geo-spectrotemporal geosampled, eco-georeferenced, sub-meter resolution, grid-stratified, *An. arabiensis* endemic transmission oriented, observations were infinitely divisible probability distributions. The directed Kullback–Leibler divergence of Pois(λ_0) from Pois(λ) was given by $D_{\mathrm{KL}}(\lambda\|\lambda_0) = \lambda_0 - \lambda + \lambda \log \frac{\lambda}{\lambda_0}$. Bounds for the tail probabilities of a Poisson random variable $X \sim \mathrm{Pois}(\lambda)$ were then derived using a Chernoff bound argument where $P(X \geq x) \leq \frac{e^{-\lambda}(e\lambda)^x}{x^x}$, for $x > \lambda$,$P(X \leq x) \leq \frac{e^{-\lambda}(e\lambda)^x}{x^x}$, for $x < \lambda$.

A model was constructed for qualitative estimation of a linear, *An. arabiensis*, aquatic, larval habitat, capture point, oviposition, endmember estimates with nested-error structure. These models were written in a matrix notation where it was n×p matrix X was a matrix of regressors. The random vectors were independent. There was no need for a zero-mean vector and covariance matrix. We employed n×n identity matrices.

We generated the inverse Wishart distribution which was a probability distribution defined by the positive-definite matrix generated from the geosampled, eco-georeferenced, sub-meter resolution, grid-stratified, *An. arabiensis*,aquatic larval habitat, endemic trasnmission-oriented predictive risk –related,capture point, geo-spectrotemporal covariates. In our Bayesian model we employed the inverse Wishart distribution to generate the conjugate prior for the covariance matrix of a multivariate normal distribution. In Bayesian probability theory, if the posterior distributions *p*(θ|*x*) are in the same family as the prior probability distribution *p*(θ), the prior and posterior are

then called conjugate distributions, and the prior is called a conjugate prior for the likelihood [2]. In this research the probability density function of the inverse Wishart was: $\frac{|\mathbf{\Psi}|^{m/2}\,|\mathbf{B}|^{-(m+p+1)/2}\,e^{-\mathrm{trace}(\mathbf{\Psi}\mathbf{B}^{-1})/2}}{2^{mp/2}\Gamma_p(m/2)}$, where B and $\mathbf{\Psi}$ were *p x p* positive definite matrices, and $\Gamma_p(\cdot)$ was the multivariate gamma function. If B follows an inverse Wishart distribution, denoted as $\mathbf{B} \sim W^{-1}(\mathbf{\Psi}, m)$, its inverse $\mathbf{B}^{-1}$ has a Wishart distribution $W(\mathbf{\Psi}^{-1}, m)$.(O'Hagan, and Forster 2004).

The multivariate Gamma function, $\Gamma_p(\cdot)$, was a generalization of the Gamma function in the aquatic, larval habitat endemic transmission-oriented, progmosticative, endmember, risk model. The Gamma function is an extension of the factorial function, with its argument shifted down by 1, to real and complex numbers and as such if *n* is a positive integer: $\Gamma(n) = (n-1)!$([2]). The gamma function appears commonly in the probability density function of the Wishart and Inverse Wishart distributions (see Neter 1992).

The distribution generated from the geosampled geo-spectrotemporal,eco-georeferenced, sub-meter resolution, grid-stratified, aquatic, larval habitat, capture point, endmember data had an inverse Wishart distribution $\mathbf{A} \sim W^{-1}(\mathbf{\Psi}, m)$.We then successfully partitioned the matrices A and $\mathbf{\Psi}$ with each other using $\mathbf{A} = \begin{bmatrix} \mathbf{A}_{11} & \mathbf{A}_{12} \\ \mathbf{A}_{21} & \mathbf{A}_{22} \end{bmatrix}$, $\mathbf{\Psi} = \begin{bmatrix} \mathbf{\Psi}_{11} & \mathbf{\Psi}_{12} \\ \mathbf{\Psi}_{21} & \mathbf{\Psi}_{22} \end{bmatrix}$ where $\mathbf{A}_{ij}$and $\mathbf{\Psi}_{ij}$ were p_i a x p_j matrices. By so doing we generated the conjugate distribution of the geosampled eco-georeferenced explanatory, aquatic, larval habitat, predictor covariates by employing a covariance probabilistic approximation matrix $\mathbf{\Sigma}$whose prior $p(\mathbf{\Sigma})$had a $W^{-1}(\mathbf{\Psi}, m)$distribution. We then performed a eigen-decomposition of a square matrix (i.e., A) into eigenvalues and eigenvectors. We defined a right eigenvector as a column vector $\mathbf{X}_R$ satisfying $\mathsf{A}\,\mathbf{X}_R = \lambda_R\,\mathbf{X}_R$, where A was a matrix, so $(\mathsf{A} - \lambda_R\,\mathsf{I})\,\mathbf{X}_R = \mathbf{0}$, which meant the right eigenvalues had zero determinant, (i.e.,). Similarly we defined a left eigenvector as a row vector $\mathbf{X}_L$ satisfying $\mathbf{X}_L\,\mathsf{A} = \lambda_L\,\mathbf{X}_L$. Taking the transpose of each side rendered$(\mathbf{X}_L\,\mathsf{A})^{\mathrm{T}} = \lambda_L\,\mathbf{X}_L{}^{\mathrm{T}}$, which in this research was rewritten as $\mathsf{A}^{\mathrm{T}}\,\mathbf{X}_L{}^{\mathrm{T}} = \lambda_L\,\mathbf{X}_L{}^{\mathrm{T}}$.We then rearranged this equation once again to obtain $(\mathsf{A}^{\mathrm{T}} - \lambda_L\,\mathsf{I})\,\mathbf{X}_L{}^{\mathrm{T}} = \mathbf{0}$, which generated $\det(\mathsf{A}^{\mathrm{T}} - \lambda_L\,\mathsf{I}) = 0$. The equation, in turn, generated $0 = \det(\mathsf{A}^{\mathrm{T}} - \lambda_L\,\mathsf{I}) = \det(\mathsf{A}^{\mathrm{T}} - \lambda_L\,\mathsf{I}^{\mathrm{T}})$,$\det(\mathsf{A} - \lambda_L\,\mathsf{I})^{\mathrm{T}}$ $\det(\mathsf{A} - \lambda_L\,\mathsf{I})$, where the last step was from the identity $\det(\mathsf{A}) = \det(\mathsf{A}^{\mathrm{T}})$. We equated these equations to 0 for A and X , which required that $\lambda_R = \lambda_L \equiv \lambda$ (see Jacob et al. 2011b). We then let $\mathbf{X}_R$ be a matrix formed by the columns of the right eigenvectors and $\mathbf{X}_L$be a matrix formed by the rows of the left eigenvectors. We then let $\mathsf{D} \equiv \begin{bmatrix} \lambda_1 & \cdots & 0 \\ \vdots & \ddots & \vdots \\ 0 & \cdots & \lambda_n \end{bmatrix}$. and as such $\mathsf{A}\,\mathbf{X}_R = \mathbf{X}_R\,\mathsf{D}$ and $\mathbf{X}_L\,\mathsf{A} = \mathsf{D}\,\mathbf{X}_L$ and $\mathbf{X}_L\,\mathsf{A}\,\mathbf{X}_R = \mathbf{X}_L\,\mathbf{X}_R\,\mathsf{D}$ while, $\mathbf{X}_L\,\mathsf{A}\,\mathbf{X}_R = \mathsf{D}\,\mathbf{X}_L\,\mathbf{X}_R$, so $\mathbf{X}_L\,\mathbf{X}_R\,\mathsf{D} = \mathsf{D}\,\mathbf{X}_L\,\mathbf{X}_R$. But this equation was of the form CD=DC where D was a diagonal matrix, so, therefore, $\mathsf{C} \equiv \mathbf{X}_L\,\mathbf{X}_R$ was also diagonal. If A is a symmetric matrix, then the left and right eigenvectors are simply each other's transpose, and if A is a self-adjoint matrix (i.e., Hermitian), then the left and right eigenvectors are adjoint matrices (Griffith 2003). In predictive, autoregressive, vector arthropod, aquatic, larval, habitat, capture point, risk modeling, a Hermitian matrix is a square matrix with complex entries that is equal to its own conjugate transpose – that is, the element in the *i*-th row and *j*-th column is equal to the complex conjugate of the element in the *j*-th row and *i*-th column, for all indices *i* and *j*: $a_{i,j} = \overline{a}_{j,i}$.[2]. Using the matrix with eigenvectors $\mathbf{x}_1$, $\mathbf{x}_2$, and $\mathbf{x}_3$and corresponding eigenvalues λ_1, λ_2, and λ_3, then an arbitrary vector $\mathbf{y}$ was written as $\mathbf{y} = b_1\,\mathbf{x}_1 + b_2\,\mathbf{x}_2 + b_3\,\mathbf{x}_3$. In this research the matrix A generated$\mathsf{A}\,\mathbf{y} = b_1\,\mathsf{A}\,\mathbf{x}_1 + b_2\,\mathsf{A}\,\mathbf{x}_2 + b_3\,\mathsf{A}\,\mathbf{x}_3 = \lambda_1\left(b_1\,\mathbf{x}_1 + \frac{\lambda_2}{\lambda_1}\,b_2\,\mathbf{x}_2 + \frac{\lambda_3}{\lambda_1}\,b_3\,\mathbf{x}_3\right)$, so $\mathsf{A}^n\,\mathbf{y} = \lambda_1^n\left[b_1\,\mathbf{x}_1 + \left(\frac{\lambda_2}{\lambda_1}\right)^n b_2\,\mathbf{x}_2 + \left(\frac{\lambda_3}{\lambda_1}\right)^n b_3\,\mathbf{x}_3\right]$.

Further, since $\lambda_1 > \lambda_2, \lambda_3$…., and $b_1 \neq 0$, it followed that $\lim_{n\to\infty} \mathsf{A}^n\,\mathbf{y} = \lambda_1^n\,b_1\,\mathbf{x}_1$, so repeated application of the regression-related matrix to an arbitrary vector resulted in a vector proportional to the eigenvector with largest eigenvalue.

International Research Journal of Computer Science and Application
Vol. 2, No. 1, March 2018, pp. 1-181
Available Online at http://acascipub.com/Journals.php

We determined probabilities for the geo-spectrotemporal geosampled, eco-georeferenced, sub-meter resolution, grid-stratified, autoregressive model. Thereafter , we used $\frac{dS_t}{S_t} = \mu' dt + \sigma\, dW_t$ where W_t was a P-standard brownian motion (i.e.,a standard brownian motion under the probability measure P) we generated: $\frac{dS_t}{S_t} = (r-g)dt + \sigma\underbrace{(dW_t + \lambda dt)}_{=\hat{W}}$ Then we employed the using the Black and Scholes model, the Q-martingale property and transferred to the value of predictor variable C in the geosampled, sub-meter resolution, grid-stratified, *An. arabiensis*, model.

Since the Girsanov theorem states that there is a probability measure Q such that $\hat{W}$ is a Q-standard brownian motion and $e^{-rt}e^{gt}S_t \;\&\; e^{-rt}e^{gt}M_t$ are Q-martingales [2]. in this research : $C(t)e^{-rt} = E_Q\left[C(T)e^{-rT}\middle|F_t\right] \Rightarrow C(t) = e^{-r(T-t)}E_Q\left[(S(T)-k)^+\middle|F_t\right]$. We then defined the *S* set by: $E = \left\{\varpi \in \Omega \middle| S(T)(\varpi) \geq k\right\} F_t\Big]$ which rendered $C(t) = e^{-r(T-t)}E_Q\left[S_T \mathrm{I}_E\middle|F_t\right] - ke^{-r(T-t)}E_Q\left[\mathrm{I}_E\middle|F_t\right]$.This quantity was computed by splitting each of its terms. The second term in the model generated $E_Q\left[\mathrm{I}_E\middle|F_t\right] = P_Q(E) = P_Q(S_T \geq k\middle|F_t)$ using $S(T) = S(t)\exp\left\{(r-\frac{\sigma^2}{2})(T-t) + \sigma\hat{W}(T-t)\right\}$ We then used the condition $S_T \geq k$ which defined $Y = -\frac{\hat{W}(T-t)}{\sqrt{T-t}} \leq d_2$. The properties of the brownian motions allowed us to write: the expression $Y \sim N(0,1)$ for the geo-spectrotemporal geosampled, eco-georeferenced, sub-meter resolution, grid-stratified. *An. arabiensis*, larval habitat, distribution model which generated $P_Q(S_T \geq k) = P_Q(Y \leq d_2) = N(d_2)$.

Using the first term $E_Q\left[S_T \mathrm{I}_E\right] = \int_k^\infty x f_{S_T}(x)dx$ we were able to generate $S(T) = S(t)\exp\left\{(r-\frac{\sigma^2}{2})(T-t) + \sigma\hat{W}(T-t)\right\}$.The log-normal property of the underlying motion rendered: $L_Q((r-\frac{\sigma^2}{2})(T-t) + \sigma\hat{W}(T-t)) = N((r-\frac{\sigma^2}{2})(T-t), \sigma\sqrt{T-t})$ and $e^{-r(T-t)}E_Q\left[S_T \mathrm{I}_E\middle|F_t\right] = S(t)N(d_1)$.

We then generated the inverse-gamma distribution which was a univariate specialization of the inverse–Wishart distribution generated using the geosampled eco-georeferenced, *An. arabiensis*, aquatic, larval habitat endemic trasnmission-oriented predictive risk –related, explanatory,endmember, predictor covariates. The pdf was $\frac{\beta^\alpha}{\Gamma(\alpha)}x^{-\alpha-1}\exp\left(\frac{-\beta}{x}\right)$ while the mean of the model was $\frac{\beta}{\alpha-1}$ for α > 1. The variance was $\frac{\beta^2}{(\alpha-1)^2(\alpha-2)}$ for α > 2. The skewness was $\frac{4\sqrt{\alpha-2}}{\alpha-3}$ for α > 3, while the kurtosis was $\frac{30\alpha-66}{(\alpha-3)(\alpha-4)}$ for α > 4 and the entropy was $\alpha+\ln(\beta\Gamma(\alpha))-(1+\alpha)\Psi(\alpha)$. The moment generating function was $\frac{2(-\beta t)^{\frac{\alpha}{2}}}{\Gamma(\alpha)}K_\alpha\left(\sqrt{-4\beta t}\right)$ while the characteristic function was $\frac{2(-i\beta t)^{\frac{\alpha}{2}}}{\Gamma(\alpha)}K_\alpha\left(\sqrt{-4i\beta t}\right)$.

The geo-spectrotemporal geosampled, eco-georeferenced, sub-meter resolution, grid-stratified model revealed that when p = 1 (i.e. univariate) and α = m / 2, $\beta = \Psi/2$ and x=B and the pdf of the inverse-Wishart distribution

became $p(x|\alpha,\beta) = \frac{\beta^{\alpha}\, x^{-\alpha-1} \exp(-\beta/x)}{\Gamma_1(\alpha)}$. The pdf of the gamma distribution was $f(x) = x^{k-1}\frac{e^{-x/\theta}}{\theta^k\,\Gamma(k)}$ and we defined the transformation $Y = g(X) = \frac{1}{X}$ then the resulting transformation was: $f_Y(y) = f_X\left(g^{-1}(y)\right)\left|\frac{d}{dy}g^{-1}(y)\right|$ $= \frac{1}{\theta^k\Gamma(k)}\left(\frac{1}{y}\right)^{k-1}\exp\left(\frac{-1}{\theta y}\right)\frac{1}{y^2} = \frac{1}{\theta^k\Gamma(k)}\left(\frac{1}{y}\right)^{k+1}\exp\left(\frac{-1}{\theta y}\right) = \frac{1}{\theta^k\Gamma(k)}y^{-k-1}\exp\left(\frac{-1}{\theta y}\right)$. Replacing *k* with α; θ^{-1} with β; and *y* with *x* results in the inverse-gamma pdf shown above $f(x) = \frac{\beta^{\alpha}}{\Gamma(\alpha)}x^{-\alpha-1}\exp\left(\frac{-\beta}{x}\right)$. The inverse gamma distribution's pdf was then defined over the support *x*>0 using the equation $f(x;\alpha,\beta) = \frac{\beta^{\alpha}}{\Gamma(\alpha)}(x)^{-\alpha-1}\exp\left(-\frac{\beta}{x}\right)$ with shape parameter α and scale parameter β. The cumulative distribution function was then quantified using the regularized gamma function $F(x;\alpha,\beta) = \frac{\Gamma\left(\alpha,\frac{\beta}{x}\right)}{\Gamma(\alpha)} = Q\left(\alpha,\frac{\beta}{x}\right)$ where the numerator in the ento-ecoepidemiological, malaria, mosquito, oviposition, aquatic, larval, habitat model was the upper incomplete gamma function and the denominator was the gamma function. The regularized gamma functions are defined by $\frac{\gamma(a,z)}{\Gamma(a)}$ and $\frac{\Gamma(a,z)}{\Gamma(a)}$, where $\gamma(a,z)$ and $\Gamma(a,z)$ are incomplete gamma functions and $\Gamma(a)$ is a complete gamma function.

We then employed methods in PROC MCMC to calculate the multivariate gamma function for the geosampled, eco-georeferenced, sub-meter resolution, grid-stratified, *An. arabiensis*, capture point, aquatic, endmember, larval habitat, endemic, trasnmission-oriented, predictive, risk model. This was constructed using $\Gamma_p(a) = \int_{S>0}\exp\left(-\mathrm{trace}(S)\right)|S|^{a-(p+1)/2}\,dS$ where S>0 and as such S was positive-definite. We used the gamma function to determine the recursive relationships in the geo-spectrotemporal, geosampled, eco-georeferenced,capture point, aquatic, larval habitat, predictor covariates using $\Gamma_p(a) = \pi^{(p-1)/2}\Gamma(a)\Gamma_{p-1}(a-\frac{1}{2}) = \pi^{(p-1)/2}\Gamma_{p-1}(a)\Gamma[a+(1-p)/2]$. Thereafter, we quantitated :$\Gamma_1(a) = \Gamma(a)$, $\Gamma_2(a) = \pi^{1/2}\Gamma(a)\Gamma(a-1/2)$ and $\Gamma_3(a) = \pi^{3/2}\Gamma(a)\Gamma(a-1/2)\Gamma(a-1)$. We then defined the multivariate digamma function in the larval habitat, endmember, forecast, vulnerability model as $\psi_p(a) = \frac{\partial \log\Gamma_p(a)}{\partial a} = \sum_{i=1}^{p}\psi(a+(1-i)/2)$ and the general polygamma function as $\psi_p^{(n)}(a) = \frac{\partial^n \log\Gamma_p(a)}{\partial a^n} = \sum_{i=1}^{p}\psi^{(n)}(a+(1-i)/2)$.

The digamma function in the capture point, oviposition, *An. arabiensis* model was defined as the logarithmic derivative of the gamma function: $\psi(x) = \frac{d}{dx}\ln\Gamma(x) = \frac{\Gamma'(x)}{\Gamma(x)}$. This equation then calculated the digamma function which was expressed as $\frac{\partial\Gamma(a+(1-i)/2)}{\partial a} = \psi(a+(i-1)/2)\Gamma(a+(i-1)/2)$. We then generated the following expression: $\frac{\partial\Gamma_p(a)}{\partial a} = \pi^{p(p-1)/4}\prod_{j=1}^{p}\Gamma(a+(1-j)/2)\sum_{i=1}^{p}\psi(a+(1-i)/2) = \Gamma_p(a)\sum_{i=1}^{p}\psi(a+(1-i)/2)$ Since in this research $\Gamma_p(a) = \pi^{p(p-1)/4}\prod_{j=1}^{p}\Gamma(a+\frac{1-j}{2})$ it followed that $\frac{\partial\Gamma_p(a)}{\partial a} = \pi^{p(p-1)/4}\sum_{i=1}^{p}\frac{\partial\Gamma(a+\frac{1-i}{2})}{\partial a}\prod_{j=1,j\neq i}^{p}\Gamma(a+\frac{1-j}{2})$.

Poissonian distribution for an interaction model was then generated. These results provided information for estimates of the prior distribution of main effect coefficients for the Bayesian analysis. The values for the geo-spectrotemporal geosampled, eco-georeferenced, sub-meter resolution, grid-stratified, *An. arabiensis*, capture point, endmember, parameter estimates and standard errors were then used as mean values and standard errors to parameterized prior expected values for the explanatory, aquatic, larval habitat, oviposition, predictor covariates. The prior expected mean value for the error term was assumed to be zero ('0'), with a standard deviation of 0.01. Initial

values for the MCMC chains were generated. Three MCMC chains estimated for the intercept which appeared to converge within the first 1,000 samples. The first 1,000 samples were discarded to allow the model to stabilize (i.e., known as "burn in"), and the next 10,000 samples were used to derive endmember, parameter estimates. The MCMC was able to numerically calculate multi-dimensional integrals. In our MCMC methods, an ensemble of "walkers" moved around randomly. At each capture point where the walker stepped, the integrand value at that point was counted towards the integral. The walker then May made a number of tentative steps around the area, looking for a place with reasonably high contribution to the integral to move into next. Random walk methods are a kind of random simulation or Monte Carlo method [2].However, whereas the random samples of the integrand used in a conventional Monte Carlo integration are generally statistically independent, those used in our MCMC were correlated[5]. A Markov chain was then constructed in such a way as to have the integrand as its equilibrium distribution. We generated an improvement in model fit, as variables are added to the Bayesian model.

All residual estimates from the geo-spectrotemporal geosampled, eco-georeferenced, sub-meter resolution, grid-stratified, *An. arabiensis* Bayesian model were then evaluated in a spatial error (SE) model. An autoregressive model was employed that used a sampled habitat variable, Y, as a function of nearby sampled habitat Y values [i.e., an autoregressive response (AR) or spatial linear (SL) specification] and/or the residuals of Y as a function of nearby Y residuals [i.e., an AR or SE specification]. Distance between sampled habitats was defined in terms of an *n*-by-*n* geographic weights matrix, C, whose c_{ij} values were 1 if the sampled *An. arabiensis*, aquatic, larval habitat,capture point, hyperproductive, unknown geolocations *i* and *j* were deemed nearby, and 0 otherwise. Adjusting this matrix by dividing each row entry by its row sum, with the row sums given by C1, converted this matrix to matrix W . The *n*-by-1 vector $x = [x_1 \cdots x_n]^T$ then contained measurements of a quantitative,capture point, endmember variable for *n* spatial units and *n*-by-*n* spatial weighting matrix W. The formulation for the Moran's index of spatial autocorrelation used in this research was: $I(x) = \frac{n\Sigma_{(2)} w_{ij}(x_i - \bar{x})(x_j - \bar{x})}{\Sigma_{(2)} w_{ij} \Sigma_{i=1}^{n} (x_i - \bar{x})^2}$ where $\sum_{(2)} \sum_{i=1}^{n} \sum_{j=1}^{n}$ with $i \neq j$The values w_{ij} were spatial weights stored in the symmetrical matrix W [i.e., ($w_{ij} = w_{ji}$)] that had a null diagonal ($w_{ii} = 0$). In this research the matrix was initially generalized to an asymmetrical matrix W. Matrix W can be generalized by a non-symmetric matrix *W** by using $W = (W^* + W^{*T})/2$ [. Moran's *I* was rewritten using matrix notation: $I(x) = \frac{n}{1^t W 1} \frac{x^T HHWHHx}{x^T HHx} = \frac{n}{1^T W 1} \frac{x^T HWHx}{x^T Hx}$ where H = ($I - 11^T/n$) was an orthogonal projector verifying that $H = H^2$, (i.e., *H* was independent). Features of matrix W for analyzing sampled covariates of the geo-spectrotemporal geosampled, eco-georeferenced, sub-meter resolution, grid-stratified, *An. arabiensis*, aquatic, larval habitats include that it: is a stochastic matrix, expresses each observed value y_i as a function of the average of habitat location *i*'s nearby habitat larval/pupal counts, and allows a single spatial autoregressive parameter, ρ, to have a maximum value of 1.

A SAR model specification was then used to describe the *An. arabiensis* larval habitat autoregressive variance uncertainty estimates. A spatial filter (SF) model specification was also used to describe both Gaussian and Poisson random variables. The resulting SAR model specification took on the following form: $\mathbf{Y} = \mu(1 - \rho)\mathbf{1} + \rho\mathbf{W}\mathbf{Y} + \varepsilon$, where μ was the scalar conditional mean of Y, and ε was an *n*-by-1 error vector whose elements were statistically independent and identically distributed (iid) normally random variates. The spatial covariance matrix for equation (3.1), using the geo-spectrotemporal, geosampled,capture point, endmember, aquatic, larval habitat covariates was $E[(Y - \mu l)'(Y - \mu l)] = \Sigma = [(I - \rho W')(I - \rho W)]^{-1}\sigma^2$, where E (●) denoted the calculus of expectations, I was the *n*-by-*n* identity matrix denoting the matrix transpose operation, and σ^2 was the error variance. However, when a mixture of positive and negative spatial autocorrelation is present in an aquatic habitat, ento-ecoepidemiological, forecast, vulnerability model, a more explicit representation of both effects leads to a more accurate interpretation of empirical results. Alternately, the excluded values may be set to zero, although if this is done then the mean and variance must be adjusted

In this research, two different spatial autoregressive parameters appeared in the spatial, covariance matrix, *An. arabiensis*, aquatic, larval, habitat, model specification, which for an SAR model specification became: $\Sigma = [(\mathbf{I} - <\rho>_{diag} \mathbf{W}')(\mathbf{I} - <\rho>_{diag} \mathbf{W})]^{-1}\sigma^2$, where the diagonal matrix of autoregressive parameters, $<\rho>_{diag}$, contained two geosampled parameters: ρ_+ for those *An. arabiensis*, aquatic,larval, habitat pairs displaying positive spatial dependency, and ρ_- for those endmember habitat pairs displaying negative spatial dependency. For example, by

letting $\sigma^2 = 1$ and employing a 2-by-2 regular square tessellation,

$$\Sigma = \left[\begin{pmatrix} 1 & 0 & 0 & 0 \\ 0 & 1 & 0 & 0 \\ 0 & 0 & 1 & 0 \\ 0 & 0 & 0 & 1 \end{pmatrix} - \begin{pmatrix} \rho_+ & 0 & 0 & 0 \\ 0 & \rho_+ & 0 & 0 \\ 0 & 0 & \rho_- & 0 \\ 0 & 0 & 0 & \rho_- \end{pmatrix} \begin{pmatrix} 0 & \frac{1}{2} & \frac{1}{2} & 0 \\ \frac{1}{2} & 0 & 0 & \frac{1}{2} \\ \frac{1}{2} & 0 & 0 & \frac{1}{2} \\ 0 & \frac{1}{2} & \frac{1}{2} & 0 \end{pmatrix} \right]^2$$

For the vector $\begin{pmatrix} y_1 \\ y_2 \\ y_3 \\ y_4 \end{pmatrix}$,enabled positing a positive relationship between the hyperproductive, geosampled, *An. arabiensis* habitats by covariates, y_1 and y_2, a negative relationship between covariates, y_3 and y_4, and, no relationship between covariates y_1 and y_3 and between y_2 and y_4. This yielded: $\mathbf{Y} = \mu(\mathbf{I} - \rho_+ < \mathbf{I}_+ >_{diag} - \rho_- < \mathbf{I}_- >_{diag})\mathbf{1} + (\rho_+ < \mathbf{I}_+ >_{diag} + \rho_- < \mathbf{I}_- >_{diag})\mathbf{WY} + \varepsilon$ (3.2)where I_+ was a binary 0-1 indicator variable which denoted those geosampled, eco-georeferenced, sub-meter resolution, grid-stratified, *An. arabiensis* habitat, endmember covariates displaying positive spatial dependency, and I_- was a binary 0-1 indicator variable denoting those geosampled habitats displaying negative spatial dependency, using $I_+ + I_- = 1$. Expressing the preceding 2-by-2 example in terms of equation (3.3) yielded:

$$\begin{pmatrix} y_1 \\ y_2 \\ y_3 \\ y_4 \end{pmatrix} = \mu \left[\begin{pmatrix} 1 & 0 & 0 & 0 \\ 0 & 1 & 0 & 0 \\ 0 & 0 & 1 & 0 \\ 0 & 0 & 0 & 1 \end{pmatrix} - \rho_+ \begin{pmatrix} 1 & 0 & 0 & 0 \\ 0 & 1 & 0 & 0 \\ 0 & 0 & 0 & 0 \\ 0 & 0 & 0 & 0 \end{pmatrix} - \rho_- \begin{pmatrix} 0 & 0 & 0 & 0 \\ 0 & 0 & 0 & 0 \\ 0 & 0 & 1 & 0 \\ 0 & 0 & 0 & 1 \end{pmatrix} \right] \begin{pmatrix} 1 \\ 1 \\ 1 \\ 1 \end{pmatrix} +$$

$$\left[\rho_+ \begin{pmatrix} 1 & 0 & 0 & 0 \\ 0 & 1 & 0 & 0 \\ 0 & 0 & 0 & 0 \\ 0 & 0 & 0 & 0 \end{pmatrix} + \rho_- \begin{pmatrix} 0 & 0 & 0 & 0 \\ 0 & 0 & 0 & 0 \\ 0 & 0 & 1 & 0 \\ 0 & 0 & 0 & 1 \end{pmatrix} \right] \begin{pmatrix} 0 & \frac{1}{2} & \frac{1}{2} & 0 \\ \frac{1}{2} & 0 & 0 & \frac{1}{2} \\ \frac{1}{2} & 0 & 0 & \frac{1}{2} \\ 0 & \frac{1}{2} & \frac{1}{2} & 0 \end{pmatrix} \begin{pmatrix} y_1 \\ y_2 \\ y_3 \\ y_4 \end{pmatrix} + \begin{pmatrix} \varepsilon_1 \\ \varepsilon_2 \\ \varepsilon_3 \\ \varepsilon_4 \end{pmatrix}.$$

If either $\rho_+ = 0$ (and hence $I_+ = 0$ and $I_- = I$) or $\rho_- = 0$ (and hence $I_- = 0$ and $I_+ = I$), then equation (3.3) reduces to equation (3.1). This eco-georeferenced, sub-meter resolution, grid-stratified, capture point, endmember, uncoalesced, geo-spectrotemporal, indicator variables classification was made in accordance with the quadrants of the corresponding Moran scatterplot generated employing the endemic, transmission-oriented, oviposition, observational, *An. arabiensis*, aquatic, larval habitat covariates geosampled in the eco-epidemiological, Mwea study site.

If positive and negative spatial autocorrelation processes counterbalance each other in a mixture, the sum of the two spatial autocorrelation parameters--($\rho_+ + \rho_-$) will be close to 0. In this research, Jacobian estimation was implemented by utilizing the differenced indicator, geosampled, eco-georeferenced, sub-meter resolution, grid-stratified, *An. arabiensis* aquatic, larval, habitat, endmember variables ($I_+ - \gamma I_-$), estimating ρ_+ and γ with maximum likelihood techniques, and setting $\hat{\rho}_- = -\hat{\gamma}\hat{\rho}_+$. The Jacobian generalizes the gradient of a scalar valued function of multiple variables which itself generalizes the derivative of a scalar-valued function of a scalar]. A more complex capture point, seasonal, hyperproductive, *An. arabiensis* habitat specification was then posited by generalizing these binary indicator variables. We used $F: R^n \rightarrow R^m$ as a function from Euclidean *n*-space to Euclidean *m*-space which was generated using the distance between sampled riverine habitat covariates. Such a function was given by *m* habitat

covariate (i.e., component functions), $y_1(x_1, xn)$, $y_m(x_1, xn)$. The partial derivatives of all these functions were organized in an *m*-by-*n* matrix, the Jacobian matrix *J* of *F*, which was as follows:

$$J = \begin{bmatrix} \frac{\partial y_1}{\partial x_1} & \cdots & \frac{\partial y_1}{\partial x_n} \\ \vdots & \ddots & \vdots \\ \frac{\partial y_m}{\partial x_1} & \cdots & \frac{\partial y_m}{\partial x_n} \end{bmatrix}$$

This matrix was denoted by $J_F(x_1, a_n)$ and $\frac{\partial(y_1,\ldots,y_m)}{\partial(x_1,\ldots,x_n)}$. The *i* Th row ($i = 1, m$) of this matrix was the gradient of the i^{th} component function y_i :(∇y_i). In these analyses p was a geosampled, *An. arabiensis*, aquatic, larval habitat, endmember covariate in R^n and *F* (i.e., geosampled larval/pupal count) was differentiable at p; its derivative was given by $J_F(p)$. The model described by $J_F(p)$) was the best linear approximation of *F* near the point p, in the sense that: $F(x) = F(p) + J_F(p)(x - p) + o(\|x - p\|)$. The spatial structuring was achieved by constructing a linear combination of a subset of the eigenvectors of a modified geographic weights matrix, using (I - 11′/n) C (I - 11′/n) that appeared in the numerator of the Moran's Coefficient (MC) Spatial autocorrelation can be indexed with a MC, a product moment correlation coefficient [

A subset of eigenvectors was then selected with a stepwise regression procedure. Because (I - 11′/n) C (I - 11′/n) = E Λ E', where E is an *n*-by-*n* matrix of eigenvectors and Λ is an *n*-by-*n* diagonal matrix of the corresponding eigenvalues the resulting geo-spectrotemporal geosampled, eco-georeferenced, sub-meter resolution, grid-stratified, *An. arabiensis* model specification was given by: $\mathbf{Y} = \mu\mathbf{1} + \mathbf{E}_k\beta + \varepsilon$, where μ the scalar mean of Y, Ek was an *n*-by-k matrix containing the subset of k <<*n* eigenvectors selected with a stepwise regression technique, and β was a *k*-by-1 vector of regression coefficients [

A number of the eigenvectors were extracted from (I - 11′/n) C (I - 11′/n), which were affiliated with geographic patterns of the geosampled *An. arabiensis* habitat, endmember covariates, in the study site, portraying a negligible degree of spatial autocorrelation. Consequently, only k of the *n* eigenvectors was of interest for generating a candidate set for a stepwise regression procedure. Candidate eigenvector represents a level of spatial autocorrelation which can account for the redundant information in orthogonal riverine larval habitat map patterns

Of note is that because the 2-by-2 square tessellation rendered a repeated eigenvalue. To identify spatial clusters of geosampled, eco-georeferenced, sub-meter resolution, grid-stratified, aquatic, *An. arabiensis* larval habitats, Thiessen polygon surface partitioning were generated to construct geographic neighbor matrices, which also were used in the spatial autocorrelation analysis. Entries in matrix were 1, if two sampled, larval habitats shared a common Thiessen polygon boundary and 0, otherwise. Next, the linkage structure for each surface was edited to remove unlikely geographic neighbors to identify pairs of sampled *An. arabiensis* aquatic larval, habitats sharing a common Thiessen polygon boundary. Attention was restricted to those map patterns associated with at least a minimum level of spatial autocorrelation, which, for implementation purposes, was defined by $|MC_j/MC_{max}| > 0.25$, where MC_j denoted the *j*th value and MC_{max}, the maximum value of MC. This threshold value allowed two candidate sets of eigenvectors to be considered for substantial positive and substantial negative spatial autocorrelation respectively. These statistics indicated that the detected negative spatial autocorrelation may be considered to be statistically significant, based upon a randomization perspective. Of note, is that the ratio of the PRESS (i.e., predicted error sum of squares) statistic to the sum of squared errors from the MC scatterplot trend line was 1.27 which was well within two standard deviations of the average standard prediction error value (roughly 1.18) for a sampled larval habitat in the Mwea study site. Because larval/pupal counts were being analyzed, a Poisson spatial filter model specification was employed in this research.

Detected overdispersion (i.e., extra-Poisson variation) results in its mean being specified as gamma distributed. The model specification was written as follows: $LN(\mu) = \alpha\mathbf{1} + \mathbf{E}_k\beta$, $\sigma_i^2 = \mu_i(1 - \eta\mu_i)$, where μ_i was the expected mean larval/pupal count for habitat location *i*, μ was an *n*-by-1 vector of expected larval/pupal counts, LN denoted the natural logarithm (i.e., the generalized linear model link function), α was an intercept term, and η was the negative

binomial dispersion parameter. This log-linear equation had no error term; rather, estimation was executed assuming a negative binomial random variable.

The eigenfunctions of a geo-spectrotemporally, spatial, weighted, geosampled, eco-georeferenced, sub-meter resolution, grid-stratified, *An. arabiensis*, aquatic, larval habitat covariance matrix were then determined. The upper and lower bounds for a spatial matrix generated using Morans indices (*I*) can be given by λ_{max} ($n/1^T W1$) and λ_{min} ($n/1^T W1$) where λ_{max} and λ_{min} which are the extreme eigenvalues of $\Omega = HWH$ .Hence, in this research, the eigenvectors of Ω were vectors with unit norm maximizing Moran's *I*. The eigenvalues of this matrix were equal to Moran's *I* coefficients of spatial autocorrelation post-multiplied by a constant. Eigenvectors associated with high positive (or negative) eigenvalues have high positive (or negative) autocorrelation.

The eigenvectors associated with eigenvalues with extremely small absolute values correspond to low spatial autocorrelation and are not suitable for defining spatial structures .The diagonalization of the spatial weighting matrix generated from the clincial, field and remote-sampled, endmember aquatic, larval habitat covariate coefficients consisted of finding the normalized vectors u_i, stored as columns in the matrix $U = [u_1 \cdots u_n]$, satisfying: $\Omega = HWH = U\Lambda U^T = \sum_{i=1}^{n} \lambda_i u_i u_i^T$ where $\Lambda = diag\ (\lambda_1 \cdots \lambda_n)$, $u_i^T u_i = \|u_i\|^2 = 1$ and $u_i^T u_j = 0$ for $i \neq j$. Note that double centering of Ω implied that the eigenvectors u_i generated from the ento-ecological, geosampled, *An. arabiensis*, immature, habitat covariates were centered and at least one eigenvalue was equal to zero. Introducing these eigenvectors in the original formulation of Moran's index lead to:

$$I(x) = \frac{n}{1^T W 1} \frac{x^T HWHx}{x^T Hx} = \frac{n}{1^T W1} \frac{x^T U\Lambda U^T x}{x^T Hx} = \frac{n}{1^T W1} \frac{\sum_{i=1}^{n} \lambda_i x^T u_i u_i^T x}{x^T Hx} \quad (3.4.)$$

Considering the centered vector $z = Hx$ and using the properties of idempotence of *H*, equation (3.5) was equivalent to: $I(x) = \frac{n}{1^T W1} \frac{\sum_{i=1}^{n} \lambda_i z^T u_i u_i^T z}{z^T z} = \frac{n}{1^T W1} \frac{\sum_{i=1}^{n} \lambda_i \|u_i^T z\|^2}{\|z\|^2}$ (3.6). We then transformed the autocorrelation indicators to geo-spectrotemporal geosampled, eco-georeferenced, sub-meter resolution, grid-stratified, capture point, correlation coefficient as the eigenvectors u_i and the vector *z* were centered the predictive, sub-meter resolution, grid-stratfiaible,LULC equation was rewritten: $I(x) = \frac{n}{1^T W1} \frac{\sum_{i=1}^{n} \lambda_i cor^2(u_i, z)\, var(z) n}{var(z) n} = \frac{n}{1^T W1} \sum_{i=1}^{n} \lambda_i cor^2(u_i, z)$ (3.7 Here,, *r* was the number of null eigenvalues of Ω ($r \geq 1$). These eigenvalues and corresponding eigenvectors were removed from Λ and *U* respectively. Equation 2.7 was then strictly equivalent to: $I(x) = \frac{n}{1^T W1} \sum_{i=1}^{n-r} \lambda_i cor^2(u_i, z)$ Moreover, it was demonstrated that Moran's index for a given eigenvector u_i was equal to $I(u_i) = (n/1^T W1)\ \lambda_i$ so the equation was rewritten: $I(x) = \sum_{i=1}^{n-r} I(u_i) cor^2(u_i, z)$ The term $cor^2(u_i, z)$ represented the part of the variance of *z* that was explained by u_i in the habitat model $z = \beta_i u_i + e_i$. This quantity was equal to $\beta_i^2 / n\ var(z)$. By definition, the eigenvectors u_i were orthogonal, and therefore, regression coefficients of the linear models $z = \beta_i u_i + e_i$ were those of the multiple,malaria, mosquito, forecast, vulnerability,ovispoition, eco-endmember, LULC, regression model $z = U\beta + \varepsilon = \beta_i u_i + \cdots + \beta_{n-r} u_{n-r} + \varepsilon$.

Next, the distribution of the error residuals in the *An. arabiensis*,capture point, aquatic, larval, habitat model, autocovariance matrix. The maximum value of *I* was obtained by all of the variation of *z*, as explained by the eigenvector u_1, which corresponded to the highest eigenvalue λ_1 in the spatial autocorrelation error matrix. Here, $cor^2(u_i, z) = 1$ (and $cor^2(u_i, z) = 0$ for $i \neq 1$) and the maximum value of *I*, was deduced for Equation 3.3), which was equal to $I_{MAX} = \lambda_1 (n/1^T W1)$. The minimum value of *me* in the error matrix was obtained as all the variation of *z* was explained by the eigenvector u_{n-r} corresponding to the lowest eigenvalue λ_{n-r} generated in the endmember habitat model. This minimum value was equal to $I_{min} = \lambda_{n-r} (n/1^T W1)$. If the ecological sampled predictor variable was not spatialized, the

part of the variance explained by each eigenvector was equal, on average, to $cor^2(u_i, z) = 1/n\text{-}1$. Because the clinical, field and remote-sampled,LULC. habitat variables in *z* were randomly permuted; it was assumed that we would obtain this result. In this research the set of *n*! Random permutations, revealed that $E_R(I) = \frac{n}{1^T W 1(n-1)} \sum_{i=1}^{n} \lambda_i = \frac{n}{1^T W 1(n-1)} trace(\Omega)$. It was easily demonstrated that $trace(\Omega) = -\frac{1^T W 1}{n}$ and it followed that $E_R(I) = -\frac{1}{n-1}$.

The geosampled, eco-georeferenced, explanatory, geo-spectrotemporal geosampled, eco-georeferenced, sub-meter resolution, grid-stratified, malaria mosquito, capture point, predictor covariates were then imput into an eigenfunction decomposition algorithm to quantify autocorrelation error coefficients in the linear residual variance estimates. Results indicated that negligible PSA was detected for the *An. arabiensis*, geo-spectrotemporal, aquatic, larval, habitat data. Eigenvectors were extracted from the matrix (I−11′/*n*) C (I−11′/*n*), employing the ento-ecological, geosampled predictor variables. In this research, denoting the autoregressive parameter captured the latent geo-spatiotemporal autocorrelation in the aquatic, larval habitat endemic transmission-oriented, predictive, risk model. This quantification involved ρ, a conditional autoregressive covariance specification, which involved the matrix (I - ρ C), where I was an *n*-by-*n* identity matrix. The residual autocorrelation error components were calculated as the matrix C raised to the power 1 (i.e., only adjacent geosampled, aquatic, larval, habitat,LULC data were involved in the autoregressive function), which was a first-order specification, with the autoregressive term being CY. An important matrix was then generated from C1, which was the vector of the number of geosampled, geo-spectrotemporal, *An. arabiensis*, aquatic, larval habitat, eco-georeferenced neighbors in the Mwea study site.

In this research, the inverse of the elements of C1 were inserted into the diagonal of a diagonal matrix, (i.e., D^{-1}) rendering matrix $W = D^{-1}C$ which became a stochastic matrix (i.e., each of its row sums equaled 1). One appealing feature of this matrix was that the autoregressive term became WY, which generated averages, rather than sums, of the neighboring geosampled larval habitat parameter estimate values. Because a covariance matrix for a vector insect larval habitat distribution model must be symmetric (Jacob et al. 2005b), we used a matrix W specification with a conditional autoregressive model by making the individual-sampled, geo-spectrotemporal geosampled, eco-georeferenced, sub-meter resolution, grid-stratified, aquatic. larval habitat variance nonconstantemploying $(I - \rho D^{-1}C)D^{-1} = (D^{-1} - \rho D^{-1}CD^{-1})$. An appealing feature of this version for the larval habitat, endemic, transmission-oriented, LULC, prognosticative, endmember, signature risk model was that it restricted values of the autoregressive parameter to the more intuitively interpretable range of $0 \leq \hat{\rho} \leq 1$. The aquatic, larval, habitat model then furnished an alternative specification which was also written in terms of matrix W. The spatial covariance was then a function of the matrix $(I - \rho CD^{-1})(I - \rho D^{-1}C) = (I - \rho W^T)(I - \rho W)$, where T denoted the matrix transpose. The resulting matrix was symmetric, and was considered a second-order specification, as it included the product of two spatial structure matrices (i.e., W^TW), which also restricted values of the autoregressive parameter to the more intuitively interpretable range of $0 \leq \hat{\rho} \leq 1$.

Positive and negative spatial autocorrelationm spatial filter, component pseudo-R^2 values were attained . These values did not exactly sum for the complete spatial filter; however, they are very close to their corresponding totals, suggesting that any induced multicollinearity was quite small. A generalized linear model (GLM) was then extended to account for quantitating latent, non-spatial , capture point, endmember, correlation effects, which allowed inferences to be drawn for a much wider range of eco-geographic sampling configurations generated from the geosampled eco-georefernced, *An. arabiensis*,capture point,seasonal, hyperproductive, aquatic, larval habitats than those utilized by employing a GLMM. The GLMM included a random effect, which was specified as a random intercept that was assumed to be normally distributed with a mean of zero, a constant variance, and zero spatial autocorrelation. This varying intercept term compensated for the non-constant mean associated with the negative binomial model general linear model specification. The spatial structuring of random effects was implemented with a conditional autoregressive model and was achieved in this research with a spatial filter. The spatial autocorrelation components revealed 11% redundant information in the ecologically sampled datasets GLMM estimation

We then listed the improvements of fit in the adjusted and unadjusted models for all model specifications and random error in the spatial analyses. The unadjusted model compared the univariate model to a model containing only the intercept term. Interactions were examined, and significant interactions were included. Improvement of fit was also

calculated for the first-order interaction models to determine whether including significant interactions improved fit compared to the full main effects model. Convergence problems prevented obtaining results of a saturated model to determine whether the presented model fit as well as the saturated model.

Bayesian inference derives the posterior probability as a consequence of two antecedents, a prior probability and a "likelihood function" derived from a probability, geo-spectrotemporal eco-georeferenced, sub-meter resolution, grid-stratified, vector arthropod-related endemic transmission oriented risk model for the geosampled, *An. arabiensis*, endemic, transmission oriented, aquatic, larval, habitat data. Bayesian inference computed the posterior probability according to Bayes' rule: $P(H|E) = \frac{P(E|H) \cdot P(H)}{P(E)}$. *H* stands for any hypothesis whose probability may be affected by data[2]. Often there are competing hypotheses, from which one chooses the most probable. The evidence *E* corresponded to the geosampled habitat data that were not used in computing the prior probability. $P(H)$, the prior probability, is the probability of *H* before *E* is observed[3]. This indicated that the previous endmember, capture point, hyperproductive, prognosticated estimate of the probability was true. Further in the residual forecasts, $P(H|E)$ was the posterior probability which was also the probability of *H* given *E*, (i.e., after *E* is observed). This allowed the probability of a hypothesis given the observed evidence. $P(E|H)$, to be determined by quantitating the probability of observing E given the likelihood estimates in the model. This indicated the compatibility of the evidence of the given hypothesis. $P(E)$ (i.e.,A Bayesian probabilistic paradym can determine explanatory endemic *An. arabiensis* –related, capture point covariates). This model was the marginal likelihood or "model evidence". Note that what affected the value of $P(H|E)$ in the risk model for different values of *H* was only the factors $P(H)$and $P(E|H)$, which both appeared in the numerator, and hence the posterior probability was proportional to both. In words, the posterior probability of a hypothesis was calculable by a combination of the inherent likeliness of a hypothesis (i.e., the prior) and the compatibility of the observed evidence with the hypothesis (i.e., the likelihood)..

We noticed that the geo-spectrotemporal geosampled, eco-georeferenced, sub-meter resolution, grid-stratified, *An. arabiensis* endemic transmission-oriented distribution had the following formula: $\mathrm{H}[\mathbf{X}] = -\ln\left(B(\mathbf{V}, n)\right) - \frac{1}{2}(n-p-1)\,\mathrm{E}[\ln|\mathbf{X}|] + \frac{np}{2}$ where $B(\mathbf{V}, n)$was the normalizing constant of the distribution: This was then expanded as follows: $\mathrm{H}[\mathbf{X}] = \frac{n}{2}\ln|\mathbf{V}| + \frac{np}{2}\ln(2) + \ln\left(\Gamma_p(\frac{n}{2})\right) - \frac{1}{2}(n-p-1)\,\mathrm{E}[\ln|\mathbf{X}|] + \frac{np}{2}$

$$\mathrm{H}[\mathbf{X}] = \frac{n}{2}\ln|\mathbf{V}| + \frac{np}{2}\ln(2) + \ln\left(\Gamma_p(\tfrac{n}{2})\right) - \frac{1}{2}(n-p-1)\,\mathrm{E}[\ln|\mathbf{X}|] + \frac{np}{2} \quad - \frac{1}{2}(n-p-1)\left(\sum_{i=1}^{p}\psi\left(\tfrac{1}{2}(n+1-i)\right) + p\ln(2) + \ln|\mathbf{V}|\right) + \frac{np}{2}$$

$$= \frac{n}{2}\ln|\mathbf{V}| + \frac{np}{2}\ln(2) + \frac{1}{4}p(p-1)\ln(\pi) + \sum_{i=1}^{p}\ln\left(\Gamma\left(\tfrac{n}{2} + \tfrac{1-i}{2}\right)\right) \quad - \left(\tfrac{1}{2}(n-p-1)\sum_{i=1}^{p}\psi\left(\tfrac{1}{2}(n+1-i)\right) + \tfrac{1}{2}(n-p-1)p\ln(2) + \tfrac{1}{2}(n-p-1)\ln|\mathbf{V}|\right) + \frac{np}{2}$$

$$= \frac{p+1}{2}\ln|\mathbf{V}| + \frac{1}{2}p(p+1)\ln(2) + \frac{1}{4}p(p-1)\ln(\pi) + \sum_{i=1}^{p}\ln\left(\Gamma\left(\tfrac{n}{2} + \tfrac{1-i}{2}\right)\right) - \frac{1}{2}(n-p-1)\sum_{i=1}^{p}\psi\left(\tfrac{1}{2}(n+1-i)\right) + \frac{np}{2}$$

The characteristic function of the Wishart distribution was then $\Theta \mapsto |\mathbf{I} - 2i\,\mathbf{\Theta V}|^{-\frac{n}{2}}$. In other words, $\Theta \mapsto \mathrm{E}\left[\exp\left(i\mathrm{tr}(\mathbf{X\Theta})\right)\right] = |\mathbf{I} - 2i\mathbf{\Theta V}|^{-\frac{n}{2}}$where E[·] denoted expectation.(Here Θ and I were te matrices which had the same size as V , I was the identity matrix; and *i* was the square root of −1. The density function of the inverse Wishart was: $\frac{|\mathbf{\Psi}|^{\frac{\nu}{2}}}{2^{\frac{\nu p}{2}}\Gamma_p(\frac{\nu}{2})}\,|\mathbf{X}|^{-\frac{\nu+p+1}{2}}\,e^{-\frac{1}{2}\mathrm{tr}(\mathbf{\Psi X}^{-1})}$ where X and $\mathbf{\Psi}$ were $p \times p$positive definite matrices, and $\Gamma_p(\cdot)$ was the multivariate gamma function.

The multivariate gamma function, $\Gamma_p(\cdot)$, is a generalization of the gamma function. It is useful in multivariate statistics, appearing in the probability density function of the and inverse Wishart distributions[2]. In this research the Bayesian endmber, autoicorrelation, prognosticative, spatial filter model possessed two equivalent definitions. One was $\Gamma_p(a) = \int_{S>0}\exp\left(-\mathrm{trace}(S)\right)|S|^{a-(p+1)/2}\,dS,$ where S>0 whenst S was positive-definite. The other one, more

useful in practice,for determining geeolocations of eco-georferenced, seasonal, hypeproductive, malaria, mosquito, oviposition foci was $\Gamma_p(a) = \pi^{p(p-1)/4} \prod_{j=1}^{p} \Gamma\left[a + (1-j)/2\right]$. From this, we have the recursive, quantitable, optimizable, non-frequentistic relationships: $\Gamma_p(a) = \pi^{(p-1)/2}\Gamma(a)\Gamma_{p-1}(a-\frac{1}{2}) = \pi^{(p-1)/2}\Gamma_{p-1}(a)\Gamma[a+(1-p)/2]$. Hence $\Gamma_1(a) = \Gamma(a), \Gamma_2(a) = \pi^{1/2}\Gamma(a)\Gamma(a-1/2)$ and $\Gamma_3(a) = \pi^{3/2}\Gamma(a)\Gamma(a-1/2)\Gamma(a-1)$

We then defined the multivariate digamma function in the seasonal, geo-spectrotemporal geosampled, eco-georeferenced, sub-meter resolution, grid-stratified, predictive endemic transmission, endmember, capture point, forecast, vulnerability rimodel as $\psi_p(a) = \frac{\partial \log \Gamma_p(a)}{\partial a} = \sum_{i=1}^{p} \psi(a + (1-i)/2),$ and the general polygamma function as $\psi_p^{(n)}(a) = \frac{\partial^n \log \Gamma_p(a)}{\partial a^n} = \sum_{i=1}^{p} \psi^{(n)}(a + (1-i)/2).$ Since $\Gamma_p(a) = \pi^{p(p-1)/4} \prod_{j=1}^{p} \Gamma(a + \frac{1-j}{2}),$ it follows that $\frac{\partial \Gamma_p(a)}{\partial a} = \pi^{p(p-1)/4} \sum_{i=1}^{p} \frac{\partial \Gamma(a + \frac{1-i}{2})}{\partial a} \prod_{j=1, j\neq i}^{p} \Gamma(a + \frac{1-j}{2}).$ By definition of the digamma function, ψ, $\frac{\partial \Gamma(a + (1-i)/2)}{\partial a} = \psi(a + (i-1)/2)\Gamma(a + (i-1)/2)$ As such it mathematically logically follows that $\frac{\partial \Gamma_p(a)}{\partial a} = \pi^{p(p-1)/4} \prod_{j=1}^{p} \Gamma(a+(1-j)/2) \sum_{i=1}^{p} \psi(a+(1-i)/2) = \Gamma_p(a) \sum_{i=1}^{p} \psi(a+(1-i)/2).$

The marginal and conditional distributions from an inverse Wishart-distributed matrix were then regressively quantitated as $\mathbf{A} \sim W^{-1}(\mathbf{\Psi}, \nu)$ which had an inverse Wishart distribution. Partition the matrices A and $\mathbf{\Psi}$ conformably with each other $\mathbf{A} = \begin{bmatrix} \mathbf{A}_{11} & \mathbf{A}_{12} \\ \mathbf{A}_{21} & \mathbf{A}_{22} \end{bmatrix}$, $\mathbf{\Psi} = \begin{bmatrix} \mathbf{\Psi}_{11} & \mathbf{\Psi}_{12} \\ \mathbf{\Psi}_{21} & \mathbf{\Psi}_{22} \end{bmatrix}$ where $\mathbf{A}_{ij}$ and $\mathbf{\Psi}_{ij}$ are $p_i \times p_j$ matrices, then we have $\mathbf{A}_{11}$ is independent of $\mathbf{A}_{11}^{-1}\mathbf{A}_{12}$ and $\mathbf{A}_{22\cdot1}$, where $\mathbf{A}_{22\cdot1} = \mathbf{A}_{22} - \mathbf{A}_{21}\mathbf{A}_{11}^{-1}\mathbf{A}_{12}$ was the Schur complement of $\mathbf{A}_{11}$ in A and $\mathbf{A}_{11} \sim W^{-1}(\mathbf{\Psi}_{11}, \nu - p_2)$. $\mathbf{A}_{11}^{-1}\mathbf{A}_{12}|\mathbf{A}_{22\cdot1} \sim MN_{p1\times p2}(\mathbf{\Psi}_{11}^{-1}\mathbf{\Psi}_{12}, \mathbf{A}_{22\cdot1} \otimes \mathbf{\Psi}_{11}^{-1})$, where $MN_{p\times q}(\cdot,\cdot)$ was a matrix normal distribution. As such $\mathbf{A}_{22\cdot1} \sim W^{-1}(\mathbf{\Psi}_{22\cdot1}, \nu)$, where $\mathbf{\Psi}_{22\cdot1} = \mathbf{\Psi}_{22} - \mathbf{\Psi}_{21}\mathbf{\Psi}_{11}^{-1}\mathbf{\Psi}_{12}$; Further, suppose we wish to make inference about a covariance matrix $\mathbf{\Sigma}$ whose prior $p(\mathbf{\Sigma})$ has a $W^{-1}(\mathbf{\Psi}, \nu)$ distribution. If the capture point,m aquatic, larval habitat, malaria mosquito, observations $\mathbf{X} = [\mathbf{x}_1, \ldots, \mathbf{x}_n]$ are independent p-variate Gaussian variables drawn from a $N(\mathbf{0}, \mathbf{\Sigma})$ distribution, then the conditional distribution $p(\mathbf{\Sigma}|\mathbf{X})$ eill have a $W^{-1}(\mathbf{A} + \mathbf{\Psi}, n + \nu)$ distribution, where $\mathbf{A} = \mathbf{X}\mathbf{X}^T$ is n times the sample covariance matrix. Because the prior and posterior distributions are the same family, we say the inverse Wishart distribution is conjugate to the multivariate Gaussian[2]. Due to its conjugacy to the multivariate Gaussian, it is possible to marginalize out (integrate out) the Gaussian's parameter $\mathbf{\Sigma}$. $P(\mathbf{X}|\mathbf{\Psi}, \nu) = \int P(\mathbf{X}|\mathbf{\Sigma})P(\mathbf{\Sigma}|\mathbf{\Psi}, \nu)d\mathbf{\Sigma} = \frac{|\mathbf{\Psi}|^{\frac{\nu}{2}}\Gamma_p\left(\frac{\nu+n}{2}\right)}{\pi^{\frac{np}{2}}|\mathbf{\Psi}+\mathbf{A}|^{\frac{\nu+n}{2}}\Gamma_p\left(\frac{\nu}{2}\right)}$ (this is useful because the variance matrix $\mathbf{\Sigma}$ is not known in practice, but because $\mathbf{\Psi}$ is known *a priori*, and A can be obtained from the data, the right hand side can be evaluated directly) The meant that $E(\mathbf{X}) = \frac{\mathbf{\Psi}}{\nu - p - 1}$. The variance of each element of X: $\mathrm{Var}(x_{ij}) = \frac{(\nu-p+1)\psi_{ij}^2 + (\nu-p-1)\psi_{ii}\psi_{jj}}{(\nu-p)(\nu-p-1)^2(\nu-p-3)}$ The variance of the diagonal uses the same formula as above with $i = j$, which simplified to: $\mathrm{Var}(x_{ii}) = \frac{2\psi_{ii}^2}{(\nu-p-1)^2(\nu-p-3)}$. The covariance of elements of X are given by: $\mathrm{Cov}(x_{ij}x_{kl}) = \frac{2\psi_{ij}\psi_{kl} + (\nu-p-1)(\psi_{ik}\psi_{jl} + \psi_{il}\psi_{kj})}{(\nu-p)(\nu-p-1)^2(\nu-p-3)}$.

The geosampled, geo-spectrotemporal eco-georeferenced, sub-meter resolution, grid-stratified, *An. arabiensis*, aquatic, larval habitats observations were independent *p*-variate Gaussian variables which were drawn from a $N(\mathbf{0}, \mathbf{\Sigma})$distribution. The conditional distribution [i.e.,$p(\mathbf{\Sigma}|\mathbf{X})$] had a $W^{-1}(\mathbf{A}+\mathbf{\Psi}, n+m)$ distribution. Thereafter, $\mathbf{A}=\mathbf{X}\mathbf{X}^T$ was used to generate the sample covariance matrix. In this research the inverse Wishart distribution was conjugate to the multivariate Gaussian. Due to its conjugacy to the multivariate Gaussian, it was possible to "integrate out" the Gaussian-based, time series, capture point, aquatic, larval, habitat parameters [i.e., $\mathbf{\Sigma}$]from the other predictor variables which in this research generated: $P(\mathbf{X}|\mathbf{\Psi}, m) = \int P(\mathbf{X}|\mathbf{\Sigma})P(\mathbf{\Sigma}|\mathbf{\Psi}, m)d\mathbf{\Sigma} = \frac{|\mathbf{\Psi}|^{\frac{m}{2}}\Gamma_p\left(\frac{m+n}{2}\right)}{\pi^{\frac{np}{2}}|\mathbf{\Psi}+\mathbf{A}|^{\frac{m+n}{2}}\Gamma_p\left(\frac{m}{2}\right)}$.This was useful as the variance matrix $\mathbf{\Sigma}$ from the sampled explanatory predictor covariates was $\mathbf{\Psi}$(i.e., the priori) and A was directly obtained from the coefficient indicator values. The mean in the endemic, transmission-oriented, vulnerability, ento-ecoepidemiological, risk model was; $E(\mathbf{B}) = \frac{\mathbf{\Psi}}{m-p-1}$.The variance of each element of B was then $\mathrm{var}(b_{ij}) = \frac{(m-p+1)\psi_{ij}^2 + (m-p-1)\psi_{ii}\psi_{jj}}{(m-p)(m-p-1)^2(m-p-3)}$ .The variance of the diagonal used in the larval habitat distribution, prognosticative, model was also generated using the same formula as above with *i* = *j*, which further simplified the model to: $\mathrm{var}(b_{ii}) = \frac{2\psi_{ii}^2}{(m-p-1)^2(m-p-3)}$.

A univariate specialization of the inverse-Wishart distribution was then the inverse-gamma distribution. With $p=1$(i.e. univariate) and $\alpha = \nu/2$, $\beta = \mathbf{\Psi}/2$and $x = \mathbf{X}$the probability density function of the inverse-Wishart distribution becomes $p(x|\alpha,\beta) = \frac{\beta^\alpha x^{-\alpha-1}\exp(-\beta/x)}{\Gamma_1(\alpha)}$. i.e., the inverse-gamma distribution, where $\Gamma_1(\cdot)$is the ordinary Gamma function. The inverse gamma distribution's probability density function is defined over the support $x>0$ $f(x;\alpha,\beta) = \frac{\beta^\alpha}{\Gamma(\alpha)}x^{-\alpha-1}\exp\left(-\frac{\beta}{x}\right)$with shape parameter $\alpha$and scale parameter β. The cumulative distribution function is the regularized gamma function $F(x;\alpha,\beta) = \frac{\Gamma\left(\alpha,\frac{\beta}{x}\right)}{\Gamma(\alpha)} = Q\left(\alpha,\frac{\beta}{x}\right)$where the numerator is the upper incomplete gamma function and the denominator is the gamma function. Many math packages allow you to compute Q, the regularized gamma function, directly.

This specification moved the investigation toward Bayesian map analysis, given that the entire clinical, field and remote-geosampled oviposition, geo-spectrotemporal geosampled, eco-georeferenced, sub-meter resolution, grid-stratified, *An. arabiensis* aquatic, larval habitat endemic trasnmission-oriented predictive risk-based explanatory predictor covariates, with the exception of the intercept, were treated as single-valued; whereas, the intercept was treated as a distribution of values and was estimated using empirical Bayes techniques. The difference in the deviances between a simple model and the more complex model provided the improvement χ^2 values. We examined all interaction between the sampled georeferenced, aquatic, larval habitat, explanatory, predictor covariates and found that an interaction model did not improve the fit therefore; no interaction terms were included in the final model.

We could not examine the improvement of fit between a saturated model and the full effects, geo-spectrotemporal geosampled, eco-georeferenced, sub-meter resolution, grid-stratified, forecast, vulnerability, ovisposition, risk model, as the number of the geosampled parameters that needed to be estimated exceeded the maximum number that could estimate. To derive the improvement of fit values listed in Table 4, the posterior mean deviance values were obtained with Deviance Information Criterion (DIC) spatial analytical tools. We focused on a spatial consideration of the local DIC measure for model selection and goodness-of-fit evaluation. We used a partitioning of the DIC into the local DIC, leverage, and deviance residuals to assess the local model fit and influence for the observations in a Bayesian framework. We also used visualization of the local DIC to assist in model selection and to visualize the global and local impacts of adding covariates or endmember, model parameters. DIC statistics were generated to identify the best fitting model. In this research, the deviance was defined as - 2 * log (likelihood), where 'likelihood' was defined as p(y | and theta), including all the normalizing constants: y comprised all stochastic node

values and theta comprised the immediate stochastic parents of y. 'Stochastic parents' are the stochastic nodes upon which the distribution of y depends, when collapsing over all logical relationships. For example, if y ~ dnorm (mu, tau), and if tau is a function of a parameter phi over which a prior distribution has been placed, then the likelihood is defined as a function of phi. The expectation $\overline{D} = \mathrm{E}^{\theta}\left[D(\theta)\right]$ was used as a measure of geo-spectrotemporal geosampled, eco-georeferenced, sub-meter resolution, grid-stratified model fitness based on the values of the sampled georeferenced explanatory predictor covariate coefficient values. The effective number of parameters included in the model was computed as $p_D = \overline{D} - D(\overline{\theta})$, where $\overline{\theta}$ was the expectation of θ. The DIC generated the following statistics: 1) the Dbar which was is the posterior mean of the deviance, 2) Dhat: the point estimate of the deviance (i.e., -2 * log(likelihood)) obtained by substituting the posterior means theta .bar of theta: thus rendering Dhat = -2 * log(p(y — theta.bar) 3) pD: this was 'the effective number of parameters which in this research this was provided by pD = Dbar – Dha and as such pD was the posterior mean of the deviance minus the deviance of the posterior means.. In normal hierarchical models, Pad = TR (H) where H is the 'hat' matrix that maps the observed data to their fitted values [25].The DIC was then calculated as: $DIC = p_D + D$. The DIC value for the final model was 931.6. The DIC value for the model was 923.4.

Median parameter values, as well as the 95% credibility intervals (2.5 percentile and 97.5 percentile values)were then derived. As the geo-spectrotemporal eco-georeferenced, sub-meter resolution, grid-stratified, *An. arabiensis* sampling sites increased based on the eco-georeferenced explanatory predictor covariate distance from the capture point, the median log-count of larval count increased. The adjusted model that assumed independence amongst the field and remote-sampled explanatory predictor covariates an of the larval counts fit better that the model that adjusted for correlation within the study site based on the root mean squared error.

We then constructed a Poisson model in SAS GEN MOD. The Poisson process in our analyses was provided by the limit of a binomial distribution of the geosampled, explanatorym endemic transmission-oriented, endmember, oviposition, *An. arabiensis* covariate coefficient estimates using $P_p(n \mid N) = \frac{N!}{n!\,(N-n)!}\, p^n (1-p)^{N-n}$. (4.1). We viewed the distribution as a function of the expected number of density larval count-oriented, variables using the sample size *N* for quantifying the fixed *p* in equation (4.1), which was then transformed into the linear equation: $P_{\nu}(n|N) = \frac{N!}{n!(N-n)!}\left(\frac{\nu}{N}\right)^{n}\left(1-\frac{\nu}{N}\right)^{N-n}$. Based on the sample size *N*, the distribution approached $P_{\nu}(n)$ was $\lim_{n\to\infty} P_{\nu}(n|N)\lim_{N\to\infty}\frac{N(N-1)\cdots(N-n+1)}{n!}\frac{\nu^{n}}{N^{n}}\left(1-\frac{\nu}{N}\right)^{N}(1-\frac{\nu}{N})^{-n}\lim_{N\to\infty}\frac{N(N-1)\cdots(N-n+1)}{N^{n}}\frac{\nu^{n}}{n!}\left(1-\frac{\nu}{N}\right)^{N}(1-\frac{\nu}{N})^{-n}=$ $1\cdot\frac{\nu^{n}}{n!}\cdot e^{-\nu}\cdot 1=\frac{\nu^{n}e^{-\nu}}{n!}$.

The GENMOD procedure then fit a GLM to the sampled data by maximum likelihood estimation of the parameter vector β. In this research the GENMOD procedure estimated the seasonal-geosampled, geo-spectrotemporal, endmember parameters of each model numerically through an iterative fitting process. The dispersion parameter was then estimated by the residual deviance and by Pearson's chi-square divided by the degrees of freedom (d.f.). Covariances, standard errors, and *p*-values were then computed for the sampled endemic transmission-oriented covariate coefficients based on the asymptotic normality derived from the maximum likelihood estimation.

Note, that the sample size *N* completely dropped out of the probability function, which in this research had the same functional form for all the geosampled district-level parameterizable, estimator indicator values (i.e., ν). As expected, the Poisson distribution was normalized so that the sum of probabilities equalled 1. The ratio of probabilities was then determined by $\sum_{n=0}^{\infty} P_{\nu}(n) = e^{-\nu}\sum_{n=0}^{\infty}\frac{\nu^{n}}{n!} = e^{-\nu}e^{\nu} = 1$which was then subsequently, asymptotically expressed as $\frac{P_{\nu}(n=i+1)}{P_{\nu}(n=i)} = \frac{\nu^{i+1}/(i+1)!}{e^{-\nu}\nu^{i}/i!} = \frac{\nu}{i+1}$.

The Poisson distribution revealed that the explanatory covariate coefficients reached a maximum when $\frac{d\,P_{\nu}(n)}{d\,n} = \frac{e^{-\nu}\,n\,(\gamma - H_n + \ln\nu)}{n!} = 0,$ where γ was the Euler-Mascheroni constant and H_n was a harmonic number, leading to the transcendental equation $\gamma - H_n + \ln\nu = 0$. The regression model also revealed that the Euler-Mascheroni constant arose in the integrals as

$g=-\int_0^{\infty} e^{-x}\ln x\,dx=-\int_0^{1}\ln\ln\left(\frac{1}{x}\right)dx=\int_0^{\infty}\left(\frac{1}{1-e^{-x}}-\frac{1}{x}\right)e^{-x}\,dx=\int_0^{\infty}\frac{1}{x}\left(\frac{1}{1+x}-e^{-x}\right)dx$ (4 .2).Commonly, integrals that render g in combination with temporal sampled constants include $\int_0^{\infty} e^{-x^2}\ln x\,dx=-\frac{1}{4}\sqrt{p}\left(g-2\ln 2\right)$ which is equal to $\int_0^{\infty} e^{-x}\left(\ln x\right)^2 dx=g^2+\frac{1}{6}p^2$ [2]. Thereafter, the double integrals in our district-level, seasonal, malaria, mosquito,capture point, eco-endmember, grid-stratifiable, regression model included $g=\int_0^{1}\int_0^{1}\frac{x-1}{\left(1-xy\right)\ln\left(xy\right)}dx\,dy$.

An interesting analog of equation (2.2) in the regression-based model was then calculated as $\ln\left(\frac{4}{p}\right)=\sum_{n=1}^{\infty}(-1)^{n-1}\left[\frac{1}{n}-\ln\frac{n+1}{n}\right]=\int_0^{1}\int_0^{1}\frac{x-1}{(1+xy)\ln(xy)}dx\,dy=0.241564...g$ This solution was also provided by incorporating Mertens theorem [i.e., $e^{g}=\lim_{n\to\infty}\frac{1}{\ln p_n}\prod_{i=1}^{n}\frac{1}{1-\frac{1}{p_i}}$] where the product was aggregated over the district-level geosampled values found in the empirical ecological datasets. Mertens' 3rd theorem: $\lim_{n\to\infty}\ln n\prod_{p\le n}\left(1-\frac{1}{p}\right)=e^{-g}$ is related to the density of prime numbers where γ is the Euler–Mascheroni constant [5].By taking the logarithm of both sides in the model, an explicit formula for γ was then derived employing $g=\lim_{x\to\infty}\left[\sum_{p\le x}\ln\left(\frac{1}{1-\frac{1}{p}}\right)-\ln\ln x\right]$. This expression was also rendered coincidently by quantifying the data series employing Euler, and equation (2.2) by first replacing $\ln n_{\,b}\ln(n+1)$, in the equation $\gamma=\sum_{k=1}^{\infty}\left[\frac{1}{k}-\ln\left(1+\frac{1}{k}\right)\right]$ and then generating $\lim_{n\to\infty}\left[\ln(n+1)-\ln n\right]=\lim_{n\to\infty}\ln\left(1+\frac{1}{n}\right)=0$.We then substituted the telescoping sum $\sum_{k=1}^{n}\ln\left(1+\frac{1}{k}\right)$ for $\ln(n+1)$ which then generated $\ln\left(1+\frac{1}{k}\right)=\ln(k+1)-\ln k$.Thereafter, our product was $\lim_{n\to\infty}\left[\sum_{k=1}^{n}\frac{1}{k}-\sum_{k=1}^{n}\ln\left(1+\frac{1}{k}\right)\right]_{\gamma}=\lim_{n\to\infty}\sum_{k=1}^{n}\left[\frac{1}{k}-\ln\left(1+\frac{1}{k}\right)\right]$.

Additionally, other series in our spectrotemporal, district-level, regression model included the equation (◇) where $g=\sum_{n=2}^{\infty}(-1)^n\frac{z(n)}{n}=\ln\left(\frac{4}{p}\right)+\sum_{n=1}^{\infty}\frac{(-1)^{n-1}z(n+1)}{2^n(n+1)}$ and $z(z)$ was $g=\sum_{n=1}^{\infty}(-1)^n\frac{[\lg n]}{n}$ plus the Riemann zeta function. The Riemann zeta function ζ(s) is a function of a complex variables that analytically continues the sum of the infinite series $\sum_{n=1}^{\infty}\frac{1}{n^s}$ which converges when the real part of *s* is greater than 1 where lg is the logarithm to base 2 and the $\lfloor x\rfloor$ is the floor function [2]. Nielsen[5] earlier provided a series equivalent to $g=1-\sum_{n=1}^{\infty}\sum_{k=2^{n-1}}^{2^n-1}\frac{n}{(2k+1)(2k+2)}$ and, thereafter $\frac{1}{(2k+1)(2k+2)}=\frac{1}{2k+1}-\frac{1}{2k+2}$ which was then added to $0=-\frac{1}{2}+\frac{1}{4}+\frac{1}{8}+\frac{1}{16}+...$ to render Vacca's formula. Gosper et al. [6] used the sums $g=\sum_{n=1}^{\infty}\sum_{k=2^n}^{\infty}\frac{(-1)^k}{k}=\sum_{k=1}^{\infty}\frac{1}{2^{k+1}}\sum_{j=0}^{k-1}\binom{2^{k-j}+j}{j}^{-1}$ with $k-j$ by replacing the undefined *I* and then rewrote the equation as a double series for applying the Euler's series transformation to each of the sampled time-series dependent explanatory covariate coefficient estimates.

International Research Journal of Computer Science and Application
Vol. 2, No. 1, March 2018, pp. 1-181
Available Online at http://acascipub.com/Journals.php

In the eco-endmember, ovisposition, malaria model $\frac{n}{}$ was used as a binomial coefficient, rearranged to achieve the conditionally convergent series in the spatiotemporal, ento-ecoepidemiological, endmeber, linear model. The plus and minus terms were first grouped in pairs of the geosampled, covariate, coefficient estimates employing the resulting series based on the actual, observational, indicator values. The double series was thereby equivalent to Catalan's integral: $\gamma = \int_0^1 \frac{1}{1+x} \sum_{n=1}^{\infty} x^{2^n-1} dx$. Catalan's integrals are a special case of general formulas due to $J_0\left(\sqrt{z^2 - y^2}\right) = \frac{1}{p} \int_0^p e^{y\cos q} \cos(z \sin q)\, dq$ where $J_0(z)$ is a Bessel function of the first kind [3]. The Bessel function is a function $Z_n(x)$ defined in a robust regression model by using the recurrence relations $Z_{n+1} + Z_{n-1} = \frac{2n}{x} Z_n$ and $Z_{n+1} - Z_{n-1} = -2\frac{dZ_n}{dx}$ [2] which more recently has been defined as solutions in linear models using the differential equation $x^2 \frac{d^2y}{dx^2} + x\frac{dy}{dx} + (x^2 - n^2)y = 0$ [6].

The Bessel function $J_n(z)$ for the LULC, malaria ,model was defined by the contour integral $J_n(z) = \frac{1}{2\pi i} \oint e^{(z/2)(t-1/t)} t^{-n-1} dt$ where the contour enclosed the origin and was traversed in a counter-clockwise direction. This explanatory, optimizable, mathematical, explanatory LULC function generated: $J_0\left(2i\sqrt{z}\right) = \frac{1}{p} \int_0^p e^{(1+z)\cos q} \cos((1-z)\sin q)\, dq$ $z \circ 1 - z$ and $y \circ 1 + z$. In mathematics, Bessel functions are canonical solutions $y(x)$ of Bessel's differential equation: $x^2\frac{d^2y}{dx^2} + x\frac{dy}{dx} + (x^2 - \alpha^2)y = 0$ for an arbitrary real or complex number α (i.e., the order of the Bessel function); the most common and important cases are for α an integer or half-integer [2]. Thereafter, to quantify the equivalence in the malarial, regression-based, capture point, aquatic, larval habitat, parameter estimators, we expanded $1/(1+x)$ in a geometric series and multiplied the sampled data feature attributes by x^{2^n-1}, and integrated the term wise as in Sondow and Zudilin [6].Other series for γ then included $g = \frac{3}{2} - \ln 2 - \sum_{m=2} (-1)^m \frac{m-1}{m} \zeta(m) - 1$ and $g = \frac{2^n}{e^{2^n}} \sum_{m=0} \frac{2^{mn}}{(m+1)!} \sum_{t=0}^{m} \frac{1}{t+1} - n\ln 2 + o\left(\frac{1}{2^n e^{2^n}}\right)$ A rapidly converging limit for γ was then provided by $g = \lim_{n\to\infty}\left[\frac{2n-1}{2n} - \ln n + \sum_{k=2}^{n}\left(\frac{1}{k} - \frac{z(1-k)}{n^k}\right)\right] = \lim_{n\to\infty}\left[\frac{2n-1}{2n} - \ln n + \sum_{k=2}^{n}\frac{1}{k}\left(1 + \frac{B_k}{n^k}\right)\right]$ and $g = \lim_{n\to\infty}\left[\frac{2n-1}{2n} - \ln n + \sum_{k=2}^{n}\left(\frac{1}{k} - \frac{z(1-k)}{n^k}\right)\right] = \lim_{n\to\infty}\left[\frac{2n-1}{2n} - \ln n + \sum_{k=2}^{n}\frac{1}{k}\left(1 + \frac{B_k}{n^k}\right)\right]$ where B_k was a Bernoulli number. Another limit formula was then provided by the equation $g = -\lim_{n\to\infty}\left[\frac{\Gamma\left(\frac{1}{n}\right)\Gamma(n+1)n^{1+1/n}}{\Gamma\left(2+n+\frac{1}{n}\right)} - \frac{n^2}{n+1}\right]$.

In mathematics, the Bernoulli numbers B_n are a sequence of rational numbers with deep connections to number theory, whereby, values of the first few explanative, time series,, geosampeld, Bernoulli numbers are $B_0 = 1$, $B_1 = \pm 1/2$, $B_2 = 1/6$, $B_3 = 0$, $B_4 = -1/30$, $B_5 = 0$, $B_6 = 1/42$, $B_7 = 0$, $B_8 = -1/30$ [2].

Jacob et al. [1] found if m and n are sampled values and $f(x)$ is a smooth sufficiently differentiable function in a seasonal, malarial-related, geo-spectrotemporal, ento-ecoepidemiological, endmember regression model which is defined for all the values of x in the interval $[m, n]$, then the integral $I = \int_m^n f(x)\,dx$ can be approximated by the sum (or vice versa) $S = \frac{1}{2}f(m) + f(m+1) + \cdots + f(n-1) + \frac{1}{2}f(n)$. The Euler–Maclaurin formula then provided expressions for quantiating the difference between the sum and the integral in terms of the higher derivatives $f^{(k)}$ at the end points of the interval m and n. The Euler–Maclaurin formula provides a powerful connection between integrals and sums which can be used to approximate integrals by finite sums, or conversely to evaluate finite sums and infinite series using integrals and the machinery of calculus [4]. Thereafter, for the capture point, oviposition, malarial-sampled values, p,

we had $S-I=\sum_{k=2}^{p}\frac{B_k}{k!}\left(f^{(k-1)'}(n)-f^{(k-1)'}(m)\right)+R$ where $B_1 = -1/2$, $B_2 = 1/6$, $B_3 = 0$, $B_4 = -1/30$, $B_5 = 0$, $B_6 = 1/42$, $B_7 = 0$, $B_8 = -1/30$, and R which was an error term. Note in this research $-B_1\left(f(n)+f(m)\right)=\frac{1}{2}\left(f(n)+f(m)\right)$.Hence, we re-wrote the regression-based formula as follows:$\sum_{i=m}^{n}f(i)=\int_m^n f(x)\,dx-B_1\left(f(n)+f(m)\right)+\sum_{k=1}^{p}\frac{B_{2k}}{(2k)!}\left(f^{(2k-1)'}(n)-f^{(2k-1)'}(m)\right)+R$ We then rewrote the equation more elegantly as$\sum_{i=m}^{n}f(i)=\sum_{k=0}^{p}\frac{1}{k!}\left(B_k f^{(k-1)'}(n)-B_k^{*}f^{(k-1)'}(m)\right)+R$ with the convention of $f^{(-1)'}(x)=\int f(x)\,dx$ (i.e. the -1th derivation of f is the integral of the function). Limits to the predictive, signature seasonal, regression model was then rendered by $g=\lim_{x\to\infty}z\left(z\left(z\right)\right)-2^{x}+\left(\frac{4}{3}\right)^{x}+1$ where $z\left(z\right)$ was the Riemann zeta function. The Bernoulli numbers appear in the Taylor series expansions of the tangent and hyperbolic tangent functions, in formulas for the sum of powers of the first positive integers, in the Euler–Maclaurin formula and in expressions for certain values of the Riemann zeta function [2].

Another connection with the primes was provided by $d\left(n\right)=s_0\left(n\right)$ for the sampled numerical values from 1 to n in the grid-stratfiable, oviposition, eco-endmember, *An. arabiensis*, endemic, transmission-oriented, parameter, estimator,LULC dataset which in this research was found to be asymptotic to $\frac{\sum_{k=1}^{n}d(k)}{n}\sim\ln n+2g-1$. De laValléePoussin [7] proved that if a large number n is divided by all primes$\leq n$, then the average amount by which the quotient is less than the next whole number is g [2]. An identity for g in our malaria, regression-based, eco-endmember, geo-spectral, forecast, vulnerability,LULC model was then provided by $g=\frac{S_0(z)-K_0(z)}{I_0(z)}-\ln\left(\frac{z}{2}\right)$ where $I_0\left(z\right)$ was a modified Bessel function of the first kind, $K_0\left(z\right)$ was a modified Bessel function of the second kind, and $S_0(z)=\sum_{k=0}^{\infty}\frac{\left(\frac{z}{2}\right)^{2k}H_k}{(k!)^2}$ where H_n was a harmonic number. For non-integer α, $Y_\alpha(x)$ is related to $J_\alpha(x)$ by: $Y_\alpha(x)=\frac{J_\alpha(x)\cos(\alpha\pi)-J_{-\alpha}(x)}{\sin(\alpha\pi)}$.[4]. In the case of integer order n, the function is defined by taking the limit as a non-integer α tends to n: $Y_n(x)=\lim_{\alpha\to n}Y_\alpha(x)$.[2]. In this research, the Bessel functions of the second kind, were denoted by $Y_\alpha(x)$, and by $N_\alpha(x)$, which were actually solutions of the Bessel differential equation employing a singularity at the origin (x = 0).This provided an efficient iterative algorithm for g for the malaria model by computing $B_k=\frac{B_{k-1}n^2}{k^2}=A_k=\frac{1}{k}\left(\frac{A_{k-1}n^2}{k}+B_k\right)=U_kV_k=U_{k-1}+A_k$ and $V_k=V_{k-1}+B_k$ with $A_0=-\ln nB_0=1U_0=A_0$ and $V_0=1$ Reformulating this identity rendered the limit $\lim_{n\to\infty}\left[\sum_{k=0}^{\infty}\frac{\left(\frac{n^k}{k!}\right)^2H_k}{\sum_{k=0}^{\infty}\left(\frac{n^k}{k!}\right)^2}-\ln n\right]=g$ Infinite products involving g also arose from the Barnes G-function using the positive integer n. In mathematics, the Barnes G-function $G(z)$ is a function that is an extension of superfactorials to the complex numbers which is related to the Gamma function [3]. In this research, this function provided $\prod_{n=1}^{\infty}e^{-1+1/(2n)}\left(1+\frac{1}{n}\right)^n=\frac{e^{1+g/2}}{\sqrt{2p}}$ and also the equation $\prod_{n=1}^{\infty}e^{-2+2/n}\left(1+\frac{2}{n}\right)^n=\frac{e^{3+2g}}{2p}$.The Barnes G-function was then linearly defined in our time-series dependent, *An. arabiensis*, regression-based,ovisposition, ento-ecoepidemiological, prognosticative, risk model which then generated

$G(z+1)=(2p)^{z/2}\exp\left(-\left(z(z+1)+g z^2\right)/2\right)\prod_{n=1}^{\infty}\left(\left(1+\frac{z}{n}\right)^n\exp\left(-z+z^2/(2n)\right)\right)$ where γ was the Euler–Mascheroni constant, exp(*x*) = e^x, and $\prod$ was capital pi notation. The Euler-Mascheroni constant was then rendered by the expressions $g=-G'(1)=-y_0(1)$ where $y_0(x)$ was the digamma function $g=\lim_{s\to 1}\left[z(s)-\frac{1}{s-1}\right]$ and the asymmetric limit form of $g=\lim_{s\to 1^+}\sum_{n=1}^{\infty}\left(\frac{1}{n^s}-\frac{1}{s^n}\right)$ and $g=\lim_{x\to\infty}\left[x-G\left(\frac{1}{x}\right)\right]$.

In mathematics, the digamma function is defined as the logarithmic derivative of the gamma function: $y(x)=\frac{d}{dx}\ln G(x)=\frac{G'(x)}{G(x)}$ where it is the first of the polygamma functions. In our model the digamma function, $\psi_0(x)$ was then related to the harmonic numbers in that $y(n)=H_{n-1}-g$ where H_n was the n^{th} harmonic number, and γ was the Euler-Mascheroni constant. In mathematics, the *n*-th harmonic number is the sum of the reciprocals of the first *n* natural numbers[2].The difference between the n^{th} convergent in equation (◇) and γ in our district-level regression-based model was then calculated by $\sum_{k=1}^{n}\frac{1}{k}-\ln n-g=\int_n^{\infty}\frac{x-\lfloor x\rfloor}{x^2}dx$ where $\lfloor x\rfloor$ was the floor function which satisfied the inequality $\sum_{k=1}^{n}\frac{1}{k}-\ln n-g=\int_n^{\infty}\frac{x-\lfloor x\rfloor}{x^2}dx$.The symbol g was then $g\approx e^g\approx 1.781072$. This led to the radical representation of the geosampled district-level, endmember, grid-stratified, sub-meter resolution, aquatic, larval habitat, covariate coefficients as $e^g=\left(\frac{2}{1}\right)^{1/2}\left(\frac{2^2}{1\times 3}\right)^{1/3}\left(\frac{2^3\times 4}{1\times 3^3}\right)^{1/4}\left(\frac{2^4\times 4^4}{1\times 3^6\times 5}\right)^{1/5}$ which was related to the double series $g=\sum_{n=1}^{\infty}\frac{1}{n}\sum_{k=0}^{n-1}(-1)^{k+1}\binom{n-1}{k}\ln(k+1)$ and $\binom{n}{k}$ a binomial coefficient. Thereafter, another proof of product in the our spatiotemporal district-level, malarial regression model was provided by the equation $\frac{p}{2}=\left(\frac{2}{1}\right)^{1/2}\left(\frac{2^2}{1\times 3}\right)^{1/4}\left(\frac{2^3\times 4}{1\times 3^3}\right)^{1/8}\left(\frac{2^4\times 4^4}{1\times 3^6\times 5}\right)^{1/16}$.The solution was then made even clearer by changing $n\to n+1$. In this research, both these regression-based formulas were also analogous to the product for *e* which was then rendered by calculating $e=\left(\frac{2}{1}\right)^{1/1}\left(\frac{2^2}{1\times 3}\right)^{1/2}\left(\frac{2^3\times 4}{1\times 3^3}\right)^{1/3}\left(\frac{2^4\times 4^4}{1\times 3^6\times 5}\right)^{1/4}$.

The Digamma was then computed in the complex plane outside negative integersusingo $\psi(z)=-\gamma+\sum_{n=0}^{\infty}\frac{z-1}{(n+1)(n+z)}=-\gamma+\sum_{n=0}^{\infty}\left(\frac{1}{n+1}-\frac{1}{n+z}\right)\qquad z\neq 0,-1,-2,-3,\ldots$ We evaluated infinite sums of rational endmember, aquatic, larval habitat, geo-spectrotemporal functions, (i.e., $\sum_{n=0}^{\infty}u_n=\sum_{n=0}^{\infty}\frac{p(n)}{q(n)}$, where *p*(*n*) and *q*(*n*) were polynomials of *n*. Performing partial fraction on u_n in the complex field, in the case when all roots of *q*(*n*) are simple roots, $u_n=\frac{p(n)}{q(n)}=\sum_{k=1}^{m}\frac{a_k}{n+b_k}$. For the series to converge, we parsimoniously robust;y employed $\lim_{n\to\infty}nu_n=0$, Hence $\sum_{k=1}^{m}a_k=0$, and $\sum_{n=0}^{\infty}u_n=\sum_{n=0}^{\infty}\sum_{k=1}^{m}\frac{a_k}{n+b_k}=\sum_{n=0}^{\infty}\sum_{k=1}^{m}a_k\left(\frac{1}{n+b_k}-\frac{1}{n+1}\right)=\sum_{k=1}^{m}\left(a_k\sum_{n=0}^{\infty}\left(\frac{1}{n+b_k}-\frac{1}{n+1}\right)\right)=-\sum_{k=1}^{m}a_k\left(\psi(b_k)+\gamma\right)=-\sum_{k=1}^{m}a_k\psi(b_k)$. With the series expansion of higher rank polygamy function a generalized formula can be given as $\sum_{n=0}^{\infty}u_n=\sum_{n=0}^{\infty}\sum_{k=1}^{m}\frac{a_k}{(n+b_k)^{r_k}}=\sum_{k=1}^{m}\frac{(-1)^{r_k}}{(r_k-1)!}a_k\psi^{(r_k-1)}(b_k)$, provided the series on the left converges[2].

International Research Journal of Computer Science and Application
Vol. 2, No. 1, March 2018, pp. 1-181
Available Online at http://acascipub.com/Journals.php

In this research the digamma function satisfied a reflection formula similar to that of the Gamma function, $\psi(1-x)-\psi(x)=\pi\cot(\pi x)$. However, the digamma function satisfies the recurrence relation $\psi(x+1)=\psi(x)+\frac{1}{x}$. in the malaria, mosquito, oviposition, ento-ecoepidemiological, endmember, forecast, vulnerability model. Thus, ia "telescope" measurement 1/x, followed since $\Delta[\psi](x)=\frac{1}{x}$ where Δ was the forward difference operator. This satisfies the recurrence relation of a partial sum of the harmonic series in the model output thus implying the formula $\psi(n) = H_{n-1}-\gamma$ where γ is the Euler-Mascheroni constant. More generally, $\psi(x+1)=-\gamma+\sum_{k=1}^{\infty}\left(\frac{1}{k}-\frac{1}{x+k}\right)$. Actually, ψ is the only solution of the functional equation $F(x+1)=F(x)+\frac{1}{x}$ that is monotone on $\mathbb{R}^+$ and satisfies $F(1)=-\gamma$[4]. This fact follows immediately from the uniqueness of the Γ function given its recurrence equation and convexity-restriction. This implies the useful difference equation : $\psi(x+N)-\psi(x)=\sum_{k=0}^{N-1}\frac{1}{x+k}$ The digamma has a Gaussian sum of the form $\frac{-1}{\pi k}\sum_{n=1}^{k}\sin\left(\frac{2\pi nm}{k}\right)\psi\left(\frac{n}{k}\right)=\zeta\left(0,\frac{m}{k}\right)=-B_1\left(\frac{m}{k}\right)=\frac{1}{2}-\frac{m}{k}$ for integers $0<m<k$. Here, ζ(*s*,*q*) is the Hurwitz zeta function and $B_n(x)$ is a Bernoulli polynomial. A special case of the multiplication theorem is $\sum_{n=1}^{k}\psi\left(\frac{n}{k}\right)=-k(\gamma+\log k)$, and a neat generalization of this is $\sum_{p=0}^{q-1}\psi(a+p/q)=q(\psi(qa)-\log(q))$, where *q* must be a natural number, but 1-*qa* not. For positive integers *m* and *k* (with *m* < *k*), the digamma function may be expressed in finite many terms of elementary functions as

The complex conjugate of a complex number $z \equiv a+b\,i$ was defined to be $\bar{z} \equiv a-b\,i.$ in the grid-stratifiable, sub-meter resolution, ento-ecoepidemiological, forecast, vulnerability model.The conjugate matrix of a matrix $\mathbf{A}=(a_{ij})$ is the matrix obtained by replacing each element a_{ij} with its complex conjugate, $\bar{\mathbf{A}}=(\bar{a}_{ij})$ (see Arfken 1985,). The complex conjugate is implemented in *Mathematica* as Conjugate[*z*]. The matrix obtained from the given matrix A by this combined operation (ie.,conjugate transpose A^H of A) ,.The terms adjoint matrix, adjugate matrix, Hermitian conjugate, and Hermitian adjoint are also used, as are the notations $\mathbf{A}^{\dagger}$ and $\mathbf{A}^{*}$. In this work, A^H was used to denote the conjugate transpose matrix and $a^{\dagger}$ was used to denote the adjoint operator in the *An. arabiensis* risk model. By definition, the complex conjugate satisfied $\bar{\bar{z}}=z$.The complex conjugate is distributive under complex addition, $\overline{z_1+z_2}=\bar{z}_1+\bar{z}_2$, since the $\overline{(a_1+i\,b_1)+(a_2+i\,b_2)}=\overline{(a_1+a_2)+i\,(b_1+b_2)}=(a_1+a_2)-i\,(b_1+b_2)=(a_1-i\,b_1)+(a_2-i\,b_2)=\overline{a_1+i\,b_1}+\overline{a_2+i\,b_2}$, and distributive over complex multiplication was $\overline{z_1\,z_2}=\bar{z}_1\,\bar{z}_2$,

There was an extremely important relationship between the autocorrelation and the Fourier transform. This may have been related to the Wiener-Khinchin theorem The Wiener–Khinchin theorem (also known as the Wiener–Khintchine theorem and sometimes as the Wiener–Khinchin–Einstein theorem or the Khinchin–Kolmogorov theorem) states that the autocorrelation function of a wide-sense-stationary random process has a spectral decomposition given by the power spectrum of that process. For continuous time, the Wiener—Khinchin theorem [2] says that if x is a wide-sense stationary process such that its autocorrelation function (i..e., autocovariance) can be defined in terms of statistical expected value E, $r_{xx}(\tau)=\mathrm{E}\left[x(t)x^*(t-\tau)\right]$ and is finite at every lag τ. As such, there exists a monotone function $F(f)$ in the frequency domain $-\infty<f<\infty$ such that $r_{xx}(\tau)=\int_{-\infty}^{\infty}e^{2\pi i\tau f}dF(f)$ is anthe integral. This is a kind of spectral decomposition of the autocorrelation function. F is called the power spectral distribution function, and is a statistical distribution function[3].

Note that the Fourier transform of $x(t)$ did not exist in the malaria model, because stationary random functions are not generally either square integrable or absolutely integrable. Nor was r_{xx} assumed to be absolutely integrable in the frequencty, signature, LULC model ouutput, so it need not have a Fourier transform either. But if $F(f)$ is absolutely continuous, for example if the process is purely in deterministic in a sub-mter resolution, malaria, mosquito,

eco-endmember model for asymptotically geo-spectrotemporally remotetly, targeting, eco-georeferenceable, un-geosampled, seasonal, hyperproductive, aquatic, larval habitat, foci then an experimenter may define the power spectral density of $x(t)$ by taking the derivative of F, and putting $S_{xx}(f) = F'(f)$ almost everywhere in the model since the theorem simplifies to $r_{xx}(\tau) = \int_{-\infty}^{\infty} S_{xx}(f) e^{2\pi i \tau f} df$. I Suppose x_n, from $n = 0$ to $N - 1$ is a time series (discrete time) with zero mean in the model forecasts. Suppose that it is a sum of a finite number of periodic habitat components (all frequencies are positive): $x_n = \sum_k [a_k \cos(2\pi \nu_k n) + b_k \sin(2\pi \nu_k n)]$. The variance of x_n is, for a zero-mean function then would be given by $\frac{1}{N} \sum_{n=0}^{N-1} x_n^2$. If these data were samples taken from an electrical signal, this would be its average power (power is energy per unit time, so it is analogous to variance if energy is analogous to the amplitude squared).Now, for simplicity, suppose the signal extends infinitely in time, so we pass to the limit as $N \to \infty$. If the average power is bounded, which is almost always the case in reality, then the following limit exists and is the variance of the data. $\lim_{N \to \infty} \frac{1}{N} \sum_{n=0}^{N-1} x_n^2$. Again, for simplicity, we will pass to continuous time, and assume that the signal extends infinitely in time in both directions. Then these two formulasbecome $x(t) = \sum_k [a_k \cos(2\pi \nu_k t) + b_k \sin(2\pi \nu_k t)]$ and $\lim_{T \to \infty} \frac{1}{2T} \int_{-T}^{T} x(t)^2 dt$.

But obviously the root mean square of either $\cos$ or $\sin$ is $1/\sqrt{2}$, so the variance of $a_k \cos(2\pi \nu_k t)$ in the malaria model was $a_k^2/2$ and that of $b_k \sin(2\pi \nu_k t)$ was $b_k^2/2$. Hence, the power of $x(t)$ which comes from the component with frequency ν_k is $(a_k^2 + b_k^2)/2$. All these contributions add up to the power of $x(t)$.Then the power as a function of frequency is obviously $(a_k^2 + b_k^2)/2$, and its statistical cumulative distribution function $F(\nu)$ will be $F(\nu) = \sum_{k:\nu_k < \nu} \frac{1}{2}(a_k^2 + b_k^2)$.

F is a step function, monotonically non-decreasing[2]. Its jumps occur at the frequencies of the periodic components of x, and the value of each jump is the power or variance of that component. The variance is the covariance of the data with itself. If we now consider the same data but with a lag of τ, we can take the covariance of $x(t)$ with $x(t + \tau)$, and define this to be the autocorrelation function c of the signal (or data) $c(\tau) = \lim_{T \to \infty} \frac{1}{2T} \int_{-T}^{T} x(t) x(t + \tau) dt$. When it exists, it is an even function of τ. If the average power is bounded, then c exists everywhere, is finite, and is bounded by $c(0)$, which is the power or variance of the data.

It is elementary to show that c can be decomposed into periodic components with the same periods as x: $c(\tau) = \sum_k \frac{1}{2}(a_k^2 + b_k^2) \cos(2\pi \nu_k \tau)$. This is in fact the spectral decomposition of c over the different frequencies, and is obviously related to the distribution of power of x over the frequencies: the amplitude of a frequency component of c is its contribution to the power of the signal now one assumes that r and S satisfy the necessary conditions for Fourier inversion to be valid[2]. the Wiener—Khinchin theorem takes the simple form of saying that r and S are a Fourier transform pair, and $S_{xx}(f) = \int_{-\infty}^{\infty} r_{xx}(\tau) e^{-2\pi i f \tau} d\tau$. [3].

Relations to other matrix operations may be possible for future, ento-ecoepidemiological, forecast, vulnerability, aquatic, larval habitat, capture point, *An. arabiensis*, endemic transmission, risk modeling. For example linearity and associativity may be quantitated employing the Kronecker product which is a special case of the tensor product, so the endemic forecasts are bilinear whereby, $\mathbf{A} \otimes (\mathbf{B} + \mathbf{C}) = \mathbf{A} \otimes \mathbf{B} + \mathbf{A} \otimes \mathbf{C}$, $(\mathbf{A} + \mathbf{B}) \otimes \mathbf{C} = \mathbf{A} \otimes \mathbf{C} + \mathbf{B} \otimes \mathbf{C}$, and also $(k\mathbf{A}) \otimes \mathbf{B} = \mathbf{A} \otimes (k\mathbf{B}) = k(\mathbf{A} \otimes \mathbf{B})$, where A, B and C are matrices and *k* is a scalar. In general A ⊗ B and B ⊗ A would be different matrices in a robust, endemic transmission, malaria, mosquito, oviposition, risk model however, A ⊗ B and B ⊗ A are permutation equivalent, meaning that there exist permutation matrices P and Q such that

$\mathbf{A} \otimes \mathbf{B} = \mathbf{P}\,(\mathbf{B} \otimes \mathbf{A})\,\mathbf{Q}$. Further, if A and B are square matrices in the endemic transmission risk model, then A ⊗ B and B ⊗ A would be even permutation similar, meaning that $P = Q^T$. Then the mixed-product property and the inverse of a Kronecker product may be determined. For example, if A, B, C and D are matrices of such size that one can form the matrix products AC and BD, then $(\mathbf{A} \otimes \mathbf{B})(\mathbf{C} \otimes \mathbf{D}) = \mathbf{AC} \otimes \mathbf{BD}$ in the vulnerability, forecasts statsically targeting the significant endemic trasnmission-oriented, seasonal geosampled explanatory, endmember, covariates this would be the mixed-product property, because it mixes the ordinary matrix product and the Kronecker product. It then follows that A ⊗ B would be invertible if and only if A and B are invertible in a dataset of grid-stratified, sub-meter resolution, aquatic, larval habitat, covariate coefficients endemic transmission risk model in which case the inverse would be given by $(\mathbf{A} \otimes \mathbf{B})^{-1} = \mathbf{A}^{-1} \otimes \mathbf{B}^{-1}$. Additionally the operation of transposition would be distributive over the Kronecker product $(\mathbf{A} \otimes \mathbf{B})^T = \mathbf{A}^T \otimes \mathbf{B}^T$. in the forecasts. As such a detrminant of the ento-ecoepiemiological, predictive, risk model may be qunatiated. For example, if we let A be an $n \times n$ matrix and let B be a $p \times p$ matrix then $|\mathbf{A} \otimes \mathbf{B}| = |\mathbf{A}|^p |\mathbf{B}|^n$. The exponent in |A| would be the order of B and the exponent in |B| would be the order of A. As such the Kronecker sum and exponentiation in the endemic transmission, risk model could be parsimoniously be regressed but only if A is $n \times n$, B is $m \times m$ and I_k denotes the $k \times k$ identity matrix. By so doing then we defines the Kronecker sum ⊕, by $\mathbf{A} \oplus \mathbf{B} = \mathbf{A} \otimes \mathbf{I}_m + \mathbf{I}_n \otimes \mathbf{B}$ in the model forecasts targeting the significant endemic trasnmission-oriented seasonal-sampled, hyperproductive, vector arthropod, aquatic, larval habitat, explanatory covariate

Further the spectrum in the endemic transmission-oriented, *An. arabiensis* seasonal geosampled, endmember, model can be quanatized For example, suppose that A and B are square matrices of size n and m respectively. If $\lambda_1, \ldots, \lambda_n$ are the eigenvalues of A and $\mu_1, \ldots, \mu_m$ are those of B listed according to multiplicity in the grid-stratified, sub-meter resolution, aquatic, larval habitat, covariate coefficient model then the eigenvalues of A ⊗ B would be $\lambda_i \mu_j, \qquad i = 1, \ldots, n,\ j = 1, \ldots, m.$ It thus follows that the trace and determinant of a optimizable Kronecker product may be optimally given by $\operatorname{tr}(\mathbf{A} \otimes \mathbf{B}) = \operatorname{tr}\mathbf{A}\,\operatorname{tr}\mathbf{B} \quad \text{and} \quad \det(\mathbf{A} \otimes \mathbf{B}) = (\det \mathbf{A})^m (\det \mathbf{B})^n$. As such singular values derived from a seasonal, endemic, transmission, oriented grid-stratified, sub-meter resolution, malaria, mosquito, aquatic, larval habitat, risk model can be generated. If A and B are rectangular matrices, singular values may also be determined. Suppose that A has r_A nonzero singular values, namely $\sigma_{\mathbf{A},i}, \qquad i = 1, \ldots, r_{\mathbf{A}}.$ Then denoting the nonzero singular values of B by $\sigma_{\mathbf{B},i}, \qquad i = 1, \ldots, r_{\mathbf{B}}$ would optimally determine any uncertainty capture point, endmember coefficients. Then the Kronecker product A ⊗ B will have $r_A r_B$ nonzero singular values, namely $\sigma_{\mathbf{A},i}\sigma_{\mathbf{B},j}, \qquad i = 1, \ldots, r_{\mathbf{A}},\ j = 1, \ldots, r_{\mathbf{B}}$. since the rank of a matrix equals the number of nonzero singular values in a seasonal, predictive, vector, arthropod-related, risk model we would then derive $\operatorname{rank}(\mathbf{A} \otimes \mathbf{B}) = \operatorname{rank}\mathbf{A}\,\operatorname{rank}\mathbf{B}$.

As such, in terms of the relation to the abstract tensor product: in an ento-ecoepidemiological, eco-georeferenceable, *An. arabiensis* dataset of seasonal, predictive, vector, arthropod-related, explanatory, endemic, transmission oriented, endmember dataset, the Kronecker product of matrices would correspond to the abstract tensor product of the risk maps delineating the endemic transmission zones. Specifically, if the vector spaces *V*, *W*, *X*, and *Y* have bases $\{v_1, \ldots, v_m\}$, $\{w_1, \ldots, w_n\}$, $\{x_1, \ldots, x_d\}$, and $\{y_1, \ldots, y_e\}$, respectively, and if the matrices *A* and *B* represent the linear transformations $S : V \to X$ and $T : W \to Y$, respectively in the appropriate bases, then the matrix $A \otimes B$ would represent the tensor product of any two . endemic transmission, larval habitat coavraite maps. Subsequently $S \otimes T : V \otimes W \to X \otimes Y$ with respect to the basis $\{v_1 \otimes w_1, v_1 \otimes w_2, \ldots, v_2 \otimes w_1, \ldots, v_m \otimes w_n\}$ of $V \otimes W$ and the similarly defined basis of $X \otimes Y$ with the property that $A \otimes B(v_i \otimes w_j)$ would equal $(Av_i) \otimes (Bw_j)$, where i and j are integers in the proper range. When *V* and *W* are Lie algebras, and $S: V \to V$ and $T: W \to W$ are Lie algebra homomorphisms, the Kronecker sum of *A* and *B* represents the induced Lie algebra homomorphisms $V \otimes W \to V \otimes W$[4]. Thereafter, based on the relations to products of the endemic, transmission-oriented, malaria mosquito, seasonal, endmember graphs, the Kronecker product of the adjacency matrices of ant two graphs outputs would be the adjacency matrix of the tensor product graph. The Kronecker sum of the adjacency matrices of two graphs would then be based on the adjacency matrix of the Cartesian product graph. The Kronecker product can be used to get a convenient representation for some matrix equations[2]

Consider for instance the equation AXB = C, where A, B and C are given matrices and the matrix X is the unknown. We can rewrite this equation as $(\mathbf{B}^\top \otimes \mathbf{A})\ \operatorname{vec}(\mathbf{X}) = \operatorname{vec}(\mathbf{AXB}) = \operatorname{vec}(\mathbf{C})$. Here, vec(X) denotes the

vectorization of the matrix X formed by stacking the columns of X into a single column vector. It now follows from the properties of the Kronecker product that the equation AXB = C has a unique solution if and only if A and B are nonsingular (see Horn & Johnson (1991, Lemma 4.3.1).

Ito's Lemma is also referred to currently as the Itō–Doeblin Theorem in recognition of the recently discovered work of Wolfgang Doeblin.[1] In its simplest form, Itō's lemma states the following: for an Itō drift-diffusion process $dX_t = \mu_t\,dt + \sigma_t\,dB_t$ and any twice differentiable function $f(t, x)$ for quantitating, any two real geo-spatiotemporal, geosampled, time series, malaria, mosquito, eco-georferenced, *An. arabiensis*, grid-stratified, sub-meter resolution, aquatic, larval habitat, covariate coefficient, eco-endmember, LULC predictor variables *t* and *x*, where one has $df(t, X_t) = \left(\frac{\partial f}{\partial t} + \mu_t\frac{\partial f}{\partial x} + \frac{\sigma_t^2}{2}\frac{\partial^2 f}{\partial x^2}\right)dt + \sigma_t\frac{\partial f}{\partial x}\,dB_t.$ This immediately implies that $f(t, X)$ is itself an Itō drift-diffusion process.

Ito's lemma explicatively states $df\,(t, X_t) = \dot{f}_t\,(t, X_t)\;dt + \nabla_{X_t}^T f \cdot dX_t + \frac{1}{2}\,dX_t^T \cdot \nabla_{X_t}^2 f \cdot dX_t$ where $X_t = (X_{t,1}, X_{t,2}, \ldots, X_{t,n})^T$ is a vector of Itō processes, $\dot{f}_t\,(t, X)$ is the partial differential w.r.t. *t*, $\nabla_X^T f$ is the gradient of *f* w.r.t. *X*, and $\nabla_X^2 f$ is the Hessian matrix of *f* w.r.t. *X*. More generally, the above formula also holds for any continuous *d*-dimensional semimartingale $X = (X^1, X^2, \ldots, X^d)$, and twice continuously differentiable and real valued function *f* on R^d. Some people prefer to present the formula in another form with cross variation shown explicitly as follows, $f(X)$ is a semimartingale satisfying $df(X_t) = \sum_{i=1}^{d} f_i(X_t)\,dX_t^i + \frac{1}{2}\sum_{i,j=1}^{d} f_{i,j}(X_t)\,d[X^i, X^j]_t.$ In this expression, the term f_i represented the partial derivative of $f(x)$ with respect to x^i, and $[X^i, X^j]$ is the quadratic covariation process of X^i and X^j.

In , Ω an open subset of $\mathbb{R}^d$, $p \in [1; +\infty]$ and $s \in \mathbb{N}$, the Sobolev space $W^{s,p}(\mathbb{R}^d)$ is defined by $W^{s,p}(\Omega) = \{f \in L^p(\Omega) : \forall\, |\alpha| \le s,\, \partial_x^\alpha f \in L^p(\Omega)\}$, where $\alpha = (\alpha_1, \ldots, \alpha_d)$, $|\alpha| = \alpha_1 + \ldots + \alpha_d$, and the derivatives $\partial_x^\alpha f = \partial_{x_1}^{\alpha_1} \cdots \partial_{x_d}^{\alpha_d} f$ are taken in a weak sense. When endowed with the norm $\|f\|_{s,p,\Omega} = \sum_{|\alpha| \le s} \|\partial_x^\alpha f\|_{L^p(\Omega)}$, $W^{s,p}(\Omega)$ is a Banach space. In the special case $p = 2$, $W^{s,2}(\Omega)$ would be denoted by $H^s(\Omega)$ in an endemic, ento-ecoepidemiological, vector arthropod, malaria, mosquito, aquatic, larval habitat, prognosticative, endmember model. This space is a Hilbert space for the inner product $\langle f, g\rangle_{s,\Omega} = \sum_{|\alpha| \le s} \langle \partial_x^\alpha f, \partial_x^\alpha g\rangle_{L^2(\Omega)} = \sum_{|\alpha| \le s} \int_\Omega \partial_x^\alpha f\, \overline{\partial_x^\alpha g}\, d\mu.$

We modeled given a function f(x) at a hypeprproductive, *An. arabiensis* capture point a in the domain a of f. The best linear approximation to f(x) near a was given by the linear function $L_a(x) = f(a) + f'(a)(x-a)$ The graph of the linear function $L_a(x)$ passed through the capture point [e.g., a,f(a)) and has slope f '(a)]. The the endmember functions f and L_a had the same value at a and they have the same derivative at a. $L_a(a) = f(a)$ $L'_a(a) = f'(a)$ Of course, the second and higher derivatives of linear functions were all zero, but a quadratic function had two nonzero derivatives. We were able to prove that quadratic function $Q_a(x)$ derived from an oviposition, endmember, forecast, vulnerability model has the properties that the functions f and Q_a have the same value, first derivative, and second dervative at a. $Q_a(a) = f(a)$ $Q'_a(a) = f'(a)$ $Q''_a(a) = f''(a)$

We vonsidered the cosine function f(x)=cos(x) and let a=0 in the malaria mosquito model It was not hard to verify that if we let $Q(x) = 1 - x^2/2$, then f and Q had the same first two derivatives at 0. In addition, the graph of Q in Table 15 resembles the graph of f very near 0.

International Research Journal of Computer Science and Application
Vol. 2, No. 1, March 2018, pp. 1-181
Available Online at http://acascipub.com/Journals.php

Table 15 The best linear approximation in a sub-mter resolution, grid-stratfiable, endmember, grid-stratfiiable malaria, mosquito, ovipsoition model to the cosine function near 0 for f(x)=cos(x), as given by $L_0(x)=1$.

f(x) = cos(x) Q(x) = 1 - $x^2/2$	f(0) = cos(0) = 1 Q(0) = 1 - 0^2 = 1
f '(x) = -sin(x) Q'(x) = -x	f '(0) = -sin(0) = 0 Q'(0) = -0 = 0
f "(x) = -cos(x) Q"(x) = -1	f "(0) = -cos(0) = -1 Q'-(0) = -1

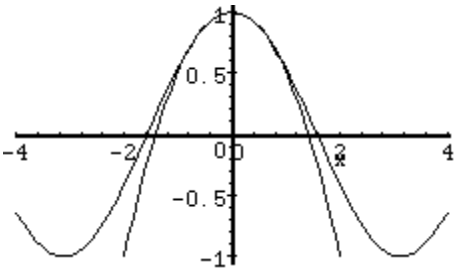

We also found a quadratic polynomial function Q(x) that had the same two first derivative capture point, seasonal, hyperproductive, aquatic, larval habitat, density count values as the natural logarithm g(x)=ln(x) at x=1. We were able to confirm that the following quadratic function could regressively quantitate to any given f and a in the model. That is, with the quadratic Qa listed below, the functions Q_a and f agree at a seasonal, eco-georferenecable, capture point, hyperproductive foci as do the derivatives Q'a and f ', as do the second derivatives Q"$_a$ and f ' in ' $Q_a(x)$ = f(a) + f '(a)(x-a) + f "(a)$(x-a)^2/2$.This model represented the best quadratic approximation to f(x) in the model.

We may define functions on discontinuous stochastic processes in an oviposition, eco-georeferenceable, aquatic ,larval habitat, geo-spectrotemporal, capture point, malaria model. For example, if a vector ecologist Let h be the jump intensity, the Poisson process model for jumps will be the probability of one jump in the interval $[t,t + \Delta t]$ which would then be $h\Delta t$ plus higher order terms. h could be a constant, a deterministic function of time, or a stochastic process. The survival probability $p_s(t)$ is the probability that no jump has occurred in the interval $[0,t]$. The change in the survival probability is $dp_s(t) = -p_s(t)h(t)\,dt.$ so $p_s(t) = \exp\left(-\int_0^t h(u)\,du\right).$ If we let $S(t)$ be a discontinuous stochastic process hen we can write $S(t^-)$ for the value of S as we approach t from the left. Write $d_jS(t)$ for the non-infinitesimal change in $S(t)$ as a result of a jump. Then $d_jS(t) = \lim_{\Delta t\to 0}(S(t+\Delta t) - S(t^-))$ If we let z be the magnitude of the jump and let $\eta(S(t^-),z)$ be the distribution of z. The expected magnitude of the jump in the oviposition, eco-georeferenceable, aquatic , larval habitat, geo-spectrotemporal, capture point, malaria model then will be $E[d_jS(t)] = h(S(t^-))\,dt\int_z z\eta(S(t^-),z)\,dz.$. A researcher can then define $dJ_S(t)$, a compensated process and martingale, as the equation $dJ_S(t) = d_jS(t) - E[d_jS(t)] = S(t) - S(t^-) - (h(S(t^-))\int_z z\eta(S(t^-),z)\,dz)\,dt.$ .Hence

$$d_jS(t) = E[d_jS(t)] + dJ_S(t) = h(S(t^-))(\int_z z\eta(S(t^-),z)\,dz)dt + dJ_S(t).$$

A medical entomologist or malariologist may also consider a function $g(S(t),t)$ of jump process $dS(t)$. If $S(t)$ jumps by Δs then $g(t)$ jumps by Δg. The Δg is drawn from distribution $\eta_g()$ which may depend on $g(t^-)$, dg and $S(t^-)$. The jump part of g is $g(t) - g(t^-) = h(t)\,dt\int_{\Delta g}\Delta g\eta_g(\cdot)\,d\Delta g + dJ_g(t).$ If S contains drift, in an eco-georeferenecable, spectrotemporal, eco-geographic, LULC, eco-endmember, malaria, mosquito, aquatic, larval habitat, forecast, vulnerability model diffusion and jump parts, then Itō's Lemma for $g(S(t),t)$ then

$$dg(t) = \left(\frac{\partial g}{\partial t} + \mu\frac{\partial g}{\partial S} + \frac{1}{2}\sigma^2\frac{\partial^2 g}{\partial S^2} + h(t)\int_{\Delta g}(\Delta g\eta_g(\cdot)\,d\Delta g)\right)dt + \frac{\partial g}{\partial S}\sigma\,dW(t) + dJ_g(t).$$

Itō's lemma for a process which is the sum of a drift-diffusion process and a jump process is just the sum of the Itō's lemma for the individual parts.

Itō's lemma can also be applied to general d-dimensional semimartingales in an oviposition, eco-georeferenceable, aquatic, larval habitat, geo-spectrotemporal, geosampled, eco-georferenced, capture point, malaria, forecast, vulnerability models which need not be continuous. In general, a semimartingale is a càdlàg process, and an additional term needs to be added to the formula to ensure that the jumps of the process are correctly given by Itō's lemma. For any cadlag process Y_t, the left limit in t is denoted by Y_{t-}, which is a left-continuous process. The jumps are written as $\Delta Y_t = Y_t - Y_{t-}$. Then, Itō's lemma states that if $X = (X^1,X^2,\ldots,X^d)$ is a d-dimensional semimartingale and f is a

twice continuously differentiable, real-valued function on R^d then $f(X)$ is a semimartingale, and therefore a malariologist or medical entomologist could then optimally generate: $f(X_t) = f(X_0) + \sum_{i=1}^{d} \int_0^t f_i(X_{s-})\, dX_s^i + \frac{1}{2} \sum_{i,j=1}^{d} \int_0^t f_{i,j}(X_{s-})\, d[X^i, X^j] + \sum_{s \le t} \left(\Delta f(X_s) - \sum_{i=1}^{d} f_i(X_{s-})\, \Delta X_s^i - \frac{1}{2} \sum_{i,j=1}^{d} f_{i,j}(X_{s-})\, \Delta X_s^i\, \Delta X_s^j \right)$. This differs from the formula for continuous semimartingales by the additional term summing over the jumps of X, which ensures that the jump of the right hand side at time t is $\Delta f(X_t)$.

A formal proof of the lemma requires us to take the limit of a sequence of random variables (e.g., ovispoition, eco-georferenecable, sub-meter resolution, grid-stratfiable, eco-georeferenceable, capture point, wavelength LULC frequnecies) which is not done here. Instead, we give a sketch of how one can derive Itō's lemma by expanding a Taylor series and applying the rules of stochastic calculus. For example, if we assume the Itō process is in the form of an expanding $f(x, t)$ in a ovispoition, forecast, vulnerability, endmember, Taylor series in x and for t we have $df = \frac{\partial f}{\partial x}\, dx + \frac{\partial f}{\partial t}\, dt + \frac{1}{2} \frac{\partial^2 f}{\partial x^2}\, dx^2 + \cdots$ Substituting $a\, dt + b\, dB$ for dx into the eco-georeferenceable, aquatic, larval habitat, geo-spectrotemporal, ento-ecoepidemiological, forecast, vulnerability, endmember, capture point, malaria model can be conducted by $df = \frac{\partial f}{\partial x}(a\, dt + b\, dB) + \frac{\partial f}{\partial t}\, dt + \frac{1}{2} \frac{\partial^2 f}{\partial x^2}(a^2\, dt^2 + 2ab\, dt\, dB + b^2\, dB^2) + \cdots$. In the limit as dt tends to 0, the dt^2 and $dt\, dB$ terms disappear, but the dB^2 term tends to dt. The latter can be shown if we prove that $dB^2 \to E(dB^2)$ since $E(dB^2) = dt$ existes in the model outputs Deleting the dt^2 and $dt\, dB$ terms, substituting dt for dB^2, and collecting the dt and dB terms, we may obtain $df = \left(a \frac{\partial f}{\partial x} + \frac{\partial f}{\partial t} + \frac{1}{2} b^2 \frac{\partial^2 f}{\partial x^2} \right) dt + b \frac{\partial f}{\partial x}\, dB$ as required for proper regression quantitation.

Finally, a process S is said to follow a geometric Brownian motion with volatility σ and drift μ if it satisfies the stochastic differential equation $dS = S(\sigma dB + \mu dt)$, for a Brownian motion B[2]. Applying Itō's lemma with $f(S) = \log(S)$ in a malaria. mosquito, aquatic, larval habitat, ento-ecoepidemiological, grid-stratifiable, ovisposition, forecast, vulnerability, endmember,prognosticative model can render $d\log(S) = f'(S)\, dS + \frac{1}{2} f''(S) S^2 \sigma^2\, dt = dX - \frac{1}{2}\, d[X]$ It follows that $\log(S_t) = \log(S_0) + \sigma B_t + (\mu - \sigma^2/2)t$, and exponentiating renders the expression for S, $S_t = S_0 \exp\left(\sigma B_t + (\mu - \sigma^2/2)t\right)$ The Doléans exponential or stochastic exponential of a continuous semimartingale X may be optimally defined as the solution to the SDE $dY = Y\, dX$ with initial condition $Y_0 = 1$which may be denoted by $\mathcal{E}(X)$ in a malaria, capture point model for geo-spatiotemporally targeting eco-georeferenceable, seasonal, hyperproductive, aquatic, larval habitats based on larval density.

Applying Itō's lemma with $f(Y) = \log(Y)$ would render $d\log(Y) = \frac{1}{Y}\, dY - \frac{1}{2Y^2}\, d[Y = dX - \frac{1}{2}\, d[X].$ in any forecast, vulnerability, geo-spectrotemporal, ento-ecoepidemiological, model. Exponentiating renders the solution $Y_t = \exp\left(X_t - X_0 - [X]_t/2\right)$.[4]. Itō's lemma can be employed to derive the Black–Scholes formula for an option. Suppose a normalized, malaria, mosquito, aquatic, larval habitat, ento-ecoepidemiological, forecast, vulnerability model follows a Geometric Brownian motion given by the stochastic differential equation $dS = S(\sigma dB + \mu\, DT)$. Then, if the value of an option at time t is $f(t,S_t)$, Itō's lemma would render $df(t, S_t) = \left(\frac{\partial f}{\partial t} + \frac{1}{2} (S_t \sigma)^2 \frac{\partial^2 f}{\partial S^2} \right) dt + \frac{\partial f}{\partial S}\, dS_t$ The term $(\partial f/\partial S)\, dS$ would represent the change in value in time dt of the trading strategy which may allow holding an amount $\partial f/\partial S$ (i.e., forecasted prolific, eco-georferenceable, capture point) If this strategy is followed, and any prevalance statistic is assumed to grow at the risk free rate r, then the total value V of this model would satisfy the SDE $dV_t = r \left(V_t - \frac{\partial f}{\partial S} S_t \right) dt + \frac{\partial f}{\partial S}\, dS_t.$ This strategy replicates the option if $V = f(t,S)$. Combining these equations would render a malaria mosquito, oviposition, endmember, sub-meter resolution, grid-stratfiable, Black-Scholes equation which may be robustly expressed as :

$$\frac{\partial f}{\partial t} + \frac{1}{2} \sigma^2 S^2 \frac{\partial^2 f}{\partial S^2} + rS \frac{\partial f}{\partial S} - rf = 0. {}^3F_2 \left[\begin{matrix} -x, -y, -z \\ n+1, -x-y-z \end{matrix} \right] = \frac{\Gamma(n+1)\Gamma(x+y+n+1)}{\Gamma(x+n+1)\Gamma(y+n+1)} \times \frac{\Gamma(y+z+n+1)\Gamma(z+x+n+1)}{\Gamma(z+n+1)\Gamma(x+y+z+n+1)}.$$

In Bayesian statistics, the posterior predictive distribution is the distribution that a new idependently distributed capture point $\tilde{x}$would have, given a set of *N* existing empirical, ento-ecoepidemiological, variables (e.g., geo-spectrotemporal, geosampled, grid-stratifiable, sub-meter resolution, *An. arabiensis* aquatic, larval habitat, oviposition endmember, observations $\mathbf{X} = \{x_1, \ldots, x_N\}$). In a frequentist context, this might be derived by computing the maximum likelihood estimate (or some other estimate) of the parameter(s) given the observed data, and then plugging them into the distribution function of the new capture point observations.However, the concept of posterior predictive distribution is normally used in a Bayesian context, where it makes use of the entire posterior distribution of the parameter(s) given the observed data — rather than simply a capture point estimate. Specifically, it is computed by marginalizing over the parameters, using the posterior distribution: $p(\tilde{x}|\mathbf{X},\alpha) = \int_\theta p(\tilde{x}|\theta)\, p(\theta|\mathbf{X},\alpha)\, \mathrm{d}\theta$ where θrepresents the parameter(s) and $\alpha$the hyperparameter(s). Any of $\tilde{x}, \theta, \alpha$may be vectors (or equivalently, may stand for multiple capture point, grid-stratifiable, oviposition, malaria, mosquito, aquatic, larval habitat, seasonal, eco-georeferenceable, hyperproductive, foci parameters).Note that this is equivalent to the expected value of the distribution of the new capture point, when the expectation is taken over the posterior distribution, (i.e.: $p(\tilde{x}|\mathbf{X},\alpha) = \mathbb{E}_{\theta|\mathbf{X},\alpha}\left[p(\tilde{x}|\theta)\right]$).

. The predictive probability of seeing a particular endemic, value of a new geo-spectrotemporal, geosampled, aquatic, larval habitat,capture point, eco-georeferenceable, observation will vary depending on the endmember parameters of the distribution of the observation. In this case, a malariologist or medical entomologist knows the exact value of the, capture point, aquatic, larval habitat, geosampled, eco-georeferenceable parameters A posterior distribution may specify what the parameters should be given the ento-ecological, time series data. Logically, then, to get "the" predictive probability, a researcher should average all of the various predictive probabilities over the different possible, grid-stratifiable, sub-meter resolution, eco-georeferened endmember, parameter estimaor values, weighting them according to how strongly he or she believes in them. This is exactly what this expected value does.

Compare this to the approach in frequentist statistics, where a single estimate of the parameters, (e.g. a maximum likelihood estimate, would be computed, and this value plugged in). This is equivalent to averaging over a posterior distribution with no variance, (i.e. where we are completely certain of the parameter having a single value (e.g, seasonal hypeprproductive, sub-meter resolution, grid-stratified,capture point, larval density count). The result would be weighted too strongly towards the mode of the posterior, and would not account of other possible values, unlike in the Bayesian approach.

The prior predictive distribution, in a Bayesian context, is the distribution of a data point (e.g., eco-georeferenced seasonal, capture point, aquatic, larval habitat) marginalized over its prior distribution. That is, if $\tilde{x} \sim F(\tilde{x}|\theta)$ and $\theta \sim G(\theta|\alpha)$, then the prior predictive distribution would be the corresponding distribution $H(\tilde{x}|\alpha)$, where $p_H(\tilde{x}|\alpha) = \int_\theta p_F(\tilde{x}|\theta)\, p_G(\theta|\alpha)\, \mathrm{d}\theta$ Note that this is similar to the posterior predictive distribution except that the marginalization is quantitatble with respect to the prior distribution instead of the posterior distribution. Further, in this research, the prior distribution $G(\theta|\alpha)$ was a conjugate prior and as such then the posterior predictive distribution belonged to the same family of distributions as the prior predictive distribution. If the prior distribution $G(\theta|\alpha)$is conjugate, then($p(\theta|\mathbf{X},\alpha) = p_G(\theta|\alpha')$, (i.e. the posterior distribution also belongs to $G(\theta|\alpha)$ but simply with a different parameter α'instead of the original parameter α.).Then, $p(\tilde{x}|\mathbf{X},\alpha) = \int_\theta p_F(\tilde{x}|\theta)\, p(\theta|\mathbf{X},\alpha)\, \mathrm{d}\theta = \int_\theta p_F(\tilde{x}|\theta)\, p_G(\theta|\alpha')\, \mathrm{d}\theta = p_H(\tilde{x}|\alpha')$ Henceforth, the posterior predictive distribution in an oviposition, sub-meter resolution, malaria, mosquito, ento-ecoepidemiological, forecast, vulnerability, grid-stratifiable model would follow the same distribution *H* as the prior predictive distribution, but with the posterior values of the hyperparameters substituted for the prior for targeting seasonal, unknown, hyperproductive, capture point, aquatic, larval habitat, foci.

The prior predictive distribution is in the form of a compound distribution, and in fact is often used to define a compound distribution, because of the lack of any complicating factors such as the dependence on the malaria empricial, oviposition, sub-meter resolution, grid-stratifiable, eco-georeferenceable, ento-eco-epidemiological, LULC data Xand the issue of conjugacy. For example, the Student's t-distribution can be defined as the prior predictive distribution of a normal distribution with known mean μ but unknown variance σ_x^2, with a conjugate prior, scaled, inverse, chi-squared distribution placed on σ_x^2, with hyperparameters v and σ^2. The resulting compound distribution $t(x|\mu,\nu,\sigma^2)$is indeed a non-standardized Student's t-distribution, and follows one of the two most common parameterizations of this distribution. Then, the corresponding posterior predictive distribution would again be Student's t, with the updated hyperparameters $\nu', \sigma^{2\prime}$that appear in the posterior distribution also directly appearing in the posterior predictive distribution. Note in some cases that the appropriate compound distribution is defined using a different parameterization than the one that would be most natural for the predictive distributions in the current problem at hand. Often this results because the prior distribution used to define the compound distribution is different from the one used in the current problem. For example, as indicated above, the Student's t-distribution of the malaria, ento-ecoepidemiological, endmember empricial, oviposition, sub-meter resolution, grid-stratifiable, frequentistic, eco-georeferenceable datatset was defined in terms of a scaled-inverse-chi-squared distribution placed on the variance. However, it is more common to use an inverse gamma distribution as the conjugate prior in this situation. The two are in fact equivalent except for parameterization; hence, the Student's t-distribution can still be used for either predictive distribution, but the hyperparameters must be reparameterized before being plugged into an ento-ecoepidemiological, geo-spectrotemporal, endmember, endemic, forecast, vulnerability model. Most, but not all, common families of distributions belong to the exponential family of distributions. Exponential families have a large number of useful properties. One of which is that all members have conjugate prior distributions — whereas very few other distributions have conjugate priors.

Another useful property is that the pdf of the compound distribution corresponding to the prior predictive distribution of an exponential family distribution may be marginalized over its conjugate prior distribution which can be determined analytically. Assume that $F(x|\boldsymbol{\theta})$is a member of the exponential family with empricial, oviposition, sub-meter resolution, grid-stratified, eco-georeferenced, malaria, mosquito, forecast, vulnerability model parameter θthat is parametrized according to the natural parameter $\boldsymbol{\eta} = \boldsymbol{\eta}(\boldsymbol{\theta})$, and is distributed as $p_F(x|\boldsymbol{\eta}) = h(x)g(\boldsymbol{\eta})e^{\boldsymbol{\eta}^{\mathrm{T}}\mathbf{T}(x)}$while $G(\boldsymbol{\eta}|\boldsymbol{\chi},\nu)$is the appropriate conjugate prior, distributed as$p_G(\boldsymbol{\eta}|\boldsymbol{\chi},\nu) = f(\boldsymbol{\chi},\nu)g(\boldsymbol{\eta})^{\nu}e^{\boldsymbol{\eta}^{\mathrm{T}}\boldsymbol{\chi}}$Then the prior predictive distribution *H* (i.e., the result of compounding *F* with *G* in a time series, multivariate, predictive, residual, geo-spectrotemporal, geosampled, eco-georeferenceable, ento-epidemiological, *An. arabiensis* aquatic, larval habitat, forecast, vulnerability, signature, frequency LULC model) may be optmally, asymptotically quantitated employing $p_H(x|\boldsymbol{\chi},\nu) = \int p_F(x|\boldsymbol{\eta})p_G(\boldsymbol{\eta}|\boldsymbol{\chi},\nu)\,\mathrm{d}\boldsymbol{\eta} = \int h(x)g(\boldsymbol{\eta})e^{\boldsymbol{\eta}^{\mathrm{T}}\mathbf{T}(x)}f(\boldsymbol{\chi},\nu)g(\boldsymbol{\eta})^{\nu}e^{\boldsymbol{\eta}^{\mathrm{T}}\boldsymbol{\chi}}\,\mathrm{d}\boldsymbol{\eta} = h(x)f(\boldsymbol{\chi},\nu)\int g(\boldsymbol{\eta})^{\nu+1}e^{\boldsymbol{\eta}^{\mathrm{T}}(\boldsymbol{\chi}+\mathbf{T}(x))}\,\mathrm{d}\boldsymbol{\eta}$
$= h(x)\frac{f(\boldsymbol{\chi},\nu)}{f(\boldsymbol{\chi}+\mathbf{T}(x),\nu+1)}$ The last line follows from the previous one by recognizing that the function inside the integral is the density function of a random variable distributed as $G(\boldsymbol{\eta}|\boldsymbol{\chi}+\mathbf{T}(x),\nu+1)$, excluding the normalizing function $f(\ldots)$. Hence the result of the integration will be the reciprocal of the normalizing function.

The above result is independent of choice of parametrization of θ, as none of θ,$\boldsymbol{\eta}$ and $g(\ldots)$appears commonly in ovisposition, ento-ecoepidmeiological, forecast, vulnerability, malaria, mosquito models. (Note that $g(\ldots)$is a function of the parameter and hence will assume different forms depending on choice of parametrization). For standard choices of *F* and *G*, it is often easier to work directly with the usual geosampled, geo-spectrotemporal, endmember, oviposition, parameter estimators rather than rewrite in terms of the natural parameters. Note also that the reason the integral is tractable in these paradigms is that it involves computing the normalization constant of a density defined by the product of a prior distribution and a likelihood. When the two are conjugate, the product is a posterior distribution, and by assumption, the normalization constant of this distribution is known [2]. Hence in a forecast, vulnerability, ento-ecoepidemiological, aquatic, larval habitat, malaria, mosquito, oviposition model the density function of the compound distribution would follow a particular form, consisting of the product of the function $h(x)$that forms part of the density function for *F*, with the quotient of two forms of the normalization "constant" for *G*, one derived from a prior distribution and the other from a posterior distribution.

The beta-binomial distribution is a good example of how this process would aid in geolocating unknown, ento-ecoendmember, seasonal hypeproductive, eco-georferenecable, LULC, sub-meter resolution,, grid-stratifiable, capture point, seasonal foci . Despite the analytical tractability of such vulnerability, distributions, they are in themselves usually not members of the exponential family. For example, the three-parameter Student's t distribution, beta-binomial distribution and Dirichlet-multinomial distribution are all predictive distributions of exponential-family distributions (the normal distribution, binomial distribution and multinomial distributions, respectively), but none are members of the exponential family. This can be due to the presence of functional dependence on $\boldsymbol{\chi} + \mathbf{T}(x)$. In an exponential-family distribution for optimally aymptotically, remotely targeting seasonal, eco-georeferenceable, capture point, malaria, mosquito, aquatic,larval habitat foci, it must be possible to separate the entire density function into multiplicative factors of three types: (1) factors containing only variables, (2) factors containing only parameters, and (3) factors whose logarithm factorizes between the uncoalesced, iterably, interpolative, aquatic, larval habitat, emissivity, sub-meter reoslution, grid-strarfiiable, ento-ecological, frequency parameters. The presence of $\boldsymbol{\chi} + \mathbf{T}(x)\chi$makes this impossible unless the "normalizing" function $f(\dots)$ either ignores the corresponding argument entirely or uses it only in the exponent of an expression.

Here, posterior predictive distribution in exponential families occurred whence a conjugate prior was employed as the posterior predictive distribution which belonged to the same family as the prior, malaria, mosquiot, habitat distribution. In the eco-georeferenceable, ento-geoclassified, forecast, vulnerability model the explanatorial, diagnostic, residual forecast was determined simply by plugging the updated hyperparameters for the posterior distribution of the unmixed, signature, LULC endmember parameter(s) into the formula for the prior predictive distribution. Using the general form of the posterior update equations for exponential-family distributions, a malariologist, medical entomologist or other experimenter may write out an explicit prognosticative, formula for the posterior, ,distribution:$p(\tilde{x}|\mathbf{X}, \boldsymbol{\chi}, \nu) = p_H(\tilde{x}|\boldsymbol{\chi} + \mathbf{T}(\mathbf{X}), \nu + N)$where $\mathbf{T}(\mathbf{X}) = \sum_{i=1}^{N} \mathbf{T}(x_i)$ [4.1]In so doing, the vulnerability forecasts may reveal that the posterior predictive distribution of a series of ungeosamped, signature, ento-ecoendmember, eco-geoclassifiable, LULC, geo-specified, capture point observations, where the observations follow an exponential family with the appropriate conjugate endmember prior has the same probability density as the compound distribution, with the capture point, parameters as specified in equation 4.1. Note in particular that the ungeosampled, eco-georeferenecable, foci observations themselves may enter only in the form $\mathbf{T}(\mathbf{X}) = \sum_{i=1}^{N} \mathbf{T}(x_i).$ This may be termed the sufficient statistic of the ento-ecoepidemioloigical, explanatorial, capture point, hyperprodcutive observations, because it would reveal everything about the observations in order to compute a robust posterior or posterior predictive distribution based on them (or, for that matter, any LULC signature, covariate based on the likelihood of the iteratable, interpolative, immature habitat, signature, wavelength eco-georeferenecable observations, such as the marginal likelihood).

In terms of a joint, predictive distribution, marginal likelihood It is also possible to consider the result of compounding a joint distribution over a fixed number of identically distributed independent endmeber, malaria, mosquito, sub-mter resolution, grid-stratfied, capture point samples with a prior distribution over a shared habitat parameter. In a Bayesian setting, this comes up in various contexts: computing the prior or posterior predictive distribution of multiple new observations, and computing the marginal likelihood of observed data (the denominator in Bayes' law), for example. When the distribution of the samples is from the exponential family and the prior distribution is conjugate, the resulting compound distribution may be tractable and follow a similar form to the expression rendered from equation 4.1. It is easy to show, in fact, that the joint compound, aquatic, larval habitat distribution of a kriged siagnture, ento-ecoendmember, frequency dataset $\mathbf{X} = \{x_1, \dots, x_N\}$ for *n* observations is$p_H(\mathbf{X}|\boldsymbol{\chi}, \nu) = \left(\prod_{i=1}^{N} h(x_i)\right) \frac{f(\boldsymbol{\chi}, \nu)}{f(\boldsymbol{\chi} + \mathbf{T}(\mathbf{X}), \nu + N)}$. This result and the above result for a single compound distribution extend trivially to the case of a distribution over a vector-valued habitat observation, such as a multivariate Gaussian distribution. Note that Bayes' rule can also be written as follows:$P(H|E) = \frac{P(E|H)}{P(E)} \cdot P(H)$where the factor $\frac{P(E|H)}{P(E)}$ represents the impact of *E* on the probability of *H*.

Further since Bayesian statistics, the Wishart distribution is the conjugate prior of the inverse covariance-matrix of a multivariate-normal random-vector, the Wishart distribution may be characterized by its posterior density function in a seasonal, predictive, vector, arthropod-related, malaria, mosquito, capture point, frequency, signature, endemic, transmission-oriented, risk model by letting $\mathbf{X}$ be a $p \times p$ symmetric matrix of the geosampeld, geo-spectrotemporal, LULC, sub-meter resolution, grid-stratifiable, eco-geoclassifiable, signature, ento-ecoendmember randomized variables that is positive definite. Then by letting V be a fixed positive definite matrix of size $p \times p$, explanatory endemic, transmission-oriented, wavelength, LULC covariate coefficient can be statistically ranked in the model's residual forecasts. Then, if $n \geq p$, $\mathbf{X}$ has a Wishart distribution with n degrees of freedom in the eco-georeferenceable prognostications (e.g., geolocations of unknown, oviposition, seasonal, hyperproductive, malaria, mosquito, capture points) as it would then have a posterior denisty function given by $\frac{1}{2^{\frac{np}{2}}|\mathbf{V}|^{\frac{n}{2}}\Gamma_p(\frac{n}{2})}|\mathbf{X}|^{\frac{n-p-1}{2}}e^{-\frac{1}{2}\mathrm{tr}(\mathbf{V}^{-1}\mathbf{X})}$ where $\Gamma_p(\cdot)$ is the multivariate gamma function [i.e., $\Gamma_p(n/2) = \pi^{p(p-1)/4}\Pi_{j=1}^{p}\Gamma\left[n/2 + (1-j)/2\right]$. This definition can be extended to any real geo-sampled $n > p-1$. If $n \leq p-2$ then the Wishart would no longer have a density—instead; it would represent a singular, capture point distribution instead. If $\mathbf{X}$ has a Wishart distribution with m degrees of freedom and variance matrix $\mathbf{V}$— in the endmember, predictive malaria, mosquito, vulnerability, endmember signature, LULC, frequency,model then $\mathbf{X} \sim \mathcal{W}_p(\mathbf{V}, m)$—and $\mathbf{C}$ would be a $q \times p$ matrix of rank q, whence $\mathbf{CXC}^T \sim \mathcal{W}_q\left(\mathbf{CVC}^T, m\right)$.

Further, if $\mathbf{Z}$is a nonzero $p \times 1$constant vector in the seasonal, predictive, *An. arabienisis*, oviposition, sub-meter resolution, geo-spectrotemrpoal, frequency, signature, LULC, risk model then $\mathbf{z}^T\mathbf{X}\mathbf{z} \sim \sigma_z^2\chi_m^2$.In this case, χ_m^2 would be the chi-squared distribution and $\sigma_z^2 = \mathbf{z}^T\mathbf{V}\mathbf{z}$ in the vulnerability residual forecasts statsitically aymptotically targeting the endemic, transmission-oriented, eco-georeferenecable, capture point, eco-endmember, signature, iteratively, interpolative covariates. Note that σ_z^2 would be a constant in the model and it would be positive because Vwould be positive definite. For example, consider the case where $\mathbf{z}^T = (0, \ldots, 0, 1, 0, \ldots, 0)$ in a seasonal, predictive, vector, arthropod-related, malaria, mosquito, sub-meter resolution, eco-geoclassifiable, endemic, transmission-oriented, malaria, risk, endmember, LULC, signature model. That is, the *j*th element is one for the geosampled, explanatory, endemic, transmission-oriented, covariate coefficients and all others are zero. This would show that $w_{jj} \sim \sigma_{jj}\chi_m^2$ and would provide the marginal distribution of each of the elements on the matrix's diagonal in the risk model. The Wishart distribution is the sampling distribution of the maximum-likelihood estimator of the covariance matrix of a multivariate normal distribution [3]. A derivation of the this estimator may then use the spectral theorem for further cofficient quantitation in the seasonal, oviposition, eco-endmember, geo-spectrotemporal, frequency, risk model . The Log-expectation may then w be $\mathrm{E}[\ln|\mathbf{X}|] = \sum_{i=1}^{p}\psi\left(\frac{1}{2}(n+1-i)\right) + p\ln(2) + \ln|\mathbf{V}|$ where ψ is the digamma function (i.e., the derivative of the log of the gamma function in the ento-ecoepidemiological model). This would play a role in variational Bayes derivations derived from robust, *An. arabiensis.*-related, seasonal, endemic, transmission-oriented, oviposition, forecast, risk models especially for Bayes networks involving the Wishart distribution.

Matrix factorization (MF) has become a common approach to collaborative filtering, due to ease of implementation and scalability to large datasets. Two existing drawbacks of the basic model for predicting seasonal ecogeorefereneceable, sub-meter resolution, ovispoition, malaria, mosquito, aquatic, larval habitat is that it does not incorporate side information on either users or items, and assumes a common variance for all users. It may be possible to extend the work of constrained probabilistic matrix factorization by deriving the Gibbs updates for the side feature vectors for. signature, eco-entoendmember malaria, mosquito, oviposition, capture point, forecastable, endemic, signature items It may be that this Bayesian treatment to the constrained probabilistic malatric factor (PMF) model outperforms other estimation methods for efficiently, remotely, asymptotically, targeting, eco-georeferenceable, seasonal, hyperproductive foci A malariologist, medical entomologist or other experimenter may consider model extensions to heteroskedastic precision as introduced in the literature such as in Lakshminarayanan, Bouchard, and Archambeau, (2011) for determining prolific, empricial, oviposition, sub-meter resolution, grid-stratifiable, eco-georeferenceable, malaria, capture points. It may be shown that overfitting in these vector eco-epidemiological forecast,

vulnerability models may be geospatially adjustable employing deterministic approximation algorithms (e.g: variational inference) whenst the observed entries in the user / item matrix are distributed in an non-uniform manner. Alternatively a truncated eco-endmember, malaria, mosquito, precision model may be proposed for asymptotically regressing, geo-spectrotemporal, geosampled, eco-georeferenceable, endmember, oviposition, malaria, mosquito, grid-stratified, sub-meter resolution, capture point, observational, uncoalesced, wavelength predictors. The experimental results may suggest that these model tends to delay overfitting based on temporal geosampled malaria mosquito data.

The use of heteroskedasticity robust covariance matrix estimators, cf. White (1980), in cross-sectional settings and of heteroskedasticity and autocorrelation consistent (HAC) covariance matrix estimators, cf. Andrews (1991), in time series contexts is extremely common in applied econometrics. The popularity of these robust, covariance matrix, rco-endmember estimators is due to their consistency under weak functional form assumptions. In particular, their use may allow a malariologist, medical entomologist or other experimenter to form valid confidence regions about a set of regressed, unmixed, sub-meter resolution, ento-geoclassifiable, grid-stratifiable, frequency, capture point, unknown, iteratively interpolated, LULC signature, parameters from a model of interest without specifying an exact process for the disturbances in the model.

With the increasing availability of panel data, it is natural that the use of robust, covariance matrix, endmember estimators for panel data settings that allow for arbitrary within individual correlation are becoming more common. A recent paper by Bertrand et al. (2004) illustrated the pitfalls of ignoring serial correlation in panel data, finding through a simulation study that inference procedures which fail to account for within individual serial correlation may be severely size distorted. As a potential resolution of this problem, Bertrand et al. (2004) suggest the use of a robust covariance matrix estimator proposed by Arellano (1987) and explored in Kezdi (2002) which may allow arbitrary within individual correlation to be optimally quantitated in a prognosticative, sub-meter resolution, grid-stratifiable, LULC, aquatic, larval habitat, model, for asymptotically targeting seasonal, unknown, hyperproductive, eco-endmember, capture point foci in a simulation study that tests frequency, signture estimators of the covariance parameters based on size

In this paper, we addressed this issue by exploring the theoretical properties of the CCM estimator in asymptotics that allow *n* and T to go to infinity jointly and in asymptotics where T goes to infinity with *n* fixed in an oviposition, empricial, sub-meter resolution, grid-stratifiable, eco-georeferenceable, malaria, mosquito, vulnerability,LULC, eco-endmember, geo-spectrotemporal, prognosticative model. We found that the CCM estimator, appropriately normalized, is consistent without imposing any conditions on the rate of growth of T (e.g., geosampled, larval, seasonal, signature, density count) relative to *n* even when the time series dependence between the aquatic larval habitat observations is left unrestricted. In this case, both the OLS estimator and the CCM estimator converge because the only information is coming from cross-sectional signature, variation. If the time series process is restricted to be strongly mixing, the OLS estimator is more consistent but, because high lags are not down weighted, and as such the robust covariance matrix estimator still converges[3]. This behavior suggests, as indicated in the simulations found in Kezdi (2002), that it is the frequency *n* dimension and not the size of n relative to T that matters for determining the properties of the CCM estimator in an oviposition, aquatic, larval habitat, ento-ecoepidemiological, geo-spectrotemporal, forecast, vulnerability, *An. arabiensis* model. It is interesting to note that the limiting behavior of seasonal eco-georeferenceable immature habitat changes ‘‘discontinuously’’ as the amount of dependence is limited. In particular, the rate of convergence changes. However, despite the difference in the limiting behavior there is no difference in the behavior of standard inference procedures based on the CCM estimator in such models. In particular, the same t and F statistics will be valid in either case (and in the n ! 1 with T fixed case) without reference to the asymptotics or degree of dependence in the empirically regressed, malaria, mosquito, eco-endmember, LULC unmixed signature datasets. A malariologist, medical entomologist or other experimeneter may derive the behavior of the CCM estimator as T ! 1 with *n* fixed, where the unmixed, signature sub-meter resolution, grid-stratfiiable, iteratively interpolative, wavelength, estimator is not consistent in an oviposition, eco-georeferenceable, malaria, mosquito, capture point model for aymptotically targeting seasonal, hyperproductive unknown foci but this model output does not have to have a limiting distribution. This result would correspond to asymptotic results for HAC estimators without truncation as found in recent work by Kiefer and Vogelsang (2002, 2005), Phillips et al. (2003), and Vogelsang (2003). While the limiting distribution in the model estimates would not be proportional to the true covariance matrix in general, it would be proportional to the covariance matrix which would aid in construction of asymptotically pivotal statistics(e.g., precise geolocations of eco-georeferenecable, ungeosampled, prolific, capture point, aquatic, larval habitats) . In fact, in this case, the standard t-statistic is not asymptotically normal in these forecast vulnerability ento-

ecoepidemiolgical, signature models but converges in distribution to a random, frequency, sub-mter resolution, grid-stratfiied, LULCvariable (e..g, discontinuous canopied endmember) which may be exactly proportional to a tn1 distribution. This behavior suggests the use of the tn1 for constructing confidence intervals in malaria mosquito, remeote sensing LULC models since the CCM estimator may be employed to provide asymptotically correct critical, capture point values under any asymptotic sequence.

Exploring the finite sample behavior of the CCM estimator and tests based upon it through a short simulation study may reveal seasonal, eco-georeferenceable, unknown, iteratively interpolated, noiseless hyperproductive, malaria, mosquito, aquatic, larval habitats. The simulation results may indicate that tests based on the robust standard error estimates generally have approximately correct size in serially correlated panel, oviposition, forecast, vulnerability, ento-ecoendmember,sub-mter resolution, grid-stratifiable, LULC signature, unmixed data even in small samples. The standard error estimates themselves are considerably more variable than their counterparts based on simple parametric models [2]. The bias of the simple, parametric, sub-meter resolution, grid-stratifiable, malaria, mosquito, eco-georeferenceable, capture point, endmember, LULC target estimators is also typically smaller in the cases where the parametric model is correct, which may suggestthat these standard error estimates are likely preferable when a malariologiost, medical entomologist or other expwerimeneter is confident in the form of the error process. The simulation, may explore the behavior in these paradigms employing an analog of White's (1980) direct test for heteroskedasticity proposed by Kezdi (2002) when constructing an oviposition, eco-georeferenceable, ento-ecoepidemiological, capture point, sub-meter resolution, grid-stratifiable, endmember, forecast, vulnerability, frequency signature model for asymptotically, targeting unknown, seasonal, hyperproductive, eco-georeferenceable, aquatic, larval habitat, capture point, ento-ecoendmember foci. The results may indicate the performance of the test is fairly good for moderate geo-spectrotemporally geosampled, *n*, though it is quite poor when *n* is small. This simulation behavior may also suggeststhat this test may be useful for choosing between the use of robust standard error estimates and standard errors estimated from a more parsimonious LULC, vector arthropod, endmebe, forecast-oriented, wavelength model when *n* is reasonably large for targeting seasonal, hyperproductive foci.

We began the ento-ecoepidemiological, geo-spectrotemporal, signature, endmember, nonlinear analysis of the *An. arabiensis*, oviposition, capture point, aquatic, larval habitat, endmember operators with definitions of differentiation. We let F(x) be a nonlinear operator acting from D(F) ⊂ X to R(F) ⊂ Y , where X and Y were real Banach spaces. We assumed D(F) was open. We noted that F(x) was differentiable in the Fr´echet sense at x0 ∈ D(F)in the model if there was a bounded, linearizable, capture point, eco-endmember, LULC operator, denoted by F (x0), such that F(x0 + h) − F(x0) = F (x0)h + ω(x0, h) for all h < ε with some ε > 0, where ω(x0, h) / h → 0 as h → 0. Then F (x0) was c the Fr´echet derivative of F(x) at x0, and dF(x0, h) = F (x0)h. Elements of nonlinear functional analysis can occur if F(x) is Fr´echet differentiable in an open domain S ⊂ D(F) of if it is Fr´echet differentiable at every point of S[4]. It was clear that the Fr´echet derivative of a continuous linear operator is the same operator in a forecast, vulnerability-oriented, sub-meter resolution, grid-stratifiable *An. arabiensis*, oviposition, signature, eco-geoclassifiable, LULC, frequency model. We also assumed y = f(x) was a vector function from Rm to Rn and f(x) ∈ (C(1)(Ω))n. We showed that this function was Fr´echet derivative at x0 ∈ Ω in an eco-georeferenceable, vector arthropod, probabistic endmember, uncoalesced, ento-ecoendmeber signature, paradigm if a Jacobi matrix , ∂fi(x0) ∂xj - i=1,...,*n* j=1,...,m is employable for quantitating the geosampled, geo-spectrotemporal,unmixed, aquatic, larval habitat, seasonal, iteratively interpolative, LULC covariates. In the construction of the Fr´echet derivative, we recognized a method of the calculus of variations, which we employed to obtain the Euler equations of a functional. The following derivative by Gˆateaux wasalso obtained. We assumed that for all h ∈ D(F) we had a limt→0 F(x0 + th) − F(x0) t = DF(x0, h), x0 ∈ D(F), where DF(x0, h) was a linear operator with respect to h in the model. In so soing, DF(x0, h) was then the Gˆateaux differential of F(x) at x0 in the ento-ecoepidmeiological, model residual derivative, signature, LULC dataset.Denoting DF(x0, h) = F (x0)h, we generated the Gˆateaux derivative F (x0). An operator is differentiable in the Gˆateaux sense in an open domain S ⊂ X if it has a Gˆateaux derivative at every point of S[4]. The definitions of the capture point, unknown, habitat, wavelength derivatives were clearly valid for the ento-ecoendmember, geo-spectrotemporal, sub-meter resolution, grid-stratified, eco-geoclassified, LULC functionals for asymptotically, optimally, remotely targeting ecogeoreferenceable, seasonal, hyperproductive, capture points.

Suppose Φ(x) is a functional which is Gˆateaux differentiable in a Hilbert space and that DΦ(x, h) is bounded at x = x0 as a linear functional in h in an endmember, oviposition,sub-meter resolution, grid-stratifiable, eco-endmember, malaria mosquito, prognosticative, eco-geoclassfied, LULC, risk model for asymptotically targeting

seasonal, unknown, hyperproductive capture points. Then, by the Riesz representation theorem, the signature aquatic, larval habitat endmebers can be represented in the form of an inner product; denoting the representing element by grad Φ(x0). In so doing a malariologist or medical entomologist may achieve DΦ(x0, h) = (grad Φ(x0), h). By this, an experimenter would have an operator grad Φ(x0) [i.e., the gradient of Φ(x) at x0] which could quanatiate any propogational, endmember interpolative uncertianities in the oviposition, ento-ecoepidemiological, signbature LULC model output dataset. If an operator F(x) in an oviposition, sub-meter resolution, grid-stratifiable, endmember, risk model from X to Y is Fr´echet differentiable at x0 ∈ D(F), then F(x) is Gˆateaux differentiable at x0 and the Gˆateaux derivative coincides with the Fr´echet derivative.

A function f is said to be Gˆateaux differentiable at x if there exists a bounded linearizable operator Tx ∈ B(X, Y) such that ∀ v ∈ X, lim t→0 f(x + tv) − f(x) t = Txv[4]. The operator Tx is called the Gˆateaux derivative of f at x[4]. If for some fixed v the limits δvf(x) := d dt t=0 f(x + tv) = limt→0 f(x + tv) − f(x) t exists, in a sub-meter resolution, grid-stratifiable, forecast, vulnerability, malaria, mosquito, signature,LULC, ento-geoclassifiable model, f will have a directional derivative at x in the direction v. Hence f is Gˆateaux differentiable at x in such an ento-ecoepidemiological, oviposition, aquatic, larval habitat, endmember, LULC, risk model for asymptotically targeting eco-georferenecable, ungeosampled, foci if and only if all the directional derivatives δvf(x) exist and form a bounded linear operator Df(x) : v → δvf(x). If the limit (in the sense of the Gˆateaux derivative) exists uniformly in v on the unit sphere of X in the model, f would be Fr´echet differentiable at x and Tx would be the Fr´echet derivative of f at x. Equivalently, if a malaiologist medical entomologist or other experimenter employs y = tv then t → 0 if and only if y → 0 occurs in the ento-ecoepidemiological model output. Thus, f is Fr´echet differentiable at x in a robust oviposition, sub-meter resolution, grid-startifiable, malaria, mosquito, capture point, eco-georeferenecable, geo-spectrotemporal, geosampled, forecast, vulnerability, eco-endmember, signature, LULC model and if for all y, f(x + y) − f(x) − Tx(y) = o(y) then Tx = Df(x) will be the derivative of f at x. Note that the distinction between the two notion of differentiability is made by how the limit is taken. The importance being that the limit in the Fr´echet case only depends on the norm of y in ento-epidemiological,eco-endmember prognosticative, ento-geoclassifiable, LULC signature, sub-meter resolution, capture point, frequency models especially when asymptotically targeting ecogeorferenceable, seasonal, hyperproductive, capture point, aquatic, larvakl habitat foci

A function which is Fr´echet differentiable at an ovipsoition, eco-geo-classifiable, malaria ,mosquito, hyperproductive, seasonal, eco-georeferenceable, sub-meter resolution, grid-stratifiable,LULC capture point , probabilistic paradigm for aymptotiically targeting prolific foci based on larval density counts may be continuous but this is not the case for Gˆateaux differentiable functions (even in the finite dimensional case). For example, the function f : R2 → R may be definable by f(0, 0) = 0 and f(x, y) which may represent x4y/(x6 + y3) for x2 + y2 > 0, as its Gˆateaux derivative at the origin, in a frequency, sub-mter resolution paradigm for optimally targeting seasonal, hyperproductive, eco-georeferenceable foci but fails to be continuous thereafter. This could provide an example of a function in these models which is Gˆateaux differentiable but not Fr´echet differentiable. Another example is the following: If X is a Banach space, and ϕ ∈ X is a discontinuous linear, explanatorial functional in an oviposition, sub-meter resolution, grid-stratifiable, eco-endmember, signature, eco-geoclassifiable, geo-spectrotemporal, LULC, malaria mosquito, ento-ecoepidemiological, risk model then the function f(x) = x ϕ(x) may be Gˆateaux differentiable at x = 0 with derivative 0. However in so doing, f(x) would not have to be Fr´echet differentiable in the output since ϕ does not have limit zero at x = 0.

Every countable collection of Lipschitz functions on a Banach space X with separable dual had a common point of Fréchet differentiability in our eco-georeferenecable, sub-meter resolution, grid-stratified, vulnerability, malaria, mosquito, capture point, geo-spectrotemporal, oviposition LULC endmember prognosticative, signature, frequency model. We show that the answer is positive for some infinite-dimensional X whence asymptotically targeting seasonal, unknown capture point, aquatic, larval habitat, malaria mosquito, hyperproductive foci based on an iteratable, interpolative, sub-meter resolution, eco-geoclassfiable, LULC eco-endmember signature Previously, even for empirical, aquatic, larval habitat sub-pixel LULC collections consisting of two functions this has been known for finite-dimensional X only (although for one function the answer is known to be affirmative in full generality). Our aims in this research were achieved by introducing a new class of null sets in Banach spaces (called Γ-null sets) which was introduced into the malaria model whose definition involved both the notions of category and measure which revealed that the required differentiability holds almost everywhere when targeting seasonal, hyperproductive, capture point,

ento-ecoepidemiological, eco-georeferenecable, endmember, capture point foci. We even obtained existence of Fréchet derivatives of Lipschitz functions between certain infinite-dimensional quasi-Banach spaces; no such results have been known previously in the literature. Our main result states that a Lipschitz map between separable Banach spaces is in a sub-meter resolution, oviposition, eco-georeferenceable, malaria, mosquito, forecast, vulnerability, grid-stratifiable, endmember,LULC model is Fréchet differentiable Γ-almost everywhere provided that it is regularly Gâteaux differentiable Γ-almost everywhere and the Gâteaux derivatives stay within a norm separable space of operators. It is easy to see that Lipschitz maps of X to spaces with the Radon-Nikod´ym property are Gâteaux differentiable Γ-almost everywhere as well in these signature prognosticative, frequency, grid-stratifiable paradigms. Moreover, Gâteaux differentiability implies regular Gâteaux differentiability with exception of another kind of negligible sets, so-called σ-porous sets. Hence every space in an oviposition, eco-georeferenecable, geo-spectrotemporal, ento-ecoendmeber, sub-meter resolution, LULC, malaria mosquito, endmember, ovipsoition, forecast, vulnerability model σ-porous set is Γ-null. Further this holds for C(K) with K countable compact, the Tsirelson space and for all subspaces Weierstrass' infinite product theorem [see 3]. Hence any given ovispsoition, geo-spectrotemrpoal, sub-meter reosolution, grid-stratifiable, eeco-geoclassifiable, malaria, mosquito, iterative \, interpolative, exploratory, ento-ecoendmember, signature, frequency, LULC sequence in the complex plane $,0,...,0,\ \alpha_1\ ,\ \alpha_2\ ,...,$ $0<|\alpha_k|\leq|\alpha_{k+1}|,\quad k=1,2,\ldots;\quad \lim_{k\to\infty}|\alpha_k|=\infty,$

there exists an entire function with zeros at the capture points α_k of this sequence and only at these points. This function may be constructed as a canonical product: $W(z)=z^{\lambda}\prod_{k=1}^{\infty}\left(1-\frac{z}{\alpha_k}\right)e^{P_k(z)},$ where λ is the multiplicity of zero in the sequence and $P_k(z)=\frac{z}{\alpha_k}+\frac{z^2}{2\,\alpha_k^2}+\ldots+\frac{z^{m_k}}{2\,\alpha_k^{m_k}}$. may reveal unknonw geolocations of eco-georeferenceable, seasonally, prolific foci. An entire function with a given sequence of complex numbers {αk}as its zeros. Suppose that the zeros αk≠0are arranged in monotone increasing order of their moduli, |αk|≤|αk+1| and have no limit point in the finite plane (a necessary condition), i.e. limk→∞αk=∞limk→∞αk=∞. Then the canonical product mayillustrate the form∏
(zαk,qk)=∏k=1∞W(zαk,qk)=∏k=1∞(1−zαk)ePk(z),∏(zαk,qk)=∏k=1∞W(zαk,qk)=∏k=1∞(1−zαk)ePk(z),where
Pk(z)=zαk+12(zαk)2+…+1qk(zαk)qk.Pk(z)=zαk+12(zαk)2+…+1qk(zαk)qk in a, sub-meter resolution, krigable, grid-stratified,, signature, wavelength, unmixed model for asymptotically targeting seasonal, hyperproductive, eco-georferenceable, ungeosampled foci of malaria mosquito, aquatic, larval habitats . The W(z/αk,qk)W(z/αk,qk) are called the elementary factors of Weierstrass[4]. The exponents qk could then be subsequently chosen so that the canonical product is absolutely and uniformly convergent on any compact set; for example, it suffices to take qk≥k−1. I these probabilistic, LULC signature, frequency paradigms . If the sequence αk|} has a discrete, explanatory, robust, finite exponent of convergence β=inf{λ>0:∑k=1∞|αk|−λ<∞},β=inf{λ>0:∑k=1∞|αk|−λ<∞}, then all the qk can be chosen to be the same, starting, from the minimal requirement that qk=q≤β≤q+1; this q is called the genus of the canonical product. If β=∞, (i.e. if ∑∞k=1|αk|−λ∑ diverges for any λ>0, then one has a canonical product of infinite genus. The order of a canonical product ρ=β (for the definition of the type of a canonical product in a sub-meter resolution, grid-stratifiable, geo-spectrotemporal, LULC, prognosticative, signature, LULC model may optimally asymptotically target, seasonal, eco-georeferenceable, aquatic, larval habitat, eco-endmember foci.

The multipliers $W\left(\frac{z}{\alpha_k};m_k\right)=\left(1-\frac{z}{\alpha_k}\right)e^{P_k(z)}$ are called Weierstrass prime multipliers or elementary factors. The exponents m_k may be chosen in a sub-meter resolution, empirical dataset of eco-georeferenecable, malaria, mosquito model so as to ensure the convergence of the an endmember product; for example, the choice $m_k=k$ may ensure the convergence of any sequence of an unknown, aquatic, larval habitat, capture point. It also follows from this theorem that any entire function $f(z)$ in a forecast vulnerability ento-ecoepidemiological, LULC, sub-pixel model with zeros would have the form $f(z)=e^{g}(z)W(z)$,where $W(z)$ is the canonical product and $g(z)$ is an entire function (see also Hadamard theorem on entire functions). If the indices $n1,n2,\ldots$, of all non-zero, ento-ecoendmember, eco-geoclassified LULC, geospecified, capture point, geosampled coefficients of the power series then f(z)=∑n=0∞anznf(z)=∑n=0∞anzn may satisfy the condition nk+1>(1+θ)nk, where θ>0. In so doing, then the boundary of the disc of convergence of this series would be its natural boundary, (i.e. the function has no analytic continuation across the boundary of this disc). This condiction is known as Hadamard's condition; the gaps which satisfy the Hadamard condition are called Hadamard gaps [2].

Weierstrass' infinite product theorem can be generalized to the case of an arbitrary domain $D \subset \mathbf{C}$: regardless of a sequence of ento-ecoendmember, iteratable, quantiatively interpolative, sub-meter resolution, malaria, mosquito, frequency signature, prognosticated, ungeosampled capture points $\{ \alpha_k \} \subset D$ (e.g., seasonal, eco-georeferenceable, geosampled, hyperproductive habitats) seasonal geolocations without limit points in *D*, but only if there exists a holomorphic function *f* in *D* with zeros at the points α_k and only at these points. The part of the theorem concerning the existence of an entire LULC function with arbitrarily specified zeros may be generalized to functions of several complex, endmember, capture point variables as follows: Let each geosampled, geo-spectrotemporal, malaria, mosquito, seasonal, eco-georeferenecable, predicte LULC signature , sub-meter resolution, grid-stratifiable, capture point α of the complex space $\mathbf{C}^n, n \geq 1$, be brought into correspondence with one of its neighbourhoods U_α and with a function f_α which is holomorphic in U_α. In so doing, prolific habitat may be seasonally identified based on simulated signatures and empirically geosampled, larval density, frequency counts Moreover, suppose this is done in such a way that if the intersection $U_\alpha \cap U_\beta$ of the neighbourhoods of the capture points $\alpha, \beta \in \mathbf{C}^n$ is non-empty, then the fraction $f_\alpha / f_\beta \neq 0$ which subsequenctly would be a holomorphic function in $U_\alpha \cap U_\beta$. Under these conditions there would exist an entire function *f* in $\mathbf{C}^n$ in the prognosticative, vector arthropod, endmember model such that the fraction f / f_α is a holomorphic function at every forecasted capture point $\alpha \in \mathbf{C}^n$. This theorem is known as Cousin's second theorem.

In mathematics, the Cousin problems are two questions in several complex variables, concerning the existence of meromorphic functions that are specified in terms of local data. Employing this theoreum et $\mathcal{U} = \{U_\alpha\}$ may robustly reveal a covering of a complex manifold *M* in an ovispoition, malaria, mosquito, sub-meter resolution, grid-stratifiable, LULC model specification for asymptotically targeting seasonal, eco-georeferenceable, hyperproductive, aquatic, larval habitat, geo-spectrotemporal foci based on the open subsets U_α, in each of which may be definable as a meromorphic function f_α; assuming that the functions $f_{\alpha\beta} = f_\alpha - f_\beta$ are holomorphic in $U_{\alpha\beta} = U_\alpha \cap U_\beta$ for all α, β(compatibility condition).There may be a requirement to construct a function *f* which is meromorphic on the entire manifold M such that the functions $f - f_\alpha$ are holomorphic in U_α for all αin these paradigms for rendering optimal vulnerability forecasts. In other words, the problem of summarizing geo-spectrotemporally adjusted, seasonal eco-georeferenceable, targeted, hyperproductive, malaria, mosquito, aquatic, larval habitat datasets based on an iteratively interpolative, endmember, sub-meter resolution, eco-geoclassified, gridded, LULC signature is to construct a global meromorphic function with locally specified polar singularities. The functions $f_{\alpha\beta}$, hence would be defined in the pairwise intersections $U_{\alpha\beta}$ of elements of $\mathcal{U}$, by then defining a holomorphic $\mathbf{1}$-cocycle for $\mathcal{U}$, (i.e. they satisfy the conditions $f_{\alpha\beta} + f_{\beta\alpha} = 0$ in $U_{\alpha\beta} f_{\alpha\beta} + f_{\beta\gamma} + f_{\gamma\alpha} = 0$ in $U_\alpha \bigcap U_\beta \bigcap U_\gamma$ for all α, β, γ).

A more general problem (known as the first Cousin problem in cohomological formulation) is the following. Given holomorphic functions $f_{\alpha\beta}$ in the intersections $U_{\alpha\beta}$, satisfying the cocycle conditions may to find functions h_α, holomorphic in U_α, such that $f_{\alpha\beta} = h_\beta - h_\alpha$ for all α, β in an ento-ecoepidemiological, forecast, vulnerability, malaria mosquito, aquatic, larval habitat model for asymptotically targeting eco-georeferenceable, seasonal, hypeproductive, malaria. mosquito, capture point foci. If the functions $f_{\alpha\beta}$ correspond to the krigable, ento-ecoendmeber LULC, signature, vector arthropod data of the first Cousin problem then the above functions h_α would exist in the model realizations as the function $f = \{f_\alpha + h_\alpha \quad \text{in } U_\alpha\}$ may be definable in the model which may reveal an output which is meromorphic throughout *M* . Further this output may reveal a solution of the first Cousin problem. Conversely, if *f* is a solution of the first Cousin problem employing the endmember ,capture point, empirically geosampled, LULC, aquatic, larval habitat, geo-spectrotemporal, data $\{f_\alpha\}$, then the holomorphic functions $h_\alpha = f - f_\alpha$ which may asymptotically optimally, geolocate seasonal, hypeproductive, unknown foci.Thus, a specific first Cousin problem is solvable if and only if the corresponding cocycle is a holomorphic coboundary in the forecast, vulnerability, ento-ecoendmember LULC model.

The first Cousin problem may also be formulated in a local version in the ento-ecoepidmeiological, geo - spectrotemporal, aquatic, larval habitat, prognosticative endmember, sub-mter resolution, signature, malaria mosquito model output (i.e.,eco-georeferenceable, geolcations of seasonally hyperproductive, oviposition foci). To each set of capture point, geosampled, eco-georeferenceable, covariates $\{U_\alpha, f_\alpha\}$ satisfying the compatibility condition there may correspond a uniquely defined global section of the sheaf $\mathcal{M}/\mathcal{O}$, where $\mathcal{M}$ and *O* are the sheaves of germs of meromorphic and holomorphic functions, respectively. The correspondence may be such that any global section

of $\mathcal{M}/\mathcal{O}$ corresponds to some first Cousin problem (the value of the section κ corresponding to a seasonal, hyperproductive foci $\{f_\alpha\}$ at a capture point $z \in U_\alpha$) which may be the element of $\mathcal{M}_z/\mathcal{O}_z$ with representative f_α. The malaria mosquito immature habitat of global sections $\phi : \Gamma(\mathcal{M}) \to \Gamma(\mathcal{M}/\mathcal{O})$ maye be mappable whence each meromorphic LULC eco-geoclassified, ento-ecoendmeber, krigabale, geo-spectrotemrpoal, function f on M to a section $^{\kappa}f$ of $\mathcal{M}/\mathcal{O}$, $^{\kappa}f(z)$ is the class in $\mathcal{M}_z/\mathcal{O}_z$ of the germ of f at the capture point $\boldsymbol{Z}$, $z \in M$. The localized first Cousin problem would then be quantatable as a global section κ of the sheaf $\mathcal{M}/\mathcal{O}$, to find a unknown habitat meromorphic function f on M (i.e. a section of $\mathcal{M}$) such that $\phi(f) = \kappa$ in the ento-ecoepidemiological, oviposition, forecast, vulnerability, endmember model output.

Theorems concerning the solvability of the first Cousin problem in an oviposition, malaria, mosquito model may be regarded as a multi-dimensional generalization of the Mittag-Leffler theorem based on the construction of a meromorphic signature LULC ento-ecoendmember function with prescribed poles. The problem in cohomological formulation, with a fixed covering $\mathcal{U}$, may be solvable (for arbitrary compatible $\{f_\alpha\}$) if and only if $H^1(\mathcal{U}, \mathcal{O}) = 0$ (the Čech cohomology for $\mathcal{U}$ with holomorphic coefficients is trivial in sub-meter resolution, grid-stratifiable, eco-geoclassifiable, forecast, vuylnberability model. The Mittag-Leffler theorem on expansion of a meromorphic function is one of the basic theorems in analytic function theory, for rendering meromorphic functions which may reveal an analogue of the expansion of a rational function into the simplest partial fractions whence asymptotically, optimally, remotely, geo-spectrotemporally targeting seasonal, unknown, aquatic, larval habitat, hyperproductive, eco-endmember, eco-geoclassifiable LULC foci .

Hence by letting {an}∞n=1be a sequence of distinct, complex, geo-spectrotemporal, geosampled, ovipsoition, ento-ecoepidemiological, malaria, mosquito, aquatic, larval habitatcapture points, ,|a1|≤|a2|≤…,limn→∞an=∞,|a1|≤|a2|≤…,limn→∞an=∞,and let {gn(z)}{gn(z)} be a sequence of rational, explicative, time series, dependent functions of the form gn(z)=∑k=1lncnk(z−an)k=,so that the aquatic, larval, geosampled, density, count variables is the unique pole of the corresponding function gn(z), then there would be explanatory, eco-georeferenecable, capture point, predicted meromorphic functions f(z) in the complex z-plane C having poles based on sample time intervals but only if there are quantaifiable principal parts of the Laurent series corresponding to the capture points.

The Laurent series is a representation of a complex function f(z) as a series. Unlike the Taylor series which expresses f(z) as a series of terms with non-negative powers of z, a Laurent series includes terms with negative powers.If $f(z)$ is analytic throughout an oviposition, eco-georeferenecable, forecast, vulnerability, geo-spectrotemrpoal, signature , LULC malaria, mosquito sub-mter resolution, grid-stratfiied, model in a riceland, agro-irrigated village K_1 and K_2 centered at $z = a$ of the radii r_1 and $r_2 < r_1$ respectively, then there exists a unique series expansion in terms of calculable positive and negative explanative powers of $(z-a)$, $f(z) = \sum_{k=0}^{\infty} a_k (z-a)^k + \sum_{k=1}^{\infty} b_k (z-a)^{-k}$, where $a_k = \frac{1}{2\pi i} \oint_{K_1} \frac{f(\zeta)\, d\zeta}{(\zeta - a)^{k+1}}$ and $b_k = \frac{1}{2\pi i} \oint_{K_2} (\zeta - a)^{k-1} f(\zeta)\, d\zeta$ (see Korn and Korn 1968).

From a oviposition, eco-georeferenecable, forecast, vulnerability, geo-spectrotemrpoal, signature , LULC malaria, mosquito Cauchy integral formula, $f(z) = \frac{1}{2\pi i} \int_C \frac{f(z')}{z'-z}\, dz' = \frac{1}{2\pi i} \int_{C_1} \frac{f(z')}{z'-z}\, dz' + \frac{1}{2\pi i} \int_{C_c} \frac{f(z')}{z'-z}\, dz' - \frac{1}{2\pi i} \int_{C_2} \frac{f(z')}{z'-z}\, dz' - \frac{1}{2\pi i} \int_{C_c} \frac{f(z')}{z'-z}\, dz' = \frac{1}{2\pi i} \int_{C_1} \frac{f(z')}{z'-z}\, dz' - \frac{1}{2\pi i} \int_{C_2} \frac{f(z')}{z'-z}\, dz'$.

$$f(z_0) = \frac{1}{2\pi i} \oint_\gamma \frac{f(z)\, dz}{z - z_0},$$

Cauchy's integral formula states that where the integral is a contour integral along the contour γ enclosing a predicted, hyperproductive, malaria, mosquito, aquatic, larval habitat, capture point z_0[1] It may be derivable in a forecast, vulnerability, sub-meter resolution, grid-stratifiable, signature LULC model by considering the contour integral $\oint_\gamma \frac{f(z)\, dz}{z - z_0}$, for defining a path γ_r as an infinitesimal counterclockwise circle around the capture point z_0, and defining the path γ_0 as an arbitrary loop with a cut line (on which the forward and reverse contributions

cancel each other out) so as to go around z_0. The total path in the model would then couls be defined by $\gamma = \gamma_0 + \gamma_r$, so $\oint_\gamma \frac{f(z)\,dz}{z-z_0} = \oint_{\gamma_0} \frac{f(z)\,dz}{z-z_0} + \oint_{\gamma_r} \frac{f(z)\,dz}{z-z_0}$. whwnce aymptotically targeting seaosnal, eco-georeferenceable, prolific capture point endmebmer foci.

From the Cauchy integral theorem, the contour integral along any path not enclosing a pole is 0[9]. If $f(z)$is analytic in some simply connected region R, then $\oint_\gamma f(z)\,dz = 0$ for any closed contour γcompletely in an oviiposition, eco-georeferenecable, predictive malaria risk model contained in R. Writing $z$as $z \equiv x + iy$and $f(z)$as $f(z) \equiv u + iv$ then gives $\oint_\gamma f(z)\,dz = \int_\gamma (u+iv)(dx+i\,dy) = \int_\gamma u\,dx - v\,dy + i\int_\gamma v\,dx + u\,dy.$ From Green's theorem,

$$\int_\gamma f(x,y)\,dx - g(x,y)\,dy = -\iint \left(\frac{\partial g}{\partial x} + \frac{\partial f}{\partial y}\right) dx\,dy, \int_\gamma f(x,y)\,dx + g(x,y)\,dy = \iint \left(\frac{\partial g}{\partial x} - \frac{\partial f}{\partial y}\right) dx\,dy,$$

so ($\diamondsuit$) becomes mathematics, Green's theorem gives the relationship between a line integral around a simple closed curve C and a double integral over the plane region D bounded by C.

$$\oint_\gamma f(z)\,dz = -\iint \left(\frac{\partial v}{\partial x} + \frac{\partial u}{\partial y}\right) dx\,dy + i\iint \left(\frac{\partial u}{\partial x} - \frac{\partial v}{\partial y}\right) dx\,dy.$$

[10]. But the Cauchy-Riemann equations will require that $\frac{\partial u}{\partial x} = \frac{\partial v}{\partial y}$ and $\frac{\partial u}{\partial y} = -\frac{\partial v}{\partial x}$, so $\oint_\gamma f(z)\,dz = 0,$ Q.E.D. for asymptotically targeting seasonal, eco-georeferenecable, aquatic, larval habitat, malaria, mosquito, capture point, hyperproductive foci.[i.e., $\oint_{C_1} f(z)\,dz = \oint_{C_2} f(z)\,dz.$].

Therefore, the first term in the above equation is 0 since γ_0 does not enclose the pole, and hence a malariologist or medical entomologist are left with $\oint_\gamma \frac{f(z)\,dz}{z-z_0} = \oint_{\gamma_r} \frac{f(z)\,dz}{z-z_0}.$ Now, let $z \equiv z_0 + re^{i\theta}$, so $dz = ire^{i\theta}\,d\theta$. Then $\oint_\gamma \frac{f(z)\,dz}{z-z_0} = \oint_{\gamma_r} \frac{f(z_0 + re^{i\theta})}{re^{i\theta}}\, ire^{i\theta}\,d\theta = \oint_{\gamma_r} f(z_0 + re^{i\theta})\,i\,d\theta.$ But an experimenter is free to allow the radius $r$to shrink in a sub-mter reoslition, grid-stratfiiable, vector arthropod, grid-stratfiiable, eco-epidemiological, LULC model for asymptotically, geo-spectrotemrpoally targeting unknown seasonal, eco-georferenecable, hyperproductive foci to 0, so $\oint_\gamma \frac{f(z)\,dz}{z-z_0} = \lim_{r\to 0} \oint_{\gamma_r} f(z_0 + re^{i\theta})\,i\,d\theta = \oint_{\gamma_r} f(z_0)\,i\,d\theta \;\; if(z_0) \oint_{\gamma_r} d\theta = 2\pi i f(z_0),$ If multiple loops are made around the capture point z_0, then the endemic equation would become $n(\gamma, z_0) f(z_0) = \frac{1}{2\pi i} \oint_\gamma \frac{f(z)\,dz}{z-z_0},$ where $n(\gamma, z_0)$is the contour winding number.

The winding number of a contour γabout a capture pointz_0, denoted $n(\gamma, z_0)$ may be definable in a sub-meter resolution, grid-stratifiable, eco-endmember, geoclassifiable, prognosticative, LULC, signature, frequency model by $n(\gamma, z_0) = \frac{1}{2\pi i} \oint_\gamma \frac{dz}{z-z_0}$.whcih may rende4r the number of times γcurve passes (counterclockwise) around an unknown, seasonal, malaria mosquito, capture point. Counterclockwise winding is assigned a positive winding number, while clockwise winding is assigned a negative winding number[2]. The winding number is also called the

index, and denoted $\mathrm{Ind}_\gamma(z_0)$[4]. The contour winding number was part of the inspiration for the idea of the Brouwer degree between two compact, oriented manifolds of the same dimension. In the language of the degree of a map, if $\gamma:[0,1]\to\mathbb{C}$ is a closed curve (i.e., $\gamma(0)=\gamma(1)$0).As such the number can be considered as a function from $\mathbb{S}^1$ to $\mathbb{C}$ in a malaria model for aymptotically geo-spectrotemporally targteing un-geosampled, seaonally prolific, aquatic, larval habitats on geoclassfiable, eco-endmember LULCs. In that context, the winding number of γaround anunknown capture point $p$in $\mathbb{C}$ may be given by the degree of the map $\frac{\gamma-p}{|\gamma-p|}$.

A similar formula may hold for the ento-cndmember LULC, malaria, mosquito, aquatic, larval, habitat, capture point, sub—meter resolution, signature, frequency derivatives of $f(z), f'(z_0)=\lim_{h\to0}\frac{f(z_0+h)-f(z_0)}{h}=\lim_{h\to0}\frac{1}{2\pi i h}\left[\oint_\gamma\frac{f(z)\,dz}{z-z_0-h}-\oint_\gamma\frac{f(z)\,dz}{z-z_0}\right]=\lim_{h\to0}\frac{1}{2\pi i h}\oint_\gamma\frac{f(z)\,[(z-z_0)-(z-z_0-h)]\,dz}{(z-z_0-h)(z-z_0)}$ which may be equivalent to $\lim_{h\to0}\frac{1}{2\pi i h}\oint_\gamma\frac{h f(z)\,dz}{(z-z_0-h)(z-z_0)}=\frac{1}{2\pi i}\oint_\gamma\frac{f(z)\,dz}{(z-z_0)^2}$. Iterating again, may reveal. $f''(z_0)=\frac{2}{2\pi i}\oint_\gamma\frac{f(z)\,dz}{(z-z_0)^3}$ in the model renderings. Continuing the process and adding the contour winding number n, may then reveal $n(\gamma,z_0)f^{(r)}(z_0)=\frac{r!}{2\pi i}\oint_\gamma\frac{f(z)\,dz}{(z-z_0)^{r+1}}$. whence optimally asymptotically geo-spectrotemporally targeting un-geosampled, seasonal, eco-georeferenceable, hyperproductive foci.

Now, since contributions from the cut line in opposite directions cancel out, hence $f(z)=\frac{1}{2\pi i}\int_{C_1}\frac{f(z')}{(z'-z_0)-(z-z_0)}dz'-\frac{1}{2\pi i}\int_{C_2}\frac{f(z')}{(z'-z_0)-(z-z_0)}dz'=\frac{1}{2\pi i}\int_{C_1}\frac{f(z')}{(z'-z_0)\left(1-\frac{z-z_0}{z'-z_0}\right)}dz'-\frac{1}{2\pi i}\int_{C_2}\frac{f(z')}{(z-z_0)\left(\frac{z'-z_0}{z-z_0}-1\right)}dz'=\frac{1}{2\pi i}\int_{C_1}\frac{f(z')}{(z'-z_0)\left(1-\frac{z-z_0}{z'-z_0}\right)}dz'+\frac{1}{2\pi i}\int_{C_2}\frac{f(z')}{(z-z_0)\left(1-\frac{z'-z_0}{z-z_0}\right)}dz'.$ in an eco-georeferenecable, forecast, vulnerability, signature, LULC malaria, mosquito sub-meter resolution, grid-stratfiable model For the first integral, $|z'-z_0|>|z-z_0|$. For the second, $|z'-z_0|<|z-z_0|$. In so doing, a Taylor series (valid for $|t|<1$) $\frac{1}{1-t}=\sum_{n=0}^{\infty}t^n$ may be parsimoniously obtainable employing the equation $f(z)=\frac{1}{2\pi i}\left[\int_{C_1}\frac{f(z')}{z'-z_0}\sum_{n=0}^{\infty}\left(\frac{z-z_0}{z'-z_0}\right)^n dz'+\int_{C_2}\frac{f(z')}{z-z_0}\sum_{n=0}^{\infty}\left(\frac{z'-z_0}{z-z_0}\right)^n dz'\right]$ which could thereafter algebraically be related $\frac{1}{2\pi i}\sum_{n=0}^{\infty}(z-z_0)^n\int_{C_1}\frac{f(z')}{(z'-z_0)^{n+1}}dz'+\frac{1}{2\pi i}\sum_{n=0}^{\infty}(z-z_0)^{-n-1}\int_{C_2}(z'-z_0)^n f(z')\,dz'$ which could be quantitated by $\frac{1}{2\pi i}\sum_{n=0}^{\infty}(z-z_0)^n\int_{C_1}\frac{f(z')}{(z'-z_0)^{n+1}}dz'+\frac{1}{2\pi i}\sum_{n=1}^{\infty}(z-z_0)^{-n}\int_{C_2}(z'-z_0)^{n-1}f(z')\,dz'$, whence the second term has been re-indexed in the model derivatives.

A Taylor series is a series expansion of a function about a point. A one-dimensional (1-D) Taylor series is an expansion of a real function $f(x)$about a capture point $x=a$is given by$f(x)=$ I $f(a)+f'(a)(x-a)+\frac{f''(a)}{2!}(x-a)^2+\frac{f^{(3)}(a)}{3!}(x-a)^3+\ldots+\frac{f^{(n)}(a)}{n!}(x-a)^n+\ldots.$ f $a=0$, the expansion is known as a Maclaurin series. Taylor's theorem (actually discovered first by Gregory) states that any function satisfying certain conditions can be expressed as a Taylor series. The Taylor (or more general) series of a function $f(x)$about a point $a$up to order $n$may be found using Series[f, {x, a, n}]. The nth term of a Taylor series of a

function f can be computed in the Wolfram Language using SeriesCoefficient[f, {x, a, n}] which may be given by the inverse Z-transform $a_n = \mathcal{Z}^{-1}\left[\frac{1}{z-a}\right](n)$. Taylor series of some common functions includeing $\frac{1}{1-x} = \frac{1}{1-a} + \frac{x-a}{(1-a)^2} + \frac{(x-a)^2}{(1-a)^3} + \dots$, $\cos x = \cos a - \sin a\,(x-a) - \frac{1}{2}\cos a\,(x-a)^2 + \frac{1}{6}\sin a\,(x-a)^3 + \dots$, $e^x = e^a\left[1 + (x-a) + \frac{1}{2}(x-a)^2 + \frac{1}{6}(x-a)^3 + \dots\right]$, $\ln x = \ln a + \frac{x-a}{a} - \frac{(x-a)^2}{2a^2} + \frac{(x-a)^3}{3a^3} - \dots$, $\sin x = \sin a + \cos a\,(x-a) - \frac{1}{2}\sin a\,(x-a)^2 - \frac{1}{6}\cos a\,(x-a)^3 + \dots$ and also the vulnarbaility, forecast, equation $\tan x = \tan a + \sec^2 a\,(x-a) + \sec^2 a \tan a\,(x-a)^2 + \sec^2 a\left(\sec^2 a - \frac{2}{3}\right)(x-a)^3 + \dots$.

To derive the Taylor series of a function $f(x)$, in an eco-georeferenecable, forecast, vulnerability, eco-endmember, signature, frequency, LULC malaria, mosquito sub-meter resolution, grid-stratified, geo-spectrotemporal model note that the integral of the $(n+1)$st derivative $f^{(n+1)}$ of $f(x)$ from the capure point x_0 to an arbitrary unknown point x may be given by $\int_{x_0}^{x} f^{(n+1)}(x)\,dx = \left[f^{(n)}(x)\right]_{x_0}^{x} = f^{(n)}(x) - f^{(n)}(x_0)$, where $f^{(n)}(x_0)$ is the nth derivative of $f(x)$ evaluated at x_0, and is therefore simply a constant. Now by integrating an interatively, interpolative,aquatic, larval habitat, malaria, mosquito, eco-endmember LULC signature, an experimenter may obtain $\int_{x_0}^{x}\left[\int_{x_0}^{x} f^{(n+1)}(x)\,dx\right]dx = \int_{x_0}^{x}\left[f^{(n)}(x) - f^{(n)}(x_0)\right]dx = \int_{x_0}^{x}\int_{x_0}^{x}\int_{x_0}^{x} f^{(n+1)}(x)\,(dx)^3 = f^{(n-2)}(x) - f^{(n-2)}(x_0) - (x-x_0)\,f^{(n-1)}(x_0) - \frac{(x-x_0)^2}{2!}f^{(n)}(x_0)$ where $f^{(k)}(x_0)$ is again a constant. Integrations then could render $\underbrace{\int\cdots\int_{x_0}^{x}}_{n+1} f^{(n+1)}(x)\,(dx)^{n+1} = f(x) - f(x_0) - (x-x_0)\,f'(x_0) - \frac{(x-x_0)^2}{2!}f''(x_0) - \dots - \frac{(x-x_0)^n}{n!}f^{(n)}(x_0)$. Rearranging this equation then would render the 1-D Taylor series $f(x) = f(x_0) + (x-x_0)\,f'(x_0) + \frac{(x-x_0)^2}{2!}f''(x_0) + \dots + \frac{(x-x_0)^n}{n!}f^{(n)}(x_0) + R_n = \sum_{k=0}^{n}\frac{(x-x_0)^k f^{(k)}(x_0)}{k!} + R_n$. Here, R_n would be a remainder term known as the Lagrange remainder, which may be given by $R_n = \underbrace{\int\cdots\int_{x_0}^{x}}_{n+1} f^{(n+1)}(x)\,(dx)^{n+1}$. Rewriting the repeated integral then would render $R_n = \int_{x_0}^{x} f^{(n+1)}(t)\,\frac{(x-t)^n}{n!}\,dt$. in the malaria model output.

Now, from the mean-value theorem for a function $g(x)$, it must be true that $\int_{x_0}^{x} g(x)\,dx = (x-x_0)\,g(x^*)$ for some $x^* \in [x_0, x]$. Therefore, integrating $n+1$ times could render the result $R_n = \frac{(x-x_0)^{n+1}}{(n+1)!}f^{(n+1)}(x^*)$ in an empirical geo-spectrotemporal, signature, frequency, sub-meter resolution dataset of vulnerability forecasts (asymptotically targeted , seasonal, hyperproductive, ento-ecoendmember, capture point foci) so the maximum error after n terms of the Taylor series is the maximum value of (18) running through all $x^* \in [x_0, x]$. Note that the Lagrange remainder R_n is also sometimes taken to refer to the remainder when terms up to the $(n-1)$st power are taken in the Taylor series.

International Research Journal of Computer Science and Application
Vol. 2, No. 1, March 2018, pp. 1-181
Available Online at http://acascipub.com/Journals.php

Taylor series can also be defined for functions of a complex eco-georeferenecable, forecast, vulnerability, geo-spectrotemporal, geoclassfiiable, LULC malaria, mosquito sub-meter resolution, explanatory model, frequency, robustifiable, gridded variable. In a Cauchy integral formula, $f(z)=\frac{1}{2\pi i}\int_C \frac{f(z')\,dz'}{z'-z}=\frac{1}{2\pi i}\int_C \frac{f(z')\,dz'}{(z'-z_0)-(z-z_0)}=\frac{1}{2\pi i}\int_C \frac{f(z')\,dz'}{(z'-z_0)\left(1-\frac{z-z_0}{z'-z_0}\right)}$. In the interior of C, $\frac{|z-z_0|}{|z'-z_0|}<1$ in the malaria model residual datatset so, employing $\frac{1}{1-t}=\sum_{n=0}^{\infty} t^n$, it would follow that $f(z)=\frac{1}{2\pi i}\int_C \sum_{n=0}^{\infty}\frac{(z-z_0)^n f(z')\,dz'}{(z'-z_0)^{n+1}}=\frac{1}{2\pi i}\sum_{n=0}^{\infty}(z-z_0)^n\int_C \frac{f(z')\,dz'}{(z'-z_0)^{n+1}}$. Using the Cauchy integral formula for derivatives, $f(z)=\sum_{n=0}^{\infty}(z-z_0)^n\frac{f^{(n)}(z_0)}{n!}$. an alternative form of the 1-D Taylor series may be obtainable by letting $x-x_0\equiv\Delta x$ so that $x\equiv x_0+\Delta x$. Substituting this result into (◇)could render $f(x_0+\Delta x)=f(x_0)+\Delta x\,f'(x_0)+\frac{1}{2!}(\Delta x)^2 f''(x_0)+\ldots.$

A Taylor series of a real function in any time series, malaria, mosquito habitat variable $f(x,y)$ may be given by : $f(x+\Delta x,y+\Delta y)=f(x,y)+\left[f_x(x,y)\Delta x+f_y(x,y)\Delta y\right]$ which when summed with $\frac{1}{2!}\left[(\Delta x)^2 f_{xx}(x,y)+2\Delta x\Delta y\,f_{xy}(x,y)+(\Delta y)^2 f_{yy}(x,y)\right]+\frac{1}{3!}\left[(\Delta x)^3 f_{xxx}(x,y)+\right.$ could be equivalent to $\left.3(\Delta x)^2\Delta y\,f_{xxy}(x,y)+3\Delta x(\Delta y)^2 f_{xyy}(x,y)+(\Delta y)^3 f_{yyy}(x,y\right.$ This can be further generalized for a real function in n variables, $f(x_1,\ldots,x_n)=\sum_{j=0}^{\infty}\left\{\frac{1}{j!}\left[\sum_{k=1}^{n}(x_k-a_k)\frac{\partial}{\partial x_k'}\right]^j f(x_1',\ldots,x_n')\right\}_{x_1'=a_1,\ldots x_n'=a_n}$. Rewriting the frequency estimator then could asymptotically, optimally, geo-spectrotemporally render $f(x_1+a_1,\ldots,x_n+a_n)=\sum_{j=0}^{\infty}\left\{\frac{1}{j!}\left(\sum_{k=1}^{n}a_k\frac{\partial}{\partial x_k'}\right)^j f(x_1',\ldots,x_n')\right\}_{x_1'=x_1,\ldots x_n'=x_n}$. Subsequently taking $n=2$ I n could then render $f(x_1,x_2)=\sum_{j=0}^{\infty}\left\{\frac{1}{j!}\left[(x_1-a_1)\frac{\partial}{\partial x_1'}+(x_2-a_2)\frac{\partial}{\partial x_2'}\right]^j f(x_1',x_2')\right\}_{x_1'=a_1,x_2'=a_2}$ which would be equivalent to $f(a_1,a_2)+\left[(x_1-a_1)\frac{\partial f}{\partial x_1}+(x_2-a_2)\frac{\partial f}{\partial x_2}\right]\quad\frac{1}{2!}\left[(x_1-a_1)^2\frac{\partial^2 f}{\partial x_1^2}+2(x_1-a_1)(x_2-a_2)\frac{\partial^2 f}{\partial x_1\partial x_2}+(x_2-a_2)^2\frac{\partial^2 f}{\partial x_2^2}\right]+\ldots.$ .Taking any eco-endmember, geoclassfiable, geosampled, LULC, signature frequency could then render

$$f(x_1+a_1,x_2+a_2,x_3+a_3)=\sum_{j=0}^{\infty}\left\{\frac{1}{j!}\left(a_1\frac{\partial}{\partial x_1'}+a_2\frac{\partial}{\partial x_2'}+a_3\frac{\partial}{\partial x_3'}\right)^j f(x_1',x_2',x_3')\right\}_{x_1'=x_1,x_2'=x_2,x_3'=x_3},$$

$$f(\mathbf{r}+\mathbf{a})=\sum_{j=0}^{\infty}\left[\frac{1}{j!}(\mathbf{a}\cdot\nabla_{\mathbf{r}'})^j f(\mathbf{r}')\right]_{\mathbf{r}'=\mathbf{r}}.$$

or, in vector form The zeroth- and first-order terms are $f(\mathbf{r})$ and $(\mathbf{a}\cdot\nabla_{\mathbf{r}'})f(\mathbf{r}')|_{\mathbf{r}'=\mathbf{r}}$, respectively. The explanative second-order term may then be $\frac{1}{2}(\mathbf{a}\cdot\nabla_{\mathbf{r}'})(\mathbf{a}\cdot\nabla_{\mathbf{r}'})f(\mathbf{r}')|_{\mathbf{r}'=\mathbf{r}}=\frac{1}{2}\mathbf{a}\cdot[\mathbf{a}\cdot\nabla_{\mathbf{r}'}(\nabla_{\mathbf{r}'}f(\mathbf{r}'))]|_{\mathbf{r}'=\mathbf{r}}$, so the first few terms of the expansion would be $f(\mathbf{r}+\mathbf{a})=f(\mathbf{r})+(\mathbf{a}\cdot\nabla_{\mathbf{r}'})f(\mathbf{r}')|_{\mathbf{r}'=\mathbf{r}}+\frac{1}{2}\mathbf{a}\cdot[\mathbf{a}\cdot\nabla_{\mathbf{r}'}(\nabla_{\mathbf{r}'}f(\mathbf{r}'))]|_{\mathbf{r}'=\mathbf{r}}$ whence aymptotically geo-spectrotemporally targeting seasonal, un-geosampled, aquatic, larval habitat, capture point, hyperproductive, eco-endmember, LULC foci.

International Research Journal of Computer Science and Application
Vol. 2, No. 1, March 2018, pp. 1-181
Available Online at http://acascipub.com/Journals.php

Re-indexing the *An. arabiesnis*, aquatic, larval habitat, sub-meter resolution, LULC again, revealed $f(z)=\frac{1}{2\pi i}\sum_{n=0}^{\infty}(z-z_0)^n\int_{C_1}\frac{f(z')}{(z'-z_0)^{n+1}}dz' \quad +\frac{1}{2\pi i}\sum_{n=-\infty}^{-1}(z-z_0)^n\int_{C_2}\frac{f(z')}{(z'-z_0)^{n+1}}dz'.$ Since the integrands, including the function $f(z)$, were analytic in the annular region defined by C_1 and C_2, the integrals were independent of the path of integration in that LULC region. We replaced paths of integration C_1 and C_2 by a circle C of radius r with $r_1 \le r \le r_2$, then

$f(z)=\frac{1}{2\pi i}\sum_{n=0}^{\infty}(z-z_0)^n\int_{C}\frac{f(z')}{(z'-z_0)^{n+1}}dz'+\frac{1}{2\pi i}\sum_{n=-\infty}^{-1}(z-z_0)^n\int_{C}\frac{f(z')}{(z'-z_0)^{n+1}}dz' =\frac{1}{2\pi i}\sum_{n=-\infty}^{\infty}(z-z_0)^n\int_{C}\frac{f(z')}{(z'-z_0)^{n+1}}dz' =$

$\sum_{n=-\infty}^{\infty}a_n(z-z_0)^n.$ Generally, the path of integration can be any path γ that lies in the annular region and encircles z_0 once in the positive (counterclockwise) direction[4].

The complex residues a_n in the malaria model were therefore defined by $a_n \equiv \frac{1}{2\pi i}\int_{\gamma}\frac{f(z')}{(z'-z_0)^{n+1}}dz'.$ Note that the annular region itself was expanded by increasing r_1 and decreasing r_2 until singularities of $f(z)$ that lay just outside C_1 or just inside C_2 a. If $f(z)$ has no singularities inside C_2, then all the b_k terms in (◇) equal zero and the Laurent series of (◇) reduces to a Taylor series with coefficients[6]'.

The Laurent generalization of a power series in non-negative integral powers of the difference $z-\alpha$ or in non-positive integral powers of $z-\alpha$ in the form $\sum_{k=-\infty}^{+\infty}c_k(z-\alpha)^k$. [2].The series (is understood as the sum of two series: $\sum_{k=0}^{+\infty}c_k(z-\alpha)^k,$ the regular part of the Laurent series, and $\sum_{k=-\infty}^{-1}c_k(z-\alpha)^k,$ the principal part of the Laurent series[6]. The series is assumed to converge if and only if its regular and principal parts converge. Properties of Laurent series include: 1) if the domain of convergence of a Laurent series contains interior points, then this domain is a circular annulus $D=\{z\in\mathbf{C}\colon 0\le r<|z-\alpha|<R\le+\infty\}$ with centre at the point $\alpha\neq\infty$; 2) at all interior points of the annulus of convergence D the series (1) converges absolutely; 3) as for power series, the behaviour of a Laurent series at points on the bounding circles $|z-\alpha|=r$ and $|z-\alpha|=R$ can be very diverse; 4) on any compact set $K\subset D$ the series converges uniformly; 5) the sum of the series (1) in D is an analytic function $f(z)$; 6) the series can be differentiated and integrated in D term-by-term; 7) the coefficients c_k of a Laurent series =may be optimally ,asymptotically, parsimoniously definable in terms of its sum $f(z)$ by the formulas $c_k=\frac{1}{2\pi i}\int_{\gamma}\frac{f(z)\,dz}{(z-\alpha)^{k+1}}, \quad k=0,\pm1,\ldots,$ in a sub-meter resolution, grid-stratifiable, eco-endmember, prognosticative, signature, frequency, eco-georeferenceable, LULC model where $\gamma=\{z\colon |z-\alpha|=\rho,\ \square r<\rho<R\}$ is any circle with centre α situated in D; and 8) expansion in a Laurent series is unique, that is, if $f(z)\equiv\phi(z)$ in D, then all the coefficients of their Laurent series in powers of $z-\alpha$ coincide[8].

For the case of a centre at a unknown, capture point at infinity, $\alpha=\infty$, the Laurent series may take the form $\sum_{k=-\infty}^{+\infty}c_kz^k,$ whence the regular part is $\sum_{k=-\infty}^{0}c_kz^k,$ while the principal part is $\sum_{k=1}^{+\infty}c_kz^k.$ The domain of convergence of this series may have the form $D'=\{z\colon 0\le r<|z|<R\le+\infty\},$ where the formulas tend to go into $c_k=-\frac{1}{2\pi i}\int_{\gamma}z^{k+1}f(z)\,dz, \quad k=0,\pm1,\ldots,$ whence $\gamma=\{z\colon |z|=\rho,\ \square r<\rho<R\}$.Otherwise all the properties would be the same as in the case of a finite centre α.The application of Laurent series is based mainly on

Laurent's theorem: Any single-valued analytic function $f(z)$ in an annulus $D=\{z\colon 0\leq r<|z-a|<R\leq+\infty\}$ can be represented in D by a convergent Laurent series [8]. In particular, in a punctured capture point, sub-meter resolution, geo-spectrotemporally, asymptotically,optimally forecasted unknown, eco-georeferenecable, geoclassifiable,aquatic, larval habitat neighbourhood $D=\{z\colon 0<|z-a|<R\}$ of a prolific,malaria, mosquito, un-geosampled, capture point a of single-valued, iteratively interpolated, LULC kriged signature character derived from an analytic function $f(z)$ may be represented by a Laurent series, which serves as the main instrument for investigating its behaviour in a neighbourhood of an isolated singularcapture point.

For holomorphic functions $f(z)$ of several complex variables $z=(z_1,\ldots,z_n)$ the following proposition can be regarded as the analogue of Laurent's theorem: Any function $f(z)$, holomorphic in the product D of annuli $D_\nu=\{z_\nu\in\mathbf{C}\colon 0\leq r_\nu<|z_\nu-a_\nu|<R_\nu\leq+\infty\}$, can be represented in D as a convergent multiple Laurent series $f(z)=\sum_{k=-\infty}^{+\infty}c_k(z-a)^k$, which the summation extends over all vector arthropod-related, geo-spectrotemporal, signature, frequency, eco- endmember, LULC, integral multi-indices $k=(k_1,\ldots,k_n)$, $|k|=k_1+\ldots+k_n$, $c_k=\frac{1}{(2\pi i)^n}\int_\gamma\frac{f(z)\,dz}{(z-a)^{k+n}}$, where γ is the product of the circles $\gamma_\nu=\{z_\nu\in\mathbf{C}\colon z_\nu=a_\nu+\rho_\nu e^{it},\ r_\nu<\rho_\nu<R_\nu,\ 0\leq t\leq 2\pi\}$, $\nu=1,\ldots,n$. The domain of convergence of the series (4) is logarithmically convex and is a relatively-complete Reinhardt domain. However, the use of multiple Laurent series is limited, since for $n\geq 2$ holomorphic functions $f(z)$ cannot have isolated singularities.domain D in the complex space $\mathbf{C}^n, n\geq 1$, with centre at a point $a=(a_1,\ldots,a_n)\in\mathbf{C}^n$, with the following property: Together with any point $z^0=(z_1^0,\ldots,z_n^0)\in D$, the probabilisc paradigm domain also may contain the set $\{z=(z_1,\ldots,z_n)\colon |z_\nu-a_\nu|=|z_\nu^0-a_\nu|,\ \nu=1,\ldots,n\}$.

A Reinhardt domain D with $a=0$ is invariant under the transformations $\{z^0\}\to\{z_\nu^0e^{i\theta_\nu}\}, 0\leq\theta_\nu<2\pi, \nu=1,\ldots,n$. The Reinhardt domains constitute a subclass of the Hartogs domains (cf. Hartogs domain) and a subclass of the circular domains, which are defined by the following condition: Together with any $z^0\in D$, the absolute forecastable, domain would contains the set $\{z=(z_1,\ldots,z_n)\colon z=a+(z^0-a)e^{i\theta}, 0\leq\theta<2\pi\}$, i.e. all malaria mosquito seasonally forecasted , hyperproductive, eco-georeferenceable ,capture points of the circle with centre a and radius $|z^0-a|=(\sum_{\nu=1}^n|z_\nu^0-a_\nu|^2)^{1/2}$ that lie on the complex line through a and z^0.A Reinhardt domain D is called a complete Reinhardt domain if together with any malaria, mosquito, geosampled eco-endmember, sub-mter resolution, geocalssified, LULC, capture point $z^0\in D$ it also contains the polydisc $\{z=(z_1,\ldots,z_n)\colon |z_\nu-a_\nu|\leq|z_\nu^0-a_\nu|,\ \nu=1,\ldots,n\}$ .A complete Reinhardt domain is star-like with respect to its centre a (cf. Star-like domain).Examples of complete Reinhardt domains are balls and polydiscs in $\mathbf{C}^n$. A circular domain D is called a complete circular domain if together with any pont $z^0\in D$ it also contains the entire disc $\{z=a+(z^0-a)\zeta\colon|\zeta|\leq 1\}$.A Reinhardt domain D is called logarithmically convex if the image $\lambda(D^*)$ of a non-heuristically optimizable aset $D^*=\{z=(z_1,\ldots,z_n)\in D\colon z_1\ldots z_n\neq 0\}$under the mapping $\lambda\colon z\to\lambda(z)=(\ln|z_1|,\ldots,\ln|z_n|)$is a convex set in the real space $\mathbf{R}^n$[9]. An important property of logarithmically-convex Reinhardt domains is the following: Every such domain in $\mathbf{C}^n$ is the interior of the set of points of absolute convergence (i.e. the domain of convergence) of some power series in $z_1-a_1,\ldots,z_n-a_n$, and conversely: The domain of convergence of any power series in $z_1,\ldots,z_n$ is a logarithmically-convex Reinhardt domain with centre $a=0$.

Hence, Let k be any field with an interpolated LULC, sub-mter resolution, eco-endmember, geo-spectrotemporal, geosampled, malaria, mosquito, forecast, vulnerability model for optimally asymptotically targeting seasonal, eco-georeferenceable, hyperproductive, aquatic, larval habitat , capture point foci . The Laurent series then

could be used to denote a formal expansion of the form $\sum_{i=-N}^{\infty} a_i X^i, \quad a_i \in k, \quad N \in \mathbf{Z}$. The expressions may be added termwise and multiplied as follows: $\left(\sum_{i=-N}^{\infty} a_i X^i\right)\left(\sum_{i=-M}^{\infty} b_i X^i\right) = \sum_{j=-N-M}^{\infty} c_j X^j$, where $c_j = \sum_{\substack{k+l=j \\ k,l \in \mathbf{Z}}} a_k b_l$ in the paradigm. The result may be a field, denoted by $k((X))$. It would be the quotient field of the ring of formal power series $k[[X]]$, and is called the field of formal Laurent series. A valuation is defined by $v(\sum_{i=-N}^{\infty} a_i X^i) = -N$ if $a_{-N} \neq 0$[9] .In so doing, $k((X))$ would be a discretely valued complete field; the ring of integers is $k[[X]]$, ansd the maximal ideal is $Xk[[X]]$ whicle the residue field is k. Subsequently, a Laurent polynomial synthesized from an empirical dataset fo geosampeld, malaria, mosquito, sub-mter resolution, eco-endmember LULC, signature estimators over k would be an expression $\sum_{i=-N}^{M} a_i X^i, -N \leq M, N, M \in \mathbf{Z}$ for optimally targeting seasonal, prolific foci.

All these functions f(z)fare representable in the form of a Mittag-Leffler expansion f(z)=h(z)+∑n=1∞[gn(z)+pn(z)],(2)(2)f(z)=h(z)+∑n=1∞[gn(z)+pn(z)], where pn(z) is a polynomial chosen in dependence of gn(z) so that a series (an uncoalesced dataset of frequency, sub-meter resolution, grid-stratified LULC datasets) is uniformly convergent (after the removal of a finite number of terms) on any compact set K⊂C where h(z) is an arbitrary entire function.The Mittag-Leffler theorem implies that any given meromorphic function f(z) in C with poles and corresponding principal parts gn(z) of the Laurent expansion of f(z) in a neighbourhood can be expanded in a capture point, malaria mosquito geosampled, geo-spectrotemporal, series where the entire function h(z) is determined by f(z). Mittag-Leffler may provide a general construction of sub-meter resolution, eco-endmember, signature, LULC polynomials pn(z) for finding the entire function h(z) relative to a given f(z). To obtain optimal forecasts (i.e, field-verifiable, seasonal, unknown eco-georeferenceable, prolific, capture point, aquatic, larval habitats) based on a kriged robust signal , methods of the theory of residues (cf. Residue of an analytic function) may be applied.

A generalization of the quoted theorem, also due to Mittag-Leffler, states that for any domain D of the extended complex plane C¯, any sequence {an} of all limit points of which are in the boundary ∂D, and corresponding principal parts (1), there is a function f(z)f(z), meromorphic in DD, having poles at {an}{an}, and only there, with the given principal parts (1). In this form the Mittag-Leffler theorem generalizes to open Riemann surfaces DD (see [7]); for the existence of meromorphic functions on compact Riemann surfaces with given singularities see Abelian differential; Differential on a Riemann surface; Riemann–Roch theorem. The Mittag-Leffler theorem is also true for abstract meromorphic functions gngn, f:D→Ff:D→F, D⊂C¯D⊂C¯, with values in a Banach space FF (see [8]).

Another generalization of the Mittag-Leffler theorem states that for any sequence {an}⊂C{an}⊂C, |a1|≤|a2|≤…|a1|≤|a2|≤…, liman=∞liman=∞, and corresponding functionsgn(z)=∑k=1∞cnk(z−an)kgn(z)=∑k=1∞cnk(z−an)k that are entire functions of the variable wn=1/(z−an)wn=1/(z−an), there is a single-valued analytic function f(z)f(z) having singular points at anan, and only there, and with principal parts gn(z)gn(z) (see [3]).

A generalization of the quoted theorem, also due to Mittag-Leffler, states that for any domain DD of the extended complex plane C¯C¯, any sequence {an}{an} of points an∈Dan∈D all limit points of which are in the boundary ∂D∂D, and corresponding principal parts (1), there is a function f(z)f(z), meromorphic in DD, having poles at {an}{an}, and only there, with the given principal parts (1). In this form the Mittag-Leffler theorem generalizes to open Riemann surfaces DD (see [7]); for the existence of meromorphic functions on compact Riemann surfaces with given singularities see Abelian differential; Differential on a Riemann surface; Riemann–Roch theorem. The Mittag-Leffler theorem is also true for abstract meromorphic functions gngn, f:D→Ff:D→F, D⊂C¯D⊂C¯, with values in a Banach space FF (see [8]).
Another generalization of the Mittag-Leffler theorem states that for any sequence {an}⊂C{an}⊂C, |a1|≤|a2|≤…|a1|≤|a2|≤…, liman=∞liman=∞, and corresponding functionsgn(z)=∑k=1∞cnk(z−an)kgn(z)=∑k=1∞cnk(z−an)kthat are entire functions of the variable wn=1/(z−an)wn=1/(z−an), there is a single-valued analytic function f(z)f(z) having singular points at anan, and

only there, and with principal parts gn(z)gn(z) (see [3]).For analytic functions of several complex variables a generalization of the Mittag-Leffler problem on the construction of a function with given singularities is the first (additive) Cousin problem (cf. Cousin problems). In this connection the following equivalent statement of the Mittag-Leffler theorem is often useful. Let Ω=∪jΩjΩ=∪jΩj, where the ΩjΩj are open sets in CC, and let there be given meromorphic functions gjgj, respectively, on the sets ΩjΩj, where the differences gj−gkgj−gk are regular functions on the intersections Ωj∩ΩkΩj∩Ωk for all jj and kk. Then there is on ΩΩ a meromorphic function ff such that the differences f−gjf−gj are regular on ΩjΩj for all jj (see [5], [6]).For the Mittag-Leffler theorem on the expansion of single-valued branches of an analytic function in a star see Star of a function element.

For analytic functions of several complex variables a generalization of the Mittag-Leffler problem on the construction of a function with given singularities is the first (additive) Cousin problem (cf. Cousin problems). In this connection the following equivalent statement of the Mittag-Leffler theorem is often useful. Let Ω=∪jΩjΩ=∪jΩj, where the Ωj are open sets in C, and let there be given meromorphic functions gj, respectively, on the sets Ωj, where the differences gj−gk are regular functions on the intersections Ωj∩Ωk for all j and k. Then there is on Ω a meromorphic function f such that the differences f−gj are regular on Ω for all j (see [5] and [6]). A specific first Cousin problem on M is solvable if and only if the corresponding section of $\mathcal{M}/\mathcal{O}$ belongs to the image of the habitat signature mapping ϕ. An arbitrary first Cousin problem on M is solvable if and only if ϕ is surjective [6]. On any complex manifold M one has an exact sequence $\Gamma(\mathcal{M}) \xrightarrow{\phi} \Gamma(\mathcal{M}/\mathcal{O}) \to H^1(M,\mathcal{O})$.

If the Čech cohomology for M with coefficients in $\mathcal{O}$ is trivial (i.e. $H^1(M,\mathcal{O})=0$) in an eco-geoclassfiied, malaria, mosquito, capture point, LULC model for asymptotically geo-spectrotemporally targeting, eco-georeferenceable, seasonal, hyperproductive, geo-spectrotemporal, capture point, eco-endmember foci, then ϕ is surjective and $H^1(\mathcal{U},\mathcal{O})=0$ for any covering $\mathcal{U}$ of M. Thus, if $H^1(M,\mathcal{O})=0$ occurs in a sub-meter resolution, grid-stratifiable, forecast, vulnerability, signature malaria, mosquito, model any first Cousin problem is solvable on M employing the classical, cohomological and local version. In particular, the problem is solvable in all domains of holomorphy and on Stein manifolds (cf. Stein manifold). If $D \subset \mathbf{C}^2$, then the first Cousin problem in D is solvable in the signature paradigms if and only if D is a domain of holomorphy. An example of an unsolvable first Cousin problem in these model outputs would be $M=\mathbf{C}^2 \setminus \{0\}, U_\alpha = \{z_\alpha \neq 0\}, \alpha = 1,2, f_1 = (z_1 z_2)^{-1}, f_2 = 0$.

Given an open covering $\mathcal{U}=\{U_\alpha\}$ of a complex manifold M and, in each U_α, a meromorphic function $f_\alpha, f_\alpha \not\equiv 0$ on each component of U_α, with the assumption that the functions $f_{\alpha\beta} = f_\alpha f_\beta^{-1}$ are holomorphic and nowhere vanishing in $U_{\alpha\beta}$ for all α, β (compatibility condition). It is required to construct a meromorphic function f on M such that the functions $f f_\alpha^{-1}$ are holomorphic and nowhere vanishing in U_α for all α.The cohomological formulation of the second Cousin problem is as follows. Given the covering $\mathcal{U}$ and functions $f_{\alpha\beta}$, holomorphic and nowhere vanishing in the intersections $U_{\alpha\beta}$, and forming a multiplicative $\mathbf{1}$-cocycle, $f_{\alpha\beta} f_{\beta\alpha} = 1$ in $U_{\alpha\beta}$; $f_{\alpha\beta} f_{\beta\gamma} f_{\gamma\alpha} = 1$ in $U_\alpha \bigcap U_\beta \bigcap U_\gamma$, it is required to find functions h_α, holomorphic and nowhere vanishing in U_α, such that $f_{\alpha\beta} = h_\beta h_\alpha^{-1}$ in $U_{\alpha\beta}$ for all α, β. If the cocycle $\{f_{\alpha\beta}\}$ corresponds to the data of a second Cousin problem and the required h_α exist, then the function $f = \{f_\alpha h_\alpha \text{ in } \square U_\alpha\}$ is defined and meromorphic throughout M and is a solution to the given second Cousin problem. Conversely, if a specific second Cousin problem is solvable, then the corresponding cocycle is a holomorphic coboundary. The localized second Cousin problem. To each set of data $\{U_\alpha, f_\alpha\}$ for the second Cousin problem there corresponds a uniquely defined global section of the sheaf $\mathcal{M}^*/\mathcal{O}^*$ (in analogy to the first Cousin problem), where $\mathcal{M}^* = \mathcal{M} \setminus \{0\}$ (with 0 the null section) is the multiplicative sheaf of germs of meromorphic functions and $\mathcal{O}^*$ is the subsheaf of $\mathcal{O}$ in which each stalk $\mathcal{O}_z^*$ consists of germs of holomorphic functions that do not vanish at z. The mapping of global sections $\Gamma(\mathcal{M}^*) \xrightarrow{\psi} \Gamma(\mathcal{M}^*/\mathcal{O}^*)$

The maps a meromorphic function f to a section κ_f^* of the sheaf $\mathcal{M}^*/\mathcal{O}^*$, where $\kappa_f^*(z)$ is the class in $\mathcal{M}_z^*/\mathcal{O}_z^*$ of the germ of f at $z, z \in M$. The localized second Cousin problem is: Given a global section κ^* of the

sheaf $\mathcal{M}^* / \mathcal{O}^*$, to find a meromorphic function f on M, $f \not\equiv 0$ on the components of M (i.e. a global section of $\mathcal{M}^*$), such that $\psi(f) = \kappa^*$.

The sections of M^* / Q^* uniquely correspond to divisors (cf. Divisor), therefore $\mathcal{M}^* / \mathcal{O}^* = \mathcal{D}$ is called the sheaf of germs of divisors[7]. A divisor on a complex manifold M is a formal locally finite sum $\sum k_j \Delta_j$, where k_j are integers and Δ_j analytic subsets of M of pure codimension 1. To each meromorphic function f corresponds the divisor whose terms are the irreducible components of the zero and polar sets of f with respective multiplicities k_j, with multiplicities of zeros considered positive and those of poles negative. Hence any iteratively interpolative, ento-ecoendmember, eco-geoclassifiable, sub-mter resolution, aquatic, larval habitat mapping ψ of each LULC function f to its signature divisor (f); (i.e., proper frequency divisors) may enable the model to target seasonal, eco-georeferenceable hyperproductive capture point foci. The second Cousin problem in terms of these signature divisors may be that a divisor Δ on the manifold M, may be optimally usable to construct a meromorphic function f on M such that $\Delta = (f)$.

Theorems concerning the solvability of the second Cousin problem may be regarded as multi-dimensional generalizations of Weierstrass' theorem on the construction of a meromorphic function with prescribed zeros and poles especially when quantitating empirical datasets of geosampled, *An. arabiensis*, eco-endmember, eco-geoclassfiiable LULC, sub-mter resolution, grid-stratifiable, aquatic, larval habitat, signature, frequency datasets. As in the case of the first Cousin problem, a necessary and sufficient condition for the solvability of any second Cousin problem in these vulnerability paradigms in cohomological version is that $H^1(M, \mathcal{O}^*) = 0$. Unfortunately, the sheaf $\mathcal{O}^*$ is not coherent, and this condition is less effective. The attempt to reduce a given second Cousin problem to a first Cousin problem in a malaria mosquito, forecast, vulnerability, eco-geoclassifiable, LULC signature model for optimally asymptotically targeting seasonal, eco-georferenecable, prolific foci may be by taking logarithms encounters an obstruction in the form of an integral 2-cocycle. In so doing an exact sequence $H^1(M, \mathcal{O}) \to H^1(M, \mathcal{O}^*) \xrightarrow{\alpha} H^2(M, \mathbf{Z})$, may be extarctable where Z is the constant sheaf based on the geosampled density, larval count, integer values. Thus, if $H^1(M, \mathcal{O}) = H^2(M, \mathbf{Z}) = 0$, any second Cousin problem is solvable on M, and any divisor is proper in these paradigms.

If M, is a Stein manifold, then α is an isomorphism; in any sub-meter resolution, eco-endmember, malaria, mosquito, ovispsoition, eco-geoclassfiable, LULC, signature model, then the topological condition $H^2(M, \mathbf{Z}) = 0$ on a Stein manifold M is necessary and sufficient for the second Cousin problem cohomological version to be solvable (i.e., parsimonious targeting of hyperproductive , aquatic, larval habitat, seasonal foci). The composite LULC mapping $c = \alpha \circ \beta, \Gamma(\mathcal{D}) \xrightarrow{\beta} H^1(M, \mathcal{O}^*) \xrightarrow{\alpha} H^2(M, \mathbf{Z})$ may illustrate each signature divisor Δ to an element $c(\Delta)$ of the group $H^2(M, \mathbf{Z})$, which may be known as the Chern class of Δ in these paradigms The specific second Cousin problem corresponding to Δ may then be solvable, assuming $H^1(M, \mathcal{O}) = 0$, if and only if the Chern class of Δ is trivial: $c(\Delta) = 0$ in the model output. On a Stein manifold, the LULV mapping c would be surjective; moreover, every ento-ecoepidemiological, sub-meter resolution, grid-stratifiable, discontinuous, capture point element in $H^2(M, \mathbf{Z})$ may be expressed as $c(\Delta)$ for some divisor Δ with positive multiplicities k_j. Thus, the obstructions to the solution of the second Cousin problem on a Stein manifold M may be completely describle in a sub-meter resolution, grid-stratifiiable, eco-geoclassifiable, iterative, interpolative, signature LULC model for optimally asymptotically identifying unknown, seasonal, hyperproductive, aquatic, larval habitat, capture point foci by the group $H^2(M, \mathbf{Z})$ but the following restrictions must be maintained:

1) $M = \mathbf{C}^2 \setminus \{z_1 = z_2, \square |z_1| = 1\}$; the first Cousin problem is unsolvable ; the second Cousin problem is unsolvable, (e.g., for the divisor $\Delta = M \cap \{z_1 = z_2, \square |z_1| < 1\}$ with multiplicity 1)

2) $M = \{|z_1^2 + z_2^2 + z_3^2 - 1| < 1\} \subset \mathbf{C}^3$, Δ may be one of the eco-endmember, components of the intersection of M, and the plane $z_2 = iz_1$ with multiplicity 1. The second Cousin problem is then unsolvable (M, is a domain of holomorphy, the first Cousin problem is solvable) in the paradigm.

3) The first and second Cousin problems are solvable in domains $D = D_1 \times \ldots \times D_n \subset \mathbf{C}^n$, where Dj are plane domains and all Dj, with the possible exception of one, are simply connected. of c0 in a LULC model specification for but it fails for Hilbert spaces.

The following list of examples is intended to be a representative sampling of some of the more useful known proximinal sets which may help malariologists, medical entomologists and other researchers to employ geoclassfiiable, grid-stratified, sub-meter resolution, eco-endmember, ento--epidemiological, malaria-related, LULC, orthogonal, or geometric mean regression models for optimally targeting seasonal, un-geosampled, hyperproductive,capture point, aquatic, laval, habitat foci:

(1) Any reflexive subspace (Klee [1949]), e.g., a finite-dimensional subspace (Riesz [1918]).
(2) Any weak* closed subset of a dual space (Phelps [1960]).
(3) Any closed convex subset of a reflexive space (Klee [1918]).
(4) The rational functions,G%J'i,n" &[a, b], 1 < p < CO(Walsh [1931],
Efimov and Stechkin lo]).
(5) The exponential sums in L,,[a, b], 1 < p < co (Hobby and Rice[1967],
6) The splines in C[u, b] of order n with k free knots
(7) Any weak-operator closed subset of the space of operators on aHilbert space, (e.g. the positive or Hermitian operators (Halmos [1972]).
The known proofs of these results exhibit a variety of techniques, although there may a common thread of "compactness" interwoven throughout the theoreums for constructing a robust, eco-geoeferenecable, sub-meter resolution, grid-stratifiable, endmember, LULC, prognosticative, vulnerability model.

In this paper we proved a simple yet general existence theorem can help quantitate an endmember, grid-stratified, oviposition, capture point, sub-meter resolution, malaria, mosquito, forecast, vulnerability, eco-georeferenecable, LULC model. To do this, we first generalized the important notion of an "approximatively compact" set (which was introduced by Efimov and Stechkin [I961]) and later extended to"approximatively weakly compact" by Breckner [1968]) to what we call "approximatively T-compact" for a "regular mode of convergence" in the model. We proved that each approximatively T-compact set of eigendecomposable, orthogonally, seasonal, ecogeoreferenceable, oviposition, hyperproductive, aquatic, larval, habitat foci, endmember explanator on a geoclassified, grid-stratifiable LULC could be proximinal to another non-prolific aquatic, larval habitat, eco-georeferenecable eigenvector-derived, foci (i.e., negative autocorrelation). Moreover, its metric projection validated checked the geo-spectrotemporal, LULC, eco-endmember, wavelength, frequency,LULC prognosticators which we noted satisfied a certain non-incessant condition in the model output.
.

The proof of the claim itself was deceptively simple to geo-spectrotemporally derive from the oviposition, eco-endmember, eco-georeferenecable, ento-ecoepidemiological, malaria, mosquito, oviposition, LULC model. For example, we considered the boundary Q = [−1, 1]n+1 ⊂ R n+1. This equation represented multivariate, LULC, grid-stratified, ecogeoreferenecd, vulnerability, capture point, orthogonal, endmember polynomials whose largest coefficient was 1. As none of these polynomials were 0 identical, by compactness $\min\{a_i\} \in \partial Q \, \|P(a0, a1, \ldots, an)\| = k > 0$. We noticed that if P was linear in the sub-meter resolution, LULC, forecast, vulnerability endmember model, then $P(\lambda a0, \lambda a1, \ldots \lambda an) = \lambda P(a0, a1, \ldots, an)$. We proved that the largest coefficient of a polynomial P in the ento-ecoepidemiological model was M, $\|P\| \geq kM$ for optimally targeting seasonal, eco-georefereneced, hypeproductive, aquatic, larval, habitat, endmember foci.

We also quantitated the sufficiency of the Chebyshev criterion in the malaria, oviposition, endmembr LULC, prognosticative, vulnerability model. Henceforth, a malariologist or medical entomologist should be able to prove if a polynomial P satisfys the Chebyshev criterion in any geo-spectrotemporal, forecast, vulnerability, malaria, mosquito, capture point, LULC, endmember, oviposition, risk model for precisely targeting seasonal, eco-georeferenecable, hyperproductive, aquatic, larval, habitat foci. Suppose polynomial Q is such that $\|f - Q\| < \|f - P\|$ in the frequency, model output. In such circumstances, a malariologist or medical entomologist may employ the polynomial P – Q for optimally quantitating an empirical dataset of malaria, mosquito, endmember, sub-meter resolution, grid-stratifiable, regressively parameterizable, LULC estimators. Suppose that at x odd, P > f while at x even, P < f in the model output. Then P – Q would be strictly positive at x odd and negative at x even. This means that there would exists P − Q in the

oviposition, regressable capture point, empirical orthogonal, eco-endmember, LULC dataset which may have zeros between all geosampled grid-stratifiable, sub-meter resolution, eco-georeferenecable seasonal hyperproductive, aquatic, larval habitats, so the paradigm would have at least n + 1 zeros. But it may be also a polynomial of degree at most geosampled capture points *n*, so it may be 0. Thus, P = Q would be identical in a geo-spectrotemporal, malaria mosquito, model, prognosticated, vulnerability residuals for targeting unknown, eco-georeferenceable, aquatic, larval, habitat, hyperproductive, seasonal foci.

α and β should be able solve the following minimization problem in any, geosampled, eco-georeferenceable, malaria, mosquito, forecast, vulnerability, hyperproductive, orthogonal, endmember, LULC, geo-spectrotemporal model by optimally quantitating argminα,βQ(α,β)arg⁡minα,βQ(α,β),whereQ(α,β)=∑i=1n(yi−α−βxi)2Q(α,β)=∑i=1n(yi−α−βxi)2.The malariologist or the medical entomologist may minimize the following function, in order to achieveα,βα,β:argminα,βP(α,β)arg⁡minα,βP(α,β)whenst P(α,β)=max1≤i≤n|yi−α−βxi|. Serious violations in homoscedasticity (e.g., assuming a distribution of oviposition, wavelength, frequency, sub-meter resolution, LULC, capture point, endmember,signatures are homoscedastic when in reality it is heteroscedastic) in a reference, signature, malaria, mosquito, ento-ecopepidemiological model may result in overestimating the goodness of fit as measured by the Pearson coefficient, a statistic commonly employed in forecast, vulnerability, vector arthropod, aquatic, larval habitat research for optimally prognosticating eco-georeferenecable,geolocations of seasonal, hyperproductive, capture point, geo-spectrotemporal, geosampled foci. For larval control to be effective, it is crucial to maximize control efforts by targeting prolific habitats (Gu and Novak 2005).Ecogeograhically, iteratively, interpolating a target orthogonal, eigendecomposable, LULC, endmember, sub-meter resolution, aquatic, larval habitat signature of an eco-georeferenecable, oviposition, mosquito, seasonal foci, parameterizable estimator may aid in geolocating unknown, hyperproductive, capture points in a sub-meter resolution, grid-stratified image.

Conclusion

In conclusion robust linear correlation estimates were generated from a PROC MIXED constructed regression which identified covariates of importance associated to prolific malaria mosquito, capture point, oviposition habitats at the Kemyan riceland agro-ecosystem study site. To fit the model in PROC NL/MIXED, the REPEATED statement was used to specify the repeated measures factor, from the geosampled dataset of *An. arabiensis* , aquatic, larval habitat explanatory predictor covariates which identified observations that were correlated and their covariance structure. We constructed an oviposition, multinomial, sub-meter resolution, aquatic, larval, habitat, LULC, ento-endmember, signature, frequency, grid-stratified dataset of quantile distribution estimators which were tabularized employing a likelihood-free, Bayesian treatment for determining unknown, eco-georeferenecable, eco-geoclassfiiable, hyperproductive, malaria, mosquito, capture point, foci regressors from an algorithmic, semi-parametric, autocorrelation, model. Subsequently a probabilistic matrix factorization was performed in which model capacity was controlled automatically by integrating over all the model hyperparameters for deducing capture point, Gaussian, LULC priors for geo-spectrotemporally, identifying unknown, hyperproductive, aquatic, larval habitats of *Anopheles arabiensis* s.s., a malaria, mosquito vector, in Karima agro-village complex in the Mwea Rice Scheme in central Kenya.

The objective function, was then minimized employing the method of steepest descent which was linear in the number of geosampled habitat observations. The dot product specific feature vectors were passed through the logistic function g(x)=1/[1+exp(−x)], which bounded the range of signature habitat predictions.We employed a simple linear-Gaussian model which made vulnerability forecasts outside of the range of the known capture point values. As well, the ratings from 1 to K were mapped to the [0,1] interval employing the function t(x)=(x−1)/(K−1). This ensured that the range of the interpolatable, habitat, LULC values matched the range of predictions made by the model. Thus, p(R|U,V,σ2)=∏Mi=1∏Nj=1[N(Rij|g(UTiVj)σ2)]. Proprieties of the posterior distribution in the model, integrated the observed, *Anopheles* data conditioned on a categorical, outcome variable (i.e., immature density count). A generative model was devised where :b∼N(0,σb)a∼N(0,σW)zn∼ (W)xn∼p(·|β,zn)tn∼Weibull[log(1+exp(z^Tna+b)]k. The latent input z_i came from a geosampled, *An. arabiensis*, capture point, regressed, LULC explanator. The seasonal, immature habitat, likelihood distribution was p(t|x)=∫zp(t|z)p(z|x)dz which accounted for all the noise in the sub-pixel, LULC, ento-epidemiological, eco-endmember paradigm employing the Bayes' theorem. In particular, a sequential Monte Carlo (SMC) algorithm that was adaptive in nature approximated a cloud of weighted, random, hyperproductive, seasonal, eco-georeferenced, capture point samples which were subsequently propagated over time. Quantile

distributions were constructed based on a copula from the iterative, Bayesian, computation algorithms. An informative prior was generated. A 2-dimensional Gaussian-Hermite moments based on a set of orthonormal, eco-georeferenceable, LULC polynomials captured rotation and translation invariants in the malaria, mosquito, model which proved that the construction forms of geometric moment invariants were valid in the linearized combinations. The moments stored the capture point, LULC, image information with minimal redundancy. A function was defined on an inner product space which possessed the rotation-invariant property. Since the moments were definable on the continuous domain, suitable transformations of the *An. arabiensis*, aquatic, larval habitat, endmember foci were needed to regressively quantitate these moments. Besides the discretization error derived from the approximation of various integrals, the inevitable uncertainty in the vulnerability forecasts were reconstructed with binary and gray-level, LULC images. The obtained results revealed the quality from Gaussian-Hermite moments were found to be superior than that from known Legendre, discrete Tchebichef and Krawtchouk moments. Habitat properties of the modified, eco-geoclassifiable, eco-georeferenecd, capture point, grid-stratifiable, LULC, ento-endmember polynomials, specifically orthogonality and orthogonal invariance revealed an interval on the center of [-1,1] covered more zeros than did that on the edge of [-1,1]. A set of octiles was trialed as well as functions which exposed the unknown, hyperproductive, capture point, LULC geolocations with all symmetrical values (e.g. uncorrelatedness, scale, skewness and kurtosis) accounted for. The summary statement revealed a broad range of temporal trend derivatives in both the mean and variance. A computation of the probability of inclusion from the SMC output was specified. Variable selection was applied to the lags in the simulation, making it possible to infer the lag order from the time series, regressed, larval count, capture point, habitat signature data simultaneously with all the other geosampled, wavelength estimators.

The probability distribution revealed capture point data conditional on a particular, discrete, aquatic, larval habitat, frequency, density, count value which was optimally devisable by $Np(\mu, A)$, whence μ and A were normalized. It may be desirable to estimate θ under the quadratic loss $L(\theta, \delta) = (\theta - \delta)tQ(\theta - \delta)$ whence geo-spectrotemporally regressively forecasting grid-stratifiable, malaria, mosquito, capture point, sub-meter resolution, sub-pixel, LULC, signature covariates for precisely asymptotically targeting unknown, hyperproductive, eco-georeferenceable, seasonal foci. Sequential estimation of iteratable, capture point, vulnerability signature, LULC ento-endmember prognosticators of unknown, seasonal, *An. arabiensis* foci may reveal risk factors to malaria transmission based on a known, orthogonal, eigenfunction eigen-decomposable, sub-pixel, LULC co-factor (e.g., Euclidean distance of a seasonal, prolific, aquatic, larval habitat, to the nearest, agro-irrigated, agro-village, remotely calculable, grid-stratifiable centroid), unless the eco-georeferenced geosampled count sequence is considered a realization of a random, zero-mean autocorrelated, diagnostic, capture point variable. Intuitively geo-spectrotemporally explicating an eigen-decomposable, eco-endmember, spatial filter, *An. arabiensis*, vulnerability regression equation into main effects and interactions may satisfy the constraint $R(\theta, \delta) \leq tr(Q\Sigma) + c, R(\theta, \delta)$. Although employing prime computing ratios of normalizing constants in common, measurable, space can define correlation and non-orthogonality in such frequency paradigms, the residuals may not equate to causality in any krigeable, ento-endmember dataset of synthetic, capture point, LULC signature eigenvectors. Maximizing the log-posterior over an unmixed, empirical eco-entomological LULC, endmember dataset of seasonal, eco-georeferenced. capture point, non-negatively autorrelated, sub-meter resolution, *An. arabiensis*, attribute features with hyperparameters (i.e. the observation noise variance and prior variances) and simulating the data in probability space may minimize the sum-of-squared-errors objective function employing quadratic regularization terms for prevention of overfitting. Here a parallelizable expectation-maximization algorithm was constructed which we found applicable to large-scale, sub-meter resolution, capture point, seasonal, malaria, mosquito, aquatic, larval, habitat, prognosticative risk, mapping applications. Regardless, our main result in this research is that an Lipschitz map quantitated between separable quasi-Banach spaces is Fréchet differentiable Γ-almost everywhere in an sub-meter resolution, grid-stratifiable, LULC, *An arabenisis*, eco-georeferenceable, capture point, eco-endmember, forecast vulnerability signature model provided that it is regularly Gˆateaux differentiable Γ-almost everywhere in the model and the residual derivatives stay within a norm separable space of operators. It is easy to see that capture point, seasonal, malaria, mosquito, LULC, sub-pixel, signature, risk maps with the Radon-Nikodym property are Gˆateaux differentiable Γ. Moreover, Gˆateaux differentiability implies regular Gˆateaux differentiability with exception of another kind of negligible sets, (i.e., σ-porous sets). An eco-georeferenceable, eco-geoclassifiable, seasonal, hyperproductive, capture point, sub-meter resolution, *An. arabiensis*, eco-endmember, LULC, signature model is positive in every space in which every σ-porous sub-set is Γ-null. We show that this holds for C(K) with K countable compact, the Tsirelson space and for all subspaces of c0, but that it fails for Hilbert spaces

The Bayesian framework allowed flexible model fitting, estimation, and mapping of all high risk georeferenced ,*An. arabiensis*, aquatic, larval habitats based on the field and remote-sampled parameters using a MCMC specification. By letting V be a fixed positive definite matrix of size $p \times p$ in a robust seasonal predictive vector arthropod-related endemic transmission oriented risk model then, if $n \geq p$, $\mathbf{X}$ and has a Wishart distribution with n degrees of freedom the reisudl forecast had a probability density function given by $\frac{1}{2^{\frac{np}{2}}|\mathbf{V}|^{\frac{n}{2}}\Gamma_p(\frac{n}{2})}|\mathbf{X}|^{\frac{n-p-1}{2}}e^{-\frac{1}{2}\mathrm{tr}(\mathbf{V}^{-1}\mathbf{X})}$ where $\Gamma_p(\cdot)$ is the multivariate gamma function defined $\Gamma_p(n/2) = \pi^{p(p-1)/4}\Pi_{j=1}^{p}\Gamma\left[n/2 + (1-j)/2\right]$. In fact the above definition can be extended to any real $n > p - 1$. The model identified the sampled explanatory predictor covariate distance from the capture point as being significantly positively associated with prolific habitats based on sampled larval abundance counts. Incorporating *An. arabiensis* larval habitats parameter estimates in a PROC NL'MIXED regression framework, a spatial filter analyses in SAS/= and a Bayesian GHLM in PROC MCMC can help generate accurate operational field maps for targeting prolific riverine habitat based on seasonal field-sampled count data These models can quantitate seasonal *An. arabiensis* endemic transmission-oriented estimators employing (a) Gaussian residuals with input-dependent variance, or (b) non-Gaussian residuals with input-dependent variance, or (c) Gaussian residuals with constant variance. We prove the main criterion for Fr´echet differentiability of Lipschitz functions in terms of Γ-null sets for a sub-meter resolution, grid-stratified, *An. arabiensis*, aquatic, larval habitat,capture point, geo-spectrotemporal, ento-ecoepidemiological, eco-georeferenecable, LULC, eco-endmember model. We did so by introducing the following simple notion. Suppose that f is a seasonal, hyperproductive, eco-georeferenceable, forecast, vulnerability, capture point, eco-endmember map from (an open set in) X to Y. Hence un-geosampled, seasonal, hyperproductive foci, capture point x would be a regular capture point of f only if for every v ∈ X for which f (x, v) exists, lim t→0 f(x + tu + tv) − f(x + tu) t = f (x, v) uniformly for u ≤ 1. Note that in the definition above it is enough to take the limit for t 0 only, since v by –v may be replaced in the model. A An. arabiensis aquatic, larval habitat Chebyshev polynomial of the first kind was related to the Bessel function of the first kind $J_n(x)$ and the modified Bessel function of the first kind $I_n(x)$ by the relations $J_n(x) = i^n T_n\left(i\frac{d}{dx}\right)J_0(x) I_n(x) = T_n\left(\frac{d}{dx}\right)I_0(x).$ Letting $x \equiv \cos\theta$ allowed the Chebyshev polynomials of the first kind to be written as $T_n(x) = \cos(n\theta) = \cos\left(n\cos^{-1}x\right).$

Our main result in this research is that an Lipschitz map quantitated between separable quasi-Banach spaces is Frechet differentiable Γ-almost everywhere in an oviposition, *An arabenisis* s,s, seasonal, grid-stratified, capture point, sub-meter resolution, signature model provided that it is regularly Gˆateaux differentiable Γ-almost everywhere in the model and the endmember derivatives stay within a norm separable space of operators. Further, an eco-georeferenceable, hyperproductive, capture point, sub-meter resolution, oviposition, *An. arabiensis*, grid-stratified, endmember, LULC signature model is positive in every space in which every σ-porous set is Γ-null.

Appendix 1

Cramer's Rule

Given a system of linear equations, Cramer's Rule is a handy way to solve for just one of the variables without having to solve the whole system of equations. Instead of solving the entire system of equations, a researcher mayuse Cramer's to solve for just one single variable.For example, let us employ the following system of equations:

2*x*	**+**	***y***	**+**	***z***	**=**	**3**
x	**–**	***y***	**–**	***z***	**=**	**0**
***x* + 2*y* + *z* = 0**						

We have the left-hand side of the system with the variables (the "coefficient matrix") and the right-hand side with the answer values. Let D be the determinant of the coefficient matrix of the above system, and let D_x be the determinant formed by replacing the x-column values with the answer-column values.

Then:

system of equations	coefficient matrix's determinant	answer column	D_x: coefficient determinant with answer-column values in x-column
$2x + 1y + 1z = 3$ $1x - 1y - 1z = 0$ $1x + 2y + 1z = 0$	$D = \begin{vmatrix} 2 & 1 & 1 \\ 1 & -1 & -1 \\ 1 & 2 & 1 \end{vmatrix}$	$\begin{bmatrix} 3 \\ 0 \\ 0 \end{bmatrix}$	$D_x = \begin{vmatrix} 3 & 1 & 1 \\ 0 & -1 & -1 \\ 0 & 2 & 1 \end{vmatrix}$

Similarly, D_y and D_z would then be:

$$D_y = \begin{vmatrix} 2 & 3 & 1 \\ 1 & 0 & -1 \\ 1 & 0 & 1 \end{vmatrix} \qquad D_z = \begin{vmatrix} 2 & 1 & 3 \\ 1 & -1 & 0 \\ 1 & 2 & 0 \end{vmatrix}$$

Evaluating each determinant, w

e get:

$$D = \begin{vmatrix} 2 & 1 & 1 \\ 1 & -1 & -1 \\ 1 & 2 & 1 \end{vmatrix} = (-2)+(-1)+(2) \\ -(-1)-(-4)-(1) = 3$$

$$D_x = \begin{vmatrix} 3 & 1 & 1 \\ 0 & -1 & -1 \\ 0 & 2 & 1 \end{vmatrix} = (-3)+(0)+(0) \\ -(0)-(-6)-(0) = -3+6 = 3$$

$$D_y = \begin{vmatrix} 2 & 3 & 1 \\ 1 & 0 & -1 \\ 1 & 0 & 1 \end{vmatrix} = (0)+(-3)+(0) \\ -(0)-(0)-(3) = -3-3 = -6$$

$$D_z = \begin{vmatrix} 2 & 1 & 3 \\ 1 & -1 & 0 \\ 1 & 2 & 0 \end{vmatrix} = (0)+(0)+(6) \\ -(-3)-(0)-(0) = 6+3 = 9$$

Cramer's Rule says that $x = D_x \div D$, $y = D_y \div D$, and $z = D_z \div D$. That is:$\boldsymbol{x = {}^{3}/_{3} = 1}$, $\boldsymbol{y = {}^{-6}/_{3} = -2}$, **and** $\boldsymbol{z = {}^{9}/_{3} = 3}$ To find whichever variable ("ß" or "beta"), a researcher must evaluate the determinant quotient $D_ß \div D$. Hence given the following system of equations, find the value of z, then

$$\begin{array}{rcrcrcr} \mathbf{2x} & + & \mathbf{y} & + & \mathbf{z} & = & \mathbf{1} \\ \mathbf{x} & - & \mathbf{y} & + & \mathbf{4z} & = & \mathbf{0} \\ \multicolumn{7}{l}{\mathbf{x + 2y - 2z = 3}} \end{array}$$

To solve only for *z*, a researcher must first find the coefficient determinant. $D=\begin{vmatrix} 2 & 1 & 1 \\ 1 & -1 & 4 \\ 1 & 2 & -2 \end{vmatrix} = (4)+(4)+(2) \\ -(-1)-(16)-(-2)=10-13=-3$ Then I will form D_z by replacing the third column of values with the answer column: $D_z=\begin{vmatrix} 2 & 1 & 1 \\ 1 & -1 & 0 \\ 1 & 2 & 3 \end{vmatrix} = (-6)+(0)+(2) \\ -(-1)-(0)-(3)=-4-2=-6$

Then I will form the quotient and simplify: $\frac{D_z}{D}=\frac{-6}{-3}=2$ **Hence *z* = 2.**

Appendix 2.

de la Vallée-Poussin theorem

The de la Vallée-Poussin theorem on the distribution of prime numbers: Let π(x)π(x) be the number of primes smaller than xx; then, if x≥1x≥1, the following equality is valid:
π(x)=li(x)+O(xexp(−Clogx−−−−√))π(x)=li(x)+O(xexp⁡(−Clog⁡x))where CC is a positive constant and li(x)li(x) is the logarithmic integral of xx. This theorem demonstrates the correctness of Gauss' hypothesis on the distribution of prime numbers, viz., as x→∞x→∞,π(x)∼xlogx .

The logarithmic integra is a special function defined, for positive real $x \neq 1$, by $\mathrm{li}\,(x)=\int_0^x \frac{dt}{\ln t}$; for $x>1$ the integrand has at $t=1$ an infinite discontinuity and the integral logarithm is taken to be the principal value $\mathrm{li}\,(x)=\lim_{\epsilon \downarrow 0}\left\{\int_0^{1-\epsilon}\frac{dt}{\ln t}+\int_{1+\epsilon}^{x}\frac{dt}{\ln t}\right\}$. The graph of the integral logarithm is given in the article Integral exponential function. For x small: $\mathrm{li}\,(x)\approx\frac{x}{\ln(1/x)}$. The integral logarithm has for positive real x the series representation $\mathrm{li}\,(x)=c+\ln|\ln x|+\sum_{k=1}^{\infty}\frac{(\ln x)^k}{k!k}, \quad k>0, \quad x\neq 1,$ where $c=0.5772\ldots$ is the Euler constant..

Euler's constant is number γ defined by
γ=limn→∞(1+12+⋯+1n−lnn)≈0.57721566490…,γ=limn→∞(1+12+⋯+1n−ln⁡n)≈0.
,considered by L. Euler (1740). Its existence follows from the fact that the sequence

1+12+⋯+1n−ln(n+1)1+12+⋯+1n−ln⁡(n+1)is monotone increasing and bounded from above. The number-theoretic nature of the Euler constant has not been studied; it is not even known (2012) whether it is a rational number or not.In fact, a relation ∑n≤x1n−lnx=γ+O(1x)

As a function of the complex variable z, $\mathrm{li}\,(z)=c+\ln(-\ln z)+\sum_{k=1}^{\infty}\frac{(\ln z)^k}{k!k}$ is a single-valued analytic function in the complex z-plane with slits along the real axis from $-\infty$ to 0 and from 1 to $+\infty$ (the

imaginary part of the logarithms is taken within the limits $-\pi$ and π). The behaviour of $\mathrm{li}\ x$ along $(1, +\infty)$ is described by $\lim_{\eta \downarrow 0} \mathrm{li}\ (x \pm i\eta) = \mathrm{li}\ x \mp \pi i, \quad x > 1$.

For x small: $\mathrm{Ci}\ (x) \approx c + \ln x$. The capture point, asymptotic representation, for x large, is: $\mathrm{Ci}\ (x) = \frac{\sin x}{x} P(x) - \frac{\cos x}{x} Q(x), P(x) \sim \sum_{k=0}^{\infty} \frac{(-1)^k (2k)!}{x^{2k}}, \quad Q(x) \sim \sum_{k=0}^{\infty} \frac{(-1)^k (2k+1)!}{x^{2k+1}}$.

The integral cosine has the series, explanatory, LULC, representation: $\mathrm{Ci}\ (x) = c + \ln x - \frac{x^2}{2!2} + \frac{x^4}{4!4} - \ldots + + (-1)^k \frac{x^{2k}}{(2k)!2k} + \ldots.$

As a function of the complex variable z, $\mathrm{Ci}\ (z)$, defined by (*), is a single-valued analytic function in the z-plane with slit along the relative negative real axis $(-\pi < \arg z < \pi)$. The value of $\ln z$ here is taken to be $\pi < \mathrm{Im} \ln z < \pi$. The behaviour of $\mathrm{Ci}\ (z)$ near the slit is determined by the limits $\lim_{\eta \downarrow 0} \mathrm{Ci}\ (x \pm i\eta) = \mathrm{Ci}\ (|z|) \pm \pi i, \quad x < 0$. The integral cosine is related to the integral exponential function $\mathrm{Ei}\ (z)$ by $\mathrm{Ci}\ (z) = \frac{1}{2} [\mathrm{Ei}\ (iz) + \mathrm{Ei}\ (-iz)]$. function li is better known as the logarithmic integral. It can, of course, be defined by the integral (as above) for $z \in \mathbf{C} \setminus \{x \in \mathbf{R}: x \leq 0 \text{ or } \square x \geq 1\}$.

The series representation for positive x, $x \neq 1$, is then also said to define the modified logarithmic integral, and is the boundary value of $\mathrm{li}\ (x + i\eta) \pm \pi i, x > 1, \eta \to 0$. For real $x > 1$ the value $\mathrm{li}\ (x)$ is a good approximation of $\pi\ (x)$, the number of primes smaller than x

References

[1] Jacob BG, Novak RJ, Toe LD, Sanfo M, Griffith DA, Lakwo Unnasch T. Ecogeographically and Non-Ecogeographically Forecasting Discontinuously Canopied Seasonally Hyperproductive Trailing Vegetation Precambrian rock *Simulium damnosum* s.l., Eco-epidemiological Capture Point Morphometrics by Geo-spectrotemporally Iteratively Stochastically Interpolating Metrizable Sub-Mixel Mean Solar Exoatmospheric Quantum Scalar Irradiance Wavelength Periodicities where θ_i is a Zenith Angle and Diatomically Etiolated Xanthophylls with Azimutually Isotropic Sources of Chloroplastic Carotenoid Zeaxanthins Stoichiometerically Extracted from a RapidEye™ Red Edge Normalized Difference Vegetation Index Reference Biosignature: A Case Study in Burkina Faso and Uganda (*Journal of Geophysics and Remote sensing* 2015 5(1);. 12-103.

[2] Cressie, NAC 1993 Statistics for Spatial Data Revised Edition. New York: John Wiley & Sons, Inc.

[3] Jacob BG, Novak RJ, Toe L, Sanfo MS, Afriyie AN, Ibrahim MA, Griffith DA, Unnasch TR. Quasi-Likelihood Techniques in a Logistic Regression Equation for *Identifying Simulium damnosum s.l.* Larval Habitats Intra-cluster Covariates in Togo. Geospatial information Science 2012;15(2):117-133.

[4]. Arellano, M. (1987), .Computing Robust Standard Errors for Within-Group Estimators,. Oxford Bulletin of Economics and Statistics, 49, 431-434Griffith D.A., "Spatial autocorrelation and spatial filtering: Gaining understanding through theory and scientific visualization," Springer-Verlag, Berlin, 2003

[5]. Hansen, C. B. (2007a), .Generalized least squares inference in panel and multilevelmodels with serial correlation and .xed e¤ects,. Journal of Econometrics, 140, 670-694

[6] Driscoll, J. C., and A. C. Kraay. 1998. Consistent Covariance Matrix Estimation with Spatially Dependent Panel Data. *Review of Economics and Statistics* 80: 549–560.

[7].Jacob BG, Griffith DA, Muturi EJ, Caamano EX, Githure JI, Novak RJ. A heteroskedastic error covoariance matrix estimator using a first-order conditional autoregressive Markov simulation for deriving asympotical efficient esetimates from ecological sampled *Anopheles arabiensis* aquatic habitat covariates. *Malaria Journal* 2009d; 8(1):216-225.

[8]. Hendricks W.A., Robey K.W. The Sampling Distribution of the Coefficient of Variation Annals of . Mathetical . Statistics. 7, (3) 129-132.

[9] O'Malley, A. J. and Zaslavsky, A. M. (2005), \Variance-covariance functions for domain meansof ordinal survey items," Survey Methodology, 31, 169{182.

[10]. Driscoll, J. C., and A. C. Kraay. 1998. Consistent Covariance Matrix Estimation with
Spatially Dependent Panel Data. *Review of Economics and Statistics* 80: 549–560.